DOCKET: EPA-HQ-OAR-2019-0534

OVERVIEW OF EPA REVIEW OF U.S. DEPARTMENT OF ENERGY 2019 WIPP COMPLIANCE RECERTIFICATION APPLICATION PERFORMANCE ASSESSMENT

U.S. Environmental Protection Agency
Office of Radiation and Indoor Air
Center for Waste Management and Regulations
1200 Pennsylvania Ave., NW
Washington, DC 20460

April 2022

PREFACE

The Waste Isolation Pilot Plant (WIPP) repository was developed by the U.S. Department of Energy (DOE or the Department) for the permanent disposal of transuranic (TRU) waste. The U.S. Environmental Protection Agency (EPA or the Agency) provides regulatory oversight of the post-closure performance of the WIPP. The DOE is required to submit a Compliance Recertification Application (CRA) to the EPA every five years that includes an updated assessment of future WIPP performance. The ability of the WIPP to meet the EPA's post-closure numerical waste isolation performance standards is determined by the results of computer modeling conducted for the DOE by Sandia National Laboratories (SNL). That modeling simulates the repository's future performance in a process called Performance Assessment (PA). The most recent assessment was included in DOE's 2019 CRA and is called the CRA-2019 PA.

The DOE's 2019 CRA was submitted to EPA in March 2019 and the CRA-2019 PA EPA reviewed was submitted to the Agency in December 2019. This PA, also called the deferred PA (DPA), was, with Agency agreement, not submitted at the same time as the recertification application. This deferred PA was previously agreed upon by EPA and DOE so that the Department could address technical issues identified in the previous CRA into CRA-2019. Because the CRA-2019 PA was not yet complete at the time the DOE's 2019 recertification application was submitted, that application referred to the Agency-approved CRA-2014 PA on an interim basis as the current baseline PA. Upon completion, the deferred CRA-2019 PA superseded the CRA-2014 PA and was regarded by the Agency as the DOE's formal, updated demonstration of continuing compliance with EPA's performance requirements.

TABLE OF CONTENTS

PREFACE 2
1.0 INTRODUCTION 7
2.0 CHANGES IN WIPP PERFORMANCE ASSESSMENT SINCE CRA-2014 8
2.1 Waste Area Design Changes 9
2.2 Additional Shaft and Associated Drifts 9
2.3 Incorporation of Brine Radiolysis 10
2.4 Refinement of the Probability of Encountering Pressurized Brine 10
2.5 Refinement of the Corrosion Rates of Steel 10
2.6 Refinement of the Effective Shear Strength of WIPP Waste 10
2.7 Refinement of Colloid Enhancement Parameters 11
2.8 Refinement of Hydromagnesite Conversion Rate 11
2.9 Removal of Iron Sulfidation Reactions 11
2.10 Correction to Length of Northernmost Panel Closure Representation 11
2.11 Updates in Drilling Rate and Plugging Pattern Parameters 11
2.12 Updates to WIPP Waste Inventory Parameters 12
2.13 Updates to Radionuclide Solubilities 12
2.14 Update to BH_OPEN:RELP_MOD Parameter 12
2.15 New Materials to Define Properties in the DRZ Surrounding Operations, Experimental, and Panel Closure Areas 13
2.16 Hardware and Computational Code Updates 13
3.0 PRINCIPAL FINDINGS IDENTIFIED BY EPA IN CRA-2019 TECHNICAL SUPPORT DOCUMENTS 13
3.1 FEPs TSD 13
3.2 APCS TSD 14
3.3 Culebra TSD 16
3.4 Borehole TSD 17
3.5 New Shaft TSD 21
3.6 Inventory TSD 24
3.7 Chemistry TSD 25
3.8 Models and Codes TSD 30
4.0 EPA SENSITIVITY STUDIES 32
4.1 PLG_PROB Analysis: Sensitivity to Borehole Plugging Frequencies 33
4.2 GCHM_S0 Analysis: Sensitivity to Actinide Baseline Solubility 34

4.3 GCHM_S1 Analysis: Sensitivity to Actinide Baseline Solubility and +III Actinide Solubility Uncertainty Distribution 36
4.4 GCHM_S2 Analysis: Sensitivity to Actinide Baseline Solubility and Actinide Colloid Parameters 37
4.5 GCHM_S3 Analysis: Sensitivity to Actinide Solubility, Colloid Parameters, and Actinide Oxidation State 38
4.6 CRA19_COMB Analysis: Sensitivity to EPA's Combined Geotechnical and Geochemical Parameter Changes 39
5.0 EPA CONCLUSIONS AND EXPECTATIONS 40
REFERENCES 42

LIST OF TABLES

Table 3.8-1. Computer Code and Library Versions Reviewed and Approved by the Agency

LIST OF FIGURES

Figure 3.4-1. Map showing wells that would have been used in the CRA-2019 PA to determine plugging frequency based on the EPA-approved methodology of considering all abandoned wells in the New Mexico part of the Delaware Basin.

Figure 3.4-2. Map showing KPLA wells used by DOE to determine plugging frequency for the CRA-2019 PA.

Figure 3.5-1. Plan view of the WIPP underground showing locations of the waste panels, exhaust shaft, and areas of limited access as of November 2016.

Figure 3.5-2. Conceptual plan view of the repository Operations Area showing the locations of the new fifth shaft and connecting drifts.

Figure 4.1-1. Mean total releases based on the Agency's approved approach (PLG_PROB curve) compared with mean total releases using DOE's new plugging pattern frequency calculation (CRA19 curve).

Figure 4.2-1. Mean DBRs calculated for the CRA-2019 PA (CRA19), the EPA revised baseline actinide solubility sensitivity calculation (GCHM_S0), and the EPA revised baseline actinide solubility plus +III actinide solubility uncertainty sensitivity calculation (GCHM_S1).

Figure 4.2-2. Mean total releases calculated for the CRA-2019 PA (CRA19), the EPA revised baseline actinide solubility sensitivity calculation (GCHM_S0), and the EPA revised baseline actinide solubility plus +III actinide solubility uncertainty sensitivity calculation (GCHM_S1).

Figure 4.4-1. Mean DBRs for the CRA-2019 PA (CRA19); the EPA revised baseline actinide solubility sensitivity calculation (GCHM_S0); the EPA revised baseline actinide solubility plus intrinsic and microbial colloid sensitivity calculations (GCHM_S2); and the EPA sensitivity calculation combining revised baseline actinide solubility, intrinsic and microbial colloid, and actinide oxidation state parameters (GCHM_S3).

Figure 4.4-2. Mean total repository releases for the CRA-2019 PA (CRA19); the EPA revised baseline actinide solubility sensitivity calculation (GCHM_S0); the EPA revised baseline actinide solubility plus intrinsic and microbial colloid sensitivity calculations (GCHM_S2); and the EPA sensitivity calculation combining revised baseline actinide solubility, intrinsic and microbial colloid, and actinide oxidation state parameters (GCHM_S3).

Figure 4.6-1. Mean total repository releases from combined geotechnical and geochemical parameter changes.

LIST OF APPENDICES

APPENDIX A. EPA Completeness Questions, DOE Responses, and EPA Evaluations of Responses

APPENDIX B. Review of Parameters Used in the CRA-2019 Performance Assessment That Have Changed Since the CRA-2014 Performance Assessment

LIST OF ACRONYMS AND ABBREVIATIONS

APCS	Abandonment of Panel Closures in the South
ASER	Annual Site Environmental Report
ATWIR	Annual TRU Waste Inventory Report
BLM	U.S. Bureau of Land Management
CCA	Compliance Certification Application
CFR	Code of Federal Regulations
CID	Comprehensive Inventory Database
CPR	Cellulosic, Plastic, and Rubber Material
CRA	Compliance Recertification Application
DBMAR	Delaware Basin Monitoring Annual Report
DBR	Direct Brine Release
DOE or The Department	U.S. Department of Energy
DPA	Deferred Performance Assessment
DRZ	Disturbed Rock Zone
EDTA	Ethylenediaminetetraacetic acid
EPA or the Agency	Environmental Protection Agency
EXP	Repository Experimental Area
FEP	Feature, Event, or Process
KPLA	Known Potash Leasing Area
LANL	Los Alamos National Laboratory
LWA	Land Withdrawal Act

LWB	Land Withdrawal Act Boundary
NROR	North Rest-of-Repository
OCD	New Mexico Oil Conservation Division
OPS	Repository Operations Area
PA	Performance Assessment
PAIR	Performance Assessment Inventory Report
RD	Requirements Document
ROM	Run-of-Mine
QA	Quality Assurance
SNL	Sandia National Laboratories
SPR	Software Problem Report
SROR	South Rest-of-Repository
TDEM	Time Domain Electromagnetic
TRU	Transuranic
TSD	Technical Support Document
WDS	Waste Data System
WIPP	Waste Isolation Pilot Plant

Support for this report was provided by SC&A, Arlington, Virginia, under Contract 68HERD20A0005, Task Order 68HERH20F0404, Task 1132-0003-001-001-02b. Although issues of both technical practice and regulatory intent are addressed in this report, final interpretation of the EPA rule and ultimate acceptance or rejection of the EPA expectations expressed in this report is only within the purview of the Agency.

1.0 INTRODUCTION

The Waste Isolation Pilot Plant (WIPP) Land Withdrawal Act (LWA) is a federal statute (Congress 1996) requiring the U.S. Department of Energy (DOE or the Department) to operate a repository for the disposal of transuranic (TRU) radioactive waste. The LWA also specifies that the U.S. Environmental Protection Agency (EPA or the Agency) is to regulate post-closure containment of TRU waste at the WIPP. EPA regulates WIPP in accordance with the radioactive waste disposal standards at Code of Federal Regulations (CFR) Title 40, Parts 191 and 194. The WIPP is located in deeply buried deposits of bedded salt in the Salado Formation within the Delaware Basin in southeastern New Mexico. The WIPP was first certified by EPA as complying with these standards and approved for TRU waste disposal in 1998. The WIPP LWA requires the DOE to submit Compliance Recertification Applications (CRAs) at five-year intervals following the first waste shipment in March 1999. The most recent CRA was submitted by DOE in March 2019 with supplemental calculations provided in December 2019 and is called the CRA-2019. EPA's decision whether to recertify the WIPP is based in part on the results of an assessment of the projected ability of the repository to meet the Agency's numerical waste isolation standards over the 10,000-year post-closure regulatory period. This Technical Support Document (TSD) provides an overview of EPA's technical evaluation of the DOE's performance assessment (PA) calculations for the CRA-2019.

Part of DOE's responsibility is to update the PA to conform with recent changes in conditions that may affect post-closure repository performance. Potential changes in conditions include, for example, the amount, types and properties of the waste, the rates of local exploratory drilling for oil and gas, and revisions to the repository design. DOE is also responsible for updating PA parameter values using current scientific information relevant to future predictions of repository performance. The Agency began its analysis of the CRA-2019 PA with a completeness review to determine whether the changes were clearly explained with adequate supporting documentation. EPA's review also determined whether the changes that had been requested by the Agency in its CRA-2014 PA review had been made.

DOE's preparation of a PA begins with a comprehensive review of a list of features, events, and processes (FEPs) potentially relevant to WIPP repository performance. Each FEP in the list is accompanied by a screening argument that describes how that FEP could affect repository performance modeling. The purpose of FEP screening is to determine which FEPs should be addressed in performance modeling. For each new recertification, past screening arguments are reviewed for continued relevance and updated as new information becomes available. The FEP screening performed by DOE for the CRA-2019 PA is described in Sosson (2019, Appendix SCR-2019).

EPA's review of the CRA-2019 PA FEPs focused on the adequacy of the Department's FEP screening process, the manner in which the relevant FEPs were incorporated into performance modeling, and the adequacy of DOE's demonstration of continued compliance. As part of its review, the Agency transmitted a series of completeness comments to DOE requesting clarifications and additional information to better understand the Department's modeling assumptions and rationale. The Agency's completeness comments, DOE responses, and the Agency's evaluations of those responses are summarized in Attachment A to this TSD. In

addition, the Agency reviewed the documentation of changes made to the parameter database since the previous CRA-2014 PA for completeness and accuracy. A summary of the Agency's database review is presented in Attachment B.

The principal findings identified by the Agency in its CRA-2019 PA review are the subjects of detailed analyses described in the following TSDs.

FEPs TSD:	*Review of Changes to WIPP Performance Assessment Features, Events, and Processes in the 2019 CRA (Docket ID No. EPA-HQ-OAR-2019-0534)*
APCS TSD:	*Review of the APCS Approach to Analyzing WIPP Repository Performance in the CRA-2019 Performance Assessment (Docket ID No. EPA-HQ-OAR-2019-0534)*
Culebra TSD:	*Review of Groundwater Flow and Radionuclide Transport Conceptualization in the Culebra Dolomite (Docket ID No. EPA-HQ-OAR-2019-0534)*
Borehole TSD:	*Review of Borehole Drilling Rate and Plugging Pattern Frequency Calculations in the CRA-2019 Performance Assessment (Docket ID No. EPA-HQ-OAR-2019-0534)*
New Shaft TSD:	*Review of DOE Planned Change Notice for a Fifth Shaft at the WIPP Repository (Docket ID No. EPA-HQ-OAR-2019-0534)*
Inventory TSD:	*Review of the Baseline Inventory Used in the Compliance Recertification Application (CRA-2019) (Docket ID No. EPA-HQ-OAR-2019-0534)*
Chemistry TSD:	*Evaluation of the Compliance Recertification Application (CRA-2019) Actinide Source Term, Gas Generation, Backfill Efficacy, Water Balance, and Culebra Dolomite Distribution Coefficient Values (Docket ID No. EPA-HQ-OAR-2019-0534)*
Models and Codes TSD:	*Review of Changes to WIPP Performance Assessment Computer Models and Codes in the CRA-2019 Performance Assessment (Docket ID No. EPA-HQ-OAR-2019-0534)*

A summary of the changes to the CRA-2019 PA that were identified by DOE is presented in Section 2 of this Overview TSD. Section 3 describes the principal findings identified by EPA in the foregoing TSDs and presents options identified by EPA for addressing those concerns. Section 4 describes the results of sensitivity studies conducted by EPA to evaluate the impacts of the Agency's principal findings. Section 5 summarizes EPA's overall response to the approach taken by DOE in assessing post-closure repository performance in the CRA-2019 PA.

2.0 CHANGES IN WIPP PERFORMANCE ASSESSMENT SINCE CRA-2014

DOE's CRA-2014 PA is the most recent Agency-approved PA and was used by Sandia National Laboratories (SNL) as the basis for identifying relevant changes to the CRA-2019 PA. The changes to the CRA-2019 PA were identified by DOE (CRA-2019, Appendix PA-2019, Section PA-1.1) and are summarized below.

2.1 Waste Area Design Changes

The WIPP repository was closed in February 2014 following an accidental release of radionuclides that contaminated the south end of the underground repository waste area. Although the repository was later reopened on a limited basis, access to the contaminated areas was prohibited and routine maintenance of ground control could not be conducted. This resulted in unsafe conditions that led to a DOE decision to withdraw from and seal off the part of the waste area designated as Panel 9 (DOE 2016). With that change, the planned installation of run-of-mine (ROM) salt panel closures in Panels 3, 4, 5, and 6 would no longer be possible because access to these panels requires access to Panel 9. Also, waste emplacement in Panel 9 would no longer be possible and a replacement for Panel 9 at an undesignated location within the underground repository was proposed. Because of these changes, in December 2017 the DOE proposed modifying the CRA-2019 PA by incorporating an Abandonment of Panel Closures in the South (APCS) approach. This approach is described in Zeitler et al. (2017) and is briefly described below. Upon review, the Agency agreed with incorporating this approach into the deferred CRA-2019 PA (Veal 2017).

The APCS approach was designed by SNL to conservatively overestimate repository releases while accounting for the abandonment of Panel 9 and the lack of ROM salt panel closures in the access drifts to four southernmost waste panels. The lack of panel closures was to be modeled by ignoring salt creep and changing the material properties for the now-open access drifts and their surrounding disturbed rock zones (DRZs) to be the same as the high porosity and permeability "open drift" properties used for the WIPP Operations and Experimental (OPS/EXP) areas. The abandoned Panel 9 continued to be modeled as waste-filled, serving as a surrogate for the replacement Panel 9. In addition, the "neighbors" relationships among waste panels were redefined such that the isolation afforded by single ROM salt panel closures, including the closures between Panels 9 and 10, was ignored. This convention allowed brine and gas to flow relatively unimpeded between adjacent panels. The rationale for these changes is presented in Zeitler et al. (2017) and is further discussed in EPA's TSD "*Review of the APCS Approach to Analyzing WIPP Repository Performance in the CRA-2019 Performance Assessment*" (Docket ID No. EPA-HQ-OAR-2019-0534).

2.2 Additional Shaft and Associated Drifts

In addition to the south end of the underground repository waste area, the accidental radionuclide release mentioned in Section 2.1 also contaminated the exhaust ventilation shaft. As a result, the DOE is planning a modified ventilation system that will provide sufficient airflow for future disposal operations (Shrader 2017). The primary components of this system are a new shaft in the north end of the repository and the associated drifts needed to connect the new shaft to the repository. A detailed review of the new shaft and connecting drifts is presented in EPA's TSD "*Review of DOE Planned Change Notice for a Fifth Shaft at the WIPP Repository*" (Docket ID No. EPA-HQ-OAR-2019-0534).

2.3 Incorporation of Brine Radiolysis

Gas generation from radiolysis of brine in the WIPP repository results primarily from the decay of americium and plutonium isotopes. Gas generation is important to repository performance because elevated gas pressure is a primary driver of all but the cuttings and cavings release pathways. The increased americium and plutonium projected for disposal in the CRA-2019 waste inventory (Kicker 2019) prompted a reevaluation of the significance of radiolysis to repository performance (Day 2019). Brine radiolysis was added to the gas generation process model in response to this evaluation and to a confirmation of the increased importance of this process to repository performance through the FEP screening process (Kirkes 2019).

2.4 Refinement of the Probability of Encountering Pressurized Brine

The WIPP PA parameter GLOBAL:PBRINE (hereafter called PBRINE) is used to specify the probability that a drilling intrusion into the waste area of the repository encounters a region of pressurized brine in the Castile Formation below the repository. SNL (Kirchner et al. 2012) developed a new distribution for this uncertain parameter and used this distribution in place of the previous distribution mandated by EPA in 1998 (Peake 1998). SNL based its distribution solely on drilling data and did not consider relevant time-domain electromagnetic (TDEM) geophysical data or hydrogeologic field investigations of known brine reservoirs. The Agency subsequently created a revised distribution for the PBRINE parameter based on a reexamination of the original TDEM and field data. DOE used the revised distribution in the CRA-2019 PA, as directed by EPA (EPA 2017a; Veal 2017).

2.5 Refinement of the Corrosion Rates of Steel

The interaction of steel in the WIPP with repository brines results in the generation of hydrogen gas from anoxic corrosion. The brine-inundated corrosion rate (STEEL:CORRMCO2) and the humid condition corrosion rate (STEEL:HUMCORR) were updated for the CRA-2019 PA. These changes were based on experimental results from Roselle (2013), the potential for enhanced corrosion at elevated pressures, the fact that some corrosion will occur in humid conditions, and the bounding CO_2 level (5 ppm) expected in the repository (Zeitler 2018a; 2018b).

2.6 Refinement of the Effective Shear Strength of WIPP Waste

WIPP PA includes scenarios in which human intrusion results in a borehole intersecting the waste area of the repository. During the intrusion, drilling mud flowing up the borehole will apply a hydrodynamic shear stress on the waste in the borehole wall. Erosion of the waste material can occur if the shear stress is high enough, resulting in radionuclides being carried up the borehole with the drilling mud and released to the accessible environment. The WIPP PA parameter BOREHOLE:TAUFAIL (hereafter called TAUFAIL) is used to represent the effective shear strength for erosion of WIPP waste. For the CRA-2014 PA, experimental results from Herrick et al. (2012) were used to determine an updated parameter distribution for TAUFAIL (Herrick and Kirchner 2013). Subsequent to the submittal of the CRA-2014, EPA requested DOE to reduce the lower bound of the TAUFAIL distribution to equal the lowest measured value

of the subset of the Herrick data included in that distribution (EPA 2017c). DOE used the revised lower bound in the CRA-2019 PA.

2.7 Refinement of Colloid Enhancement Parameters

Changes were made to intrinsic, humic, and microbial colloid enhancement parameters based on new laboratory and literature data since the CRA-2014 PA. These parameters are used to calculate mobilized radionuclide concentrations (Reed et al. 2019; Mariner 2019). In addition, the basis for the CAPMIC (maximum concentration of actinides on microbial colloids) parameterization changed for the CRA-2014 PA from a toxicity to a biomass approach (Reed et al. 2013), but the PANEL code was not correspondingly updated. For the CRA-2019 PA, the PANEL code has been updated and there is now consistency between the parameterization of the CAPMIC property and PA calculations (Sarathi 2019).

2.8 Refinement of Hydromagnesite Conversion Rate

The reaction of hydromagnesite to form magnesite was included along with an associated reaction rate in the CRA-2014 PA. Subsequent to the submittal of the CRA-2014, EPA requested that the DOE change the uncertainty distribution for the reaction rate and revise its range to account for a specified range of reaction rates, including the possibility of no conversion to magnesite via a lower rate bound of zero (U.S. EPA 2017b). DOE accepted these changes and applied them in the CRA-2019 PA (Zeitler 2019b).

2.9 Removal of Iron Sulfidation Reactions

Iron and iron hydroxide sulfidation reactions were included as part of the repository brine and gas production/consumption calculations in the CRA-2014 PA. Subsequent to the submittal of the CRA-2014, the EPA requested that the DOE remove these chemical reactions from WIPP PA by setting the appropriate stoichiometric coefficients to zero (EPA 2017b; Zeitler 2019b). The DOE used these changes in the CRA-2019 PA.

2.10 Correction to Length of Northernmost Panel Closure Representation

Three separate panel closure areas are represented in the BRAGFLO Salado Flow model: the "northernmost" panel closure area between the Operations area and the North Rest-of-the-Repository (NROR), the "middle" panel closure area between the NROR and the South Rest-of-the-Repository (SROR), and the "southernmost" panel closure area between the SROR and the Waste Panel. As part of the DOE/EPA completeness determination discussions for CRA-2014, the northernmost panel closure in the BRAGFLO grid was identified by the Agency as representing the length of one set of panel closures instead of the two sets of closures included in the repository design. The DOE corrected this error by doubling the length of the northernmost panel closure area in the BRAGFLO grid for the CRA-2019 PA. The impact of this change on the pressures and brine saturations in the waste areas was found to be negligible (Zeitler 2015).

2.11 Updates in Drilling Rate and Plugging Pattern Parameters

EPA regulations (40 CFR 194.33) require that deep borehole drilling rates and plugging pattern frequencies be updated with current data for each WIPP recertification. The data supporting these updates are developed by the DOE through annual surveys of drilling and plugging activities in the Delaware Basin as documented in annual reports. Survey results through September 2018 were used as the basis for the updates in the CRA-2019 PA and are documented in the 2018 Delaware Basin Monitoring Annual Report (DBMAR) (DOE 2018). In addition to updating the rates and frequencies, the DOE also changed the methodology for calculating the plugging pattern frequencies by analyzing plugging practices of abandoned boreholes over a smaller area and therefore using a smaller database than previously used. Both the drilling rate and plugging pattern frequency parameters have changed substantially since the CRA-2014 PA due to a combination of increased exploratory drilling for hydrocarbon resources in the Delaware Basin and the aforementioned change in calculating plugging patterns. Because these changes are potentially impactful on PA results, they have been separately evaluated by the Agency in the TSD "*Review of Borehole Drilling Rate and Plugging Pattern Frequency Calculations in the CRA-2019 Performance Assessment*" (Docket ID No. EPA-HQ-OAR-2019-0534).

2.12 Updates to WIPP Waste Inventory Parameters

In addition to borehole drilling and plugging practices, the current and projected WIPP waste inventory at repository closure are also updated for each recertification. The waste inventory used in the CRA-2019 PA is described in the 2018 Performance Assessment Inventory Report (PAIR-2018) (Van Soest 2018). Van Soest (2018) presents inventory information collected through the cutoff date of December 31, 2017.

2.13 Updates to Radionuclide Solubilities

The solubilities of actinide elements are influenced by the chemical components of the waste and by the disposal environment. Updated information on the chemical components in the waste was provided in the PAIR-2018 (Van Soest 2018). Based upon this information, discussions between the DOE and EPA, and updates to the thermodynamic database used to calculate actinide solubility values, the parameters used to represent actinide solubilities were updated in the CRA-2019 PA. The updates included correlating dissolved actinide concentrations with waste panel brine volumes (Sosson 2019, Appendix GEOCHEM, Section 1.2.5.4; Domski 2019a). Additionally, uncertainty ranges and probability distributions for actinide solubilities were recalculated using an updated thermodynamic database (Domski and Sisk-Scott 2019). Baseline solubility parameters for the CRA-2019 PA are summarized in Domski (2019b).

2.14 Update to BH_OPEN:RELP_MOD Parameter

Errors in the BRAGFLO code related to the calculation of capillary pressure were discovered and corrected by DOE, as detailed in software problem report (SPR) 18-002 (Day 2018). These errors were determined to have an insignificant effect on repository performance results. One of the corrections prompted a change in the relative permeability model used when simulating flow in an open borehole (parameter BH_OPEN:RELP_MOD). The relative permeability model number was changed from 5 (the value used in the CRA-2014 PA) to 11 (for the CRA-2019 PA). This change was made because the code correction introduced capillary effects into RELP_MOD

= 5 that resulted in a positive capillary pressure within the open borehole, which is physically unrealistic. The use of RELP_MOD = 11 for the BH_OPEN material assumes no capillary effects and is consistent with the relative permeability and (zero) capillary pressure implemented for other "open" repository areas such as the OPS/EXP Areas.

2.15 New Materials to Define Properties in the DRZ Surrounding Operations, Experimental, and Panel Closure Areas

As part of its review of the CRA-2014, the Agency directed DOE to conduct multiple sensitivity studies that investigated the impacts of parameter changes to the OPS/EXP and panel closure areas and their associated DRZs. To facilitate those analyses, DOE introduced new material names for the DRZs to provide flexibility in specifying material properties independently across areas for which material properties in the CRA-2014 PA were identical. DOE chose to retain this flexibility by keeping these new material names in the CRA-2019 PA. These new materials represented the DRZs for the OPS/EXP Areas for times -5 to 0 years (DRZ_OE_0) and 0 to 10,000 years (DRZ_OE_1), the DRZs for active panel closures for times -5 to 0 years (DRZ_PC_0) and 0 to 10,000 years (DRZ_PC_1), and the -5 to 0 year startup material for the active panel closures (CAVITY_5). Although the material names have changed, the parameter values for these areas of the BRAGFLO grid have not changed since the CRA-2014 PA (DOE 2019, Appendix PA, Section PA-1.1.15).

2.16 Hardware and Computational Code Updates

Calculations for the CRA-2014 PA were performed on the WIPP PA Alpha Cluster, which consisted of HP AlphaServer hardware running the OpenVMS operating system (Long 2013). WIPP PA codes were later migrated to the WIPP PA Solaris Cluster, which consists of Intel hardware running the Solaris operating system (Kirchner et al. 2014; 2015). The CRA-2019 PA was run on the WIPP PA Solaris Cluster. The code migration and subsequent updates did not involve any changes to the FEPs baseline or screening arguments and are included here as changes that occurred since the CRA-2014 PA for completeness.

3.0 PRINCIPAL FINDINGS IDENTIFIED BY EPA IN CRA-2019 TECHNICAL SUPPORT DOCUMENTS

3.1 FEPs TSD

The FEPs TSD describes EPA's evaluation of DOE's updating of features, events, and processes relevant to the CRA-2019 PA. The FEPs TSD, titled *Review of Changes to WIPP Performance Assessment Features, Events, and Processes in the 2019 CRA,* can be accessed from the Agency's Docket EPA-HQ-OAR-2019-0534. EPA concluded that SNL's FEP review successfully identified most FEPs that have changed since the 2014 FEP baseline was completed and addressed the principal modeling changes that were necessary to achieve the purpose of the CRA-2019 PA.

A description of SNL's 2019 FEP baseline review is presented in Kirkes (2019). Thirteen out of the 84 FEPs identified by SNL as changed for the CRA-2019 PA were identified by EPA as having unsatisfactory screening arguments. Three of those 13 FEPs (N71 *Microbes*, H31 *Natural Borehole Fluid Flow*, and W23 *Subsidence*) were flagged as deserving special attention from DOE when preparing the CRA-2024 PA because of their potentially greater significance for repository performance. In addition, five FEPs or groups of FEPs that were not considered by SNL to have changed were identified by EPA as meriting updated evaluations or arguments. One of those (H26 *Groundwater Extraction*) may have a greater significance for repository performance and should also be given special attention. Consequently, EPA expects DOE to address and resolve the issues raised by the Agency in the Department's 2024 FEP review for all FEPs identified in the FEPs TSD as having residual concerns, with special attention given to the following:

FEP N71 Microbes. The role of microbes in facilitating radionuclide transport is a potentially important feature of the Culebra release pathway. The DOE conclusion that microbes are rapidly filtered out in the Culebra needs to be reevaluated and better supported in the CRA-2024 PA.

FEP H26 Groundwater Extraction. Recent pumping from a private well on the Mills Ranch may alter groundwater flow directions in the Culebra in a manner that is not currently anticipated in WIPP PA. The potential impact of this type of groundwater extraction on the Culebra release pathway needs to be reevaluated for the CRA-2024 PA. Additional discussion of this concern is presented in Section 3.3.

FEP H31 Natural Borehole Fluid Flow. A new method for calculating borehole plugging frequencies introduced by DOE in the CRA-2019 PA has not been accepted by EPA. EPA expects DOE to revert to the previously-approved methodology for calculating plugging pattern probabilities in the CRA-2024 PA, or otherwise propose alternative methods that may be approved by EPA prior to that time. Additional discussion of this concern is presented in Section 3.4.

FEP W23 Subsidence. DOE's assumption that the effects of subsidence due to repository excavations are intrinsically incorporated in the Culebra transmissivity fields is inadequately supported. EPA is unaware of any documentation describing how Culebra transmissivity fields based on geohydrologic field data have been modified to account for subsidence due to repository excavations that has not yet fully occurred. EPA expects that the screening argument for this FEP will be reevaluated for the CRA-2024 PA.

In conclusion, EPA accepts SNL's updated FEP baseline as sufficient for the CRA-2019 PA and expects DOE to address and resolve the issues raised by the Agency as part of the Department's 2024 FEP baseline review. This expectation applies to all FEPs identified by EPA as having residual concerns with special attention given to the four FEPs identified above as having potentially greater significance for repository performance.

3.2 APCS TSD

The APCS TSD describes EPA's evaluation of DOE's interim use of the "APCS approach" in the CRA-2019 PA. "APCS" stands for *Abandonment of Panel Closures in the South*. The APCS TSD, titled *Review of the APCS Approach to Analyzing WIPP Repository Performance in the*

CRA-2019 Performance Assessment, can be accessed from the Agency's Docket EPA-HQ-OAR-2019-0534.

The WIPP repository was closed between February 2014 and January 2017 following an accidental release of radionuclides that contaminated the south end of the underground repository waste area. During that time access to the contaminated areas was prohibited or limited and routine ground control could not be conducted. This resulted in unsafe conditions that led to a DOE decision to seal off and abandon the part of the waste area designated as Panel 9, to cancel the planned installation of run-of-mine (ROM) salt panel closures in Panels 3, 4, 5, and 6, and to identify the need for a replacement for Panel 9 at an undesignated location. DOE addressed the impacts of these design changes in the CRA-2019 PA using the APCS approach.

The APCS PA approach incorporated conservative assumptions that were intended to estimate somewhat higher repository releases than would be expected given that no waste will actually be emplaced in Panel 9. DOE proposed this interim approach for the CRA-2019 PA because the Department had not identified a location for the replacement Panel 9 at the time the calculations needed to be started, and also because of the long lead time required to develop replacement models in addition to developing a new repository design. The primary elements of this approach were to treat the abandoned Panel 9 as a surrogate for its replacement by modeling the abandoned panel as though waste had actually been emplaced in it, and to treat the now-empty waste panel access drifts as having relatively high porosities and permeabilities for the 10,000-year EPA regulatory period. In addition, to help ensure that repository releases would not be underestimated by this approach, the isolation functions of the remaining single ROM salt panel closures, including the important closures between Panels 9 and 10, were not modeled. A comprehensive description of the APCS approach is presented in Zeitler et al. (2017).

Upon review, EPA found that the assumptions in the APCS approach were not physically realistic but did compensate for inherent uncertainties in modeling the design changes. In accepting the APCS approach, EPA also considered DOE's plans to develop a parallel model that assumed all panel access drifts without constructed closures would immediately creep close and have the very low porosity and permeability properties of intact halite, to develop a qualified 3D replacement for the 2D BRAGFLO model, and to perform numerical and laboratory studies of creep closure of empty rooms with and without roof falls for the purpose of informing future PAs. The first of these efforts, development of the parallel CRA19_CL model, has been completed. This model is documented in Zeitler et al. (2019, Appendix A). The other two efforts are in progress.

DOE's CRA19_CL model was intended to demonstrate that treating waste panel access drifts without constructed closures as immediately creep closing resulted in lower calculated repository releases than if the drifts were treated as remaining open, thereby demonstrating the conservatism of the APCS approach. This model did calculate lower repository releases than DOE's CRA-2019 PA model, but the Agency found that the model did not address the consolidation and healing of the DRZs surrounding the empty drifts. EPA considered that if the access drifts creep closed and healed to approach the properties of intact halite, the surrounding DRZs would heal in a like manner. EPA separately analyzed the effects of DRZ healing using the Agency's CRA19_COMP model. This model treated the DRZs as immediately creep closing

to the same properties of intact halite as the empty drifts. The results confirmed that the APCS approach overestimated calculated repository releases as compared with empty drifts that were assumed to creep close with low porosity and permeability endpoints similar to intact halite.

3.3 Culebra TSD

Modeling the transport of radionuclides through the Culebra Dolomite Member of the Rustler Formation (hereafter referred to as the Culebra) is one component of the PA performed for the CRA-2019. The EPA's Culebra TSD, titled *Review of Groundwater Flow and Radionuclide Transport Conceptualization in the Culebra Dolomite* can be accessed from the Agency's Docket EPA-HQ-OAR-2019-0534.

The Culebra Hydrogeology Conceptual Model describes the overall hydrogeologic framework of the Culebra and is of significance to the WIPP PA because it provides the basis for development of transmissivity (T) fields used in numerical calculations of radionuclide transport through the Culebra. At the time of the CCA, the Culebra conceptual model was found to be "inadequate, but of no consequence" by the Conceptual Models Peer Panel because the numerical model was based on hydraulic field data with little conceptual geological support. Since the CCA, DOE strengthened the conceptual model by establishing basic relationships between Culebra hydraulic properties and geological factors. In 2008, a Peer Review Panel concluded that as long as the focus of this conceptual model is primarily one of flux (i.e., groundwater volumetric flow) and not velocity, a porous representation of the transmissivity fields is appropriate. However, transport modeling in PA requires flow velocity results from the Culebra groundwater flow model.

More recent information, including water-level monitoring data and modeling the potential impacts on groundwater flow and radionuclide transport from a private pumping well located to the southwest of the WIPP LWB, has raised some additional questions regarding the current conceptualization of the Culebra, particularly with respect to the potential impact of discrete fractures on radionuclide transport.

DOE monitors monthly water-level measurements in all accessible wells completed within the Culebra, with results reported in the Annual Site Environmental Reports (ASERs) and collects both periodic water-level measurements and continuous measurement (typically at 1-hour intervals) of fluid pressure in wells instrumented with downhole pressure gauges.
Water level elevations in four Culebra wells in the north central portion of the WIPP Site decreased beginning in 2013 through 2016. Individual wells saw a total decrease of approximately 2 to 5 m during this period. These drawdowns are related to pumping at a privately owned well at Mills Ranch, located about 2.25 km southwest of the LWB, that began in September 2013 and continued until mid-January 2017.

DOE observed that the effects of the pumping at Mills Ranch on the Culebra have been like a very large-scale uncontrolled pumping test and that the data could be used to better understand the flow models used in WIPP performance assessment and to validate the system using a dataset not used in the system calibration (Thomas et al. 2017). Furthermore, DOE notes that wells SNL-

13 and SNL-17 are both responding to the pumping at Mills Ranch in ways that are not typical, but they are also different from one another (Kuhlman and Corbet 2017).

The measured drawdowns in several Culebra monitor wells are more than 25 meters, which is inconsistent with the current conceptual model in which groundwater levels are not expected to fluctuate markedly, except in response to long-term climatic changes, with response times on the order of hundreds to thousands of years. Furthermore, the markedly fluctuating water-levels reflect an aspect of the Culebra hydrogeology that has not been adequately captured in the current conceptual model. For instance, it may be that the Culebra has lower storage values or more discrete fractures than currently conceptualized, which lead to greater pressure responses.

DOE modeled the impact of pumping at the Mills Ranch well to improve confidence in hydrologic analyses intended to provide quantitative predictions for the 10,000-year regulatory timescale by evaluating the impact of unanticipated anthropogenic impacts on the Culebra groundwater flow system. DOE quantified the impact of the well by (a) estimating the well pumping rate, (b) simulating drawdown associated with the pumping, and (c) simulating and comparing advective particle paths and travel times for cases with and without pumping. Although the pumping, assumed to be constant for 10,000 years, was not found to dramatically affect average particle travel distance, it did shift the intersection of the particle track with the LWA boundary more than 2 km to the west. DOE also observed that despite the relatively low hydraulic conductivity values along the average path for particles influenced by pumping, the steepened hydraulic gradients reduced the average travel time by half.

The observations and modeling associated with this pumping raises questions about radionuclide transport within the Culebra that will need to be further considered, especially in the western part of the site where additional panels are planned.

3.4 Borehole TSD

The Borehole TSD describes EPA's evaluation of DOE's methodology for calculating borehole intrusion rates and plugging frequencies in the CRA-2019 PA. The Borehole TSD, titled *Review of Borehole Drilling Rate and Plugging Pattern Frequency Calculations in the CRA-2019 Performance Assessment,* can be accessed from the Agency's Docket EPA-HQ-OAR-2019-0534.

The only significant pathways for post-closure releases of WIPP waste are those created by the inadvertent intrusion of the repository by future exploratory boreholes. Those releases may occur at the time a borehole first penetrates repository waste as well as after a borehole has been plugged. The rate at which boreholes are drilled and the locations of plugs that are installed in boreholes have significant effects on projections of future repository performance.

The WIPP site is located in the northern part of the Delaware Basin of southeast New Mexico and western Texas. EPA regulations in 40 CFR 194.33 treat the drilling practices and technology currently used in the Delaware Basin as analogues for projecting future drilling and abandonment practices in WIPP PA. The "drilling rate" represents the future number of boreholes per unit area that could be drilled each year at the WIPP site. The rate is calculated

based upon EPA requirements in 40 CFR 194.33 and assumes that the average annual rate for all borehole drilling in the Delaware Basin over the past 100 years was to continue for the next 10,000 years. Also, based on local regulatory considerations, future borehole plugging practices have been assumed to be the same as plugging practices in the New Mexico portion of the Delaware Basin since 1988. DOE compiles information on current borehole drilling and plugging practices obtained from state and federal agencies and maintains a database that is updated annually. The borehole data used to support the CRA-2019 PA are presented in DOE (2018).

Drilling Rates. Drilling rates are separately calculated by DOE for shallow and deep boreholes. For purposes of WIPP PA, deep wells are defined as those that extend below the 2,150-foot depth of the WIPP repository and consist almost entirely of boreholes drilled for exploration and recovery of oil and gas resources. Shallow wells are those that do not extend below the depth of the repository. This distinction is important because only deep boreholes are considered to have a potential effect on future repository performance.

DOE's approach for calculating drilling rates begins by categorizing wells as either deep, shallow, or drilling/waiting on paperwork. Wells in this last category generally have unknown depths because of incomplete documentation at the time they are first reported. DOE's practice has been to initially assume that all wells of unknown depth were shallow and if they were later found to be deep, they would be reclassified as deep wells. This reclassification typically occurs 1 to 2 years later when complete documentation becomes available. At any given time, the categorization of unknown wells as shallow wells creates a data lag that underestimates drilling rates for deep wells. DOE's approach led to a calculated drilling rate of 99.0 boreholes/km^2 for the CRA-2019 PA. By comparison, the deep drilling rate used for CRA-2014 was 67.3 boreholes/km^2 and was based on data reported through September 2012.

The Agency accepts DOE's drilling rate for CRA-2019 but requests that DOE reconsider its drilling rate methodology for CRA-2024 because significantly increased oil and gas activity over the past decade has created a larger discrepancy or lag between the actual number of boreholes drilled in the Delaware Basin at a given time and the drilling rate as it is captured in PA.

Plugging Pattern Frequencies. Prior to abandonment, boreholes are sealed by placing concrete plugs at various depth intervals in the borehole. The depth of placement and lengths of plugs create plugging patterns that control the ability of fluids to flow vertically within boreholes after abandonment. With regard to the WIPP, certain patterns promote waste isolation while other patterns do not. The frequencies of occurrence of the various plugging patterns that are currently used in the Delaware Basin are used in WIPP PA as analogues for patterns that would be placed in future boreholes that penetrate WIPP waste. Performance assessments conducted prior to the CRA-2019 PA used plugging frequencies based on all plugged boreholes in the New Mexico portion of the Delaware Basin. Although the WIPP is on federal land where the plugging requirements of the U.S. Bureau of Land Management (BLM) would apply, the DOE chose to include all abandoned boreholes to obtain a larger sample. This approach was supported by the close similarity between BLM requirements and those of the New Mexico Oil Conservation Division (OCD) that apply to state and private lands (DOE 1996, Appendix MASS, Attachment MASS 15-5). This approach was approved by EPA as providing an appropriate regulatory and

geologic analogue and was used by DOE in the 1996 CCA and in all subsequent CRAs until the CRA-2019. The locations of plugged and abandoned wells in the New Mexico portion of the Delaware Basin as of 2018 are shown in Figure 3.4-1. These are the wells that would have been used to calculate plugging frequencies for the CRA-2019 PA if DOE had not changed its approach.

In the CRA-2019 the DOE changed its approach to consider only plugged and abandoned boreholes in the part of the Delaware Basin within the Known Potash Leasing Area (KPLA). This approach is described in DOE (2018). The area used to calculate plugging frequencies for the CRA-2019 PA and the locations of plugged and abandoned boreholes within that area are shown in Figure 3.4-2. This area is within the New Mexico part of the Delaware Basin. The DOE justified this change because the WIPP site is within the KPLA and the KPLA could therefore be considered to represent an appropriate regulatory and geologic analogue for future plugging practices at the WIPP. This change resulted in a tenfold increase, from 4% to 40%, in the frequency of continuous plugs over that calculated for the CRA-2014 PA and had the effect of significantly reducing calculated releases in WIPP PA. This is because essentially no releases of WIPP waste can occur through boreholes with continuous plugs.

Borehole plugging in the KPLA is controlled by OCD Order R-111-P (OCD 1988). This order allows the OCD District Supervisor to waive the continuous plug requirement in barren areas within the KPLA where economic grade potash ore is absent. EPA found that waivers to the requirement for continuous plugs are frequently granted by the OCD because 60% of the boreholes in the KPLA used non-continuous plugs according to DOE's database for CRA-2019. In preparing the 1996 CCA, DOE found that the repository is in a "barren" area without economical potash reserves and would therefore qualify for a waiver (DOE 1996, Appendix MASS, Attachment MASS 15-5). The DOE's CRA-2019 approach does not directly consider that the WIPP is in a barren area or that boreholes at the WIPP site would qualify for a waiver. Because WIPP is in a barren area, EPA expects that a borehole through the WIPP repository would likely be granted a waiver from the continuous plug requirement so that the probability of such a borehole being abandoned with a continuous plug would be much less than 40% as used in the CRA-2019 PA. In addition, the new approach ignores a number of abandoned boreholes directly southeast of WIPP but just outside the KPLA that may otherwise be relevant geological analogues.

EPA concludes that the new approach used by DOE to calculate plugging pattern frequencies is not adequately supported by regulatory considerations in the KPLA (the authority to grant exemptions to the solid plugging requirement), or by the current practice (the frequent granting of exemptions), or by the location of the WIPP waste panels in a barren area. It further fails to consider representative, relevant boreholes in the vicinity of WIPP. EPA expects DOE to revert to the previously approved methodology for calculating plugging pattern probabilities in the CRA-2024 PA, or otherwise propose alternative methods that may be approved by EPA prior to that time.

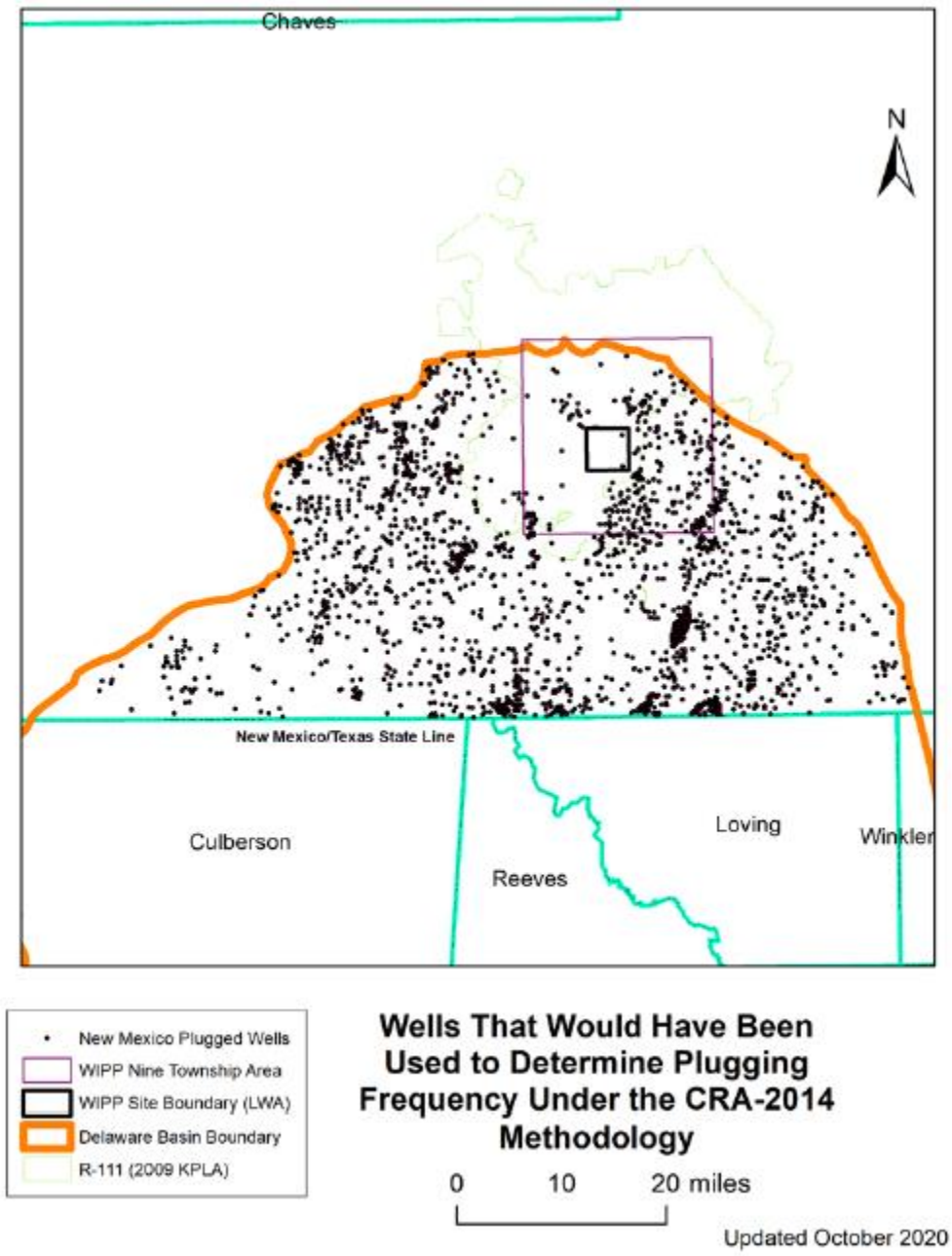

Figure 3.4-1. Map showing wells that would have been used in the CRA-2019 PA to determine plugging frequency based on the EPA-approved methodology of considering all abandoned wells in the New Mexico part of the Delaware Basin (from Response to EPA Completeness Question CC5-33-5c; see Appendix A).

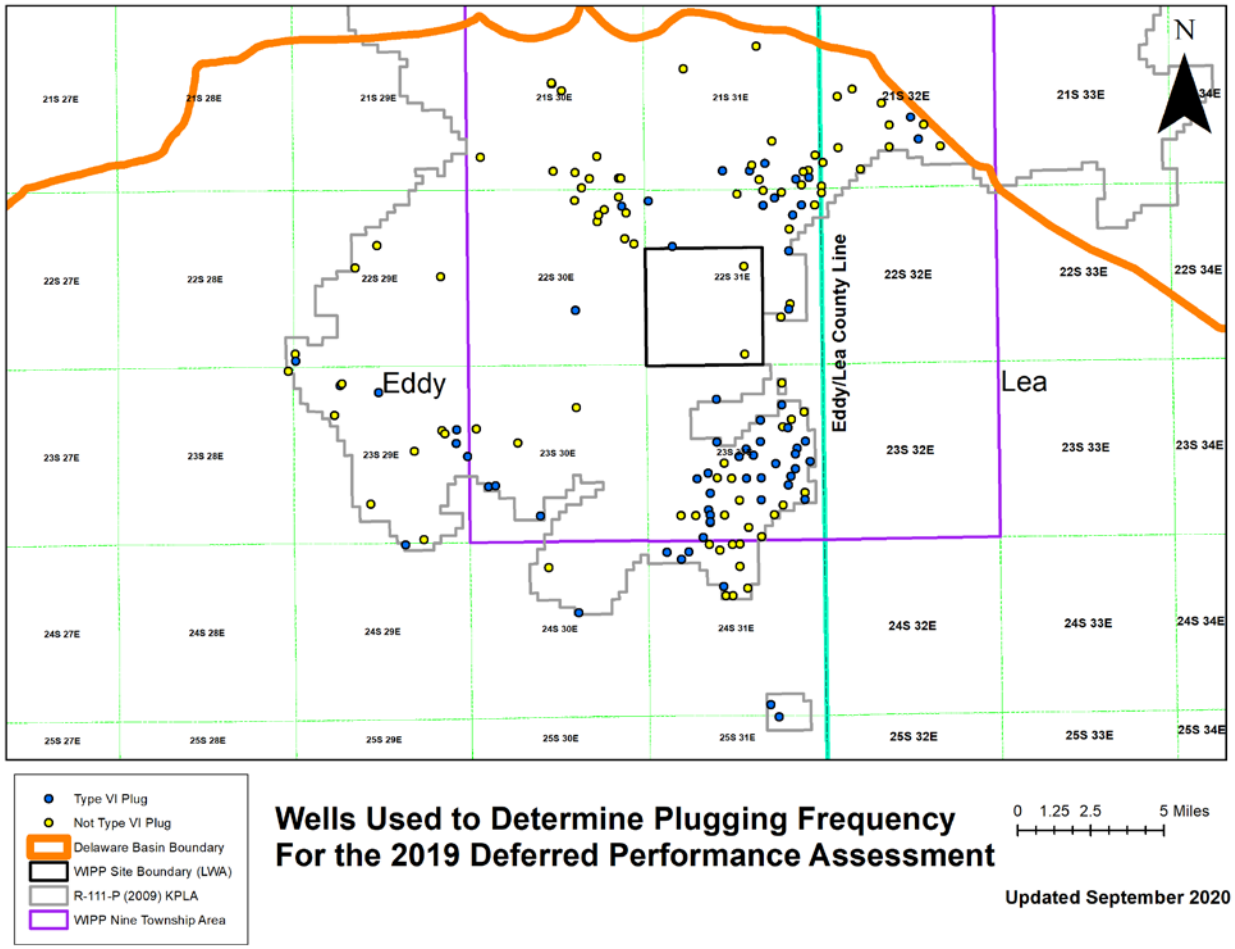

Figure 3.4-2. Map showing KPLA wells used by DOE to determine plugging frequency for the CRA-2019 PA (from Response to EPA Completeness Question CC5-33-5a; see Appendix A).

3.5 New Shaft TSD

The New Shaft TSD describes EPA's evaluation of DOE's proposal to sink a new shaft at the WIPP site and to excavate connecting drifts between the new shaft and the existing underground workings. The New Shaft TSD, titled *Review of DOE Planned Change Notice for a Fifth Shaft at the WIPP Repository*, can be accessed from the Agency's Docket EPA-HQ-OAR-2019-0534.

In February 2014 an exothermic reaction occurred in a waste drum that had recently been emplaced in Panel 7 in the WIPP repository, resulting in rapid pressure buildup and a breach of the drum. Radioactive dust blown from the drum was entrained in the ventilation system air and dispersed down gradient into the southern half of the repository's Waste Area and back to the exhaust ventilation shaft. Dust particles that settled out in transit contaminated all surfaces along this flow path as well as the exhaust ventilation shaft.

Containment of the radionuclide contamination requires additional HEPA filtration of ventilation air from the exhaust shaft and a reduction in air flow rates until the required additional filtration capacity can be installed. During this interim, the lower air flow rates required reducing underground mining, maintenance, and waste emplacement operations. A plan view of the WIPP

underground showing the locations of the waste panels, exhaust shaft, and areas with restricted or prohibited access is shown in Figure 3.5-1. The new shaft and connecting drifts would be built in conjunction with a new filter building for the exhaust shaft. These upgrades would expand the capacity of the ventilation system and support resumption of concurrent, full-scale underground operations. The new shaft would supplement the four existing shafts accessing the WIPP repository. The locations of the new shaft (identified as Shaft #5) and drifts (in red) are shown in Figure 3.5-2.

DOE evaluated the effect of the new shaft on repository performance by modifying the BRAGFLO Salado Flow model based on preliminary shaft and drift designs to account for adding a fifth shaft to the four existing shafts and increasing the volume of the repository Operations Area to account for the volume of the new connecting drifts (Camphouse 2014). The results were compared with those of the CRA-2014 performance assessment and showed no indication that significant changes in repository releases would occur. Later design updates increased the diameter of the shaft and decreased the volume of the connecting drifts. Radionuclide releases through the four existing shafts have been negligible in all past performance assessments. EPA expects releases through the shafts to remain negligible with the addition of a fifth shaft despite the increase in shaft diameter because the new shaft would be plugged and sealed upon repository closure in the same manner as the existing shafts.

EPA believes that DOE's analyses have adequately demonstrated that the new shaft and connecting drifts would not significantly affect repository performance The Agency concluded that these design changes would not result in non-compliance with the terms of WIPP certification and did not object to the shaft construction (Veal 2020).

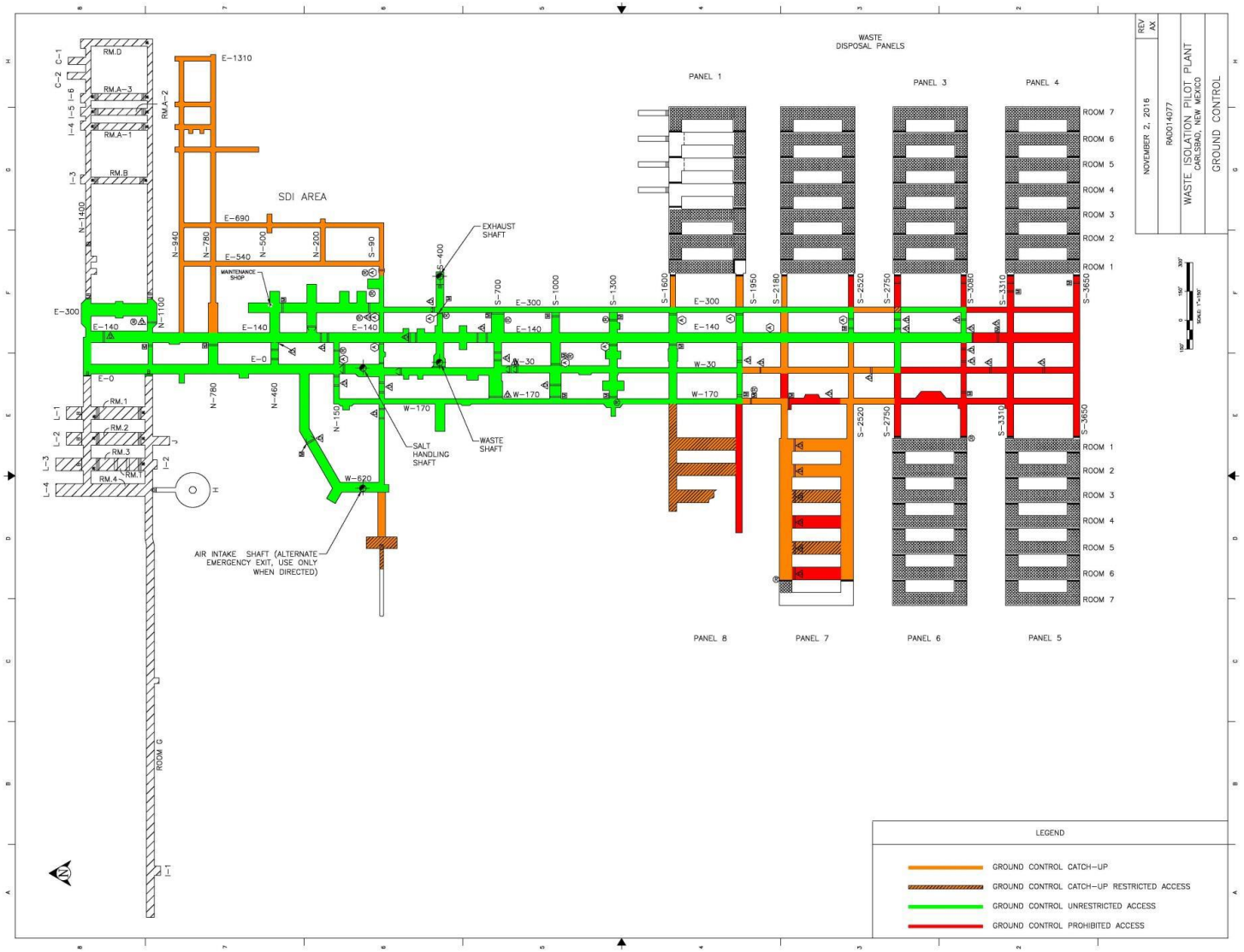

Figure 3.5-1. Plan view of the WIPP underground showing locations of the waste panels, exhaust shaft, and areas of limited access as of November 2016 (from DOE-NWP 2019, Enclosure 1).

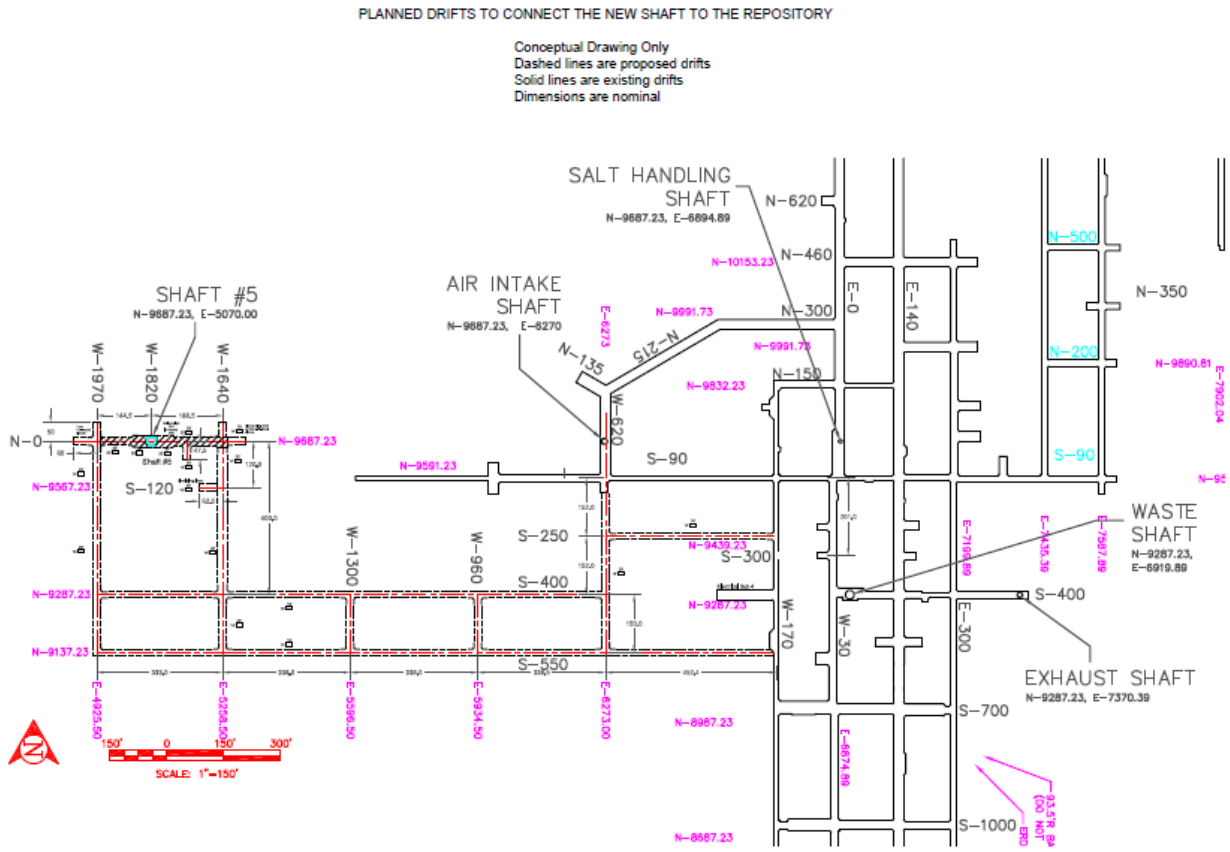

Figure 3.5-2. Conceptual plan view of the repository Operations Area showing the locations of the new fifth shaft and connecting drifts. (from Shrader 2017, Enclosure 1)

3.6 Inventory TSD

The Inventory TSD describes EPA's evaluation of DOE's waste inventory as updated for the CRA-2019 PA. The expected inventory of TRU waste and waste packaging materials upon repository closure is updated by DOE for every CRA. These updates are reviewed by EPA to assure compliance with the requirements of relevant portions of 40 CFR 194.24(a), (b), and (c)(1), and 194.15. The Inventory TSD, titled *Review of the Baseline Inventory Used in the Compliance Recertification Application (CRA-2019)*, can be accessed from the Agency's Docket EPA-HQ-OAR-2019-0534.

The DOE's Comprehensive Inventory Database (CID) is used to store and manage all WIPP inventory data. The CID is updated annually using data from DOE's Waste Data System (WDS) for emplaced WIPP waste and data from the waste generator sites for anticipated waste. The CID data are used by DOE to prepare the Annual TRU Waste Inventory Reports (ATWIRs) using CID-generated reports of waste volumes, waste material parameters, decayed radionuclides, and chemical components. Performance Assessment Inventory Reports (PAIRs) are provided by DOE for each WIPP PA, which scale the inventory data from an ATWIR to a full repository and provide the inventory data in the format needed for PA. The PAIRs also include calculations that provide quantities of complexing agents, oxyanions, solidified cements, and emplacement

materials. DOE developed the waste inventory used in the CRA-2019 PA using data provided in ATWIR (2018) and PAIR 2018 (Van Soest 2018).

The Agency's review of DOE's inventory update process and documentation included the procedures for annual transfer of emplaced waste data from the WDS to the CID and procedures for annual updates to the stored and projected waste from the transuranic (TRU) waste generator sites to the CID. EPA also conducted QA and waste characterization inspections, observations, and technical reviews between January 2013 and December 2017 to evaluate compliance with the requirements of 40 CFR 194.8 and 40 CFR 194.24. EPA found that based on the DOE's inventory updating process, inventory reporting is being conducted in a manner that should produce an inventory suitable for use in PA. However, EPA did identify areas where DOE must improve inventory documentation in future CRAs.

CRA-2019 Section 24 (DOE 2019) used ATWIR (2017) as the data source for Tables 24-2, 24-3, 24-4, 24-5, and 24-6. ATWIR (2017) has a data cutoff date of 12/31/2016. However, ATWIR (2018) with a data cutoff date of 12/31/2017 was used as the data source for the PAIR (2018) and for the CRA-2019 PA. The difference is due to the timing of the CRA submission, which occurred nine months before the submission of the supporting PA. As such, data included in the deferred PA differed from the data provided in Section 24. The inclusion of ATWIR (2017) data in CRA-2019 Section 24 served no purpose because these data were not used in compliance calculations and creates the potential for confusion. Although EPA believes this was a unique situation, for future CRAs, DOE should include the same data in Section 24 of the CRA as is used in the accompanying PA.

DOE is required by 40 CFR 194.24(b) to identify and assess all waste characteristics for their impact on disposal system performance, and to submit an analysis that supports decisions to exclude consideration of a waste characteristic or components. The tables that describe the inclusion or exclusion of these waste characteristics and components were last updated for the CRA-2004 (DOE 2004, Tables TRU WASTE-4 through TRU WASTE-6). These tables contain entries that are inconsistent with the CRA-2019 PA. DOE should also provide an updated listing of all waste characteristics and components that are included or excluded from consideration along with substantiating analyses in all future CRAs.

On the basis of its review, EPA concludes that DOE has appropriate QA procedures in place to accurately document the WIPP waste inventory on an annual basis. EPA further concludes that the ATWIR (2018)/PAIR (2018) inventory is appropriate for use in the CRA-2019 PA calculations.

3.7 Chemistry TSD

The Chemistry TSD describes EPA's review of DOE's projections of post-closure chemical conditions in the WIPP repository, as updated for the CRA-2019 PA. The Chemistry TSD, titled *Evaluation of the Compliance Recertification Application (CRA-2019) Actinide Source Term, Gas Generation, Backfill Efficacy, Water Balance, and Culebra Dolomite Distribution Coefficient Values,* can be accessed from the Agency's Docket EPA-HQ-OAR-2019-0534.

Chemical conditions and processes in the WIPP repository resulting from the emplacement of TRU waste will be affected by the interaction of brine with the radionuclide inventory, waste chemical components, waste container materials, waste emplacement materials, and MgO backfill. Repository chemical conditions and processes will also be influenced by the geologic setting, including the Salado mineralogy, Salado and Castile brine chemistry, hydrostatic pressure, and lithostatic pressure. Chemical processes expected to influence repository conditions and releases include gas generation, backfill reactions, radionuclide solubilities, association of radionuclides with mobile colloids, and radionuclide sorption during transport through the Culebra Dolomite to the LWB.

3.7.1 Radiolytic Gas Generation and Related Issues

Radiolytic gas generation was not considered in previous WIPP PAs but was included in the CRA-2019 PA because of an increased plutonium radionuclide inventory. Gas generation from brine radiolysis was assumed to occur only in brine from dissolved and colloidal radionuclides and from radiolysis of brine by wetted solids. Brunell (2019) determined that inclusion of gas generation by brine radiolysis likely contributed to increased waste area brine pressures and saturations, causing increased normalized repository releases in the CRA-2019 PA compared to the CRA-2014 PA.

DOE demonstrated that radiolysis of CPR and other wastes would not significantly affect repository releases for the CRA-2019 PA. However, there are uncertainties associated with gas generation by CPR radiolysis that EPA expects DOE to consider for CRA-2024:

- The potential effects of higher total gas generation rates in the first 1,000 years post-closure before matrix depletion decreases gas generation rates from CPR radiolysis,
- Whether CPR polymer property changes caused by radiolysis could increase microbial gas generation rates, and
- The fraction of radiolysis caused by radionuclides in wetted waste that will cause gas generation from brine versus from CPR.

Gas generation by radiolysis of water adsorbed on waste under unsaturated conditions was not included in the CRA-2019 PA. DOE (Knerr 2020) agrees there is evidence that radiolysis of water adsorbed on waste could contribute to $H_2(g)$ generation at a rate similar to the rates already considered from brine radiolysis by dissolved, colloidal, and wetted radionuclides. EPA expects that DOE will evaluate the potential importance of gas generation by radiolysis of adsorbed water for the CRA-2024. Brine consumption by radiolysis of water adsorbed on waste materials for CRA-2024 could affect the repository water balance in addition to gas generation rates. EPA expects DOE to continue investigating radiolytic gas generation and brine consumption, including the relative importance and timing of radiolysis of brine by dissolved, colloidal, and wetted radionuclide solids, radiolysis of water adsorbed on waste, and CPR radiolysis.
The increase in plutonium in the waste inventory is due to the addition of a single waste stream, SR-KAC-PuOx, which represents about 3.5% of the total waste volume but contains approximately 30% of the radionuclides that are predicted to cause radiolytic gas generation and brine consumption in the CRA-2019 PA. If this waste stream is placed in a limited number of panels, these panels may exhibit higher gas generation rates and greater brine consumption than

other panels. EPA expects DOE to evaluate the potential effects on repository releases of placing waste stream SR-KAC-PuOx in a limited number of panels.

3.7.2 Actinide Oxidation States

Americium, curium, thorium, plutonium, neptunium, and uranium are included in dissolved actinide solubility and mobile colloidal actinide calculations for WIPP PA. Americium and curium are expected to be present in repository solids and aqueous species only as Am(III) and Cm(III), and thorium is expected to be present only as Th(IV). Plutonium, neptunium, and uranium have been assumed to be present in one of two oxidation states but it was uncertain at the time of the CCA which state would predominate. This uncertainty was addressed by assuming that reducing conditions with Pu(III), Np(IV), and U(IV) oxidation states will occur in half of WIPP PA realizations, and slightly less-reducing conditions will occur in the other half of PA realizations, with Pu(IV), Np(V), and U(VI) oxidation states.

Oxidation states affect the solubilities of actinide solids, with lower predicted solubilities for Pu(IV), Np(IV), and U(IV) than for Pu(III), Np(V), and U(VI). High H_2(g) pressures, ranging from approximately 79 atm to 149 atm, will exist in the WIPP repository under conditions where a DBR could occur. These high H_2(g) pressures, combined with the presence of iron metal and corrosion products that contain Fe(II) [e.g., $Fe(OH)_2$(s)], will create strongly reducing conditions. Under these reducing conditions, the most reduced oxidation states [Pu(III), Np(IV), and U(IV)] will predominate in WIPP solid phases and aqueous species. Because higher solubilities are predicted for Pu(III) solids, using the Pu(IV) oxidation state for half of the PA realizations underestimates total mobilized plutonium and underpredicts plutonium releases through DBRs or by transport through the Culebra or Salado. Under the highly reducing conditions in the WIPP repository, the evidence reviewed by EPA demonstrates that the lowest oxidation states [Pu(III), Np(IV), and U(IV)] will be the predominant oxidation states. DOE should have these reduced actinides dominate solubility and mobilization calculations for all CRA-2024 PA realizations. Pending more robust technical justification by DOE for its current or an alternative approach, DOE should assume Pu(III) solids control dissolved Pu concentrations in future calculations.

3.7.3 Dissolved Actinide Concentrations

Dissolved actinide source term baseline concentrations are calculated for WIPP PA using the EQ3/6 geochemical modeling code and an associated thermodynamic database. The DATA0.FM4 thermodynamic database used by DOE for the CRA-2019 PA baseline dissolved actinide solubility calculations was revised from the version used for the CRA-2014 PA (DATA0.FM1). EPA reviewed DATA0.FM4 and determined that issues related to the aqueous stability constants for $CaEDTA^{2-}$, $MgEDTA^{2-}$, and $AmEDTA^{-}$, and to the derivation and testing of some of the $EDTA^{4-}$ Pitzer parameters, resulted in significant underprediction of the baseline dissolved +III concentrations calculated for the CRA-2019 PA. EPA also identified issues with some of the revised citrate, oxalate, acetate, iron, and lead data, but these issues are expected to have negligible effects on the actinide solubilities calculated for the CRA-2019 PA. The calculated baseline dissolved actinide concentrations and associated uncertainties influence both the dissolved actinide concentrations and the concentrations of actinide humic and microbial colloids mobilized in WIPP repository brines. EPA expects that DOE will revise the EDTA

stability constants and Pitzer parameters and correct other issues in the EQ3/6 database before the CRA-2024.

CRA-2019 PA baseline actinide solubility calculations included the assumption that calcite would precipitate to equilibrium, causing predicted precipitation of large quantities of Phase 5 [$Mg_3(OH)_5Cl•4H_2O$] and extensive water consumption. The calculated baseline actinide solubilities were not greatly affected by these processes. However, the formation of large quantities of solids and the consumption of a large proportion of the available water in brine are inconsistent with the existing Chemical Conditions conceptual model, they are not represented in the rest of the PA, and they have implications for MgO efficacy and rock mechanics. EPA recommends that DOE assume a reasonable degree of calcite oversaturation in actinide solubility calculations to prevent unrealistic amounts of Phase 5 precipitation and solvent water consumption. EPA also recommends that DOE determine whether Phase 5 formation could affect the water balance calculations after re-evaluating its solubility and investigating its formation in Martin Marietta MgO hydration experiments.

3.7.4 Actinide Solubility Uncertainty Distributions

Uncertainty distributions are sampled for the +III and +IV actinide solubilities to bound the upper and lower limits of the dissolved actinide concentrations used in WIPP PA. The actinide solubility uncertainty distributions are developed by comparing measured actinide solubilities in published studies to DOE's modeled concentrations under the experimental conditions of the studies, calculating the differences between the measured values and modeled baseline results, and accumulating the difference values into uncertainty distributions that are sampled to adjust the modeled baseline solubilities.

The published studies used to develop the actinide solubility uncertainty distributions are included or excluded from the evaluation based on a set of selection criteria. DOE used selection criteria for the CRA-2019 PA that included an October 31, 2011 cutoff date for published experimental solubility data, which was an earlier cutoff date than for CRA-2019. During completeness discussions, EPA requested DOE to evaluate additional studies published through December 2020 (i.e., since the last CRA, Knerr 2021). This evaluation did not identify additional +IV actinide studies for inclusion in the +IV actinide solubility uncertainty distribution, but did identify three additional solubility studies for inclusion in the +III actinide solubility uncertainty distribution. Inclusion of solubility data from these three studies increased the mean, median, and maximum difference values of the distribution, and would increase predicted repository releases through DBRs.

The revised +III actinide solubility uncertainty distribution contains significantly more solubility data for microcrystalline or amorphous solids than for crystalline solids. As a result, the revised +III actinide solubility uncertainty distribution may overestimate the likely persistence of less-crystalline, more-soluble +III actinide solids in the long-term WIPP repository. DOE should determine whether the availability of more actinide solubility data for some conditions (e.g., less-crystalline, more-soluble solid phases) may bias the resulting actinide uncertainty distributions, and whether a defensible approach is available to address this potential effect.

Although the current approach used for WIPP PA provides uncertainty distributions that adequately represent the potential ranges of dissolved actinide solubilities, a review of other possible approaches and the relative advantages and disadvantages of these alternatives would strengthen the defensibility of the current approach for addressing +III and +IV actinide solubility uncertainties.

3.7.5 Colloidal Actinide Concentrations

Mineral fragment, intrinsic, humic, and microbial colloids are assumed to form in WIPP repository brines and contribute to actinide mobilization. Constant values are used in WIPP PA for the actinide concentrations associated with mineral fragment and intrinsic colloids. Actinide concentrations associated with humic and microbial colloids are based on proportionality constants (moles of colloidal actinide per mole of dissolved actinide) multiplied by the dissolved actinide concentrations. Humic and microbial colloidal concentrations are also bounded by maximum values. Mineral fragment colloid parameters have remained unchanged for all WIPP PAs, and these parameters are consistent with the available data. For CRA-2019, DOE updated the intrinsic, humic, and microbial colloid parameters.

DOE used experimental filtration data to establish the intrinsic colloid parameters used in the CRA-2019 PA. EPA's evaluation of the data for plutonium, neptunium, and uranium indicates the parameters used in the CRA-2019 PA for intrinsic colloid concentrations are consistent with the available data. However, the Am(III) intrinsic colloid concentration used in the CRA-2019 PA should be increased for the next PA to provide an appropriate upper bound for the available data, and the Th(IV) intrinsic colloid concentration should be increased to be consistent with WIPP-specific data and available literature data.

The humic colloid parameters were recalculated for the CRA-2019 PA and these parameters provide reasonable upper bounds for the actinide concentrations associated with humic colloids. Because the parameter calculations used data from humic colloid experiments with solutions that contained EDTA, DATA0.FM4 database issues related to EDTA may have slightly affected the calculated humic colloid parameters. EPA expects that for the next PA, DOE will make appropriate corrections to the EDTA stability constants and Pitzer parameters in the EQ3/6 database and recalculate the humic colloid proportionality constants.

DOE revised the microbial colloid proportionality constants and maximum actinide concentrations associated with microbial colloids for the CRA-2019 PA. EPA evaluated the data provided by DOE and also surveyed the available scientific literature to determine the potential ranges for the microbial colloid proportionality constants and maximum actinide concentrations. EPA concluded that the CRA-2019 PA parameters do not reflect the large variability reported in the literature because the CRA-2019 PA parameters were determined using a single organism. EPA found that proportionality constant values from the CCA and from EPA's investigation, as well as maximum microbial colloid-associated actinide concentrations recalculated from data provided by Papenguth (1996), bound most values from the literature. For future PAs, unless DOE proposes an acceptable alternative, DOE should use microbial colloid proportionality constants that adequately address the variability in the literature and CCA-based microbial colloid maximum values.

3.8 Models and Codes TSD

The Models and Computer Codes TSD describes the results of EPA's review of Performance Assessment (PA) computer code development and testing activities performed by DOE in support of their 2019 CRA. The ability of the WIPP facility to meet the Agency's certification requirements was demonstrated, in part, using a series of PA computer codes that are documented in Appendix PA of the 2019 CRA. The Models and Computer Codes TSD, titled *Review of Changes to WIPP Performance Assessment Computer Codes in the CRA-2019 Performance Assessment,* can be accessed from the Agency's Docket EPA-HQ-OAR-2019-0534.

DOE conducted a PA to show compliance with the Agency's disposal regulations as part of the WIPP certification process. DOE must demonstrate on an ongoing basis that PA computer software complies with regulations outlined in §194.22 – Quality Assurance and §194.23 – Models and Computer Codes. Examples of software that must comply with these regulations include:

- Scientific or engineering software used to assess the performance of a site
- Scientific or engineering software used to analyze data for, or produce input (parameters) to, a PA calculation
- Software that is used in managing information or augmenting mission-essential decisions
- Software used to collect data (e.g., far-field, near-field, engineered barriers)

DOE executes the PA conceptual models through software applications with parameter value inputs on an infrastructure composed of computers and operating systems that are periodically updated.

Software Qualification. To demonstrate that computer software complies with disposal regulations outlined in §194.22, DOE established a life-cycle management process for software used to support their PA. The qualification approach for the software follows the life-cycle phases outlined in ASME NQA-2a-1990 addenda, part 2.7, as follows:

- Planning
- Requirements
- Design
- Implementation
- Validation
- Installation and Checkout
- Maintenance
- Retirement

DOE implements life-cycle phases using an iterative or sequential approach and each phase has associated documentation (e.g., Software QA Plan, Functional Requirements, Verification and Validation Plan).

Current Status. CRA-2014 PA calculations were done on the WIPP PA computing cluster running a VMS operating system. WIPP PA codes have since been migrated to a cluster running a Solaris operating system. Subsequent to the migration of codes to the Solaris system, SNL made and documented additional code changes for the CRA-2019 PA to account for bug fixes, added functionality, and the addition of two codes to the Software Baseline that were previously qualified and used under SNL's Nuclear Waste Management Procedure NP 9-1: Analyses (SCREEN_NUTS and CCDFVECTORSTATS). The PA codes were qualified on the Solaris system. The CRA19 PA was run on the WIPP PA Solaris Cluster.

The Agency's Review Approach. The Agency's review was conducted by a team consisting of Agency and contractor personnel. The review was initiated with preparatory activities and assembly of background information. Except for computer codes associated with the inventory database, for which Los Alamos National Laboratory (LANL) is responsible, all of the computer codes are maintained in Carlsbad by the Department's WIPP science advisor, SNL.

The Agency's review was conducted in several stages, recognizing that changes in the assessment approach might be required, depending upon results obtained. The following preparatory activities were conducted before conducting on-site reviews:

- Tabulation of the Agency's code acceptance criteria developed by the Agency during the CCA
- Preparation of a list of computer code life-cycle documentation (e.g., VVPs, Change Control and Error Reporting forms) that the Agency needed to review
- Preparation of a draft checklist for reviewing the ability of the PA codes to meet the QA criteria

The following on-site review activities were conducted by the Agency:

- Received overview presentations by SNL and LANL personnel describing the computer code migration activities
- Obtained and reviewed the adequacy of documentation describing the computer code migration activities
- Reviewed the adequacy of testing performed to demonstrate consistency of code output under different operating/hardware systems
- Reviewed and evaluated the traceability of the code migration information
- Reviewed the ability of PA codes to accurately reproduce output obtained under the software/hardware configurations in place during the CCA and subsequent CRAs

In addition to the on-site reviews, off-site reviews were conducted that included relevant documents (e.g., Change Control and Error Reporting Forms, Code Tracking Sheets, Validation Documents) and the DIFFERENCE files for all tests cases for each of the computer codes. Based on this most current review, the Agency approved 33 WIPP PA codes for compliance calculations on the Solaris Blade platform with SunOS 5.11. The Agency concludes that the versions of the computer codes specified in Table 3.8-1 are approved for use in PA compliance calculations on the Solaris cluster with the SunOS operating system.

Table 3.8-1. Computer Code and Library Versions Reviewed and Approved by the Agency

Computer Code	CCA	2004 CRA 2004 PABC	2009 CRA 2009 PABC	2014 CRA	2019 CRA
ALGEBRACDB	2.35	2.35	2.35	2.36	2.36
BLOTCDB	--	--	1.37	1.38	1.38
BRAGFLO	4.0	5.0	6.0	6.02	7.0
CCDFGF	1.01	5.0A	5.02	6.02	7.03
CCDFGFVECTOR_STATS	---	---	---	---	1.01
CCDFSUM	1.01	2.00	2.00	2.0	2.0
CUTTINGS_S	5.03	5.04A	6.02	6.03	6.03
DRSPALL	NA	1.0	1.10	1.22	1.22
DTRKMF	NA	1.0	1.0	1.01	1.01
EPAUNI	1.14	1.15A	1.15A	1.16	1.19
GENMESH	6.08	6.08	6.08	6.09	6.10
GROPECDB	2.12	2.12	2.12	2.13	2.13
ICSET	2.21	2.22	2.22	2.23	2.23
LHS	2.32Z0	2.41	2.42	2.43	2.44
MATSET	9.0	9.10	9.10	9.21	9.24
MODFLOW2000	NA	1.60	1.60	1.70	1.70
MWT3D	---	---	2.51	2.51	2.51
NONLIN	---	---	2.01	2.02	2.02
NUTS	2.02	2.05A	2.05C	2.06	2.06
PANEL	3.6	4.02	4.03	4.04	5.0
PEST	NA	5.51	9.11	9.12	9.12
POSTBRAG	4.00	4.00	4.00	4.02	4.02
POSTLHS	4.07	4.07	4.07A	4.08	4.08
POSTSECOTP2D	1.02	1.04	1.04	1.05	1.05
PREBRAG	6.0	7.00	8.00	8.03	9.0
PRECCDFGF	1.0	1.00B	1.01	2.0	2.0
PRELHS	2.10	2.10	2.30	2.40	2.44
PRESECOTP2D	1.20	1.22	1.22	1.23	1.23
RELATE	1.43	1.43	1.43	1.45	1.45
SCREENNUTS	---	---	---	---	1.02
SECOTP2D	1.30	1.41	1.41A	1.43	1.43
STEPWISE	2.20	2.21	2.21	2.22	2.22
SUMMARIZE	2.10	2.20	3.01	3.02	3.02

Note: The test methodology and acceptance criteria for validating code migration are described in SNL Analysis Plan (AP-089) 2002. "Upgrade of Operating System to OpenVMS 7.3-1 and Hardware to HP Alpha ES45." Sandia National Laboratories. Sandia WIPP Central Files ERMS #523491.

4.0 EPA SENSITIVITY STUDIES

For the CRA-2019, EPA performed its own set of model calculations to determine the sensitivity of releases to the issues EPA identified in its review. The sensitivity studies were fully qualified under the Agency's Quality Assurance Project Plan (QAPP), allowing the results to be used in supporting regulatory decisions. A copy of the EPA's QAPP, *Quality Assurance Project Plan for: Modeling Analysis and Verification of PHREEQC Databases and Input Files Performed to Support EPA's Review of DOE's Compliance Recertification Application 2019 (CRA-2019) at*

the Waste Isolation Pilot Plant, is archived in Docket ID No. EPA-HQ-OAR-2019-0534. Summaries of EPA's sensitivity calculations are presented below. The results are expressed as changes in mean total repository releases in EPA units as compared with the DOE's CRA-2019 results. For reference, the EPA release limits are 1.0 EPA units with an exceedance probability of 0.1 (the upper compliance point) and 10.0 EPA units with an exceedance probability of 0.001 (the lower compliance point). The exceedance probability is the probability that the mean calculated release is actually greater than the calculated amount.

The sensitivity analyses are:

a) Sensitivity to Creep Closure of Empty Rooms (CRA19_COMP Analysis)
b) Sensitivity to Borehole Plugging Frequency (PLG_PROB Analysis)
c) Sensitivity to Actinide Solubility (GCHM_S0 Analysis)
d) Sensitivity to Actinide Solubility and Colloid Parameters (GCHM_S2 Analysis)
e) Sensitivity to Actinide Solubility, Colloid Parameters, and Actinide Oxidation State (GCHM_S3 Analysis)
f) Sensitivity to Combined Geotechnical and Geochemical Parameter Changes (CRA19_COMB Analysis)

4.1 PLG_PROB Analysis: Sensitivity to Borehole Plugging Frequencies

DOE's new approach to calculating borehole plugging frequencies is described in Section 3.4, above. This approach is based only on wells within the KPLA portion of the New Mexico part of the Delaware Basin and was found by EPA to be an inappropriate analogue for use in WIPP PA. EPA's sensitivity analysis compares the results of DOE's new approach with results based on all plugged and abandoned wells in the New Mexico part of the Delaware Basin. This latter approach was used in all WIPP recertifications until the CRA-2019 and has been approved by the Agency. The 822 abandoned boreholes that would have been used to calculate plugging frequencies in the CRA-2019 PA under EPA's previously approved methodology are shown in Figure 3.4-1.

The sensitivity of mean total repository releases to using the prior EPA-approved methodology for calculating abandoned borehole plugging frequencies in comparison to DOE's CRA-2019 PA calculation is shown in Figure 4.2 as a noticeable rightward shift in the results. The primary impact of this methodology change was on spallings and direct brine releases. The results showed that DOE's new approach underestimated repository releases. Mean total releases using the prior EPA-approved methodology (the PLG_PROB analysis) increased from 0.0685 in DOE's CRA-2019 analysis to 0.07924 EPA units at the EPA's upper compliance point and from 0.7505 to 0.8954 EPA units at the EPA's lower compliance point.

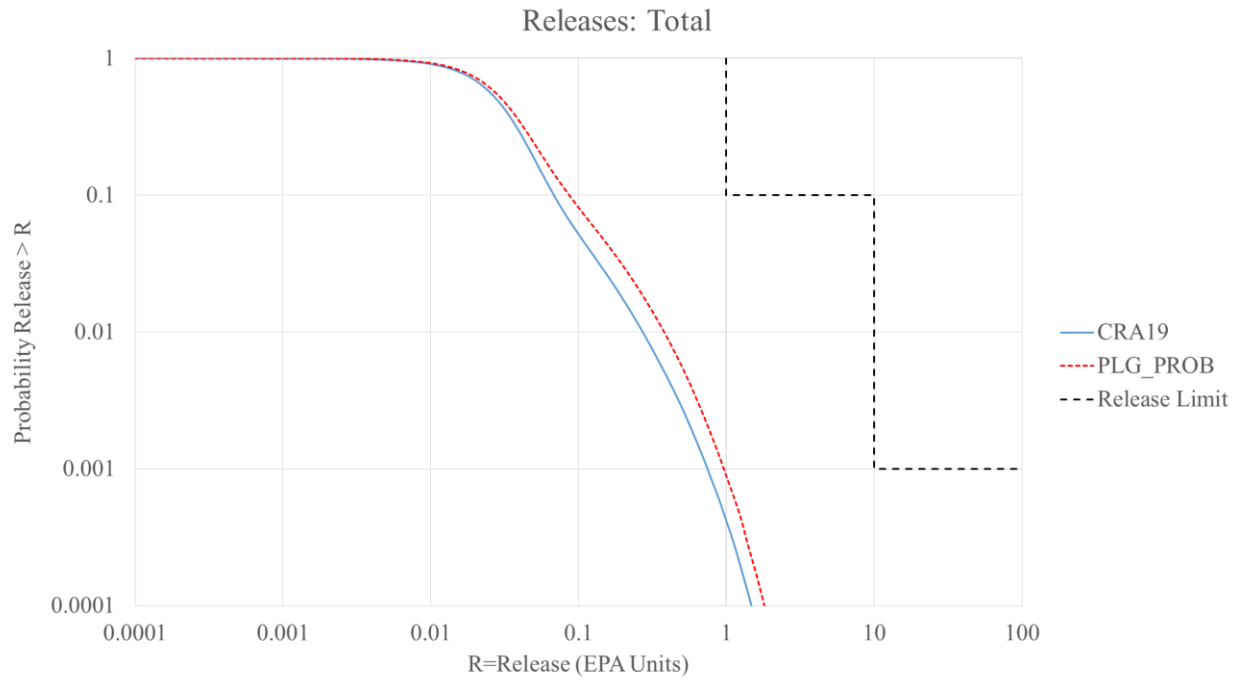

Figure 4.1-1. Mean total releases based on the Agency's approved approach (PLG_PROB curve) compared with mean total releases using DOE's new plugging pattern frequency calculation (CRA19 curve).

4.2 GCHM_S0 Analysis: Sensitivity to Actinide Baseline Solubility

The geochemistry parameters evaluated in EPA's sensitivity calculations affect the actinide concentrations mobilized in WIPP brines, which could affect DBRs and releases through the Culebra. However, releases through the Culebra did not contribute significantly to total repository releases for the CRA-2019 PA. The chemistry parameter changes do not affect cuttings and cavings or spallings releases. As a result, the chemistry parameter changes in the sensitivity calculations only affected DBRs, which significantly contributed to total repository releases for the CRA-2019 PA.

Changes in total mobilized neptunium and uranium concentrations do not significantly contribute to DBRs or to total repository releases. Consequently, only the chemistry parameter changes that affect the predicted mobilization of Am(III), Pu(III), or Pu(IV) in WIPP brines cause significant changes in releases.

EPA reviewed the CRA-2019 PA baseline actinide solubility calculations and the DATA0.FM4 database used by DOE to perform those calculations (see Section 3.7.3, above). EPA determined that issues related to aqueous stability constants and Pitzer parameters for some EDTA species resulted in significant underprediction of the baseline dissolved +III actinide concentrations calculated for the CRA-2019 PA. EPA also found that the predicted precipitation of large amounts of calcite and Phase 5 [$Mg_3(OH)_5Cl{\bullet}4H_2O$], and consumption of a large fraction of water in the calculations, are inconsistent with DOE's Chemical Conditions conceptual model. EPA recalculated the baseline actinide solubilities to correct for these issues, which resulted in

an increase of approximately an order of magnitude in baseline +III actinide solubilities and in relatively small changes to baseline +IV actinide solubilities.

The mean DBRs and total repository releases calculated with the revised baseline actinide solubilities in EPA's GCHM_S0 sensitivity calculation are compared to the CRA-2019 PA results in Figures 4.2-1 and 4.2-2. The increased baseline +III actinide solubilities resulted in increased DBRs compared to the CRA-2019 PA (Figure 4.2-1). Total releases increased relative to the CRA-2019 PA at low probabilities (Figure 4.2-2) because total releases are dominated by DBRs at lower probabilities. These results show that DBRs and total repository releases are sensitive to baseline dissolved Am(III) and Pu(III) concentrations and that CRA-2019 PA DBRs and total repository releases were underpredicted. Because of the importance of the baseline actinide solubilities to total mobilized actinide concentrations in WIPP PA, the revised +III and +IV baseline actinide solubilities were included in all EPA chemistry parameter sensitivity calculations. Mean total releases in the GCHM_S0 analysis increased from 0.06853 in DOE's CRA-2019 analysis to 0.07788 EPA units at the EPA's upper compliance point and from 0.7505 to 1.186 EPA units at the EPA's lower compliance point.

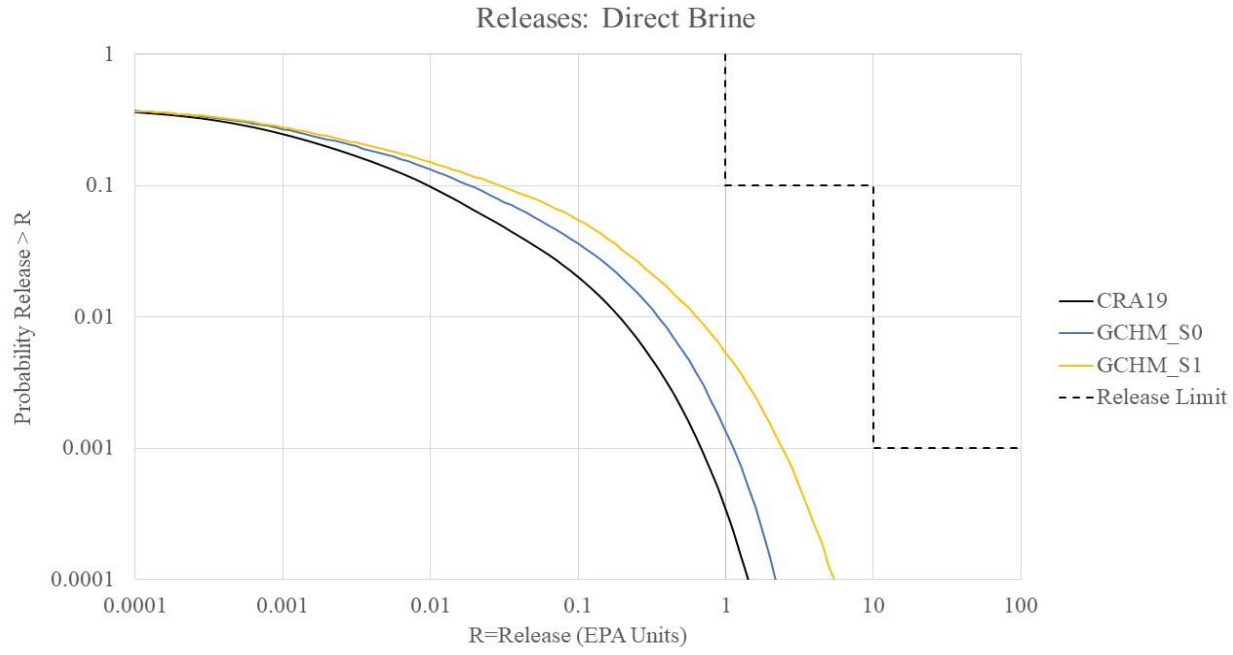

Figure 4.2-1. Mean DBRs calculated for the CRA-2019 PA (CRA19), the EPA revised baseline actinide solubility sensitivity calculation (GCHM_S0), and the EPA revised baseline actinide solubility plus +III actinide solubility uncertainty sensitivity calculation (GCHM_S1).

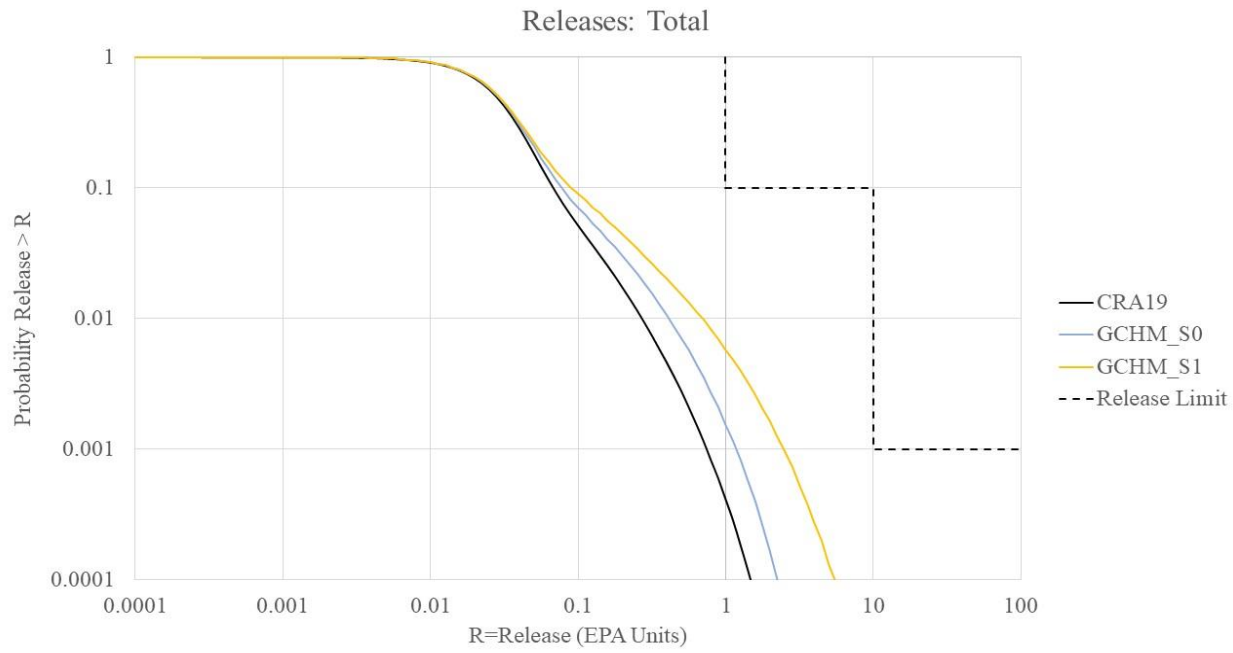

Figure 4.2-2. Mean total releases calculated for the CRA-2019 PA (CRA19), the EPA revised baseline actinide solubility sensitivity calculation (GCHM_S0), and the EPA revised baseline actinide solubility plus +III actinide solubility uncertainty sensitivity calculation (GCHM_S1).

4.3 GCHM_S1 Analysis: Sensitivity to Actinide Baseline Solubility and +III Actinide Solubility Uncertainty Distribution

In response to a request from EPA, DOE (Knerr 2021) provided an updated +III actinide solubility uncertainty distribution that included additional data from experimental investigations published through December 2020 (see Section 3.7.4, above). EPA performed a sensitivity calculation to assess the effects of the recalculated baseline actinide solubilities (Section 4.3.1, above) combined with the updated +III actinide solubility uncertainty distribution (GCHM_S1). The differences in DBRs and total repository releases between the GCHM_S0 calculation (revised baseline actinide solubilities only) and GCHM_S1 calculation (Figures 4.2-1 and 4.2-2) are caused by the updated +III actinide solubility uncertainty distribution.

The significant effects of the +III actinide solubility uncertainty distribution on repository releases are consistent with the regression analysis results of Zeitler (2019a), who identified the +III actinide solubility uncertainty parameter as an important contributor to variability in repository releases. The combination of the increased baseline actinide solubilities and updated +III actinide solubility uncertainty distribution significantly increased total repository releases compared to the CRA-2019 PA results but predicted total repository releases remained below regulatory limits (Figure 4.2-2).

EPA does not recommend using the revised +III actinide solubility uncertainty distribution from Knerr (2021) in future WIPP PA calculations because the updated distribution likely provides an excessively conservative estimate of the uncertainty associated with the baseline +III actinide solubilities (see Section 3.7.4, above). However, the results of the GCHM_S1 sensitivity

calculation demonstrate the importance of this parameter. The importance of the revised +III actinide solubility uncertainty distribution for repository releases indicates that DOE should consider whether there is a defensible approach for limiting potential bias in the actinide solubility uncertainty distributions (see Section 3.7.4, above). In addition, the defensibility of the current approach for determining actinide solubility uncertainty distributions would be enhanced by an assessment of the relative advantages and disadvantages of alternative approaches.

4.4 GCHM_S2 Analysis: Sensitivity to Actinide Baseline Solubility and Actinide Colloid Parameters

EPA reviewed the actinide colloid parameters used in the CRA-2019 PA and found that the Am(III) and Th(IV) intrinsic colloid parameters should be increased to adequately represent the WIPP-specific experimental data and literature data (see Section 3.7.3, above). The GCHM_S2 sensitivity results illustrate the combined effects of the increased baseline actinide solubilities and intrinsic colloid and microbial colloid parameter changes on DBRs and total repository releases (Figures 4.4-1 and 4.4-2). The differences between the GCHM_S0 and GCHM_S2 results are caused by the actinide colloid parameter changes.

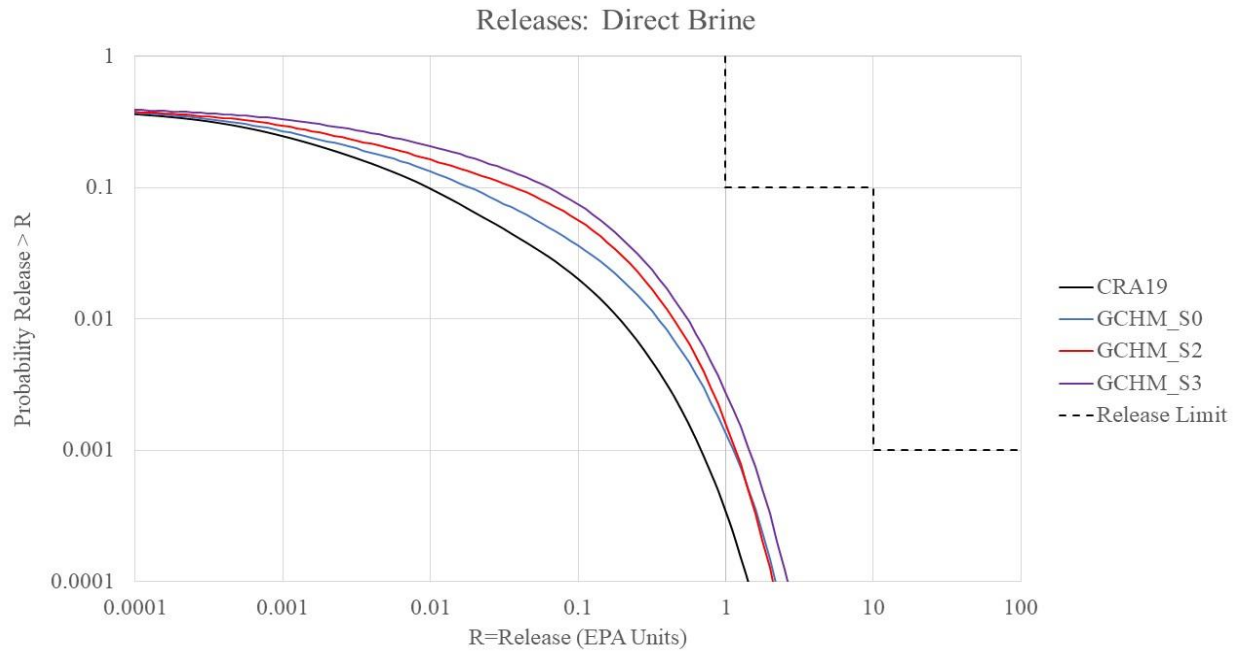

Figure 4.4-1. Mean DBRs for the CRA-2019 PA (CRA19); the EPA revised baseline actinide solubility sensitivity calculation (GCHM_S0); the EPA revised baseline actinide solubility plus intrinsic and microbial colloid sensitivity calculations (GCHM_S2); and the EPA sensitivity calculation combining revised baseline actinide solubility, intrinsic and microbial colloid, and actinide oxidation state parameters (GCHM_S3).

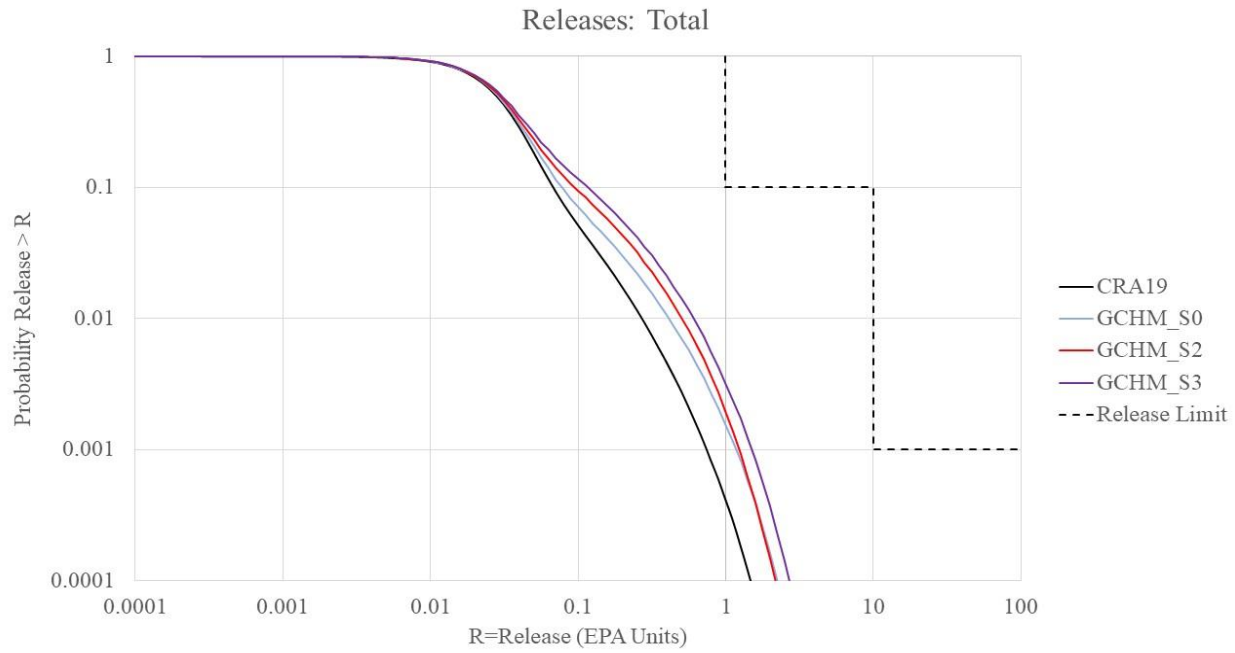

Figure 4.4-2. Mean total repository releases for the CRA-2019 PA (CRA19); the EPA revised baseline actinide solubility sensitivity calculation (GCHM_S0); the EPA revised baseline actinide solubility plus intrinsic and microbial colloid sensitivity calculations (GCHM_S2); and the EPA sensitivity calculation combining revised baseline actinide solubility, intrinsic and microbial colloid, and actinide oxidation state parameters (GCHM_S3).

The actinide colloid parameter changes affect DBRs at probabilities greater than 0.001 (Figure 4.4-1). The minimal effects on DBRs at the lowest probabilities in the GCHM_S2 analysis are likely caused by the actinide concentrations associated with microbial colloids reaching the maximum mobilized concentration (CAPMIC) values in WIPP PA and by the decreasing importance of the constant Am(III) intrinsic colloid concentration because higher dissolved concentrations are produced for realizations that include above-median sampled +III actinide uncertainty values.

Total releases in the GCHM_S2 analysis (Figure 4.4-2) are barely changed at high probabilities because cuttings and cavings releases are the most important to total releases at high probabilities. The increased total releases in the probability range from 0.001 to ~ 0.5 demonstrates that total releases are sensitive to the intrinsic and microbial colloid parameter changes. Mean total releases in the GCHM_S2 analysis increased from 0.06853 in DOE's CRA19 analysis to 0.09497 EPA units at the EPA's upper compliance point and from 0.7505 to 1.238 EPA units at the EPA's lower compliance point.

4.5 GCHM_S3 Analysis: Sensitivity to Actinide Solubility, Colloid Parameters, and Actinide Oxidation State

EPA's review of actinide oxidation states in the WIPP environment established that the lowest oxidation states should be assumed to control the solubilities and aqueous speciation of actinide solids in WIPP brines (see Section 3.7.2, above). EPA's GCHM_S3 sensitivity calculation

combined the revised baseline actinide solubilities, revised intrinsic and microbial colloid parameters, and a revised actinide oxidation state parameter to maintain the Pu(III), Np(IV), and U(IV) oxidation states in all realizations.

The GCHM_S3 results show the combined effects of the geochemistry parameter changes on DBRs and total repository releases (Figures 4.4-1 and 4.4-2). DBRs were consistently increased at both high and low probabilities by the oxidation state parameter change relative to the GCHM_S2 results (Figure 4.4-1) because of the predicted higher total mobilized Pu(III) concentration compared to total mobilized Pu(IV). The combined results of these changes (Figure 4.4-2) showed that the chemical conditions assumed by the DOE in the CRA-2019 PA underestimated repository releases. Mean total releases in the GCHM_S3 analysis increased from 0.06853 in DOE's CRA-2019 analysis to 0.1165 EPA units at the EPA's upper compliance point and from 0.7505 to 1.516 EPA units at the EPA's lower compliance point. The results of this sensitivity study showed that, although the combined effects of EPA's geochemistry parameter changes materially increased calculated repository releases, the mean total repository releases remained below the regulatory limits.

4.6 CRA19_COMB Analysis: Sensitivity to EPA's Combined Geotechnical and Geochemical Parameter Changes

CRA19_COMB is a comprehensive analysis that includes all changes made by EPA in the PLG_PROB and GCHM_S3 analyses. This analysis was conducted to evaluate the cumulative effects on repository performance by simultaneously changing the values of several parameters that the Agency questioned in its review. This analysis provides significant insights as to the degree to which some parameter values that are of interest to the EPA impact releases. This sensitivity study was based on the CRA-2019 PA but with the following parameter changes:

- Use previously approved plugging pattern methodology (Section 3.4);
- Use revised actinide baseline solubility parameters (Section 3.7.3);
- Use revised colloid parameters (Section 3.7.5);
- Use revised actinide oxidation state parameters (Section 3.7.2).

The results of EPA's CRA19_COMB analysis are shown in Figure 4.6-1. The cumulative effects of the changes were to increase calculated total mean repository releases from 0.06853 in DOE's CRA-2019 analysis to 0.1669 EPA units at the EPA's upper compliance point and from 0.7505 to 1.766 EPA units at the EPA's lower compliance point. However, the combined results and the upper 95% confidence limit on those results remained below the regulatory limits of 1.0 EPA units at the upper compliance point and 10.0 EPA units at the lower compliance point.

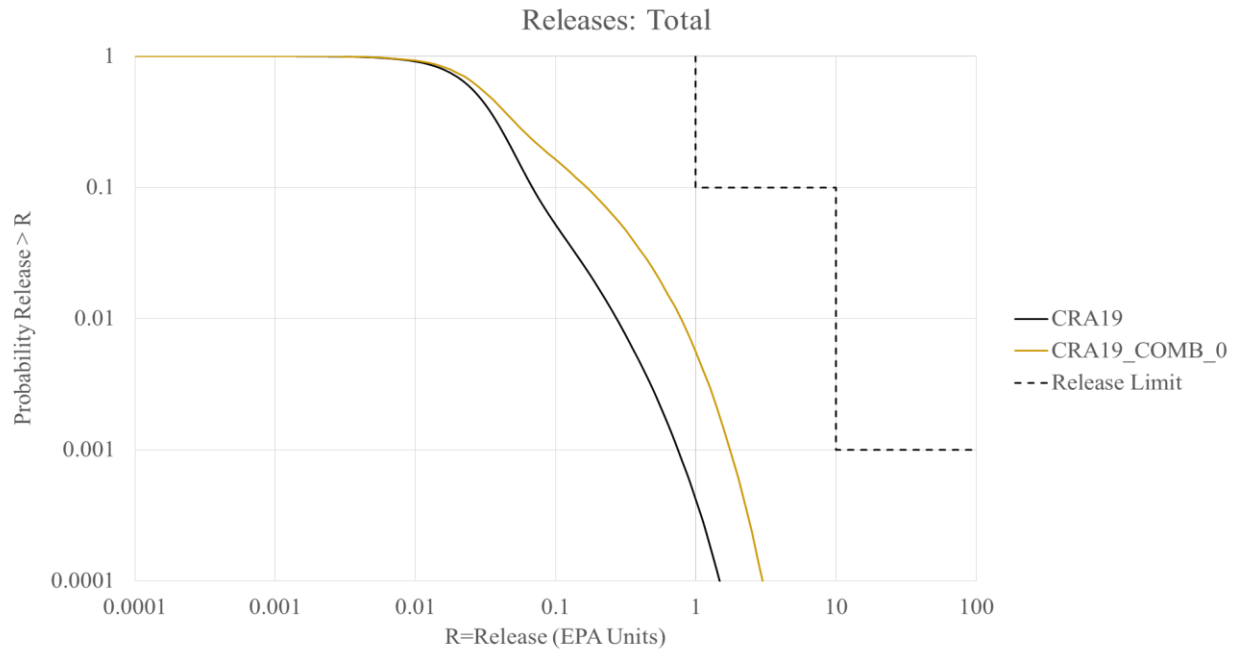

Figure 4.6-1. Mean total repository releases from combined geotechnical and geochemical parameter changes.

5.0 EPA CONCLUSIONS AND EXPECTATIONS

The EPA's sensitivity studies demonstrated that WIPP performance is sensitive to each of the Agency's parameter changes but that the combined results as well as the upper 95% confidence limit on those results remained below the EPA's regulatory limits. The EPA expects the DOE to incorporate the parameter changes made in these sensitivity studies in the CRA-2024 PA. These are:

- Use previously approved plugging pattern frequency methodology (Boreholes TSD)
- Use revised actinide baseline solubility parameters (Chemistry TSD)
- Use revised colloid parameters (Chemistry TSD)
- Use revised actinide oxidation state parameters (Chemistry TSD)

EPA's sensitivity studies examined the technical issues in the CRA-2019 PA that potentially had the most significant impact on repository releases. Additional EPA concerns are identified in this Overview TSD and in the individual focused TSDs that will also need to be addressed by the DOE in future CRAs. These concerns are grouped below by priority based on potential importance to repository release calculations.

High Priority:

- Revise the EQ3/6 database, especially to resolve issues related to the EDTA data, possible inconsistencies in Am(III) stability constants and Pitzer parameters, Th(IV)-carbonate aqueous speciation, Phase 5 solubility, addition of missing iron-sulfate data, and removal of lead data, as well as other issues outlined in Attachment B of the Chemistry TSD

- Revert to previously approved methodology for calculating borehole plugging pattern probabilities (Borehole TSD)
- Incorporate creep closure of empty rooms with and without roof falls in WIPP PA as soon as feasible (APCS TSD)
- Develop a qualified three-dimensional replacement for the two-dimensional flow and transport models currently used in WIPP PA as soon as feasible (APCS TSD)
- Reevaluate the impact of groundwater extraction from the Culebra on the Culebra release pathway (Culebra TSD) and develop a peer-reviewed and approved transport model for the Culebra (Culebra TSD)

Moderate Priority:

- Determine whether the availability of more actinide solubility data for some conditions (e.g., less-crystalline solid phases) may bias the resulting actinide solubility uncertainty distributions, and consider whether a defensible approach is available to counter this potential effect (Chemistry TSD)
- Strengthen the defensibility of the current approach for addressing +III and +IV actinide solubility uncertainties (Chemistry TSD)
- Reevaluate borehole drilling rate calculation methodology (Borehole TSD)
- Evaluate the potential importance of brine consumption by radiolysis of water adsorbed on waste materials and the effects of the different hydration rates of MgO obtained from different vendors on PA water balance calculations (Chemistry TSD)
- Reevaluate the screening argument for microbe-facilitated radionuclide transport in the Culebra (FEP TSD)
- Reevaluate the impact of repository-induced subsidence on Culebra flow and transport (FEP TSD)
- Provide an updated, comprehensive listing of all waste characteristics and components that are included or excluded from consideration along with substantiating analyses (Inventory TSD)
- Present the same data in the CRA demonstrations of compliance as are used in the accompanying PA compliance calculations (Inventory TSD)
- Update the cutoff date for publications used to develop the +III and +IV actinide solubility uncertainty distributions to the most recent date that can be implemented (Chemistry TSD)
- Evaluate whether the current PA calculations adequately address the radiolytic effects of SR-KAC-PuOx waste on brine consumption, gas generation, and repository releases if this waste is placed in a single panel (Chemistry TSD)
- Evaluate the potential importance of gas generation by radiolysis of adsorbed water, uncertainties associated with higher total gas generation rates in the first 1,000 years post-closure, and uncertainties associated with the radiolysis of CPR (Chemistry TSD)

The major issues identified in EPA's review primarily influence the importance of the direct brine release pathway and how the performance assessment simulates those releases. EPA found that direct brine releases are strongly influenced by the degree of waste panel isolation. By treating the now-empty waste panel access drifts as retaining high permeability and porosity for the 10,000-year EPA regulatory period and discounting most of the isolation capabilities of the constructed panel seals that remained, the DOE's APCS methodology, described in Section 3.2

above, did not simulate the isolation of waste panels that is likely to occur. As a result, DOE's use of the APCS methodology in the 2019 CRA provided an unlikely starting point for evaluating the sensitivity of releases to EPA concerns. When the non-conservative borehole plugging, chemistry, and microbial assumptions in the 2019 CRA were removed in EPA's sensitivity analyses, the conservative overestimates of the APCS approach remained. Because of this, EPA believes that the sensitivity study results also conservatively overestimated repository releases compared to a more realistic approach to modeling waste panel isolation. The Agency has a reasonable expectation that WIPP will contain radionuclides within regulatory limits as required by EPA's radioactive waste disposal regulations.

REFERENCES

Brunell, S. 2019. *Analysis Package for Normalized Releases in the 2019 Compliance Recertification Application Performance Assessment (CRA-2019 PA).* Sandia National Laboratories, Carlsbad, New Mexico, ERMS 571373.

Camphouse, R.C. 2014. *Impact Assessment of an Additional WIPP Shaft*, Revision 0. ERMS 562973. Sandia National Laboratories, Carlsbad, New Mexico. November.

Congress, U.S., 1996. Public Law 102-579. Waste Isolation Pilot Plant Land Withdrawal Act of 1992, as Amended by Public Law 104-201, 1996.

Day, B. 2018. *Impact Analysis for BRAGFLO 6.03 Software Problem Report*, SPR 18-002. Carlsbad, NM: Sandia National Laboratories. ERMS 570325.

Day, B. 2019. *Reassessment of Need and Parameter Justification for Modeling Gas Generation due to Radiolysis of Brine and Cellulose/Plastic/Rubber in WIPP for CRA-2019*. Carlsbad, NM: Sandia National Laboratories. ERMS 570873.

DOE 1996. *Title 40 CFR 191 Compliance Certification Application for the Waste Isolation Pilot Plant.* DOE/CA0-1996-2184. U.S. Department of Energy, Carlsbad Area Office, Carlsbad, New Mexico.

DOE 2016. WIPP UPDATE: October 14, 2016, *Plans Call for Controlled Withdrawal from South End of Underground*.

DOE 2018. *Delaware Basin Monitoring Annual Report, September 2018.* DOE/WIPP-18-2308 Rev. 1. Carlsbad Field Office, Carlsbad, New Mexico. September.

DOE 2019. *Title 40 CFR 191 Subparts B and C, Compliance Certification Application 2019 for the Waste Isolation Pilot Plant.* DOE/WIPP-19-3609, Rev. 0. U.S. Department of Energy, Carlsbad Area Office, Carlsbad, New Mexico. March.

DOE-NWP 2019. *Class 3 Permit Modification Request. Excavation of a New Shaft and Associated Connecting Drifts*. WIPP Permit Number NM4890139088-TSDF. Waste Isolation Pilot Plant, Carlsbad, New Mexico. August.

Domski, P.S. 2019a. *Official Release of the Qualified Pitzer Thermodynamic Database, DATA0.FM4, for EQ3/6 under AP-183*, Revision 1Carlsbad, NM: Sandia National Laboratories. ERMS 571051.

Domski, P. 2019b. *Th(IV), Np(V), and Am(III) Baseline Solubilities and Th(IV) and Am(III) Solubility Uncertainties for the CRA-2019 PA*. 2019. Carlsbad, NM: Sandia National Laboratories. ERMS 571169.

Domski, P., and C. Sisk-Scott 2019. *Prediction of Baseline Actinide Solubilities for CRA 2019 with and Updated EQ3/6 Pitzer Thermodynamic Database, DATA0.FM4*. Carlsbad, NM: Sandia National Laboratories. ERMS 571178.

EPA 2017a. *Probability of Encountering Castile Brine beneath the WIPP Waste Panels Using the TDEM Block Method*. June, 2017. Office of Radiation and Indoor Air, Docket EPA-HQ-OAR-2014-0609-0047.

EPA 2017b. *Technical Support Document for Section 194.24, Evaluation of the Compliance Recertification Actinide Source Term, Gas Generation, Backfill Efficacy, Water Balance and Culebra Dolomite Distribution Coefficient Values*. June, 2017. Office of Radiation and Indoor Air, Docket EPA-HQ-OAR-2014-0609-0054.

EPA 2017c. *Technical Support Document for Section 194.23, EPA Review of Proposed Modification to the Waste Shear Strength Parameter TAUFAIL*. July, 2017. Office of Radiation and Indoor Air, Docket EPA-HQ-OAR-2014-0609-0052.

Herrick, C.G., M.D. Schuhen, D.M. Chapin, and D.C. Kicker 2012. *Determining the Hydrodynamic Shear Strength of Surrogate Degraded TRU Waste Materials as an Estimate for the Lower Limit of the Performance Assessment Parameter TAUFAIL*. Carlsbad, NM: Sandia National Laboratories. ERMS 558479.

Herrick, C.G. and T. Kirchner 2013. *Memorandum to C. Camphouse. Subject: Follow-up to Questions Concerning TAUFAIL Flume Testing Raised during the November 14-15, 2012 Technical Exchange Between the DOE and EPA*. January 23, 2013. Carlsbad, NM: Sandia National Laboratories. ERMS 559081.

Kicker, D. 2019. *Radionuclide Inventory Screening Analysis for the 2019 Compliance Recertification Application Performance Assessment (CRA-2019 PA).* Carlsbad, NM: Sandia National Laboratories. ERMS 571244.

Kirchner, T., T. Zeitler, and R. Kirkes 2012. *Memorandum to Records Center. Subject: Evaluating the Data in Order to Derive a Value for GLOBAL:PBRINE*. December 11, 2012. Carlsbad, NM: Sandia National Laboratories. ERMS 558724.

Kirchner, T., A. Gilkey, and J. Long 2014. *Summary Report on the Migration of the WIPP PA Codes from VMS to Solaris, AP-162* Revision 1. Carlsbad, NM: Sandia National Laboratories. ERMS 561757.

Kirchner, T., A. Gilkey, and J. Long 2015. *Addendum to the Summary Report on the Migration of the WIPP PA Codes*. Carlsbad, NM: Sandia National Laboratories. ERMS 564675.

Kirkes, R. 2019. *Features, Events, and Processes Assessment for the 2019 Compliance Recertification Application Performance Assessment (CRA-2019 PA).* Carlsbad, NM: Sandia National Laboratories. ERMS 571366.

Knerr, R. 2020. *Response 7 to U.S. Environmental Protection Agency's 2019 Compliance Recertification Application Completeness Comments Letters dated May 6, 2020, June 12, 2020, July 17, 2020 and September 11, 2020 from Tom Peake to Mike Brown*. U.S. Department of

Energy, Carlsbad Field Office, Carlsbad, New Mexico. Letter to L.B. Veal, U.S. Environmental Protection Agency Radiation Protection Division, Washington, D.C. December 1, 2020.

Knerr, R. 2021. *Supplementary Information as Requested by U.S. Environmental Protection Agency During Technical Exchange Meeting on June 22, 2020*. U.S. Department of Energy, Carlsbad Field Office, Carlsbad, New Mexico. Letter to L.B. Veal, U.S. Environmental Protection Agency Radiation Protection Division, Washington, D.C. July 8, 2021.

Kuhlman K.L., and T.F. Corbet. 2017. *Memo to Records Center (Subject: WIPP Milestone Report: 2016 Culebra Groundwater Level Fluctuations).* May 19, 2017. Carlsbad, NM: Sandia National Laboratories. ERMS 568172

Long, J. 2013. *Execution of Performance Assessment Codes for the CRA-2014 Performance Assessment.* Carlsbad, NM: Sandia National Laboratories. ERMS 560016.

Mariner, P. 2019. *A Summary of Humic Colloid Parameter Values to be Implemented in the CRA-2019 Deferred Performance Assessment*. Albuquerque, NM: Sandia National Laboratories. ERMS 571250.

OCD (New Mexico Oil Conservation Division; Energy, Minerals, and Natural Resources Department) 1988. *Order R-111-P, Potash Areas of Eddy and Lea Counties, NM.* Case 9316, Revision to Order R-111-P. April 21, 1988. Santa Fe, New Mexico.

Papenguth, H.W. 1996. *Parameter Record Package for Colloidal Actinide Source Term Parameters. Mobile-Colloidal-Actinide Source Term. 4. Microbes.* Memorandum to C.T. Stockman, Sandia National Laboratories, Albuquerque, New Mexico, May 7, 1996, ERMS 235856.

Peake, T. 1998. *Technical Report Review of TDEM Analysis of WIPP Brine Pockets*. Washington, DC: U. S. Environmental Protection Agency, Office of Radiation and Indoor Air.

Reed, D.T., J.S. Swanson, J.F. Lucchini, and M.K. Richmann 2013. *Intrinsic, Mineral, and Microbial Colloid Enhancement Parameters for the WIPP Actinide Source Term*. Los Alamos National Laboratory; Carlsbad, NM. LCO-ACP-18, LA-UR-13-20858.

Reed, D.T., J.S. Swanson, and F. Stanley 2019. *LANL/ACRSP Parameter Recommendations for the CRA-2019 Deferred Performance Assessment*, Rev. 1. Los Alamos National Laboratory, Carlsbad, NM. ERMS 571296.

Roselle, G.T. 2013. *Determination of Corrosion Rates from Iron/Lead Corrosion Experiments to be used for Gas Generation Calculations*. Carlsbad, NM: Sandia National Laboratories. ERMS 559077.

Sarathi, R. 2019. *Explanation of CAPMIC Definition and Usage in PA Calculations*. Carlsbad, NM: Sandia National Laboratories. ERMS 570685.

Shrader, Todd 2017. *Planned Change Notice Regarding the Excavation and Construction of a New Ventilation Shaft and Associated Connecting drifts at the Waste Isolation Pilot Plant*. U.S. Department of Energy Carlsbad Field Office. CBFO:OEP:GTB:AC:17-1064:UFC 5486.00. Carlsbad, New Mexico. September 29.

Sosson, Gregory 2019. *Deferred Performance Assessment for the Compliance Recertification Application 2019.* Letter 19-0279 from Gregory Sosson (U.S. Department of Energy) to Lee Veal (U.S. Environmental Protection Agency). Carlsbad, New Mexico. December.

Thomas, M.A., Kuhlman, K.L., and Ward, A.L. 2017. Anthropogenic influences on groundwater in the vicinity of a long-lived radioactive waste repository. *Hydrological Processes*, 31(14). 2637-2647.

Van Soest, G.D. 2018. *Performance Assessment Inventory Report – 2018*. Los Alamos National Laboratory Carlsbad Operations. Carlsbad, NM. LA-UR-18-31882, December 12, 2018.

Veal, Lee 2017. Letter from Lee Veal (EPA) to Todd Shrader (DOE). U.S. Environmental Protection Agency, Office of Air and Radiation, Washington, D.C. December 4.

Veal, Lee. 2020. Letter from Lee Veal (EPA) to R. Knerr (DOE). *EPA Comments and Determination on Shaft Planned Change Notification re: WIPP CRA-2019*. U.S. Environmental Protection Agency, Office of Air and Radiation, Washington, D.C. September 28. EPA-HQ-OAR-2019-0534-0021.

Zeitler, T.R. 2015. *Memo to Records. Subject: BRAGFLO calculations for updated northern-most ROMPCS representation*. Carlsbad, NM: Sandia National Laboratories. ERMS 563875.

Zeitler, T.R., B. Day, J. Bethune, R. Sarathi, and J. Long. 2017. *Assessment of Abandoned Panel Closures in South End of Repository and Lack of Waste Emplacement in Panel 9*. Carlsbad, NM: Sandia National Laboratories. ERMS 568459.

Zeitler, T.R. 2018a. *Cumulative Distribution for STEEL:CORRMCO2 for the CRA-2019 PA*. Carlsbad, NM: Sandia National Laboratories. ERMS 570869.

Zeitler, T.R. 2018b. *Bounding Calculation of the Cumulative Distribution for STEEL:HUMCORR*. Carlsbad, NM: Sandia National Laboratories. ERMS 569807.

Zeitler, T.R. 2019a. *Analysis Package for the Sensitivity of Releases to Input Parameters in the 2019 Compliance Recertification Application Performance Assessment (CRA-2019 DPA) Revision 0*. Sandia National Laboratories, Carlsbad, New Mexico, ERMS 571374.

Zeitler, T.R. 2019b. *A Summary of EPA/DOE Defined Parameters to be Implemented in the CRA-2019 PA*. Carlsbad, NM: Sandia National Laboratories. ERMS 570879.

Zeitler, T.R., J. Bethune, S. Brunell, B. Day, D. Kicker, J. Long, and R. Sarathi, 2019. *Summary Report for the 2019 Compliance Recertification Application Performance Assessment (CRA-2019 PA)*. Carlsbad, NM: Sandia National Laboratories. ERMS 571376.

APPENDIX A

EPA COMPLETENESS QUESTIONS, DOE RESPONSES, AND EPA EVALUATIONS OF RESPONSES

Table of Contents

Table 1: EPA Completeness Comments, DOE Responses, and EPA Evaluations for CRA-2019 6
Table 2: List of EPA Docket Items, EPA Completeness Comments, and DOE Response Packages 15
Select copies of EPA Completeness Comments, DOE Responses, and EPA Evaluations not included in separate Technical Support Documents 18
CC1-GEN-1 Closure Dates 18
CC1-34-1 Request for Figures from PA Results 18
CC1-34-1a 19
CC1-34-1b 19
CC1-34-1c. 20
CC1-34-1d. 21
CC1-34-1e. 22
CC1-34-1f. 23
CC1-34-2 Repository Conditions Completeness Request 23
34-2a. 23
34-2b. 32
34-2d 37
34-2e. 37
34-2f. 37
34-2g. 37
CC1-34-7 Corrections to Relative Permeability Models 49
34-7a. 49
34-7b. 49
34-7c. 50
34-7d. 50
34-7e. 50
CC1-42-1 Question regarding changes in CRA-2019 DPA and MONPAR analysis 51
CC1-51/52-1 CRA-2019 changes' impact on IGP 54
CC1-MASS-1 Definition of Conservative 55
CC1-MASS-2 Identification of conservative assumptions leading to lower releases. 56
CC2-34-9 Borehole Drilling Conceptual Model Clarification 57
CC2-MON-3 Seismicity and Seismic Monitoring Data 58
MON-1a. 58
MON-1b. 59
MON-1c. 60
Copies of EPA Completeness Comments, DOE Responses, and EPA Evaluations Not Included in the Geochemistry or Inventory Technical Support Documents 61

CC1-24-1 Documentation Inconsistencies or Errors 61
CC1-24-1a. 61
CC1-24-1b. 61
CC1-GEOCHEM-1 Modify Cut-Off Date for Actinide Solubility Uncertainty Evaluation Literature Search 62
Geochem-1a 62
Geochem-1b 62
Geochem-1c. 62
CC1-GEOCHEM-2 Inaccurate Statement Regarding Sampling of Parameter BIOGENFC 64
CC1-SOTERM-2 Incomplete Evaluation of Borate Aqueous Speciation and Solubility Data 64
CC1-SOTERM-3 Incomplete Evaluation of Am(III) Aqueous Speciation and Solubility Data 73
CC1-SOTERM-4 Incomplete Evaluation of Th(IV) Aqueous Speciation and Solubility Data 88
CC2-GEN-2 Cutoff Dates 102
CC2-24-2 Table Updates 103
CC2-24-2a. 103
CC2-24-2b. 105
CC2-24-2c 111
CC2-GEOCHEM-8 Clarification of data source information in Domski (2019) 111
GEOCHEM-8a 111
GEOCHEM-8b. 112
GEOCHEM-8c. 112
CC2-GEOCHEM-10 Testing of Revised EDTA Stability Constants and Pitzer Ion-Interaction Parameters 113
GEOCHEM-10a. 113
GEOCHEM-10b. 113
GEOCHEM-10c. 113
GEOCHEM-10d. 113
GEOCHEM-10e. 113
GEOCHEM-10f. 113
GEOCHEM-10g. 113
CC2-GEOCHEM-11 Data Used to Derive Ca2EDTA·7H2O(s) Solubility Product and Evaluation of the Solubility Product 122
GEOCHEM 11a 123
GEOCHEM 11b 123
GEOCHEM 11c 123
CC2-GEOCHEM-12 Evaluation of Revised Citrate Equilibrium Constants 130
GEOCHEM-12a. 130

GEOCHEM-12b. 130
GEOCHEM-12c. 130
GEOCHEM-12d. 130
GEOCHEM-12e. 130
GEOCHEM-12f. 130
CC2-GEOCHEM-13 Omission of Earlandite from DATA0.FM4 134
CC2-GEOCHEM-15 Effects of Selected G Value for H2(g) Production by Brine Radiolysis 136
CC2-GEOCHEM-16 Omission of RH Waste Gamma Irradiation from Radiolysis Evaluation 138
CC3-GEOCHEM-17 Plutonium Particle Sizes Used in Radiolytic Gas Generation Calculations 141
GEOCHEM-17a. 141
GEOCHEM-17b. 141
GEOCHEM-17c. 142
GEOCHEM-17d. 150
CC3-GEOCHEM-19 Evaluation of Matrix Depletion and Radiolytic Gas Generation for Cellulosics, Plastics, and Rubber Radiolysis 151
GEOCHEM-19a. 151
GEOCHEM-19b. 154
CC3-GEOCHEM-20 Gas Generation in Unsaturated Repository 170
CC3-GEOCHEM-21 Gas Generation by Radiolysis of Non-CPR Waste Materials 173
CC4-SOTERM-8 Pu(III) Intrinsic Colloid Concentrations 177
CC4-SOTERM-8a. 177
CC-4 SOTERM-8b. 178
CC4-SOTERM-8c. 178
CC4- SOTERM-9 Th(IV) Intrinsic Colloid Concentrations Error 179
CC4- SOTERM-10 Th(IV) Concentration Data Revisions 183
CC4- SOTERM-11 Th(IV) Mineral Fragment Colloid Parameter 185
CC4- SOTERM-12 Actinide(IV)-Silica Colloids 186
CC5-GEOCHEM-24 Inclusion of Calcite Precipitation in EQ3/6 Calculations 188
CC5-GEOCHEM-25 Effects of Polyhalite on Modeled Brine Chemistry 196
CC5-GEOCHEM-26 Effects of Cements on Brine Chemistry 198
CC5-GEOCHEM-27 Incomplete Documentation Related to Pitzer Parameter Errors in DATA0.FM4 199
GEOCHEM-27a. 199
GEOCHEM-27b. 200
GEOCHEM-27c. 200
GEOCHEM-27d. 201

CC6-GEOCHEM-28 Iron-Sulfate Pitzer Parameters and Solid Phases Not Included in DATA0.FM4 202
CC6-GEOCHEM-29 Adequacy of Lead Parameterization in DATA0.FM4 204
CC6-GEOCHEM-31 Comparison of Modeled and Experimental Glushinskite Data 206
CC6- GEOCHEM-32 Effects of Shielded Containers on Steel Surface Area per Unit Volume 208
CC6- GEOCHEM-33 Humid Steel Corrosion Parameter 210
CC6- GEOCHEM-35 Omission of Brine Radiolysis Effects from Appendix GEOCHEM Discussions of Radiolysis and the Brine Production Model 212
FC1-CCR-SOTERM-8, 9, 10 Nd(III) Colloids Data 213
FC2-CCR-GEOCHEM-32 Number of Shielded Containers Emplaced Up to December 31, 2017 217

Table 1: EPA Completeness Comments, DOE Responses, and EPA Evaluations for CRA-2019
Summary of EPA Completeness Questions and DOE Responses

Question	Topic	DOE Response Set	Evaluation/Resolution	Discussion/ Documentation
Round 1 (CC1) Submitted March 2020				
CC1-GEN-1	Closure dates	#1 (6/10/20)	DOE postponed response, will provide later	**Appendix A**
CC1-24-1 a,b	Waste characterization	#1 (6/10/20)	satisfactory	Inventory TSD; **Appendix A**
CC1-27-1	Peer Review references	#1 (6/10/20)	satisfactory, references provided	-
CC1-33-1 a,b	Borehole plugging	#1 (6/10/20)	satisfactory, text updated and corrected	Boreholes TSD
CC1-33-2 a-d	borehole plugging maps and additional info	#1 (6/10/20)	satisfactory, information provided	Boreholes TSD
CC1-33-3 a-d	borehole plugging database	#2 (7/8/20)	satisfactory, data provided	Boreholes TSD
CC1-34-1 a-f	results of PA figures requested	#1 (6/10/20)	satisfactory, figures provided	**Appendix A**
CC1-34-2 a-g	repository conditions figures requested	#3 (8/13/20)	satisfactory, figures provided	**Appendix A**
CC1-34-3 a-e	frequency of borehole intrusions	#3 (8/13/20)	satisfactory; graphs provided plus additional information were helpful	**Appendix A**
CC1-34-4	panel closure design	#2 (7/8/20)	satisfactory	**Appendix A**
CC1-34-5	panel closure design construction	#2 (7/8/20)	satisfactory	**Appendix A**
CC1-34-6	rock mechanics studies update	#1 (6/10/20)	satisfactory; DOE committed to future technical exchange	APCS TSD
CC1-34-7 a-e	corrections to relative permeability values	#2 (7/8/20)	satisfactory	**Appendix A**
CC1-34-8	BRAGFLO representation of shaft seals	#2 (7/8/20)	satisfactory, provided charts and figures	New Shaft TSD
CC1-42-1	changes in PA and MONPAR analysis	#2 (7/8/20)	satisfactory	**Appendix A**
CC1-43-1	passive institutional controls incomplete sentence	#1 (6/10/20)	satisfactory, correction noted	-

Question	Topic	DOE Response Set	Evaluation/Resolution	Discussion/ Documentation
CC1-46-1	Appendix WRAC	#1 (6/10/20)	satisfactory, DOE added documentation to website	-
CC1-51/52-1	CRA-2019 impact on IGP	#2 (7/8/20)	satisfactory	**Appendix A**
CC1-PA-1	PA missing or mislabeled references	#1 (6/10/20)	satisfactory	-
CC1-GEOCHEM-1 a-c	cutoff dates actinide solubility	#1 (6/10/20)	postponed in first response, DOE later provided a satisfactory evaluation	Chemistry TSD; **Appendix A**
CC1-GEOCHEM-2	BIOGENFC inaccurate statement	#1 (6/10/20)	satisfactory, acknowledged in errata	Chemistry TSD, Attachment A**;** **Appendix A**
CC1-GEOCHEM-3	MgO hydration rate inaccurate statement	#1 (6/10/20)	satisfactory, acknowledged in errata	Chemistry TSD, Attachment A
CC1-GEOCHEM-4	typographic error	#1 (6/10/20)	satisfactory, acknowledged in errata	Chemistry TSD, Attachment A
CC1-GEOCHEM-5	typographic error	#1 (6/10/20)	satisfactory, acknowledged in errata	Chemistry TSD, Attachment A
CC1-GEOCHEM-6	missing discussion An(III)	#1 (6/10/20)	satisfactory, additional information provided	Chemistry TSD, Attachment A
CC1-SOTERM-1	document request Van Soest	#1 (6/10/20)	satisfactory, reference provided	Inventory TSD; Chemistry TSD, Attachment A
CC1-SOTERM-2	borate aqueous speciation	#6 (10/26/20)	satisfactory	Chemistry TSD, Attachment B; **Appendix A**
CC1-SOTERM-3	Am(III) aqueous speciation	SOTERM-3 (5/20/21)	satisfactory	Chemistry TSD, Attachment B**;** **Appendix A**
CC1-SOTERM-4	Th(IV) aqueous speciation	#6 (10/26/20)	satisfactory	Chemistry TSD, Attachment B; **Appendix A**
CC1-SOTERM-5	incomplete iron inventory data	#1 (6/10/20)	satisfactory, acknowledged in errata	Inventory TSD;

Question	Topic	DOE Response Set	Evaluation/Resolution	Discussion/ Documentation
				Chemistry TSD, Attachment A
CC1-MASS-1	definition of conservative	#2 (7/8/20)	satisfactory, explanation provided	**Appendix A**
Round 2 (CC2) Submitted May 2020				
CC2-GEN-2	Cutoff Dates	#3 (8/13/20)	partially adequate; DOE needs to provide more specific information	Inventory TSD; **Appendix A**
CC2-22-1	(Quality Assurance) QA Audits	#3 (8/13/20)	satisfactory	
CC2-24-2 a-c	(Waste Characterization) Table updates	#4 (9/15/20)	satisfactory	**Appendix A;** Inventory TSD
CC2-34-9	Borehole Drilling Conceptual Model Clarification	#3 (8/13/20)	satisfactory	**Appendix A**
CC2-34-10	Clarification of "Neighbor" Relationships in the CRA19_CL Analysis	#3 (8/13/20)	satisfactory	APCS TSD
CC2-34-11	Results of Granular Salt Reconsolidation Study.	#4 (9/15/20)	satisfactory; DOE committed to future technical exchange	APCS TSD
CC2-GEOCHEM-7	Missing Reference	#3 (8/13/20)	satisfactory; references provided	Chemistry TSD, Attachment A
CC2-GEOCHEM-8 a-c	Clarification of data source information in Domski (2019)	#6 (10/26/20)	satisfactory, data source and documentation identified	Chemistry TSD, Attachment B; **Appendix A**
CC2-GEOCHEM-9	Typographical Errors in Table GEOCHEM-21	#3 (8/13/20)	satisfactory; acknowledged in errata	Chemistry TSD, Attachment A
CC2-GEOCHEM-10 a-g	Testing of Revised EDTA Stability Constants and Pitzer Ion-Interaction Parameters	#4 (9/15/20)	adequate response, additional investigation required for future PAs	Chemistry TSD, Attachment B; **Appendix A**
CC2-GEOCHEM-11 a-c	Data Used to Derive Ca2EDTA·7H2O(s) Solubility Product and Evaluation	#3 (a) #5 (b,c)	satisfactory (a); adequate response (b,c), Ca2EDTA·7H2O(s) solubility product rejected by EPA	Chemistry TSD, Attachment B; **Appendix A**
CC2-GEOCHEM-12 a-f	Evaluation of Revised Citrate Equilibrium Constants	#4 (9/15/20)	adequate response, additional investigation required for future PAs	Chemistry TSD,

Question	Topic	DOE Response Set	Evaluation/Resolution	Discussion/ Documentation
				Attachment B; **Appendix A**
CC2-GEOCHEM-13	Omission of Earlandite from DATA0.FM4	#6 (10/26/20)	satisfactory; DOE acknowledged omission and calculations demonstrated no effects on actinide solubility modeling results	Chemistry TSD, Attachment B; **Appendix A**
CC2-GEOCHEM-14	Supporting Files for Actinide Solubility Calculations	#3 (8/13/20)	satisfactory, files provided	Chemistry TSD
CC2-GEOCHEM-15	Effects of Selected G Value for H2(g) Production by Brine Radiolysis	#7 (12/1/20)	satisfactory	Chemistry TSD
CC2-GEOCHEM-16	Omission of RH Waste Gamma Irradiation from Radiolysis Evaluation	#7 (12/1/20)	satisfactory	Chemistry TSD
CC2-MON-1 a-c	Seismicity and seismic monitoring data	#5 (10/19/20)	satisfactory (a-b); partially adequate (c), not fully answered; EPA will look at earlier documentation	**Appendix A**
Round 3 (CC3) Submitted June 2020				
CC3-GEN-3	CRA-2019 (Deferred) PA a Bounding Analysis	#6 (10/26/20)	satisfactory, DOE provided explanation	APCS TSD
CC3-GEOCHEM-17 a-d	Plutonium Particle Sizes Used in Radiolytic Gas Generation Calculations	#7 (12/1/20)	satisfactory	Chemistry TSD; **Appendix A**
CC3-GEOCHEM-18	Reference Request	#5 (10/19/20)	satisfactory; reference provided	Chemistry TSD; **Attachment A**
CC3-GEOCHEM-19 a-b	Evaluation of Matrix Depletion and Radiolytic Gas Generation for Cellulosics, Plastics, and Rubber Radiolysis	#7 (12/1/20)	satisfactory, additional investigation required for future PAs	Chemistry TSD; **Appendix A**
CC3-GEOCHEM-20	Gas Generation in Unsaturated Repository	#7 (12/1/20)	satisfactory, additional investigation required for future PAs	Chemistry TSD; **Appendix A**

Question	Topic	DOE Response Set	Evaluation/Resolution	Discussion/ Documentation
CC3-GEOCHEM-21	Gas Generation by Radiolysis of Non-CPR Waste Materials	#7 (12/1/20)	satisfactory	Chemistry TSD; **Appendix A**
CC3-HYDRO-1	Radionuclide Transport Questions Answered by Radiokrypton Analyses	#5 (10/19/20)	satisfactory; will be a discussion topic of an upcoming Technical Exchange.	Culebra TSD
CC3-HYDRO-2	Corrections to Atmospheric Pressure	#5 (10/19/20)	satisfactory	Culebra TSD
CC3-HYDRO-3	Response of Water Levels to Precipitation	#6 (10/26/20)	satisfactory; will be a discussion topic of an upcoming Technical Exchange	Culebra TSD
CC3-HYDRO-4	Inventory of Pumping Wells Potentially Impacting Water Levels in the Culebra	#7 (12/1/20)	satisfactory; will be a discussion topic of an upcoming Technical Exchange	Culebra TSD
CC3-HYDRO-5 a-b	Additional Understanding of Water-Level Changes in the Culebra	#5 (10/19/20)	satisfactory; future work is not being considered as a completeness issue in CRA-2019 but will be a discussion topic of an upcoming Technical Exchange	Culebra TSD
CC3-HYDRO-6	Quality Assurance Requirements for Thomas et. al. (2017)	#5 (10/19/20)	satisfactory	Culebra TSD
CC3-HYDRO-7	Additional Understanding of Water-Level Changes in the Bell Canyon	#7 (12/1/20)	satisfactory	Culebra TSD
CC3-SCR-1	Supplemental Information for FEP N71 Microbes	#6 (10/26/20)	partially adequate; information on microbial size provided, but much less discussion on filtration	FEPs TSD
CC3-SCR-2	Supplemental Information for FEP W22 Roof Falls	#6 (10/26/20)	satisfactory, screening argument expanded	FEPs TSD
CC3-SCR-3	Updates for FEP W23 Subsidence	#6 (10/26/20)	partially adequate, updated discussion deferred to CRA-2024	FEPs TSD
CC3-SCR-4	Supplemental Information for FEP W28 Nuclear Explosions	#6 (10/26/20)	satisfactory; screening argument will be updated in CRA-2024	FEPs TSD

Question	Topic	DOE Response Set	Evaluation/Resolution	Discussion/ Documentation
CC3-SCR-5 a-b	Supplemental Information for FEP N12 Seismic Activity	#6 (10/26/20)	satisfactory; discussion should be expanded for CRA-2024	FEPs TSD
Round 4 (CC4) Submitted July 2020				
CC4-GEOCHEM-22	Appendix GEOCHEM Colloid Parameter Table	#7 (12/1/20)	satisfactory	Chemistry TSD, Attachment A
CC4-MON-2	Updated map of potash mining	#6 (10/26/20)	partially adequate; updated map of potash leases provided, but not mined areas	Boreholes TSD
CC4-MON-3	Status of proposed new potash mine east of WIPP	#6 (10/26/20)	satisfactory	Boreholes TSD
CC4-SCR-6 a-b	N FEPs updates	#7 (12/1/20)	satisfactory; additional information and discussion will be provided in CRA-2024	FEPs TSD
CC4-SOTERM-6 a-b	Comparison of PROPMIC Values to Literature Values	#7 (12/1/20)	incomplete initial response led to technical exchange held December 2020, calculations and data comparisons performed by EPA	Chemistry TSD
CC4-SOTERM-7	Missing Reference	#6 (10/26/20)	satisfactory; reference provided	Chemistry TSD, Attachment A
CC4-SOTERM-8 a-c	Pu(III) Intrinsic Colloid Concentrations	#7 (12/1/20)	adequate response, technical exchange held Dec 2020	Chemistry TSD; **Appendix A**
CC4-SOTERM-9	Th(IV) Intrinsic Colloid Concentrations Error	#7 (12/1/20)	partially adequate response, technical exchange held December 2020, EPA performed additional assessment	Chemistry TSD; **Appendix A**
CC4-SOTERM-10	Th(IV) Concentration Data Revisions	#7 (12/1/20)	satisfactory	Chemistry TSD; **Appendix A**
CC4-SOTERM-11	Th(IV) Mineral Fragment Colloid Parameter	#7 (12/1/20)	satisfactory	Chemistry TSD; **Appendix A**
CC4-SOTERM-12	Actinide(IV)-Silica Colloids	#6 (10/26/20)	partially adequate response; technical exchange held December 2020; additional investigation required for future PAs	Chemistry TSD; **Appendix A**
Round 5 (CC5) Submitted Sept 2020				

Question	Topic	DOE Response Set	Evaluation/Resolution	Discussion/ Documentation
CC5-33-5 a-c	Borehole Location Maps and Plugging Exemptions	#8 (1/13/21)	satisfactory (a), partially adequate (b,c); descriptions and maps don't agree	Boreholes TSD
CC5-33-6	Apparent conflict in descriptions of areas used for determining plugging patterns	#8 (1/13/21)	partially adequate; does not match map provided	Boreholes TSD
CC5-33-7	Clarification of data discrepancies between DBMAR 2018 ("Rev. 0") and DBMAR 2018 Rev. 1	#8 (1/13/21)	satisfactory; data availability problem, added to erratum	Boreholes TSD
CC5-33-8	Categorization of boreholes of unknown depth and/or incomplete information	#8 (1/13/21)	satisfactory; request reevaluation for future	Boreholes TSD
CC5-GEOCHEM-23	Humic Colloid PHREEQC Input, Output, and Database Files	#7 (12/1/20)	satisfactory, files provided	Chemistry TSD, Attachment A
CC5-GEOCHEM-24	Inclusion of Calcite Precipitation in EQ3/6 Calculations	#8 (1/13/21) & #12 (5/27/21)	satisfactory; follow up call held with DOE Feb 2021	Chemistry TSD; **Appendix A**
CC5-GEOCHEM-25	Effects of Polyhalite on Modeled Brine Chemistry	#8 (1/13/21) & #12 (5/27/21)	satisfactory; follow up call held with DOE Feb 2021	Chemistry TSD; **Appendix A**
CC5-GEOCHEM-26	Effects of Cements on Brine Chemistry	#8 (1/13/21) & #12 (5/27/21)	satisfactory; follow up call held with DOE Feb 2021	Chemistry TSD; **Appendix A**
CC5-GEOCHEM-27 a-d	Incomplete Documentation Related to Pitzer Parameter Errors in DATA0.FM4	#8 (1/13/21)	satisfactory, requested data provided	Chemistry TSD, Attachment B; **Appendix A**
CC5-HYDRO-8	Explanation of pressure response in SNL-13	#11 (4/23/21)	satisfactory; will be a discussion topic of an upcoming Technical Exchange	Culebra TSD
CC5-HYDRO-9	Explanation of pressure response in H-09bR	#11 (4/23/21)	satisfactory; will be a discussion topic of an upcoming Technical Exchange	Culebra TSD
CC5-HYDRO-10	Validity of Groundwater Flow and Radionuclide Transport Assumptions in the Culebra	#11 (4/23/21)	satisfactory; will be a discussion topic of an upcoming Technical Exchange	Culebra TSD

Question	Topic	DOE Response Set	Evaluation/Resolution	Discussion/ Documentation
CC5-HYDRO-11	Investigations to better understand pressure responses in Magenta monitoring wells	#11 (4/23/21)	satisfactory	Culebra TSD
CC5-MON-4 a-m	Data errors and anomalies in Delaware Basin Drilling Surveillance Program	#9 (3/4/21)	satisfactory; DOE has committed to audit program, take corrective action	Boreholes TSD
CC5-MON-5	Response rate of Delaware Basin Drilling Surveillance Program surveys of area operators	#9 (3/4/21)	satisfactory	Boreholes TSD
CC5-MON-6	Uncounted shallow sulfur exploration holes previously identified from New Mexico	#9 (3/4/21)	satisfactory	Boreholes TSD
CC5-SCR-7	Effects of Cementitious Components of Repository Shaft Seals (FEPs W8 and W56)	#9 (3/4/21)	partially adequate; screening arguments should be revised	FEPs TSD
CC5-SCR-8	Screening Argument for Galvanic Coupling Within the Repository (FEP W50)	#10 (3/30/21)	satisfactory; discussion should be updated and expanded for CRA-2024	FEPs TSD, Chemistry TSD
CC5-SCR-9	Screening Decision for Gas Generation by Lead Corrosion (FEPs W5 and W49)	#10 (3/30/21)	satisfactory; calculations provided	FEPs TSD, Chemistry TSD
CC5-SCR-10 a-c	N FEPs and related updates	#10 (3/30/21)	partially adequate; DOE did not directly acknowledge or answer all questions; screening arguments should be reviewed and updated for CRA-2024	FEPs TSD
CC5-TFIELD-1	Recalculation of TFIELDs	#10 (3/30/21)	satisfactory; will be a topic of conversation of an upcoming Technical Exchange	Culebra TSD
Round 6 (CC6) Submitted Nov 2020				
CC6-24-3	ATWIR 2018 inventory documents request	#8 (1/13/21)	satisfactory, documents provided	Inventory TSD

Question	Topic	DOE Response Set	Evaluation/Resolution	Discussion/ Documentation
CC6-GEOCHEM-28	Iron-sulfate Pitzer parameters and solid phases not in DATA0.FM4	#10 (3/30/21)	adequate response, omitted data should be added to database for future PAs	Chemistry TSD, Attachment B; **Appendix A**
CC6-GEOCHEM-29	adequacy of lead parameterization in DATA0.FM4	#10 (3/30/21)	adequate response, lead data rejected by EPA	Chemistry TSD, Attachment B; **Appendix A**
CC6-GEOCHEM-30	Jang and Kim (2016) report request	#9 (3/4/21)	satisfactory, reference provided	Chemistry TSD, Attachment A
CC6-GEOCHEM-31	Comparison of Modeled and Experimental Glushinskite Data	#10 (3/30/21)	satisfactory	Chemistry TSD, Attachment B; **Appendix A**
CC6-GEOCHEM-32	Effects of Shielded Containers on Steel Surface Area per Unit Volume	#9 (3/4/21)	adequate response	Chemistry TSD; **Appendix A**
CC6-GEOCHEM-33	Humic Steel Corrosion Parameter	#9 (3/4/21)	satisfactory	Chemistry TSD; **Appendix A**
CC6-GEOCHEM-34	Incorrect Units for Gas Generation and Brine Production Rates	#9 (3/4/21)	satisfactory, acknowledged in errata	Chemistry TSD, Attachment A
CC6-GEOCHEM-35	Omission of Brine Radiolysis Effects from Appendix GEOCHEM Discussions of Radiolysis and the Brine Production Model	#9 (3/4/21)	satisfactory, acknowledged in errata	Chemistry TSD; **Appendix A**
CC6-HYDRO-12	Modeling Performed by Thomas, et. al. (2017)	#10 (3/30/21)	satisfactory; will be a discussion topic of an upcoming Technical Exchange	Culebra TSD
CC6-SCR-11	Updates to seismic activity FEPs	#10 (3/30/21)	partially adequate; additional, updated information and discussion should be provided in CRA-2024	FEPs TSD
Follow Up Completeness Comments 1 (FC1) Submitted Jan 2021 (email) EPA-HQ-OAR-2019-0534-0041				
FC1-CCR-SOTERM-8, 9, 10	Nd (III) Colloids Data	#11 (4/23/21)	satisfactory	Chemistry TSD; **Appendix A**

Question	Topic	DOE Response Set	Evaluation/Resolution	Discussion/ Documentation
Follow Up Completeness Comments 2 (FC2) Submitted Apr 2021 (email) EPA-HQ-OAR-2019-0534-0042				
FC2-CCR-GEOCHEM-32	steel surface area (number of shielded containers)	#13 (5/18/21)	satisfactory	Chemistry TSD; **Appendix A**

Table 2: List of EPA Docket Items, EPA Completeness Comments, and DOE Response Packages

WIPP CRA-2019 EPA Docket numbers corresponding to EPA Completeness Question Sets and DOE Response Packages

Docket Number	Item
EPA Completeness Questions	
EPA-HQ-OAR-2019-0534-0005	Letter to DOE/M. Brown - EPA Completeness Comments #1 on the CRA-2019 (3/23/20)
EPA-HQ-OAR-2019-0534-0006	Letter to DOE/M. Brown - EPA Completeness Comments #2 on the CRA-2019 (5/6/20)
EPA-HQ-OAR-2019-0534-0007	Letter to DOE/M. Brown - EPA Completeness Comments #3 on the CRA-2019 (6/12/20)
EPA-HQ-OAR-2019-0534-0008	Letter to DOE/M. Brown - EPA Completeness Comments #4 on the CRA-2019 (7/17/20)
EPA-HQ-OAR-2019-0534-0009	Letter to DOE/M. Brown - EPA Completeness Comments #5 on the CRA-2019 (9/11/20)
EPA-HQ-OAR-2019-0534-0010	Letter to DOE/M. Brown - EPA Completeness Comments #6 on the CRA-2019 (11/13/20)
EPA-HQ-OAR-2019-0534-0011	E-mail Correspondence between EPA/J. Santillan and DOE/R. Patterson, re: Actinide Solubility Uncertainty related to the CRA-2019
EPA-HQ-OAR-2019-0534-0040	Email from I. Rosencrantz to A Ward *EPA follow up completeness comments #1 (1/7/21)*

EPA-HQ-OAR-2019-0534-0041	Email from E. Santillan to A Ward *EPA follow up completeness comments #2 (4/15/21)*
DOE Responses	
EPA-HQ-OAR-2019-0534-0012	Letter to EPA/L. Veal - DOE Response to EPA Completeness Comments #1 on the CRA-2019 (6/10/20)
EPA-HQ-OAR-2019-0534-0013	Letter to EPA/L. Veal - DOE Response to EPA Completeness Comments #2 on the CRA-2019 (7/8/20)
EPA-HQ-OAR-2019-0534-0014	Letter to EPA/L. Veal - DOE Response to EPA Completeness Comments #3 on the CRA-2019 (8/13/20)
EPA-HQ-OAR-2019-0534-0015	Letter to EPA/L. Veal - DOE Response to EPA Completeness Comments #4 on the CRA-2019 (9/15/20)
EPA-HQ-OAR-2019-0534-0016	Letter to EPA/L. Veal - DOE Response to EPA Completeness Comments #5 on the CRA-2019 (10/19/20)
EPA-HQ-OAR-2019-0534-0017	Letter to EPA/L. Veal - DOE Response to EPA Completeness Comments #6 on the CRA-2019 (10/26/20)
EPA-HQ-OAR-2019-0534-0018	Letter to EPA/L. Veal - DOE Response to EPA Completeness Comments #7 on the CRA-2019 (12/1/20)
EPA-HQ-OAR-2019-0534-0024	Letter to EPA/L. Veal - DOE Response 8 to EPA Completeness Comments on the CRA-2019 (1/13/21)
EPA-HQ-OAR-2019-0534-0025	Letter to EPA/L. Veal - DOE Response 9 to EPA Completeness Comments on the CRA-2019 (3/4/2021)
EPA-HQ-OAR-2019-0534-0026	Letter to EPA/L. Veal - DOE Response 10 to EPA Completeness Comments on the CRA-2019 (3/30/21)
EPA-HQ-OAR-2019-0534-0027	Letter to EPA/L. Veal - DOE Response (SOTERM) to EPA Completeness Comments on the CRA-2019 (5/20/21)
EPA-HQ-OAR-2019-0534-0028	Letter to EPA/L. Veal - DOE Response 12 to EPA Completeness Comments on the CRA-2019 (5/27/21)
EPA-HQ-OAR-2019-0534-0029	Letter to EPA/L. Veal - DOE Response 13 to EPA Completeness Comments on the CRA-2019 (5/18/21)

EPA-HQ-OAR-2019-0534-0030	Letter to EPA/L. Veal - DOE Response 14 to EPA Completeness Comments (via June 201 Technical Exchange) on the CRA-2019 (6/10/20)
EPA-HQ-OAR-2019-0534-0031	Letter to EPA/L. Veal - DOE Response 11 to EPA Completeness Comments on the CRA-2019 (4/23/21)

NOTE: A separate pdf file compiled from all of DOE's completeness comment responses and their full text is included in the CRA-2019 Docket ID No. EPA-HQ-OAR-2019-0534.

Select copies of EPA Completeness Comments, DOE Responses, and EPA Evaluations not included in separate Technical Support Documents

CC1-GEN-1 Closure Dates

WIPP Compliance Recertification Application 2019

EPA Question (from EPA Completeness Comment Package 1)

Please provide an update of the currently projected facility life span and closure date, projected closure dates for individual waste panels, and a summary of DOE's approach for incorporating the impacts of an extended facility life into the performance assessment (PA). In other words, please explain and reconcile the different closure dates found in available compliance documents.

> *EPA is aware that the DOE and NWP have provided NMED with a draft Ten-Year Renewal Application of the RCRA Hazardous Waste Facility Permit for the WIPP that proposes to extend the waste disposal phase to September 2052 and also provides specific closure dates for individual waste panels. An extension beyond the current closure date of 2033 may impact current assumptions regarding time-sensitive initial conditions for post-closure PA modeling. These assumptions include the extent of radioactive decay, creep closure, and sealing of the underground facilities at the time of closure.*

DOE Response (from DOE Response Package 1)

A formal decision and subsequent announcement of a new closure date for the Waste Isolation Pilot Plant (WIPP) has not been made by the U.S. Department of Energy (DOE). Therefore, the CRA-2019 submittal to the U.S. Environmental Protection Agency (EPA) on March 5, 2019 and the deferred performance assessment submitted to EPA on December 20, 2019 are based on a closure date of 2033, which is consistent with all previous compliance recertification applications (CRAs) for WIPP. In addition, closure dates were removed from the Ten-Year Renewal Application submitted to the New Mexico Environment Department (NMED) on March 31, 2020.

Once a revised closure date for WIPP is approved for use by DOE, future compliance calculations and compliance documentation will reflect this change.

EPA Evaluation of Response

The DOE response was adequate, but postpones addressing the main question to a later date. Beyond the reasons stated in EPA's original question, this is one of the most commonly communicated stakeholder concerns. EPA is aware of many different factors and organizations involved in these decisions, but appreciates more proactive communications about future plans where possible.

CC1-34-1 Request for Figures from PA Results

40 CFR §194.34 Results of Performance Assessments

EPA Question (from EPA Completeness Comment Package 1)

Please provide the following figures for Scenario S3-BF:

CC1-34-1a***. Overall Means of WP Pressure***

DOE Response (from DOE Response Package 1)

Below is a plot of the overall means of WP (waste panel) pressure, S3-BF, for CRA14 and CRA19.

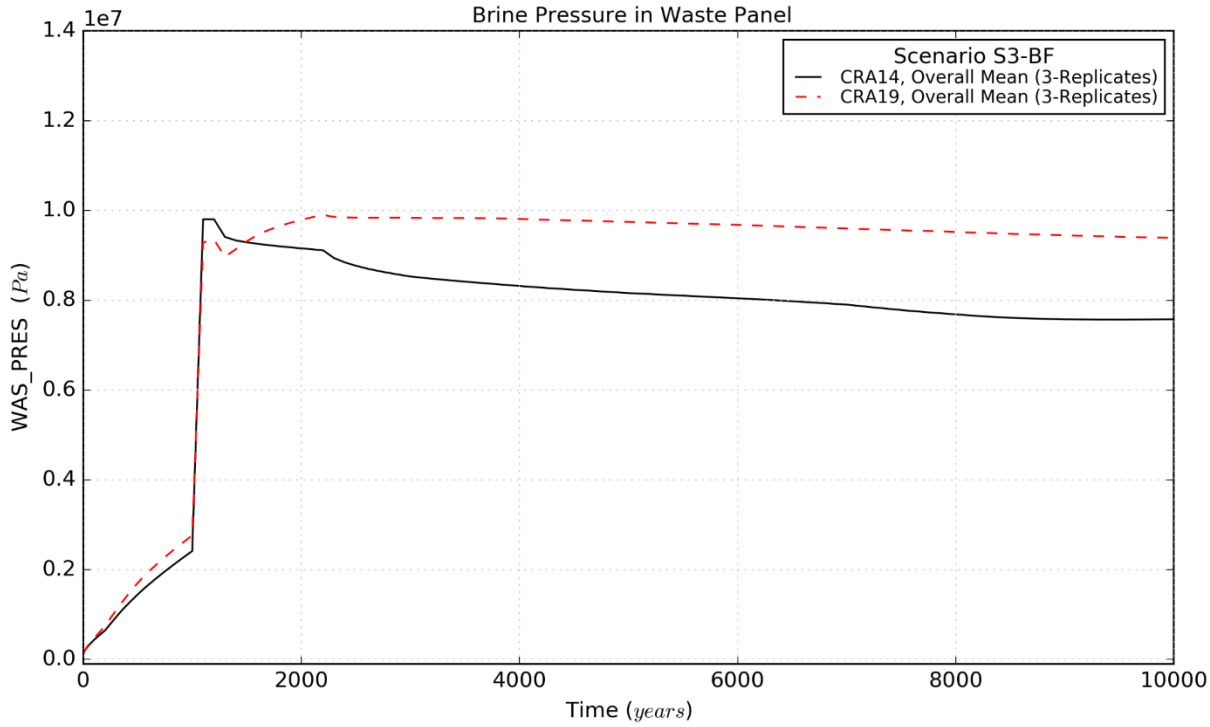

CC1-34-1b***. Overall Means of SROR Pressure***

DOE Response

Below is a plot of the overall means of SROR (south rest-of-repository) pressure, S3-BF, for CRA14 and CRA19

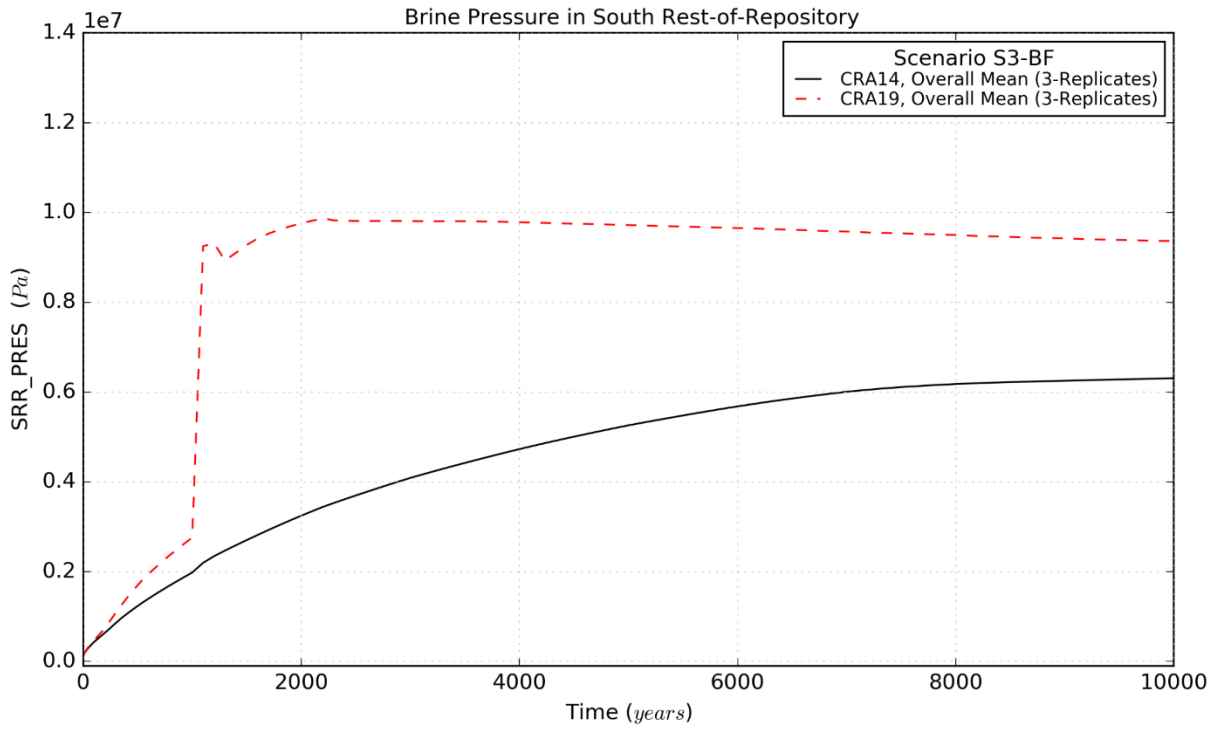

CC1-34-1c. ***Overall Means of NROR Pressure***

DOE Response

Below is a plot of the overall means of NROR (north rest-of-repository) pressure, S3-BF, for CRA14 and CRA19.

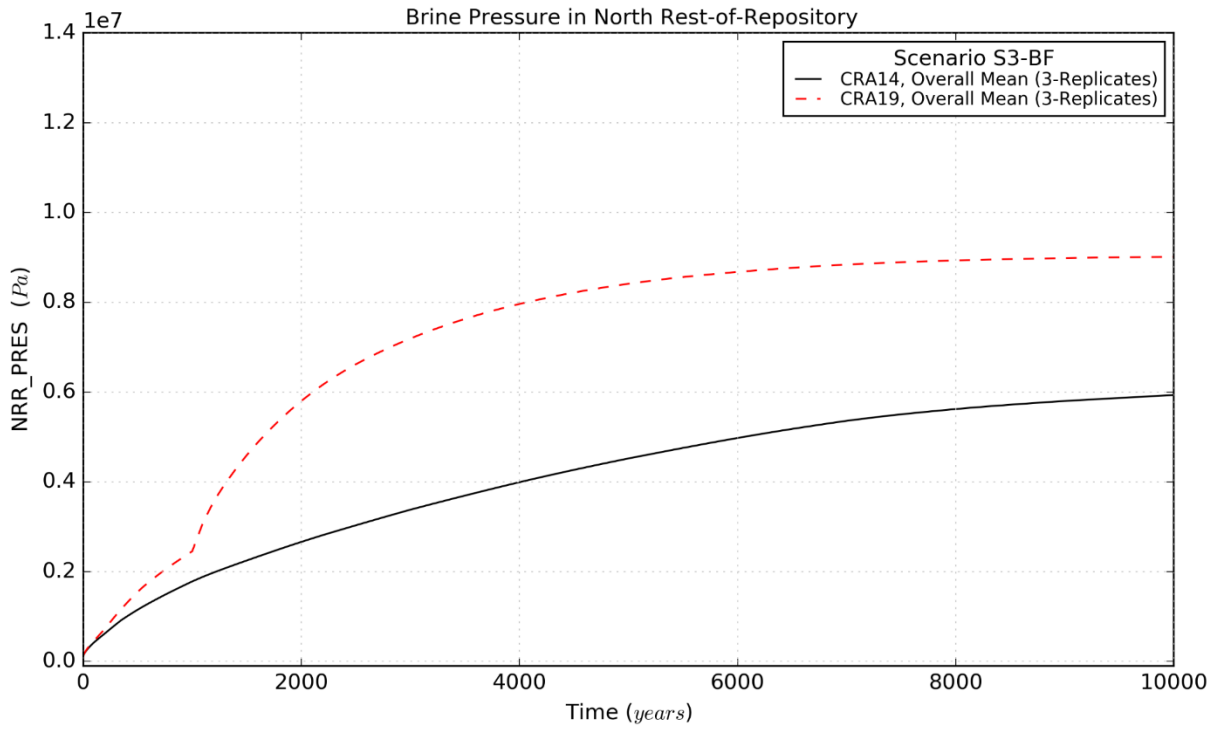

CC1-34-1d. ***Overall Means of WP Brine Saturation***

DOE Response

Below is a plot of the overall means of WP brine saturation, S3-BF, for CRA14 and CRA19.

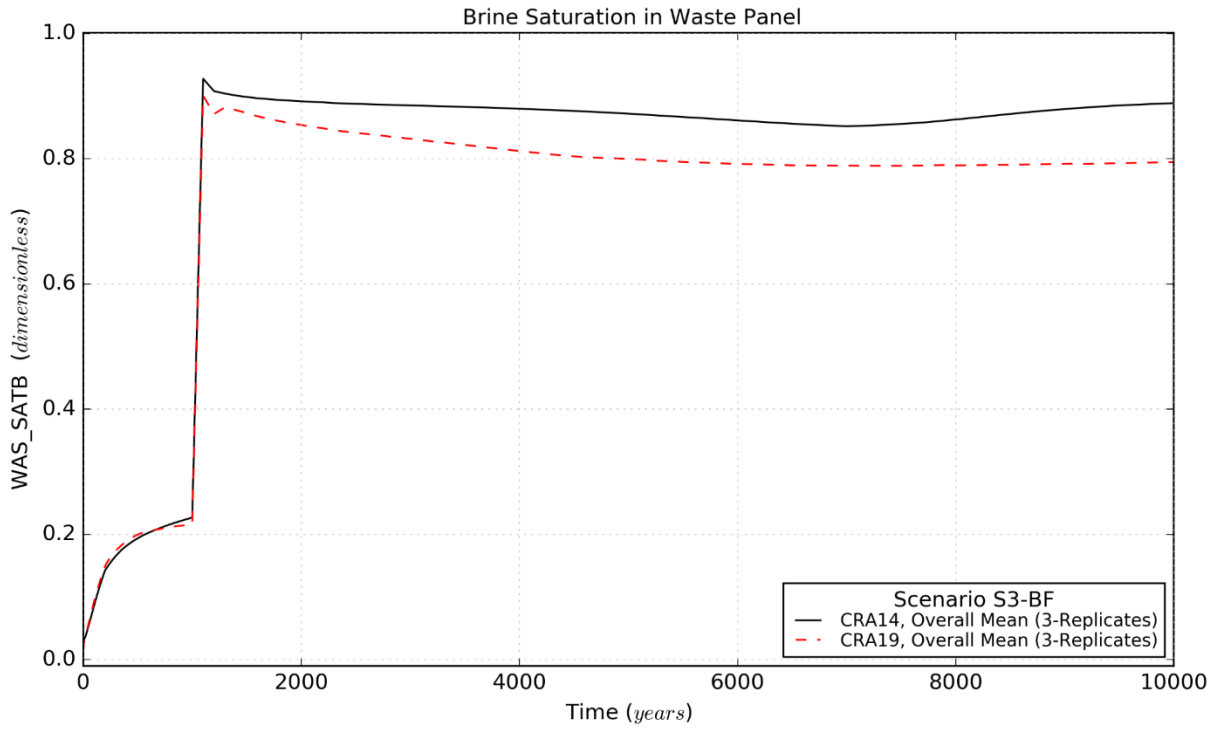

CC1-34-1e. ***Overall Means of SROR Brine Saturation***

DOE Response

Below is a plot of the overall means of SROR brine saturation, S3-BF, for CRA14 and CRA19.

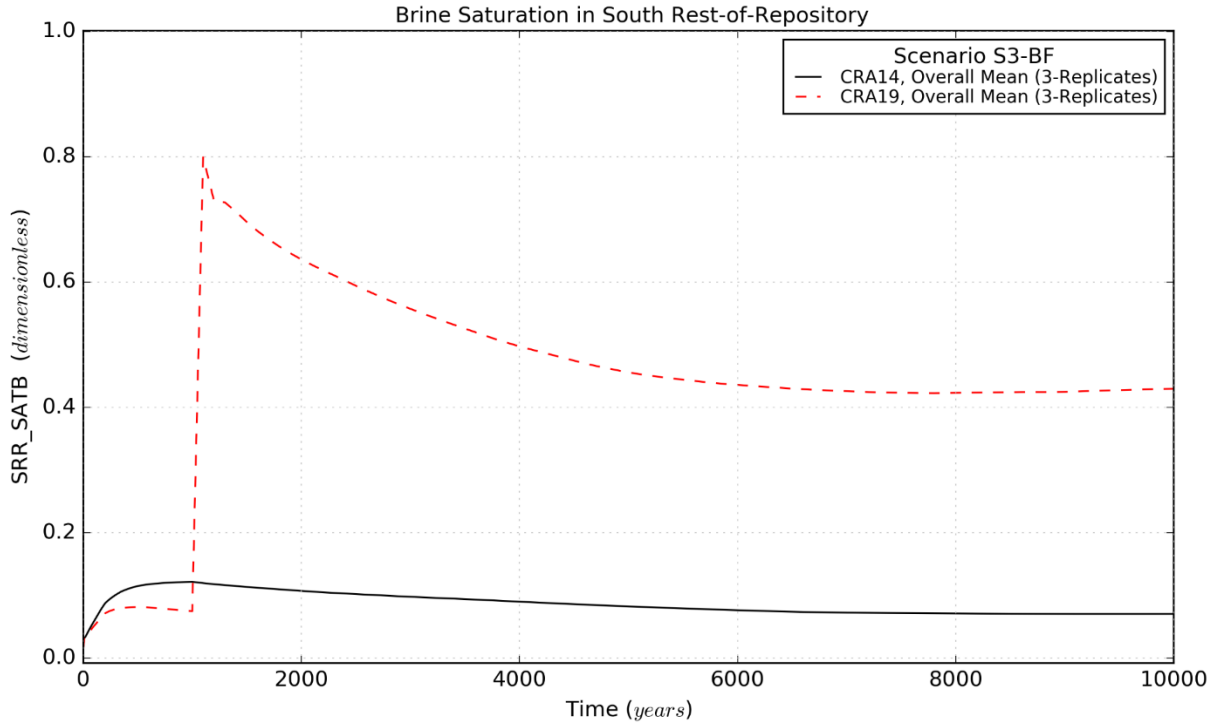

CC1-34-1f. ***Overall Means of NROR Brine Saturation***

DOE Response

Below is a plot of the overall means of NROR brine saturation, S3-BF, for CRA14 and CRA19.

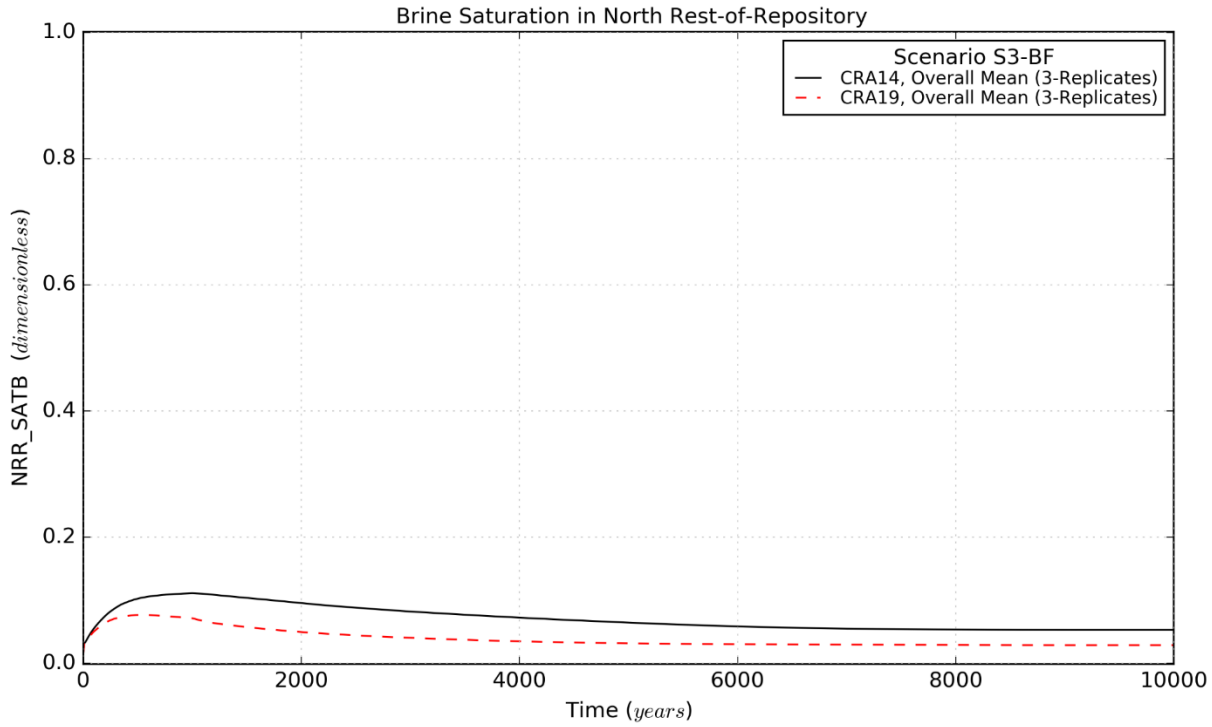

EPA Evaluation of Response

The DOE response was satisfactory. The figures were provided as requested and useful to EPA for understanding brine saturation over time.

CC1-34-2 Repository Conditions Completeness Request

40 CFR §194.34 Results of Performance Assessments

EPA Question (from EPA Completeness Comment Package 1)

Please provide calculations, figures, and explanations of how the following information is determined for an example realization selected by DOE that resulted in a DBR. EPA is seeking explanations of how the results requested in Question 34-2a are used to determine repository pressures and brine saturations at times other than 350 and 1,000 years post-closure.

34-2a. ***Figures showing pressure and brine saturation vs time for the example realization for Scenarios S2-BF and S3-BF for the WP, SROR, and NROR.***

DOE Response (from DOE Response Package 3)

Vector 001 of Replicate 1 is used as an example realization. Figure 1 through Figure 3 show the brine pressure and saturation results for this vector in the waste panel (WP), south rest of repository (SROR), and north rest of repository (NROR) areas. Scenario S2-BF and S3-BF results from the 10,000-year BRAGFLO simulation scenario are plotted together for each repository area. Scenario S2-BF is defined with an intrusion into the Castile at 350 years and scenario S3-BF is defined with an intrusion into the Castile at 1000 years. The brine pressure and saturation responses from the intrusions can clearly be seen at the intrusion times in the figures. Figure 4 through Figure 6 plot the brine pressure and saturation results for all 100 vectors of Replicate 1 S2-BF along with the mean value at each point in time. Corresponding results for S3-BF are shown in Figure 7 through Figure 9.

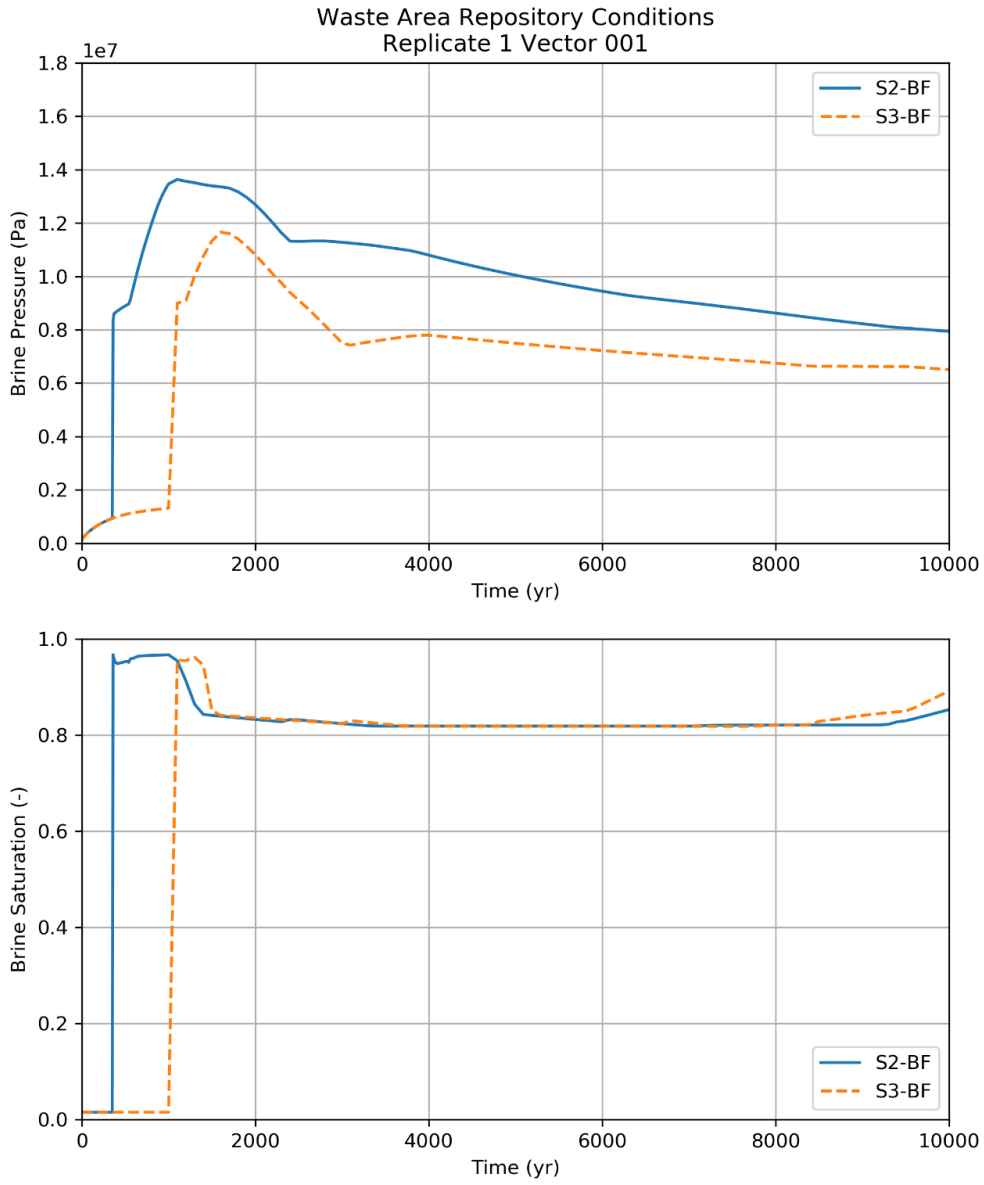

Figure 1 Waste Panel Repository Conditions for Vector 001 of Replicate 1

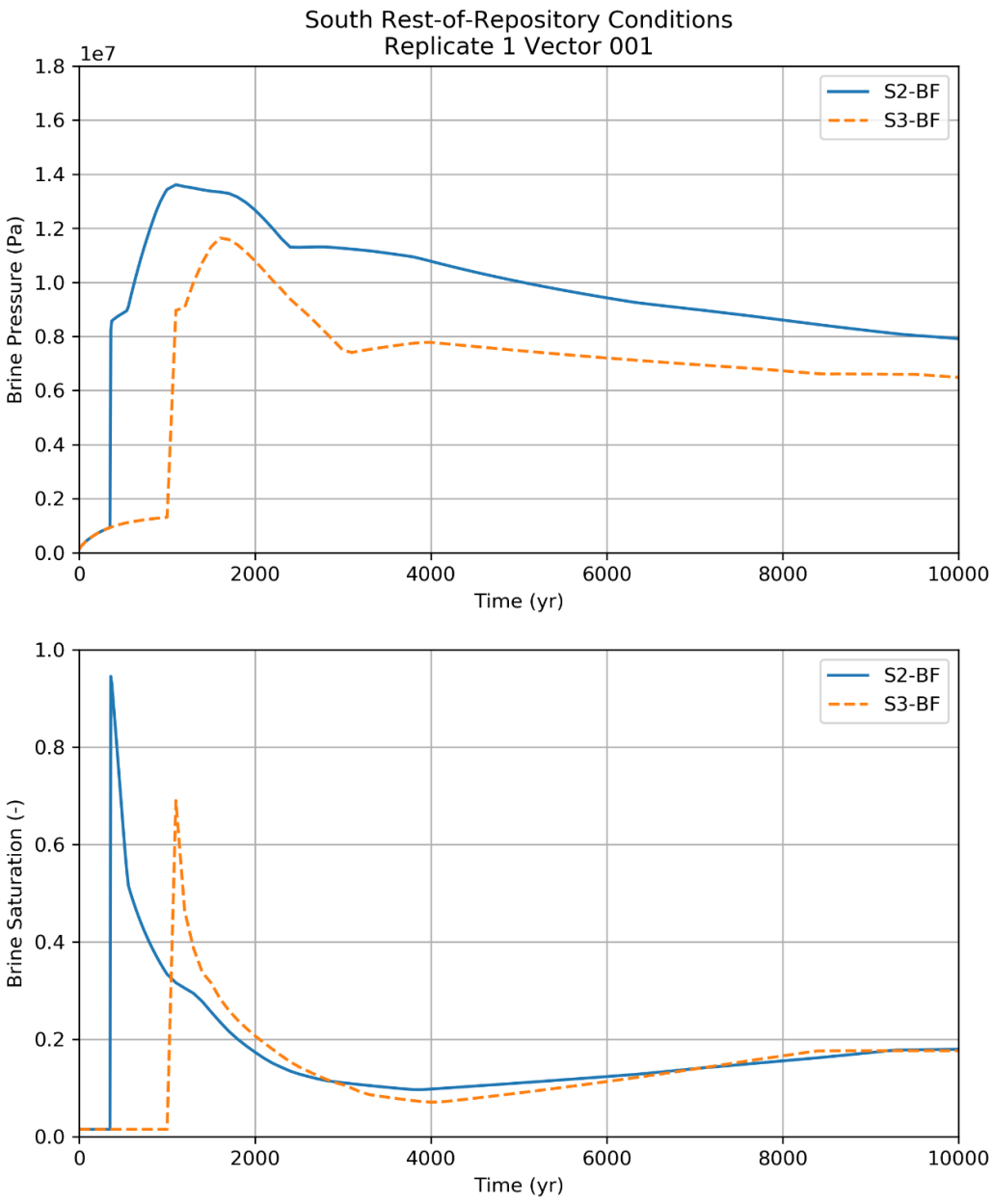

Figure 2 South Rest-of-Repository Conditions for Vector 001 of Replicate 1

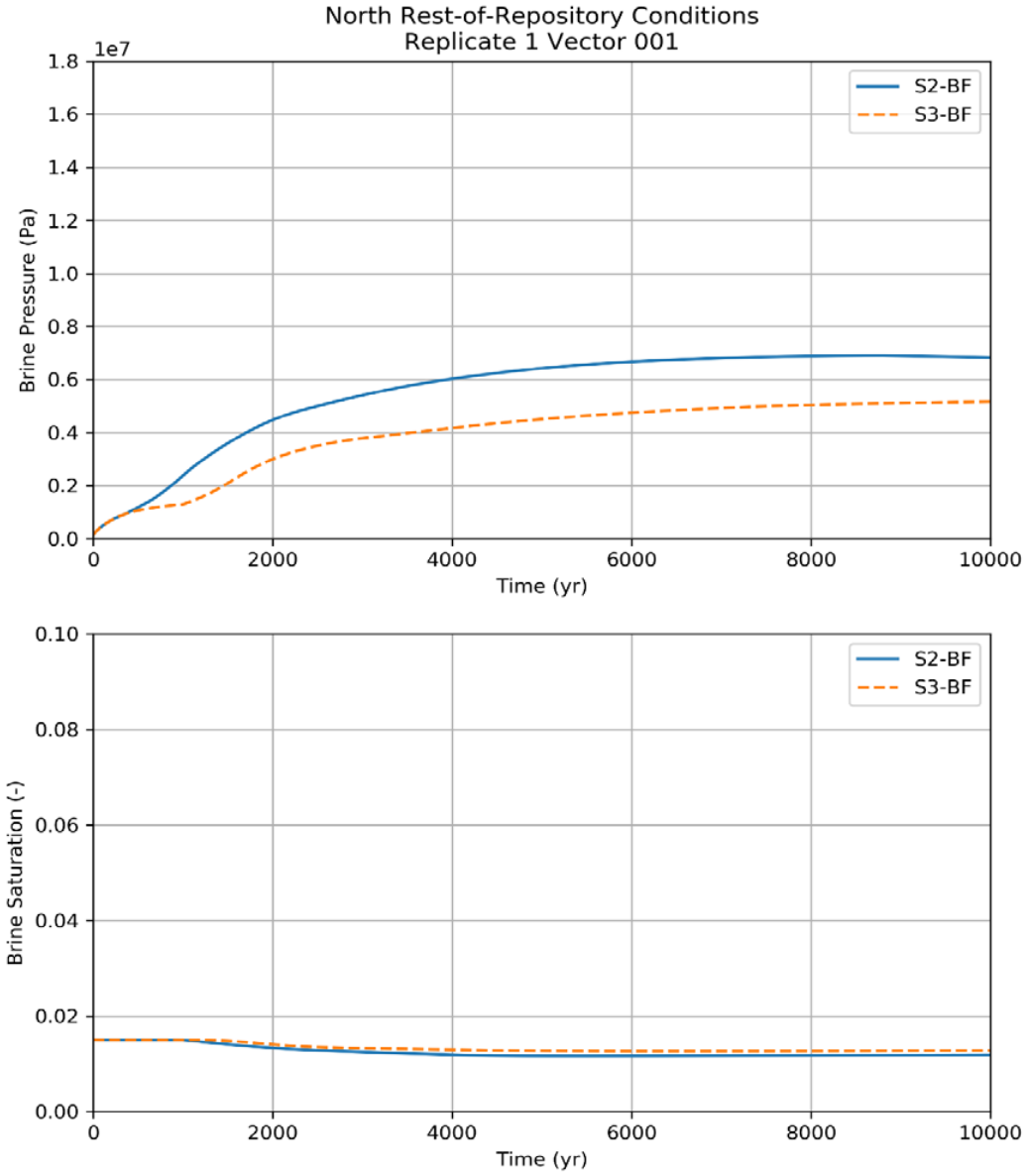

Figure 3 North Rest-of-Repository Conditions for Vector 001 of Replicate 1[1]

[1] Note when comparing other regions the Brine Saturation axis has been scaled from 0 to 0.1 to better show results in this area.

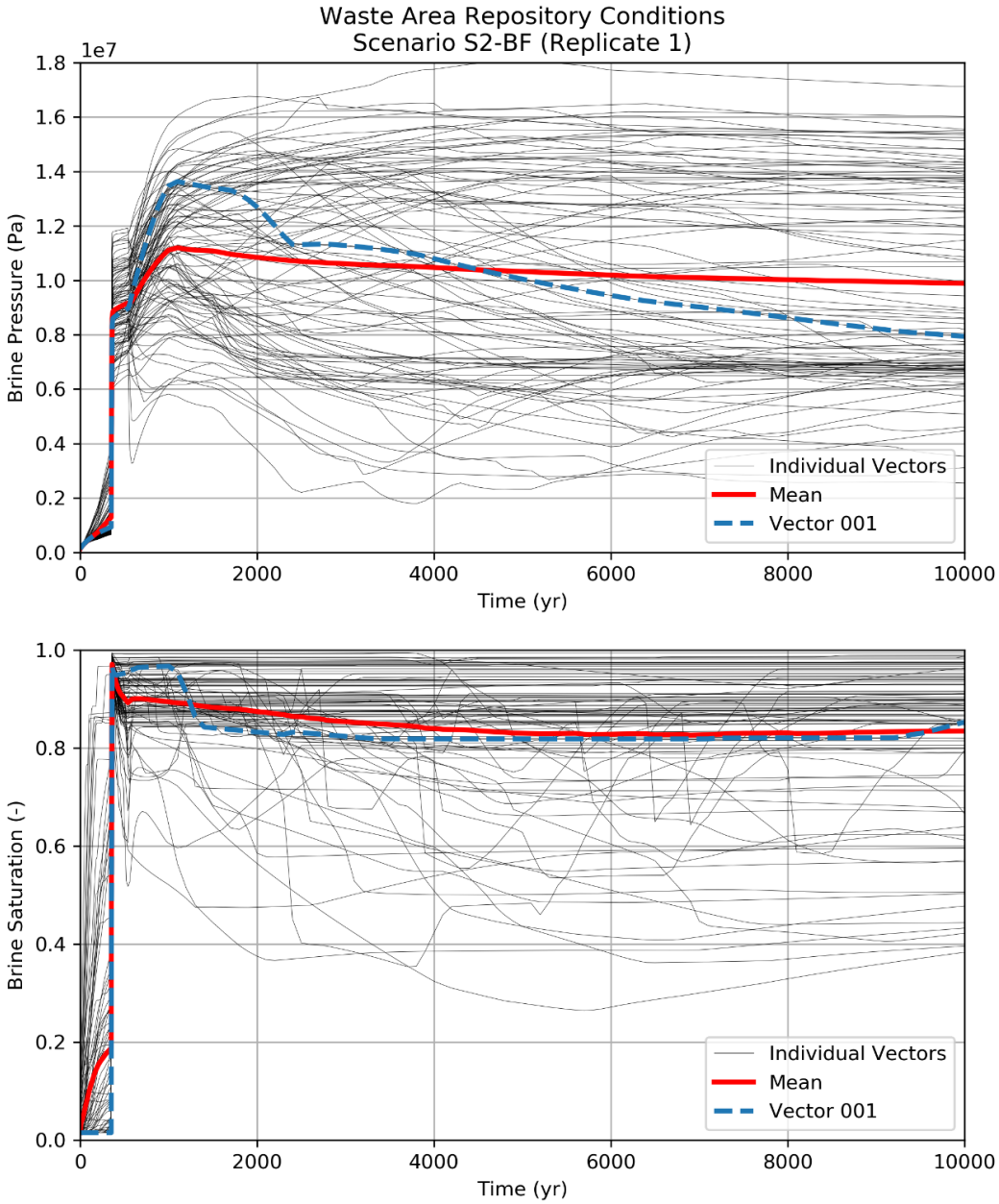

Figure 4 Waste Panel S2-BF Repository Conditions for all Replicate 1 Vectors

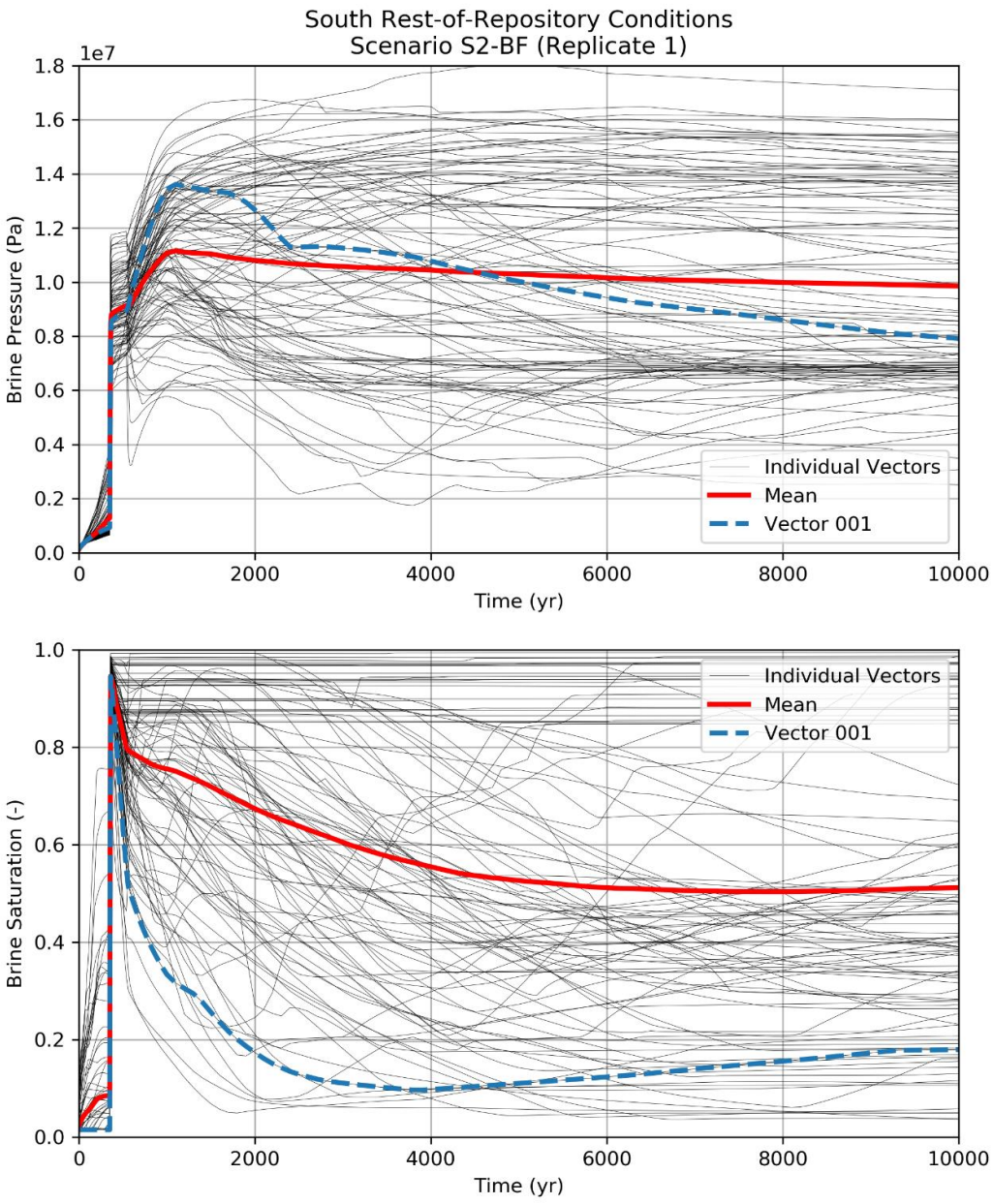

Figure 5 South Rest-of-Repository S2-BF Conditions for all Replicate 1 Vectors

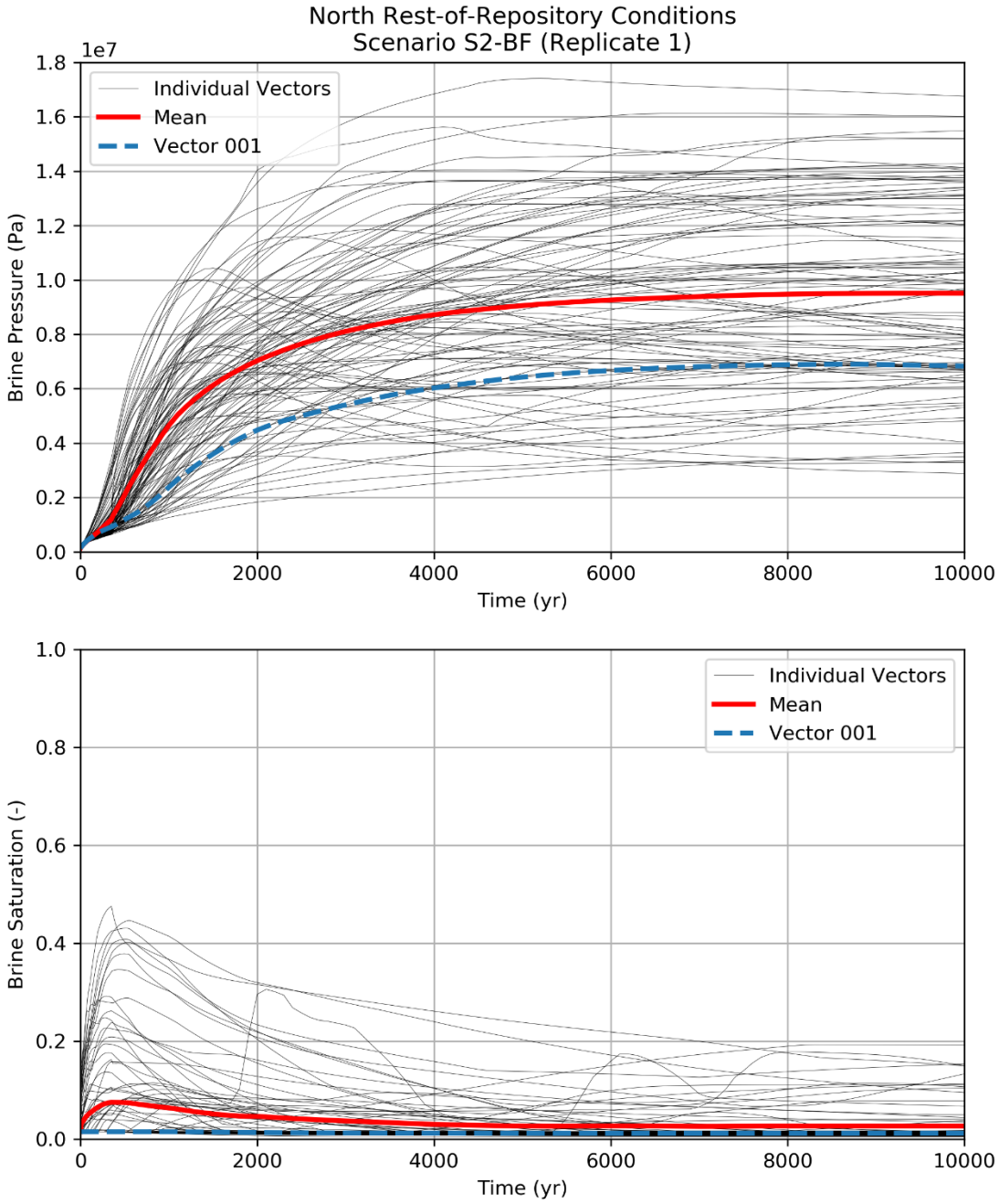

Figure 6 North Rest-of-Repository S2-BF Conditions for all Replicate 1 Vectors

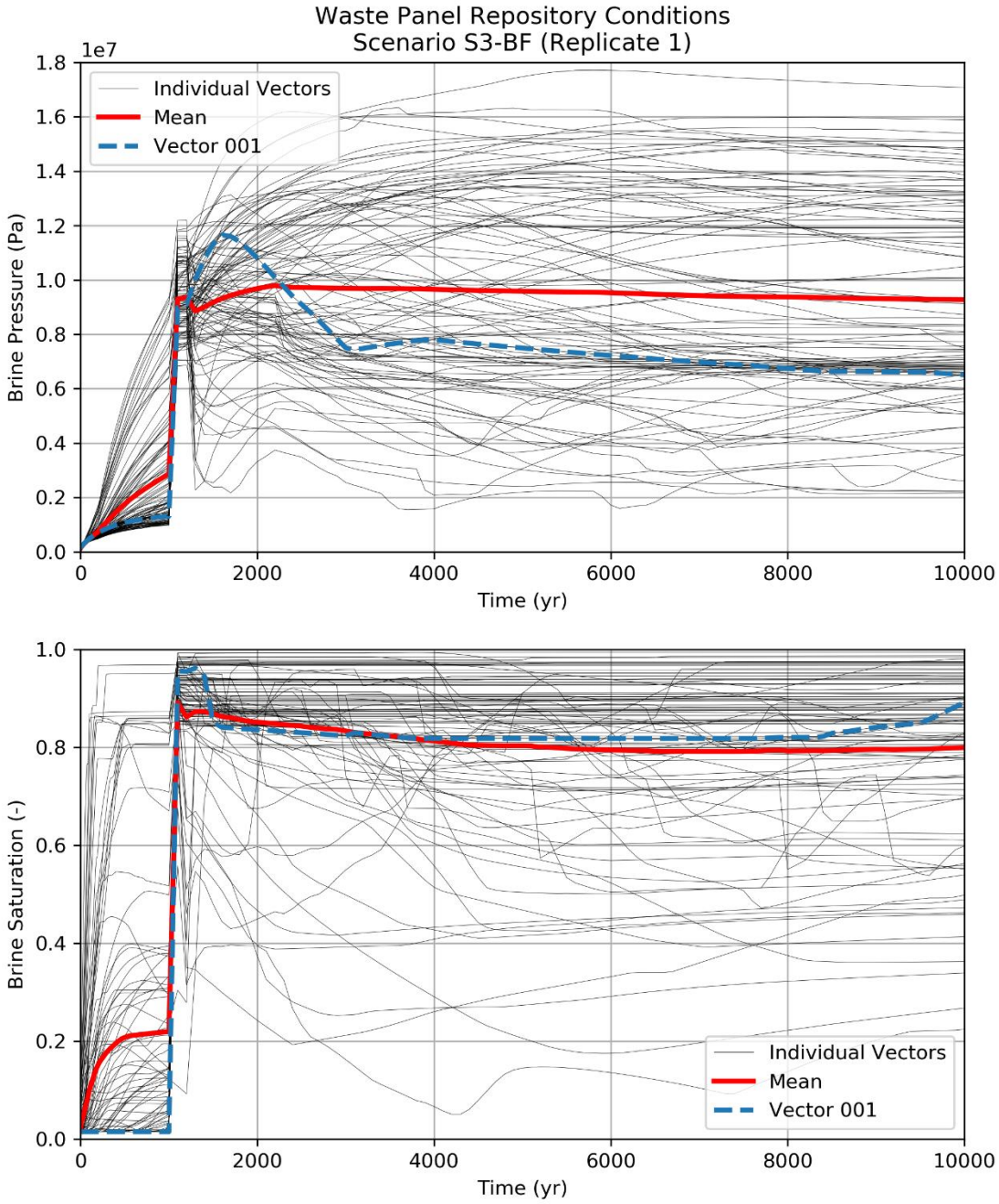

Figure 7 Waste Panel S3-BF Repository Conditions for all Replicate 1 Vectors

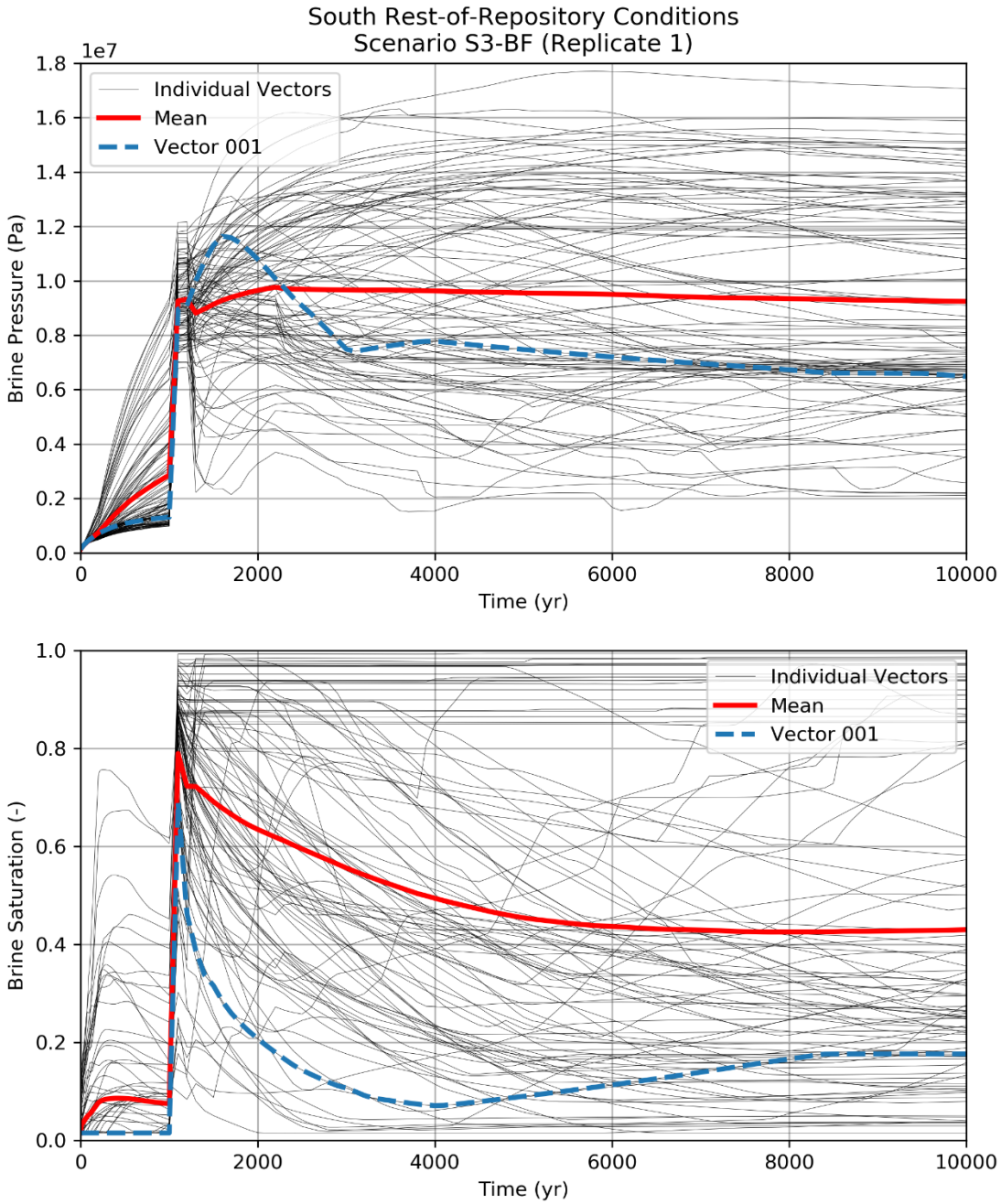

Figure 8 South Rest-of-Repository S3-BF Conditions for all Replicate 1 Vectors

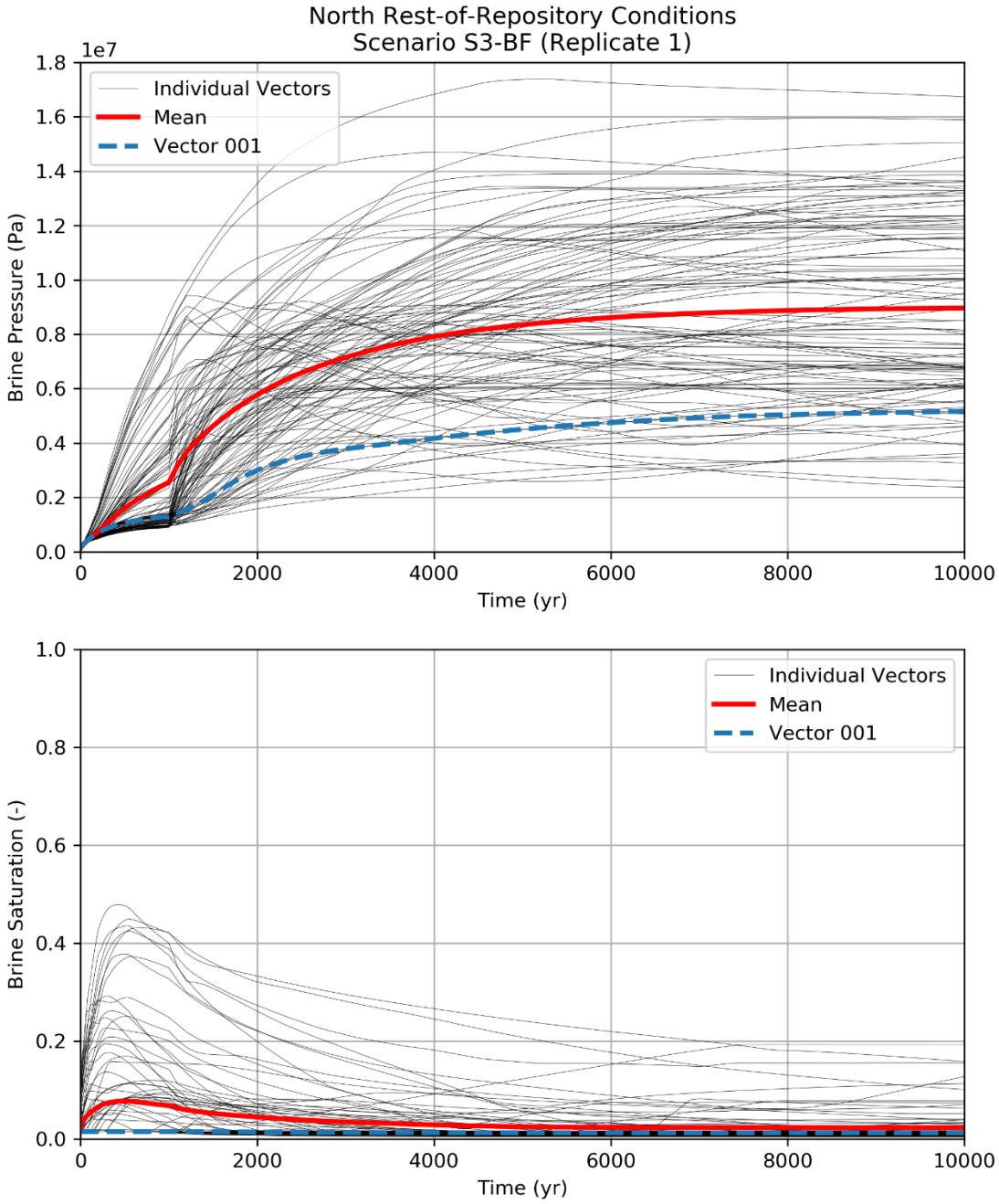

Figure 9 North Rest-of-Repository S3-BF Conditions for all Replicate 1 Vectors

34-2b. ***The repository pressure and brine saturation encountered by a first E1 borehole penetrating the WP at 200 years post-closure.***

DOE Response (from DOE Response Package 3)

In the Waste Isolation Pilot Plant (WIPP) performance assessment (PA), repository conditions (i.e., brine pressure and saturation) are calculated for six specific scenarios using the Salado flow model implemented in the BRAGFLO code. Next, direct brine release (DBR) volumes are calculated for specific intrusion times, using the BRAGFLO DBR code with initial conditions taken from the results of the Salado flow model. DBR volumes are put into look-up tables. When calculating the release at a random intrusion time, the CCDFGF code interpolates on the DBR volumes, not on the underlying repository conditions. This calculation is described in PA-6.8.2 of Appendix PA as well as sections 5.4 and 5.5 of the CCDFGF Design Document and User's Manual (SNL 2010). Figure 10 illustrates the flow of scenario information from BRAGFLO to the CCDFs. Note that this PA methodology for CRA-2019 has not changed since the CRA-2014 PA.

In the case of an initial E1 intrusion at 200 years, this is the first borehole so the calculated releases will be based on the S1-DBR scenario results. Scenario S1-DBR calculates direct brine release volumes at a number of intrusion times, including 100 years and 350 years which are the two nearest bracketing times to the 200 year intrusion time. The release at 200 years is linearly interpolated between the releases at 100 years and 350 years.

The S1-BF results would calculate the repository conditions at 200 years post-closure, but the releases for this intrusion would be based on the interpolation of *releases* at other times, not these *repository conditions* at 200 years.

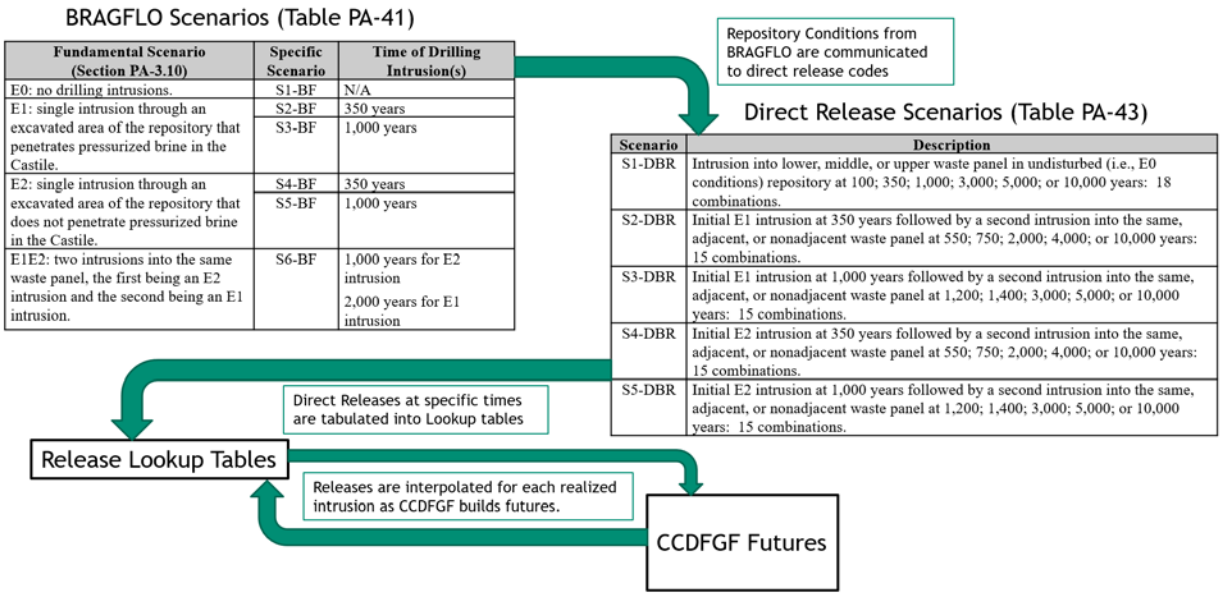

Figure 10 Flow of Data in WIPP PA calculations

34-2c. The repository pressure and brine saturation encountered by a second borehole penetrating the WP at 500 years post-closure following a first E1 borehole penetrating the WP at 200 years postclosure.

DOE Response (from DOE Response Package 3)

As a reminder, when calculating the direct brine release at a random intrusion time, the CCDFGF code interpolates on pre-calculated direct brine release (DBR) volumes, not on the underlying repository conditions. This PA methodology for CRA-2019 has not changed since the CRA-2014 PA.

Direct release scenario S1-DBR calculates direct brine releases from an initial intrusion into an undisturbed repository at a sequence of times. Direct release scenarios S2-DBR through S5-DBR assume an initial intrusion at either 350yr or 1000yr, and calculate direct brine releases for a second intrusion occurring in one of three representative locations and at a sequence of later times (Figure 10). The results of the direct release scenario are referred to as time series, where the time series comprises the direct brine release at each initial intrusion time (scenario S1-DBR) or the direct brine release at the second intrusion time (scenarios S2-DBR through S5-DBR). When organizing the direct brine releases from the S2-DBR through S5-DBR direct release scenarios into lookup tables, the PRECCDFGF code constructs additional time series of direct brine releases from the available scenarios by time-shifting to earlier or later initial intrusion times (SNL 2009). The first of these additional time series has an initial intrusion at 100 years and the last has an initial intrusion at 10,000 years. Time shifting is done by setting the first intrusion time equal to the desired initial intrusion time, and setting secondary intrusion times based on the elapsed time between the first and second intrusions. A final secondary intrusion time is set at 10,000 years for every time series. This is designed so releases from any intrusion time can be found from interpolation on these time series without a need for extrapolation.

To calculate a direct brine release from a second intrusion the algorithm in the CCDFGF code is as follows:

1. The state of the repository (E0, E1, or E2) is determined based on the type of earlier intrusions. The repository state is E0 if all earlier intrusions into the repository have been fully plugged (including an undisturbed repository); E1 if any earlier intrusion introduces Castile brine into the repository; and E2 otherwise (SNL 2010). The repository state determines which direct release scenario is used for later intrusions: S1- DBR for E0 conditions, S2-DBR and S3-DBR for E1 conditions, and S4-DBR and S5-DBR for E2 conditions.

2. The representative waste panel (Same, Adjacent or Non-adjacent) for the current intrusion is determined based on the panel randomly selected for the current intrusion and previously intruded panels (see Table 9 of CC2-34-10 for neighbor relationships).

3. From the set of time series of direct brine release volumes for the repository condition and representative waste panel, two time series of release volumes are selected such that the initial intrusion times for these series bracket the initial intrusion time in the future being simulated. As described above these time series could have been constructed by time-shifting the results of the direct release scenarios.

4. The time difference, Δt = current intrusion time – initial intrusion time, is calculated.

5. Within each time series, a release volume is interpolated at the time series' initial intrusion time plus Δt.

6. A release volume for the current intrusion is found by interpolating between the two release volumes found for each time series (see Figure 11 which is based on Figure 12 in CCDFGF documentation (SNL 2010)).

7. The direct brine release volume is multiplied by the radionuclide concentration, which itself has been interpolated to the intrusion time (Figure 12). The product is the direct brine release for the current intrusion.

This process will now be walked through for the situation of a 200 year initial E1 intrusion and a 500 year subsequent intrusion in the same panel. For a second intrusion, the panel state (E0, E1, or E2) is determined by the type of the earlier intrusion (E1 in this case). Releases from a second intrusion at 500 years are determined by interpolation on the results of the S2-DBR scenario, as illustrated in Figure 11 (based on Figure 12 in (SNL 2010)). Since both intrusions are occurring in the same panel, the "Lower" representative waste panel will be used.

For the direct brine releases at the 500 year subsequent intrusion, the two series that contain initial intrusion times bracketing the specified initial intrusion are: 1) the S2-DBR scenario timeshifted -250 years, which places an initial intrusion at 100 years, and 2) the base S2-DBR scenario which has an initial intrusion at 350 years. The S2-DBR scenario is selected rather than the S4-DBR because the repository state is E1. The time difference Δt from initial intrusion at 200 years to second intrusion at 500 years is 300 years. A direct brine release volume from the first time series (initial intrusion at 100 years) is interpolated at $100 + \Delta t = 400$ years. The result of this interpolation corresponds to point I1 in Figure 11.

A brine release volume from the second time series (initial intrusion at 350 years) is interpolated at $350 + \Delta t = 650$ years, resulting in a value corresponding to point I2 in Figure 11.

The direct brine release volumes indicated by points I1 and I2 are used to interpolate a release volume at $200 + \Delta t = 500$ years (point BH2 on Figure 11). Radionuclide concentration is interpolated to the volume of brine in the intruded panel at the time of the intrusion, then interpolated to the intrusion time. This direct brine release volume is then multiplied by the radionuclide concentrations to obtain radionuclide release (Figure 12).

Interpolating with this approach makes calculating releases computationally feasible over the many intrusions, futures, and replicates of a full performance assessment (PA) calculation.

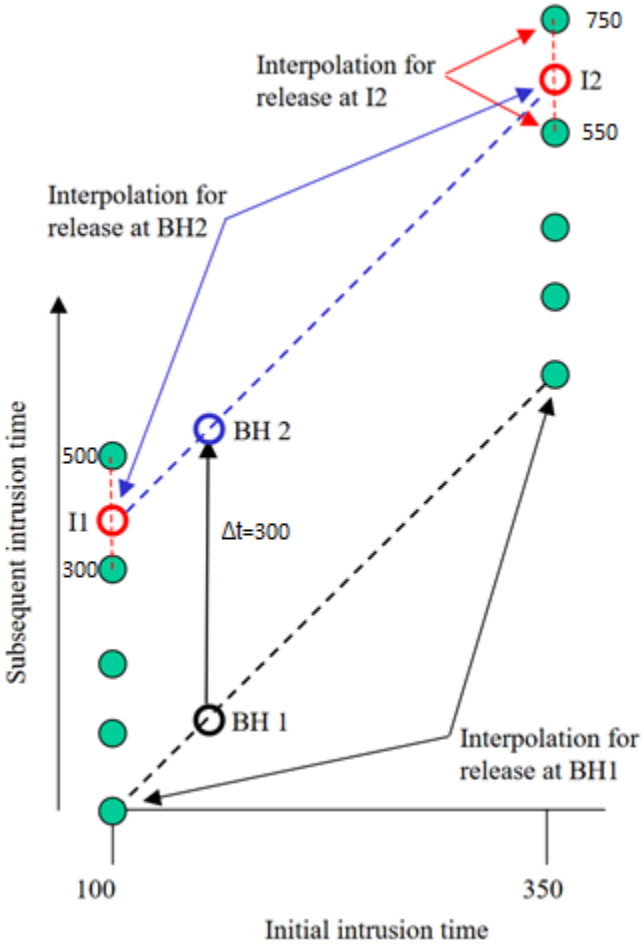

Figure 11 Direct Release Interpolation Logic (SNL 2010)

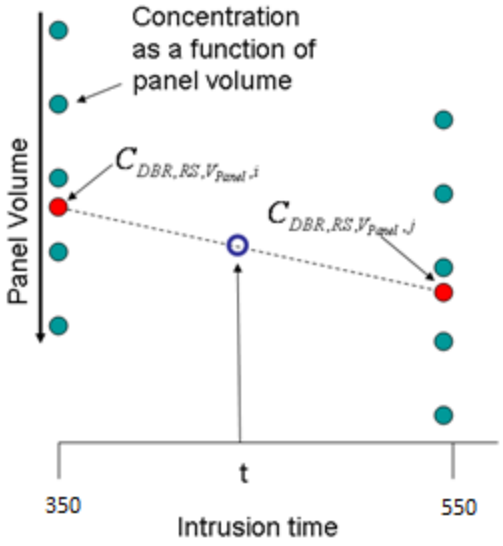

Figure 12 Concentration Interpolation Logic (SNL 2010)

34-2d. ***The repository pressure and brine saturation encountered by a second borehole penetrating the WP at 2,000 years post-closure following a first E1 borehole penetrating the WP at 200 years postclosure.***

DOE Response (from DOE Response Package 3)

See response for 34-2c. The only change in this situation is the time to the subsequent intrusion Δt = 1,800 years, and therefore the use of different points in time series used for the interpolations.

34-2e. ***The repository pressure and brine saturation encountered by a second borehole penetrating Panel 1 at 500 years post-closure following a first E1 borehole penetrating Panel 6 at 200 years postclosure.***

DOE Response (from DOE Response Package 3)

See response to 34-2c. In this situation the representative waste panel for the second intrusion is the "Upper" waste panel (rather than the "Lower" waste panel), based on the panel neighboring relationship between Panels 1 and 6. All other steps are the same as described in the response to 34-2c.

34-2f. ***The repository pressure and brine saturation encountered by a second borehole penetrating Panel 1 at 2,000 years post-closure following a first E1 borehole penetrating Panel 6 at 200 years postclosure.***

DOE Response (from DOE Response Package 3)

See responses for 34-2c, d, and e. In this situation, the release volume for the second intrusion is modeled by the "Upper" waste panel, and Δt = 1,800 years. Otherwise, the calculation is the same as described in the response to 34-2c.

34-2g. ***The repository pressure and brine saturation encountered by a third borehole penetrating Panel 3 at 3,000 years post-closure following a second borehole penetrating Panel 5 at 2,000 years post-closure following a first E1 borehole penetrating Panel 6 at 200 years post-closure.***

DOE Response (from DOE Response Package 3)

From section 6.8.2.3 of Appendix PA, "Brine releases from the third and subsequent intrusions are computed as if the current intrusion was the second intrusion into the repository". Therefore, a selection of what constitutes the "initial intrusion" needs to be made from the two previous intrusions (it is not necessarily the most recent intrusion). From Section 5.3.2 of the CCDFGF Design Document and User's Manual (SNL 2010), "The previous intrusion is selected by finding the closest panel (same, adjacent, non-adjacent) whose intrusion condition, excluding the current intrusion, is equal to the repository condition. The time of the previous intrusion is the time of the most recent intrusion having the greatest consequence and closest distance." The consequence is defined by the intrusion type, with E1 intrusions having larger consequence over E2 intrusions. Panel 3 is non-adjacent to both panels 5 and 6, so the second intrusion at 2,000 years will be considered as the initial intrusion if it was an E1 intrusion; in this case the two time series are based on the S3-DBR scenario. If the 2000 year intrusion

was not an E1, the first intrusion at 200 years would be considered as the initial intrusion, and the two time series from question 34-2f would be used with a new Δt = 2,800 years.

References

Sandia National Laboratories (SNL). 2009. User's Manual for PRECCDFGF. Sandia National Laboratories, Carlsbad, NM. ERMS 552576.
Sandia National Laboratories (SNL). 2010. Design Document and User's Manual for CCDFGF. Sandia National Laboratories, Carlsbad, NM. ERMS 554046.

EPA Evaluation of Response

The DOE response was satisfactory. The information was provided as requested and useful for understanding the repository model response to borehole intrusion scenarios.

CC1-34-3: Frequency of Borehole Intrusions

40 CFR §194.34 Results of Performance Assessments

EPA Question (from EPA Completeness Comment Package 1)

Please provide the following information:

Question 34-3a. Graphical and tabular displays of the number of first E1 borehole intrusions in 20-Year increments for the first 500 years following repository closure for Replicate 1.

DOE Response (from DOE Response Package 3 (DOE RP3 2020))

These are statistics not normally tracked in the Waste Isolation Pilot Plant (WIPP) performance assessment (PA), but the CCDFGF code has the capability to produce a text file (a diagnostic output file) containing raw information about drilling intrusions. For the official CRA19 run, information was produced for a limited number of futures. For this request, CCDFGF was re-run on Replicate 1, and produced information for all 10,000 futures for each of the 100 vectors (1,000,000 total possible futures) which were then written to a text file. Python scripts were then developed to extract the requested information out of this text file.

The data provided is for the timing of intrusions on a repository-wide basis for a given future, and not discussed panel-by-panel. By regulation, active institutional controls prevent intrusions for the first 100 years post-closure.

Table 1 contains the number of first E1 intrusions in 20-year increments for the first 500 years following repository closure for Replicate 1, as well as the total number summed over all bins. Figure 13 is a histogram representing the same information. These data show approximately 2,000 intrusions per bin, which indicates about 0.2% of the simulated 1,000,000 futures have a first E1 intrusion in any given 20-year time period during the first 500 years, or, an annual probability of a first E1 intrusion of about 1×10^{-4}.

Table 1 Number of First E1 Intrusions, 1,000,000 futures, first 500 years each, CRA19 Replicate 1

Time Interval Years	Bin Count	Time Interval Years	Bin Count
0 – 20	0	260 – 280	2,133
20 – 40	0	280 – 300	2,142
40 – 60	0	300 – 320	2,193
60 – 80	0	320 – 340	2,097
80 – 100	0	340 – 360	2,074
100 – 120	2,226	360 – 380	2,141
120 – 140	2,089	380 – 400	2,084
140 – 160	2,161	400 – 420	2,060
160 – 180	2,123	420 – 440	2,095
180 – 200	2,284	440 – 460	2,153
200 – 220	2,226	460 – 480	2,024
220 – 240	2,246	480 – 500	2,103
240 – 260	2,205	**Total:**	**42,859**

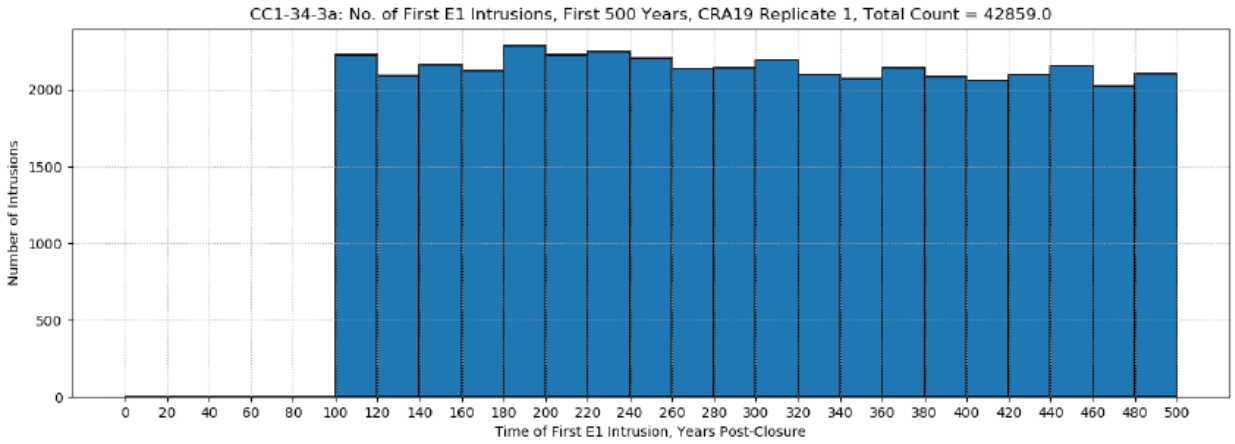

Figure 13 Number of First E1 Intrusions, 1,000,000 futures, first 500 years each, CRA19 Replicate 1

EPA Evaluation of Response

The DOE response was satisfactory. The information was provided as requested and the supplemental interpretations that were not requested were appreciated.

Question 34-3b. Graphical and tabular displays of the number of second E1 borehole intrusions in 20-year increments for the first 500 years following repository closure for Replicate 1.

DOE Response (from DOE Response Package 3 (DOE RP3 2020))

Table 2 presents the number of second E1 intrusions in 20-year increments for the first 500 years following repository closure for Replicate 1, as well as the total number summed over all bins. These data are presented in the form of a histogram in Figure 14.

Table 2 Number of Second E1 Intrusions, 1,000,000 futures, First 500 years Each, CRA19 Replicate 1

Time Interval Years	Bin Count	Time Interval Years	Bin Count
0 – 20	0	260 – 280	50
20 – 40	0	280 – 300	60
40 – 60	0	300 – 320	57
60 – 80	0	320 – 340	71
80 – 100	0	340 – 360	69
100 – 120	3	360 – 380	78
120 – 140	8	380 – 400	85
140 – 160	13	400 – 420	92
160 – 180	21	420 – 440	95
180 – 200	21	440 – 460	101
200 – 220	33	460 – 480	109
220 – 240	41	480 – 500	121
240 – 260	46	**Total:**	**1,174**

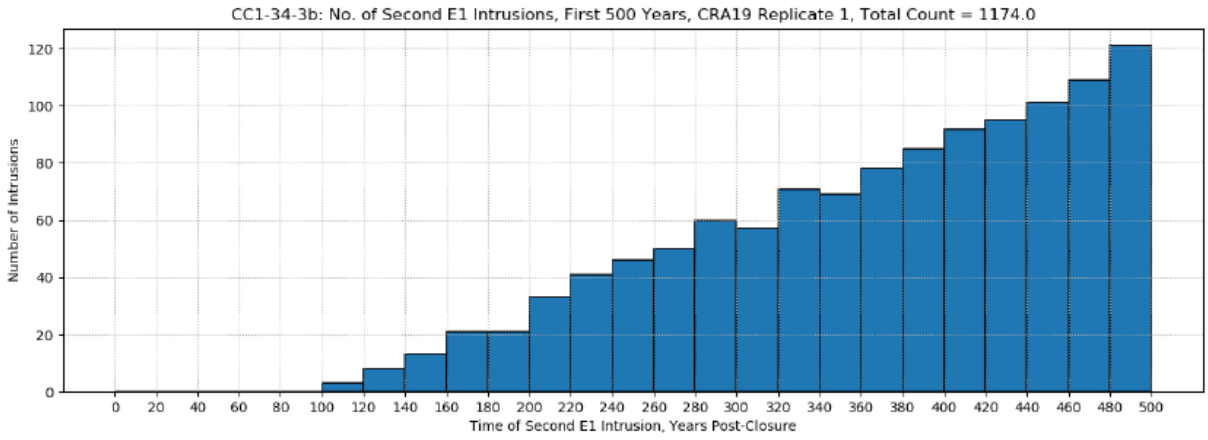

Figure 14 Number of Second E1 Intrusions, 1,000,000 futures, First 500 Years Each, CRA19 Replicate 1

EPA Evaluation of Response

The DOE response was satisfactory. The information was provided as requested.

Question 34-3c. Graphical and tabular displays of the number of first E1 borehole intrusions in 200-year increments over the 10,000-year regulatory period for Replicate 1.

DOE Response (from DOE Response Package 3 (DOE RP3 2020))

Table 3 contains the observed number of first E1 intrusions in 200-year increments over the 10,000-year regulatory period for Replicate 1, as well as the total number summed over all bins. Figure 15 is a graphical representation of this information.

Table 3 Observed Number of First E1 Intrusions, 1,000,000 Futures, 10,000 Years Each, CRA19 Replicate 1[2]

Time Interval Years	Bin Count
0 – 200	10,883
200 – 400	21,541
400 – 600	20,754
600 – 800	20,557
800 – 1,000	19,581
1,000 – 2,000	19,190
1,200 – 1,400	18,651
1,400 – 1,600	17,999
1,600 – 1,800	17,571
1,800 – 2,000	17,237
2,000 – 2,200	16,676
2,200 – 2,400	16,268
2,400 – 2,600	16,060
2,600 – 2,800	15,496
2,800 – 3,000	15,227

Time Interval Years	Bin Count
3,000 – 3,200	14,726
3,200 – 3,400	14,557
3,400 – 3,600	14,200
3,600 – 3,800	13,636
3,800 – 4,000	13,272
4,000 – 4,200	13,361
4,200 – 4,400	12,791
4,400 – 4,600	12,506
4,600 – 4,800	12,209
4,800 – 5,000	11,953
5,000 – 5,200	11,694
5,200 – 5,400	11,334
5,400 – 5,600	10,795
5,600 – 5,800	10,680
5,800 – 6,000	10,499

Time Interval Years	Bin Count
6,000 – 6,200	10,113
6,200 – 6,400	10,177
6,400 – 6,600	9,610
6,600 – 6,800	9,499
6,800 – 7,000	9,327
7,000 – 7,200	9,282
7,200 – 7,400	8,903
7,400 – 7,600	8,702
7,600 – 7,700	8,442
7,800 – 8,000	8,344
8,000 – 8,200	8,038
8,200 – 8,400	7,878
8,400 – 8,600	7,692
8,600 – 8,800	7,688
8,800 – 9,000	7,366

Time Interval Years	Bin Count
9,000 – 9,200	7,306
9,200 – 9,400	7,100
9,400 – 9,600	6,873
9,600 – 9,800	6,738
9,800 – 10,000	6,637
Total:	617,619

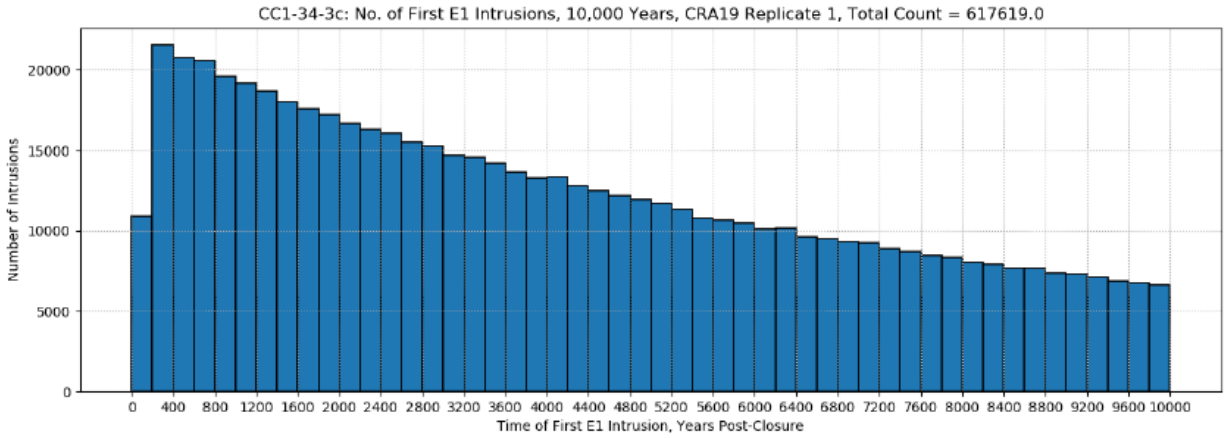

Figure 15 Number of First E1 Intrusions, 1,000,000 Futures, 10,000 Years Each, CRA19 Replicate 1[2]

Since these statistics are not typically tracked, a series of additional steps were performed to verify the accuracy of this data. There are 1,000,000 total possible futures represented by Replicate 1, but only 617,619 futures are represented as having a first E1 intrusion over the 10,000 year regulatory period (Table 3 and Figure 15).

There are two possible reasons that a future has no E1 intrusion: 1) there are no intrusions in the future that intersects a brine pocket within the excavated area; or 2) the intrusion intersects a brine pocket in the excavated area but does not have plugging pattern 2. All futures that fall into each category were first counted. 617,619 futures have at least one E1 intrusion, 287,582 futures were excluded based on selected plugging pattern, and 94,799 were excluded based on intrusions into non-excavated areas only. The sum of these three quantities is equal to the total number of futures (1,000,000).

Next, two random futures with no E1 intrusion from each category were examined to insure the accuracy of the recorded information, and no inconsistencies were found.

Additionally, a theoretical calculation was performed to verify that the data retrieved from the diagnostic output file is reasonable. Since drilling intrusions are modeled as randomly occurring at a constant mean rate, the probability that a first E1 intrusion will occur during any given time interval can be modeled by a Poisson distribution.

The probability mass function for a Poisson distribution is

$$f(k;\lambda) = \Pr(X = k) = \frac{\lambda^k e^{-\lambda}}{k!}$$

where *X* denotes the number of events in a unit time interval, specified here as one year, and the rate parameter λ is the expected number of E1 intrusions in that time interval.

Table 4 lists the parameter values used in CRA-2019 which determine the number of E1 intrusions in a given time interval.

Table 4 CRA-2019 Parameters Affecting E1 Drilling Intrusion Timing

Material	Property	Description	Units	Value
GLOBAL	LAMBDAD	Drilling rate	$km^{-2}\ yr^{-1}$	9.90×10^{-3}
REFCON	ABERM	Area of the berm at the land surface	m^2	628,500
REFCON	AREA_CH	Area occupied by contact-handled waste	m^2	111,500
REFCON	AREA_RH	Area occupied by remote-handled waste	m^2	15,760
GLOBAL	TWOPLG	Probability that a borehole uses a two-plug configuration	(-)	0.331
GLOBAL	PBRINE	Probability that a borehole encounters pressurized brine in the Castile	(-)	Cum. distribution as summarized in U.S. EPA (2017) and Zeitler (2019)

A borehole results in an E1 intrusion if the borehole is in the excavated area, has a two-plug configuration, and encounters pressurized brine. Accordingly, the rate of E1 intrusions per year is given by

$$\lambda_i = 9.9 \times 10^{-3} \times 0.331 \times \frac{628{,}500}{1{,}000{,}000} \times \frac{111{,}500 + 15{,}760}{628{,}500} \times PBRINE_i$$
$$= 4.17 \times 10^{-4} \times PBRINE_i$$

where $PBRINE_i$ is the value of GLOBAL:PBRINE for the ith vector.

The probability that a first E1 intrusion occurs in an interval [y0,1] in the ith vector is given by

$$Pr(\text{First E1 in } [y_0, y_1]; \lambda_i) = Pr(0 \text{ E1 in } [100\text{yr}, y_0]) \times Pr(1 \text{ or more E1 in } [y_0, y_1])$$
$$= f\left(0; \lambda_i \times (y_0 - 100)\right) \times \left(1 - f\left(0; \lambda_i \times (y_1 - y_0)\right)\right)$$

To verify the accuracy of the observed number of intrusions in each 200-year time interval in Table 3, the expected number of intrusions for each time interval can now be calculated; results are shown in Table 5. The total number of first E1 intrusions observed 617,619 (from Table 4) closely matches the expected number of first E1 intrusions 617,388 (from Table 5).

The expected number of futures with a given number (k) of intrusions can also be computed using the LHS sample from the CRA-2019 as

$$\sum_{i=1}^{100} 10{,}000 \times f(k; \lambda_i)$$

Table 5 Expected Number of First E1 Intrusions, 1,000,000 Futures, 10,000 Years Each, CRA19 Replicate 1[2]

Time Interval Years	Bin Count
0 – 200	10,960
200 – 400	21,476
400 – 600	20,902
600 – 800	20,345
800 – 1,000	19,800
1,000 – 2,000	19,280
1,200 – 1,400	18,773
1,400 – 1,600	18,271
1,600 – 1,800	17,797
1,800 – 2,000	17,331
2,000 – 2,200	16,880
2,200 – 2,400	16,446
2,400 – 2,600	16,014
2,600 – 2,800	15,611
2,800 – 3,000	15,207

Time Interval Years	Bin Count
3,000 – 3,200	14,822
3,200 – 3,400	14,447
3,400 – 3,600	14,082
3,600 – 3,800	13,731
3,800 – 4,000	13,387
4,000 – 4,200	13,052
4,200 – 4,400	12,725
4,400 – 4,600	12,416
4,600 – 4,800	12,099
4,800 – 5,000	11,805
5,000 – 5,200	11,524
5,200 – 5,400	11,235
5,400 – 5,600	10,974
5,600 – 5,800	10,707
5,800 – 6,000	10,451

Time Interval Years	Bin Count
6,000 – 6,200	10,204
6,200 – 6,400	9,962
6,400 – 6,600	9,725
6,600 – 6,800	9,492
6,800 – 7,000	9,268
7,000 – 7,200	9,059
7,200 – 7,400	8,848
7,400 – 7,600	8,639
7,600 – 7,700	8,441
7,800 – 8,000	8,248
8,000 – 8,200	8,063
8,200 – 8,400	7,873
8,400 – 8,600	7,705
8,600 – 8,800	7,530
8,800 – 9,000	7,353

Time Interval Years	Bin Count
9,000 – 9,200	7,199
9,200 – 9,400	7,037
9,400 – 9,600	6,879
9,600 – 9,800	6,729
9,800 – 10,000	6,584
Total:	**617,388**

These expected values can then be compared to the observed values (Table 6). By comparing the observed number of futures with no E1 intrusion (382,381) to the expected number (382,612), it can be shown that these values are consistent.

Table 6 Observed vs. Expected Number of E1 Intrusions per Future, 1,000,000 Total Futures

Number of E1 Intrusions	Expected Number of Futures	Observed Number of Futures
0	382,612	382,381
1	322,221	322,831
2	175,418	174,960
3	77,475	77,285
4	29,156	29,387
5	9,504	9,500
6	2,719	2,748
7	691	726
8	158	142
9	32	35
10	6	5

EPA Evaluation of Response

The DOE response was satisfactory. The information was provided as requested and the supplemental explanations that were not requested were appreciated and were very interesting.

Question 34-3d. Graphical and tabular displays of the number of second E1 borehole intrusions in 200-year increments over the 10,000-year regulatory period for Replicate 1.

DOE Response (from DOE Response Package 3 (DOE RP3 2020))

Table 7 contains the number of second E1 intrusions in 200-year increments over the 10,000-year regulatory period for Replicate 1, as well as the total number summed over all bins. Figure 16 is a histogram representing that same information.

Table 7 Number of Second E1 intrusions, 1,000,000 Futures, 10,000 Years Each, CRA19 Replicate 1[2]

Time Interval Years	Bin Count	Time Interval Years	Bin Count	Time Interval Years	Bin Count	Time Interval Years	Bin Count
0 – 200	66	3,000 – 3,200	5,848	6,000 – 6,200	7,355	9,000 – 9,200	7,371
200 – 400	590	3,200 – 3,400	5,829	6,200 – 6,400	7,402	9,200 – 9,400	7,165
400 – 600	1,107	3,400 – 3,600	6,107	6,400 – 6,600	7,408	9,400 – 9,600	7,175
600 – 800	1,617	3,600 – 3,800	6,327	6,600 – 6,800	7,452	9,600 – 9,800	7,148
800 – 1,000	2,148	3,800 – 4,000	6,417	6,800 – 7,000	7,421	9,800 – 10,000	7,129
1,000 – 2,000	2,539	4,000 – 4,200	6,484	7,000 – 7,200	7,342	**Total:**	**294,788**
1,200 – 1,400	2,942	4,200 – 4,400	6,827	7,200 – 7,400	7,591		
1,400 – 1,600	3,428	4,400 – 4,600	6,751	7,400 – 7,600	7,407		
1,600 – 1,800	3,699	4,600 – 4,800	7,046	7,600 – 7,700	7,528		
1,800 – 2,000	4,095	4,800 – 5,000	6,876	7,800 – 8,000	7,241		
2,000 – 2,200	4,427	5,000 – 5,200	7,142	8,000 – 8,200	7,453		
2,200 – 2,400	4,604	5,200 – 5,400	7,248	8,200 – 8,400	7,405		
2,400 – 2,600	4,864	5,400 – 5,600	7,290	8,400 – 8,600	7,317		
2,600 – 2,800	5,197	5,600 – 5,800	7,295	8,600 – 8,800	7,404		
2,800 – 3,000	5,407	5,800 – 6,000	7,387	8,800 – 9,000	7,470		

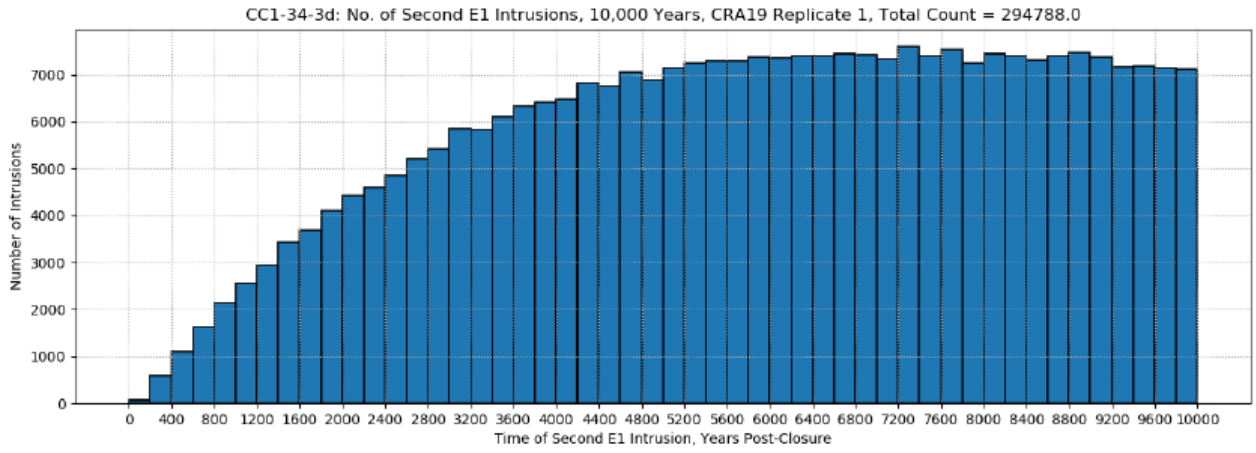

Figure 16 Number of Second E1 intrusions, 1,000,000 Futures, 10,000 Years Each, CRA19 Replicate 1[2]

A similar examination to that described in 34-3c was run to examine the number of futures with no second E1 intrusion and verify the accuracy of the presented data. It was determined that of the possible 1,000,000 futures, 382,381 have no E1 intrusion, 322,831 have only one E1 intrusion, 294,788 have more than one E1 intrusion (Table 7 and Figure 16). This information is also summarized in detail in Table 6.

EPA Evaluation of Response

The DOE response was satisfactory. The information was provided as requested and the supplemental explanations that were not requested were appreciated and were very interesting.

Question 34-3e. Graphical and tabular displays of the total number of waste area borehole intrusions per 10,000-year realization for Replicate 1.

DOE Response (from DOE Response Package 3 (DOE RP3 2020))
Table 8 contains a tabular representation of the total number of borehole intrusions into the waste area in 200-year increments for all 1,000,000 simulated futures in Replicate 1, where each future covers a 10,000-year duration. The total number of intrusions summed over all bins is presented at the end of Figure 8. Figure 17 is a histogram representing this same information. There are a total of 12,476,580 simulated intrusions across all 1,000,000 futures, which translates to approximately 12.5 borehole intrusions for a single 10,000-year future.

Table 8 Total Number of Intrusions for 1,000,000 Futures, 10,000 Years Each, CRA19 Replicate 1[2]

Time Interval Years	Bin Count
0 – 200	126,236
200 – 400	252,668
400 – 600	251,809
600 – 800	252,348
800 – 1,000	251,876
1,000 – 2,000	251,248
1,200 – 1,400	251,056
1,400 – 1,600	251,972
1,600 – 1,800	250,983
1,800 – 2,000	251,713
2,000 – 2,200	251,681
2,200 – 2,400	251,641
2,400 – 2,600	252,690
2,600 – 2,800	251,808
2,800 – 3,000	250,999

Time Interval Years	Bin Count
3,000 – 3,200	251,649
3,200 – 3,400	251,771
3,400 – 3,600	252,711
3,600 – 3,800	252,058
3,800 – 4,000	251,708
4,000 – 4,200	251,934
4,200 – 4,400	251,830
4,400 – 4,600	252,037
4,600 – 4,800	252,778
4,800 – 5,000	252,130
5,000 – 5,200	252,370
5,200 – 5,400	252,727
5,400 – 5,600	251,817
5,600 – 5,800	251,282
5,800 – 6,000	252,376

Time Interval Years	Bin Count
6,000 – 6,200	252,539
6,200 – 6,400	252,720
6,400 – 6,600	252,647
6,600 – 6,800	252,300
6,800 – 7,000	251,923
7,000 – 7,200	252,993
7,200 – 7,400	251,088
7,400 – 7,600	252,439
7,600 – 7,700	252,186
7,800 – 8,000	251,908
8,000 – 8,200	252,541
8,200 – 8,400	253,043
8,400 – 8,600	251,768
8,600 – 8,800	252,138
8,800 – 9,000	251,949

Time Interval Years	Bin Count
9,000 – 9,200	252,353
9,200 – 9,400	251,268
9,400 – 9,600	251,874
9,600 – 9,800	251,800
9,800 – 10,000	253,197
Total:	**12,476,580**

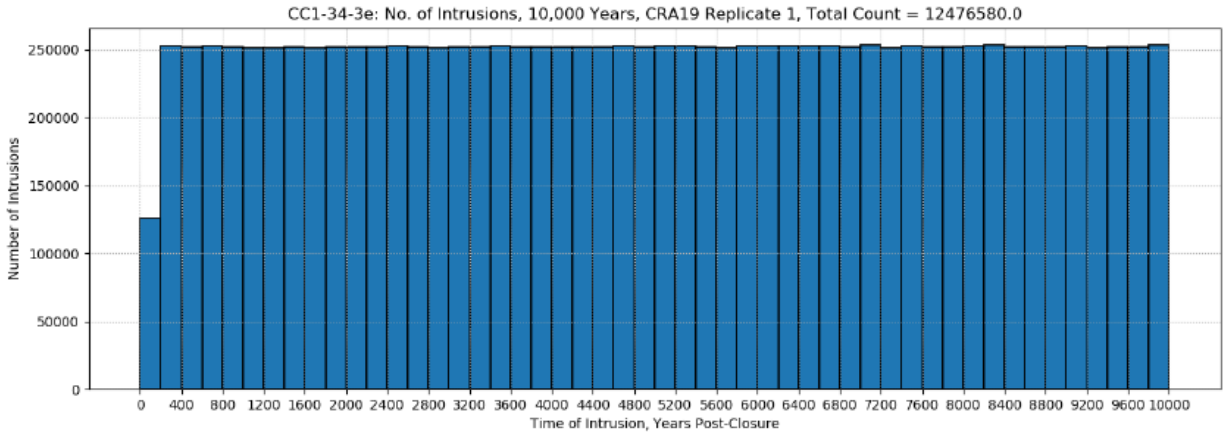

Figure 17 Total Number of Intrusions for 1,000,000 Futures, 10,000 Years Each, CRA19 Replicate 1[2]

DOE References:

U.S. Environmental Protection Agency (EPA). 2017. Probability of Encountering Castile Brine Beneath the WIPP Waste Panels Using the TDEM Block Method. June 2017. Office of Radiation and Indoor Air, Docket EPA-HQ-OAR-2014-0609-0047.

Zeitler, T.R. 2019. A Summary of EPA/DOE Defined Parameters to be implemented in the CRA-2019 PA. Sandia National Laboratories. Carlsbad, NM. ERMS 570879.

EPA Evaluation of Response

The DOE response was satisfactory. The information was provided as requested.

CC1-34-4: Panel Closure Designs

40 CFR §194.34 Results of Performance Assessments

EPA Question (from EPA Completeness Comment Package 1)

Please provide as-built descriptions and illustrations of the ROM salt and bulkhead components for each of the four panel closure systems installed between Panels 9 and 10.

DOE Response (from DOE Response Package 2 (DOE RP2 2020))

The closures installed between Panels 9 and 10 were constructed in accordance with the EPA approved Run of Mine Salt Closure Panel Closure System (EPA 2014). The installed ROMPCS consists of two standard steel ventilation bulkheads with a minimum of 100 feet of run-of-mine (ROM) salt between them, filling the drift from floor to ceiling. The panel closures were built as shown in the illustration provided below (Figure 1). The panel closures were installed in the north-south mains (E-300, E-140, W-30, and W-170) between Panels 9 and 10. Attached is the survey plat showing the location of the installed closures (Figure 2, zoom in for a clearer view).

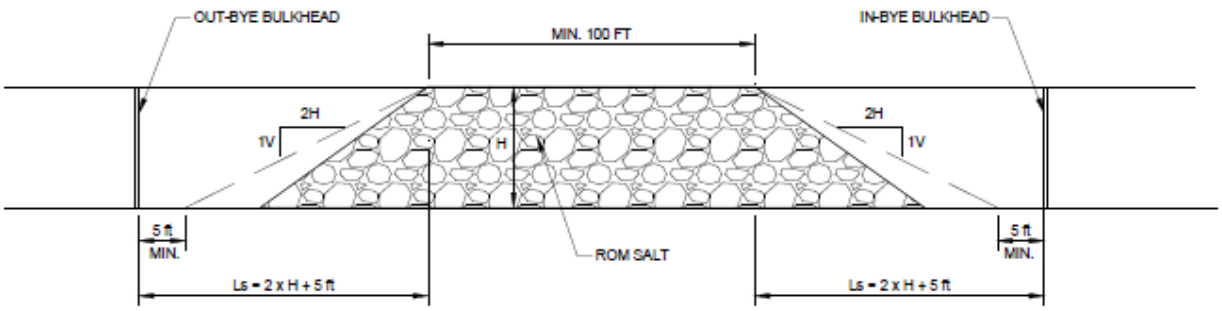

RUN-OF-MINE SALT PANEL CLOSURE SYSTEM
NOT TO SCALE

Figure 1: Run-of-Mine Salt Panel Closure System

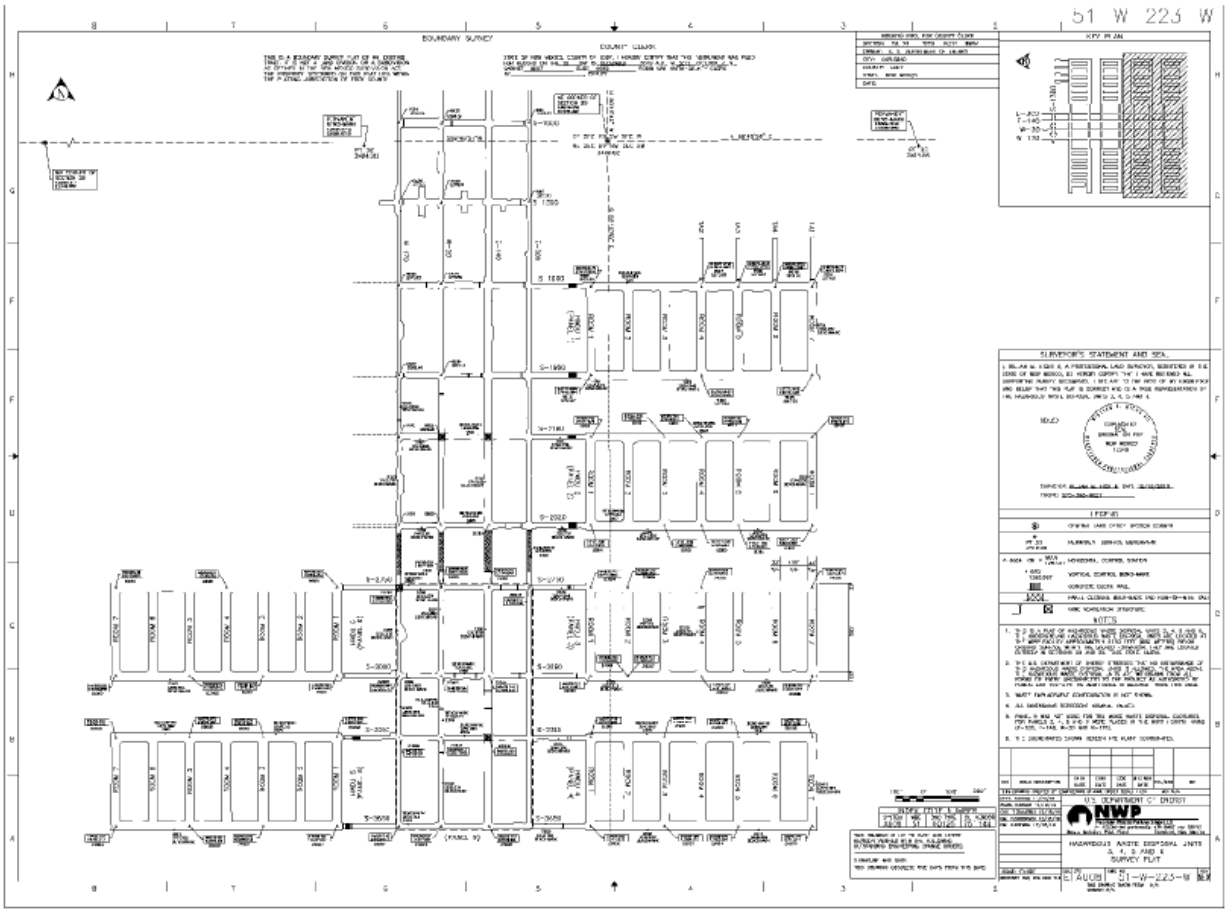

Figure 2: Survey Plat Showing Location of Installed Closures

DOE Reference

U.S. Environmental Protection Agency (EPA). 2014. Criteria for the Certification and Recertification of the Waste Isolation Pilot Plants Compliance with the Disposal Regulations; Panel Closure Redesign; Final Rule. September 30, 2014. Washington D.C., Office of Radiation and Indoor Air. EPA-HQ-OAR-2013-0684.

EPA Evaluation of Response

The DOE response was satisfactory. The information was provided as requested.

CC1-34-5: Panel Closure Designs and Construction

40 CFR §194.34 Results of Performance Assessments

EPA Question (from EPA Completeness Comment Package 1)

Please provide descriptions and illustrations of the panel closure systems planned to be installed at each of the access drifts to Panels 1, 2, 7, and 8 or identify whether the existing closure design (e.g., 100 feet of run-of-mine salt) will be used.

DOE Response (from DOE Response Package 2 (DOE RP3 2020))

For Panels 1, 2, 7 & 8, the installation of run-of-mine salt panel closures as previously described in the panel closure rulemaking (EPA 2014) are planned. No official change had been decided upon at the time of the CRA-2019 and DPA-2019.

DOE Reference

U.S. Environmental Protection Agency (EPA). 2014. Criteria for the Certification and Recertification of the Waste Isolation Pilot Plants Compliance with the Disposal Regulations; Panel Closure Redesign; Final Rule. September 30, 2014. Washington D.C., Office of Radiation and Indoor Air. EPA-HQ-OAR-2013-0684.

EPA Evaluation of Response

The DOE response was satisfactory. The information was provided as requested.

CC1-34-7 Corrections to Relative Permeability Models

40 CFR §194.34 Results of Performance Assessments

EPA Question (from EPA Completeness Comment Package 1)

Please provide the following information:

34-7a. ***Issue Summary and Assessment For Issue Affecting Model KRP = 2***

The three relative permeability issues identified by Day (2018, ERMS 570325, p. 1) were stated to affect relative permeability models KRP = 1, 2, 5, 6, 7, and 8. However, in the SPR18-002 Issue Summary and Assessment section of Day's document, none of the three issues assessed model KRP = 2. Please provide an Issue Summary and Assessment for the issue that affected model KRP = 2.

DOE Response (from DOE Response Package 2)

There is a typographical error on page 1 of the ERMS 570325 (Day 2018). As described in issue summary and assessment section of the ERMS 570325 , there was no issue found with relative permeability model KRP = 2. The first and second issues affected KRP = 1 and KRP = 8, respectively, while the third issue affected KRP = 5, 6, and 7 which was identified with the capillary pressure model KCP = 2.

34-7b. ***Explanation why Errors Affecting Model KRP Did Not Affect the Other Three Models.***

Model KRP = 2 is one of four models based on variations of the Brooks-Corey relative permeability model. The other three are KRP = 3, 4, and 12. Please explain why the errors that affected model KRP = 2 did not also affect these other three models.

DOE Response

See response for 34-7a. No issues with the variation of the Brooks-Corey relative permeability models KRP = 2, 3, 4, and 12 have been found.

34-7c. ***Results of Review of KRP = 3, 4, 11, and 12 for Errors.***

All relative permeability models except models KRP = 3, 4, 11, and 12 were reviewed by DOE and found to have errors related to capillary pressures. Were these four remaining models similarly reviewed for errors and if so, what were the findings? If they were not reviewed, please explain why not.

DOE Response

All relative permeability models were reviewed, no errors were found with models KRP = 2, 3, 4, 11, and 12.

34-7d. ***Identification and Description of Materials used in CRAs 2014 and 2019.***

For each of the relative permeability models affected by the errors identified in Day (2018, ERMS 570325), please identify and describe the materials used in PAs CRA_2014, CRA14_SEN3, CRA14_SEN4, and CRA_2019 that were assigned to those models.

DOE Response

The Performance Assessment (PA) code LHS samples a value for S_MB139:RELP_MOD with an equal probability of taking on a KRP of 1 or 4. This sampled KRP model is used for the Salado Marker Bed 138 (S_MB138), Salado anhydrite beds A and B (S_ANH_AB), and Salado Marker Bed 139 (S_MB139), so for each vector all three materials use the same KRP model. These are the only materials that use KRP = 1. This is true for all four analyses CRA-2014, CRA14_SEN3, CRA14_SEN4, and CRA-2019.

The unrestricted borehole (BH_OPEN) used KRP = 5 prior to CRA-2019. In CRA-2019 the unrestricted borehole was changed to use KRP = 11.

No materials use KRP = 6, 7, or 8 in any of the four analyses CRA-2014, CRA14_SEN3, CRA14_SEN4, and CRA-2019.

34-7e. ***Values Assigned to Properties PCT_1, PCT_EXP, and KCP for Materials Identified in CC1-34-7d***

For each of the materials and each of the PAs identified in response to Question 34-7d, please provide the values assigned to properties PCT_A, PCT_EXP, and KCP.

DOE Response

Table 1 Relative Permeability Model Parameter Values

Material	Description	RELP_MOD(KRP)	PCT_A	PCT_EXP	CAP_MOD(KCP)
S_MB139	Marker Bed 139	1,4 (50%, 50%)	0.26	-0.348	2
S_ANH_AB	Anhydrite AB	1,4 (50%, 50%)	0.26	-0.348	2
S_MB138	Marker Bed 138	1,4 (50%, 50%)	0.26	-0.348	2
BH_OPEN (CRA-2014, CRA14_SEN3, CRA14_SEN4)	Unrestricted Borehole	5	0	0	1
BH_OPEN (CRA-2019)	Unrestricted Borehole	11	0	0	1

Reference

Day, B. 2018. Impact Analysis for BRAGFLO 6.03 Software Problem Report, SPR 18-002. Sandia National Laboratories. Carlsbad, NM. ERMS 570325

EPA Evaluation of Response

The DOE response was satisfactory. The information was provided as requested and useful for understanding the permeability models in BRAGFLO.

CC1-42-1 Question regarding changes in CRA-2019 DPA and MONPAR analysis

40 CFR §194.42 Monitoring

EPA Question (from EPA Completeness Comment Package 1)

Please describe whether the changes introduced in the CRA-2019 DPA are captured in the current monitoring programs. Do the changes in the CRA-2019 DPA impact the MONPAR analysis and conclusions presented in Wagner 2018?

The Wagner 2018 reassessment of the MONPAR Analysis states that no PA changes were assessed because the CRA-2014 PA would be used as the compliance PA baseline. This document was created prior to the CRA-2019 DPA and as such, does not include this analysis.

Wagner, S.W. 2018. Reassessment of MONPAR Analysis for Use in the 2019 Compliance Recertification Application. Carlsbad, NM: Sandia National Laboratories. ERMS 569616.

DOE Response (from DOE Response Package 2)

The MONPAR reassessments are performed under SP-9-8, Monitoring Parameter Assessment per 40 CFR 194.42 (Wagner 2017). The assessment is used to determine if elements of the Waste Isolation Pilot Plant (WIPP) program that have changed since the last recertification affect

the “parameters” used in the MONPAR analysis (U.S. DOE 1996). The specific disposal system elements that are evaluated in the assessment include:

1. Monitoring Results
2. Experimental Activities
3. Performance Assessment Changes – Methodology/Parameters/Implementation
4. WIPP Operational Changes
5. Proposed changes to activities and conditions approved by EPA

The MONPAR reassessment (Wagner 2018) referenced in the CRA-2019 Section 42 was completed prior to the CRA-2019 Deferred Performance Assessment (DPA) and did not consider the potential impacts on the monitoring program due to “Performance Assessment Changes” (the third item listed above) implemented in the DPA. Wagner 2018 did evaluate the remaining four items listed above and stated, *“The conclusions of the MONPAR Analysis remain valid and its conclusions continue to be adequate for inclusion in the CRA-2019.”* The following is an evaluation of the impacts on the monitoring parameter assessment in MONPAR due to Performance Assessment Changes in the CRA-2019 DPA and was performed under SP-9-8.

The Performance Assessment (PA) changes since the CRA-2014 PA incorporated in the CRA-2019 DPA are listed in Table PA-1 and include the following:

1. Abandonment of Planned Panel Closures in Entrances to Panels, 3, 4, 5 & 6, and Abandonment of Waste in Panel 9
2. Additional Shaft and Drifts
3. Brine Radiolysis
4. Probability of Encountering Pressurized Brine during Drilling Intrusion
5. Steel Corrosion Rates
6. Waste Shear Strength
7. Colloid Enhancement Parameters
8. Hydromagnesite to Magnesite Conversion Rate
9. Iron Sulfidation
10. Northernmost Panel Closure Representation Correction
11. Drilling Rate and Plugging Pattern Probabilities
12. Waste Inventory Information
13. Radionuclide Solubility and their Uncertainties
14. Borehole Permeability Model Parameter Update
15. BRAGFLO Grid Flexibility
16. Hardware and Code Updates

Of the 16 changes listed, 10, 15 & 16 are PA modeling changes and are not applicable to monitoring parameters. Change 14 corrected a modeling error and is also not applicable to monitoring parameters. Of the remaining 12, items 4, 11 & 12 are current monitoring parameters under the Compliance Monitoring Program (COMP) and their monitoring assessments for the period since the CRA-2014 did not indicate that changes to these monitoring parameters were warranted in the annual COMPs reports. The remaining 10 items will be discussed further to determine if the impacts of these changes impact the conclusion of the original MONPAR analysis.

PA Changes 1 & 2: Changes to PA to account for the inclusion of an additional shaft and abandonment of panel closures and waste in Panel 9 were implemented through changes to the BRAGFLO grid and neighbor relationships. While model representation of these features was not assessed in the original MONPAR analysis, waste and repository induced properties were assessed. Specifically, the shaft seal system was assessed in the MONPAR analysis which determined that this system could not be monitored during the operational period and would be detrimental to performance if monitored during the post-closure period. An additional shaft would not impact the original determination. The original MONPAR analysis did not identify waste area or drift area properties as significant and were not retained for monitoring. Therefore, abandonment of planned panel closures and waste and an additional shaft would not impact the original MONPAR determination.

PA Changes 3 & 5: The PA change to include additional gas generation from brine radiolysis impacts the gas generation PA assumptions. While experimental investigations of these processes have been performed by the WIPP project and other scientific communities, no gas generating processes were identified for operational or post-closure monitoring in the MONPAR analysis. That analysis also assessed gas generation from steel corrosion (item 5) which was also not identified for monitoring.

PA Change 6: Waste shear strength was not assessed in the original MONPAR analysis. This property was determined through experimental analyses and is an important PA parameter. It is not practical to monitor during the operational phase because the properties of the waste that are used in the PA model are those of compressed and degraded waste, which will not occur until sometime after closure.

PA Change 7: Changes to the colloidal enhancement factor are discussed in the original MONPAR relating to radionuclide transport and retardation. Monitoring of this property was not justified. Specifically, MONPAR states, "*Transport* [of dissolved and colloidal radionuclides] *into the Salado or the Culebra will not occur during the active control period, thus monitoring in the operational or early post-closure periods will not provide useful information."* See also the later discussion on item 13, Radionuclide Solubility and their Uncertainties.

PA Change 8: Change to the Hydromagnesite to Magnesite Conversion Rate impacts gas generation and water balance assumptions in PA. The timeframe for this conversion cannot occur until after repository closure and potential hydration of the magnesium oxide (MgO) backfill. As such, it cannot be monitored during operations and is not possible after closure. Hydromagnesite to Magnesite Conversion rate was not analyzed in the original MONPAR and past MONPAR reassessments.

PA Change 9: Iron Sulfidation was included in gas generation assumptions in previous PAs; however, it was removed from the CRA-2019 PA. As such there is no impact on monitoring, as gas generation processes were not identified in the original MONPAR as important.

PA Change 13: Radionuclide Solubility and their Uncertainties (item 13) were included in the original MONPAR assessment of Repository Chemical Conditions. Specifically, MONPAR states, *"The closed repository will not achieve the long-term chemical conditions (brine composition, dissolved actinide concentrations, or colloidal actinide concentrations) used in performance assessment during the operational or active control periods. Therefore, monitoring the chemical conditions will not provide relevant information or verify assumptions used in performance assessment. Chemical conditions in the repository cannot be monitored after decommissioning without jeopardizing repository integrity. Thus, these parameters will not be monitored during the operational period nor during the post-closure periods."*

In addition to the assessment document in Wagner 2018, the evaluation described above determined that the "Performance Assessment Changes" incorporated in the CRA-2019 DPA do not impact the conclusions and determination of monitoring parameters documented in the original MONPAR analysis.

References

Wagner, S. W. 2017. Monitoring Parameter Assessment per 40 CFR 194.42, SP 9-8, Revision 2, Carlsbad, NM: Sandia National Laboratories. ERMS 568069

Wagner, S.W. 2018. Reassessment of MONPAR Analysis for Use in the 2019 Compliance Recertification Application. Carlsbad, NM: Sandia National Laboratories. ERMS 569616.

U.S. DOE. 1996. Title 40 CFR Part 191 Compliance Certification Application (October); Appendix MONPAR, Carlsbad, NM: Carlsbad Field Office. DOE/CAO 1996-2184

EPA Evaluation of Response

DOE response was satisfactory. The information was provided as requested and useful for understanding the relationship between MONPAR and other compliance documentation.

CC1-51/52-1 CRA-2019 changes' impact on IGP

40 CFR §194.51/52 Consideration of Protected Individual and Exposure Pathways

EPA Question (from EPA Completeness Comment Package 1)

Please provide calculations, figures, tables, and/or explanations which reflect the changes in CRA-2019 for the compliances of individual and groundwater protection requirements.

> *1. For the 2019 recertification, DOE uses the CRA-2014 compliance assessment (CRA- 2014 Appendix IGP-2014) as the baseline, instead of conducting a new compliance assessment (CRA-2019 Appendix IGP-2019).*
>
> *2. Changes in CRA-2019 PA included:*
>
> > *a. CRA-2019 PA reflects the operational decisions to not emplace panel closures in Panels 3, 4, 5, and 6, and to not emplace waste in Panel 9;*
> > *b. Enlarged BRAGFLO grid for additional Shaft and Drifts (EXP area);*
> > *c. New and updated chemical and microbial process and parameters;*
> > *d. Updates to WIPP Waste Inventory Parameters (e.g. increased Pu isotopes).*

DOE Response (from DOE Response Package 2)

In support of the CRA-2019, the U.S. Department of Energy (DOE) reviewed and updated information provided in the Compliance Certification Application (CCA) (DOE 1996) and previous Compliance Recertification Applications (CRAs) sections relating to Individual and Groundwater Protection Requirements (Section 51/52). The updated material was provided in Appendix IGP- 2019. Changes or new information pertaining to the CRA-2019 Deferred Performance Assessment (DPA) are listed in Table

PA-1 of Appendix Performance Assessment (PA). The impacts of these changes are included in the PA results and result in the following impacts on compliance with Section 51/52 requirements.

1. The CRA-2019 DPA evaluation showed that for the undisturbed performance scenario, none of the 300 modeling system realizations resulted in radionuclide concentrations greater than zero reaching the accessible environment through the anhydrite interbeds in the Salado Formation over the 10,000-year compliance period (Appendix PA-2019, Section PA-7.2). As with all previous CRAs, the CCA calculations bound the CRA-2019 results and are used to demonstrate continued compliance with the 40 CFR § 191.15(a) individual protection standard.

2. Because there were no realizations with concentrations greater than zero reaching the accessible environment, an updated evaluation of maximum potential ^{226}Ra and ^{228}Ra concentrations was unnecessary. Therefore, the PA results demonstrate continued compliance with the 40 CFR § 141.66(b) groundwater protection standard because they are below the 5-pCi/L regulatory limit.

3. For the CRA-2019 evaluation, the gross alpha particle activity, including ^{226}Ra and excluding radon and uranium at the boundary of the accessible environment, was zero. Continued compliance with the groundwater protection standard limit defined in 40 CFR § 141.66(c) of 15 pCi/L was therefore demonstrated.

EPA Evaluation of Response

The DOE response was satisfactory. The information was provided as requested to clarify documentation relating to individual and groundwater protection.

CC1-MASS-1 Definition of Conservative

WIPP Compliance Recertification Application 2019 Appendix-MASS (Modeling Assumptions)

EPA Question (from EPA Completeness Comment Package 1)

Please explain why the definition of "conservative" has fundamentally changed from previous CRA's.

In CRA-2019 Appendix MASS (p. MASS-2) the text states "The DOE has not attempted to bias the overall results of PA toward a conservative outcome. However, the DOE has chosen to use conservative assumptions where data or models are impractical to obtain, or where effects on performance are not expected to be significant enough to justify development of a more complicated model." The text further states "The designator C (conservative) indicates that the DOE considers the assumption (i.e. model inputs) may overestimate a process or effect.[1]

[1]*Conservatism in model inputs may result in lower or higher releases." In contrast, the analogous text from CRA-2014 the text states (p.MASS-12) "The designator C (conservative) indicates that the DOE considers the assumption (i.e. model inputs) may overestimate a process or effect that may contribute to releases to the accessible environment".*

DOE Response (from DOE Response Package 2)

The definition of "conservative" used to assign conservative (*C*) and reasonable (*R*) designators to the modeling assumptions in Appendix MASS has not changed from MASS-2014. However, an attempt was made in MASS-2019 to clarify that, while the *C* designation indicates that the given modeling assumption tends to overestimate risk, as measured by average releases, there is not a guarantee that a conservative assumption overestimates releases for all realizations in performance assessment calculations. Due to the interconnected nature of the process models implemented in Waste Isolation Pilot Plant (WIPP) Performance Assessment (PA), there exists the possibility that a process or effect that is considered conservative may lead to lower releases for certain combinations of input parameter values.

To clarify the text in MASS-2019, the sentence in question should be changed to the following:

The designator *C* (conservative) indicates that the DOE considers the assumption may overestimate a process or effect.[1]

1. The *C* designator indicates that the modeling assumption tends to overestimate releases averaged over uncertainties. The *C* designator does not guarantee that this is the case for all realizations in performance assessment calculations. Due to the interconnected nature of the process models implemented in WIPP PA, there exists the possibility that a process or effect that is considered conservative may lead to lower releases for certain combinations of input parameter values.

EPA Evaluation of Response

The DOE response was satisfactory. The explanation was useful and the sentence in question was clarified.

CC1-MASS-2 Identification of conservative assumptions leading to lower releases.

WIPP Compliance Recertification Application 2019 Appendix-MASS (Modeling Assumptions)

EPA Question (from EPA Completeness Comment Package 1)

Please identify the modeling assumptions classified as "conservative" in Table MASS-1 that lead to lower releases.

DOE Response (from DOE Response Package 2)

The response to comment MASS-1 above has attempted to clarify the use of the conservative (*C*) designator in MASS-2019 and point out that the overestimation of a process or effect may not lead to increased releases for all realizations of WIPP PA calculations. There are parts of WIPP PA that rely on interplay among different process models to calculate a release. A conservative process model that is overestimated will overwhelmingly tend to result in increased releases. However, the possibility exists that it may result in lower or higher releases depending on other sampled parameters; i.e., there are enough differences among the sampled realizations (vectors) that it is not always possible to predict ahead of time (prior to running PA calculations) if the overestimation will lead to increased releases for all cases considered in WIPP PA. A conservative assumption (i.e., one that may overestimate a process or effect) may lead to increased or decreased releases for different PA realizations depending on

sampled parameter values. None of the assumptions classified as "conservative" in Table MASS-1 are known to always result in lower releases. However, some of the assumptions may, under specific circumstances, result in lower releases.

One approach to investigate the degree of conservatism associated with each assumption with a *C* designator from Table MASS-1 is to perform a calculation that isolates the impact of the implementation of a given assumption for all realizations in a given compliance calculation. However, those calculations are not necessary because the overall tendency of these assumptions has already been established to lead to an overestimation of releases. Based on the interplay among WIPP PA process models, it is known that there is the potential for the implementation of some process models to result in an underestimation of releases in limited cases.

Examples of conservative assumptions that could potentially result in an underestimation of releases in some realizations (despite an overall tendency to overestimate releases) are those related to gas generation (e.g., Assumptions 33, 36, 41, 42). Those assumptions overestimate the gas generation process, overestimating the amount of gas produced in the repository. However, increased gas generation does not necessarily lead to increased releases for all realizations, since there may be realizations in which increased gas generation results in sufficient consumption of brine such that DBRs (direct brine releases) decrease—this is because DBRs are also dependent on the sampled residual brine saturation values. In those specific cases, it is possible that by increasing brine consumption and gas generation, the waste saturation will decrease below the threshold for a DBR, resulting in no direct brine release. In this way, overestimating the gas generation process may lead to decreased releases for specific realizations, despite an overall tendency to overestimate releases.

EPA Evaluation of Response

The DOE response was satisfactory. The information in combination with the previous question explained DOE's position.

CC2-34-9 Borehole Drilling Conceptual Model Clarification

40 CFR §194.34 Results of Performance Assessments

EPA Question (from EPA Completeness Comment Package 2)

Please clarify whether the conceptual model for E2 boreholes that may intersect the waste area continues to assume they are drilled in a search for natural resources below the repository horizon and are not assumed to terminate at the floor of the Waste Panel. If this conceptual model has not changed, please clarify the description of Scenario S4-BF in Day (2019, ERMS 571368, p. 36) and other similar scenarios regarding borehole termination.

> *Day (2019, ERMS 571368, p. 36) describes Scenario S4-BF (an E2 intrusion at 350 years), for example, as a "Borehole intrusion terminating at the floor of the Waste Panel…", It is EPA's understanding that the conceptual model for future E2 boreholes assumes they are drilled for the purpose of exploring for natural resources below the repository horizon. Such boreholes would therefore extend well below the floor of the waste panel and would intersect MB 139, the lower Salado, as well as deeper formations. EPA believes that the aforementioned text statement may*

be intended to CC1-GEN-1: Closure Dates describe a modeling assumption and should be distinguished as such from the underlying conceptual model.

DOE Response (from DOE Response Package 3)

Conceptually all wellbore intrusions would be in the pursuit of natural resources and extend through the lower Salado. E2 intrusions are intrusions that do not intersect a pressurized brine pocket in the Castile formation. With all intersected formations underlying the repository at hydrostatic pressure there is very little influence on repository performance from the wellbore below the repository. Therefore, a simplifying assumption is made not to model the portion of the wellbore below the repository. This simplifying assumption has not changed since the CRA-2014 PA. Day's (2019) description of E2 intrusions could be clarified by saying *"Borehole intrusion modeled as terminating at the floor of the Waste Panel…"*

Reference

Day, B. 2019a. Analysis Package for Salado Flow in the 2019 Compliance Recertification Application Performance Assessment (CRA-2019 PA). Carlsbad, NM: Sandia national Laboratories. ERMS 571368.

EPA Evaluation of Response

The DOE response was satisfactory. Clarifying information was provided.

CC2-MON-3 Seismicity and Seismic Monitoring Data

WIPP Compliance Recertification Application 2019 Appendix-MON (Monitoring)

EPA Question (from EPA Completeness Comment Package 2)

MON-1a. ***Confirmation of Earthquake Magnitude Scale***

Please confirm which earthquake magnitude scale is being used to report seismic events found in Section 2.8 "Seismic Activity in the Delaware Basin" and the corresponding Table (e.g. Table 9 for the 2018 report) in the Delaware Basin Monitoring Annual Reports that are referenced in Appendix MON, and indirectly in Appendix SCR, CRA-2019 Section 42, etc.

The data table in the Delaware Basin Monitoring Report seems to suggest a standard seismic magnitude scale is being used, but it is not specified. EPA assumes it is one of the common seismic magnitude scales (e.g. M0 moment magnitude, mb body wave magnitude, ML local or Richter magnitude, etc.) which are based on energy release and instrumental readings. Trends and comparisons of historic seismicity are 1*difficult without specifying and calibrating the scale used. The key explanation provided below the table is somewhat useful, but potentially misleading, and no reference is provided. Is seems to align intensity measures (i.e. Modified Mercalli scale (MM or MMI) intensity, or perhaps the USGS Instrumental Intensity scale) to earthquake magnitude. This conversion of earthquake magnitude in energy to damage or ground impacts is dependent on depth and distance to hypocenter, plus site characteristics. Thus, reporting both seismic intensity (based on local ground shaking and damage) and seismic magnitude together is potentially misleading and should be qualified, reportedly separately, or explained better.*

DOE Response (from DOE Response Package 5)

The Waste Isolation Pilot Plant (WIPP) Seismic Network, operated by the New Mexico Institute of Mining and Technology (NMIMT), only records and reports earthquake magnitudes within 300 km of the WIPP site using the Duration Magnitude Scale (Md). The Delaware Basin Monitoring Annual Reports (DBMAR) summarize seismic events in the Delaware Basin obtained from the NMIMT quarterly reports. Therefore, the seismic magnitudes in the DBMARs are in Md.

Reference

Litherland, M. 2020. A Report on the Seismicity of the WIPP Site for the Period October 1, 2019 through December 31, 2019. U.S. Department of Energy. DOE13-PO507726.

This reference is included in Enclosure 4.

MON-1b. ***Request for Copies of 2017 and 2018 Reports on Seismicity:***

Please provide copies of the quarterly "A Report on the Seismicity of the WIPP Site from the New Mexico for the Period ___" by the New Mexico Institute of Mining and Technology (NMIMT) for 2017 and 2018 that are data sources for the Delaware Basin Monitoring program.

DOE Response

The requested references are included in Enclosure 4.

References

Ingate, S. 2017. A Report on the Seismicity of the WIPP Site for the Period January 1, 2017 through March 31, 2017. U.S. Department of Energy. DOE13-PO506942.

Ingate, S. 2017. A Report on the Seismicity of the WIPP Site for the Period April 1, 2017 through June 30, 2017. U.S. Department of Energy. DOE13-PO506942.

Ingate, S. 2017. A Report on the Seismicity of the WIPP Site for the Period July 1, 2017 through September 30, 2017. U.S. Department of Energy. DOE13-PO506942.

Litherland, M. 2019. A Report on the Seismicity of the WIPP Site for the Period October 1, 2017 through December 31, 2017. U.S. Department of Energy. DOE13-PO507726.

Litherland, M. 2018. A Report on the Seismicity of the WIPP Site for the Period January 1, 2018 through March 31, 2018. U.S. Department of Energy. DOE13-PO507726.

Litherland, M. 2018. A Report on the Seismicity of the WIPP Site for the Period April 1, 2018 through June 30, 2018. U.S. Department of Energy. DOE13-PO507726.

Litherland, M. 2018. A Report on the Seismicity of the WIPP Site for the Period July 1, 2018 through September 30, 2018. U.S. Department of Energy. DOE13-PO507726.

Litherland, M. 2019. A Report on the Seismicity of the WIPP Site for the Period October 1, 2018 through December 31, 2018. U.S. Department of Energy. DOE13-PO507726.

MON-1c. ***Magnitude of Completeness (Mc)***

What is the magnitude of completeness (Mc) of the WIPP seismic network catalog in the WIPP region currently, and what has it been in the past, from the initial site characterization phase and through the following decades? What methods were used to estimate Mc?

DOE Response

The current magnitude of completeness (Mc) for the Waste Isolation Pilot Plant (WIPP) seismic network catalog is 1.5.

The time period from 2005 - 2019 was analyzed. Change in Mc during that 14 year time period was negligible. Mc calculations performed by the New Mexico Institute of Mining and Technology prior to 2005 and in time intervals shorter than the 14-year period are not available because they were not analyzed.

Mc is estimated using the maximum curvature technique and goodness of fit technique as described in Mignan and Woessner, 2012.

References

Mignan, A. and Woessner, J. 2012. Understanding Seismicity Catalogs and their Problems: Estimating the magnitude of completeness for earthquake catalogs, Community Online Resource for Statistical Seismicity Analysis.

This reference is included in Enclosure 4.

EPA Evaluation of Responses

The DOE response to parts a and b were satisfactory. Clarifying information was provided in the text and supporting documentation provided and/or listed. Part c was addressed, but an estimate of magnitude of completeness prior to 2005 was not provided because it apparently has not been analyzed by the operator of the WIPP seismic network, New Mexico Institute of Mining and Technology. EPA will look at earlier documentation for an estimate.

Copies of EPA Completeness Comments, DOE Responses, and EPA Evaluations Not Included in the Geochemistry or Inventory Technical Support Documents

CC1-24-1 Documentation Inconsistencies or Errors

40 CFR §194.24 Waste Characterization

EPA Question (from EPA Completeness Comment Package 1)

CC1-24-1a. ***Status of WIPP Waste Information System***

Please note that the status of the WIPP Waste Information System (WWIS) on page 24-8 of Section 194.24 is inconsistent with the WDS User's manual.

Section 24 (Waste Characterization) of the CRA-2019 states on page 24-8 that the WWIS was retired in December 2009 and replaced with the Waste Data System (WDS). The WDS User's Manual (DOE 2019, page 12) states that the WWIS is a subsystem of the WDS.

DOE Response (from DOE Response Package 1)

The following is a revision to the first two sentences of CRA-2019, Section 24.3.4. The revised text has been changed to read:

In December 2009, the WDS replaced the WIPP Waste Information System, which became a subsystem of the WDS. The WDS provides the Department of Energy (DOE) with a modern approach to process controls and data sharing as described in CRA-2014, Section 24.8.7.

This change is included in Enclosure 2, CRA-2019 Errata Tracking.

CC1-24-1b. ***Current Version of the Waste Data System User's Manual***

Please note that the cited Waste Data System User's Manual Revision 17 (USDOE, 2018b) should be updated to Revision 19 (USDOE, 2019).

In Section 194.24.3.4, DOE cites Revision 17 of the Waste Data System User's Manual (USDOE, 2018b). Revision 19 (USDOE, 2019), which predates the CRA-2019, is the most recent version.

USDOE (U.S. Department of Energy). 2018b. Waste Data System User's Manual. Revision 17 (January). Carlsbad Field Office, Carlsbad, NM. DOE/WIPP-09-3427.

USDOE (U.S. Department of Energy). 2019. Waste Data System User's Manual. Revision 19 (January 10, 2019). Carlsbad Field Office, Carlsbad, NM. DOE/WIPP-09-3427.

DOE Response

At the time of writing Section 24 of the CRA-2019, Revision 17 of the Waste Data System (WDS) User's Manual was the latest revision available. Revision 19 was released on January 10, 2019, after the CRA-2019 application was completed.

EPA Evaluation of Response

The DOE response was satisfactory. The applicable text from 1a was revised and noted in errata. For 1b, DOE explained that the manual revision occurred after CRA-2019 was completed.

CC1-GEOCHEM-1 Modify Cut-Off Date for Actinide Solubility Uncertainty Evaluation Literature Search

WIPP Compliance Recertification Application 2019 Appendix-GEOCHEM (Geochemistry)

EPA Question (from EPA Completeness Comment Package 1)

Please evaluate the effects of including actinide solubility data from reports and journal articles published between November 2011 and December 2018 on the +III and +IV actinide solubility uncertainty distributions used in the CRA-2019 PA:

Geochem-1a***.*** *Please identify all additional published +III and +IV experimental solubility data appropriate for inclusion in the uncertainty distributions using a Criterion G1 cutoff date of December 2018 and the other criteria established for selection of experimental solubility data (EPA 2017).*

Geochem-1b***.*** *If additional actinide solubility data are identified that meet the criteria, please calculate the difference values (log D) for each solubility value and provide revised uncertainty distributions for the solubilities of the +III and +IV actinides that include these additional data. DOE should also provide an assessment of the effects of the revised actinide solubility uncertainty distributions on PA results.*

Geochem-1c. *Please provide all EQ3/6 input and output files and Excel spreadsheets used to calculate the +III and +IV actinide solubility uncertainty distributions, ensuring that the log D values calculated for each experimental solubility data point are clearly identified.*

Domski (2019) performed the actinide solubility uncertainty distribution literature search using a search cut-off date of November 2011, stating that "…the CRA-2014 was limited to January 1990 to November 2011, and at EPA's direction no additional literature search was done for the CRA-2019." Alternatively, Appendix GEOCHEM states that the end date for the experimental solubility data literature search for the actinide solubility uncertainty distributions was December 18, 2018 (Page GEOCHEM-105, Criterion G-1). Including results available through calendar year 2018 in the actinide solubility uncertainty distributions is reasonable and would allow DOE to include as much data as possible while allowing time to process the data before performing the CRA-2019 PA calculations.

Assigning a fixed November 2011 data cut-off date in Criterion G1 conflicts with the 40CFR194.15(a) requirement that each CRA must include significant information not previously included in a compliance certification or recertification application. EPA expects that the cut-off date for Criterion G1 will be updated to the latest practical date for each CRA PA, including the CRA-2019 DPA.

Domski, P. S. 2019. Uncertainty Analysis of Actinide Solubilities for CRA 2019. Sandia National Laboratories, Carlsbad, New Mexico. ERMS 571179.

EPA (U.S. Environmental Protection Agency) 2017. Evaluation of the Compliance Recertification Actinide Source Term, Gas Generation, Backfill Efficacy, Water Balance and Culebra Dolomite Distribution Coefficient Values. Docket No. EPA-HQ-OAR-2014- 0609. U.S. Environmental Protection Agency. Washington, DC.

Peake, T., 2018. Status of PA Issues 2 and 3, Actinide Uncertainty Distribution and Microbial Colloids. Letter to US DOE November 20, 2018.

DOE Response (from DOE Response Package 1)

At the technical exchange in Albuquerque, New Mexico, on February 13-15, 2018, the U.S. Environmental Protection Agency (EPA) indicated that the U.S. Department of Energy (DOE) should base the +III and +IV actinide solubility uncertainty distributions for the CRA-2019 on the same selection criteria and the same experimental data that EPA identified for the SEN4 calculation (EPA, 2016). There was one exception for the experimental data: DOE recommended and EPA later concurred (Peake 2018) that the data from (Khalili et al. 1994) should be excluded from consideration.

EPA made significant changes to the experimental data for +III and +IV actinides that are the basis for the SEN4 uncertainty distributions (EPA, 2016). Given that EPA developed and approved the SEN4 approach, adding new experimental data might lead to changes that are inconsistent with the EPA's original intent for SEN4 or that might ultimately require additional performance assessment (PA) calculations.

The DOE approach is consistent with our understanding of EPA's intent, and is consistent with an email from Ingrid Rosencrantz to Russ Patterson dated October 18, 2018:

> "*Based on the questions and discussions we had at the September technical exchange, and given the time constraints DOE currently has preparing for the upcoming CRA, EPA would be willing to accept DOE's use of the criteria laid out in the SEN4 study for CRA-2019, minus the Khalili study discussed in the February exchange. If DOE chooses this approach, we will count the issue as resolved …. We would also be willing to discuss updates, changes, or new directions after CRA 2019 is complete about the uncertainty distribution for CRA-2024 and onward.*"

For CRA-2024, DOE agrees that the actinide solubility uncertainty distributions should consider all relevant data up to the data cutoff date, estimated to be January 3, 2023.

The statement on page GEOCHEM-99, Criterion G-1, regarding the end date for the literature search for experimental solubility data for the deferred PA is a typographical error; the end date will be corrected to November 2011. This change is included in Enclosure 2, CRA-2019 Errata Tracking.

References

EPA, 2016. *Reference and Data Selection for the CRA-2014 PABC Actinide Solubility Uncertainty Distributions*. September 16, 2016. ERMS 567126

Khalili, F.K., V. Symeopoulos, J.F. Chen and G.R. Choppin. 1994. *Solubility of Nd in brine.* Radiochimica Acta 66/67:51-54.

Peake, Tom, 2018. Letter from Mr. Tom Peake, Director, Center for Waste Management and Regulations, U.S. Environmental Protection Agency, to Mr. Mike Brown, Office of Environmental Protection, Carlsbad Field Office, U.S. Department of Energy. December 17, 2018.

EPA Evaluation of Response

The DOE response was initially postponed in first response, but DOE later provided a satisfactory evaluation.

CC1-GEOCHEM-2 Inaccurate Statement Regarding Sampling of Parameter BIOGENFC

WIPP Compliance Recertification Application 2019 Appendix-GEOCHEM (Geochemistry)

EPA Question (from EPA Completeness Comment Package 1)

Please confirm that the parameter WAS_AREA:BIOGENFC was sampled for the CRA-2019 PA.

Appendix GEOCHEM includes the statement that parameter BIOGENFC would be set equal to 1 for CRA 2019 (page GEOCHEM-28, lines 1-2). Appendix PA-2019 states that WAS_AREA:BIOGENFC is uniformly sampled from 0 to 1 (page SOTERM-92). Kim and Feng (2019) lists WAS_AREA:BIOGENFC as an LHS sampled parameter for the CRA- 2019 in Table 1 (page 17) and Table 4 (page 53), and also provides a summary of the sampled values in Table A.60 (pages 317-319).

Kim and Feng. 2019. Input Parameter Report for the 2019 Compliance Recertification Application Performance Assessment (CRA-2019 PA), Revision 1. Sandia National Laboratories, Carlsbad, New Mexico. ERMS 571660.

DOE Response (from DOE Response Package 1)

The parameter WAS_AREA:BIOGENFC was sampled from a uniform 0 to 1 distribution, as indicated in Appendix PA-2019. When Kim and Feng state it is a Latin Hypercube Sampling (LHS) sampled parameter, they are referring to the Performance Assessment (PA) code named LHS that samples the value.

This is a typographical error on page GEOCHEM-28 lines 1-2 in section GEOCHEM-2.4.2. The text will be corrected to read, "B_{fc} is an uncertainty factor defining the probability that microbial activity will occur. B_{fc} will be uniformly sampled from 0 to 1" for CRA-2019.

This change is included in Enclosure 2, CRA-2019 Errata Tracking.

EPA Evaluation of Response

The DOE response was satisfactory and the correct parameter values acknowledged in errata.

CC1-SOTERM-2 Incomplete Evaluation of Borate Aqueous Speciation and Solubility Data

WIPP Compliance Recertification Application 2019 Appendix-SOTERM (Actinide Chemistry Source Term)

EPA Question (from EPA Completeness Comment Package 1)

Please provide a summary and review of all available WIPP-relevant borate aqueous speciation and solubility data published through December 2018. As part of the review, please include an evaluation of the significance of the available data for modeling predictions of WIPP repository brine chemistry.

Appendix SOTERM, Section 5.8.2 discusses investigations of the potential interactions of borate and tetraborate with An(III) species (Borkowski et al. 2010, Hinz et al. 2015) and Section SOTERM-5.5.1.3 addresses investigations related to the role of borate in aqueous U(VI) aqueous speciation (Lucchini et al. 2013a, 2013b). Additional borate aqueous speciation and solubility data that may be relevant to WIPP have been published, including the citations listed below, but these publications were not reviewed in Appendix SOTERM. Because of the 40 CFR194.15(a) requirement that each CRA must include significant information not previously included in a compliance certification or recertification application, all such data must be addressed in the CRA-2019, including the potential implications of these investigations for modeling predictions of WIPP repository brine chemistry.

Borkowski, M., M. Richmann, D. T. Reed, and Y. Xiong. 2010. Complexation of Nd(III)with Tetraborate Ion and Its Effect on Actinide(III) Solubility in WIPP Brine. Radiochimica Acta. 98:577-582.

Hinz, K., M. Altmaier, X. Gaona, T. Rabung, D. Schild, M. Richmann, D. Reed, E. Alekseev, and H. Geckeis. 2015. Interaction of Nd(III) and Cm(III) with Borate in Dilute to Concentrated Alkaline NaCl, MgCl2, and CaCl2 Solutions: Solubility and TRLFS Studies. New Journal of Chemistry 39:1-30.

Hinz, K., D. Fellhauer, X. Gaona, M. Vespa, K. Dardenne, D. Schild, T. Yokosawa, M.A. Silver, D.T. Reed, T.E. Albrecht-Schmitt, M. Altmaier, and H. Geckeis. 2020. Interaction of Np(V) with borate in alkaline, dilute-to-concentrated, NaCl and MgCl2 solutions.

Lucchini, J.-F., M.K. Richmann, M. Borkowski. 2013a. Uranium (VI) Solubility in WIPP Brine. Los Alamos National Laboratory; Carlsbad, NM. LCO-ACP-14. LA-UR-13-20786.

Lucchini, J.-F., M. Borkowski, M.K. Richmann, and D.T. Reed. 2013b. Uranium(VI) Solubility in Carbonate-Free WIPP Brine. Radiochimica Acta 101: 391-398.

Schott, J., J. Kretzschmar, M. Acker, S. Eidner, M.U. Kumke, B. Drobot, A. Barkleit, S. Taut, V. Brendler and T. Stumpf. 2014. Formation of a Eu(III) borate solid species from a weak Eu(III) borate complex in aqueous solution. Dalton Transactions 43:11516-11528.

Xiong, Y.L. 2015. Modeling Equilibrium Constant for AmHB4O7 2+ by reevaluation of the Nd(III) data for NdHB4O7 2+, and its Associated Pitzer Parameters to be Consistent with the WIPP Thermodynamic Model. Sandia National Laboratories, Carlsbad, NM, ERMS 564857.

Xiong, Y. 2017a. Nd(III)/Am(III) interactions with borate in NaCl solutions: speciation and solubility as a function of pHm. ABC-Salt Workshop V, March 26-29, 2017, Ruidoso, New Mexico.

Xiong, Y. 2017b. Solution chemistry for actinide borate species to high ionic strengths: equilibrium constants for AmHB4O7 2+ and AmB9O13(OH)4(cr) and their importance to nuclear

waste management. Scientific Basis for Nuclear Waste Management XL, Vol.2:741-746, Materials Research Society (MRS) Fall Meeting, November 27-December 2, 2016, Boston, Massachusetts.

Xiong, Y., L. Kirkes, T. Westfall and T. Olivas. 2011. Experimental determination of solubilities of sodium tetraborate (borax) in NaCl solutions to high ionic strengths, and thermodynamics of NaB(OH)4(aq).

Xiong, Y.L., L. Kirkes and T. Westfall. 2013. Experimental determination of solubilities of sodium tetraborate (borax) in NaCl solutions, and a thermodynamic model for the Na-B(OH)3-Cl-SO4 system to high-ionic strengths at 25ºC. American Mineralogist 98:2030-2036.

Xiong, Y., Kirkes, C. Marrs and J. Knox. 2017a. Nd(III)/Am(III) Interactions with borate: experimental investigations of Nd(OH)3(micro c) solubility in NaCl solutions in equilibrium with borax. 6th East Asia Forum on Radwaste Management, November 27-29, 2017, Osaka Japan.

Xiong, Y., L. Kirkes, J. Knox, and C. Marrs. 2017b. Experimental determination of solubilities of sodium polyborates in $MgCl_2$ solutions: solubility constant of di-sodium hexaborate tetrahydrate, and implications for diagenetic formation of ameghinite. The Canadian Mineralogist 55:1001-1008.

Xiong, Y., L. Kirkes, and T. Westfall. 2018a. Experimental determination of solubilities of brucite [$Mg(OH)_2$(cr)] in Na_2SO_4 solutions with borate to high ionic strengths:interactions of $MgB(OH)_4^+$ with Na_2SO_4. Journal of Solution Chemistry 47:595-610.

Xiong, Y., L. Kirkes, T. Westfall, J. Knox, C. Marrs and H. Burton. 2018b. A Pitzer Model for Lead Oxide Solubilities in the Presence of Borate to High Ionic Strength Journal of Solution Chemistry 47:1905-1925.

Xiong, Y., L. Kirkes, J. Knox, C. Marrs and H. Burton. 2018c. Experimental determination of stability constant of ferrous iron borate complex [$FeB(OH)_4^+$] at 25ºC from solubility measurements: implications for transport of iron in reducing environments. Chemical Geology 493:16-23.

Xiong, Y., L. Kirkes, J. Knox, C. Marrs and H. Burton. 2018d. Experimental determination of solubilities of magnesium borates: solubility of boracite [$Mg_3B_7O_{13}Cl$(cr)] and aksaite [$MgB_6O_7(OH)_6 \cdot 2H_2O$(cr). Chemical Geology 483:254-260.

DOE Response (from DOE Response Package 6)

The Environmental Protection Agency (EPA) is correct in pointing out that the subject of borate complexation is not discussed in Appendix SOTERM as a stand-alone section. The various impacts of borate on actinide speciation were however discussed in the individual actinide Sections. Lucchini et at. (2013 a and b) were discussed in SOTERM 5.5.1 (Uranium Chemistry). Hinz et al. (2015) and Borkowski et al. (2009; 2010) were discussed in SOTERM 5.8.2 (Americium and Curium Chemistry). A short discussion of the status of the WIPP borate model was given in Appendix GEOCHEM, Section GEOCHEM 3.2.6. A broader more comprehensive discussion of the borate issue is provided in this response. The status of

this chemistry, based on current literature publications and WIPP-relevant research through May 2020, is also summarized.

Borate, which has a relatively complex chemistry, is indigenous to WIPP brine and is present at concentrations that range from 62 to 186 mM (Lucchini et al., 2013c; CRA-2014, Appendix SOTERM, Table SOTERM-4). There is no predicted impact on this concentration due to TRU waste emplacement. The polyborate species that predominate at the higher borate concentrations can form complexes with An(III), An(V) and An(VI) actinides under WIPP-relevant conditions. This overall chemistry is relatively complex and continues to be the subject of ongoing studies within the WIPP project.

Overview of Borate chemistry

The Department of Energy's (DOE's) position on borate speciation in the WIPP was clarified in CRA-2014 (See CRA-2014, DOE response to EPA question 3-C-2 entitled "Boron Species in WIPP Brine"). The borate species that are potentially present in WIPP, based on the speciation scheme developed by Anderson et al. (1964), are given below. The overall speciation diagram for these species is given in Figure 1. This predicts the tetraborate species to be predominant in the pH range (pH ~ 8-10) and $[B]_{total}$ ~ 160 mM of interest to the WIPP.

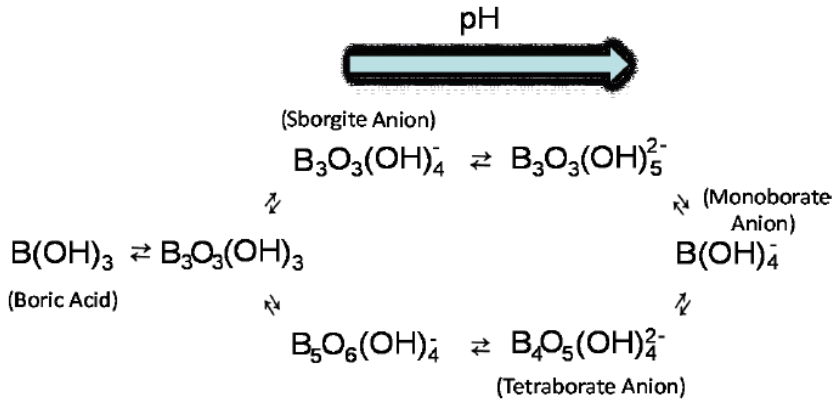

This borate chemistry was extended to high ionic-strength Na-K-Ca-Mg-H-Cl-SO_4-CO_3 brine systems (up to I ~ 14 M) in a study of borate mineral equilibria in Searles Lake (Felmy and Weare, 1986). The important role of polyborates, in particular the tri ($B_3O_3(OH)^-$) and tetra ($B_4O_5(OH)^{2-}$) borate species in the aqueous speciation was affirmed. A set of Pitzer interaction parameters to describe this chemistry were also developed (see Tables 3 and 4 in Felmy and Weare, 1986). These remain the most accepted interaction parameters for this complex aqueous system.

WIPP-specific data appear to confirm the importance of polyborate species and, in general, this speciation scheme. The key borate species, with respect to impact on actinide complexation, was proposed to be the tetraborate species (Borkowski et al., 2009; 2010). This opinion was based on the following observations and evidence:

- The predominance scheme, as shown in Figure 1, and the expectation that the di-anion is the strongest complexant.
- The correlation of the borate complexation effect and pH dependency with what is observed in the speciation/solubility of the An(III) and An(V) actinides (see later discussion) – this mirrors the speciation of tetraborate in that the impacts occur between pC_{H^+} 8 and 10.

- A tetraborate solid phase, regardless of the way in which borate was introduced to the brine, was evaporatively precipitated under WIPP-relevant conditions and identified by X-ray diffraction (XRD).

Overall, however, there remains a significant amount of uncertainty about the borate speciation and the resolution of this chemistry remains an obstacle to the development of a comprehensive actinide-borate WIPP-relevant model.

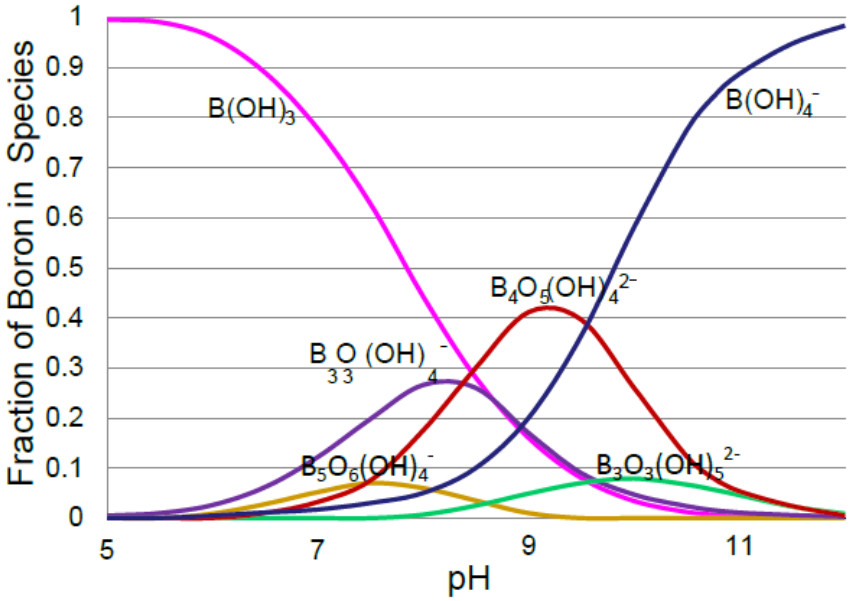

Figure 2 Speciation of borate species as a function of pH (Anderson et al., 1964). This shows the tetraborate ($B_4O_5(OH)_4^{2-}$) species to predominate at pH ~ 9 when calculated for a total [B] = 160 mM.

Impacts of Borate on Actinide Speciation

The potential impact of borate on metal speciation and, more importantly for the WIPP project, actinide/analog speciation was not recognized until the WIPP-relevant studies on neodymium solubility were performed in the early 2000s (Borkowski et al., 2009; 2010). These studies identified a relatively small (~ factor of 3) increase in solubility in simulated WIPP brine due to borate complexation. This has since been shown to be due to the formation of metastable polyborate (presumably tetraborate) complexation that affirms the key role of polyborates established in the Felmy and Weare 1986 study. The effect of tetraborate was observed at moderately high pH (pC_{H+} = 8.5-9.5) and in many ways mirrors the pH dependencies often associated with carbonate complexation. Since the neodymium study (Borkowski et. al., 2009; 2010), it has also been shown that tetraborate impacts Np(V) and U(VI)/Pu(VI) speciation. Additionally, many actinide borate solid phases have been synthesized by Albrecht-Schmitt's group at Florida State University (FSU). These FSU results were reviewed elsewhere: An(III) borate phases in Polinski et al. (2012); and their overall progress in understanding actinide borate chemistry in Wang et al. (2011).

An(III)-Borate Speciation

The complexation of An(III) with borate only occurs at high borate concentration (> 100 mM) where polyborate species are predominant (see Figure SOTERM 1). In Borkowski et al. (2009; 2010) the tetraborate species was proposed as the likely complexant according to the following:

$$Nd^{3+} + HB_4O_7^{1-} \leftrightarrow NdHB_4O_7^{2+} \quad (1)$$

In hindsight, this reaction should have been written as a combination of the following two reactions:

$$Nd^{3+} + B_4O_5(OH)_4^{2-} \leftrightarrow Nd\,B_4O_5(OH)_4^{1+} \quad (2)$$
$$Nd3+ + B_3O_3(OH)_5^{2-} \leftrightarrow Nd\,B_3O_3(OH)_5^{1+} \quad (3)$$

Pitzer interaction parameters were also established in sodium chloride media. These analyses were based on solubility/equilibrium measurements made in long-term studies performed in WIPP brine (Borkowski et al., 2009; CRA-2014, Appendix SOTERM, Section 3.7).

These initial results were extended in two areas. First, low pH (pH <6) solubility studies at I ~ 0.1 M were performed with Eu(III) as the An(III) analog (Schott et al., 2014). The monoborate complex was confirmed to be fairly weak (Log [□11] ~ 2-3) with a relatively small effect on the aqueous speciation. A borate phase, however, was formed when polyborate species were known to be present at high borate concentrations. The speciation proposed by the authors, based on time resolved laser-induced fluorescence (TRLFS), was tri- and penta-borate Eu complexes and the solid phase was shown to consist of penta-borate units that were XRD amorphous. A follow-up study using organoborates was performed (Schott et al., 2015) to evaluate the structural relationships on the borate complex. This study showed that the complex was not greatly influenced by the functional group present. These studies together confirm the importance of polyborates, albeit at low pH, and were the first to note the presence of a borate phase as the solubility-controlling phase.

Second and more relevant to the conditions expected in the WIPP, is the solubility and speciation study (Hinz et al., 2015) in NaCl, $MgCl_2$ and $CaCl_2$ simplified brines. This was done collaboratively between the WIPP project and the Institute for Nuclear Waste Disposal (INE) and established the solubility of neodymium, as the An(III) analog, from over and under saturation at moderately high pH as a function of ionic strength. These data were supported by Cm(III) TRLFS experiments to interrogate the speciation and the presence of two complexes at high borate concentration were proposed based on these data. At low borate concentration, where the mono-borate species predominated, there was essentially no effect of borate on the solubility meaning that the borate complex did not outcompete hydrolysis. At high borate concentrations, however, phase alteration of the starting amorphous neodymium hydroxide phase to a borate phase was noted. This borate phase formed on the surface of the hydroxide starting material and led to a 1-2 order of magnitude decrease in solubility (even with the hydroxide phase present). All the phases formed under these conditions were XRD amorphous. These results were believed to be consistent with the Felmy/Weare Pitzer speciation model where the tri- and tetra-borate complexes formed at high borate concentrations accounted for the speciation and subsequent solubility-controlling phase formation.

An(IV)-Borate Speciation

There has been no effect of borate speciation on the An(IV) system observed or reported in the literature. For this oxidation state, hydrolysis likely predominates under all WIPP-relevant conditions. The difference between this oxidation state and the An(III), An(V) and An(VI) oxidation state is best

explained by the relative strength of borate complexation vs. the much stronger hydrolytic tendencies toward complexation/precipitation.

An(V)-Borate Speciation

There are significant but relatively new results on the effects of borate complexation on the solubility and speciation of An(V) under WIPP-relevant conditions. Although the complexation of Np(V) with borate species has been informally discussed since CRA-2014, the first publication of these data was by Hinz et al. (2020) which is the result of a collaborative effort between the WIPP project and INE (Germany). In this study, the solubility of Np(V) was established from over and under saturation across a moderately high pH range (7-10), in dilute to concentrated NaCl and $MgCl_2$ systems, and as a function of total borate concentration. There are a number of highly relevant results reported:

At low borate concentration (~ 0.04 M), where the mono-borate species would predominate, no effect of borate on the solubility of NpO_2OH (am) was observed.

- At high total borate concentrations (~ 0.16 M), in contrast, there were many effects noted:
    - In 5 M NaCl, there was a rapid (~ 2 weeks) transformation of the Np amorphous phase to a crystalline borate solubility-controlling phase (white-greyish color) that was proposed to be $NpO_2[B_5O_6(OH)_4].2NaOH$. This resulted in a 3-4 order of magnitude decrease in the observed neptunium solubility.
    - In 0.25 M $MgCl_2$, a similar precipitated phase was noted that was proposed to be $NpO_2[B_5O_6(OH)_4].3Mg(OH)_2$. The precipitate was not observed at higher magnesium chloride concentrations due to the stabilization against precipitation by the Mgborate complexes formed. This also explains the slow formation of borate phases in high magnesium WIPP brines.
    - Borate complexation was noted in the absorption spectra but these were shown to be complex and could not be de-convoluted meaningfully.

These data, taken as a whole, are very analogous to the results discussed for the An(III)-borate systems where the effects of borate complexation were also shown to be a result of the polyborate species and associated chemistry that is typically only observed at high borate concentrations (> 0.1 M) and moderately high pH. Most importantly for the WIPP project, the presence of these species led to the formation of borate-containing phases that significantly decreased the solubility of Np(V).

An(VI)-Borate Speciation

The An(VI) oxidation state, primarily associated with U(VI) in WIPP PA, is also known to form complexes with borate. A weak complex with U(VI) was noted in Lucchini et al. (2013 a and b). Two borate species were also noted in absorption spectra of Pu(VI) (Reed, 2020). The effects of borate on this oxidation state, however, have not been systematically investigated. Similar trends to those observed for both the An(III) and An(V) systems are likely, but this needs to be confirmed under WIPP-relevant conditions.

Status of model development

The WIPP does not currently have a borate model that accounts for its impact on actinide speciation and solubility (CRA-2019, Appendix GEOCHEM, Section 3.2.6). A number of studies were, however, completed to construct a Pitzer database in WIPP-relevant brine systems. The ionic strength

dependency of borate speciation in NaCl (Xiong et al., 2011; Xiong et al., 2013) and magnesium systems (Xiong et al., 2017a; Xiong et al., 2018 a and b) were re-evaluated. This was extended to determine the interaction parameters in the presence of sulfate (Xiong et al., 2018a). The interaction parameters with Fe^{2+} (Xiong et al., 2018c) and Pb^{2+} (Xiong et al., 2018d) metals were also established. Lastly, the An(III)-borate interaction parameters were also investigated by the reevaluation of the Nd^{3+} data (Xiong, 2015; Xiong 2017 a and b). These many data obtained are not yet fully evaluated by the WIPP project.

WIPP-relevant data since CRA-2014

There has been much progress in the understanding of the role of borate and the Pitzer modeling of borate interactions since the CRA-2014. A number of key brine-chemistry interaction parameters were established. The Pitzer parameters for the An(III) actinide system were re-evaluated. Lastly, the WIPP project worked collaboratively with INE to perform longterm studies using Nd and Cm in simplified brines and at variable borate concentrations and ionic strengths.

The experimental studies, in particular, provide key and critical input to the understanding the role of borate under WIPP-relevant conditions. The important role of polyborates was confirmed. Perhaps more importantly, the polyborates led to the formation of solubility controlling phases that are 2-3 orders of magnitude lower than the comparable amorphous hydroxide solids. This phase formation was always seen in low-magnesium simplified brines. Even in high magnesium systems, the polyborates are either tied up as a magnesium complex or available to form precipitates. This positive effect on the mobile concentration of the actinides makes the understanding of borate and the completion of a comprehensive model less critical and is an added conservatism to an already very conservative model.

References

References with hyperlinks were provided in prior CRAs. The remainder of the reference documents will be provided in Enclosure 4 or as otherwise noted.

Anderson, J., E. Eyring and M. Whittaker. 1964. Temperature Jump Rate Studies of Polyborate Formation in Aqueous Boric Acid. The Journal of Physical Chemistry, (68) pp. 1128-1132.

Borkowski, M. J-F. Lucchini, M. Richmann and D. Reed. 2009. Actinide (III) Solubility in WIPP Brine: Data Summary and Recommendations. Los Alamos, NM: Los Alamos National Laboratory. Report LA-14360.

Borkowski, M., M. Richmann, D. Reed and Y. Xiong. 2010. Complexation of Nd(III) with Tetraborate Ion and Its Effect on Actinide(III) Solubility in WIPP Brine. Radiochimica Acta 98:577-582.

Felmy, A. and J. Weare. 1986. The Prediction of Borate Mineral Equilibria in Natural Waters: Application to Searles Lake, California. Geochimica et Cosmochimica Acta (50), pp. 2771-2783.

Hinz, K., M. Altmaier, X. Gaona, T. Rabung, D. Schild, M. Richmann, D. Reed, E. Alekseev and H. Geckeis. 2015. Interaction of Nd(III) and Cm(III) with Borate in Dilute to Concentrated Alkaline NaCl, $MgCl_2$ and $CaCl_2$ Solutions: Solubility and TRLFS Studies. New Journal of Chemistry (39), pp. 849-859.

Hinz, K., D. Fellhauer, X. Gaona, M. Vespa, K. Dardenne, D. Schild, T. Yokosawa, M. Silver, D. Reed, T. Albrecht-Schmitt, M. Altmaier and H. Geckeis. 2020. Interaction of Np(V) with borate in alkaline, dilute-to-concentrated, NaCl and $MgCl_2$ solutions. Dalton Transactions (49) 1570- 1582.

Lucchini, J.-F., M. Richmann, M. Borkowski. 2013a. Uranium (VI) Solubility in WIPP Brine. Los Alamos National Laboratory; Carlsbad, NM. LCO-ACP-14. LA-UR-13-20786.

Lucchini, J.-F., M. Borkowski, M. Richmann, and D. Reed. 2013b. Uranium(VI) Solubility in Carbonate-Free WIPP Brine. Radiochimica Acta 101: 391-398.

Lucchini, J.-F., M. Borkowski, H. Khaing, M. Richmann, J. Swanson, K. Simmons and D. Reed. 2013c. WIPP Actinide-Relevant Brine Chemistry. LCO-ACP-15, LANL\ACRSP Report. Los Alamos National Laboratory, Los Alamos, NM. LA-UR 13-20620.

Polinski, M., S. Wang, E. Alekseev, W. Depmeier, G. Liu, R. Haire and T. Albrecht-Schmitt. 2012. Curium (III) Borate Shows Coordination Environments of Both Plutonium(III) and Americium(III) Borates. Angewandte (124), pp. 1905-1908.

Reed, D. 2020. Complexation of Np(V) and Pu(VI) with Borate, Los Alamos – Carlsbad Operations, Carlsbad NM. Los Alamos National Laboratory Report LA-UR-2020.

Schott, J., J. Kretzchmar, M. Acker, S. Eidner, M. Kumke, B. Drobot, A. Barkleit, S. Taut, V. Brendler and T. Stumpf. 2014. Formation of a Eu(III) Borate Solid Species from a Weak Eu(III) Borate Complex in Aqueous Solution. Dalton Trans (43), pp. 11516-11528.

Schott, J., J. Kretzchmar, S. Tsushima, B. Drobot, M. Acker, A. Barkleit, S. Taut, V. Brendler and T. Stumpf. 2015. The Interaction of Eu(III) with organoborates – a further Approach to Understand the Complexation in the An/Ln(III)-Borate System. Dalton Trans (44), pp. 11095- 11108.

Wang, S., E. Alekseev, W. Depmeier and T. Albrecht-Schmitt. 2011. Recent Progress in Actinide Borate Chemistry. Chemical Communications (47), pp. 10874-10885.

Xiong, Y. 2015. Modeling Equilibrium Constant for $AmHB_4O^{2+}$ by reevaluation of the Nd(III) data for $NdHB_4O^{2+}$, and its Associated Pitzer Parameters to be Consistent with the WIPP Thermodynamic Model. Sandia National Laboratories, Carlsbad, NM. ERMS 564857.

Xiong, Y. 2017a. Nd(III)/Am(III) interactions with borate in NaCl solutions: speciation and solubility as a function of pH_m. ABC-Salt Workshop V, March 26-29, 2017. Ruidoso, New Mexico.

Xiong, Y. 2017b. Solution chemistry for actinide borate species to high ionic strengths: equilibrium constants for $AmHB_4O^{2+}$ and AmB O (OH) (cr) and their importance to nuclear waste management. Materials Research Society (MRS) Fall Meeting, November 27-December 2, 2016, Boston, Massachusetts. Scientific Basis for Nuclear Waste Management XL, Vol.2:741- 746.

Xiong, Y., L. Kirkes, T. Westfall and T. Olivas. 2011. Experimental determination of solubilities of sodium tetraborate (borax) in NaCl solutions to high ionic strengths, and thermodynamics of $NaB(OH)_4(aq)$.

Xiong, Y., L. Kirkes and T. Westfall. 2013. Experimental Determination of Solubility of Sodium Tetraborate (borax) in NaCl solutions and a Thermodynamic Model for the $Na\text{-}B(OH)_3\text{-}Cl\text{-}SO_4$ System to High-Ionic Strength at 25°C. American Mineralogist (98), pp. 2030-2036.

Xiong, Y., Kirkes, C. Marrs and J. Knox. 2017a. Nd(III)/Am(III) Interactions with borate: experimental investigations of $Nd(OH)_3$(micro c) solubility in NaCl solutions in equilibrium with borax. 6th East Asia Forum on Radwaste Management, November 27-29, 2017, Osaka, Japan.

Xiong, Y., L. Kirkes, J. Knox, and C. Marrs. 2017b. Experimental determination of solubilities of sodium polyborates in $MgCl_2$ solutions: solubility constant of di-sodium hexaborate tetrahydrate, and implications for diagenetic formation of ameghinite. The Canadian Mineralogist 55:1001-1008.

Xiong, Y., L. Kirkes, and T. Westfall. 2018a. Experimental determination of solubilities of brucite [$Mg(OH)_2$(cr)] in Na_2SO_4 solutions with borate to high ionic strengths:interactions of $MgB(OH)^{1+}$ with Na_2SO_4. Journal of Solution Chemistry 47:595-610.

Xiong, Y., L. Kirkes, J. Knox, C. Marrs and H. Burton. 2018b. Experimental determination of solubilities of magnesium borates: solubility of boracite [$Mg_3B_7O_{13}Cl$(cr)] and aksaite [$MgB_6O_7(OH)_6{\cdot}2H_2O$(cr). Chemical Geology 483:254-260.

Xiong, Y., L. Kirkes, J. Knox, C. Marrs and H. Burton. 2018c. Experimental determination of stability constant of ferrous iron borate complex [$FeB(OH)_4^{1+}$] at 25ºC from solubility measurements: implications for transport of iron in reducing environments. Chemical Geology 493:16-23.

Xiong, Y., L. Kirkes, T. Westfall, J. Knox, C. Marrs and H. Burton. 2018d. A Pitzer Model for Lead Oxide Solubilities in the Presence of Borate to High Ionic Strength. Journal of Solution Chemistry 47:1905-1925.

EPA Evaluation of Response

The DOE response was satisfactory. The information was provided as requested.

CC1-SOTERM-3 Incomplete Evaluation of Am(III) Aqueous Speciation and Solubility Data

WIPP Compliance Recertification Application 2019 Appendix-SOTERM (Actinide Chemistry Source Term)

EPA Question (from EPA Completeness Comment Package 1)

Please provide a summary and review of all available WIPP-relevant Am(III)/Nd(III)/Cm(III) aqueous speciation and solubility data published through December 2018, including Xiong et al. (2017) and Kim et al. (2018). As part of this review, please evaluate the significance of all available data for modeling predictions of WIPP repository brine chemistry.

> *Because of the 40 CFR 194.15(a) requirement that each CRA must include significant information not previously included in a compliance certification or recertification application, all such data must be addressed in the CRA-2019. Although much of the available aqueous speciation and solubility data for the +III actinides are discussed in Appendix SOTERM, Section SOTERM-5.8, this discussion is incomplete because it omits investigations by Xiong et al. (2017) and Kim et al. (2018). The review also is incomplete because it does not address whether data published since the last revision of the Am(III) aqueous speciation and solubility data in the EQ3/6 database (Giambalvo 2002a) will have significant implications for modeling predictions of WIPP repository brine chemistry.*

Giambalvo, E.R. 2002a. Recommended Parameter Values for Modeling An(III)Solubility in WIPP Brines. Memorandum to L.H. Brush, Sandia National Laboratories, Carlsbad, New Mexico. ERMS 522982.

Kim, H.-K., S. Choi, E.C. Jung, H.-R. Cho, J.I. Yun and W. Cha. 2018. TRLFS study of hydrolyzed Eu(III) species. Journal of Luminescence 202:469-474.

Xiong, Y, L. Kirkes and C. Marrs. 2017. Long-Term experimental determination of solubilities of micro-crystalline Nd(III) hydroxide in high ionic strength solutions: applications to nuclear waste management. Aquatic Geochemistry 23:359–375.

DOE Response (from DOE Response Package SOTERM-3 (5/20/21))

The U.S. Department of Energy (DOE) understood by this comment that the U.S. Environmental Protection Agency (EPA) was requesting both the inclusion of the specific two papers cited in the comment (Xiong et al., 2017; Kim et al., 2018) to the Compliance Recertification Application (CRA)-2019 documentation as well as a general summary of the key data generated since the Giambalvo 2002 description of the Waste Isolation Pilot Plant (WIPP) An(III) model. The An(III) model was discussed in the CRA-2019 documentation provided (Appendix SOTERM, Section 6.5.1; Appendix GEOCHEM, Sections 4.2.1 and 4.3.1).

A review of the two papers cited by the EPA and a summary of key new data since the Giambalvo 2002 memos are provided in this response.

Review and Comment on the two EPA-cited Papers

Kim et al., 2018: "TRLFS of hydrolyzed Eu(III) species"

This paper was not included in the CRA-2019 Appendix SOTERM review for two reasons: 1) the experimental conditions were judged to be well outside of what is typically viewed as WIPP relevant, and 2) its focus was on a lanthanide (Eu) that is outside the usual scope of the WIPP An(III) CRA update and reviews (it is multivalent and has a somewhat higher charge/volume ratio than Am(III) and Pu(III) actinides). In this paper (Kim at al., 2018), the formation constant and lifetime of the first hydrolysis constant ($EuOH^{2+}$) and the spectral qualities of the initial hydroxide solid precipitate noted ($Eu(OH)_{3\,(s)}$) were determined. This was performed at low ionic strength (I = 0.1 M sodium perchlorate) at pH 2-8.5 using laser-induced breakdown detection (LIBD) to measure the presence of colloids and time-resolved laser fluorescence spectroscopy (TRLFS) to interrogate the aqueous and solid speciation. Only the first hydrolysis constant could be determined due to the low solubility and prevalence of colloid formation noted at pH > 8.3. The formation constant determined, based on the measurements made, was $\log^*\beta_{1,1} = -7.87 \pm 0.22$, and was extrapolated to zero ionic strength using the specific ion interaction theory (SIT) approach. This value was within experimental uncertainty of the Nuclear Energy Agency-Thermodynamic Data Base project (NEA-TDB) selected value of -7.2 ± 0.5 that was determined for americium and curium (Grenthe et al., 2020).

This investigation, as a whole, shows a good application of laser spectroscopic techniques to a luminescent Eu(III) lanthanide system. With respect to the thermodynamic data measured, there is little

added value to the WIPP project because it does not address ionic strength effects and is focused on the lower-pH first hydrolysis reaction rather than the higher-pH hydrolysis species that would predominate under WIPP-relevant conditions. Additionally, this formation constant is already well established for Am^{3+} (Grenthe et al., 2020) which is more directly relevant to WIPP. With respect to the higher pH data where colloids were predominant, it is unlikely that their observations would extend to the higher ionic strengths that are typically found in WIPP brine. Nonetheless, this paper shows a good way to directly evaluate this potential contribution using LIBD.

Xiong et al., 2017: "Long-term experimental determination of solubilities of micro-crystalline Nd(III) hydroxide in high ionic strength solutions: Applications to nuclear waste management" This paper was not included in the CRA-2019 Appendix SOTERM or Appendix GEOCHEM review because its application to WIPP-specific systems was still being evaluated by the DOE (WIPP project) at the time these appendices were written. This WIPP project study on the solubility of Nd(III) at high pH and high ionic strength should have clear relevance to the current An(III) WIPP model and these data may be considered in future model/database updates.

In this investigation (Xiong et al., 2017), micro-crystalline neodymium hydroxide, $Nd(OH)_3$(micro-cr), solid phase was synthesized and its solubility was measured in long-term experiments (1146 days) at 25 °C in 4.4 and 5.0 m NaCl brine. The dissolution-process was evaluated at pH_m 9.5 and 9.9. In these studies, it was argued that the initial crystalline phase was preserved throughout the experiment. The solubility data were obtained using 0.2µm filtration and relatively high scatter was observed in the concentration data. At this pH (note discussion above in Kim et al., 2018) colloidal formation could have been predominant which would have over-estimated the measured solubility. A much smaller-sized filtration approach, typically 10K Dalton (~5 nm) or 100K Dalton (~ 20 nm) filtration sizes, would better distinguish between the solubility and colloidal contributions (if present). These data were shown to be essentially the same as those in experiments where an amorphous hydroxide phase was used and believed to be the solubility-controlling phase. The measured $Log_{10} K_{s0}^0 = 16.85 \pm 0.2$ is the same as that selected by the NEA-TDB review (Grenthe et al., 2020) of 16.9 ± 0.8 for amorphous phases but somewhat higher than the value of 15.6 ± 0.6 selected for crystalline phases. The WIPP Pitzer model was used to assess/analyze the relevant literature data to confirm and validate the model predictions.

These data and modeling results appear to show that the current WIPP An(III) model does a good job of predicting the measured solubility of $An(III)(OH)_3$ which is the most likely solubility controlling phase under WIPP-relevant conditions. These "crystalline" data agree very well with the NEA-TDB selected value as well as published results for the amorphous phase solubility. The filtration that was used in these experiments does not permit the full evaluation of the potential presence of colloidal species at the pH_m investigated.

General Overview of the WIPP An(III) Model since 2002 (Giambalvo, 2002)

The EPA correctly notes that the last extensive update of the WIPP An(III) model/database was done in 2002 by Giambalvo (Giambalvo, 2002 a and b). The currently implemented An(III) model, as already mentioned, is described in CRA-2019 (Appendix GEOCHEM, Sections 4.2.1 and 4.3.1; Appendix SOTERM, Section 5.8). The DOE continues to support this model as compliant and adequate for the CRA-2019 documentation that has been provided.

To address the EPA question, however, a short summary in three key areas is given in this part of the response. These are: 1) Basis of the Giambalvo model and WIPP project updates; 2) Comparison of the WIPP An(III) database to the ThermoChimie database, the THEREDA database, and the NEA-TDB selected database; and 3) New Pitzer Interaction Data Since the 2002 Giambalvo An(III) Update.

1) Basis of the Giambalvo model and WIPP project updates

The 2002 An(III) model/database update is well documented in WIPP project reports which identify and list the changes from the Compliance Certification Application (CCA) model that were adopted at this time. Generally speaking, the performance assessment verification test (PAVT) model used in the CCA was largely based on WIPP-project data generated at PNNL (Rai et al, 1992; Felmy et al., 1989; Felmy et al., 1990; Rai et al. 1995; Rao et al., 1996) and some analysis of research done on the Institute for Nuclear Waste Management (INE, Karlsruhe) data (Novak 1995; 1996). This was updated to reflect newer data (Fanghänel et al., 1994; 1995; 1998; 1999; Könnecke et al., 1997) generated at the institute and/or reviewed by the NEA-TDB (Silva, 1995) in their data selection process. Most importantly, this was a major update of the Pitzer interaction parameters that were largely missing in the PAVT modeling data set. Key features of this update were:

- Two shortcomings of the PAVT An(III) model/database were addressed: a) as stated by Giambalvo, the Fanghänel et al. (1994) parameters "are appropriate for use in simulating WIPP brines, but their inclusion in the PAVT database was awkwardly implemented" in the hydrolysis model, and b) the range of ionic strengths considered was extended to more WIPP-relevant conditions.
- Conceptually, the CCA implementation that relies on data from three actinides (Pu, Am and Cm) and one analog (Nd), was continued. These four metals are expected to have very similar chemistries (i.e. very similar charge to volume ratios in the III oxidation state) and all, but plutonium, are essentially oxidation-state invariant.
- Americium is the actinide used to represent the An(III) TRU actinides. This americium (III) model, in summary, consisted of the following:
    - First, second and third hydrolysis constants. First and second are based on Cm fluorescence data (Fanghänel 1994; Könnecke et al. 1997); Third is based on the formation constant recommended by the NEA-TDB review (Silva et al. 1995) and the Pitzer coefficients from Könnecke et al. (1997).
    - Chloride interactions are included and based on Cm data (Fanghänel et al., 1995).
    - Carbonate speciation is addressed based on Cm data (Fanghänel et al., 1999).
    - Sulfate complexation is added based on Cm data (Paviet et al., 1996) and the Pitzer coefficients from Fanghänel and Kim (1998).
- Four phases are included to define solubility: 1) The amorphous hydroxide phase $Am(OH)_3(s)$ which was based on a compilation of americium solubility data from the literature (Morss and Williams, 1994); 2) the crystalline ternary americium hydroxy carbonate phase ($AmOHCO_3(c)$) that was based on solubility data (Felmy et al., 1990); 3) the $NaAm(CO_3)_2 \cdot 6\ H_2O$ (c) phase that is based on neodymium data (Rao et al., 1996); and 4) the americium phosphate phase ($AmPO_4(c)$) based on americium solubility data (Rai et al., 1992). In the notation adopted by Giambalvo, (s) stands for "solid" but implies an amorphous or disordered phase and (c) stands for "crystalline" and was used to designate a crystalline phase.
- Additionally, complexation with five organic complexants were reviewed and updated: acetate, oxalate, lactate, citrate, and ethylenediaminetetraacetic acid (EDTA). The changes from the

PAVT model were very minor and both versions of the model are based on the same data (fully published as Choppin et al., 2001).

This Giambalvo 2002 updated model/database was used for CRA-2004, CRA-2009, CRA-2014 and CRA 2019. Two changes, the addition of an An(III)-borate model and an update to the Am- EDTA data, were considered as part of CRA-2014 (this is in the DATA0.FM2 database) but in the end these changes were not accepted by the EPA and these are not part of DATA0.FM4 used in CRA-2019.

2) Comparison of the WIPP An(III) database to the ThermoChimie database, the THEREDA database, and the NEA-TDB Selected Database

Since the 2002 WIPP model/database update, other repository models were developed and the NEA-TDB continues to update its list of selected thermodynamic data. The ThermoChimie database (ThermoChimie 2020), which is widely used in low ionic-strength repository applications, is based on the NEA-TDB selected values for thermodynamic data but incorporates additional reactions and data that were not selected. The THEREDA database (THEREDA 2020), although still under development, provides a more direct comparison as this is intended for a salt repository application using the Pitzer approach and has an implemented An(III) model. The NEA-TDB just published an actinide data update blue book (Grenthe et al., 2020). In this part of the DOE response, the WIPP An(III) database is compared to these new models and database updates to assess the completeness of the list of reactions (so appropriateness of the WIPP reaction set) and the acceptability of the Log K values used for the various reactions.

The key observations and differences noted in these data sets were:

Solid Phases:

Four solid phases are currently in the WIPP model: $Am(OH)_3$ (s), $AmOHCO_3$ (s), $NaAm(CO_3)_2 \cdot 6H_2O$ (s) and $AmPO_4$ (c). Key comparisons are:

- There are small differences between the WIPP and the THEREDA database – mostly due to new information about the solid phases since 2002. THEREDA includes both an amorphous and crystalline hydroxide phase. The americium hydroxy-carbonate phase ($Am(OH)CO_3 \cdot 0.5 H_2O$ (c)) and the sodium americium carbonate phase ($NaAm(CO_3)_2 \cdot 5 H_2O$ (c)) are formulated slightly differently than in the WIPP database (per NEA-TDB recommendations). It does not include a crystalline americium phosphate phase although various amorphous phosphate phases were included.
- The ThermoChimie database includes all the phases found in THEREDA (these are both rooted in the NEA-TDB recommendations) with the addition of the following: an amorphous $Am(OH)(CO_3)$ (s) phase (so same as WIPP) and a crystalline Am_2O_3 (c) phase because it considers a wider range of redox conditions.
- Table 1 shows a comparison of the Log K data for the hydroxide phase which is the most important in defining An(III) solubility.

Table 1. Comparison of the Log K Values for the Formation of Am(OH)3 Solid Phase

Reaction	WIPP An(III) Model	NEA-TDB, THEREDA and ThermoChimie Model
$Am^{3+} + 3OH^- \leftrightarrow Am(OH)_3$ (s)	27.5	25.1 ± 0.8
$Am^{3+} + 3OH^- \leftrightarrow Am(OH)_3$ (c)	N/A	26.4 ± 0.6

Overall, these results show that the WIPP model/database continues to do a good job of identifying key reactions/relationships with respect to solid phase formation. There, however, has been some clarity in the Log Ks and phase definitions since 2002 that are reflected in the NEA-TDB activities/reviews (also used in the THEREDA and ThermoChimie databases) that are not currently found in the DATA0.FM4 database. The impact of this on the actual calculated solubilities would also encompass the associated Pitzer interactions parameters. A direct comparison with the THEREDA An(III) database, which also uses the Pitzer approach, for the solubility of americium hydroxide in 5.6 m NaCl is shown in Figure 1. This Figure shows, for this very simplified system, that the WIPP model under-predicts An(III) solubility across a wide pH range by over an order of magnitude. This is consistent with and readily explained by the differences in the Log K values shown in Table 1 and is not corrected even when accounting for the Pitzer interaction coefficients used in each database. Under more WIPP-relevant conditions, where organic complexation and a complex WIPP brine system is modeled, better agreement would be expected meaning that the Pitzer interaction coefficients effectively correct for the underprediction imposed on the modeling by starting with a Log K value that is too low.

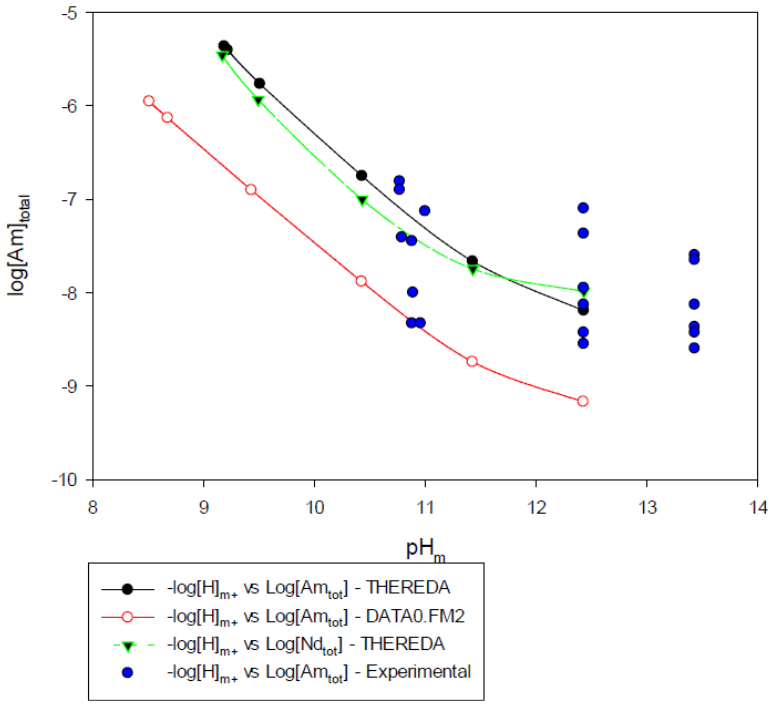

Figure 1. Calculation of Americium Speciation with the WIPP DATA0.FM2 Database and THEREDA Database in 5.6 m NaCl Compared to Experiment as f(pH_m) (Richmann 2021). Solubility Data are from Neck et al. (2009).

Aqueous Inorganic Reactions:

The WIPP An(III) database accounts for hydrolysis, carbonate complexation, chloride complexation and sulfate complexation (Appendix SOTERM, Section 6.5.1, Reactions SOTERM-

21 through SOTERM-31). These same processes are in the THEREDA database although there are some differences. In addition to this, the THEREDA database includes ternary Ca hydroxide species and Na carbonate species that are not in the WIPP database. All of these differences are also in the ThermoChimie database except for the ternary Na carbonate species. These differences are compared in more detail in Table 2.

Table 2. Comparison of Aqueous Reactions in the WIPP, THEREDA and ThermoChimie Databases

Reaction	Present in the Database (Y/N)? Log K Used		
	WIPP	THEREDA/ ThermoChimie	Comparison with WIPP
Hydrolysis			
$Am^{3+} + OH^- \leftrightarrows AmOH^{2+}$	Y; 6.4	Y; 6.8 ± 0.5 (1)	within uncertainty
$Am^{3+} + 2OH^- \leftrightarrows Am(OH)_2^+$	Y; 12.3	Y; 12.9 ± 0.7 (1)	within uncertainty
$Am^{3+} + 3OH^- \leftrightarrows Am(OH)_3(aq)$	Y; 16.3	Y; 15.8 ± 0.5 (1)	within uncertainty
$Am^{3+} + 4OH^- \leftrightarrows Am(OH)_4^-$	N	Y; 15.3 ± 0.7 (1)	not present in model
Carbonate complexation			
$Am^{3+} + CO_3^{2-} \leftrightarrows AmCO_3^+$	Y; 8.1	Y; 8 ± 0.4 (2)	within uncertainty
$Am^{3+} + 2CO_3^{2-} \leftrightarrows Am(CO_3)_2^-$	Y; 13.0	Y; 12.9 ± 0.6 (3)	within uncertainty
$Am^{3+} + 3CO_3^{2-} \leftrightarrows Am(CO_3)_3^{3-}$	Y; 15.2	Y; 15 ± 1 (4)	within uncertainty
$Am^{3+} + 4CO_3^{2-} \leftrightarrows Am(CO_3)_4^{5-}$	Y; 13.0	N	Only in WIPP model
$Am^{3+} + CO_3^{2-} + H_2O \leftrightarrows AmHCO_3^{2+} + OH^-$	N	Y; 27.4 ± 0.3 (1)	not present in model
$2Am^{3+} + 3CO_3^{2-} \leftrightarrows Am_2(CO_3)_3$	N	Y; 33.4 ± 2.2 (1)	not present in model
$Am^{3+} + 5CO_3^{2-} \leftrightarrows Am(CO_3)_5^{6-} + e$	N	Y; -5.1 ± 1.35 (5)	not present in model
Chloride complexation			
$Am^{3+} + Cl^- \leftrightarrows AmCl^{2+}$	Y; 0.24	Y; 0.24 ± 0.03 (1)	within uncertainty
$Am^{3+} + 2Cl^- \leftrightarrows AmCl_2^+$	Y; -0.74	Y; -0.74 ± 0.05 (1)	within uncertainty
Sulfate complexation			
$Am^{3+} + SO_4^{2-} \leftrightarrows Am(SO_4)^+$	Y; 3.25	Y; 3.3 ± 0.15 (6)	Agrees with THEREDA, not ThermoChimie
$Am^{3+} + 2SO_4^{2-} \leftrightarrows Am(SO_4)_2^-$	Y; 3.7	Y; 3.7 ± 0.15 (7)	Agrees with THEREDA, not ThermoChimie
Ternary Complexes			
$2\ Ca^{2+} + Am^{3+} + 4H_2O \leftrightarrows Ca_2[Am(OH)_4]^{3+} + 4\ H^+$	N	-37.2 ± 0.6 (1)	not present in model
$3\ Ca^{2+} + Am^{3+} + 6H_2O \leftrightarrows Ca_3[Am(OH)_6]^{3+} + 6\ H^+$	N	-60.7 ± 0.5 (1)	not present in model
$Ca^{2+} + Am^{3+} + 3H_2O \leftrightarrows Ca[Am(OH)_3]^{2+} + 3\ H^+$	N	-26.3 ± 0.5 (1)	not present in model

Y = Yes, N = No
(1) Same value is used in ThermoChimie
(2) this is 7.9 ± 0.4 in ThermoChimie
(3) this is 12.6 ± 0.6 in ThermoChimie
(4) this is 14.6 ± 1 in ThermoChimie
(5) Only in ThermoChimie
(6) this is 3.45 ± 0.13 in ThermoChimie
(7) this is 4.57 ± 0.44 in ThermoChimie

As shown in Table 2, there are both significant agreements and significant differences between the three databases compared. All are in complete agreement as to the reactions and Log Ks for the two chloride reactions. There is good agreement with the hydrolysis reactions except a

fourth hydrolysis reaction is absent in the WIPP model. This omission is not significant given the predicted pH of the WIPP repository. There is good agreement on the sulfate reactions for all three models. The sulfate reaction Log Ks of the WIPP database are in complete agreement with the THEREDA database, but ThermoChimie has slightly different values.

The two areas where there exists the most disagreement are the carbonate and calcium ternary-species data. For the carbonate reactions, there is good agreement with 1:1, 1:2, and 1:3 carbonate complexes. The WIPP database includes the formation of an $Am(CO_3)_4^{5-}$ species that is not included in the other two models. Additionally, there are three carbonate reactions not included in the WIPP model. As is well recognized, the MgO engineered barrier will sequester CO_2, removing carbonates that would normally form complexes with An(III) and increase solubility. Thus, these differences in carbonate reactions, should not have a significant effect on An(III) solubility in the WIPP. Lastly, the calcium ternary species are absent in the WIPP model.

The aqueous reactions that have been reviewed/selected by the NEA-TDB (meaning that there are high quality data that support the log Ks reported) are listed in Table 3.

Table 3. NEA-TDB Selected Species and Log K.[1]

Species	Log K	THEREDA/ThermoChimie	WIPP Database
$AmOH^{2+}$	6.8 ± 0.6	Same as THEREDA/ThermoChimie	within uncertainty
$Am(OH)_2^{+}$	12.9 ± 0.7	Same as THEREDA/ThermoChimie	within uncertainty
$AmCl^{2+}$	0.24 ± 0.35	Same as THEREDA/ThermoChimie	Agreement
$AmCl_2^{+}$	-0.81 ± 0.35	Slightly different than what is used for both models (-0.74± 0.05)	within uncertainty
$Am(SO_4)^{+}$	3.5 ± 0.3	Same as THEREDA/ThermoChimie	within uncertainty
$Am(SO_4)_2^{-}$	5.0 ± 1	Recently updated in NEA, so slightly different from all three models	Does not agree
$AmCO_3^{+}$	8.0 ± 0.40	Same as THEREDA, slightly different in ThermoChimie	within uncertainty
$Am(CO_3)_2^{-}$	12.9 ± 0.60	Same as THEREDA, slightly different in ThermoChimie	within uncertainty
$Am(CO_3)_3^{3-}$	15.0 ± 0.50	Same value in THEREDA but ± 1 uncertainty, slightly different in ThermoChimie	within uncertainty
$Am(CO_3)_5^{6-}$	-20.1 ± 0.90	Not applicable, this needs to be coupled with a redox assumption	Not in WIPP
$AmHCO_3^{2+}$	3.1 ± 0.30	This is 13.4 ± 0.3 in the same reaction form at THEREDA/ThermoChimie – so agrees with THEREDA; slightly different uncertainty in ThermoChimie	Not in WIPP

[1] Species missing from this list do not have selected values meaning that the data supporting the log K were not of sufficient quality.

In the future, the DOE plans to evaluate the applicability of the NEA-TBD values for Log K to aqueous speciation in the WIPP chemistry model. However, it is important to note that most of the WIPP values are still within the uncertainty ranges reported in the NEA dataset. Although an assessment of the carbonate data, in light of what is being done in models elsewhere, could be performed, this is not expected to significantly change the calculated solubilities as carbonate complexes are not the major contributor to An(III) solubility. The WIPP project, in light of relatively new data on the Ca ternary species, may further evaluate these species especially if Ca

continues to be an important factor in defining actinide solubility under WIPP-relevant conditions.

Organic Complexation Reactions:

The WIPP database (Appendix SOTERM, Reactions SOTERM-32 to SOTERM-36) accounts for the complexation of five organic complexes with An(III) as americium: Acetate, oxalate, lactate, citrate and EDTA. In all cases, the reactions relate to the formation of the 1:1 complex for each organic complexant. These were all added by Giambalvo in 2002 as described (Giambalvo 2002b) and there have been no changes to the model/database since that time. There are no organic complexes included in the THEREDA An(III) database so the only comparison that can be made is to the ThermoChimie database and the NEA-TDB database. The reactions in these two models along with those selected by the NEA-TDB are given in Table 4.

A comparison between the NEA, ThermoChimie, and WIPP data show the following:

Acetate: There are no selected data from the NEA-TDB. Both WIPP and ThermoChimie have the 1:1 complex and these are within experimental error of each other. The WIPP database does not include the 1:2 and 1:3 complex reactions that are in ThermoChimie but acetate has already been shown by the WIPP project to be an unimportant complex for An(III) (U.S. DOE, 2014, Appendix SOTERM, Figure SOTERM-21).

Lactate: Only the WIPP database has the 1:1 Am-Lactate formation constant. This is not in ThermoChimie and was not part of the NEA-TDB review.

Oxalate: There are selected data for the 1:1, 1:2, and 1:3 Am-oxalate complex in the NEATDB database. These selected values and associated reactions are used in ThermoChimie. The WIPP database only has the 1:1 complex with a Log K value that is approximately the same as the selected value but slightly lower (6.16 vs. 6.51 ± 0.15).

Citrate: There are selected data for the 1:1 and 1:2 citrate and hydrogen citrate americium complex in the NEA-TDB database. These are also used in ThermoChimie. The WIPP database only has the 1:1 americium citrate complex with a Log K value that is slightly higher than the NEA-TDB selected value (8.80 vs. 8.55 ± 0.1).

EDTA: There are selected data for the 1:1 EDTA and hydrogen EDTA americium and plutonium complexes in the NEA-TDB database. These are both present in the ThermoChimie database. The WIPP database only has the 1:1 complex with a Log K value that is almost a log unit lower than the selected value (18.97 vs. 19.67 ± 0.11 for Am and 20.18 ± 0.37 for Pu).

Table 4. List and Comparison of An(III) Organic Reactions in the WIPP, ThermoChimie and NEA-TDB

Reaction	WIPP (Y/N) Log K	ThermoChimie (Y/N) Log K	NEA-TDB
Acetate			
$Am^{3+} + Acetate^{-} \leftrightarrows AmAcetate^{2+}$	Y 2.74	Y 2.94 ± 0.5	not selected
$Am^{3+} + 2Acetate^{-} \leftrightarrows Am(Acetate)_2^{+}$	N	Y 5.07 ± 0.5	not selected
$Am^{3+} + 3Acetate^{-} \leftrightarrows Am(Acetate)_3$	N	Y 6.54 ± 0.5	not selected
Lactate			
$Am^{3+} + Lactate^{-} \leftrightarrows AmLactate^{2+}$	Y 3.71	N	No data reviewed
Oxalate			
$Am^{3+} + Oxalate^{2-} \leftrightarrows AmOxalate^{+}$	Y 6.16	Y 6.51 ± 0.15	6.51 ± 0.15
$Am^{3+} + 2Oxalate^{2-} \leftrightarrows Am(Oxalate)_2^{-}$	N	Y 10.71 ± 0.2	10.71 ± 0.200
$Am^{3+} + 3Oxalate^{2-} \leftrightarrows Am(Oxalate)_3^{-3}$	N	Y 13.00 ± 1.00	13.00 ± 1.00
Citrate			
$Am^{3+} + Citrate^{3-} \leftrightarrows AmCitrate(aq)$	Y 8.80	Y 8.55 ± 0.2	8.55 ± 0.2
$Am^{3+} + Citrate^{3-} \leftrightarrows Am(Citrate)_2^{3-}$	N	Y 13.9 ± 1.00	13.9 ± 1.00
$Am^{3+} + Citrate^{3-} + H^{+} \leftrightarrows AmHCitrate^{+}$	N	Y 12.86 ± 1.00	12.86 ± 1.00
$Am^{3+} + 2Citrate^{3-} + 2H^{+} \leftrightarrows Am(HCitrate)_2^{-}$	N	Y 23.52 ± 1.00	23.52 ± 1.00
EDTA			
$Am^{3+} + EDTA^{4-} \leftrightarrows AmEDTA^{-}$	Y 18.97	Y 19.67 ± 0.11	19.67 ± 0.11
$Am^{3+} + EDTA^{4-} + H+ \leftrightarrows AmHEDTA$	N	Y 21.84 ± 0.27	21.84 ± 0.27
$Pu^{3+} + EDTA^{4-} \leftrightarrows PuEDTA^{-}$	NA	Y 20.18 ± 0.37	20.18 ± 0.37
$Pu^{3+} + EDTA^{4-} + H+ \leftrightarrows PuHEDTA$	NA	Y 22.02 ± 0.26	22.02 ± 0.26

Overall, the WIPP model/database does a good job of estimating the effects of organics on the An(III) actinides. There are no Pitzer data for the higher-order complexes found in ThermoChimie and the NEA-TDB database. Accuracy could be improved by adopting the selected values recommended by the NEA TDB for the Log K values and, to a lesser extent, adding the 1:2 and 1:3 complexes, which could contribute to the overall speciation found at WIPP-relevant pH (but this may not be a significant improvement for the calculated An(III) solubilities and requires a determination of the relevant Pitzer interaction parameters). The hydrogen complexes (e.g. $HCitrate^{-2}$ and $HEDTA^{-3}$), although present in solution at this pH, will not contribute significantly because of their low tendency to form complexes at this pH. The DOE will consider the benefit of dropping the lactate complexation reaction from its database since significant amounts of lactate are not expected to be present in WIPP and lactate is a relatively weak complexant. All of these relatively small changes could require a recalculation of the associated Pitzer parameters.

3) <u>New Pitzer Interaction Data Since the 2002 Giambalvo An(III) Update</u>

There have been three major reviews and updates of the An(III) data since 2002. These were:

A. Update on the Chemical Thermodynamics of Uranium, Neptunium, Plutonium, Americium, and Technetium. This was an NEA-TDB blue book updated published in 2003 (Guillaumont et al., 2003).
   - Available literature was reviewed; associated thermodynamic data updated
   - Pitzer interaction parameters were outside the scope of this review

B. International Union of Pure and Applied Chemistry-National Institute of Standards and Technology (IUPAC-NIST) Solubility Data Series. 84. Solubility of Inorganic Actinide Compounds. This was an IUPAC review that was published in 2007 (Hàla and Miyamoto, 2007).
   - This reviewed Pu(III) and Am/Cm(III) data through 1994
   - Pitzer interaction parameters were outside the scope of this review

C. Second Update on the Chemical Thermodynamics of Uranium, Neptunium, Plutonium, Americium, and Technetium. This was an NEA-TDB update blue book published in 2020 (Grenthe et al., 2020).
   - Available literature was reviewed; associated thermodynamic data updated
   - Pitzer interaction parameters were outside the scope of this review

The NEA-TDB selection process updated the set of reactions that were judged to have qualified data and the associated Log K values and thermodynamic data. These data updates were discussed earlier in this review (see Tables 1, 3, and 4). In all cases, these general reviews and updates did not look in detail at high ionic strength data where the Pitzer approach would be used so there are no new data in these reviews on this aspect of the WIPP Pitzer model.

In this section, however, the focus is on publications since 2002 that may be useful in reassessing the Pitzer coefficients used in the WIPP model. The coefficients currently used in the WIPP An(III) database were developed by Giambalvo and are listed in the CRA-2019 Appendix GEOCHEM (Appendix GEOCHEM, Table GEOCHEM-47). It is important to note, as has already been discussed, that this 2002 model/database update relied on WIPP project data and those obtained outside the project (Giambalvo, 2002 a and b). In all cases the analyses were extended beyond I = 4m.

A list of publications, that may contain data that could be useful if it is decided to reassess the An(III) Pitzer interaction parameters – listed in the order of publication date, are the following:

1) Roy, R.N., et al. 2005. Thermodynamics of Electrolyte Mixtures: HCl + $NdCl_3$ + H_2O from 5 to 55 °C. Journal of Solution Chemistry **34**:1033-1044.
2) Neck, V., et al. 2009. Thermodynamics of Trivalent Actinides and Neodymium in NaCl, $MgCl_2$, and $CaCl_2$ solutions: Solubility, Hydrolysis, and Ternary Ca-M(III)-OH Complexes. Pure and Applied Chemistry **81**(9):1555-1568.
3) Rai, D., et al. 2010. $PuPO_4$(cr, hyd.) Solubility Product and Pu^{3+} Complexes with Phosphate and Ethylenediaminetetraacetic Acid. Journal of Solution Chemistry **39**:778-807.
4) Thakur, P., et al. 2012. Thermodynamic Modeling of Trivalent Am, Cm and Eu-citrate Complexation in Concentrated $NaClO_4$ Media. Radiochimica Acta **100**:165-172.

5) Thakur, P., et al. 2014. Improved Thermodynamic Model for Interaction of EDTA with Trivalent Actinides and Lanthanide to Ionic Strength of 6.60 m. Geochimica et Cosmochimica Acta **133**:299-312.
6) Zalupski, P.R. and R. McDowell. 2014. Isopiestic Determination of the Osmotic Coefficients of $NaNO_3$ + $Eu(NO_3)_3$ + H_2O at 298.15 K and Representation with an Extended Ion-Interaction (Pitzer) Model. J. Chem. Eng. Data **59**:1574-1582.
7) Chatterjee, S., et al 2015. Aqueous Binary Lanthanide(III) Nitrate $Ln(NO_3)_3$ Electrolytes Revisited: Extended Pitzer and Bromley Treatments. J. Chem. Eng. Data **59**:2974-2988.
8) Herm, M., et al. 2015. Solubility and Spectroscopic Study of An(III)/Ln(III) in Dilute to Concentrated Na-Mg-Ca-Cl-NO_3 Solutions. Pure and Applied Chemistry **87**(5):487-502.
9) Thakur, P., Y. Xiong, and M. Borkowski. 2015. An Improved Thermodynamic Model for the Complexation of Trivalent Actinides and Lanthanide with Oxalic Acid Valid to High Ionic Strength. Chemical Geology **413**:7-17.
10) Xiong, Y, L. Kirkes and C. Marrs. 2017. Long-Term Experimental Determination of Solubilities of Micro-crystalline Nd(III) Hydroxide in High Ionic Strength Solutions: Applications to Nuclear Waste Management. Aquatic Geochemistry **23**:359–375.
11) Oakes, C., A. Ward, N. Chugunov, and J. Icenhower. 2021. A Speciated, Conventional Pitzer Ion-interaction Model for the Aqueous Nd^{3+}-H^+-Na^+-K^+-Ca^{2+}-Cl^--OH^- System at 298 K and 0.1 MPa. Geochimica et Cosmochimica Acta **297**:308-327.

These publications have varying importance, relative to the WIPP chemistry model, and their potential usefulness will be further evaluated in future model/database updates. In particular, the Roy (reference 1), Neck (reference 2), Herm (reference 8), Xiong (reference 10), and Oakes (reference 11) would have direct application to An(III) solubility. Further evaluation of the An(III)-EDTA complex, which remains a key complexant for this oxidation state, could be done with data from Rai (reference 3), and Thakur (reference 5). Additional data in this area, particularly for the gaps identified in section 2, would likely be needed to make future improvements to the WIPP chemistry model.

Overall Summary of Observations of Database Comparisons

A key and over-arching conclusion that needs to be restated is that the DOE continues to support the CRA-2019 WIPP An(III) model and believes this model to be sufficiently compliant for recertification.

The WIPP An(III) model/database update implemented in 2002 by Giambalvo was a good and needed update that was based on the best understanding of the time. This core An(III) model was used in CRA 2004, 2009, 2014, and 2019 although there have been some indirect changes to the WIPP database/model over time that impact the predicted results for An(III) solubility (e.g., changes in the calculated pH, speciation and availability of organic complexants, brine composition, and influences of increased Ca). In this context this core model has served the project well for almost 20 years.

Since this last WIPP An(III) model/database update, however, there are many new data and assessments of An(III) data that are not reflected in the current WIPP model. Periodic updates of a repository model/database are a good problem that is inevitable for successful longrunning repository programs such as WIPP. This is most evident in the comparisons of the WIPP An(III) database to the newer NEA, THEREDA, and ThermoChimie databases. The most important observations from this comparison were:

1) A reassessment of the Log Ks for the four solid phases in the WIPP model is justifiable. It appears that the phosphate phase, added to the WIPP chemistry model at the time of the CCA when a lower pH may have been thought to be possible in WIPP, is no longer needed. Most importantly the Log K for the hydroxide phase, which is the key solubility controlling phase, should be adjusted to the currently accepted NEA-TDB value for the amorphous phase (25.1±0.8). The current value is an order of magnitude lower than the crystalline hydroxide phase (so two orders of magnitude below the amorphous phase). Using the amorphous phase, rather than the crystalline phase, is consistent with the WIPP An(III) model recommended in the Giambalvo update and will apply to the Pu(III) phase where only amorphous phases appear to exist at high pH.
2) An evaluation of the benefit of revising the aqueous phase reactions and Log K values to those recommended by the NEA-TDB is justifiable. In many cases, the WIPP values are within the stated uncertainty of the NEA selected values. This agreement is a strong data point that supports the current implementation and defensibility of the WIPP chemistry model. That being said, since the values are mostly in agreement, the provenance and accuracy of the database would be improved by using the NEA-TDB selected values, which were last updated in 2020 and are based on a wider assessment of the available data. It should also be noted that the speciation of some reactions (see Table 2) has been further clarified based on newer data so this could also be changed for the same reason.
3) Thermodynamic data for organic complexants are a known data gap/deficiency in the nuclear repository field. In the WIPP chemistry model, at $pH_m \sim 9$, citrate and EDTA are the organic complexants that are most impactive on An(III) speciation. The DOE will continue to evaluate the speciation, Log K values, and associated Pitzer interaction coefficients for these key reactions (along with their associated brine chemistry).
4) A possible future update of the An(III) model by the DOE along the lines of the first three observations just noted would lead to some re-assessments of the Pitzer interaction coefficients used to model the An(III) system at the I > 5 m ionic strengths in WIPP-relevant brine systems. If this is done, it should be done in a self-consistent way that addresses all key interactions. There are new data and new approaches available for this fitting process that could be considered.

References

Fanghänel, T., J. Kim, P. Paviet, R. Klenze, and W. Hauser. 1994. Thermodynamics of Radioactive Trace Elements in Concentrated Electrolyte Solutions: Hydrolysis of Cm^{3+} in NaCl-Solutions. Radiochimica Acta 66/67: 81-87.

Fanghänel, T., J. Kim, R. Klenze, and Y. Kato. 1995. Formation of Cm(III) Chloride Complexes in $CaCl_2$ Solutions. Journal of Alloys and Compounds 225:308-311.

Fanghänel, T. and J. Kim. 1998. Spectroscopic Evaluation of Thermodynamics of Trivalent Actinides in Brines. Journal of Alloys and Compounds 271-273:728-737.

Fanghänel, T., T. Könnecke, H. Weger, P. Paviet-Hartmann, V. Neck, and J. Kim. 1999. Thermodynamics of Cm(III) in Concentrated Salt Solutions: Carbonate Complexation in NaCl Solution at 25°C. Journal of Solution Chemistry 28:447-462.

Felmy, A., D. Rai, J. Schramke, and J. Ryan. 1989. The Solubility of Plutonium Hydroxide in Dilute Solution and in High-Ionic Strength Chloride Brines. Radiochimica Acta 48: 29–35.

Felmy, A., D. Rai, and R. Fulton. 1990. The Solubility of $AmOHCO_3$(cr) and the Aqueous Thermodynamics of the System Na_{+}-Am_{3+}-HCO_{3-}-CO_3^{2-}-OH_{-}-H_2O. Radiochimica Acta 50: 193– 204.

Giambalvo, E. 2002a. Recommended Parameter Values for Modeling An(III)Solubility in WIPP Brines. Memorandum to L.H. Brush, Sandia National Laboratories, Carlsbad, New Mexico. ERMS 522982.

Giambalvo, E. 2002b. Recommended Parameter Values for Modeling Organic Ligands in WIPP Brines. Memorandum to L.H. Brush, Sandia National Laboratories, Carlsbad, New Mexico. ERMS 522981.

Grenthe, I., X. Gaona, A. Plyasunov, L. Rao, W. Runde, B. Grambow, R. Konings, A. Smith, and E. Moore. 2020. Second Update on the Chemical Thermodynamics of Uranium, Neptunium, Plutonium, Americium and Technetium. OECD Nuclear Energy Agency, Data Bank, Boulogne-Billancourt, France. Chemical Thermodynamics Volume 14.

Guillaumont, R., T. Fanghänel, J. Fuger, I. Grenthe, V. Neck, D. Palmer, and M. Rand. 2003. Update on the Chemical Thermodynamics of Uranium, Neptunium, Plutonium, Americium and Technetium. F.I. Mompean, M. Illemassene, C. Domenech-Orti, and K. Ben Said, eds. Amsterdam: Elsevier. Chemical Thermodynamics. Vol. 5

Hàla, J. and H. Miyamoto. 2007. IUPAC-NIST Solubility Data Series. 84. Solubility of Inorganic Actinide Compounds. J. Phys. Chem. Ref. Data 36 (4):1417-1736.

Kim, H.K., S. Choi, E. Jung, H.R. Cho, J. Yun, and W. Cha. 2018. TRLFS Study of Hydrolyzed Eu(III) Species. Journal of Luminescence 202:469-474.

Könnecke, T., T. Fanghänel, and J. Kim. 1997. Thermodynamics of Trivalent Actinides in Concentrated Electrolyte Solutions: Modelling the Chloride Complexation of Cm(III). Radiochimica Acta 76:131-135.

Morss, L. and C. Williams. 1994. Synthesis of Crystalline Americium Hydroxide, $Am(OH)_3$, and Determination of its Enthalpy of Formation; Estimation of the Solubility-product Constants of Actinide(III) Hydroxides. Radiochimica Acta 66/67:89-93.

Novak, C. 1995. A Data Base for Thermodynamic Modeling of +III Actinide Solubility in Concentrated Na-Cl-$S0_4$-$C0_3$-$P0_4$ Electrolytes. Sandia National Laboratories, Albuquerque, NM. 17 pp. SAND95-2010C.

Novak, C. 1996. Parameter Values for +III Actinide Hydrolysis Species, Memo to R. V. Bynum. June 11, 1996. Albuquerque: Sandia National Laboratories. WPO 40692

Neck, V., M. Altmaier, T. Rabung, J. Lützenkirchen, and T. Fanghanel. 2009. Thermodynamics of Trivalent Actinides and Neodymium in NaCl, MgCl(2), and CaCl(2) Solutions: Solubility, Hydrolysis, and Ternary Ca-M(III)-OH Complexes. Pure Appl. Chem. 81:1555-1568.

Paviet, P., T. Fanghänel, R. Klenze, and J. Kim. 1996. Thermodynamics of Curium(III) in Concentrated Electrolyte Solutions: Formation of Sulfate Complexes in NaCl/Na_2S0_4 solutions. Radiochimica Acta 74:99-103.

Rai, D., A. Felmy, and R. Fulton. 1995. Nd_{3+} and Am_{3+} Ion Interaction with Sulfate Ion and Their Influence on $NdPO_4$(c) Solubility. Journal of Solution Chemistry 24:879–95.

Rai, D., J. Ryan, D. Moore, and R. Strickert. 1983. Am(III) Hydrolysis Constants and Solubility of Am(III) Hydroxide. Radiochimica Acta 33:201–206.

Rai, D., A. Felmy, and R. Fulton. 1992. Solubility and Ion Activity Product of $AmP0_4 \cdot xH_20$(am). Radiochimica Acta 56:7-14.

Rai, D., A. Felmy, and R. Fulton. 1995. Nd_{3+} and Am_{3+} Ion Interactions with Sulfate Ion and their Influence on $NdP0_4$(c) Solubility. Journal of Solution Chemistry 24:879-895.

Rai, D., R. Strickert, D. Moore, and J. Ryan. 1983. Am(III) Hydrolysis Constants and Solubility of Am(Ill) Hydroxide. Radiochimica Acta, 33:201-206.

Rao, L., D. Rai, A.R. Felmy, R.W. Fulton, and C.F. Novak. 1996. Solubility of $NaNd(CO_3)_3 \cdot 6H_2O$(c) in Concentrated Na_2CO_3 and $NaHCO_3$ Solutions. Radiochimica Acta 75:141–147.

Richmann, M.K. 2021. Los Alamos Data Package for the Comparison of the WIPP DATA0.FM2 database and the THEREDA thereda_2020_gwb_jan19 database using Geochemists Workbench.

Silva, R., G. Bidoglio, M. Rand, P. Robouch, H. Wanner, and I. Puigdomenech. 1995. Chemical Thermodynamics of Americium. Nuclear Energy Agency OECD, Amsterdam. THEREDA 2020. Database thereda_2020_gwb_jan19 found on www.thereda.de ThermoChimie 2020. Database version 10a (TC10a) found at www.thermochimie-tdb.com

U.S. Department of Energy (DOE). 1996. Title 40 CFR Part 191 Compliance Certification Application for the Waste Isolation Pilot Plant (October). 21 vols. Carlsbad Field Office, Carlsbad NM. DOE/CAO-1996-2184.

U.S. Department of Energy (DOE). 1996. Title 40 CFR Part 191, Compliance Certification Application for the Waste Isolation Pilot Plant, Appendix SOTERM. Title 40 CFR Part 191, Subparts B and C, Actinide Chemistry Source Term. 1996. United States Department of Energy/Waste Isolation Pilot Plant. Carlsbad Field Office, Carlsbad, NM. DOE/CAO-1996-2184.

U.S. Department of Energy (DOE). 2004. Title 40 CFR Part 191, Compliance Recertification Application for the Waste Isolation Pilot Plant (March). 10 vols. Carlsbad Field Office, Carlsbad, NM. DOE/WIPP 2004-3231.

U.S. Department of Energy (DOE). 2009. Title 40 CFR Part 191, Subparts B and C, Compliance Recertification Application 2009, Appendix PA, Attachment SOTERM. Carlsbad Field Office, Carlsbad, NM. DOE/WIPP 2009-3424.

U.S. Department of Energy (DOE). 2014. Title 40 CFR Part 191, Subparts B and C, Compliance Recertification Application for the Waste Isolation Pilot Plant (March). Carlsbad Field Office, Carlsbad, NM. DOE/WIPP 2014-3503.

U.S. Department of Energy (DOE). 2019. Title 40 CFR Part 191, Subparts B and C, Compliance Recertification Application for the Waste Isolation Pilot Plant (March). Carlsbad Field Office, Carlsbad, NM. DOE/WIPP-19-3609.

Xiong, Y, L. Kirkes and C. Marrs. 2017. Long-Term Experimental Determination of Solubilities of Micro-crystalline Nd(III) Hydroxide in High Ionic Strength Solutions: Applications to Nuclear Waste Management. Aquatic Geochemistry 23:359–375.

EPA Evaluation of Response

The DOE response was satisfactory. The information was provided as requested.

CC1-SOTERM-4 Incomplete Evaluation of Th(IV) Aqueous Speciation and Solubility Data

WIPP Compliance Recertification Application 2019 Appendix-SOTERM (Actinide Chemistry Source Term)

EPA Question (from EPA Completeness Comment Package 1)

Please provide an evaluation of the expected effects of all available WIPP-relevant Th(IV) aqueous speciation and solubility data on modeling predictions of WIPP repository brine chemistry.

Appendix SOTERM Section SOTERM-5.4 provides a review of Th(IV) aqueous speciation and solubility data that has become available since the last update of the WIPP EQ3/6 database (Giambalvo 2002b, Nowak 2005). However, an assessment is not provided of the expected effects of the new data on modeling predictions of WIPP repository brine chemistry.

Giambalvo, E.R. 2002b. Recommended Parameter Values for Modeling An(IV) Solubility in WIPP Brines. Memorandum to L.H. Brush, Sandia National Laboratories, Carlsbad, New Mexico. ERMS 522986.

Nowak, E.J. 2005. Recommended Change in the FMT Thermodynamic Data Base. Memorandum to L.H. Brush, Sandia National Laboratories, Carlsbad, New Mexico. ERMS 539227.

DOE Response (from DOE Response Package 6)

The U.S. Department of Energy (DOE), to address this U.S. Environmental Protection Agency (EPA) completeness request, has completed a comprehensive review and assessment of the available thorium

data since the Giambalvo (2002 a-c) and Nowak (2005) memos that underpin the current Waste Isolation Pilot Plant (WIPP) An(IV) model. The main conclusions/observations of this review are summarized within this response.

It is important to also note that the DOE has always reviewed newly-available WIPP project and open literature thorium data in the three re-certifications of the WIPP since the 2004 Compliance Recertification Application (CRA) (CRA-2009, Appendix SOTERM, Section 3.2; CRA- 2014, Appendix SOTERM, Section 3.3; CRA-2019, Appendix SOTERM, Section 5.4; CRA-2019, Appendix GEOCHEM Sections 4.2.2 and 4.3.2). Additionally, the DOE previously assessed the thorium model with particular emphasis on comparisons with the thermodynamic data in the Nuclear Energy Agency (NEA) database (Rand et al. 2008) and the potential need and importance of including additional ternary Th-OH-CO_3 species to the WIPP model for CRA-2009 (Borkowski and Richmann 2009). Based on all these documents and data sources, it continues to be the DOE position that the currently implemented An(IV) thorium model remains conservative for two key reasons:

1) The calculated solubilities over-predict the solubilities of U(IV), Np(IV) and Pu(IV) which are the An(IV) oxidation states that are most critical to WIPP Performance Assessment (PA) release calculations. (Altmaier et al. 2017)
2) As currently implemented, the high uncertainty associated with Th(IV) solubilities exaggerates the impact of An(IV) on transuranic (TRU) release from the WIPP. (Altmaier et al. 2017)

This prevailing conservatism preserves the defensibility of the approach implemented in the CRA-2019 PA.

Basis of the Current WIPP An(IV) Model

The overall approach to modeling the An(IV) oxidation state was established at the time of the Compliance Certification Application (CCA) and has not significantly changed since that time (see CRA-2019, Appendix SOTERM, Section 6.5.2). The CCA approach used Th(IV) as the analog for U(IV), Np(IV), and Pu(IV), based on the conservativeness with respect to the calculated solubilities of Th(IV), which was a low activity redox-invariant analog with many experimental advantages, and the availability of thorium Pitzer data for the WIPP model. This model is best documented in a series of memos published to support CRA-2004 by Giambalvo (Giambalvo 2002a, Giambalvo 2002b, Giambalvo 2002c) and augmented by a recommendation for a minor revision of the μ_0/RT (reduced free energy; μ_0 = standard free energy change per mole, R = ideal gas constant) value of $Th(OH)_{4(aq)}$ (Nowak 2005).

The first of these memos (Giambalvo 2002a) and Nowak's recommendation (Nowak 2005) discuss parameter values for modeling An(IV) solubility in WIPP brines. Specifically, the WIPP approach to address thorium hydrolysis, carbonate complexation, sulfate complexation, and chloride complexation in equilibrium with $ThO_{2(am)}$ are presented. These memos outline the basis for the parameters of the An(IV) speciation and solubility model (Novak 1996, 1997), and recommend two changes to the model:

1) Updating ternary interactions of $Th(CO_3)^{6-}$, Cl^-, Na^+ (θ, ψ) from a peer-reviewed article (Felmy and Rai 1999)
2) Updating the μ_0/RT value of $Th(OH)_{4(aq)}$ as calculated from the data in two peer-reviewed articles (Ryan and Rai 1987, Felmy et al. 1991) and subsequently to a log $*\beta^o_{1,4}$ = -17.5 ± 1.0.

The experimental basis of these reactions are largely from the following publications (mainly late 80's to mid 90's):

Ryan and Rai 1987: Thorium solubility/hydrolysis
Felmy et al. 1991: Thorium solubility/hydrolysis
Pitzer and Mayorga 1973: Th – chloride Pitzer parameters
Felmy et al. 1997: Th-carbonate system
Felmy and Rai 1992: Th-sulfate system
Roy et al. 1992: Th-chloride system

The second two Giambalvo memos discuss updates to parameter values for modeling organic ligands in WIPP brines. Specifically, the complexation of thorium by ethylenediaminetetraacetic acid (EDTA), acetate and lactate (Giambalvo 2002b) and oxalate (Giambalvo 2002c) are addressed. Most of these data were taken from Choppin et al. 2001 and peer-reviewed publications derived from this experimental data on oxalate (Borkowski et al. 2001). Parameters describing thorium complexation with acetate are included based on the Choppin et al. data. Additionally, Th-EDTA complexation is included from the Choppin et al. data with the caveat that Th hydrolysis species and Na-EDTA complexes contribute to the recommended stability constant of $Th(EDTA)_{(aq)}$ of log β = 23.6. The calculated and observed trend of the log β vs NaCl molality differ slightly, perhaps indicating that the log β value chosen is incorrect or that more species are responsible for the prediction of Th complexation with EDTA (**Figure 1**).

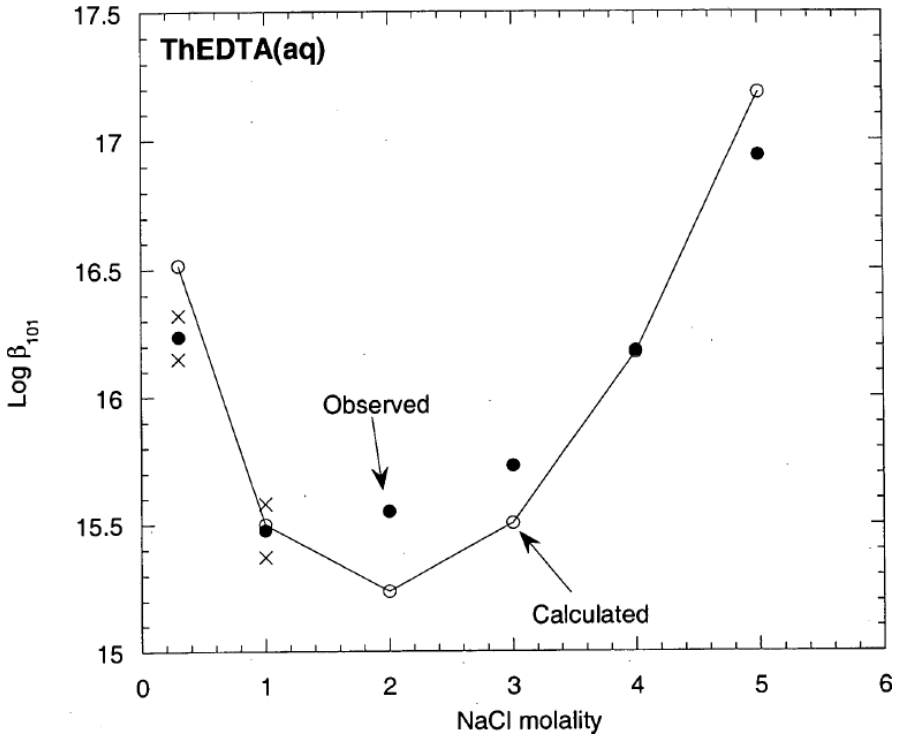

Figure 1. Log β versus NaCl molality of Th(EDTA). Filled circles represent values from Choppin et al. 2001, points at 0.3 and 1 m NaCl are average values calculated from values plotted with X; open circles represent model prediction. Taken from Giambalvo 2002b.

Th(IV) as an analog for An(IV)

The most important aspect of the Th(IV) model is its simulation of U(IV), Np(IV) and Pu(IV) solubility under WIPP specific conditions. Plutonium, in particular, is the element of most concern when predicting actinide mobility and release in the WIPP. Th was chosen as the model for all An(IV) solubilities due to its redox invariant nature, as it only forms the +4 ion under environmental conditions, low activity, and its solubility being higher than the other An(IV) species. Only forming one stable oxidation state in solution allows a wide variety of experimental conditions to be used without the addition of redox controlling reagents or conditions. Of the other +4 actinides, U(IV) and Np(IV) can be stabilized with the use of redox buffers, which allows them to be used as analogs for Pu(IV) in long-term studies under WIPP relevant conditions. Using thorium to simulate An(IV) solubility has been an acceptable strategy within the WIPP project, as well as many high level waste (HLW) nuclear programs, since it has the highest solubility of the +4 actinides. Thorium, however, is not a good analog for colloidal behavior, redox-related studies, and pH-dependent hydrolysis behavior. This issue was well discussed in an Institute for Nuclear Waste Disposal (INE, Karlsruhe, Germany) report (Altmaier et al. 2017) prepared for the DOE that fully assessed the use of Np(IV) and U(IV), in combination with redox-controlling buffers, as improved analogs for Pu(IV) in high ionic strength brine systems. Generally speaking, thorium chemistry is an outlier when compared to the oxidation-state specific chemistry of U(IV), Np(IV) and Pu(IV), which behave very similarly to each other.

The divergence between thorium and the other An(IV) actinide chemistry is best illustrated in the hydrolysis trends which correlate with the electrostatic interaction energy of the actinides and hydroxide ions (Neck and Kim 2001; Altmaier et al. 2017). As shown in Figure 2, the thorium hydrolysis stability constants are much lower than that of U(IV), Np(IV), and Pu(IV) and do not correlate as well with effective charge. This explains the higher solubility usually noted and the much higher tendency towards colloidal formation in aqueous systems.

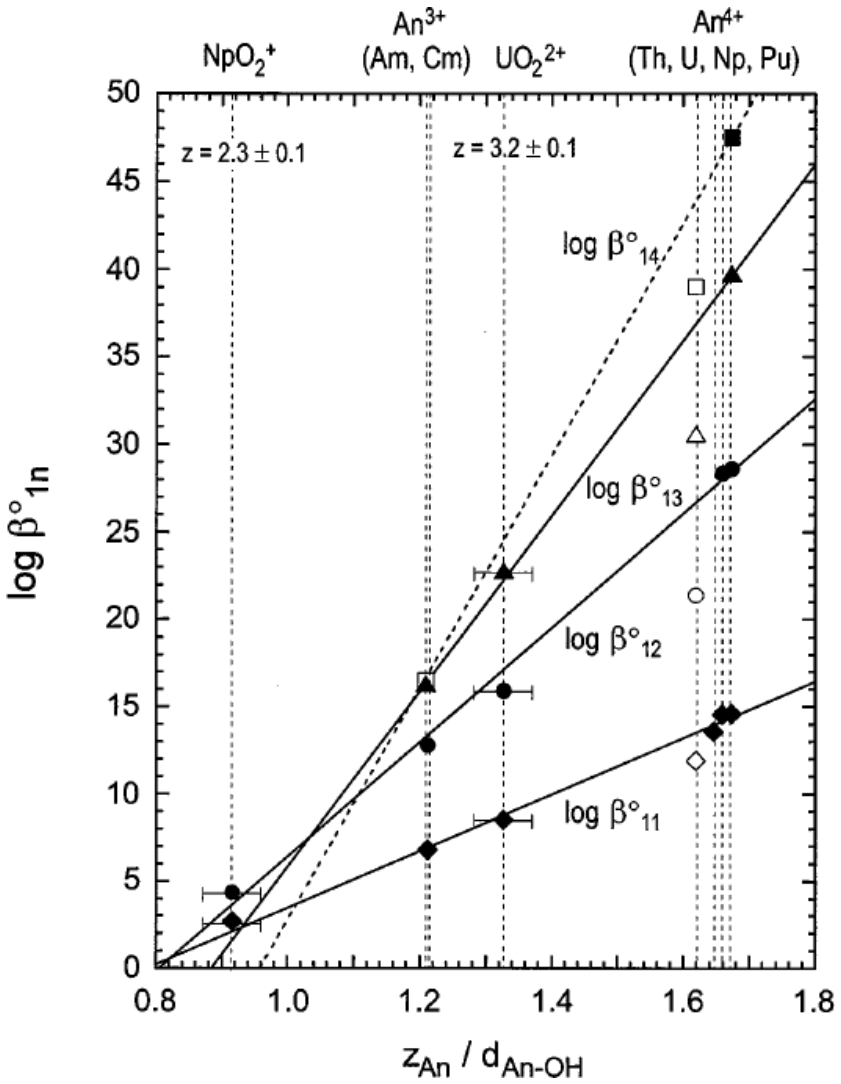

Figure 2. Correlation of the formation constants log ß$_{ln}$° of actinide hydroxide complexes with the electrostatic interaction energy $_{el}E_{An\text{-}OH}$ between the actinide and OH^- ions (taken from Neck and Kim 2001). Thorium hydrolysis, shown as open symbols do not follow the trend of U(IV), Np(IV), and Pu(IV).

Review of Specific Thorium Complexes

Thorium Carbonate Complexes

In the current WIPP model, thorium complexation with carbonate is included through the use of two complexes, $Th(OH)_3(CO_3)^-$ and $Th(CO_3)_6^{6-}$. The inclusion of these two species was based off solubility studies in concentrated $NaHCO_3$ and Na_2CO_3 solutions (Östholls et al. 1994, Felmy et al. 1997). Two more recent studies from INE (Altmaier et al. 2004, Altmaier et al. 2006), include the species $Th(OH)(CO_3)_4^{5-}$ and $Th(OH)_2(CO_3)_2^{2-}$ as the species most responsible for predicting the solubility of ThO_2(am,hyd) with smaller contributions from $Th(OH)_2(CO_3)$, $Th(OH)_3(CO_3)^-$ and $Th(OH)_4(CO_3)_2^{2-}$. X-ray absorption fine structure (XAFS) studies at I = 0.5 M and $C_{tot} \leq 0.1$ M show that the formation of $Th(CO_3)_6^{6-}$ is insignificant, but can be formed at higher $[CO_3^{2-}]$ or $[HCO_3^-]$. The NEA and ThermoChimie databases have selected data for all of the complexes listed above:

$Th^{4+} + 5\ CO_3^{2-} \leftrightharpoons Th(CO_3)_5^{6-}$

log K = 31.00 ± 0.70, $\Delta_r G°_m$ = -176.948 ± 3.996 kJ/mol, $\Delta_f G°_m$ = -3521 ± 6.917 kJ/mol
ε $Na^+/Th(CO_3)_5^{6-}$ = -0.30 ± 0.15

$Th^{4+} + CO_{2-} + 2\ H\ O \leftrightharpoons Th(OH)\ (CO\ ) + 2\ H^+$

log K = 2.50 ± 0.60, $\Delta_r G°_m$ = -14.270 ± 3.425 kJ/mol, $\Delta_f G°_m$ = -1721.233 ± 6.321 kJ/mol

$Th^{4+} + CO_{2-} + 3\ H\ O \leftrightharpoons Th(OH)\ (CO\ )^- + 3\ H^+$

log K = -3.70 ± 0.70, $\Delta_r G°_m$ = 21.120 ± 3.996 kJ/mol, $\Delta_f G°_m$ = -1922.983 ± 6.648 kJ/mol
ε Na^+ / $Th(CO_3)(OH)^-$ = -0.05 ± 0.20

$Th^{4+} + CO_{2-} + 4\ H\ O \leftrightharpoons Th(OH)\ (CO\ )_{2-} + 4\ H^+$

log K = -15.60 ± 0.60, $\Delta_r G°_m$ = 89.045 ± 3.425 kJ/mol, $\Delta_f G°_m$ = -2092.198 ± 6.323 kJ/mol
ε Na^+ / $Th(CO_3)(OH)_{2-}$ = -0.10 ± 0.20

$Th^{4+} + 2\ CO_{2-} + 2\ H\ O \leftrightharpoons Th(OH)\ (CO\ )_{2-} + 2\ H^+$

log K = 8.80 ± 0.50, $\Delta_r G°_m$ = -50.230 ± 2.854 kJ/mol, $\Delta_f G°_m$ = -2285.093 ± 6.068 kJ/mol
ε Na^+ / $Th(CO_3)_2(OH)_{2-}$ = -0.10 ± 0.20

$Th^{4+} + 4\ CO_{2-} + H\ O \leftrightharpoons Th(OH)(CO\ )_{5-} + H^+$

log K = 21.60± 0.50, $\Delta_r G°_m$ = -123.293 ± 2.854 kJ/mol, $\Delta_f G°_m$ = -3176.816 ± 6.216 kJ/mol
ε Na^+/ $Th(CO_3)_4(OH)_{5-}$= -0.22 ± 0.13

The data selected by the NEA and ThermoChimie databases for $Th(OH)_3(CO_3)^-$ is consistent with the value selected in CRA-2019. However, the data selected for $Th(CO\ )_{6-}$ (log K = 26.9), is two orders of magnitude higher than that in CRA-2019 (log K = 24.6) and therefore over-estimates the impact of carbonate on the solubility.

<u>Thorium Sulfate Complexes</u>

Thorium sulfate complexes were initially included prior to the CCA when the pH of the WIPP system was not well understood. The addition of MgO to sequester free carbonate buffers the WIPP pH to be alkaline (pH 8-10). A recent investigation into the Th-PO4-SO4-H2O system (Kim and Osseo-Asare 2012), has shown that thorium sulfate complexes are not stable above pH 4, where ThO2 dominates the Pourbaix diagram at sulfate concentrations from 0.01 -1 M. Both the Castille and Salado brines have [SO_4^{2-}] in the range of 0.1 M. The inclusion of these species and the double salts is unnecessary for prediction of An^{4+} solubility under WIPP conditions.

The NEA and ThermoChimie databases have selected data for the following thorium sulfate species:

$Th^{4+} + SO_4^{2-} \leftrightharpoons Th(SO_4)^{2+}$

log K = 6.17 ± 0.32, $\Delta_r G°_m$ = -35.218 ± 1.827 kJ/mol, $\Delta_f G°_m$ = -1484.005 ± 5.620 kJ/mol
$\Delta_r H°_m$ = -20.920 ± 0.740 kJ/mol, $\Delta_f H°_m$ = -1657.120 ± 2.449 kJ/mol
$\Delta_r S°_m$ = 188.289 ± 6.610 J/mol·K, $\Delta_f S°_m$ = -216.311 ± 20.566 J/mol·K
ε $Cl^-/Th(SO_4)^{2+}$ = 0.14 ± 0.15

ε $ClO_4^-/Th(SO_4)_2$ = 0.30 ± 0.10

$Th^{4+} + 2\ SO_4^{2-} \leftrightharpoons Th(SO_4)_2$

log K = 9.69 ± 0.27, $\Delta_r G°_m$ = -55.311 ± 1.541 kJ/mol, $\Delta_f G°_m$ = -2248.102 ± 5.581 kJ/mol
$\Delta_r H°_m$ = 40.380 ± 1.080 kJ/mol, $\Delta_f H°_m$ = -2547.000 ± 2.664 kJ/mol
$\Delta_r S°_m$ = 320.948 ± 6.312 J/mol·K, $\Delta_f S°_m$ = -65.154 ± 20.747 J/mol·K

$Th^{4+} + SO\ _{2-} + 9\ H\ O \leftrightharpoons Th(SO\ ) \cdot 9\ H\ O$

log K = 11.25 ± 0.10, $\Delta_r G°_m$ = -64.215 ± 0.571 kJ/mol, $\Delta_f G°_m$ = -4391.266 ± 5.406 kJ/mol

$Th^{4+} + 3\ SO\ _{2-} \leftrightharpoons Th(SO\ )\ _{2-}$

log K = 10.75 ± 0.07, $\Delta_r G°_m$ = -61.361 ± 0.400 kJ/mol, $\Delta_f G°_m$ = -2998.156 ± 5.459 kJ/mol
ε $Na_+/Th(SO\ )\ _{2-}$ = -0.091 ± 0.038

These values differ slightly from those included in WIPP PA: log K $[Th(SO_4)_2]$ = -11.6, log K $[Th(SO_4)_2 \cdot 9H_2O]$ = -13.0, and log K $[Th(SO\ )\ _{2-}]$ = -12.4. The sign difference between these reactions and those listed in Appendix GEOCHEM are due to the NEA reactions being shown as formation and GEOCHEM shown as dissociation. These differences are however inconsequential to the overall solubility calculations as sulfate complexation does not have a significant impact.

Thorium Colloidal Species

Thorium is well known for its colloidal behavior in high-ionic strength alkaline solutions (see the many discussions of this in CRA-2014 and CRA-2019 Appendix SOTERM). These colloids are usually small (<10 nm, and often ~1-2 nm) and can be treated as thermodynamically stable species. Unlike Pu(IV) colloids, Th colloids are stable for years in solution (Borkowski et al. 2012). Th colloids have been measured at concentrations of 10^{-6} M in NaCl, $NaClO_4$, and $MgCl_2$ solutions independent of ionic strength and pH (al. 2004). This exceeds the typical solubility at pH 8-10 by roughly two orders of magnitude. Modeling these colloids can be accomplished through the use of polymeric species $Th_x(OH)_{y4x-y}$, several of these species have thermodynamic data included in the NEA and ThermoChimie Databases as follows:

$2\ Th^{4+} + 2\ H_2O \leftrightharpoons Th_2(OH)_2^{6+} + 2\ H_+$

log K = -5.90 ± 0.50, $\Delta_r G°_m$ = 33.677 ± 2.854 kJ/mol, $\Delta_f G°_m$ = -1850.169 ± 10.974 kJ/mol
$\Delta_r H°_m$ = 58.300 ± 5.700 kJ/mol, $\Delta_f H°_m$ = -2050.760 ± 7.325 kJ/mol
$\Delta_r S°_m$ = 82.585 ± 21.380 J/mol·K, $\Delta_f S°_m$ = -623.714 ± 44.264 J/mol·K
ε $Cl^-/Th_2(OH)_2$
$^{6+}$ = 0.40 ± 0.16
ε $ClO_4^-/Th_2(OH)_2$
$^{6+}$ = 1.22 ± 0.24
ε $NO_3^-/Th_2(OH)_2$
$^{6+}$ = 0.69 ± 0.26

$2\ Th^{4+} + 3\ H_2O \leftrightharpoons Th_2(OH)_3^{5+} + 3\ H_+$

log K = -6.80 ± 0.20, $\Delta_r G°_m$ = 38.814 ± 1.142 kJ/mol, $\Delta_f G°_m$ = -2082.172 ± 10.658 kJ/mol
ε $Cl^-/Th_2(OH)_3$
$^{5+}$ = 0.29 ± 0.09
ε $ClO_4^-/Th_2(OH)_3$
$^{5+}$ = 0.91 ± 0.21
ε $NO_3^-/Th_2(OH)_2$
$^{5+}$ = 0.69 ± 0.25

$4\ Th^{4+} + 8\ H_2O \leftrightharpoons Th_4(OH)_8^{8+} + 8\ H^+$

log K = -20.40 ± 0.40, $\Delta_r G°_m$ = 116.443 ± 2.283 kJ/mol, $\Delta_f G°_m$ = -4599.809 ± 21.317 kJ/mol
$\Delta_r H°_m$ = 243.000 ± 21.300 kJ/mol, $\Delta_f H°_m$ = -5118.440 ± 23.204 kJ/mol
$\Delta_r S°_m$ = 424.473 ± 71.850 J/mol·K, $\Delta_f S°_m$ = -708.330 ± 105.703 J/mol·K
ε $Cl^-/Th_4(OH)_8^{8+}$ = 0.70 ± 0.20
ε $ClO^-/Th(OH)^{8+}$ = 1.69 ± 0.42
ε $NO^-/Th(OH)^{8+}$ = 1.59 ± 0.51

$4\ Th^{4+} + 12\ H_2O \leftrightharpoons Th_4(OH)^{4+} + 12\ H^+$

log K = -26.60 ± 0.20, $\Delta_r G°_m$ = 151.833 ± 1.142 kJ/mol, $\Delta_f G°_m$ = -5512.979 ± 21.228 kJ/mol
ε $Cl^-/Th_4(OH)^{4+}$ = 0.25 ± 0.20
ε $ClO^-/Th(OH)^{4+}$ = 0.56 ± 0.42
ε $NO^-/Th(OH)^{4+}$ = 0.42 ± 0.50

$6\ Th^{4+} + 14\ H_2O \leftrightharpoons Th_6(OH)^{10+} + 14\ H^+$

log K = -36.80 ± 1.20, $\Delta_r G°_m$ = 210.055 ± 6.850 kJ/mol, $\Delta_f G°_m$ = -7338.603 ± 32.523 kJ/mol
ε $Cl^-/Th_6(OH)^{10+}$ = 0.8 ± 0.3
ε $ClO^-/Th(OH)^{10+}$ = 2.2 ± 0.3
ε $NO^-/Th(OH)^{10+}$ = 2.9 ± 0.5

$6\ Th^{4+} + 15\ H_2O \leftrightharpoons Th_6(OH)^{9+} + 15\ H^+$

log K = -36.80 ± 1.50, $\Delta_r G°_m$ = 210.055 ± 8.562 kJ/mol, $\Delta_f G°_m$ = -7575.743 ± 32.927 kJ/mol
$\Delta_r H°_m$ = 472.800 ± 22.000 kJ/mol, $\Delta_f H°_m$ = -8426.850 ± 25.977 kJ/mol
$\Delta_r S°_m$ = 881.252 ± 79.180 J/mol·K, $\Delta_f S°_m$ = -608.106 ± 140.699 J/mol·K
ε $Cl^-/Th_6(OH)^{9+}$ = 0.72 ± 0.30
ε $ClO^-/Th(OH)^{9+}$ = 1.85 ± 0.74
ε $NO^-/Th(OH)^{9+}$ = 2.20 ± 0.77

Of these species, $Th_4(OH)^{8+}$ and $Th(OH)^{9+}$, along with the hydrolysis species $Th(OH)^{4-x}$ ($x \leq 4$) were all found to be important for describing the solubility of ThO2 in 1 M HClO4 (Ekberg et al.2000). The NEA review of this literature explicitly states that Pitzer parameters derived from Rai et al. 1997 should not be combined with solubility and hydrolysis constants selected in the review due to the absence of hydrolysis in their model.

These modeled hydrolysis and polynuclear species were expressly excluded in the CCA based on a study that was able to simulate Th solubility in up to 3 M NaCl solutions (Felmy et al. 1991). This view, however, was changed in CRA-2014 based on WIPP-specific experimental results. In this context, the current WIPP PA approach overestimates An(IV) colloidal contributions by using sequential filtration data from long-term WIPP specific data (Reed et al. 2013) rather than the use of detailed high ionic-strength models for colloidal behavior.

<u>Thorium EDTA Complexes</u>

A 2001 report generated for Sandia National Laboratories explored the complexation of thorium with several organic ligands (Choppin et al. 2001). The Th-EDTA data included the effects of interferences due to the presence of Th hydrolysis species and Na-EDTA competition. The authors recommended that the value of log β [Th(EDTA)] = -17 be used for performance assessment purposes, as it included the effects of the additional species. A more recent study on the solubility of ThO_2(am) in the aqueous Na^+-H^+-OH^-–NO_3^--H_2O-EDTA system has been published (Xia et al. 2003). The results of this study indicate that between pH 4.2 and 8.2, the 1:1 complex Th(EDTA) is the only species controlling Th solubility. Above

pH= 9, the solubility decreased and hydrolyzed Th(EDTA) complexes $Th(OH)_2EDTA^{2-}$ and $Th(OH)_3EDTA^{3-}$ contribute to the solubility. This is in contrast to earlier work which attributed the decrease in solubility to the formation of $Th(OH)EDTA^-$ and $[Th(OH)EDTA]_2$ (Martell and Smith 1995). XAFS analysis of the high pH solutions showed no indication of Th-Th bonding, excluding the presence of any polynuclear Th species (Martell and Smith 1995). Equilibrium constants for the two hydrolysis species were given as:

$ThO_2(am) + EDTA^{4-} + 2\ H_2O \leftrightharpoons Th(OH)_2(EDTA)^{2-} + 2\ OH^-$, log K = -6.0

$ThO_2(am) + EDTA^{4-} + 2\ H_2O \leftrightharpoons Th(OH)_3(EDTA)^{3-} + OH^-$, log K = -7.5

The ThermoChimie database selects the two complexes from Martell and Smith:

$Th^{4+} + EDTA^{4-} + H_2O \leftrightharpoons Th(EDTA)(OH)^- + H^+$

log K = 19.50 ± 0.42, $\Delta_r G°_m$ = -111.306 ± 2.397 kJ/mol

$2\ Th^{4+} + 2\ EDTA^{4-} + 2\ H_2O \leftrightharpoons [Th(EDTA)(OH)]_2^{2-} + 2\ H^+$

log K = 43.70 ± 0.50, $\Delta_r G°_m$ = -249.440 ± 2.854 kJ/mol

There is still disagreement on the speciation of Th-EDTA at high pH in high ionic strength brines although it is clear that EDTA complexation can impact the high-pH speciation of U(IV), Np(IV) and Pu(IV) under some circumstances that are WIPP-relevant. This is perhaps a case where the very different colloidal/hydrolysis behavior of thorium masks the impacts of hydrolyzed EDTA complexes on the other An(IV) solubilities. This effect and concern is somewhat mitigated when the complexation of EDTA with Ca^{2+}, Na^+, and Mg^{2+} is taken into account as EDTA complexation with actinides is significantly reduced. This was confirmed when the solubility of Th in Ca(OH)2 solution was shown to be independent of the presence of EDTA, indicating that Ca-EDTA complexes were preferentially formed (Felipe-Sotelo et al. 2015).

Thorium Oxalate Complexes

One thorium oxalate complex is included in the WIPP source term, $Th(Ox)^{2+}$. This was determined from the data in Choppin et al. 2001. In an earlier study, stability constants were determined for multiple thorium oxalate complexes in 1-9 M $NaClO_4$ solutions at a pH range of 1.3-4, well below that of the WIPP system (Erten et al. 1994). This study found four species: $Th(Ox)^{2+}$, $Th(HOx)^{3+}$, $Th(Ox)_2$, and $Th(HOx)2^{2+}$, however they did not obtain sufficient data for Pitzer parameter determination of these complexes. Log K of $Th(Ox)^{2+}$ is given as -11.4 in the WIPP model, this differs slightly from the value selected by the ThermoChimie database that is based on NEA data:

$Th^{4+} + ox^{2-} \leftrightharpoons Th(ox)^{2+}$

log K = 9.70 ±0.10, $\Delta_r G°_m$ = -55.368 ± 0.571 kJ/mol, $\Delta_f G°_m$ = -1440.285 ± 5.634 kJ/mol

Additional reactions supporting the speciation proposed in Erten et al. 1994 are also selected:

$Th^{4+} + 2\ ox^{2-} \leftrightharpoons Th(ox)_2$

log K = 16.00 ±0.60, $\Delta_r G°_m$ = -91.328 ± 3.425 kJ/mol, $\Delta_f G°_m$ = -2156.379 ± 7.292 kJ/mol

$Th^{4+} + H^+ + ox^{2-} \leftrightharpoons Th(Hox)^{3+}$

log K = 11.00, $\Delta_r G°_m$ = -62.788 kJ/mol, $\Delta_f G°_m$ = -1447.705 kJ/mol

$Th^{4+} + 2\ H^+ + 2\ ox^{2-} \leftrightharpoons Th(Hox)^{2+}$

log K = 18.13, $\Delta_r G°_m$ = -103.486 kJ/mol, $\Delta_f G°_m$ = -2168.537 kJ/mol

Overall, Th-oxalate complexation is not expected to have a significant impact on the An(IV) solubility in the WIPP when compared to the effects of hydrolysis and the presence of stronger organic complexes (e.g., EDTA and Citrate).

Thorium Acetate Complexes

Thorium acetate complex formation was studied in Choppin et al. 2001. They determined stability constants for $Th(ac)_{3+}$ and $Th(ac)_{2+}$ in 0.3 to 5 M NaCl. The stability constants derived from these data match closely to that of Rao et al. 2005. In this study, stability constants for three additional Th-acetate complexes, $Th(ac)_{+}$, Th(ac) , and $Th(ac)_{-}$ were determined by titration potentiometry and calorimetry in 1 M $NaClO_4$ (Rao et al. 2005).

Th_{4+} + acetate$_{-}$ ⇋ Th(acetate)$_{3+}$

log K = 3.79 ± 0.02, $\Delta_r G°_m$ = -21.6 kJ/mol, $\Delta_r H°_m$ = 12.2 ± 0.18 kJ/mol, $\Delta_r S°_m$ = 114 ± 1 J/mol·K

Th_{4+} + 2 acetate$_{-}$ ⇋ Th(acetate)$_{2+}$

log K = 6.79 ± 0.02, $\Delta_r G°_m$ = -38.8 kJ/mol, $\Delta_r H°_m$ = 16.9 ± 0.27 kJ/mol, $\Delta_r S°_m$ = 187 ± 1 J/mol·K

Th_{4+} + 3 acetate$_{-}$ ⇋ Th(acetate)$_{+}$

log K = 8.71 ± 0.13, $\Delta_r G°_m$ = -49.7 kJ/mol, $\Delta_r H°_m$ = 30.8 ± 0.7 kJ/mol, $\Delta_r S°_m$ = 270 ± 3 J/mol·K

Th_{4+} + 4 acetate$_{-}$ ⇋ Th(acetate)$_4$

log K = 10.17 ± 0.25, $\Delta_r G°_m$ = -58.0 kJ/mol, $\Delta_r H°_m$ = 30.7 ± 1.4 kJ/mol, $\Delta_r S°_m$ = 298 ± 7 J/mol·K

Th_{4+} + 5 acetate$_{-}$ ⇋ Th(acetate)$_{-}$

log K = 11.41 ± 0.22, $\Delta_r G°_m$ = -65.1 kJ/mol, $\Delta_r H°_m$ = 38.9 ± 0.8 kJ/mol, $\Delta_r S°_m$ = 349 ± 5 J/mol·K

A more recent study determined the stability constants of thorium acetate complexes using capillary electrophoresis coupled to inductively coupled plasma mass spectrometry (ICP-MS) (Willberger et al. 2019). This work determined the stability constants for the same five species as Rao et al. 2005, but with values roughly one log unit higher. The values selected in the ThermoChimie database are about two log units higher than those determined by Rao and Choppin (Richard et al. 2011).

Both of these newer sets of data show that the current WIPP model may underestimate the impact of acetate on thorium solubility. This, however, is largely inconsequential for the same reasons discussed in the case of oxalate: strong hydrolysis at pH ~9 and competition with EDTA and citrate. Additionally, the survival of acetate in the WIPP environment is unlikely due to its high likelihood to undergo biodegradation.

Thorium Citrate Complexes

WIPP PA currently includes one Th-citrate complex, $Th(citrate)_{+}$, with log K = 15.2 (Choppin et al. 2001). A more recent publication has studied the interaction of thorium with citrate in 0.5-6 M $NaNO_3$ in neutral to basic conditions (Felmy et al. 2006). Two sets of experiments were performed to explain the effects of both pH and citrate on the solubility of ThO_2. The first set of experiments were performed with a fixed concentration of citrate while varying pH. Above pH = 8 the solubility decreases with a slope of -1, indicating that the forward reaction would only contain one proton. The second set of experiments studied the effect of citrate concentration on the solubility. These results indicated that between two and three citrate ligands were present around each thorium atom, again determined by slope analysis of the solubility curve. The results of these two sets of experiments led to the proposed

species $Th(OH)_3(H_{-1}Cit)^{5-}$, $Th(H_{-1}Cit)^{2-}$ $Th(OH)(Cit)^{5-}$ and $Th(OH)(Cit)_8H$ Cit indicates that the hydroxyl proton is also removed from the citrate group. The two species without hydroxyl deprotonation were also used to describe ThO_2 solubility in saturated $Ca(OH)_2$ solution (Felipe-Sotelo et al. 2015). Equilibrium constants were given for those species as follows:

$$ThO_2(am) + H_2O + 3\ Cit^{3-} + H^+ \leftrightharpoons Th(OH)_3(Cit)^{8-};\ \log K = -2.4$$

$$ThO_2(am) + 3\ Cit^{3-} + H^+ \leftrightharpoons Th(H_{-1}Cit)^{8-} + 2\ H_2O;\ \log K = -2.4$$

$$ThO_2(am) + H_2O + 2\ Cit^{3-} + H^+ \leftrightharpoons Th(OH)_3(Cit)^{5-};\ \log K = -4.5$$

$$ThO_2(am) + 2\ Cit^{3-} + H^+ \leftrightharpoons Th(OH)_3(H_{-1}Cit)^{5-};\ \log K = -4.5$$

The WIPP model does not currently have these high pH species for citrate (a similar problem was observed for EDTA). The potential impact of citrate, however, is likely mitigated by the competition of hydrolysis and other cations (Mg, Ca, Fe and Pb).

Summary of Overall Assessment

The WIPP An(IV) model, based on thorium, remains a conservative and defensible approach as currently implemented in the CRA-2019 WIPP PA and over-predicts An(IV) solubility as well as the uncertainty associated with this solubility.

That being said, there are new data and insights that if used would strengthen the already conservative WIPP An(IV) model, for example:

- There is really no need to continue to consider any Th-sulfate species in the WIPP model. These species have essentially no impact on the solubility of An(IV) at the pH ~ 9 or higher expected in the WIPP.
- Thorium hydrolysis and carbonate effects on solubility: this could be revised slightly by considering the more recent INE and NEA-selected data for these two systems. This would improve the credibility of the WIPP model but would not be likely to have a significant impact on the solubilities calculated.
- The impacts of organics: the WIPP model could be revised to model Th-organic interactions and the interactions of all the organics with other cations (Mg, Ca, Fe and Pb) to model the impacts of organics. However, when the brine system is fully modeled, the expectation is that the cation-competition effect will mitigate the organic complexation effect so there would be little to no effect on the net solubilities calculated. This is more an issue of the completeness of the model rather than the omission of key potential impacts on the releases calculated in WIPP PA.
- The WIPP An(IV) core model could be based on U(IV) and/or Np(IV) data rather than Th(IV). This would improve the relevance of the model for predicting the solubility and colloidal behavior of Pu(IV) under WIPP relevant conditions, which is the most important An(IV) species in assessing the performance of the WIPP.

References

References with hyperlinks were provided in prior CRAs. The remainder of the reference documents will be provided in Enclosure 4 or as otherwise noted.

Altmaier, M., V. Neck and Th. Fanghanel. 2004. Solubility and colloid formation of Th(IV) in concentrated NaCl and $MgCl_2$ solution. Radiochimica Acta. 2004(92), 537-543.

Altmaier, M., V. Neck, M.A. Denecke, R. Yin and Th. Fanghanel. 2006. Solubility of $ThO_2 \cdot xH_2O$(am) and the formation of ternary Th(IV) hydroxide-carbonate complexes in $NaHCO_3$- Na_2CO_3 solutions containing 0-4 M NaCl. Radiochimica Acta. 2006(94), 495-500.

Altmaier, M., D. Fellhauer, X. Gaona and E. Yalcintas. 2017. Assessment of Np(IV) and U(IV) as Improved Analogs for Pu(IV) in High Ionic-Strength Brine Systems. Karlsruhe Institute of Technology Report. Karlsruhe, Germany. KIT/INE Report.

Borkowski, M., R.C. Moore, M.G. Bronikowski, J. Chen, O.S. Pokrovsky, Y. Xia and G.R. Choppin. 2001. Thermodynamic Modeling of Actinide Complexation with Oxalate at High Ionic Strength. J. Journal of Radioanalytical and Nuclear Chemistry. 2017(248), 467-471.

Borkowski, M. and M. Richmann. 2009. Comparison of Recent Thorium Thermodynamic Data with those used in the WIPP FMT_050405.CHEMDAT Database. Los Alamos National Laboratory Report ACP-0911-01-03-01. LA UR 09-07298.

Borkowski, M., M. Richmann and J.-F. Lucchini. 2012. *Solubility of An(IV) in WIPP Brine: Thorium Analog Studies in WIPP Simulated Brine*. Los Alamos National Laboratory; Carlsbad, NM. LCOACP- 17. LA-UR-12-24417.

Choppin, G., A. Bond, M. Borkowski and M.G. Bronikowski, J.F. Chen, S. Lis, J. Mizera, O. Pokrovsky, N. Wall, Y. Xia and R.C. Moore. 2001. Waste Isolation Pilot Plane Actinide Source Term Test Program: Solubility Studies and Development of Modeling Parameters. Sandia National Laboratories Report. ERMS 518556 SAND99-0943.

Ekberg, C., Y. Albinsson, M. Comarmond and P. Brown. 2000. Studies on the Behavior of Thorium(IV). Journal of Solution Chemistry 2000(29), 63-86.

Erten, H., A. Mohammed and G.R. Choppin. 1994. Variation of Stability Constants of Thorium and Uranium Oxalate Complexes with Ionic Strength. Radiochimica Acta 1994 (66/67), 123-128.

Felipe-Sotelo, M., M. Edgar, T. Beattie, P. Warwick, N.D.M. Evans and D. Read. 2015. Effect of Anythropogenic Organic Complexants on the Solubility of Ni, Th, U(IV) and U(VI). Journal of Hazardous Material 2015(300), 553-560.

Felmy, A., D. Rai and M.J. Mason. 1991. The Solubility of Hydrous Thorium(IV) Oxide in Chloride Media: Development of an Aqueous Ion-Interaction Model. Radiochimica Acta (55), 177-185.

Felmy, A. and D. Rai. 1992. An aqueous Thermodynamic Model for a High Valence 4:2 Electrolyte Th^{4+}-SO_4^{2-} in the System Na^+-K^+-Li^+-NH_4^+-Th^{4+}-SO_4^{2-}-HSO_4^--H O to High Concentration. Journal of Solution Chemistry 1992(21), 407-423.

Felmy, A., D. Rai, S.M. Sterner, M.J. Mason, N.J. Hess and S.D. Conradson. 1997. Thermodynamic Models for Highly Charged Aqueous Species: Solubility of Th(IV) Hydrous Oxide in Concentrated $NaHCO_3$ and Na_2CO_3 Solutions. Journal of Solution Chemistry 1997(26), 233-248.

Felmy, A. and D. Rai. 1999. Application of Pitzer's Equations for Modeling the Aqueous Thermodynamics of Actinide Species in Natural Waters: A Review. Journal of Solution Chemistry 1999(28), 533-553.

Felmy, A., H. Cho, D.A. Dixon, Y. Xia, N.J. Hess and Z. Wang. 2006. The Aqueous Complexation of Thorium with Citrate under Neutral to Basic Conditions. Radiochim. Acta. 2006(94), 205-212.

Giambalvo, E. 2002a. Recommended Parameter Values for Modeling An(IV) Solubility in WIPP Brines. Memo to L.H. Brush. Sandia National Laboratories. ERMS 522986

Giambalvo, E. 2002b. Recommended Parameter Values for Modeling Organic Ligands in WIPP Brines. Memo to L.H. Brush. Sandia National Laboratories. ERMS 522981.

Giambalvo, E. 2002c. Recommended μ_0/RT Values for Modeling the Solubility of Oxalate Solids in WIPP Brines. Memo to L.H. Brush. Sandia National Laboratories. ERMS 523057.

Kim, E. and K. Osseo-Asare. 2012. Aqueous stability of thorium and rare earth metals in monazite hydrometallurgy: Eh-pH diagrams for the systems Th-, Ce-, La-, Nd- (PO_4)- (SO_4)- H_2O at 25 °C. Hydrometallurgy 2012(113-114), 67-78.

Martell, A. and R. Smith. 1995. Critically Selected Stability Constants of Metal Complexes Database. Version 2.0 NIST Standard Reference Data Program. Gaithersburg, MD.

Neck, V. and J. Kim. 2001. J.I. Solubility and hydrolysis of tetravalent actinides. Radiochimica Acta 2001(89), 1-16.

Novak, C. 1996. Preliminary Inorganic Model for Thorium Solubility in WIPP Brines. Memo to E.J. Nowak. Sandia National Laboratories. ERMS 230930.

Novak, C. 1997. Calculation of Actinide Solubilities in WIPP SPC and ERDA-6 Brines under MgO Backfill Scenarios Containing either Nesquehonite or Hydromagnesite as the Mg-CO_3 Solubility limiting Phase. Memo to R. V. Bynum. Sandia National Laboratories. ERMS 246124.

Nowak, E. 2005. Recommended Change in the FMT Thermodynamic Data Base. Memorandum to L.H. Brush, Sandia National Laboratories, Carlsbad, New Mexico. ERMS 539227.

Nuclear Energy Agency, Thermochemical Database (TDB). 2003. Organization for Economic Cooperation and Development, Accessed at https://www.oecd-neat.org/dbtdb/tdb2.

Östhols, E., J. Bruno and I. Grenthe. 1994. On the Influence of Carbonate on Mineral Dissolution III. The Solubility of Microcrystalline ThO_2 in CO_2-H_2O Media. Geochimica. Et Cosmochimica Acta 1994(58), 613-623.

Pitzer, K.S. and G. Mayorga. 1973. Thermodynamics of Electrolyes. II. Activity and Osmotic Coefficients for Strong Electrolytes with One or Both Ions Univalents. Journal of Physical Chemistry 1973 (77), 2300-2308.

Rai, D., A. Felmy, S. Sterner, D. Moore and M. Mason. 1997. The Solubility of Th(IV) and U(IV) Hydrous Oxides in Concentrated NaCl and $MgCl_2$ Solutions. Radiochimica Acta 1997(79), 239- 247.

Rand, M.H., J. Fuger, I. Grenth, V. Neck and D. Rai. 2008. Chemical Thermodynamics of Thorium. OECD-NEA Chemical Thermodynamics Series, Volume 11.

Rao, L., P. Zanonato and P. Di Bernardo. 1995. Interaction of Actinides with Carboylates in Solutions: Complexation of U(VI), Th(IV), and Nd(III) with Acetate at Variable Temperature. Journal of Nuclear and Radiochemical Sciences 1995(6), 31-37.

Reed, D.T., J. Swanson, J-F. Lucchini and M. Richmann. 2013. Intrinsic, Mineral, and Microbial Colloid Enhancement Parameters for the WIPP Actinide Source Term. Report LCO-ACP-18, Carlsbad, NM: Los Alamos National Laboratory. LA-UR 13-20858.

Richard, L., M. Grieve and L. Duro. 2011. Selection of Formation Constants for Acetate Complexes of Ca and Radionuclides. *ANDRA-TDB7 Task 3 Organics.*

Roy, R., K. Vogel, C. Good, W. Davis, L. Roy, D. Johnson, A. Felmy and K. Pitzer. 1992. Activity Coefficients in Electrolyte Mixtures: HCl + ThCl4 + H2O for 5-55 C. Journal of Physical Chemistry 1992 (96), 11065-11072.

Ryan, J. and D. Rai. 1987. Thorium(IV) Hydrous Oxide Solubility. Inorganic Chemistry 1987(26), 4140-4142.

U.S. Department of Energy (DOE). 1996. Title 40 CFR Part 191 Compliance Certification Application for the Waste Isolation Pilot Plant (October). 21 vols. Carlsbad Field Office, Carlsbad, NM. DOE/CAO-1996-2184

U.S. Department of Energy (DOE). 2004. Title 40 CFR Part 191 Compliance Recertification Application for the Waste Isolation Pilot Plant (March). 10 vols. Carlsbad Field Office, Carlsbad, NM. DOE/WIPP 2004-3231.

U.S. Department of Energy (DOE). 2009. Subparts B and C Compliance Recertification Application 2009, Appendix PA, Attachment SOTERM, DOE Carlsbad Field Office, Carlsbad, NM.

U.S. Department of Energy (DOE). 2014. Title 40 CFR Part 191 Subparts B and C. Compliance Recertification Application for the Waste Isolation Pilot Plant (March 26, 2019 and December 18, 2019). Appendix SOTERM. Carlsbad Field Office, Carlsbad, NM. DOE/WIPP 2019-3609.

U.S. Department of Energy (DOE). 2019. Title 40 CFR Part 191 Subparts B and C. Compliance Recertification Application for the Waste Isolation Pilot Plant (March 26, 2019 and December 18, 2019). Carlsbad Field Office, Carlsbad, NM. DOE/WIPP 2019-3609.

Willberger, C., D. Leichtfuβ, S. Amayri and T. Reich. 2019. Determination of the Stability Constants of the Acetate Complexes of the Actinides Am(III), Th(IV), Np(V), and U(VI) Using Capillary Electrophoresis-Inductively Coupled Plasma Mass Spectrometry. Inorganic Chemistry 2019(58), 4851-4858.

Xia, Y., A. Felmy, L. Rao, Z. Wang and N. Hess. 2003. Thermodynamic Model for the Solubility of ThO_2(am) in the aqueous Na_+-H_+-OH–NO –H O-EDTA System. Radiochimica Acta 2003(91), 751-760.

EPA Evaluation of Response

The DOE response was satisfactory. The information was provided as requested.

CC2-GEN-2 Cutoff Dates

WIPP Compliance Recertification Application 2019

EPA Question (from EPA Completeness Comment Package 2)

How do the data cutoff dates used for DPA-2019 affect the compliance conclusions presented in the CRA-2019? For example, ATWIR-2017 has a data cutoff date of 12/31/2016 and was used to present the waste characteristics data in Section 24. However, the ATWIR used to make the PAIR for the DPA uses ATWIR-2018, with a data cutoff date of 12/31/2017 and the data from this document is used to generate scaled waste values and other data related to Section 24. Please provide a separate explanation with supporting rationale for each occurrence.

DOE Response (from DOE Response Package 3)

Each Compliance Recertification Application (CRA) documents the most up-to-date information available to demonstrate the Waste Isolation Pilot Plant's (WIPP) continued compliance with the U.S. Environmental Protection Agency's (EPA) disposal regulations. This approach is mandated by 40 CFR 194.15(a) which requires the Department of Energy (DOE) to report any new WIPP-relevant information and data that have become available since the last CRA. In order for the DOE to develop, review and submit CRA documentation to the EPA every five years in accordance with the WIPP Land Withdrawal Act (LWA), a data cutoff date 14 to 15 months prior to submittal is necessary. Historically, the DOE has submitted a CRA and subsequently submitted updated performance assessment (PA) documentation (i.e., a Performance Assessment Baseline Calculation [PABC], for CRA-2004 and CRA-2009) in the same recertification cycle. In such cases, the CRA and the PABC used different dates for the cutoff of data used in PA calculations, but collectively presented the most current information available.

Data cutoffs are also routinely used for the Annual Transuranic Waste Inventory Report (ATWIR). The ATWIR is updated on a yearly cycle to provide the latest inventory data for managing the Transuranic (TRU) waste complex and for performing compliance-related calculations, including PA calculations submitted with the CRA and other regulatory calculations, such as the Deferred PA (DPA). The ATWIR uses a cutoff date of December 31 for data gathered from all the active TRU waste generator sites during the prior calendar year. The inventory data provided with the CRA-2019 is based on ATWIR-2017, the most recent ATWIR before the CRA data cutoff. The DPA-2019 uses ATWIR-2018 which is the most recent ATWIR available at the time calculations were performed. The data from the ATWIR's are used to scale the inventory data to a full repository and are presented in the Performance Assessment Inventory Report (PAIR) that supports the PA's.

The CRA-2019 was submitted in two parts 1) the main body of the application submitted in March 2019, and 2) the DPA-2019 submitted in December 2019. The CRA-2019 and the subsequent DPA-2019 use different data cutoff dates, but collectively document updates and changes since the current regulatory baseline, the CRA-2014. Based on information presented in both the CRA-2019 main body and

subsequent DPA-2019, the DOE continues to demonstrate continued compliance with certification regulations, and neither affects the compliance conclusions presented in either document.

EPA Evaluation of Response

The DOE response was partially adequate. The response was more general than expected, however EPA was able to later ask for more specific information.

CC2-24-2 Table Updates

40 CFR §194.24 Waste Characterization

EPA Question (from EPA Completeness Comment Package 2)

CC2-24-2a. ***Request to Update Tables 24-2, 24-3, 24-4, 24-5 and 24-6 to reflect the ATWIR-2018***

Please update Tables 24-2, 24-3, 24-4, 24-5, and 24-6 to reflect the ATWIR-2018, rather than the ATWIR-2017 since ATWIR-2018 is the version used for the DPA submission.

Section 24a of CRA-2019 cites ATWIR-2017 to make tables 24-2, 24-3, 24-4, 24-5, and 24-6. ATWIR-2017 has a data cutoff date of 12/31/2016. However, the ATWIR used to make the PAIR for the DPA uses ATWIR-2018, with a data cutoff date of 12/31/2017.

DOE Response (from DOE Response Package 4)

> As described in the U.S. Department of Energy (DOE) response to CC2-GEN-2 Cutoff Dates (DOE 2020), the 2019 Compliance Recertification Application (CRA-2019) was submitted in two parts, each with different data cutoff dates. Section 24, *Waste Characterization*, of the CRA-2019 application presented data from the Annual Transuranic Waste Inventory Report - 2017 (ATWIR-2017), because at the time of submittal, it reported the latest data that had become available since the CRA-2014.
>
> The transuranic (TRU) waste inventory information used for performance assessment in the CRA-2014 and the CRA-2019 Deferred Performance Assessment (DPA) is provided in Table 1 below. Please note that no changes will be made to Tables 24-2, 24-3, 24-4, 24-5, and 24-6 in Section 24 of the CRA-2019 application as a result of this response.

Table 1. Waste Characteristics Reported in the CRA-2014 and CRA-2019 Deferred Performance Assessment

		CRA-2014 Inventory Cutoff Date 12/31/2011		CRA-2019 DPA Inventory Cutoff Date 12/31/2017	
		ATWIR-2012	PAIR-2012 (Scaled)	ATWIR-2018	PAIR-2018 (Scaled)
Volume (m^3)	CH	147,000	168,000	154,000	168,000
	RH	3,840	7,080	2,980	7,080
Activity (Ci)	CH	3,480,000	2,700,000	5,480,000	5,120,000
	RH	1,200,000	936,000	1,070,000	1,010,000
Waste Materials including Cement(kg)		45,700,000	56,700,000	52,700,000	62,700,000
Packaging Materials (kg)		33,900,000	40,500,000	46,800,000	66,200,000
Emplacement/Operational Materials (kg)		Not Available	1,510,000*	Not Available	1,780,000*
Organic Ligands (kg)		19,500	50,700*	18,900	55,400*
Oxyanions (kg)		1,070,000	2,380,000*	721,000	2,420,000*

Note: Numerical values in this table are rounded to three significant figures.
* Includes estimates of emplaced mass derived through separate analyses.

The TRU waste inventory information presented in the ATWIR-2012 reflects the collection date for all TRU waste emplaced, stored, or projected to be generated through calendar year (CY) 2033. At the direction of DOE/Carlsbad Field Office (CBFO), the ATWIR-2018 focused on all TRU waste emplaced, stored, and projected to be generated through CY 2033 in order to reflect the Waste Isolation Pilot Plant (WIPP) facility closure date for the CRA-2019 DPA (Shrader 2018). The Performance Assessment Inventory Reports (PAIRs) are based on the annual inventory collected from the TRU waste sites and documented in an ATWIR, which is then scaled to simulate the WIPP repository filled to its legislated capacity. The PAIR-2012 and PAIR-2018 both report TRU waste emplaced, stored, and projected to be generated through CY 2033.

The radionuclide activity reported for the ATWIR-2012 and ATWIR-2018 is decayed through the data collection years of 2011 and 2017, respectively. The radionuclide activity reported for both the PAIR-2012 and PAIR-2018 is decayed through the common year of 2033.

The waste materials in the TRU waste containers and the packaging materials associated with the WIPP-approved containers were reported in both the ATWIRs and the PAIRs. The emplacement and operational materials are “Not Available” in the ATWIRs, but are reported in the PAIRs because a supplemental analysis (Callicoat 2018) was performed to derive the total scaled emplacement and operational material estimates. These estimates were determined using the reported emplaced, stored, and projected container types identified in the ATWIRs and the WIPP Waste Data System (WDS).

The ATWIR-2012 and ATWIR-2018 report the unscaled stored and projected mass of organic ligands and oxyanions. The PAIR-2012 and PAIR-2018 includes the total scaled (estimated emplaced, stored, and projected) organic ligand and oxyanion mass. Since the emplaced organic

ligand and oxyanion mass is not tracked by the WDS, the estimated mass was derived through analyses (Young 2018).

References

Callicoat, J. 2018. Estimation of Cellulose, Plastic, and Rubber Emplacement and Operational Materials in the Waste Isolation Pilot Plant. INV-SAR-51, Revision 0. December 13, 2018. LANLCO, Carlsbad, NM.

Shrader, T. 2018. Assumption for the WIPP Facility Closure Date for the Purpose of Preparing the 2018 Annual TRU Waste Inventory Report and Performance Assessment Inventory Report for use in the Compliance Recertification Application – 2019. August 28, 2018, CBFO:OEP:MRB:AC:18-0345:UFC 5486.00. Carlsbad Field Office, Carlsbad, NM.

U.S. Department of Energy. 2020. R. Knerr to L. Veal. Response 3 to U.S. Environmental Protection Agency's 2019 Compliance Recertification Application Completeness Comments Letters dated March 23, 2020 and May 6, 2020 from Tom Peake to Mike Brown. August 13, 2020.

Young, J. 2018. Chemical and Cement Components 2017 Inventory Estimates. INV-SAR-50, Revision 0. December 13, 2018. LANL-CO, Carlsbad, NM.

EPA Question

CC2-24-2b. ***Request to Update Enclosure 2 List of Waste Characteristics from Sosson (2019)***

Enclosure 2 of Sosson (2019) provides a list of waste characteristics being examined for the PA (as required by 40 CFR 194.24(b)(1)) that is incomplete. Please update the list to include colloidal suspensions, waste compactability, and any new characteristics that have been used for the PA. Additionally, please include references to where these characteristics have been addressed.

DOE has provided a crosswalk (Enclosure 2, Sosson 2019) to indicate where different sections of the CRA are addressed with the submission of the DPA. Section 24(b)(1) of the crosswalk provides citations for the following parameters:

- *Radioactivity in curies*
- *Solubility*
- *Organic ligands*
- *Metals, CPR, oxyanions*
- *Steel corrosion, Fe sulfidation*
- *Gas production*
- *Waste shear strength*

Absent from this list are colloids and compactability. In previous CRAs, these characteristics were given a full discussion in Section 24 as they applied to the PA, such as with the 2014-CRA. Furthermore, if any other new parameters were added for the 2019-CRA, EPA would like to know as the Sosson et al. (2019) enclosure does not mention it.

Sosson, G. 2019. Deferred Performance Assessment for the Compliance Recertification Application 2019, Letter to L. Veal, U.S. Environmental Protection Agency, December 20, 2019.

DOE Response

The following changes were included in the CRA-2019 Deferred Performance Assessment (DPA) that relate to compliance with Section 24(b)(1).

Table 1 Significance of the Changes in Waste Components and Characteristics

Waste Component or Characteristic Used in PA	Increase or Decrease From CRA-2014 to CRA-2019	Significance
Radioactivity (Ci/m^3)	Increase (Kicker 2019a)	Required to calculate potential releases and compliance release limits
Solubility	Increase or decrease, depending on species and oxidation state (SOTERM Table 32 & 33, Domski and Sisk 2019)	Higher solubility can lead to higher releases
Organic Ligands-complexing agents	Increase (Van Soest 2018)	Higher Organic Ligand concentrations could lead to increases in actinide solubility
Amount of Ferrous Metals	Increase (Van Soest 2018)	Maintains reducing environment; increased amounts may increase potential gas generation
Lead Inventory	Increase (Van Soest 2018)	May increase gas generation and impact actinide solubilities
Amount of CPR	Increase (Van Soest 2018)	May increase gas generation from microbial processes
Oxyanions: nitrate, sulfate, and phosphate	Increase or decrease (Van Soest 2018)	May increase actinide solubility and provide microbial nutrients that lead to higher gas generation rates
Cement	Decrease (Van Soest 2018)	Significant volume changes may lead to increases in actinide solubilities
Shear Strength[1]	Decrease (Zeitler 2019; Appendix PA, Section PA-1.1.6)	Lesser waste strength may result in greater potential drilling releases
Formation of Colloidal Suspensions	Increase and/or decrease (GEOCHEM Table 61; SOTERM Tables 8 and 9; SOTERM Section 3.5.1)	Increases in colloidal content of the actinide source term will increase DBR release and may facilitate transport in the far field

1 The EPA comment identifies “compactability” as a change. The CRA-2019 DPA did not include changes to modeling waste compaction. In the CCA Appendix WCA, Table WCA-2, “compressibility and shear strength” were
identified as a characteristic. The DOE believes that EPA is referring to the changes made to the “shear strength”
parameter.

Assessment of Waste Components or Waste Characteristics and Performance Assessment Input Parameters

In the Compliance Certification Application (CCA), the U.S. Department of Energy (DOE) originally identified several waste characteristics as being potentially important to Performance Assessment (PA) (CCA Appendix WCA; DOE 1996). The CRA-2014 Section 24 provided the historical background for changes to these parameters since the CCA. The CRA-2014 identified the same important characteristics as in the CCA. As was first done in the CRA-2004, the CRA-2019 DPA continues to assert that organic ligands could be important to solubility and therefore organic ligands are included in the solubility calculations (Domski and Sisk-Scott 2019, GEOCHEM 2019-3.2.5). Additionally, the impacts of lead and iron have been added to the solubility calculations (GEOCHEM 2019-3.2.7 and 3.2.8). These changes impacted the chemical conditions process model for the CRA-2019 DPA, however there were no changes to the conceptual models.

CRA-2019 Radioactivity in Curies

The DOE used the information from the Performance Assessment Inventory Report 2018 (PAIR; Van Soest 2018) as the basis for the PA radionuclide inventory for the CRA-2019 DPA. The CRA-2019 DPA Radionuclide Inventory Screening Analysis (Kicker 2019) discusses the methodology used by the DOE to determine the Waste Isolation Pilot Plant (WIPP) repository radionuclide inventory information for use in CRA-2019 DPA calculations. The parameters for the initial radionuclide inventory decayed to the WIPP facility closure date, and those calculated based on the initial radionuclide inventories such as the Waste Unit Factor (WUF), and the initial lumped radionuclide inventories were updated for use in the CRA 2019 DPA (Kicker 2019a & b, Kim and Feng 2019).

CRA-2019 Solubility

The CRA-2019 DPA includes new solubility values for An(IV), An(V) and An(III) (Domski and Sisk-Scott 2019), and new solubility uncertainty factors (Domski 2019a). The DOE utilized EQ3/6, Version 8.0A, and the thermodynamic database DATA0.FM4 (Domski 2019b). More details are provided in CRA-2019 Appendix GEOCHEM-4.0 on the refinement of the baseline solubilities and solubility uncertainties and in Appendix MASS-2014, Section MASS-2.6.10 on the implementation of variable brine volume.

CRA-2019 Organic Ligands

In the CRA-2014, the DOE implemented a new method for calculating the organic ligand concentrations for the multiple minimum brine volumes for a Direct Brine Release (DBR) by adding additional parameters (Camphouse 2013). This method was also used for the CRA-2019 DPA.

CRA-2019 Parameters Related to Metals, CPR, and Oxyanions

The CRA-2019 DPA used the inventory described in Tables 6-3, 6-5 & 6-6 of the Performance Assessment Inventory Report (PAIR)-2018 (Van Soest 2018) to update the parameters related to

metals, cellulose, plastics, and rubbers (CPRs), and oxyanions. The PAIR-2018 reports the masses of the waste and packaging materials.

CRA-2019 Production of Gas from the Waste

Three changes related to the gas generation from the waste were implemented in the CRA-2019 DPA: the inclusion of radiolysis, the removal of sulfidization and parameters for anoxic steel corrosion were updated. Each change is discussed below.

Radiolysis

Radiolytic factors have been reconsidered in the CRA-2019 DPA to reflect the increase in plutonium inventory and changes in the screening argument (Day 2019). This directly leads to a small increase in total gas generation. Gas generation due to radiolysis of brine from radionuclides in solution and in wetted-solid form was included in the CRA-2019 DPA. Radiolytic brine gas generation impacts repository pressure and brine saturation conditions in the repository and is modeled within BRAGFLO. Gas generation due to radiolysis of CPR continues to be screened-out for the CRA-2019 DPA and is not expected to have a significant impact on the performance of the repository due to matrix depletion (CRA 2019 Appendix SCR-6.5.1.6).

Table 2 Gas Generation Parameters Added or Modified

Material:Property	Description
(AM241, PU238, PU239, PU240, PU242):DECAYNRG	Added for Radiolysis
GLOBAL:GH2SAVG	Added for Radiolysis
GLOBAL:GDEPFAC	Added for Radiolysis
GLOBAL:SRADO2	Added for Radiolysis
STEEL:HUMCORR	Updated humid corrosion rate
STEEL:CORRMCO2	Updated steel corrosion rate w/o CO_2
REFCON:(STCO_31, STCO_32, STCO_35, STCO_36, STCO_43, STCO_46)	Updated to remove sulfidation

Removal of Sulfidization Reactions from CRA-2019

For the CRA-2014, the sulfidation reactions with iron and iron hydroxide were included as part of the repository brine and gas production/consumption calculations. In response to U.S. Environmental Protection Agency (EPA) comments on the CRA-2014, the EPA requested that the DOE remove the sulfidization chemical reactions from WIPP PA by setting the appropriate stoichiometric coefficients (i.e., REFCON:STCO_31, REFCON:STCO_32, REFCON: STCO_35, REFCON:STCO_36, REFCON:STCO_43, and REFCON:STCO_46) to zero (Zeitler 2019). The DOE made these changes for the CRA-2019 DPA.

Refinement of Steel Corrosion Rates

The anoxic corrosion of steel in the WIPP repository will result in the formation of H_2 gas. Two steel corrosion rates were updated for the CRA-2019 DPA, STEEL:CORRMCO2 and STEEL:HUMCORR (Zeitler 2018a & b). The DOE has previously updated both the distribution type and values for the parameter STEEL:CORRMCO2 for the CRA-2014 PA based on the experimental corrosion data reported by Roselle (Roselle 2013).

CRA-2019 Parameter Related to Waste Shear Strength

The parameter related to the waste shear strength was revised for the CRA-2014. Based on the recommendations of Herrick and Kirchner (Herrick and Kirchner 2013), the DOE included a refined distribution for the parameter BOREHOLE:TAUFAIL in the CRA-2014 PA calculations (Appendix PA-2014, Section PA-1.1.5). In response to EPA comments on the CRA-2014, the DOE has revised the TAUFAIL parameter for the CRA-2019 DPA (Zeitler 2019). The lower end of the sampled parameter was changed from 2.22 Pa to 1.60 Pa and the distribution was changed to uniform.

CRA-2019 Formation of Colloidal Suspensions

The colloid enhancement parameters were re-examined for the CRA-2019 DPA (Appendix GEOCHEM 2019, Section GEOCHEM-5.4) and discussed in SOTERM (Section 3.5.1: SOTERM 5.3 through 5.8 for individual actinides). Based on the recommendations of Reed et al. (2019) and Mariner (2019), the DOE has updated the PA colloid parameters. Specifically, the PA parameter properties CONCINT, PROPMIC, CAPMIC, PHUMSIM and PHUMCIM were changed. These values are shown in Appendix GEOCHEM-2019, Table GEOCHEM-61 and Appendix SOTERM-2019, Sections SOTERM-8 and 9.

40 CFR §§ 194.24(b)(2) and (b)(3)

The CRA-2019 DPA identifies the same important waste characteristics as in the CCA, and identifies organic ligands as being potentially important to PA. The CRA-2019 DPA includes organic ligands in the solubility calculations (Domski and Sisk-Scott 2019). Most of the inventory amounts of the listed components have changed since the CRA-2014; these are described in the PAIR-2018 (Van Soest 2018).

References

Camphouse, R. 2013. Analysis Package for Salado Flow Modeling Done in the 2014 Compliance Recertification Application Performance Assessment (CRA-2014 PA). Carlsbad, NM: Sandia National Laboratories. ERMS 559980

Day, B. 2019. Reassessment of Need and Parameter Justification for Modeling Gas Generation due to Radiolysis of Brine and Cellulose/Plastic/Rubber in WIPP for CRA-2019. Carlsbad, NM. Sandia National Laboratories ERMS 570873

Domski, P. S., 2019a. Uncertainty Analysis of Actinide Solubilities for CRA 2019. Sandia National Laboratories, Carlsbad, New Mexico. ERMS 571179

Domski, P. S., 2019b. An Update to the EQ3/6 Pitzer Thermodynamic Database DATA0.FM1 with the Creation of DATA0.FM4. Sandia National Laboratories. Carlsbad, New Mexico. ERMS 571052

Domski, P. and C. Sisk-Scott. 2019. Prediction of Baseline Actinide Solubilities for CRA 2019 with and Updated EQ3/6 Pitzer Thermodynamic Database, DATA0.FM4. Carlsbad, NM: Sandia National Laboratories. ERMS 571178

Herrick, C.G. and T. Kirchner. 2013. Memorandum to C Camphouse (Subject: Follow-up to Questions Concerning TAUFAIL Flume Testing Raised during the November 14-15, 2012 Technical Exchange Between the DOE and EPA). (January 24, 2013). Carlsbad, NM: Sandia National Laboratories. ERMS 559081

Kicker, D. 2019a. Analysis Package for Inventory EPA Units in the 2019 Compliance Recertification Application Performance Assessment (CRA-2019 PA). Carlsbad, NM: Sandia National Laboratories. ERMS 571372

Kicker, D. 2019b. Radionuclide Inventory Screening Analysis for the 2019 Compliance Recertification Application Performance Assessment (CRA-2019 PA). Carlsbad, NM: Sandia National Laboratories. ERMS 571659

Kim, S. and L. Feng. 2019. Parameter Summary Report for the 2019 Compliance Recertification Application, Rev. 1. Carlsbad, NM: Sandia National Laboratories ERMS 571660

Mariner, P. E. 2019. Memo. A summary of humic colloid parameter values to be implemented in the CRA-2019 Deferred Performance Assessment. April 15, 2019. Sandia National Laboratories, Carlsbad, New Mexico. ERMS 571250

Reed, D. T., J. Swanson, and F. Stanley. 2019. LANL/ACRSP Parameter Recommendations for the CRA-2019 Deferred Performance Assessment, Los Alamos National Laboratory, Los Alamos, NM. LANL-CO ACRSP/CP-ACP-24. LA-UR-19-22787

Roselle, G. T. 2013c. Determination of Corrosion Rates from Iron/Lead Corrosion Experiments to be used for Gas Generation Calculations (Revision 1). Analysis Report, January 23, 2013. Sandia National Laboratories, Carlsbad, NM. ERMS 559077

Van Soest, G.D. 2018. Performance Assessment Inventory Report – 2018. Los Alamos National Laboratory Carlsbad Operations. Carlsbad, NM. INV-1812-09-01-01

Zeitler, T.R. 2018a. Cumulative Distribution for STEEL:CORRMCO2 for the CRA-2019 PA. Carlsbad, NM: Sandia National Laboratories. ERMS 570869

Zeitler, T.R. 2018b. Bounding Calculation of the Cumulative Distribution for STEEL:HUMCORR. Carlsbad, NM: Sandia National Laboratories. ERMS 569807

Zeitler, T.R. 2019. A Summary of EPA/DOE Defined Parameters to be Implemented in the CRA-2019 PA. Carlsbad, NM: Sandia National Laboratories. ERMS 570879

EPA Question

CC2-24-2c ***Updated table of waste characteristics and components excluded from PA consideration***

Please provide an updated table of waste characteristics and components that are excluded from consideration in the PA as required by 40 CFR 194.24(b)(3). The list currently referenced is Table WCA-4 of Appendix-WCA of the CCA which is currently outdated as it includes brine radiolysis and organic ligands which are now included in PA.

> *The DPA cites Table WCA-4 of Appendix-WCA of the CCA for a table of waste characteristics excluded in the PA. Besides the change in screening for organic ligands and brine radiolysis, does this list remain the same for CRA-2019?*

DOE Response

> There were no changes to the decision to include or exclude important waste components and characteristics for consideration in Performance Assessment (PA) since the CRA-2014 recertification decision. The historical background that explains changes to important waste characteristics that are accounted for or excluded in PA is presented in Section 24 of the CRA-2014. The CRA-2019 referenced this historical information in compliance with 40 CFR 194.15.
>
> Note: This was numbered CC2-24-1C in the U.S. Environmental Protection Agency (EPA) letter but was the third subpart of Comment 2 and was renumbered as 24-2C in this response.

EPA Evaluation of Response

The DOE response was satisfactory. The explanatory information was provided as requested and significantly helped EPA's review of waste inventory and geochemistry.

CC2-GEOCHEM-8 Clarification of data source information in Domski (2019)

WIPP Compliance Recertification Application 2019 Appendix-GEOCHEM (Geochemistry)

EPA Question (from EPA Completeness Comment Package 2)

Domski (2019, page 14) states that the systems used to reproduce the fitted parameters in DATA0.FM4 included the "Na – Ca – Cl – EDTA system, Na – Mg – Cl – Oxalate system, and the Na – Fe – Cl – CO_3 system" but references for the data were not provided. The full document citations for the comments referenced are listed below the questions/comments.

GEOCHEM-8a***. Na – Ca – Cl – EDTA System Data Source***

Were the Na – Ca – Cl – EDTA system data obtained from Table 4 of Xiong (2018), as stated by Domski (2018)?

DOE Response (from DOE Response Package 6)

The source of the Na – Ca – Cl – EDTA data referenced by Domski (2018) are from Table 4 of

Xiong (2018).

References

References with hyperlinks were provided in prior CRAs.

Domski, P.S. 2018. Memo on the estimation of the solubility product (Log K_{sp}) for $Ca_2EDTA.7H_2O$, and Pitzer parameters for the Na_+ / $CaEDTA_{2-}$ pair. Sandia National Laboratories, Carlsbad, New Mexico. ERMS 570202.

Xiong, Y.-L. 2018. Experimental determination of solubilities of lead oxalate (PbC_2O_4), dicalcium ethylenediaminetetraacetic acid hydrate ($Ca_2EDTA•7H_2O(s)$) in $MgC1_2$-H_2O system, and earlandite ($Ca_3[C_3H_5O(COO)_3]_2•4H_2O$) in NaCl-$H_2O$ and $MgC1_2$-H_2O systems, and their respective Pitzer interaction parameters. Revision 3. Supersedes ERMS 567810. Sandia National Laboratories, Carlsbad, New Mexico. ERMS 570088. (This reference was provided with DOE Response Letter 3, Enclosure 4)

GEOCHEM-8b. ***Please identify the source of the Na – Mg – Cl – Oxalate system data.***

DOE Response

The original data source was Jang and Kim (2016) (Table IV.2-11 and Table IV.2-14). These data were slightly modified by inclusion and averaging of additional measurements of oxalate at Sandia National Laboratories, which are included with the records package for AP-182 (Jang, 2019). The additional data were collected to ensure the reproducibility of the oxalate measurements presented in Jang and Kim (2016).

References

Jang, J. 2019. Analysis plan for derivation and addition of equilibrium constants and Pitzer interaction parameters to the WIPP Geochemical Thermodynamic Database. AP-182, Revision 0. ERMS 571074. (Reference previously provided to EPA)

Jang, J. and S. Kim. 2016. Derivation of Pitzer Interaction Parameters and Thermodynamic Properties for the Aqueous Species of Ferrous Iron and their pairs, Revision 2. Sandia National Laboratories, Carlsbad, New Mexico. ERMS 567283. (Reference is included in Enclosure 4.)

GEOCHEM-8c. ***Please identify the source of the Na – Fe – Cl – CO_3 system data.***

Domski, P.S. 2018. Memo on the estimation of the solubility product (Log K_{sp}) for $Ca_2EDTA.7H_2O$, and Pitzer parameters for the Na_+ / $CaEDTA_{2-}$ pair. Sandia National Laboratories, Carlsbad, New Mexico. ERMS 570202.
Domski, P.S. 2019. An update to the EQ3/6 Pitzer thermodynamic database DATA0.FM1 with the creation of DATA0.FM4. Sandia National Laboratories, Carlsbad, New Mexico. ERMS 571052.

Xiong, Y.-L. 2018. Experimental determination of solubilities of lead oxalate (PbC_2O_4), di-calcium ethylenediaminetetraacetic acid hydrate ($Ca_2EDTA•7H_2O(s)$) in $MgC1_2$-H_2O system, and earlandite ($Ca_3[C_3H_5O(COO)_3]_2•4H_2O$) in NaCl-$H_2O$ and $MgC1_2$-H_2O systems, and their respective Pitzer interaction

parameters. Revision 3, Supersedes ERMS 567810. Sandia National Laboratories, Carlsbad, New Mexico. ERMS 570088.

DOE Response

The source of the Na – Fe – Cl – CO_3 system data is Table 5 in Kim et al. (2017).

Reference

The following reference was provided with submittal of the Compliance Recertification Application 2019.

Kim, S., C. Marrs, M. Nemer and J-H Jang. 2017. Solubility Model for Ferrous Iron Hydroxide, Hibbingite, Siderite, and Chukanovite in High Saline Solutions of Sodium Chloride, Sodium Sulfate, and Sodium Carbonate. ACS Earth and Space Chemistry 1: 647−663

EPA Evaluation of Response

The DOE response was satisfactory. The information was provided as requested along with explanatory text.

CC2-GEOCHEM-10 Testing of Revised EDTA Stability Constants and Pitzer Ion-Interaction Parameters

WIPP Compliance Recertification Application 2019 Appendix-GEOCHEM (Geochemistry)

EPA Question (from EPA Completeness Comment Package 2)

Please provide a comparison of the apparent stability constants as a function of ionic strength: 1) reported by Choppin et al. (2001), 2) calculated using the DATA0.FM1 database, and 3) calculated using the DATA0.FM4 database for the following reactions. Although most of these modifications were small and would be expected to have minor individual effects, DOE has not demonstrated whether the EQ3/6 database used for the CRA-2019 PA actinide solubility calculations yields speciation results consistent with the available high-ionic-strength data for aqueous EDTA species (Choppin et al. 2001) or whether these changes result in improvements in the ability to simulate the data compared to using DATA0.FM1.

GEOCHEM-10a. *Acid dissociation reaction $H_4EDTA(aq) \leftrightarrow H^+ + H_3EDTA^-$ (Choppin et al. 2001, Tables 1 – 7)*
GEOCHEM-10b. *Acid dissociation reaction $H_3EDTA^- \leftrightarrow H^+ + H_2EDTA^{2-}$ (Choppin et al. 2001, Tables 1 – 7)*
GEOCHEM-10c. *Acid dissociation reaction $H_2EDTA^- \leftrightarrow H^+ + HEDTA^{3-}$ (Choppin et al. 2001, Tables 1 – 7)*
GEOCHEM-10d. *Acid dissociation reaction $HEDTA^- \leftrightarrow H^+ + EDTA^{4-}$ (Choppin et al. 2001, Tables 1 – 7)*
GEOCHEM-10e. *Thorium complexation with EDTA (Choppin et al. 2001, Tables 8 – 13)*
GEOCHEM-10f. *Americium complexation with EDTA (Choppin et al. 2001, Tables 26 – 31)*
GEOCHEM-10g. *Magnesium complexation with EDTA (Choppin et al. 2001, Tables 32 – 37)*

- *Modification of the previously approved EQ3/6 database DATA0.FM1 to create the DATA0.FM4 database used for CRA-2019 included numerous changes to the data for EDTA aqueous species, and Pitzer parameters (Sisk-Scott and Domski 2019):*
- *Replacement of the acid dissociation constants for EDTA (Giambalvo 2002) with values from Hummel et al. (2005)*
- *Addition of the Ca2EDTA·7H2O(s) dissolution reaction (Domski 2018a)*
- *Addition of aqueous stability constants for NaEDTA3-, MgHEDTA–, and CaHEDTA– (Hummel et al. 2005)*
- *Replacement of the aqueous stability constants for MgEDTA2- and CaEDTA2- (Giambalvo 2002) with values from Hummel et al. (2005)*
- *Replacement of Pitzer parameters for Na+ - EDTA4- and K+ - EDTA4- (Giambalvo 2002) with values from Felmy and Mason (2003)*
- *Replacement of Pitzer parameters for Na+ - CaEDTA2- and K+ - CaEDTA2- (Giambalvo 2002) with values from Domski (2018b)*
- *Addition of Pitzer parameters for Na+ - NaEDTA3- from Felmy and Mason (2003)*
- *Addition of Pitzer parameters for Ca2+ - EDTA4-, Mg2+ - CaEDTA2-, Mg2+ - MgEDTA2-, from Domski (2018b)*
- *Deletion of the Pitzer parameters for Na+ - MgEDTA2- and K+ - MgEDTA2-*

Choppin, G.R., A.H. Bond, M. Borkowski, M. Bronikowski, J.-F. Chen, S. Lis, J. Mizera, O.S. Pokrovsky, N.A. Wall, Y.X. Xia, and R.C. Moore. 2001. Waste Isolation Pilot Plant Actinide Source Term Test Program: Solubility Studies and Development of Modeling Parameters. Sandia National Laboratories, Albuquerque, New Mexico, April 2001, SAND99-0943. ERMS 518556

Domski, P.S. 2018a. Memo on the estimation of the solubility product (Log Ksp) for Ca2EDTA·7H2O, and Pitzer parameters for the Na+/CaEDTA2- pair. Sandia National Laboratories, Carlsbad, New Mexico. ERMS 570202.

Domski, P.S. 2018b. Memo on the estimation of Pitzer parameters for the Mg2+ / CaEDTA2- Mg2+ / MgEDTA2-, and Ca2+ / EDTA4- pairs. Sandia National Laboratories, Carlsbad, New Mexico. ERMS 570855.

Felmy, A.R., and M.J. Mason. 2003. An Aqueous Thermodynamic Model for the Complexation of Sodium and Strontium with Organic Chelates Valid to High Ionic Strength. I. Ethylenedinitrilotetraacetic Acid (EDTA). Journal of Solution Chemistry 31:283.

Giambalvo, E.R. 2002. Letter to L.H. Brush. Subject: Recommended Parameter Values for Modeling Organic Ligands in WIPP Brines. July 25, 2002. Carlsbad, New Mexico. Sandia National Laboratory. ERMS 522981.

Hummel, W., G. Anderegg, I. Puigdomenech, L. Rao, and O. Tochiyama. 2005. Chemical Thermodynamics of Compounds and Complexes of U, Np, Pu, Am, Tc, Zr, Ni and Se with Selected Organic Ligands. Chemical Thermodynamics, Volume 9, OECD Nuclear Energy Agency, Data Bank, Issy-les-Moulineaux, France, Elsevier BB Amsterdam, The Netherlands, P. 1088.

Sisk-Scott, C. and P. Domski. Analysis plan to update the WIPP geochemical thermodynamic database (DATA0.FM1) to DATA0.FM4 for CRA-2019. AP-183, Revision 1. Sandia National Laboratories, Carlsbad, New Mexico. ERMS 571001.

DOE Response (from DOE Response Package 4)

The U.S. Environmental Protection Agency (EPA) has asked the U.S. Department of Energy (DOE) for a comparison of the apparent stability constants as a function of ionic strength from the following sources: 1) reported by Choppin et al. (2001), 2) calculated using the DATA0.FM1 database, and 3) calculated using the DATA0.FM4 database. The EPA has asked the DOE to verify that the changes made to the DATA0.FM1 database that now reside in the DATA0.FM4 database (see Sisk-Scott and Domski 2019) yield speciation calculated results consistent with the available high-ionic-strength data (Choppin et al., 2001) for aqueous-ethylenediaminetetraacetic acid (EDTA) species. The DOE interprets this question in the following way: the EPA has asked the DOE to compare the results of EQ3/6 calculations using DATA0.FM1 and DATA0.FM4 to the results given in Choppin et al. (2001), using a methodology similar to that performed in Choppin et al. (2001) and Giambalvo (2002). In particular, calculate the negative logarithm of the apparent equilibrium constants for EDTA deprotonation (pKa_i) and the logarithm of the apparent dissociation constants for EDTA complexation with thorium, americium, and magnesium (log βs). The DOE further interprets the EPA's question as asking the DOE to provide comparisons of these systems as a function of increasing sodium chloride concentration.

To address CC2-GEOCHEM Comment 10, EQ3NR input files were created and run using two databases, DATA0.FM1 and DATA0.FM4 to reproduce Choppin et al.'s (2001) models (i.e., apparent log Ks) that were derived from data collected at Florida State University for the WIPP Actinide Source Term Program. Mapping Choppin et al.'s (2001) model(s) to the EPA's questions: Comments 10a through 10d relate to the sequential deprotonation of H_4EDTA(aq); Comment 10e relates to thorium (Th(IV)) complexation with EDTA; Comment 10f relates to americium (Am(III)) complexation with EDTA; Comment 10g concerns magnesium complexation with EDTA.

GEOCHEM 10a, 10b, 10c, 10d Acid Dissociation Reactions Comment Response

From Choppin et al. (2001), page 68:

Acid dissociation constants, K_{ai} of an n-protic acid, vary as a function of ionic strength and temperature. For a general acid dissociation reaction:

$$H_{n-i+1}A_{(i-1)-} = H_+ + H_{n-i}A_{i-}, \text{ (1)}$$

where i = 1, 2, …, n, the apparent equilibrium constants (K_{ai}'s) for Reaction (1) is defined as:

$$K_{ai} = ([H_+]\,[H_{n-i}A_{i-}]) / [H_{n-i+1}A_{(i-1)-}]$$

And reported as $pK_{ai} = -\log K_{ai}$

Thus,

$$pK_{ai} = -\log[H_+] - \log[H_{n-i}A_{i-}] - (-\log[H_{n-i+1}A_{(i-1)-}]).$$

To answer CC2-GEOCHEM-10a through 10d, the calculation of pK_{ai} for the deprotonation of H_4EDTA(aq) was performed following the calculation methodology shown above from Choppin et al. (2001), using

the output from EQ3NR. For example, the first deprotonation of $H_4EDTA(aq)$ follows the following reaction

$$H_4EDTA(aq) = H^+ + H_3EDTA^-, \quad (2)$$

where n = 4 and i = 1 in Reaction (1). Thus, following Choppin et al. (2001),

$$pK_{a1} = -\log[H^+] - \log[H_3EDTA^-] - (-\log[H_4EDTA(aq)]). \quad (3)$$

Note that quantities contained between square brackets [-] are in units of molality (m) not molarity. Using DATA0.FM1 at NaCl = 0.1m, and $EDTA^{4-}$ = 1.0E-3m (concentration used in Choppin et al., 2001), EQ3NR calculates the EDTA speciation to be that shown in Table 1.

Table 1. EQ3NR Output Using DATA0.FM1 with NaCl = 0.1m and $EDTA^{4-}$ = 1.0E-3m.*

--- Distribution of Aqueous Solute Species ---

Species	Molality	Log Molality	Log Gamma	Log Activity
Na+	1.0000E-01	-1.0000	-0.1104	-1.1104
Cl-	1.0000E-01	-1.0000	-0.1107	-1.1107
H+	1.4539E-03	-2.8375	-0.0975	-2.9349
H2EDTA--	5.4908E-04	-3.2604	-0.4784	-3.7388
H3EDTA-	3.5503E-04	-3.4497	-0.1366	-3.5863
H4EDTA(aq)	9.5645E-05	-4.0193	0.0000	-4.0193
HEDTA---	2.4731E-07	-6.6068	-1.0764	-7.6831
OH-	1.1277E-11	-10.9478	-0.1154	-11.0632
EDTA----	5.6659E-14	-13.2467	-2.0722	-15.3189

*Shaded cells are values subsequently used in Equation (4).

Thus, using the DATA0.FM1 database with EQ3NR,

$$pKa_1 = 2.8375 + 3.4497 - 4.0193 = 2.2679. \quad (4)$$

Similar EQ3NR calculations were carried out for pKa_1 ($H_4EDTA(aq)$), pKa_2 (H_3EDTA^-), pKa_3 (H_2EDTA^{2-}) and pKa_4 ($HEDTA^{3-}$) at NaCl concentrations of 0.1, 0.3, 0.5, 1.0, 2.0, 3.0, and 5.0 molal using both the DATA0.FM1 and DATA0.FM4 databases.

The results of the EQ3NR calculations for EDTA deprotonation are displayed in Figure 1. There is agreement; the pKa values calculated using DATA0.FM1 and DATA0.FM4 match with the pKa values of Choppin et al. (2001), Tables 1 – 7, for all of the pKa values except for pKa_4 for DATA0.FM4, which deviates from the other two data sources. A cause of this deviation is the inclusion of the sodium-EDTA complex, $NaEDTA^{3-}$, in DATA0.FM4, the source of which is Hummel et al. (2005). In a sodium chloride system, the addition of this complex to DATA0.FM4 sets up an equilibrium between $EDTA^{4-}$ and $NaEDTA^{3-}$ with the sodium-EDTA complex dominating, thus partly accounting for the observed deviation. The apparent pKa_4 is calculated via the expression:

$$pK_{a4} = -\log[H^+] - \log[HEDTA^{3-}] - (-\log[EDTA^{4-}]). \quad (5)$$

The molality values of the pertinent EDTA complexes are provided in Table 2 for both the DATA0.FM1 and the DATA0.FM4 databases for the calculation of pKa_4. Table 2 shows that the concentration of the $EDTA^{4-}$ complex is significantly less in calculations using DATA0.FM4 compared to that calculated using DATA0.FM1. The concentration of the complex $NaEDTA^{3-}$ obtained in calculations using DATA0.FM4 is similar to the concentration of the $EDTA^{4-}$ complex obtained using DATA0.FM1.

Table 2. Molalities of EDTA Complexes Used to Calculated pKa_4.

Database	DATA0.FM1	DATA0.FM4	DATA0.FM1	DATA0.FM4	DATA0.FM1	DATA0.FM4	DATA0.FM4
NaCl (m)	H^+ Log (m)		$HEDTA^{3-}$ Log (m)		$EDTA^{4-}$ Log (m)		$NaEDTA^{3-}$ Log (m)
0.1	-2.84	-2.83	-6.61	-6.55	-13.25	-14.10	-13.18
0.3	-2.81	-2.81	-6.42	-6.35	-12.74	-13.89	-12.58
0.5	-2.80	-2.80	-6.38	-6.31	-12.57	-13.92	-12.37
1	-2.79	-2.79	-6.42	-6.35	-12.43	-14.14	-12.22
2	-2.79	-2.79	-6.64	-6.57	-12.51	-14.60	-12.34
3	-2.79	-2.79	-6.89	-6.82	-12.75	-15.07	-12.63
5	-2.82	-2.82	-7.38	-7.31	-13.49	-16.10	-13.36

The use of log K values from Hummel et al. (2005) was jointly agreed to by the DOE and the EPA during a technical exchange in Albuquerque in September 2018. The mixing of SIT-based log K values from Hummel et al. (2005) with the Pitzer approach introduces additional model bias that may be a factor in the observed deviation at high ionic strength. In addition, changes to related Pitzer interaction parameters for DATA0.FM4 compared to DATA0.FM1, as defined in the nine bullets in the EPA comments (see pages 11 and 12 of this response), also contributed to the deviation.

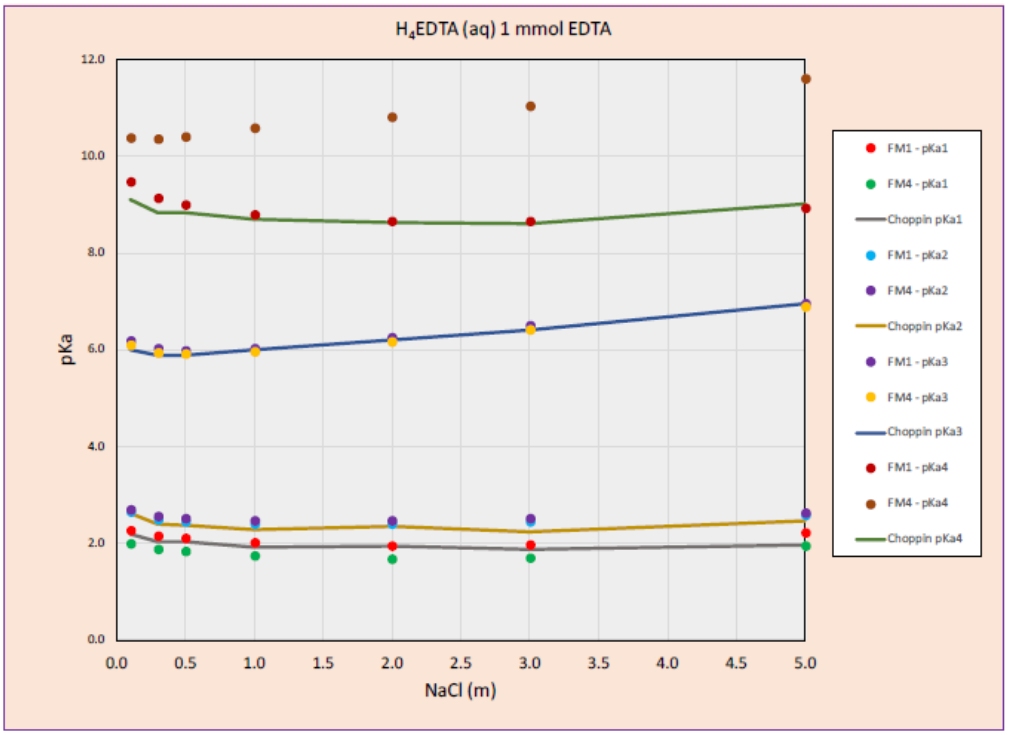

Figure 1. $H_4EDTA(aq)$ Acid Dissociation Constants (pKa) as a Function of Sodium Chloride Concentration.

GEOCHEM 10e, 10f, 10g Thorium Complexation with EDTA Comment Responses

The apparent dissociation constants, β, (log β) for aqueous complexes may be calculated from the molalities of the aqueous complex components. For the thorium-EDTA complex, the reaction is given by

$$ThEDTA(aq) = Th^{4+} + EDTA^{4-}. \quad (6)$$

Then β and log β are calculated from

$$\beta = [Th^{4+}]\,[EDTA^{4-}] / [ThEDTA(aq)] \quad (7)$$

$$\log \beta = \log[Th^{4+}] + \log[EDTA^{4-}] - \log[ThEDTA(aq)] \quad (8)$$

These same formulas apply to the $AmEDTA^-$ and $MgEDTA^{2-}$ complexes. Herein, β is used as the comparison metric between EQ3NR calculation results and the results given in Choppin et al. (2001), similar to the methodology performed in Giambalvo (2002). Using DATA0.FM1 at NaCl = 0.3m, Th^{4+} = 7.1E-07m, and $EDTA^{4-}$ = 1.0E-3m, EQ3NR calculates the thorium speciation as shown in Table 3.

Table 3. EQ3NR Output Using DATA0.FM1 with NaCl = 0.3m and $EDTA^{4-}$ = 1.0E-3m.*

--- Distribution of Aqueous Solute Species ---

Species	Molality	Log Molality	Log Gamma	Log Activity
Cl-	3.0000E-01	-0.5229	-0.1510	-0.6739
Na+	3.0000E-01	-0.5229	-0.1509	-0.6738
H+	1.5505E-03	-2.8095	-0.1122	-2.9217
H2EDTA--	6.2012E-04	-3.2075	-0.6952	-3.9028
H3EDTA-	3.0911E-04	-3.5099	-0.2272	-3.7371
H4EDTA(aq)	6.9685E-05	-4.1569	0.0000	-4.1569
ThEDTA(aq)	7.0988E-07	-6.1488	0.0290	-6.1199
HEDTA---	3.8251E-07	-6.4174	-1.4430	-7.8604
Th++++	1.2284E-10	-9.9106	-4.2568	-14.1675
OH-	1.2146E-11	-10.9156	-0.1638	-11.0793
EDTA----	1.8055E-13	-12.7434	-2.7660	-15.5094
Th(OH)4(aq)	1.0040E-20	-19.9983	0.0000	-19.9983

*Shaded cells are values subsequently used in Equation (8).

Thus, for DATA0.FM1

$$\log \beta_{ThEDTA(aq)} = -9.9106 + (-12.7434) - (-6.1488) = -16.5052 \quad (9)$$

The $\log \beta_{ThEDTA(aq)}$ provided by Choppin et al. (2001), Tables Th55 - 63, are given for the apparent stability constants of the complex, and thus have the opposite sign as the dissociation constant calculated above.

The $\log \beta_{ThEDTA(aq)}$ values were calculated using EQ3NR using both the FM1 and FM4 databases at 0.3, 1.0, 2.0, 3.0, 4.0, and 5.0 molal NaCl solutions to reproduce Choppin et al.'s (2001) experiments and model. The results are displayed in Figure 2.

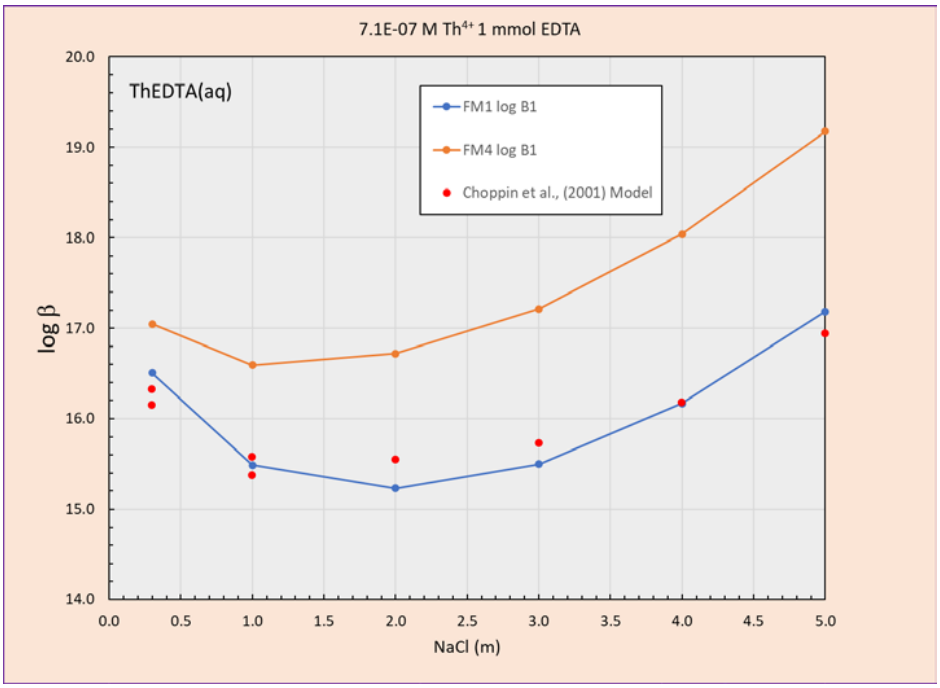

Figure 2. Log $\beta_{ThEDTA(aq)}$ as a Function of Sodium Chloride Concentration.

Figure 2 shows that DATA0.FM1 and the Choppin et al. (2001) model (apparent log Ks) are in agreement, as expected because Choppin et al. (2001) model (apparent log Ks) was used to parameterize the Waste Isolation Pilot Plant (WIPP) thorium model included in DATA0.FM1. The log $\beta_{ThEDTA(aq)}$ values calculated using DATA0.FM4 deviate from both the FM1 simulated data and the Choppin data, although both DATA0.FM1 and DATA0.FM4 use the same log K for ThEDTA(aq) as calculated by Giambalvo (2002) using Choppin et al.'s (2001) data. The deviation is a cumulative effect of several changes to DATA0.FM4 relative to DATA0.FM1, for example, (i) the use of SIT-based log K values for $H_4EDTA(aq)$ deprotonation (Hummel et al., 2005), and (ii) changes to some of the relevant Pitzer parameter data, as shown in the nine EPA bullets on pages 11 and 12 of this response.

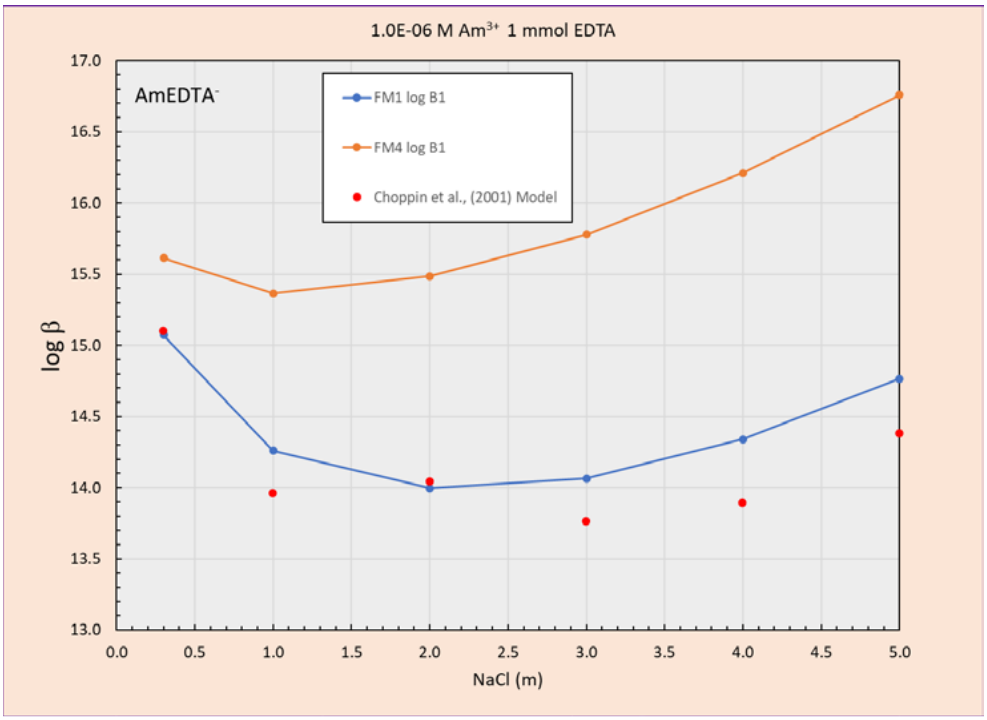

Figure 3. Log β_{AmEDTA} as a Function of Sodium Chloride Concentration.

Figure 3 shows the (log) apparent stability constants for $AmEDTA^-$ as a function of NaCl concentration. Deviation is noticeable for the DATA0.FM4-based calculations although the same log K for $AmEDTA^-$ was used in both DATA0.FM1 and DATA0.FM4. The cause of the deviation is the same as described in the text associated with Figure 2.

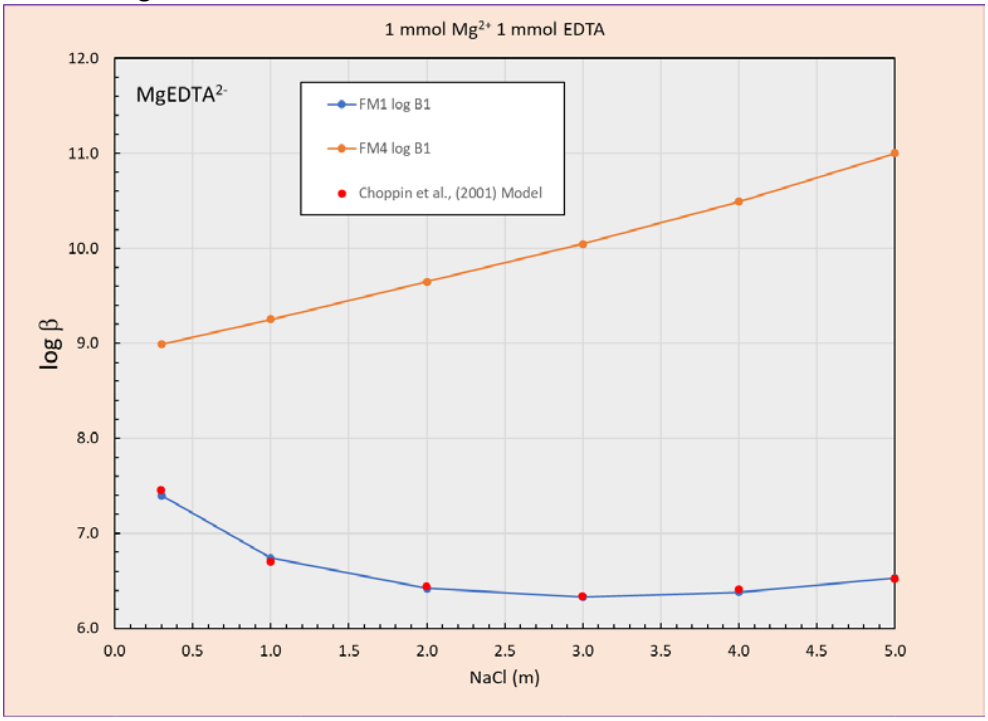

Figure 4. Log $\beta_{MgEDTA^{2-}}$ as a Function of Sodium Chloride Concentration.

Figure 4 shows the (log) apparent stability constants for $MgEDTA^{2-}$ as a function of NaCl concentration. The observed deviation is due in part to the use of different log K values for $MgEDTA^{2-}$ in DATA0.FM1 (-10.13) and DATA0.FM4 (-10.90), but also to the cumulative effect of other changes to the relevant Pitzer interaction parameters.

In summary, it was shown in the responses to comments 10a through 10d that the addition of thermodynamic data for $NaEDTA^{3-}$ to DATA0.FM4 causes a deviation in the calculated $H_4EDTA(aq)$ system. This deviation is expected because the EDTA thermodynamic data included in the DATA0.FM1 database was based on the Choppin et al.'s (2001) model (apparent log Ks) and does not include the sodium-EDTA complex. The DATA0.FM4 EDTA thermodynamic data is based on a different data set and model, that of Hummel et al. (2005), which included the sodium-EDTA complex. Apparent (log) equilibrium constants, pKa_i values, are metrics composed of a mix of modeling and experimental results. Because the model of Choppin et al. (2001) and Hummel et al. (2005) are different there should be no expectation of agreement between the pKa_i's based on different models.

For the Th-EDTA, Am-EDTA, and Mg-EDTA systems, the deviations calculated between the DATA0.FM1 and DATA0.FM4 modeled systems are a cumulative effect of several differences in DATA0.FM4 relative to DATA0.FM1. As noted by the EPA (CC2-GEOCHEM-10) these changes include:

- *Modification of the previously approved EQ3/6 database DATA0.FM1 to create the DATA0.FM4 database used for CRA-2019 included numerous changes to the data for EDTA aqueous species, and Pitzer parameters (Sisk-Scott and Domski 2019):*
- *Replacement of the acid dissociation constants for EDTA (Giambalvo 2002) with valuesfrom Hummel et al. (2005)*
- *Addition of aqueous stability constants for $NaEDTA^{3-}$, $MgHEDTA^{-}$, and $CaHEDTA^{-}$ (Hummel et al. 2005)*
- *Replacement of the aqueous stability constants for $MgEDTA^{2-}$ and $CaEDTA^{2-}$ (Giambalvo 2002) with values from Hummel et al. (2005)*
- *Replacement of Pitzer parameters for Na^{+} - $EDTA^{4-}$ and K^{+} - $EDTA^{4-}$ (Giambalvo 2002) with values from Felmy and Mason (2003)*
- *Addition of Pitzer parameters for Na^{+} - $NaEDTA^{3-}$ from Felmy and Mason (2003)*
- *Addition of Pitzer parameters for Ca^{2+} - $EDTA^{4-}$, Mg^{2+} - $CaEDTA^{2-}$, Mg^{2+} - $MgEDTA^{2-}$, from Domski (2018b)*
- *Deletion of the Pitzer parameters for Na^{+} - $MgEDTA^{2-}$ and K^{+} - $MgEDTA^{2-}$*

All files used in addressing CC2-GEOCHEM-10 will be stored at the following location: /cvs/CVSLIB/WIPP_EXTERNAL/CRA19_comments. The files are also included in Enclosure 4.

EPA Evaluation of Response

The DOE response was satisfactory. The data source and documentation was identified as requested.

CC2-GEOCHEM-11 Data Used to Derive Ca2EDTA·7H2O(s) Solubility Product and Evaluation of the Solubility Product

WIPP Compliance Recertification Application 2019 Appendix-GEOCHEM (Geochemistry)

EPA Question (from EPA Completeness Comment Package 2)

Please provide the following additional information about the data used to derive the $Ca_2EDTA{\cdot}7H_2O(s)$ solubility product and associated Pitzer parameters:

GEOCHEM 11a***. Please explain whether the data Domski (2018) used to develop the solubility product for $Ca_2EDTA{\cdot}7H_2O(s)$ and $\beta_{(0)}$ and $\beta_{(1)}$ Pitzer parameters for Na^+ / $CaEDTA^{2-}$ were from Table 4 of Xiong et al. (2018), and if the EDTA concentrations were assumed equal to half of the measured calcium concentrations.***

DOE Response (from DOE Response Package 3)

The data used by Domski (2018) to fit the solubility product for $Ca_2EDTA{\cdot}7H_2O(s)$, and β(0)and β(1) Pitzer parameters for Na^+ / $CaEDTA^{2-}$ were the average values of pmH and the average calcium concentrations (molal) as measured on day 1431, and listed in Table 4 of Xiong (2018). EPA is correct in that Domski (2018) used one half of the average calcium concentration as measured on day 1431 to represent the ethylenediaminetetraacetic acid (EDTA) concentration for the purpose of fitting the $Ca_2EDTA{\cdot}7H_2O(s)$ solubility product.

References

Domski, P.S. 2018. Memo on the estimation of the solubility product (Log K_{sp}) for $Ca_2EDTA.7H_2O$, and Pitzer parameters for the Na^+ / $CaEDTA^{2-}$ pair. Sandia National Laboratories, Carlsbad, New Mexico. ERMS 570202.

Xiong, Y.-L. 2018. Experimental determination of solubilities of lead oxalate (PbC_2O_4), dicalcium ethylenediaminetetraacetic acid hydrate ($Ca_2EDTA{\bullet}7H_2O(s)$) in $MgCl_2$-H_2O system, and earlandite ($Ca_3[C_3H_5O(COO)_3]_2{\bullet}4H_2O$) in NaCl-$H_2O$ and $MgCl_2$-H_2O systems, and their respective Pitzer interaction parameters. Revision 3, Supersedes ERMS 567810. Sandia National Laboratories, Carlsbad, New Mexico. ERMS 570088.

EPA Question

GEOCHEM 11b***. Please use the data in Kirkes et al. (2014, Table 3-57) including pmH data calculated from the reported pH measurements, to calculate apparent log K_{sp} values as a function of ionic strength for $Ca_2EDTA{\cdot}7H_2O(s)$ in NaCl solutions. Please compare these measured apparent log K_{sp} values to apparent log K_{sp} values calculated using the DATA0.FM4 database.***

GEOCHEM 11c***. Please use the data in Kirkes et al. (2014, Table 3-59) including pmH data calculated from the reported pH measurements, to calculate apparent log K_{sp} values as a function of ionic strength for $Ca_2EDTA{\cdot}7H_2O(s)$ in $MgCl_2$ solutions. Please compare these measured apparent log K_{sp} values to apparent log K_{sp} values calculated using the DATA0.FM4 database.***

The data set used to derive the solubility product (log K_{sp}) for $Ca_2EDTA{\cdot}7H_2O(s)$ and the $\beta_{(0)}$ and $\beta_{(1)}$ values for the Na+ / $CaEDTA^{2-}$ pair (Domski 2019) appears to be the data listed in Table 4 of Xiong (2018) (see GEOCHEM-8 and GEOCHEM-9, above). However, this table lists only the calcium concentrations and pmH values measured in the $Ca_2EDTA{\cdot}7H_2O(s)$ solubility experiments performed in 0.01 to 5 m NaCl solutions

and does not include the EDTA concentrations. Full data sets are provided in Kirkes et al. (2014, Table 3-57), including pH, and sodium, calcium, EDTA, and chloride concentrations. Additional $Ca_2EDTA{\cdot}7H_2O(s)$ solubility experiments were conducted in 0.01 to 2.5 m $MgCl_2$ solutions, and data listed for these experiments includes pH, magnesium, calcium, EDTA and chloride (Kirkes et al. 2014 Table 3-59). Domski (2018) compared the measured and modeled calcium concentrations and pmH values for the $Ca_2EDTA{\cdot}7H_2O(s)$ solubility experiments carried out in NaCl solutions but did not provide comparisons of the apparent measured and log K_{sp} values for NaCl solutions, or an evaluation of the $MgCl_2$ solubility experiment data.

Domski, P.S. 2018. Memo on the estimation of the solubility product (Log K_{sp}) for $Ca_2EDTA{\cdot}7H_2O(s)$, and Pitzer parameters for the Na_+ / $CaEDTA_{2-}$ Pair. Sandia National Laboratories, Carlsbad, New Mexico. ERMS 570202.

Domski, P.S. 2019. An date to the EQ3/6 Pitzer thermodynamic database DATA0.FM1 with the creation of DATA0.FM4. Sandia National Laboratories, Carlsbad, New Mexico. ERMS 570202.

Kirkes, L., T. Olivas, J.-H. Jang, S. Kim, and Y.-L. Xiong. 2014. Third milestone report on Test Plan TP 08-02, "Iron, Lead, Sulfide and EDTA Solubilities" Revision 2. Sandia National Laboratories, Carlsbad, New Mexico. ERMS 562497.

Xiong, Y.-L. 2018. Experimental determination of solubilities of lead oxalate (PbC_2O_4), di-calcium ethylenediaminetetraacetic acid hydrate ($Ca_2EDTA{\bullet}7H_2O(s)$) in $MgC1_2$-H_2O system, and earlandite ($Ca_3[C_3H_5O(COO)_3]_2{\bullet}4H_2O$) in NaCl-$H_2O$ and $MgC1_2$-H_2O systems, and their respective Pitzer interaction parameters, Revision 3, Supersedes ERMS 567810. Sandia National Laboratories, Carlsbad, New Mexico. ERMS 570088.

DOE Response (from DOE Response Package 5)

The DOE responses to CC2-GEOCHEM-11b and 11c require that apparent Log K values for $Ca_2EDTA{\bullet}7H_2O(s)$ be calculated from the analytical data as presented in Kirkes et al. (2014) in Tables 3-57 and 3-59, respectively. On June 12, 2020 the U.S. Department of Energy (DOE) (Patterson, 2020), in an email, asked the U.S. Environmental Protection Agency (EPA) for clarification on CC2-GEOCHEM-11b and CC2-GEOCHEM-11c. The EPA (Santillan, 2020) responded in an email on June 16, 2020 with the following:

> *To compare the results of EQ3/6 calculations performed using the DATA0.FM4 to the experimental solubility data, we are requesting that DOE perform solubility calculations for $Ca_2EDTA{\cdot}7H_2O(s)$ at the pmH and NaCl concentrations of the experiments reported in Kirkes et al. (2014,Table 3-57). The results of these calculations will include the total calcium (all modeled species) and total EDTA (all modeled species) concentrations in equilibrium with $Ca_2EDTA{\cdot}7H_2O(s)$, which should be used to calculate the apparent solubility product. Comparison of the measured and predicted apparent solubility products as a function of NaCl concentration and pmH should then be performed to assess the ability of the model to predict the measured concentrations.*

Per the EPA's clarification, the DOE will calculate the base-10 logarithm of the apparent solubility product, Log $K_{sp,app}$, from the un-speciated analytical measurements of the total molality values of calcium and ethylenediaminetetraacetic acid (EDTA) as they appear in Kirkes et al. (2014). For

completeness, the DOE will calculate the Log $K_{sp,app}$ values from the measured data using both the reported EDTA concentrations from Tables 3-57 and 3-59 of Kirkes et al. (2014), and EDTA concentrations equal to 50% of the reported calcium concentration[1] reported in Tables 3-57 and 3-59 of Kirkes et al. (2014) as were used in the analysis of Domski (2018). These Log $K_{sp,app}$ values will be compared to those calculated from EQ3/6 (an aqueous solution speciation-solubility modeling code) output using the DATA0.FM4 database at the specified pmH, sodium chloride, or magnesium chloride concentration.

Note, in Domski (2018) the EDTA concentration was set equal to half of the average calcium concentration(m) as measured on day 1431. The necessity of maintaining the 2:1, Ca:EDTA, mole ratio for mass and charge balance in the inverse-fitting model calculation (Domski, 2018) using EQ3NR were the reasons for taking this approach.

To calculate the Log $K_{sp,app}$ values the experimental data was screened for outlier data points, either non-steady state or spurious data points using visual-inspection methods; more complex methods were not considered necessary because the variability in the data was small. The data screening for total calcium (m) was done in Excel by plotting the concentration data as a function of time for each NaCl or $MgCl_2$ concentration and excluding the outlier data by visual inspection and calculating the mean total Ca concentration at each NaCl or $MgCl_2$ concentration. The pH, calcium, and EDTA data were screened using the calcium data to determine which data were to be included. The data screening for both Comment 11b and 11c are included in the Excel spreadsheet *Comment-11_Ca2EDTA_logK_New.xlsx*, and are included with the records package which is located here: /cvs/CVSLIB/WIPP_EXTERNAL/CRA19_comments.

_____

[1]In the remainder of the document these will be referred to as “50% Ca”

This excel spreadsheet is included in Enclosure 4.

The log of the apparent solubility product, Log $K_{sp,app}$, for the dissolution of $Ca_2EDTA•7H_2O$ follows the reaction

$$Ca_2EDTA•7H_2O(s) = 2Ca^{2+} + EDTA^{4-} + 7H_2O. \quad (1)$$

The apparent solubility product is then calculated by

$$K_{sp,app} = [Ca^{2+}]_T^2 [EDTA^{4-}]_T . \quad (2)$$

By definition, the mole fraction of a pure solid is 1. The mole fraction of water is purposely set to be 1 for simplicity of calculation of $K_{sp,app}$. Note the square brackets ([-]) indicate concentration in units of molality (m). Subscript T stands for the total Ca^{2+} and $EDTA^{4-}$ concentrations. The log of the apparent solubility product then follows from equation (2),

$$\text{Log } K_{sp,app} = 2\text{Log } [Ca^{2+}]_T + \text{Log } [EDTA^{4-}]_T. \quad (3)$$

Tables 11-1 and 11-2 provide the pmH, calcium, and EDTA molalities used to calculate the log $K_{sp,app}$ values for $Ca_2EDTA•7H_2O$ as a function of NaCl and $MgCl_2$ concentration, as well as the log $K_{sp,app}$ values for the two values of EDTA concentrations.

Table 11-1. Log $K_{sp,app}$ Values for $Ca_2EDTA•7H_2O$ in NaCl Solutions from Table 3-57 of Kirkes et al. (2014)

			Measured		50% Ca(m)	
NaCl (m)	pmH	Ca (m)	EDTA (m)	App Log K	EDTA (m)	App Log K
0.01	7.9	7.298E-02	5.640E-02	-3.52	3.649E-02	-3.71
0.10	7.9	8.580E-02	6.733E-02	-3.30	4.290E-02	-3.50
1.00	7.9	1.223E-01	9.192E-02	-2.86	6.114E-02	-3.04
2.10	8.1	1.217E-01	9.131E-02	-2.87	6.086E-02	-3.05
3.20	8.2	1.094E-01	8.379E-02	-3.00	5.471E-02	-3.18
4.40	8.3	9.441E-02	7.359E-02	-3.18	4.720E-02	-3.38
5.00	8.2	8.385E-02	6.686E-02	-3.33	4.192E-02	-3.53

Table 11-2. Log $K_{sp,app}$ Values for $Ca_2EDTA•7H_2O$ in $MgCl_2$ Solutions from Table 3-59 of Kirkes et al. (2014)

			Measured		50% Ca(m)	
$MgCl_2$ (m)	pmH	Ca (m)	EDTA (m)	App LogK	EDTA (m)	App LogK
0.01	7.8	7.684E-02	5.978E-02	-3.45	3.842E-02	-3.64
0.10	7.6	1.145E-01	8.622E-02	-2.95	5.725E-02	-3.12
1.00	7.57	1.757E-01	4.257E-02	-2.88	8.786E-02	-2.57
1.50	7.6	2.237E-01	3.758E-02	-2.73	1.119E-01	-2.25
2.00	7.6	2.303E-01	4.685E-02	-2.60	1.151E-01	-2.21
2.50	7.7	2.961E-01	8.115E-02	-2.15	1.480E-01	-1.89

To address EPA's CC2-GEOCHEM-11b and 11c, EQ3/6 input files were created to simulate the experimental conditions outlined in Kirkes et al. (2014) Section 3.29 for the Ca – Na – Cl – EDTA – H_2O system (Comment 11b), and Section 3.30 for the Ca – Mg – Cl – EDTA – H_2O system (Comment 11c). EQ3NR and EQ6 were used to simulate the chemical system using the data in Tables 11-1 and 11-2. For the model calculations, each sodium chloride, or magnesium chloride concentration, as well as the pH were used to create individual EQ3NR input files. The EQ3NR input files for each sodium chloride, or magnesium chloride concentration was executed and EQ3 pickup files (*.3p files) were generated. These pickup files contain the important solution properties for each sodium chloride, or magnesium chloride concentration and are used as part of the EQ6 input files. The EQ6 input files, in addition to the EQ3 pickup files, specified $Ca_2EDTA•7H_2O(s)$ as a reactant which the EQ6 code "titrates" into the initial solution composition until equilibrium conditions were achieved. This calculational method was used because it most closely simulates the actual laboratory experiment. The equilibrium concentrations of ΣCa^{2+} and $\Sigma EDTA^{4-}$ were extracted from the EQ6 output files to calculate the apparent log values as a function of sodium chloride or magnesium chloride concentration. The EQ3NR and EQ6 input and output files are included in the records package and may be found at the following location: /cvs/CVSLIB/WIPP_EXTERNAL/CRA19_comments.

The input and output files are included in Enclosure 4.

The results of the EQ3/6 simulations were extracted into an Excel spreadsheet (*Comment-11_Ca2EDTA_logK_New.xlsx)* using the macro GetEqData.xlsx, and the pertinent data, total $[Ca^{2+}]$ and total $[EDTA^{4-}]$ were used to calculate the apparent solubility products ($K_{sp,app}$), as outlined above, for $Ca_2EDTA•7H_2O$ at each NaCl or $MgCl_2$ concentration.

The results of the EQ3/6 simulations of $Ca_2EDTA \bullet 7H_2O$ at increasing NaCl concentrations are tabulated in Table 11-3, these results are displayed in Figure 11-1.

Table 11-3. EQ3/6 Output for $Ca_2EDTA \bullet 7H_2O$ Solubility in NaCl Solutions

NaCl (m)	pmH	Ca (m)	EDTA (m)	App LogK
0.01	7.8	7.07E-02	3.53E-02	-3.75
0.10	7.9	8.80E-02	4.40E-02	-3.47
1.00	8.0	1.24E-01	6.21E-02	-3.02
2.10	8.2	1.21E-01	6.05E-02	-3.05
3.20	8.4	1.10E-01	5.50E-02	-3.18
4.40	8.6	9.67E-02	4.84E-02	-3.34
5.00	8.6	9.05E-02	4.52E-02	-3.43

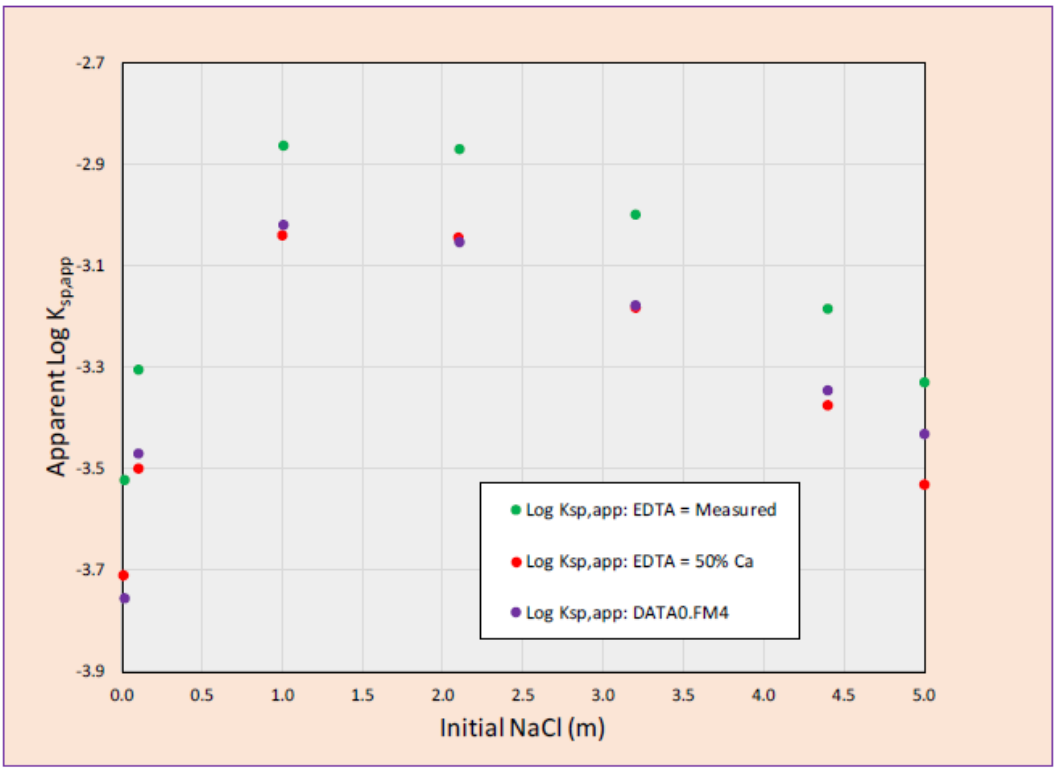

Figure 11-1. Log $K_{sp,app}$ for $Ca_2EDTA \bullet 7H_2O$ as a Function of Sodium Chloride Concentration

Figure 11-1 shows the apparent log K values for $Ca_2EDTA \bullet 7H_2O(s)$ as a function of increasing NaCl concentration as calculated using the laboratory measured EDTA concentrations (green points), the apparent log K values calculated using the measured calcium concentration with the EDTA concentration set equal to 50% of calcium concentration (red points), and finally, the $Ca_2EDTA \bullet 7H_2O(s)$ apparent log K values calculated from the EQ3/6 output using the DATA0.FM4 database (purple points). The close agreement between the red points and the purple points is easily explained by the fact that the log K value included in DATA0.FM4 for $Ca_2EDTA \bullet 7H_2O(s)$ was derived using this dataset (red points) (Domski, 2018). The apparent log K values for $Ca_2EDTA \bullet 7H_2O(s)$ calculated using the laboratory measured EDTA values (green points) fall above the other two datasets. These data were included in Figure 11-2 for

completeness as requested by EPA, and do not reflect on the solubility model of $Ca_2EDTA•7H_2O(s)$ included in DATA0.FM4. Note that the EDTA budget used in the baseline solubility model which provides actinide concentration data to performance assessment is set in the waste inventory and not via equilibrium reactions with $Ca_2EDTA•7H_2O(s)$. Furthermore, the solubility limit of $Ca_2EDTA•7H_2O(s)$ was never reached in any of the 2019 Compliance Recertification Application (CRA-2019) baseline solubility simulations. In other words, the amount of available EDTA is inventory limited.

The results of the EQ3/6 simulations of $Ca_2EDTA•7H_2O$ equilibrium at specified $MgCl_2$ concentrations are listed in Table 11-4, and displayed graphically in Figure 11-2.

Table 11-4. DATA0.FM4 EQ3NR Output for $Ca_2EDTA•7H_2O$ Solubility in $MgCl_2$ Solutions.

$MgCl_2$ (m)	pmH	Ca (m)	EDTA (m)	App LogK
0.01	7.8	7.70E-02	3.85E-02	-3.64
0.10	7.7	1.27E-01	6.33E-02	-2.99
1.00	7.9	3.96E-01	1.98E-01	-1.51
1.50	8.1	5.20E-01	2.60E-01	-1.15
2.00	8.1	6.53E-01	3.26E-01	-0.86
2.50	8.2	8.35E-01	4.18E-01	-0.54

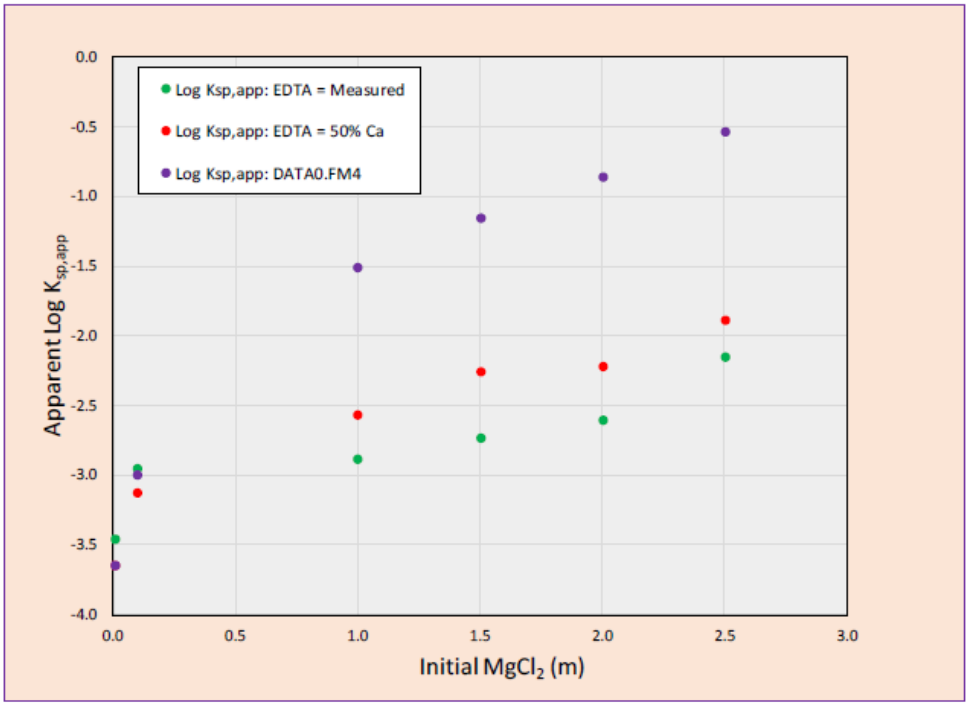

Figure 11-2. Log $K_{sp,app}$ for $Ca_2EDTA.7H_2O$ as a Function of Magnesium Chloride Concentration.

Figure 11-2 shows the log $K_{sp,app}$ values for $Ca_2EDTA•7H_2O(s)$ as a function of increasing $MgCl_2$ concentration as calculated from the EQ3/6 output using the DATA0.FM4 database (purple points), for the experimental data where the EDTA concentration was set equal to 50% of the calcium concentration (red points), and for the measured calcium and EDTA concentrations (green points). It should be noted that the log K_{sp} for $Ca_2EDTA•7H_2O(s)$ that is included in DATA0.FM4 was not derived from either of the datasets displayed in Figure 11-2. The enhanced apparent solubility of the DATA0.FM4 model (purple

points) for $Ca_2EDTA•7H_2O(s)$ as displayed in Figure 11-2 can be attributed, to some extent, to the formation of the strong Mg-EDTA aqueous complex, the stability constant (log β) of which was updated in DATA0.FM4 with the value of Hummel et al., (2005). The formation of Mg-EDTA complexes in solution acts to enhance the solubility of $Ca_2EDTA•7H_2O(s)$, and thus its apparent log K values. Note that for the purposes of the baseline solubility model, which provides the actinide concentrations for performance assessment, the EDTA budget is set by the waste inventory and the solubility of $Ca_2EDTA•7H_2O(s)$ has no effect on the amount of EDTA available to complex with the actinides or any other metals in solution. Furthermore, the solubility limit of $Ca_2EDTA•7H_2O(s)$ was never reached in any of the CRA-2019 baseline solubility simulations. In other words, the amount of available EDTA is inventory limited.

References

The reference documents are provided in Enclosure 3 unless a footnote is designated.

Domski, P.S. 2018. Memo on the estimation of the solubility product (Log K_{sp}) for $Ca_2EDTA·7H_2O$, and Pitzer parameters for the Na_+ / $CaEDTA_{2-}$ Pair. Sandia National Laboratories, Carlsbad, New Mexico. ERMS 570202. [1]

Domski, P.S. and C. Sisk-Scott. 2019. Prediction of baseline actinide solubilities for CRA 2019 with an updated EQ3/6 Pitzer thermodynamic database DATA0.FM4. Sandia National Laboratories, Carlsbad, New Mexico. ERMS 571178.[1]

Hummel, W., G. Anderegg, I. Puigdomenech, L. Rao, and O. Tochiyama. 2005. Chemical Thermodynamics of Compounds and Complexes of U, Np, Pu, Am, Tc, Zr, Ni and Se with Selected Organic Ligands. Chemical Thermodynamics, Vol. 9, OECD Nuclear Energy Agency, Data Bank, Issy-les-Moulineaux, France, Elsevier B.B. Amsterdam, The Netherlands, p. 1088. [1]

Peake, T. 2020. *Second Round of CRA-2019 Completeness Comments.* Letter to M. Brown, Carlsbad Field Office, U.S. Department of Energy. May 6, 2020. [1]

Patterson, R. 2020. *Re: Clarification from EPA*. Email to Tom Peake, U.S. Environmental Protection Agency. June 12, 2020.

Santillan, E-F. 2020. Response to Email from Russ Patterson to Tom Peake Sent on June 12, 2020 Re: Question CC2-GEOCHEM-11 from "Second Round of CRA-2019 Completeness Comments", Letter to Mike Brown Sent on May 6, 2020. Docket ID EPA-HQ-OAR-2019-0534. U.S. Environmental Protection Agency. June 16, 2020.

[1] Reference Documents were provided with CRA-2019, DPA-2019 or a prior DOE Response to EPA Completeness Comments for CRA-2019.

EPA Evaluation of Response

The DOE response was satisfactory for part a) and adequate for parts b & c. However, the Ca2EDTA·7H2O(s) solubility product is rejected by EPA.

CC2-GEOCHEM-12 Evaluation of Revised Citrate Equilibrium Constants

WIPP Compliance Recertification Application 2019 Appendix-GEOCHEM (Geochemistry)

EPA Question (from EPA Completeness Comment Package 2)

Please provide as a function of ionic strength a comparison of the apparent stability constants: 1) reported by Choppin et al. (2001), 2) calculated using the DATA0.FM1 database, and 3) calculated using the DATA0.FM4 database for the following reactions:

GEOCHEM-12a. *Acid dissociation reaction $H_3Citrate(aq) \leftrightarrow H_+ + H_2Citrate_-$ (Choppin et al. 2001, Tables 1 – 7)*
GEOCHEM-12b. *Acid dissociation reaction $H_2Citrate_- \leftrightarrow H_+ + HCitrate_{2-}$ (Choppin et al. 2001, Tables 1 – 7)*
GEOCHEM-12c. *Acid dissociation reaction $HCitrate_{2-} \leftrightarrow H_+ + Citrate_{3-}$ (Choppin et al. 2001, Tables 1 – 7)*
GEOCHEM-12d. *Thorium complexation with citrate (Choppin et al. 2001, Tables 8 – 13)*
GEOCHEM-12e. *Americium complexation with citrate (Choppin et al. 2001, Tables 26 – 31)*
GEOCHEM-12f. *Magnesium complexation with citrate (Choppin et al. 2001, Tables 32 – 37)*

Modification of the previously approved EQ3/6 database DATA0.FM1 to create the DATA0.FM4 database used for CRA-2019 included several changes to the data for citrate aqueous species, and Pitzer parameters (Sisk-Scott and Domski 2019):

- *Replacement of the acid dissociation constants for citrate (Giambalvo 2002) with values from Hummel et al. (2005)*
- *Addition of aqueous stability constants for MgHCitrate(aq), $MgH_2Citrate(aq)$, CaHCitrate(aq), and $CaH_2Citrate(aq)$ (Hummel et al. 2005)*
- *Replacement of the aqueous stability constants for $MgCitrate_-$ and $CaCitrate_-$ (Giambalvo 2002) with values from Hummel et al. (2005)*

Although most of these modifications were small and would be expected to have minor individual effects, DOE has not demonstrated whether the EQ3/6 database used for the CRA-2019 PA actinide solubility calculations yields speciation results consistent with the available high-ionic-strength data for aqueous EDTA species (Choppin et al. 2001) or whether these changes result in improvements in the ability to simulate the data compared to using DATA0.FM1.

Choppin, G.R., A.H. Bond, M. Borkowski, M. Bronikowski, J.-F. Chen, S. Lis, J. Mizera, O.S. Pokrovsky, N.A. Wall, Y.X. Xia, and R.C. Moore. 2001. Waste Isolation Pilot Plant Actinide Source Term Test Program: Solubility Studies and Development of Modeling Parameters. Sandia National Laboratories, Albuquerque, New Mexico, April 2001, SAND99-0943.

Giambalvo, E.R. 2002. Recommended Parameter values for modeling organic ligands in WIPP brines. Memorandum to L.H. Brush, July 25, 2002, ERMS 522981.

Hummel, W., G. Anderegg, I. Puigdomenech, L. Rao, and O. Tochiyama. 2005. Chemical Thermodynamics of Compounds and Complexes of U, Np, Pu, Am, Tc, Zr, Ni and Se with Selected Organic Ligands. Chemical Thermodynamics, Volume 9, OECD Nuclear Energy Agency, Data Bank, Issy-les-Moulineaux, France.

DOE Response (from DOE Response Package 4)

The U.S. Environmental Protection Agency (EPA) has asked the U.S. Department of Energy (DOE) for a comparison of the apparent stability constants as a function of ionic strength from the following sources: 1) reported by Choppin et al. (2001), 2) calculated using the DATA0.FM1 database, and 3) calculated using the DATA0.FM4 database. The DOE interprets this question in the following way: the EPA has asked the DOE to calculate, using EQ3/6, apparent equilibrium constants for citrate deprotonation and apparent dissociation constants for citrate complexes of thorium, americium, and magnesium. The EPA has asked the DOE to compare these calculated results using DATA0.FM1 and DATA0.FM4 to the results given in Choppin et al. (2001), using a methodology similar to that performed in Choppin et al. (2001) and Giambalvo (2002). The methodologies used herein to calculate apparent pKa values for citrate deprotonation (comment 12a-c), and apparent stability constants for thorium, americium, and magnesium citrate complexation (and their 10-based logarithms, log β) (comment 12d-g) are given in the DOE response to CC2-GEOCHEM-10a-d, and 10e-g, respectively and will not be repeated for this comment response.

GEOCHEM 12a, 12b, 12c Acid Dissociation Reactions Comment Response

Tables 1-7 of Choppin et al. (2001) provide the apparent pKa values for citric acid; pKa_1 for $H_3Citrate(aq)$, pKa_2 for $H_2Citrate^-$, and pKa_3 for $HCitrate^{2-}$, at seven sodium chloride concentrations ranging from 0.1m (molality) to 5m. These pKa values are the basis of the thermodynamic model for the sequential deprotonation of citric acid, $H_3Citrate(aq)$, implemented in DATA0.FM1. The pKa values are model parameters derived from laboratory titration data also reported in Choppin et al. (2001). To address this comment, EQ3NR input files were generated to approximate the conditions of Choppin's experiments in order to provide model outputs which could be used to calculate the apparent pKa values for comparison purposes with those reported in Choppin et al. (2001). These EQ3NR input files were executed using both the DATA0.FM1 and DATA0.FM4 databases, and the results from each database were extracted into a Microsoft® Excel spreadsheet using the macro GetEqData.xlsx. The pKa values were subsequently calculated from the molal concentrations of the appropriate aqueous species.

Figure 12-1 shows the pKa values calculated from the EQ3NR output using DATA0.FM1 and DATA0.FM4 plotted with Choppin et al.'s (2001) apparent pKa values for $H_3Citrate(aq)$ deprotonation. The results for all of the models are in agreement, with DATA0.FM1 having slightly closer agreement with Choppin's apparent pKa values than DATA0.FM4.

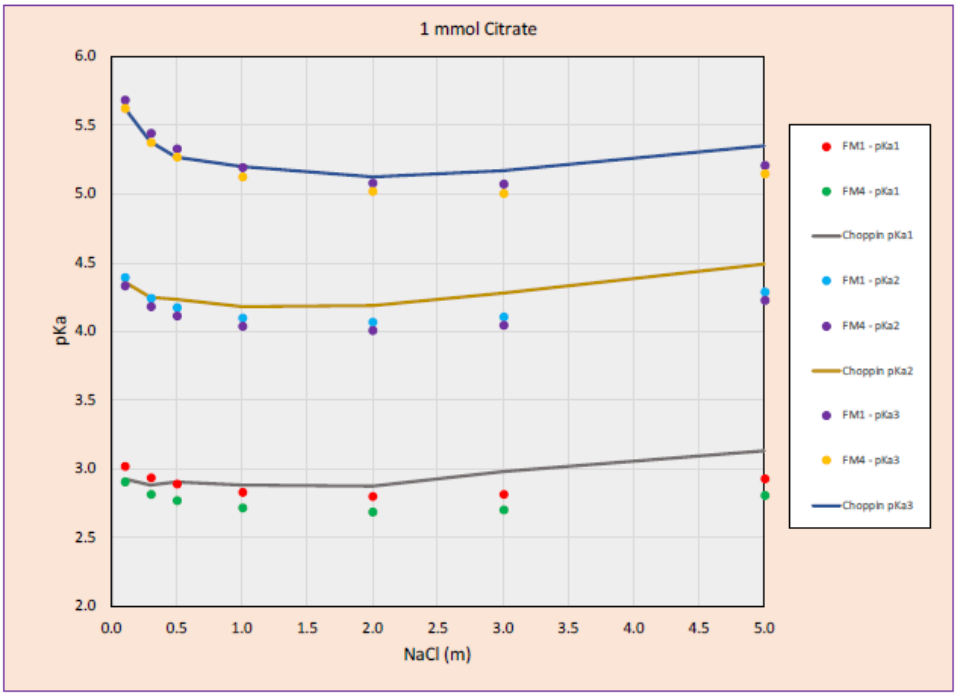

Figure 12-1. H_3Citrate(aq) Acid Dissociation Constants (pKa) as a Function of Sodium Chloride Concentration.

GEOCHEM 12d, 12e, 12f Thorium, Americium, Magnesium Complexation with Citrate Comment Response

Similar to the response for comment 12a – c above, EQ3NR input files were created to match the experimental conditions of Choppin et al. (2001) for $ThCitrate^+$ (Comment 12d), AmCitrate(aq) (Comment 12e), and MgCitrate- (Comment 12f) at six sodium chloride concentrations from 0.3m to 5.0m, with each input concentration executed using DATA0.FM1 and DATA0.FM4. The results of the EQ3NR simulations were extracted into a Microsoft® Excel spreadsheet using the macro GetEqData.xlsx, and the pertinent aqueous species data were used to calculate apparent log β values for each NaCl concentration. The method used to calculate apparent log β values is described in CC2-GEOCHEM-10e and will not be repeated in this section. Figures 12-2 and 12-3 show the comparison of the three models (Choppin et al (2001), DATA0.FM1, DATA0.FM4) for $ThCitrate^+$ and AmCitrate(aq), respectively. There are two outstanding features displayed in these two figures, 1) the results of the DATA0.FM1 simulations do not provide a good fit to Choppin's model, and 2) the results of DATA0.FM1 and DATA0.FM4 are virtually identical. Neither of the log K values for $ThCitrate^+$ or AmCitrate(aq) were updated in DATA0.FM4 relative to DATA0.FM1. Therefore, it may be concluded that although the H_3Citrate(aq) model was updated in DATA0.FM4 from DATA0.FM1, the changes to the log K values of the deprotonation of citric acid did not impact the model performance. Both DATA0.FM1 and DATA0.FM4 underestimate the formation of $ThCitrate^+$ at [NaCl] > 3.0 m. Both DATA0.FM1 and DATA0.FM4 overestimate the formation of AmCitrate(aq) at [NaCl] > 3.0 m.

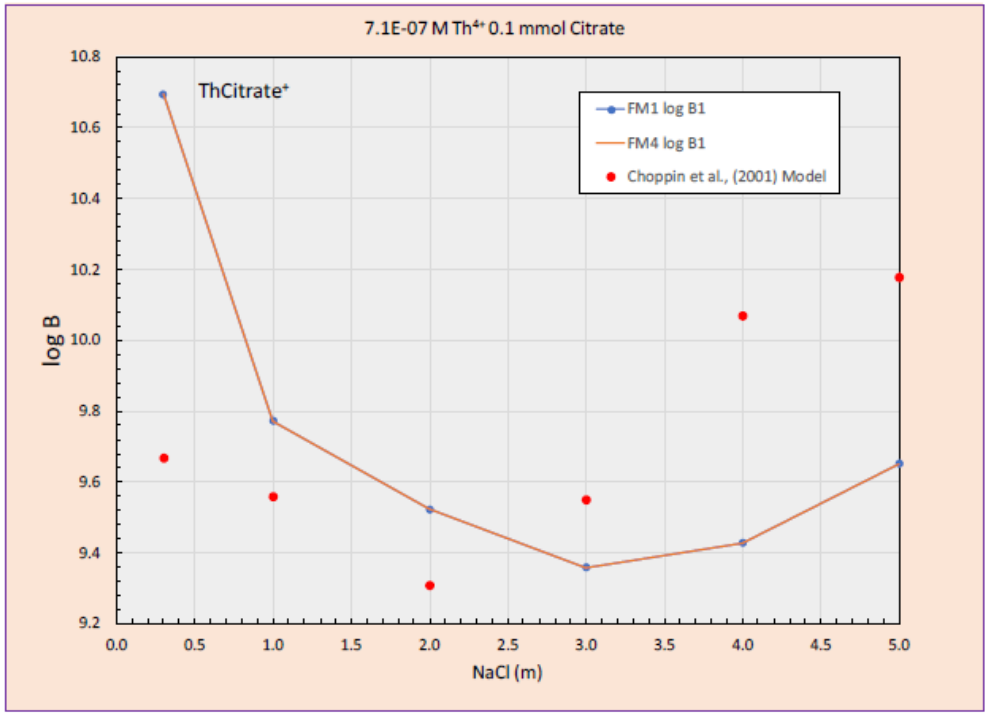

Figure 12-2. Log $\beta_{ThCitrate^+}$ as a Function of Sodium Chloride Concentration.

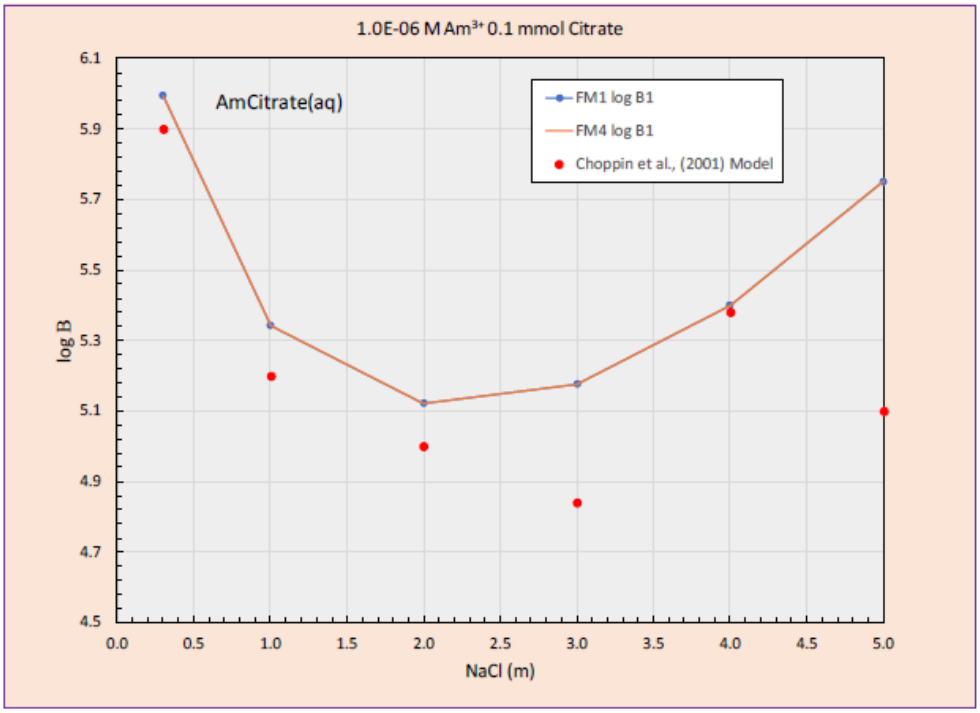

Figure 12-3. Log $\beta_{AmCitrate(aq)}$ as a Function of Sodium Chloride Concentration.

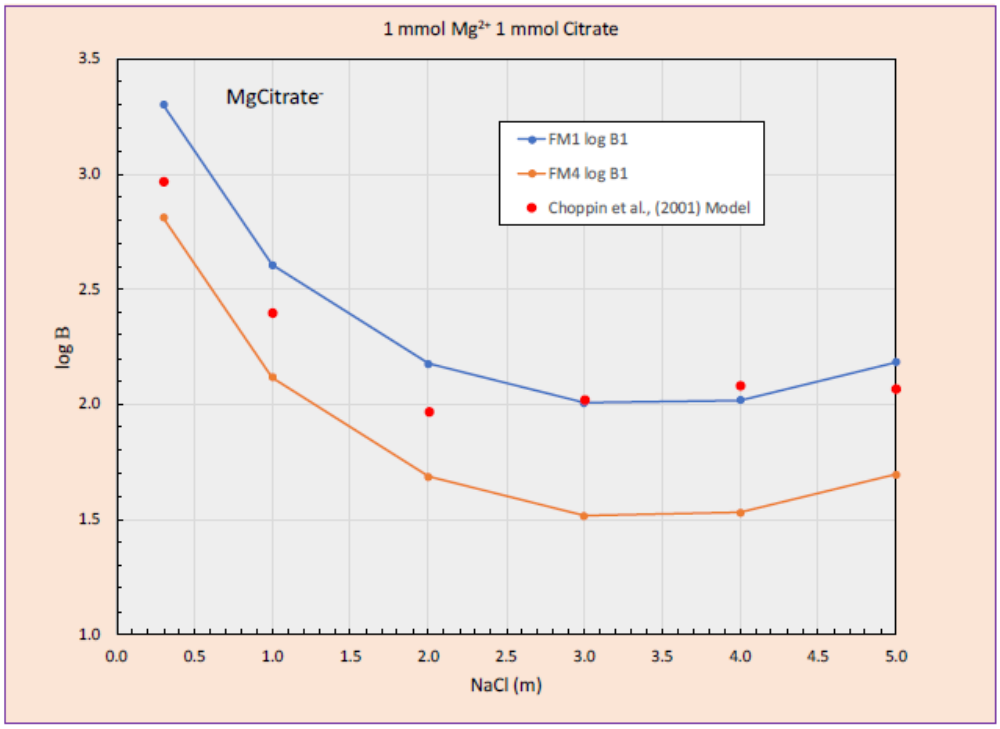

Figure 12-4. Log $\beta_{MgCitrate^-}$ as a Function of Sodium Chloride Concentration.

A comparison of the $MgCitrate^-$ models is displayed in Figure 12-4. The observed deviation of the DATA0.FM4 model is caused by the replacement of the Giambalvo (2002) log K for dissociation of the $MgCitrate^-$ (-5.30) complex in DATA0.FM1 with that of Hummel et al. (2005) in DATA0.FM4 (-4.81), as well as the inclusion of MgHCitrate(aq) and $MgH_2Citrate^+$ of Hummel et al. (2005) in the DATA0.FM4 database. The apparent stability constants reported in Choppin et al. (2001) and those calculated using DATA0.FM1 show better agreement than those calculated using DATA0.FM4. This is to be expected because the DATA0.FM1 was formulated based on the apparent stability constants reported in Choppin et al. (2001). As explained in CC2-GEOCHEM-10, log β values are metrics composed of a mixture of modeling and experimental results. Because the model of Choppin et al. (2001) and Hummel et al. (2005) are different, the disagreement noted in Figure 12-4 are due to the fact that different models were used.

Note that all EQ3/6 input, output and processed output files can be found in the WIPP records center in the following location: /cvs/CVSLIB/WIPP_EXTERNAL/CRA19_comments.

EPA Evaluation of Response

The DOE response was adequate, but additional investigation will be required for future PAs.

CC2-GEOCHEM-13 Omission of Earlandite from DATA0.FM4

WIPP Compliance Recertification Application 2019 Appendix-GEOCHEM (Geochemistry)

EPA Question (from EPA Completeness Comment Package 2)

Please note that although the log K_{sp} for earlandite [$Ca_3(Citrate)_2 \cdot 4H_2O(s)$] is included in Table GEOCHEM-22, the solubility reaction for earlandite was not included in DATA0.FM4.

Appendix GEOCHEM, Table GEOCHEM-22 includes the earlandite dissolution reaction in the list of parameter changes made to the EQ3/6 database [DATA0.FM4] used for the CRA-2019 PA. This reaction is included by Domski (2019, Table 4) and by (Sisk-Scott 2019, Table 4) in the list of equilibrium constants implemented for the CRA-2019. However, this solubility reaction was not included in DATA0.FM4.

DOE Response (from DOE Response Package 6)

The U.S. Environmental Protection Agency (EPA) has correctly noted the absence of Earlandite in DATA0.FM4.

An effort was made to determine if the absence of Earlandite in DATA0.FM4 had an effect that was adverse to quality for the 2019 Compliance Recertification Application (CRA-2019) Deferred Performance Assessment (DPA). This was accomplished by cloning DATA0.FM4 and adding Earlandite and renaming the database DATA0.ERL. The DATA0.ERL database was used only to address this comment. Baseline solubility input files for the minimum-volume cases for Energy Research and Development Administration (WIPP Well) 6 (ERDA-6) and Generic Weep Brine (GWB) brines, which have the maximum organic ligands concentrations, were prepared and run with EQ3/6. Using the maximum anticipated organic ligands concentrations in these brines, specifically citrate, facilitate a determination of whether Earlandite reaches supersaturation during the reaction-path simulations, and thus precipitates from solution. Precipitation of Earlandite from solution would effectively lower citrate concentration to its solubility from the system, lessening its effect on actinide solubility.

The following data block was added to DATA0.ERL:

```
+------------------------------------------------------------------------

Earlandite              Ca3Citrate2:4H2O

     sp.type =  solid
*    EQ3/6   =  hmo
     revised =  16-oct-2006
*    mol.wt. =   570.5008 g/mol
     V0PrTr  =     0.000 cm**3/mol [source:          ]
****
     4 element(s):
     12.0000 C             18.0000 H             18.0000 O
      3.0000 Ca
****
     4 species in aqueous dissociation reaction:
     -1.0000  Earlandite                   3.0000  Ca++
      2.0000  Citrate---                   4.0000  H2O
*
**** logK grid [0-25-60-100C @1.0132bar; 150-200-250-300C @Psat-H2O]:
        500.0000  -17.9000  500.0000  500.0000
        500.0000  500.0000  500.0000  500.0000
+------------------------------------------------------------------------
```

The CRA-2019 input files for ERDA-6 and GWB were executed using the DATA0.ERL database and the results of the EQ3/6 simulations were extracted into the spreadsheet, *Earlandite_SI.xlsx*, using the macro *GetEQdata.xlsx*. The results show that the maximum saturation index (SI) (Log Q/K) for ERDA-6 brine was -2.83, and -4.46 for GWB. Negative values of SI indicate undersaturation, a zero value indicates saturation, and positive values indicate supersaturation. Thus, Earlandite never attained saturation in either brine and total citrate concentration was not solubility limited (in either brine). Therefore, the oversight of Earlandite not being included in DATA0.FM4 did not create a situation adverse to quality and there was no impact on the CRA-2019 DPA.

The files used to address this comment are contained in the zip file *CC2-GEOCHEM-13.zip*, the individual files are listed in Table 1, and are stored at this location:
/cvs/CVSLIB/WIPP_EXTERNAL/CRA19_comments

Table 1. Files and Description Contained in the Zip File *CC2-GEOCHEM-13.zip*

List of Included files	File Description
DATA0.ERL	Non-QA EQ3/6 Database with Earlandite
Earlandite_SI.xlsx	EQ6 Output spreadsheet
ERDA6_1x.3i	ERDA-6 EQ3NR Input file
erda6_1x.3p	ERDA-6 EQ3NR pickup file
ERDA_1X.6i	ERDA-6 EQ6 Input file
erda_1x.6o	ERDA-6 EQ6 Output file
GWB_1x.3i	GWB EQ3NR Input file
gwb_1x.3p	GWB EQ3NR pickup file
GWB_1x.6i	GWB EQ6 Input file
gwb_1x.6o	GWB EQ6 Output file

The elimination of references to earlandite in the Appendix GEOCHEM have been added to Enclosure 2, CRA-2019 Errata Tracking.

EPA Evaluation of Response

The DOE response was satisfactory. DOE acknowledged the omission and calculations demonstrated no effects on actinide solubility modeling results.

CC2-GEOCHEM-15 Effects of Selected G Value for H2(g) Production by Brine Radiolysis

WIPP Compliance Recertification Application 2019 Appendix-GEOCHEM (Geochemistry)

EPA Question (from EPA Completeness Comment Package 2)

Please provide justification for selecting a single G value (1.4 molecules/100 eV) for the production of H_2(g) by alpha radiolysis by evaluating the effects on repository releases of using this single, higher-range value compared to a sampled range of values.

> *Day (2019) selected a G value of 1.4 molecules/100 eV for modeling radiolytic H_2(g) production, which is near the high end of the range of values (0.6 – 1.5 molecules/100 eV) reported by Reed et al. (1993) based on experiments in WIPP brines. The justification for selecting a relatively high G value and its likely effects on releases from the repository compared to using sampled values from the reported range in WIPP brines was not provided. Selection of a relatively high G value increases gas production and may yield higher pressures, which could increase spallings releases. Relatively large G values also increases brine consumption, which could decrease direct brine releases. Consequently, the potential effects on overall repository releases of using a relatively high H_2(g) G value are unclear.*
>
> *Day, B. 2019. Reassessment of need and parameter justification for modeling gas generation due to radiolysis of brine and cellulose/plastic/rubber in WIPP for CRA-2019. Sandia National Laboratories, Carlsbad, New Mexico. ERMS 570873.*

DOE Response (from DOE Response Package 7)

The G value for molecular hydrogen in water is 1.56 molecules (molec)/100 electron Volts (eV) (0.163 moles [mol]/joules [J]) and is well established for ~ 5 MeV alpha particle irradiation (Spinks and Woods, 1990; Table 7.4). The Waste Isolation Pilot Plant (WIPP) experiments (Reed et al., 1993) were performed to evaluate the potential effects of the high concentrations of cations present in WIPP-relevant brine (e.g., sodium, potassium, and magnesium) on H_2 yield as these could interfere with the solvated electron chemistry to lower or raise the molecular hydrogen yield. These experiments were difficult to perform. Sampling of the small volume of produced gas in a high liquid:gas volume experiment, relatively long experimental times, use of WIPP-relevant brines and relatively low Pu-239 concentrations made deriving results more complicated. Some precipitation was noted at longer times which effectively lowered the dose to solution in the experiment. For these reasons, the best-value yields recommended are biased towards the initial higher-value data obtained: 1.4 ± 0.1, 0.9 ± 0.2, 1.3 ± 0.1, and 1.3 ± 0.1 molec/100 eV for Brine A, ERDA-6, DH-36, and G8-B WIPP brines respectively (Table 1 in Reed et al., 1993). Since these WIPP-specific studies, the hydrogen yield was theoretically calculated to be 1.52 molec/100 eV for 5 molar (M) sodium chloride (Kelm et al., 1999) based on measured hypochlorite production rates. All of these data, taken together, confirm that the cations present in WIPP brine lead to a relatively small impact on the pure water-hydrogen yield and this is the basis of the G_{H2} = 1.4 ± 0.1 value considered for use in WIPP Performance Assessment (PA).

The main uncertainty in the radiolytic hydrogen production rates used in PA is in the assumptions and calculational approach used to model energy deposition. This uncertainty is accounted for in the broad range of the energy deposition probability for wetted solid radionuclides (GLOBAL:GDEPFAC), which is sampled uniformly between 0 and 0.5. The range of values used for the energy deposition probability covers uncertainty in the G value, as well as other uncertainties such as adherence and coating by non-hydrogenous materials and particle size based self attenuation (Day 2019, Table 3 page 7). The uncertainty in energy deposition probability is much greater than the uncertainty in G value. Adding an additional uncertain variable to PA calculations that attempts to capture the impact of the small variability in G value relative to the variability in GLOBAL:GEDPFAC would be superfluous.

The energy deposition probability parameter (GLOBAL:GDEPFAC) was shown to not have substantial impact on the variability of any release mechanism or total releases in CRA-2019 PA results (Zeitler 2019), so it is not expected that PA results would be impacted by uncertainty in the G value.

References

Kelm, M., I. Pashalidis and J.I. Kim. 1999. Spectroscopic Investigation on the Formation of Hypochlorite by Alpha Radiolysis in Concentrated NaCl Solutions. Applied Radiation and Isotopes 51: 637–642.

Reed, D., S. Okajima, L. Brush and M. Molecke. 1993. Radiolytically-Induced Gas Production in Plutonium-Spiked WIPP Brine, Scientific Basis for Nuclear Waste Management XVI, Materials Research Society Symposium Proceedings, Boston, MA, November 30 – December 4, 1992. C.G. Interrante and R.T. Pabalan, eds. SAND92-7283C. ERMS 228637. Materials Research Society, Pittsburgh, PA. Vol. 294, pp. 431–438

Spinks, J. and R. Woods. 1990. An Introduction to Radiation Chemistry, Third Edition, John-Wiley and Sons, Inc., New York, Toronto. 574 Seiten, Preis: DM 91, 45. ISBN 0-471-61403-3.

Zeitler, T. 2019. Analysis Package for the Sensitivity of Releases to Input Parameters in the 2019 Compliance Recertification Application Performance Assessment (CRA-2019 PA). ERMS 571374. Carlsbad, NM: Sandia National Laboratories.

EPA Evaluation of Response

The DOE response was satisfactory. The information was provided as requested.

CC2-GEOCHEM-16 Omission of RH Waste Gamma Irradiation from Radiolysis Evaluation

WIPP Compliance Recertification Application 2019 Appendix-GEOCHEM (Geochemistry)

EPA Question (from EPA Completeness Comment Package 2)

Please explain the omission of the potential effects of gas generation from gamma radiation from RH waste on performance assessment.

Day (2019, page 2) states that lower G(H2) values for gamma radiation combined with low gamma dose rates associated with contact-handled waste supports consideration of only gas generation by alpha radiolysis for performance assessment. However, the effects of gamma radiation from RH waste on gas generation is not directly addressed.

Day, B. 2019. Reassessment of need and parameter justification for modeling gas generation due to radiolysis of brine and cellulose/plastic/rubber in WIPP for CRA-2019. Sandia National Laboratories, Carlsbad, New Mexico. ERMS 570873.

DOE Response (from DOE Response Package 7)

When screening radionuclides for inclusion in the radiolysis model, both contact-handled (CH) and remote-handled (RH) inventories were considered (Kicker 2019). The radionuclide disintegration energy

used in the PA calculation given by Kicker (2019) is the Total Emitted Energy from the International Commission on Radiological Protection (ICRP) ICRP-07 Collection (ICRP 2008, Appendix A); meaning that the disintegration energy used is the sum of the alpha, beta, and gamma disintegration energy for each radionuclide. The ICRP-07 Collection includes the disintegration energy for each decay type, meaning a similar methodology used by Kicker (2019, Appendix C) to screen radionuclides can be used to compare decay types to total decay heat of the Compliance Recertification Application (CRA)-2019 Inventory. Where Kicker uses the total disintegration energy to calculate the total decay heat of the inventory, this analysis uses each decay type disintegration energy to calculate a decay heat for that decay type. Dividing each decay heat type by the total decay heat gives the percent contribution of that decay type to the total decay heat. The results of breaking the radionuclide disintegration energy into decay type in watts, for the CRA-2019 Inventory are shown in Table 1. At repository closure, alpha decay accounts for 97% of the total decay heat. As the inventory decays through time, alpha decay becomes even more dominant over beta and gamma decay. By 2133 (100 years post-closure), alpha decay accounts for over 99% of the total inventory decay heat. The total inventory decay heat at the end of the 10,000-year regulatory period is completely dominated by alpha decay.

A more complex model for radiolysis with a separate gamma decay calculation would have a gamma-specific G value and energy deposition factor. While it is expected that the (dimensionless) energy deposition factor would be larger for gamma decay as the emitted photons would have less self-attenuation, as noted in Day (2019) the G value for gamma decay would be smaller (0.43 vs 1.4 molec/100 eV) than the G value used for alpha decay. This larger energy deposition factor and smaller G value would mostly cancel out leaving the fractional decay-heat contribution from the inventory as the primary difference factor between alpha and gamma decay radiolysis. As shown in Table 1, the heat contribution of gamma irradiation is no more than 1% of the total decay heat. This small contribution is the basis of the radiolytic gas generation model being focused on alpha decay.

Table 1 Decay Heat for CRA-2019 Inventory

Year	Decay Type	CH Waste (watts)	RH Waste (watts)	CH + RH (watts)	Decay Type % of Total Decay heat[1]
2033 (Closure Date)	Alpha	1.06E+05	2.61E+03	1.08E+05	97.1%
	Beta (Electron)	4.35E+02	1.70E+03	2.13E+03	1.9%
	Gamma (Photon)	2.24E+02	8.63E+02	1.09E+03	1.0%
	Total (α+β+γ)	1.06E+05	5.17E+03	1.11E+05	100.0%
2133 (100 years post closure)	Alpha	8.44E+04	1.04E+03	8.54E+04	99.1%
	Beta (Electron)	3.12E+02	1.54E+02	4.66E+02	0.5%
	Gamma (Photon)	1.93E+02	8.62E+01	2.79E+02	0.3%
	Total (α+β+γ)	8.49E+04	1.28E+03	8.62E+04	100.0%
12033 (10,000 years post-closure)	Alpha	2.37E+04	1.49E+02	2.39E+04	99.8%
	Beta (Electron)	3.76E+01	9.64E-01	3.85E+01	0.2%
	Gamma (Photon)	6.70E+00	4.00E-01	7.10E+00	0.0%
	Total (α+β+γ)	2.38E+04	1.51E+02	2.39E+04	100.0%

[1] (CH+RH)/Total(alpha + beta + gamma)

References

ICRP, 2008. Nuclear Decay Data for Dosimetric Calculations. ICRP Publication 107. Ann. ICRP 38

Kicker, D. 2019. Radionuclide Inventory Screening Analysis for the 2019 Compliance Recertification Application Performance Assessment (CRA-2019 PA). Sandia National Laboratories, Carlsbad, NM. ERMS 571244.

EPA Evaluation of Response

The DOE response was satisfactory. Clarifying information was provided.

CC3-GEOCHEM-17 Plutonium Particle Sizes Used in Radiolytic Gas Generation Calculations

WIPP Compliance Recertification Application 2019 Appendix-GEOCHEM (Geochemistry)

EPA Question (from EPA Completeness Comment Package 3)

Please compare the general composition and particle sizes of the Pu materials used in the Narlesky et al. (2012) study with the surplus Pu waste stream SR-KAC-PuOx and other WIPP wastes by addressing the questions below. The composition and particle size of the waste can have important impacts on the extent of radiolytic gas generation.

GEOCHEM-17a. **SR-KAC-PuOx Material Originating Site**

Please indicate whether the SR-KAC-PuOx material originated at the same sites as the material in the Narlesky et al. (2012) study (Hanford, Rocky Flats, and Los Alamos National Laboratory).

DOE Response (from DOE Response Package 7)

> The Narlesky et al. (2012) report describes representative materials for DOE-STD-3013, the U.S. Department of Energy (DOE) standard that provides guidance on the stabilization, packaging, and storage of plutonium-bearing materials (the current version is DOE 2018). All materials dispositioned as part of the SR-KAC-PuOx waste stream have been processed (i.e., stabilized by heating to 950C in an oxidizing atmosphere or approved equivalent) to meet this standard. All of the material in SR-KCAC-PuOx may originate from processes represented in the Narlesky document.
>
> A large fraction of the plutonium dispositioned as SR-KAC-PuOx originated at the specific sites identified in Narlesky et al. (2012) – Rocky Flats, Hanford, and Los Alamos National Laboratory (LANL). There are also materials in the SR-KAC-PuOx waste stream that originated at Savannah River Site (SRS) and Lawrence Livermore National Laboratory (LLNL). However, each of the materials originating from SRS or LLNL is represented by specific items in the Narlesky report based on processing history or impurities present in the material following stabilization (see references 4-10, as cited in the Material Representation of Narlesky et al. 2012). The processes identified in Narlesky (e.g., metal oxidation, aqueous processing, etc.) represent the full range of processes supplying materials for surplus plutonium disposition as part of SR-KAC-PuOx.
>
> References
>
> U.S. Department of Energy. 2018. Stabilization, Packaging and Storage of Plutonium-Bearing Materials. DOE-STD-3013-2018
>
> Narlesky, J., M. Stroud, P. Smith, D. Wayne, R. Mason and L. Worl. 2012. Characterization of representative materials in support of safe, long term storage of surplus plutonium in DOE-STD-3013 Containers. Los Alamos National Laboratory, Los Alamos, New Mexico. LA-UR-12-23790.

EPA Question

GEOCHEM-17b. **Process or Processes Producing SR-KAC-PuOx**

Please identify the process or processes that produced the SR-KAC-PuOx (e.g., aqueous processing, metal oxidation, or other processes).

DOE Response

Materials in the SR-KAC-PuOx waste stream may originate from any of the five categories identified in Table 1 of Narlesky et al. (2012); i.e., aqueous processing, metal oxidation, mixed actinide operations, molten salt operations, or miscellaneous (as defined in the Narlesky report).

References

Narlesky, J., M. Stroud, P. Smith, D. Wayne, R. Mason and L. Worl. 2012. Characterization of representative materials in support of safe, long term storage of surplus plutonium in DOE-STD-3013 Containers. Los Alamos National Laboratory, Los Alamos, New Mexico. LA-UR-12-23790,

EPA Question

GEOCHEM-17c. **Effects of Particle Size Reduction During Repackaging Process**

Please evaluate the effects of particle size reduction during the repackaging process on the SR-KAC-PuOx waste stream and other plutonium wastes in the WIPP inventory on radiolytic gas generation. In this evaluation, please assess the additional modeling uncertainty introduced as a result of a higher proportion of smaller particle sizes than the distribution Narlesky et al. (2012) has reported.

DOE Response

The implementation of a model for gas generation due to brine radiolysis in the CRA-2019 PA was based, in part, on assumptions about waste particle sizes in WIPP waste (Day 2019). Particle size in the transuranic (TRU) waste emplaced at WIPP is uncertain and is not tracked as part of typical waste stream data. The best available distribution of waste particle sizes for PuO_2 waste is from Narlesky et al. (2012) and is based on Pu waste derived from a variety of processes used throughout the DOE complex. The Narlesky data was used in parameterizing the brine radiolysis model in Day (2019). The DOE continues to support the CRA-2019 PA approach, and the parameter values used for brine radiolysis

The particle size distribution derived by Narlesky et al. (2012) was assumed by Day (2019) to be representative of the radionuclide-bearing wastes that contribute substantially to gas generation from brine radiolysis. Pu contributes a majority (>96%) of the WIPP alpha-emitting inventory disintegration energy (the contribution to disintegration energy was confirmed by wattage calculations in Appendix C of Kicker 2019).

The SR-KAC-PuOx waste stream was not created at the time of the Narlesky et al. (2012) report, but as established in parts 17a and 17b above, the material in this waste stream is derived by the same processes as the material examined in Narlesky et al. (2012). The fissile content of this waste stream is largely comprised of Pu and represents about 29% of the TRU waste in terms of U.S. Environmental Protection Agency (EPA) units, by far the greatest percentage of any of the 607 waste streams (Kicker 2019).

The waste in the SR-KAC-PuOx waste stream will undergo repackaging (McAlhany 2018). However, the particle size distribution reported in Narlesky et al. (2012) should not be altered by the repackaging process at SRS because in the process used by Narlesky et al. at LANL, the particle size analysis included agitating a sample in an electrolyte solution using an ultrasonic bath prior to measurement. This processing is intended to break down any agglomerates of particles prior to particle size analysis and thus resulted in particles of minimal size. On the other hand, dilute and dispose operations utilize the minimum mechanical processing necessary to break down agglomerates containing plutonium-bearing materials to pass a 2 millimeter (mm) sieve (i.e., #10). This size reduction step is performed to ensure adequate mixing of the plutonium-bearing materials with adulterant used in the dilute and dispose approach. The processing steps required for dilute and dispose packaging should not change the particle size defined by a laser scattering analysis with particle sizes in the sub 100 micrometer (µm) range. For the above reasons, the Narlesky particle size distribution is a reasonable representation of WIPP waste in general for the purposes of brine radiolysis.

An evaluation of the potential effects of particle size reduction on radiolytic gas generation, as implemented in WIPP PA, is provided below.

A reduction in waste particle size would increase the percent of energy released as shown in Figure 2 of Day (2019), which depicts the fractional energy released as a function of particle diameter (reproduced below as Figure 1). Within the PA calculation, an increase in the amount of energy would be modeled as an increase in the energy deposition probability (parameter GLOBAL:GDEPFAC). For the CRA-2019 PA, the distribution for the energy deposition probability parameter was derived in part from an assumed particle diameter of 20.5 µm, corresponding to a fractional energy release of 45%. The fractional energy release was not the only factor used in deriving the energy deposition probability (Day 2019), other processes such as additional attenuation due to adherence to and coating by non-hydrogenous materials were also included. The energy deposition probability (GLOBAL:GDEPFAC) parameter was sampled uniformly from 0 to 0.5 in the CRA-2019 PA.

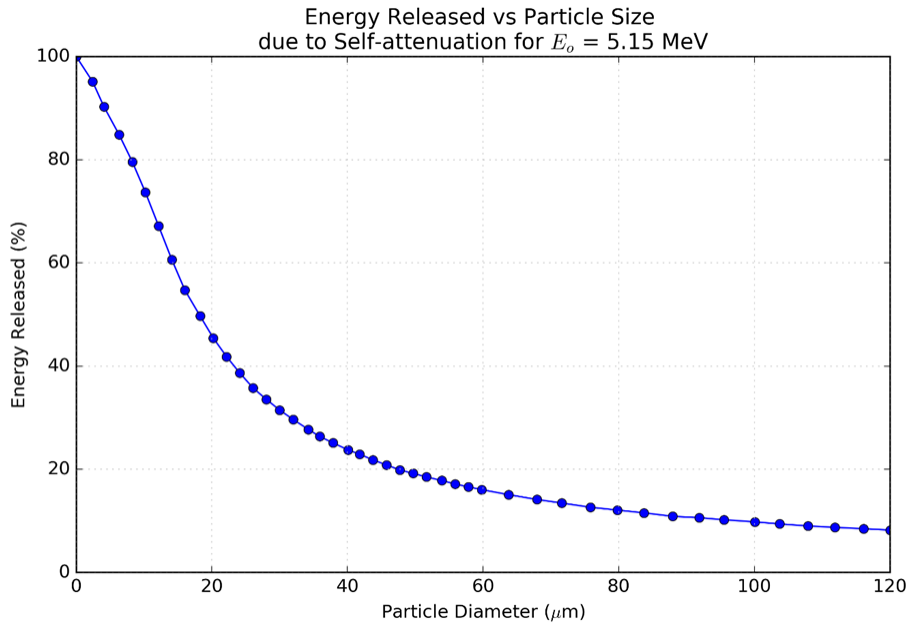

Figure 1 Fractional Energy vs. Particle Diameter for PuO2 (from Figure 2 from Day 2019)

To evaluate the effects of increasing the energy deposition probability, two additional PA calculations have been run for the 100 vectors of replicate 1 of the CRA-2019 PA. In the first calculation (denoted as GDEPF01), the energy deposition probability has been sampled uniformly between 0 and 1, the theoretical minimum and maximum values[2]. In the second calculation (denoted as GDEPFAC), the energy deposition probability has been set to a constant value of 1, the theoretical maximum value, corresponding to a maximized energy release associated with a minimized particle diameter[3]. A summary of the energy deposition probability parameter values used in the three calculations is provided in Table 2. Comparisons of average results over the 100 vectors among the CRA19, GDEPF01, and GDEPFAC calculations are provided in Figure 2 through Figure 7 for gas generation and estimated releases.

Table 2 Summary of Energy Deposition Probability (GLOBAL:GDEPFAC parameter) Values Used in the CRA19, GDEPF01, and GDEPFAC Calculations

Calculation Name	GLOBAL:GDEPFAC Parameter			
	Distribution Type	Minimum	Maximum	Mean
CRA19	Uniform	0	0.5	0.25
GDEPF01	Uniform	0	1	0.5
GDEPFAC	Constant	1	1	1

[2] Files associated with the GDEPF01 calculation are archived on the WIPP PA cluster at /nfs/data/CVSLIB/WIPP_EXTERNAL/CRA19_comments/CC3-GEOCHEM-17-21/GDEPF01.tar.gz.
[3] Files associated with the GDEPFAC calculation are archived on the WIPP PA cluster at /nfs/data/CVSLIB/WIPP_EXTERNAL/CRA19_comments/CC3-GEOCHEM-17-21/GDEPFAC.tar.gz.

The gas generation process model implemented in WIPP PA consists of three mechanisms: brine radiolysis, iron corrosion, and the biodegradation of cellulosics, plastics, and rubber (CPR). All of these processes are modeled as generating hydrogen gas in the repository waste areas which results in increased repository pressure. All three mechanisms are assumed to generate more gas at higher brine saturations. The brine radiolysis and iron corrosion mechanisms are assumed to consume water as gas is generated, but the CPR degradation mechanism is assumed to generate water.

Figure 2 shows a comparison of average gas generation in moles over time from the brine radiolysis model implemented in the BRAGFLO code for the 100 vectors in each of three calculations. The comparison is made for scenario S2-BF, the scenario in which an intrusion intersects both the repository and the pressurized Castile below the repository at 350 years postclosure. This scenario was chosen for comparison because it has the highest brine saturations of the six BRAGFLO scenarios. Higher brine saturation promotes higher gas generation due to brine radiolysis being driven, in part, by brine availability. As such, the comparison using this scenario shows the maximum effect of the changes to the GLOBAL:GDEPFAC parameter.

Because both the GDEPF01 and GDEPFAC calculations have, on average, greater values of the GLOBAL:GDEPFAC parameter, gas generation has increased compared to CRA-2019, as expected. Also as expected, gas generation in the GDEPFAC calculation exceeds that of the GDEPF01 calculation due to the increased value of the GLOBAL:GDEPFAC parameter. The results of the GDEPFAC calculation show the impact of maximizing gas generation due to brine radiolysis. Figure 3 shows a comparison of mean gas generation in moles over time for all three gas generation mechanisms included in BRAGFLO for scenario S2-BF across the 100 vectors in each of three calculations. The same trend of increased overall gas generation for increased values of the GLOBAL:GDEPFAC parameter holds here as well, despite the increased consumption of brine leading to reduced brine saturations, and therefore, reduced gas generation from the other two gas generation mechanisms.

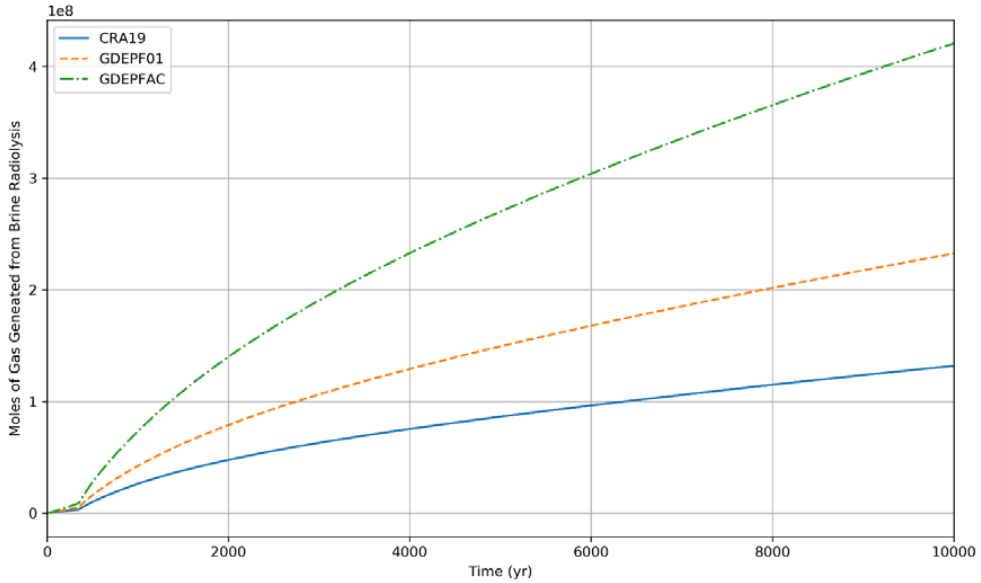

Figure 2 Mean H2 Generation from Brine Radiolysis for S2-BF

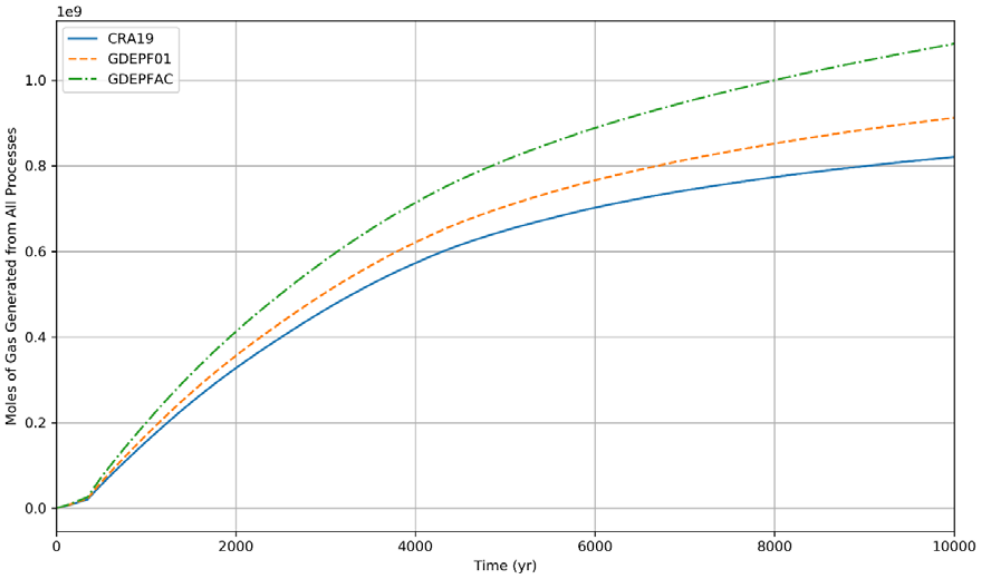

Figure 3 Mean H_2 Generation for S2-BF Across All Gas Generation Processes

Figure 4 shows a comparison of the average brine pressures and saturations through time in each of three waste areas in the BRAGFLO grid. As gas generation increased in the GDEPF01 and GDEPFAC analyses, the pressure in the waste areas also increased. The increase in brine radiolysis increased brine consumption, lowering the brine saturation across the GDEPF01 and GDEPFAC analyses.

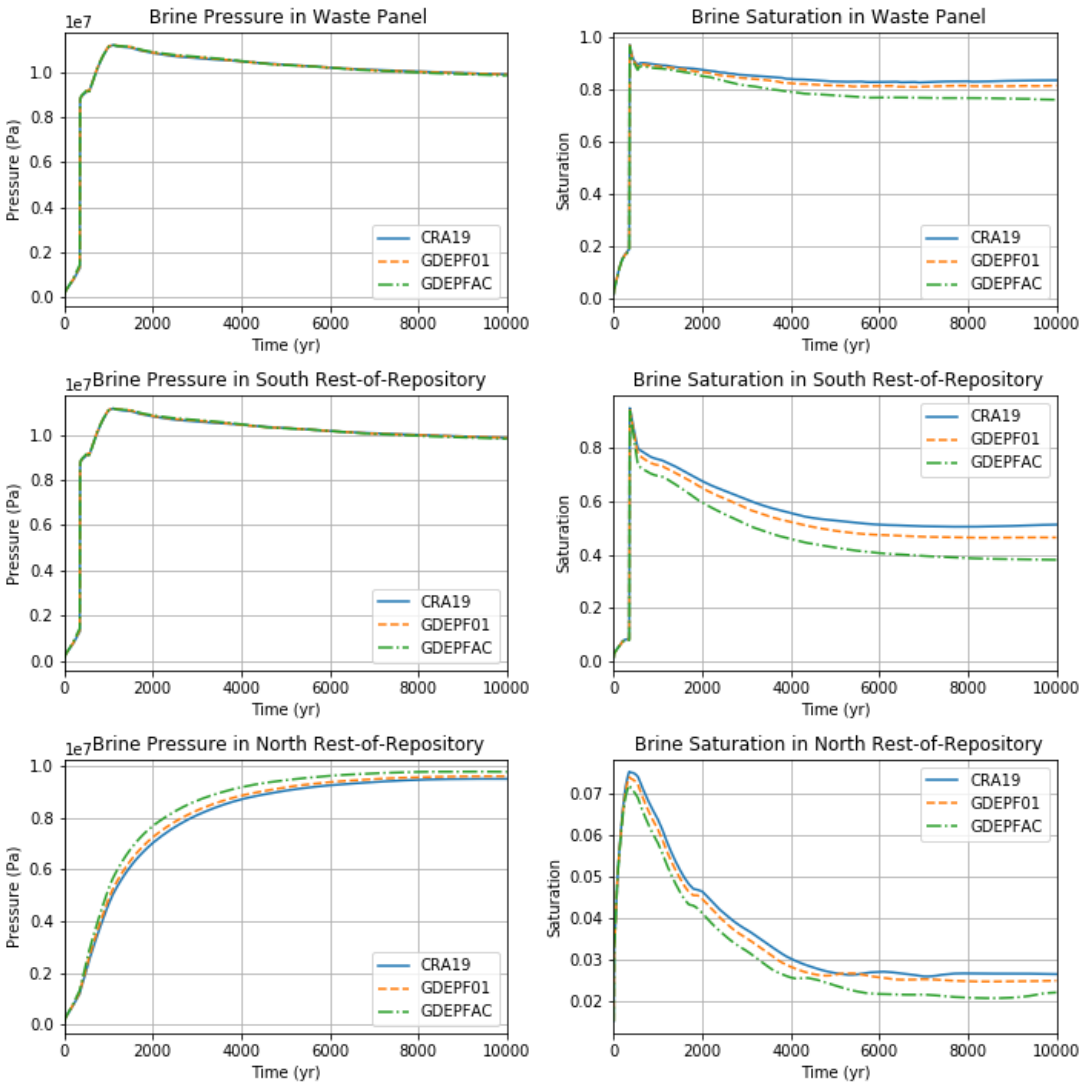

Figure 4 Mean Brine Pressure and Saturation in the Waste Areas for S2-BF.

Figure 5 shows the mean complementary cumulative distribution function (CCDF) for total releases for these two calculations compared to replicate 1 of the CRA-2019 PA. These results show that increasing the average energy deposition probability, and therefore increasing the average gas generation from brine radiolysis, has led to decreased average total releases. The effect is observed primarily for mean releases at lower probability, while mean release at higher probability are not significantly impacted much. From these results, we may generalize that mean releases decrease with increased radiolytic gas generation resulting from decreased particle size.

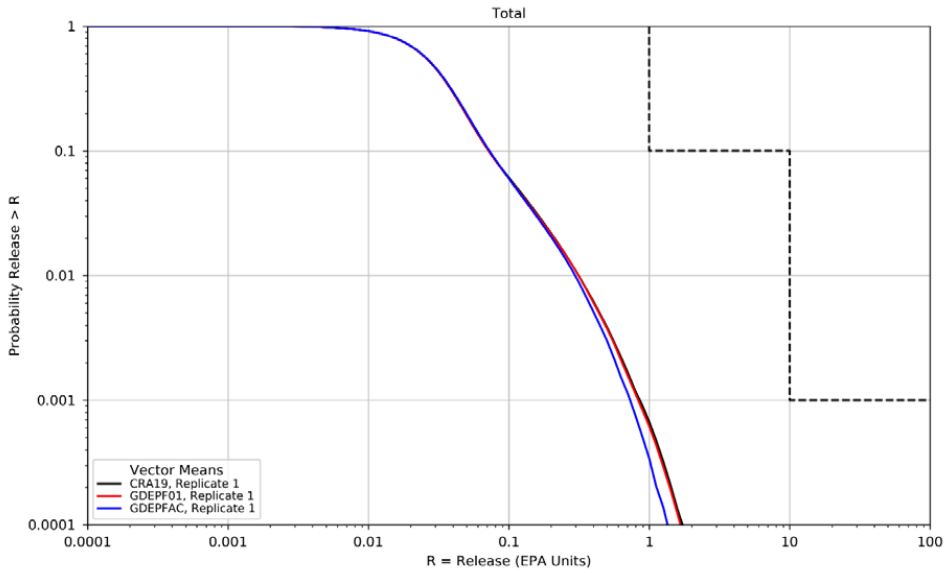

Figure 5 Mean CCDF for Total Release for Replicate 1

Further investigation show that direct brine releases (DBRs) are the primary driver for total releases in the area of the total release curve where the decrease is seen. Figure 6 shows the mean CCDF for DBRs for the two calculations compared to CRA-2019. The DBRs decrease with the increased gas generation due to brine radiolysis. DBRs generally increase with increased repository pressure and increased brine saturation but are also dependent on uncertain parameters such as residual brine saturation in the waste areas (WAS_AREA:SAT_RBRN). Thus, the relative impacts of changes in pressure and saturation vary across vectors as well. Because brine radiolysis results in increased pressures (due to gas generation), but decreased saturations (due to brine consumption), DBRs may increase or decrease depending on the specific combination of pressures and saturations for a given vector. However, when averaged over all vectors, mean DBR releases tend to decrease with increasing gas generated from radiolysis as indicated in Figure 6.

Figure 7 shows the mean CCDFs for spallings releases. Spallings releases are driven by repository pressures and are independent of brine saturation; increased pressures result in increased spallings releases. For the three calculations considered here, an increase in spallings releases is seen with the increases in brine radiolysis, as expected. Spallings releases are overshadowed by DBRs in the total release curve, so this increase in spallings releases does not impact the total release curves. Cuttings and cavings releases are independent of pressures and saturations, and thus independent of brine radiolysis parameterization. Releases from the Culebra show even less sensitivity to the changes in brine radiolysis than do spallings and DBRs. The results for these release mechanisms, are therefore not shown here.

In summary, the effects of particle size reduction were examined by considering the potential of additional gas generation due to brine radiolysis for smaller particles. A higher proportion of smaller particle sizes would effectively increase the percentage of energy released, which can be accounted for by skewing the GLOBAL:GDEPFAC (i.e., energy deposition factor) parameter distribution to higher values. The impact of changing the distribution of GLOBAL:GDEPFAC was assessed in two additional analyses, one of which raised the upper bound of the distribution

from 0.5 to 1 (GDEPF01 analysis) and the other of which assumed a constant value of 1 for all vectors (GDEPFAC analysis). In both analyses, the increased energy deposition probability results in decreased DBRs and increased spallings, leading to a net decrease in total releases. The DOE continues to support the uniform 0 to 0.5 distribution of GLOBAL:GDEPFAC used in the CRA-2019 PA.

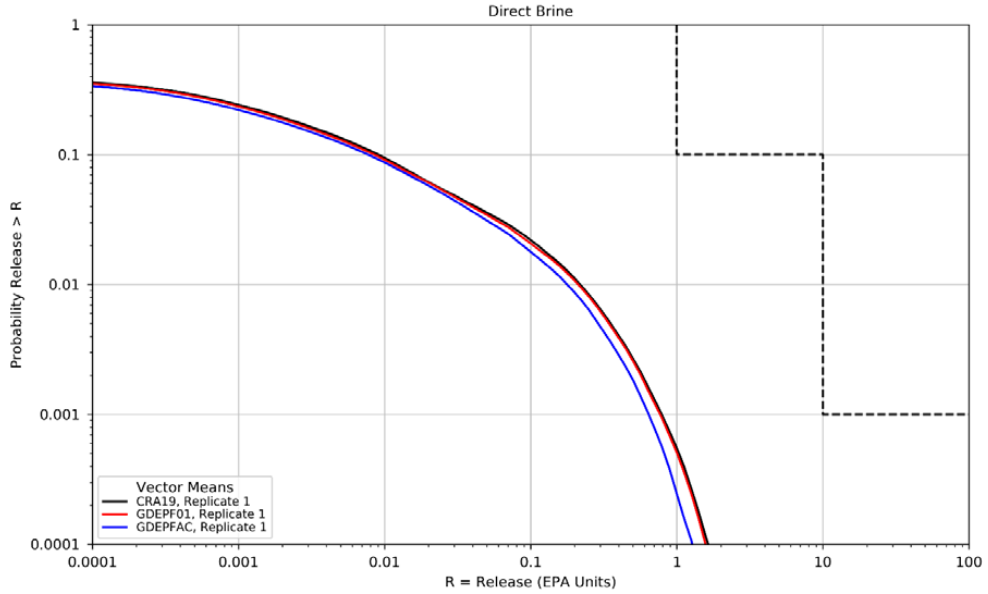

Figure 6 Mean CCDF for Direct Brine Release for Replicate 1

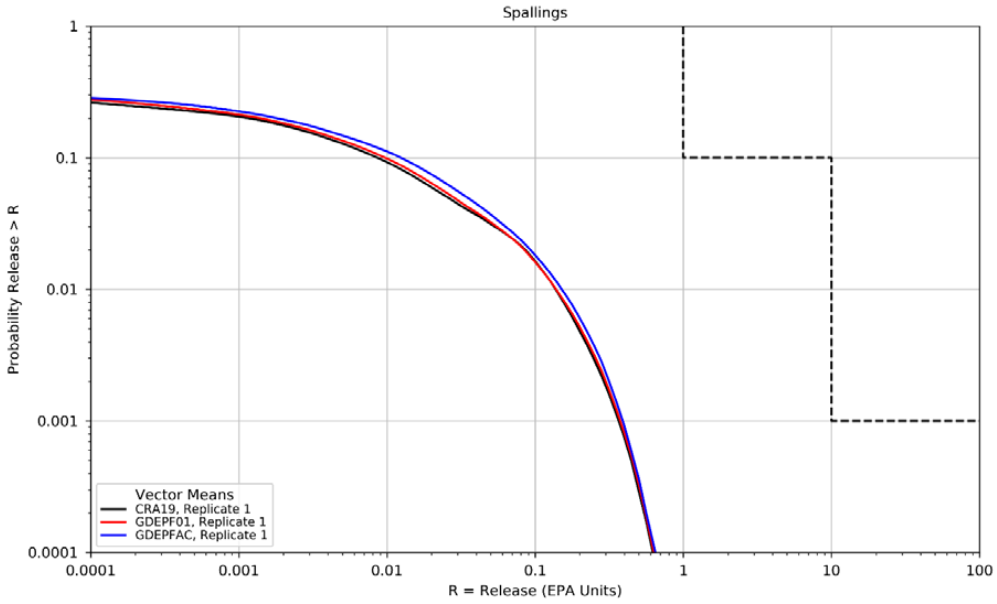

Figure 7 Mean CCDF for Spallings Release for Replicate 1

References

Day, B. 2019. Reassessment of Need and Parameter Justification for Modeling Gas Generation due to Radiolysis of Brine and Cellulose/Plastic/Rubber in WIPP for CRA-2019. Carlsbad, NM. Sandia National Laboratories ERMS 570873.

McAlhany, S. 2018. Surplus plutonium disposition – dilute and dispose approach. National Nuclear Security Administration. February 23, 2018. M3-SR-18-0012, Revision 0.

Kicker, D. 2019. Analysis Package for Inventory EPA Units in the 2019 Compliance Recertification Application Performance Assessment (CRA-2019 PA). Carlsbad, NM: Sandia national Laboratories. ERMS 571372.

Narlesky, J., M. Stroud, P. Smith, D. Wayne, R. Mason and L. Worl. 2012. Characterization of representative materials in support of safe, long term storage of surplus plutonium in DOE-STD-3013 Containers. Los Alamos National Laboratory, Los Alamos, New Mexico. LA-UR-12-23790.

Van Soest, G. 2018. Performance Assessment Inventory Report – 2018. Los Alamos National Laboratory, Carlsbad Operations. Carlsbad, NM. LA-UR-18-31882.

EPA Question

GEOCHEM-17d. **Assess uncertainty Introduced into Particle Sze Ranges and Distributions and Radiolytic Gas Generation Calculations**

Please assess the uncertainty introduced into the particle size ranges and distributions and the radiolytic gas generation calculations by the presence in the WIPP inventory of plutonium wastes that were not included in the Narlesky et al. (2012) investigation, such as incinerator ash, contaminated soils, and plutonium contamination on waste materials surfaces.

Day (2019) used data provided by Narlesky et al. (2012) to estimate and justify the particle size distribution of plutonium in the WIPP inventory for use in calculations of radiolytic gas generation rates. The materials characterized by Narlesky et al. (2012) are representative of plutonium stored in DOE-STD-3013 containers. These materials are product and byproducts produced by aqueous processing, metal oxidation, mixed actinide operations, and molten salt operations at Hanford, Rocky Flats, and Los Alamos National Laboratory (LANL) and were originally destined for conversion to mixed oxide fuel. However, plutonium-bearing wastes from other sites are present in the WIPP inventory, and the inventory also includes other forms of plutonium-bearing waste such as incinerator ash from Hanford, Rocky Flats, LANL, and Savannah River Site (Behrens et al. 1995), and other wastes such as contaminated soils. The materials examined by Narlesky et al. (2012) were characterized after passing through 40 mesh (0.42 mm) sieves but were not reported to be crushed or ground. On the other hand, waste stream SR-KACPuOx material appears to have been ground and sieved during processing at Savannah River (McAlhany 2018). Crushing or grinding of other wastes prior to repackaging for WIPP has also been reported (e.g., Hopkins et al. 2003). Smaller grain sizes would be expected to increase the rate of gas generation by brine radiolysis.

Day, B. 2019. Reassessment of need and parameter justification for modeling gas generation due to radiolysis of brine and cellulose/plastic/rubber in WIPP for CRA-2019. Sandia National Laboratories, Carlsbad, New Mexico. ERMS 570873.

Hopkins, A.M., C. Sutter, G. Julse and J. Teal. 2003. Disposal of TRU waste from the Plutonium Finishing Plant in pipe overpack containers to WIPP including new security requirements. WM '03 Conference, February 23-27, Tucson, Arizona.

McAlhany, S. 2018. Surplus plutonium disposition – dilute and dispose approach. National Nuclear Security Administration, M3-SR-18-0012, Revision 0. February 23, 2018.

Narlesky, J.E., M.A. Stroud, P.H. Smith, D. M. Wayne, R. E. Mason and L.A Worl, 2012. Characterization of representative materials in support of safe, long term storage of surplus plutonium in DOE-STD-3013 Containers, LA-UR-12-23790, Los Alamos National Laboratory, Los Alamos, New Mexico.

DOE Response

Particle size in the TRU waste emplaced at WIPP is uncertain and is not tracked as part of typical waste stream data. The best available distribution of waste particle sizes for PuO_2 waste is from Narlesky et al. (2012) and is based on Pu waste derived from a variety of processes used throughout the DOE complex. Additional processes may generate waste with smaller particle sizes. As discussed in the response to GEOCHEM-17c, a decrease in assumed waste particle diameter could be implemented in WIPP PA by increasing the uncertainty range (toward the higher side) on the GLOBAL:GDEPFAC parameter, which represents the energy deposition probability. By moving that parameter distribution toward higher average values, the distribution in particle diameters would skew toward smaller particles and a higher percent of energy released, resulting in increased gas generation due to brine radiolysis. However, the results of the two calculations performed for GEOCHEM-17c, in which gas generation due to brine radiolysis was increased, show decreased total releases compared to the CRA-2019 PA results. As such, we concluded that the range of the GLOBAL:GDEPFAC parameter distribution implemented in the CRA-2019 PA calculations is conservative with respect to releases.

EPA Evaluation of Response

The DOE response was satisfactory.

CC3-GEOCHEM-19 Evaluation of Matrix Depletion and Radiolytic Gas Generation for Cellulosics, Plastics, and Rubber Radiolysis

WIPP Compliance Recertification Application 2019 Appendix-GEOCHEM (Geochemistry)

EPA Question (from EPA Completeness Comment Package 3)

Please support the assertion that matrix depletion will result in insignificant amounts of gas production by CPR radiolysis compared to other processes by providing additional calculations described in the following questions. There was more Pu per kilogram of waste in the Zerwekh (1979) study than that of the WIPP. This higher concentration may have resulted in in faster matrix depletion. In contrast, matrix depletion rates at WIPP may be slower, and gas generation values may potentially be underestimated. Furthermore, G-values from Zerwekh (1979) appear to asymptotically reach the value of 0.3 moles/100 eV, indicating a possible upper bound value for prediction of gas generation from CPR radiolysis.

GEOCHEM-19a. **Evaluation of Higher Plutonium Concentrations**

Please evaluate whether the much higher plutonium concentrations used by Zerwekh (1979) accelerated the experimentally observed matrix depletion in the experiments. Zerwekh (1979) used high Pu-238 concentrations (~20 Ci/kg) in an experimental investigation of radiolytic gas generation from organic materials. This concentration is significantly higher than the average Ci/kg in the WIPP waste material and packaging material inventory (USDOE 2018,). Additionally, please include an analysis of the effects on the predicted G values over time for CPR radiolysis if the effects of matrix depletion on G values for CPR in the WIPP repository are adjusted to be consistent with the much lower radionuclide concentrations in the inventory.

DOE Response (from DOE Response Package 7)

Zerwekh (1979) uses approximately 40 times the maximum allowable loading rate of activity for waste to compress 20 years of gas generation into six month experiments. This assumes a linear relationship between energy input and G-value evolution. Following the linear relationship that Zerwekh proposes, the G-values around 0.3 moles/100 eV at five years would correspond to Gvalues at 200 years for the activity concentrations of WIPP waste.

Zerwekh's experiments were extended beyond the six months originally planned. Zerwekh had five test cylinders where the experiments continued to nearly five years, measuring the time span required to reach a specified pressure increase and calculating the realized G-value from the measured time span. Four of the test cylinders contained cellulosics (cylinders 22, 1, 26, and 27) and one cylinder contained a mixture of cellulosics, plastics, and rubbers (cylinder 24). A curve was fit for the changing G-values through time for each cylinder. Those curve fit equations are shown in Table 3.

Table 3 G-Value Equations from Zerwekh (1979) Experiments.

Cylinder #	G-Value fit equation
22	$G(gas) = 1.4726e^{-0.00079x}$
1	$G(gas) = 1.6006e^{-0.00098x}$
26	$G(gas) = \frac{1}{1.45 + 0.00176x}$
24	$G(gas) = 1.414e^{-0.0011x}$
27	$G(gas) = \frac{1}{0.9526 + 0.0012x}$
Where x is the number of days the material has been exposed to ionizing radiation.	

Applying the 1/40 time scaling expected from the lower energy input from WIPP waste gives G-value equations shown in Table 4.

Table 4 G-Value Equation Scaled to WIPP Waste Concentrations

Cylinder #	G-Value fit equation
22	$G(gas) = 1.4726e^{-0.00079x/40} = 1.4726e^{-0.00001975x}$
1	$G(gas) = 1.6006e^{-0.00098x/40} = 1.6006e^{-0.0000245x}$
26	$G(gas) = \frac{1}{1.45 + 0.00176x/40} = \frac{1}{1.45 + 0.000044x}$
24	$G(gas) = 1.414e^{-0.0011x/40} = 1.414e^{-0.0000275x}$
27	$G(gas) = \frac{1}{0.9526 + 0.0012x/40} = \frac{1}{0.9526 + 0.00003x}$
Where x is the number of days the material has been exposed to ionizing radiation.	

With the 1/40 time scaling applied, considering the 10,000 year regulatory lifetime of the WIPP repository, the G-value would be less than 5% (i.e., 2.85E-02/1.25E+00 molec/100eV) of the initial observed G-value for 90% (i.e., 9000/10000 years) of the repository regulatory timeframe. The 1/40 time scaling of G-value evolution for CPR calculated from the equations in Table 4 is displayed in Table 5 and Figure 8.

As described in Day (2019), the reduction in G-value over time is understood as a matrix depletion, where there is less hydrogen available for release by radiolysis in the CPR inventory through time (INEEL 1990). The CPR inventory in the WIPP is also assumed to undergo biodegradation which could reduce the available CPR inventory for radiolysis faster than the experimentally observed values where only radiolysis was depleting the CPR inventory. The GRATMIC2, GRATMIC4, and GRATMIC8 analyses described in CC3-GEOCHEM-19b failed to double the amount of gas generated by CPR biodegradation after increasing the rate of CPR biodegradation by factors of two, four, and eight. This is attributed to a limited CPR inventory. This would indicate that the total gas generated from CPR material from both biodegradation and radiolysis would be limited by CPR inventory, not a G-value related to CPR radiolysis. With respect to the total amount of gas that can be generated by CPR material, the SMIC2 analysis described in CC2-GEOCHEM-19b could be considered bounding independent of G-value; as it forces more gas to be generated than appears possible from the CPR inventory. With this CPR inventory limit, a larger G-value will shift the gas generation earlier in time, but not increase the total gas generation.

Table 5 Matrix Depletion G-values for CPR with 1/40-time Scaling

Elapsed Time		G(gas) for Test Cylinder-Contents					G(gas)	G(gas)/ G_o(gas)
Years	Days	Cyl 22 - cellulosics	Cyl 1 - cellulosics	Cyl 26 - cellulosics	Cyl 24 - cellulosics, plastics, rubbers	Cyl 27 - cellulosics	Average (molecules/ 100 eV)	Percent
0.001	0.365	1.47E+00	1.60E+00	6.90E-01	1.41E+00	1.05E+00	1.25E+00	100%
1	365	1.46E+00	1.59E+00	6.82E-01	1.40E+00	1.04E+00	1.23E+00	99%
5	1825	1.42E+00	1.53E+00	6.53E-01	1.34E+00	9.93E-01	1.19E+00	95%
10	3650	1.37E+00	1.46E+00	6.21E-01	1.28E+00	9.42E-01	1.14E+00	91.1%
100	36500	7.16E-01	6.55E-01	3.27E-01	5.18E-01	4.88E-01	5.41E-01	43.4%
1000	365000	1.09E-03	2.09E-04	5.71E-02	6.18E-05	8.40E-02	2.85E-02	2.3%
10000	3650000	7.26E-32	2.33E-39	6.17E-03	3.62E-44	9.05E-03	3.04E-03	0.2%

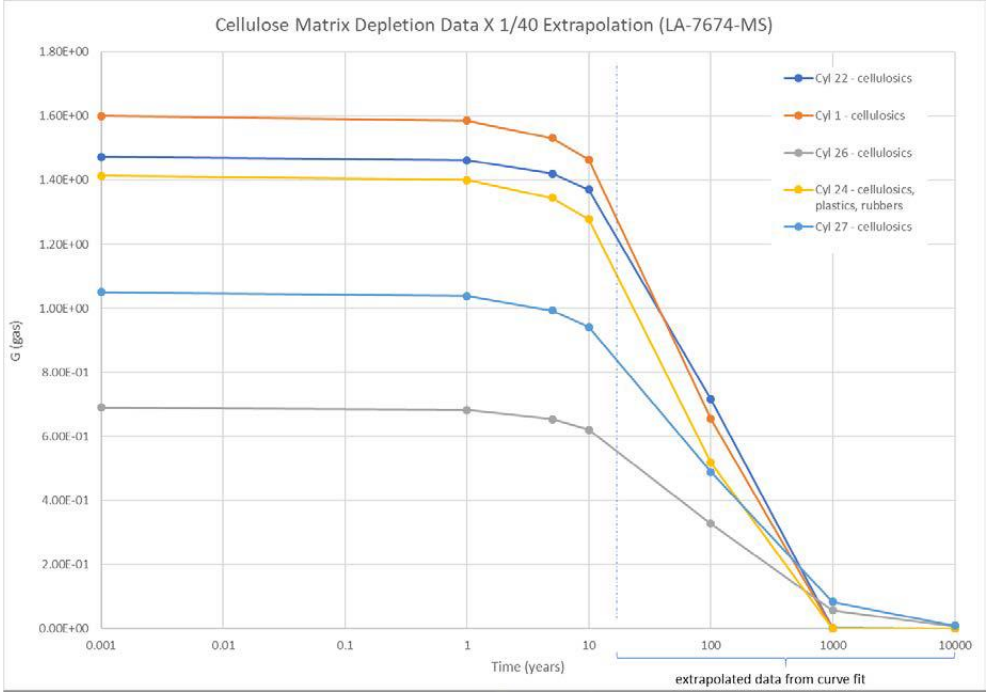

Figure 8 Extrapolated Matrix Depletion Data with 1/40-time Scaling

References

Day, B. 2019. Reassessment of Need and Parameter Justification for Modeling Gas Generation due to Radiolysis of Brine and Cellulose/Plastic/Rubber in WIPP for CRA-2019. Carlsbad, NM. Sandia National Laboratories ERMS 570873.

Idaho National Engineering and Environmental Laboratory. 1990. TRUPACT-II Matrix Depletion Program Final Report, prepared for the U.S. Department of Energy, Idaho Operations Office, Idaho Falls, Idaho. INEL/EXT-98-00987, Rev. 1

Zerwekh, A. 1979. Gas Generation from Radiolytic Attack of TRU-Contaminated Hydrogenous Waste. Los Alamos National Laboratory, Los Alamos, NM. LA-7674-MS.

GEOCHEM-19b.**Bounding Analysis for Gas Generation from CPR Radiolysis**

Please provide a bounding analysis of the amount of gas generation from CPR radiolysis in the WIPP repository by assuming a constant G value of 0.3 moles/100 eV throughout the repository regulatory period. Zerwekh (1979) provided equations that were fitted to the gas generation data, and these equations were used by Day (2019) to project extremely low radiolytic gas generation rates after approximately 100 years (Day 2019, Figure 3). However, examination of the G values as a function of time indicates that the data may be asymptotically approaching a G value of approximately 0.3 molecules/100 eV at the end of the 4.9-year experiments (Zerwekh 1979, Figures 20 – 28).

The radiolytic production of gas from organic materials such as cellulosics, plastics, and rubber (CPR) can decrease over time because of a process called matrix depletion. When an alpha source material is present in waste in dispersed, particulate form, only a small, spherical volume of the surrounding

material is affected because of the relatively short distance that alpha particles can travel in solid materials. Over time, the nearby material is depleted and the effective G value (molecules/100 eV) decreases to a limit that is characteristic of the affected matrix (INEEL 1999).

Day (2019) evaluated the time-dependent G values for CPR measured by Zerwekh (1979) and concluded that because of matrix depletion, radiolysis of CPR would result in insignificant amounts of gas production compared to other processes in the WIPP repository. However, the plutonium concentrations per kg of waste used in the Zerwekh (1979) experiments were extremely high compared to concentrations in WIPP waste, and these high concentrations would be expected to increase the rate at which matrix depletion occurs. That approach could tend to underestimate gas generation resulting from radiolysis.

The equations used to extrapolate G values from the Zerwekh (1979) will produce predicted G values with an associated uncertainty that is expected to increase with increasing time. Visual inspection of graphs of the G values reported by Zerwekh (1979) as a function of time indicate that the G values may have been asymptotically approaching constant values of approximately 0.3 molecules/100 eV after about 5 years. This constant G value of 0.3 molecules/100 eV can be used to develop an upper-bound prediction of gas generation from CPR radiolysis for an evaluation of its likely significance to gas generation during the repository regulatory period. If the gas generation rate by CPR radiolysis calculated using this upperbound G value would not significantly contribute to repository gas pressure, then radiolytic gas generation from CPR could be defensibly excluded from PA.

Day, B. 2019. Reassessment of need and parameter justification for modeling gas generation due to radiolysis of brine and cellulose/plastic/rubber in WIPP for CRA-2019. Sandia National Laboratories, Carlsbad, New Mexico. ERMS 570873.

INEEL (Idaho National Engineering and Environmental Laboratory). 1999. TRUPACT-II Matrix Depletion Program Final Report. Prepared for the U.S. Department of Energy, Idaho Falls, Idaho, INEL/EXT-98-00987.

USDOE (U.S. Department of Energy). 2018. Annual Transuranic Waste Inventory Report – 2018. U.S. Department of Energy Carlsbad Field Office, DOE/TRU-18-3425, Revision 0.

Van Soest, G.D. 2018. Performance Assessment Inventory Report. Los Alamos National Laboratory, Carlsbad, New Mexico, INV-PA-18, Revision 0.

Zerwekh, A. 1979. Gas Generation from Radiolytic Attack of TRU-Contaminated Hydrogenous Waste. Los Alamos National Laboratory, Los Alamos, New Mexico, LA-7674-MS.

DOE Response

It is the DOE's position that a constant G-value model for CPR radiolysis will not accurately represent the conditions in the WIPP or produce meaningful results for PA. The bounding calculation suggested by the EPA was performed and the result show that the CPR inventory in the WIPP does not support the model. It also shows that PA result would not be significantly impacted by the overestimated gas generation that this model predicts such that the DOE continues to screen out CPR radiolysis from PA.

Introduction

From a modeling perspective, the amount of gas generated from radiolysis of CPR material must be limited by the amount of CPR material available for radiolysis. Even when ignoring the matrix depletion effect, where less hydrogen-bearing material is exposed to each short-range alpha-emitting source, a constant G-value model will continue to produce gas after all CPR material has been consumed by other processes. A bounding calculation is presented below on the amount of gas that a constant CPR radiolysis model could generate, and the effects that gas generation would have on PA results; however this model is an unrealistic overestimation of gas generation potential due to CPR radiolysis. As seen in the DOE response to GEOCHEM-17c, overestimations of gas generation has the potential to lead to lower estimations of releases, although the case of CPR radiolysis differs from that of brine radiolysis in that brine is not consumed.

In order to perform the requested bounding analysis, a model for CPR radiolysis has been defined with the prescribed constant G-value of 0.3 Molecules/100 eV. The BRAGFLO code does not have the ability to decrease the amount of available CPR as the process of CPR radiolysis proceeds because the analysis of Day (2019) determined that CPR radiolysis would not contribute substantially to gas generation. An alternative approach to account for gas generation due to CPR radiolysis is used for this bounding analysis.

To investigate how much gas could be generated from CPR radiolysis, the gas generation rate from CPR radiolysis will be calculated using a defined relationship to the brine radiolysis gas generation rate, in a two-step process. First, the relationship between brine radiolysis and CPR radiolysis rates is established and the amount of gas generated from CPR radiolysis is compared to the other gas generation mechanisms. Then, to quantify the effect of CPR radiolysis on repository performance, the gas generation rate for CPR degradation is increased to account for the amount of gas generated by CPR radiolysis.

Model derivation

As a starting point, we note that the radiation source for radiolysis (i.e., alpha energy) is constant, independent of whether CPR radiolysis is assumed to occur—in other words, the radionuclide inventory may contribute to radiolysis of brine and CPR, but to avoid double counting, we assume that only the radionuclide inventory that does not already contribute to brine radiolysis may contribute to CPR radiolysis. With the disintegration energy from radionuclides in solution and wetted solid radionuclides being accounted for in brine radiolysis, we therefore make the assumption that CPR radiolysis will only depend on the disintegration energy from non-wetted solid radionuclides. The quantity of non-wetted radionuclides resulting from radionuclide decay is the complement of the wetted radionuclides found in Day (2019) and can be found following the same methodology.

The radionuclide decay constant λ is a function of the radionuclide half life $T_{1/2:}$

$$\lambda = \left(\frac{ln(2)}{T_{1/2}}\right)$$

(1)

The total quantity of each radionuclide decay *M(t)* [mol] is:

$$M(t) = M_0 \times e^{-\lambda t}$$

(2)

A closed-form solution of the Bateman (1910) equations is implemented to determine the decay and ingrowth for radionuclides and their associated daughters.

The mole fraction of a radionuclide with respect to other radionuclides of the same element (mf_i) is defined as:

$$mf_i = \frac{M(t)_i}{\sum_{j=1}^{n} M(t)_j}$$

(3)

where *i* is the index of radionuclides in the inventory, *j* is the index of radionuclides of an element in the inventory, and n is the total number of radionuclides of an element in the inventory.

The quantity of dissolved and sorbed (onto suspended colloids) radionuclides $M(t)_{sol}$ [mol] is defined as:

$$M(t)_{sol,i} = V_{waste} \times \varphi \times S_w \times S_{sol,i} \times mf_i$$

(4)

where φ is the porosity of the waste, S_w is the brine saturation, and $S_{sol,I}$ [mol/m3] is the radionuclide mobilization potential.

The quantity of non-wetted solid radionuclides $M(t)_{dry,\,I}$ [mol], is the difference between the total inventory and the inventory in solution multiplied by the gas saturation (which is found with one minus the brine saturation).

$$M(t)_{dry,i} = \left(M(t)_i - M(t)_{sol,i}\right) \times (1 - S_w)$$

(5)

With this, the gas generation rate due to CPR radiolysis ($R_{CPR,i}$) is defined as:

$$R_{CPR,i} = \left(M(t)_{dry,i} \times P_{dep}\right)\left(\lambda_i \times E_{dis,i} \times G(H_2)_{CPR}\right)$$

(6)

where P_{dep} is the energy deposition probability (assumed equal to the energy deposition probability for brine radiolysis here, the GLOBAL:GDEPFAC parameter), and $E_{dis,I}$ is the disintegration energy of radionuclide *i*.

From this model, the CPR gas generation rate can now be related to the brine radiolysis gas generation rate. Noting the relationship between wetted and non-wetted radionuclides as:

$$M(t)_{dry,i} = \frac{(1 - S_W)}{S_W} M(t)_{wet,i}$$

(7)

Manipulating the equation for CPR radiolysis (equation 6) using the definition of wetted solid radionuclides (equation 7) and the G-value for brine radiolysis ($G(H_2)_{brine}$), the gas generation rate due to CPR radiolysis $R_{CPR,i}$ can also be expressed as:

$$R_{CPR,i} = \frac{(1 - S_W)}{S_W} \times \left(M(t)_{wet,i} \times P_{dep}\right)\left(\lambda_i \times E_{dis,i} \times G(H_2)_{brine}\right) \times \frac{G(H_2)_{CPR}}{G(H_2)_{brine}} \quad (8)$$

Noting the gas generation for brine radiolysis $R_{CPR,i}$ (from Day (2019), equation 7) as:

$$R_{brine,i} = \left(M(t)_{sol,i} + M(t)_{wet,i} \times P_{dep}\right)\left(\lambda_i \times E_{dis,i} \times G(H_2)_{brine}\right) \quad (9)$$

The gas generation rate for CPR radiolysis in equation 8 contains the brine radiolysis gas generation rate (equation 9) except for the radionuclides in solution term ($M(t)_{sol,i}$). With all terms concerned being positive, adding the radionuclides in solution to the wetted radionuclides will give an upper bound on the gas generation from CPR radiolysis, allowing the gas generation rate from CPR radiolysis to be expressed in terms of the gas generation rate of brine radiolysis.

$$R_{CPR,i} \leq \frac{(1 - S_W)}{S_W} \times \left(M(t)_{sol,i} + M(t)_{wet,i} \times P_{dep}\right)\left(\lambda_i \times E_{dis,i} \times G(H_2)_{brine}\right) \times \frac{G(H_2)_{CPR}}{G(H_2)_{brine}}$$
$$= \frac{(1 - S_W)}{S_W} R_{brine,i} \frac{G(H_2)_{CPR}}{G(H_2)_{brine}} \quad (10)$$

Comparison of gas generation

With this upper bound to the gas generation rate from CPR radiolysis, the CRA-2019 PA results can be used to approximate the amount of gas generation that the CPR radiolysis model could produce. In Figure 9, the mean cumulative gas generation from CPR radiolysis (labeled as CPR Rad) for replicate 1 of CRA-2019 is calculated using equation 10 and the CRA-2019 brine radiolysis gas generation. This is compared with the CRA-2019 cumulative gas generation from iron corrosion (Iron), biodegradation of CPR (Bio CPR), brine radiolysis (H_2O Rad), and total CRA-2019 gas generation rate (Total), where the total is a sum of iron corrosion, biodegradation, and brine radiolysis. Four scenarios are shown in the subplots of Figure 9, S1-BF is the undisturbed scenario, S2-BF has an E1 (i.e., Castile brine) intrusion at 350 years, S4-BF has an E2 (i.e., no Castile brine) intrusion at 350 years, and S6-BF has an E2 intrusion at 1000 years and an E1 intrusion at 2000 years. A complete description of the scenarios can be found in Day (2019a).

Modeling effects of additional gas generation

To see the effects that gas generation from this CPR radiolysis model would have on the Salado flow model and PA calculated releases, the BRAGFLO code is rerun with the amount of gas generated by the CPR biodegradation model doubled to account for gas generation from CPR radiolysis.

To model a doubling of the CPR biodegradation gas generation independent of any CPR inventory limitation, the H_2 stoichiometric coefficient for biodegradation was doubled for a bounding analysis (named SMIC2)[4]. The 100 vectors of replicate 1 were ran for this bounding analysis, the mean results are plotted along with mean results of the same vectors from CRA-2019. Figure 10 shows the cumulative gas generation from biodegradation of CPR materials in this bounding analysis (labeled SMIC2) compared to the values from CRA-2019. As the figures

show, this method of doubling the stochiometric coefficient was successful in doubling the gas generation rate of biodegradation. Figure 11 shows the total cumulative gas generation from all sources for this bounding analysis alongside the gas generation from CRA-2019.

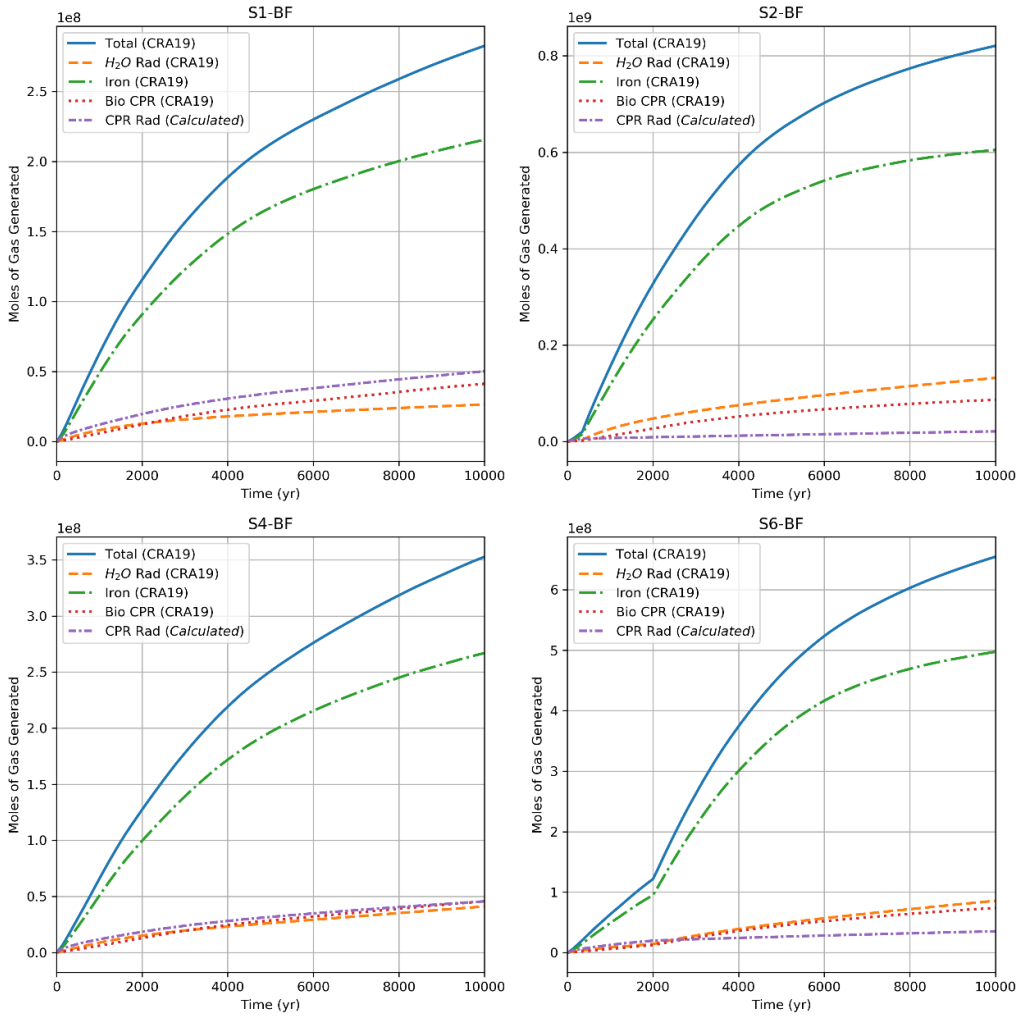

Figure 9 Mean Gas Generation Rate Approximation for CPR Radiolysis Compared to Existing CRA19 Gas Generation Rates for S1-BF, S2-BF, S4-BF, and S6-BF.

The results in Figure 9 show that the CPR radiolysis approximation is closest to the already existing CPR biodegradation rates in the CRA-2019 PA for scenarios without an E1 intrusion (S1-BF and S4-BF), and less than the CPR biodegradation rates in cases with an E1 intrusion (S2-BF and S6-BF).

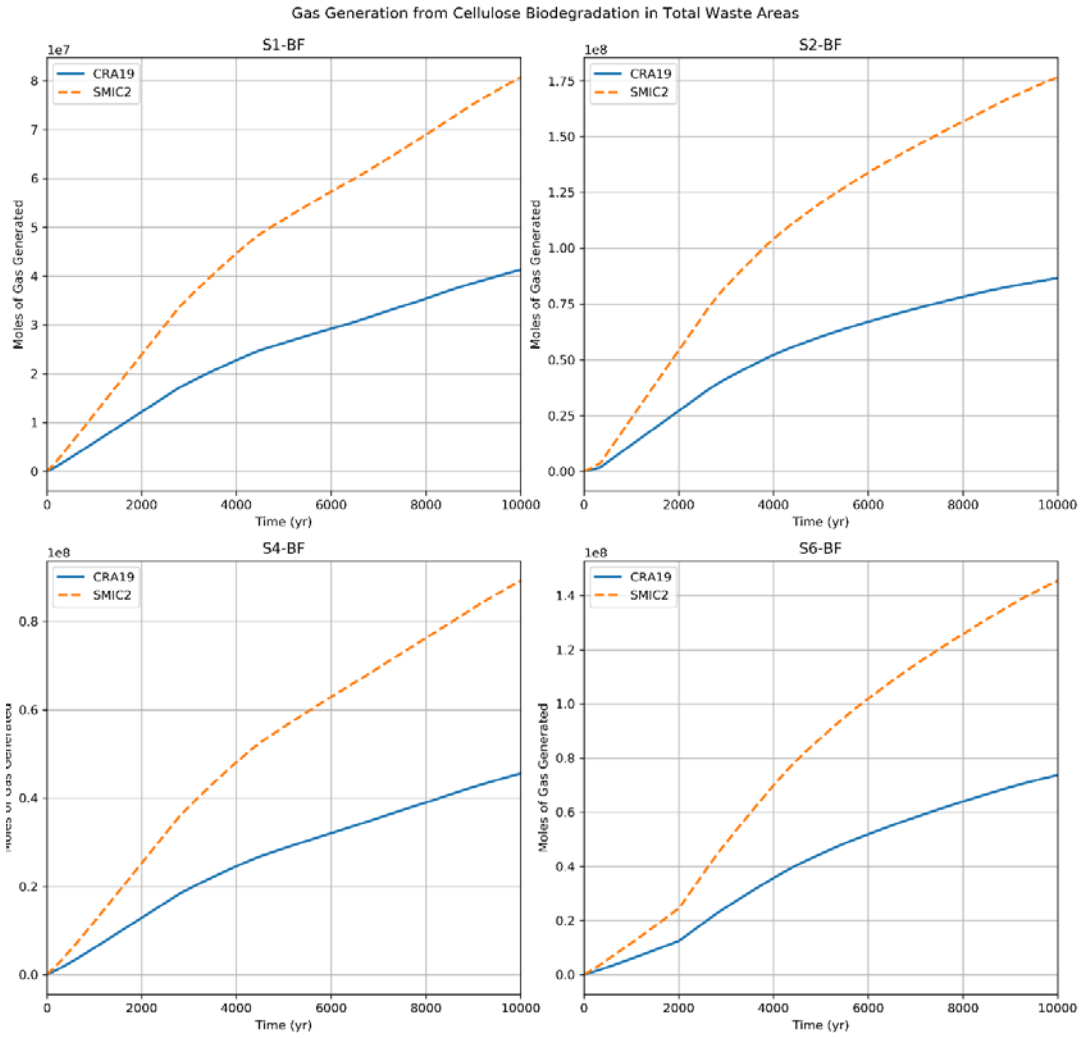

Figure 10 Mean gas generation from Biodegradation of CPR material in bounding analysis (SMIC2) and CRA-2019 for S1-BF, S2-BF, S4-BF, and S6-BF.

---

[4] Files associated with the SMIC2 calculation are archived on the WIPP PA cluster at /nfs/data/CVSLIB/WIPP_EXTERNAL/CRA19_comments/CC3-GEOCHEM-17-21/SMIC2.tar.gz.

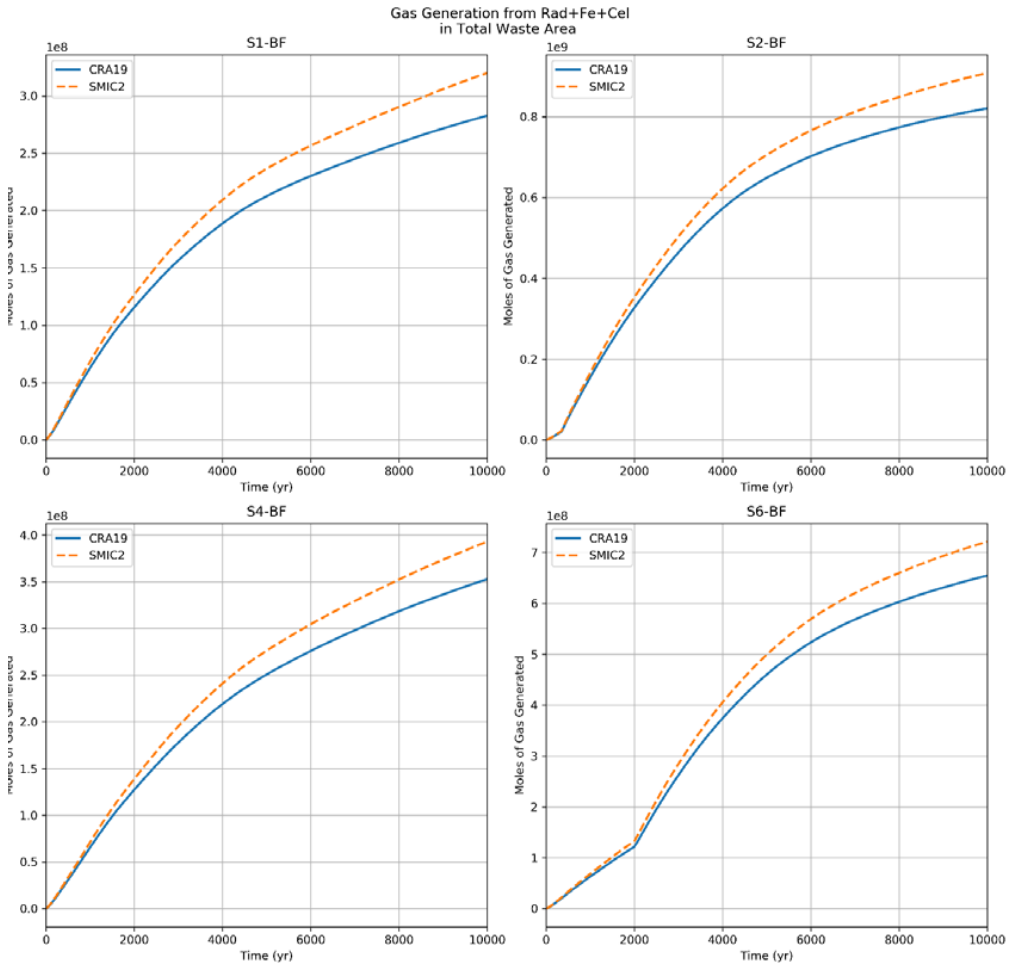

Figure 11 Mean Total Gas Generation for Bounding Analysis (SMIC2) and CRA-2019 for S1-BF, S2-BF, S4-BF, and S6-BF.

The mean brine pressure in the three repository waste areas (Waste Panel, South Rest-of-Repository, and North Rest-of-Repository) are shown in Figure 12 through Figure 14. An increase in pressure is seen from the additional gas generation in the bounding analysis (SMIC2) compared to the CRA-2019 (CRA19) results.

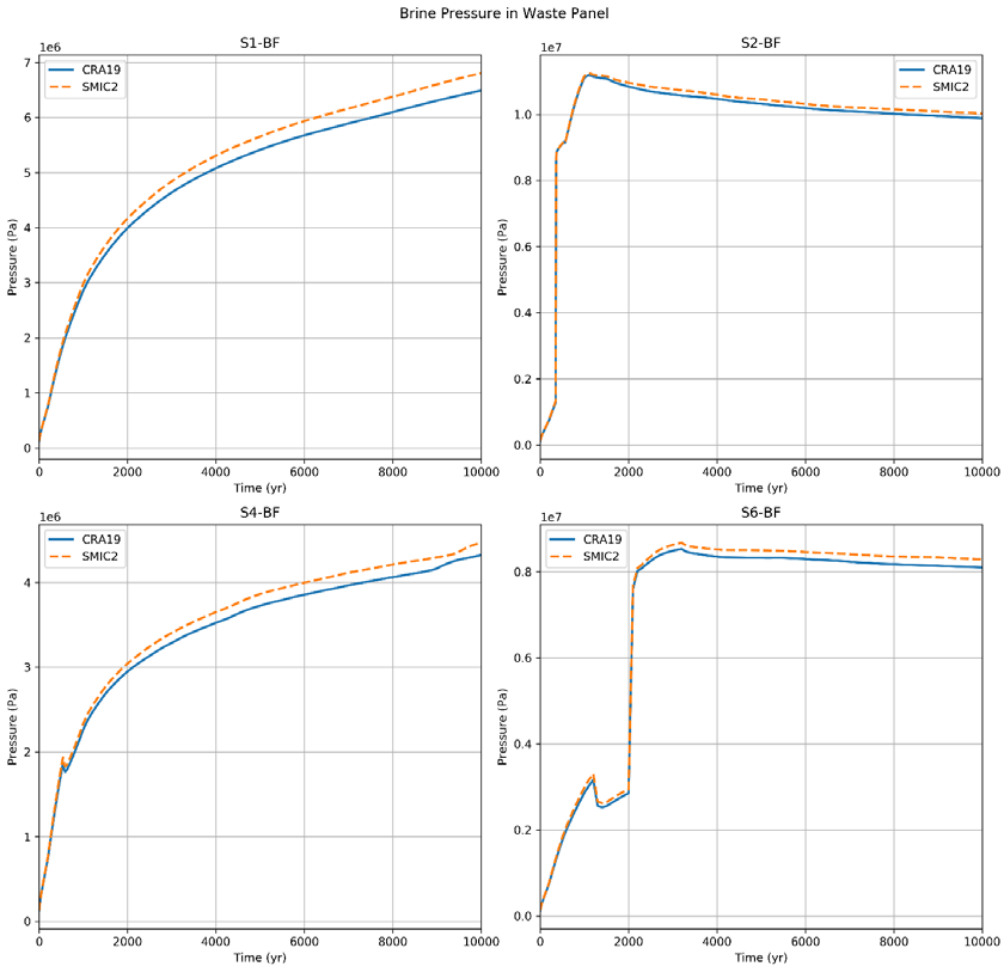

Figure 12 Mean Brine Pressure in the Waste Panel Area for the Bounding Analysis and CRA-2019 for S1-BF, S2-BF, S4-BF, and S6-BF.

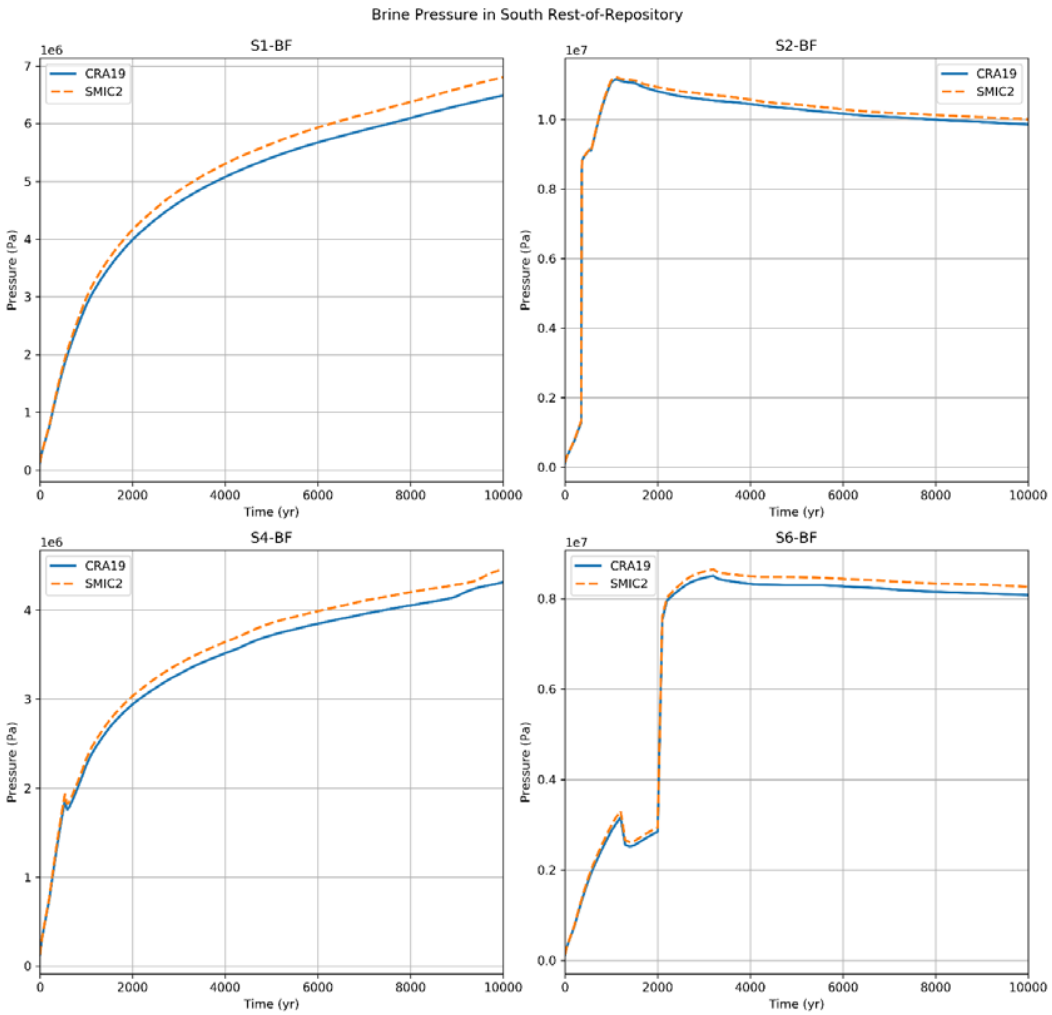

Figure 13 Mean Brine Pressure in the South Rest-of-Repository for the Bounding Analysis and CRA- 2019 for S1-BF, S2-BF, S4-BF, and S6-BF.

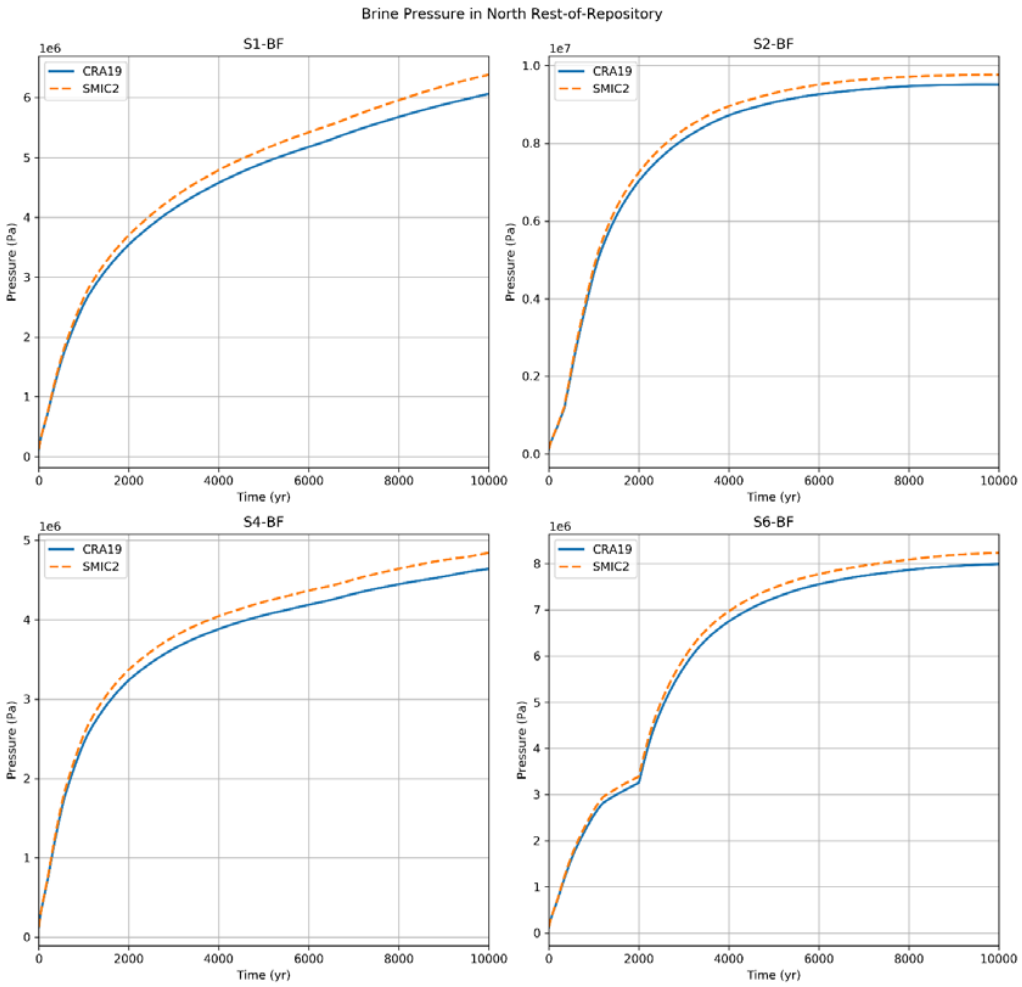

Figure 14 Mean Brine Pressure in the North Rest-of-Repository for the Bounding Analysis and CRA-2019 for S1-BF, S2-BF, S4-BF, and S6-BF.

Brine saturation in the three repository waste areas are shown in Figure 15 through Figure 17 for the bounding analysis (SMIC2) and CRA-2019 (CRA19). The brine saturation is generally decreased from the additional gas generation. Although this increased gas generation doesn't consume brine (such as increasing iron corrosion or brine radiolysis would), the increased pressure inhibits brine flow into the repository, reducing brine saturation.

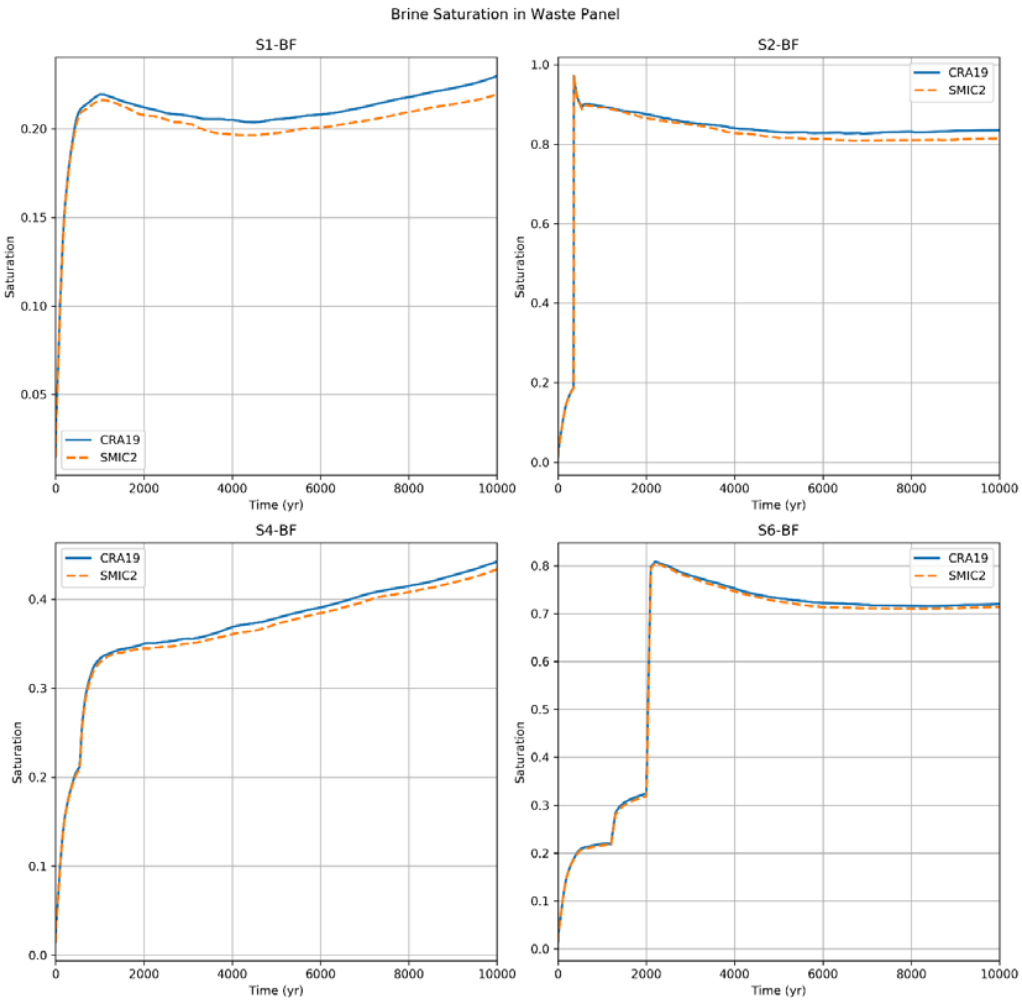

Figure 15 Mean Brine Saturation in the Waste Panel Area for the Bounding Analysis and CRA-2019 for S1-BF, S2-BF, S4-BF, and S6-BF.

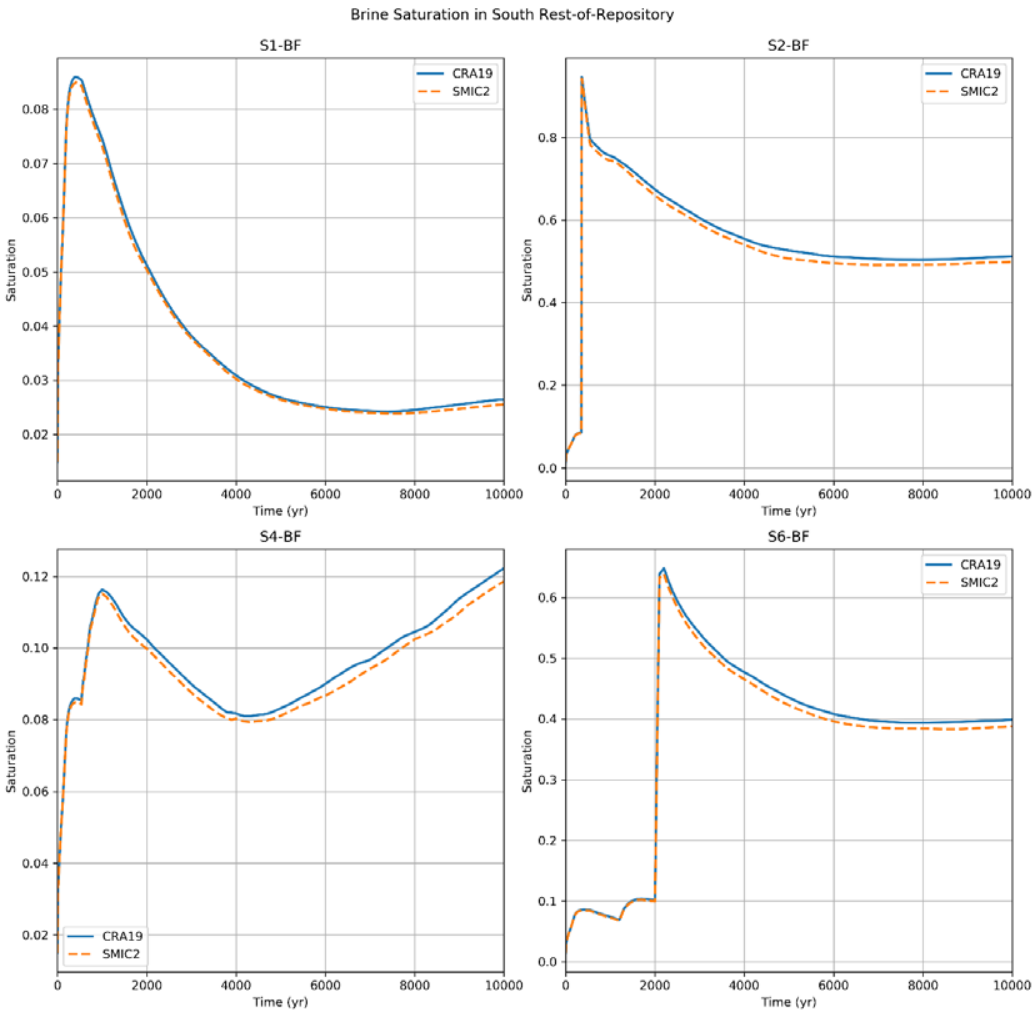

Figure 16 Mean Brine Saturation in the South Rest-of-Repository for the Bounding analysis and CRA-2019 for S1-BF, S2-BF, S4-BF, and S6-BF.

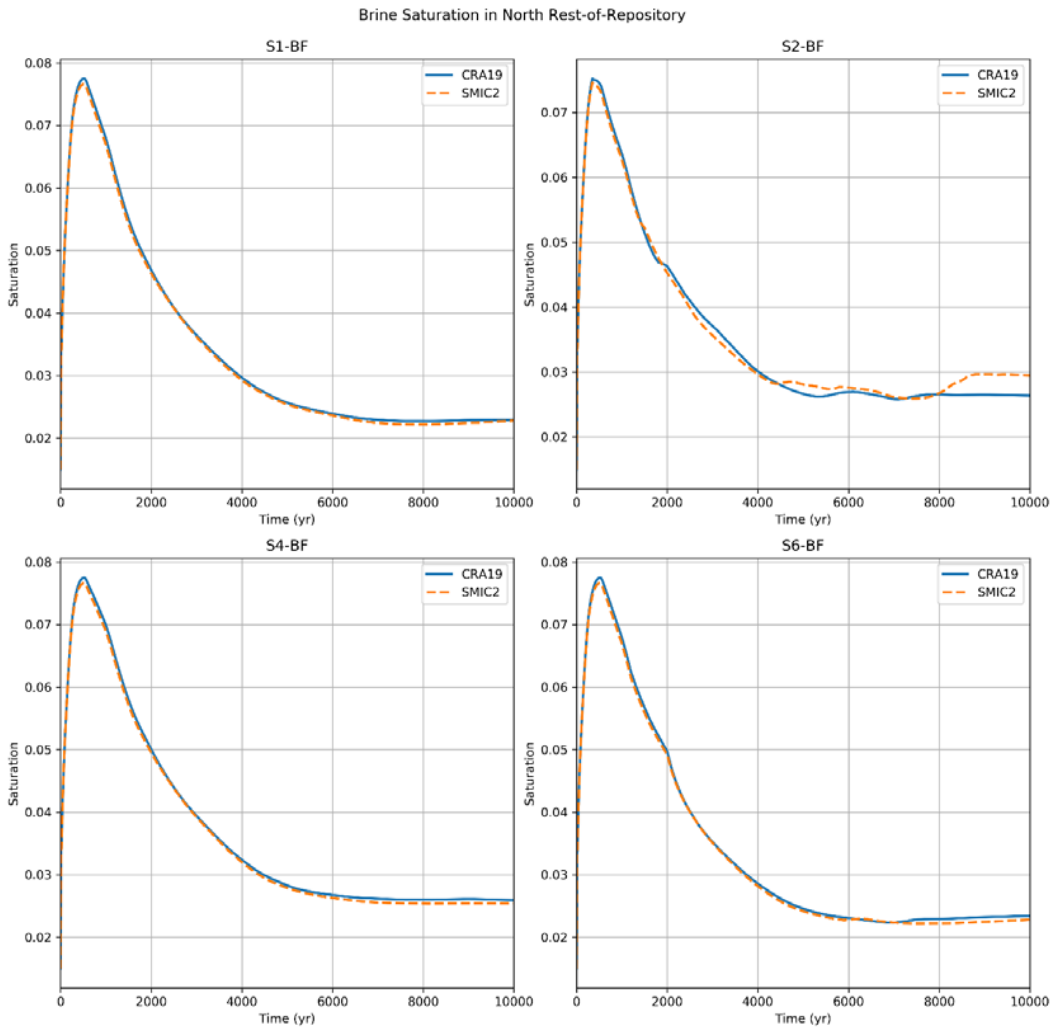

Figure 17 Mean Brine Saturation in the North Rest-of-Repository for the Bounding analysis and CRA-2019.

The Salado flow results show some increases in brine pressure and decreases in brine saturation due to the additional gas generation. The pressure increase has the potential to increase DBRs and spallings releases, however the decreased brine saturation has a competing potential effect of lowering DBRs. To see the impact of these changes on releases, releases were calculated for this bounding analysis. The mean total release CCDF curves for replicate 1 of the bounding analysis is displayed in Figure 18 alongside the same results for CRA-2019. The results show the increased gas generation in the bounding analysis has very little effect on releases. The small effect of adding a large overestimate of possible gas generation due to CPR radiolysis indicates that CPR radiolysis is not substantially impactful.

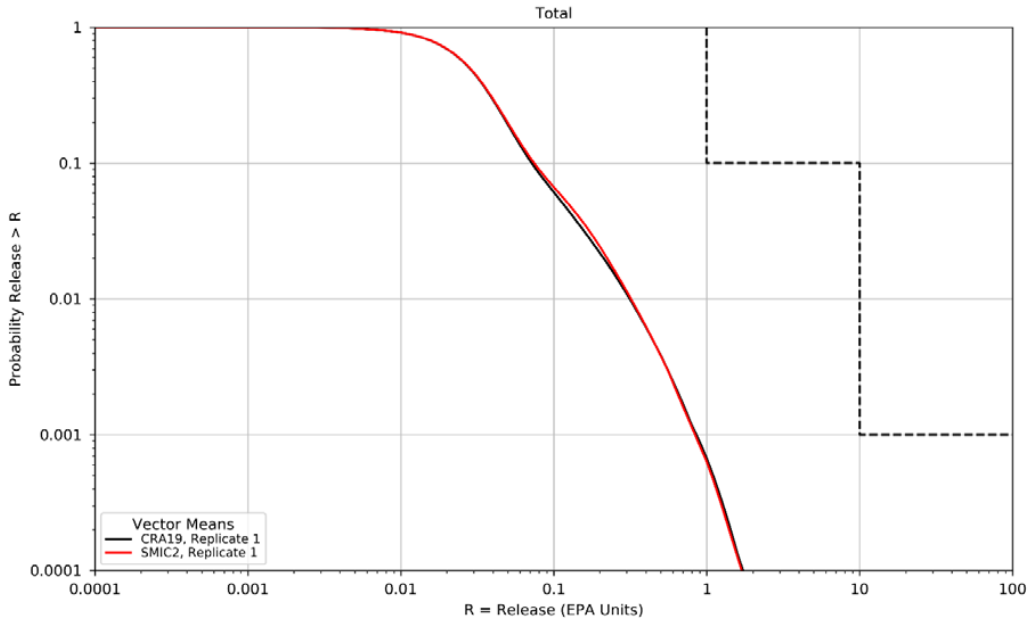

Figure 18 Mean CCDF Curve for Total Releases for the Bounding Analysis (SMIC2) and CRA-2019

To evaluate how the amount of the CPR inventory would limit gas generation from both CPR radiolysis and biodegradation, calculations were done with the biodegradation rate multiplied by a factor of two, four, and eight (labeled GRATMIC2, GRATMIC4, and GRATMIC8 respectively)[5]. Each calculation includes the 100 vectors of replicate 1, and the mean results are compared to the mean results of the CRA-2019. Figure 19 compares the gas generation from CPR biodegradation for CRA-2019 to analyses with the biodegradation rate multiplied by factors of two, four, and eight. In these plots it can be seen that the early time rate of gas generation is increased by approximately the biodegradation rate multiplication factor, however the rates drop off between 1,000 and 4,000 years leaving the total gas generated from biodegradation less than double the CRA-2019 gas generation. While each of these biodegradation rate increases increased the gas generation from biodegradation, the biodegradation model is limited by the CPR inventory, and the CPR inventory in an increasing number of vectors becomes depleted prior to the end of the simulation. This observation supports the argument that a CPR radiolysis model needs to account for CPR inventory and the model is an overestimation of the actual gas produced by CPR radiolysis.

---

[5] Files associated with the GRATMIC2, GRATMIC4, and GRATMIC8 calculations are archived on the WIPP PA cluster at /nfs/data/CVSLIB/WIPP_EXTERNAL/CRA19_comments/cc3-GEOCHEM-17-21/GRATMIC2.tar.gz.

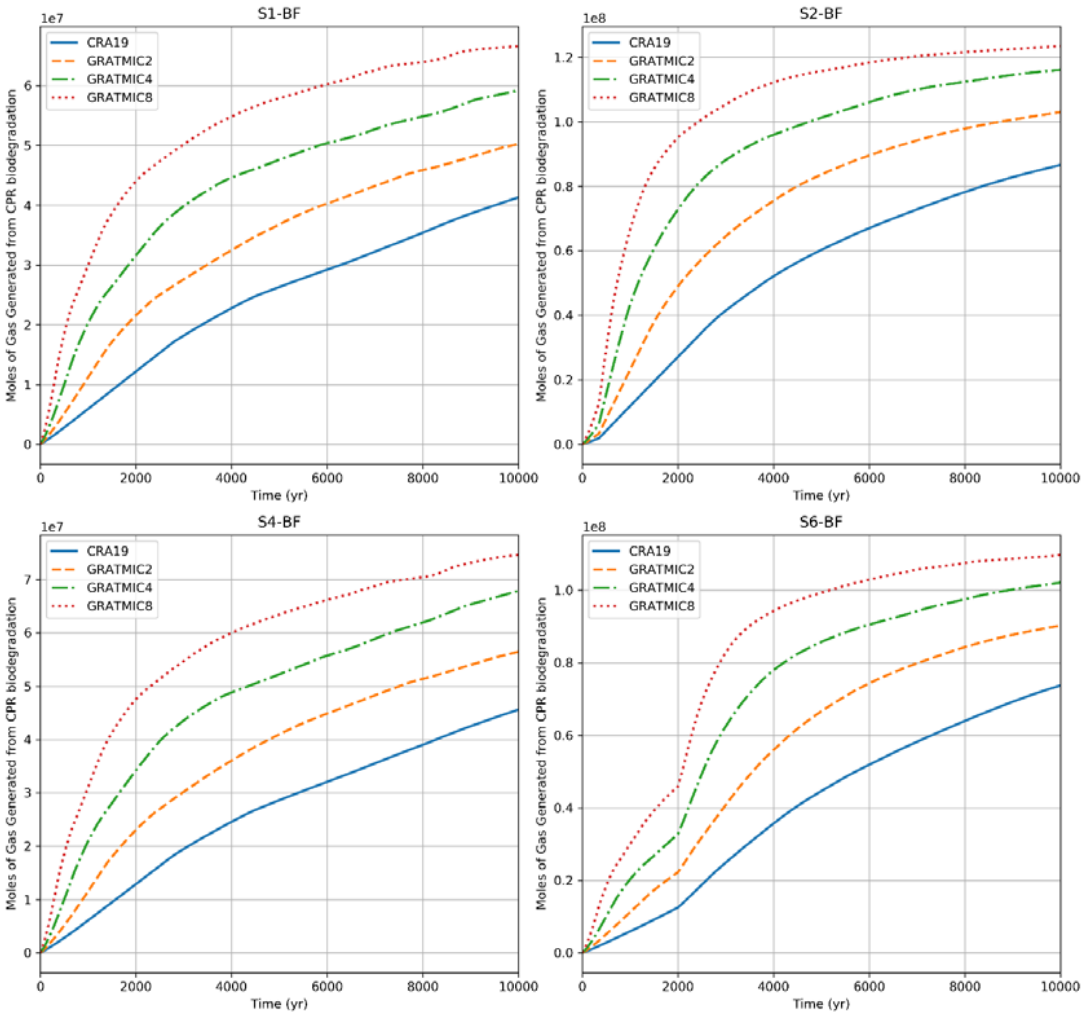

Figure 19 Mean Gas Generation from CPR Biodegradation for Multiple Biodegradation Rates.

Summary

A model of gas generation due to CPR radiolysis with the prescribed G-value was defined. Due to limitations of the BRAGFLO code, this model is represented by adjusting parameters for other gas generation models implemented within BRAGLO. A PA calculation was done with gas generation increased to be equivalent to that estimated by the CPR radiolysis model with the prescribed Gvalue. The results of this PA calculation show that the CRA-2019 releases are not substantially impacted by CPR radiolysis, justifying the screening out of CPR radiolysis from WIPP PA. A constant G-value model that does not account for CPR inventory limitations will greatly overestimate gas generation.

These results support DOE's position to screen out CPR radiolysis from CRA-2019. The results also support DOE's position that the suggested constant G-value model is unrealistic under WIPP conditions due to CPR inventory limitations.

References

Bateman, H. 1910. The solution of a system of differential equations occurring in the theory of radioactive transformations. In Proc. Cambridge Philos. Soc. (Vol. 15, No. pt V, pp. 423–427).

Day, B. 2019. Reassessment of Need and Parameter Justification for Modeling Gas Generation due to Radiolysis of Brine and Cellulose/Plastic/Rubber in WIPP for CRA-2019. Carlsbad, NM. Sandia National Laboratories. ERMS 570873.

Day, B. 2019a. Analysis Package for Salado Flow in the 2019 Compliance Recertification Application Performance Assessment (CRA-2019 PA). Carlsbad, NM. Sandia National Laboratories. ERMS 571368.

Zerwekh, A. 1979. Gas Generation from Radiolytic Attack of TRU-Contaminated Hydrogenous Waste. Los Alamos National Laboratory, Los Alamos, NM. LA-7674-MS.

EPA Evaluation of Response

The DOE response was satisfactory. However, additional investigation will be required for future PAs.

CC3-GEOCHEM-20 Gas Generation in Unsaturated Repository

WIPP Compliance Recertification Application 2019 Appendix-GEOCHEM (Geochemistry)

EPA Question (from EPA Completeness Comment Package 3)

Please evaluate whether radiolysis of adsorbed water on waste surfaces in humid areas of the WIPP repository could significantly affect the rates of radiolytic gas generation.

The radiolytic hydrogen gas generation rate calculated for WIPP PA includes two processes: brine radiolysis due to dissolved and colloidal radionuclides in brine, and brine radiolysis caused by wetted solid radionuclides (Day 2019). Implementation of these processes in WIPP PA requires the presence of brine in the repository. Hydrogen gas production due to radiolysis of water adsorbed on various surfaces has also been reported in the literature (e.g., Laverne and Tandon 2003, La Caër 2011, Veirs et al. 2012). These data indicate that hydrogen gas yields at the oxide surface can be higher than in bulk water, due to the efficient energy transfer that can occur at the interface. The likely rates of hydrogen gas production due to radiolysis of adsorbed water on waste material surfaces should be evaluated to justify omitting this process from the gas generation calculations used in WIPP PA.

Day, B. 2019. Reassessment of need and parameter justification for modeling gas generation due to radiolysis of brine and cellulose/plastic/rubber in WIPP for CRA-2019. Sandia National Laboratories, Carlsbad, New Mexico. ERMS 570873.

LaVerne, J. and L. Tandon. 2003. H_2 production in the radiolysis of water on UO_2 and other oxides. Journal of Physical Chemistry B 107:13623-13628.

Le Caër, S. 2011. Water radiolysis: influence of oxide surfaces on H_2 production under ionizing radiation. Water 3:235-253.

Viers, D., J. Berg and M. Crowder. 2012. The effect of plutonium dioxide water surface coverage on the generation of hydrogen and oxygen. MIS Program Report, Los Alamos National Laboratory, LAUR-12-22377.

DOE Response (from DOE Response Package 7)

The current DOE position is that radiolytic gas generation from adsorbed water is a low consequence effect that will have no impact on the WIPP performance assessment conclusions and is therefore not modeled.

Introduction

Prior to the CRA-2019 PA, gas generation due to brine radiolysis was excluded from PA calculations based on arguments in the Features, Events, and Processes (FEPs) analyses. The FEPs argument was based on calculations showing relatively low gas generation. That argument considered gas generated by radionuclides in solution (FEP W52 in Appendix SCR, DOE 2014) with solubility chosen such that the entire inventory of Pu was in solution. A reassessment of gas generation due to brine radiolysis has been made in which contributions were considered for radionuclides in solution, as well as wetted radionuclides (Day 2019). As a result, in the brine radiolysis gas generation model implemented in the CRA-2019 PA, it is assumed that H2 is generated only from radionuclides dissolved in brine and any inventory in contact with brine (i.e., wetted, based on brine saturation). The EPA question proposes an additional contribution to gas generation from the remaining (i.e., non-wetted) inventory that would have a few layers of adsorbed water present on the surface of oxide particles due to humidity in the repository.

The work of Laverne and Tandon (2003), Le Caër (2011), and Veirs et al. (2012) provide evidence of radiolysis of water at the surface of non-wetted particles that can result in H2 generation at a higher rate (i.e., higher G-value) than from dissolved or wetted particles. To assess the completeness of the radiolysis model implemented in WIPP PA, the inventory assumed to contribute to brine radiolysis in the current model is compared to the inventory of non-wetted radionuclides.

Assumptions Regarding Input Parameters for Comparison of Inventories

The radiolysis model includes the contribution from dissolved radionuclides, which varies by orders of magnitude across PA vectors due to the modeled uncertainty in radionuclide solubilities. The radiolysis model also includes the contribution from wetted radionuclides, the mass of which is assumed to be the total mass of non-dissolved radionuclides multiplied by the brine saturation (which varies in time). Thus, the relative amounts of dissolved/wetted/nonwetted radionuclides changes with time and varies across vectors. For the purposes of estimating the potential contribution of non-wetted radionuclides to brine radiolysis, we assume average amounts of dissolved and wetted radionuclides based on CRA-2019 PA results.

For simplicity, we only consider the inventory of Pu-238, Pu-239, and Pu-240 at the time of closure, which are estimated to comprise ~62% of the total wattage at closure (Am-241 is estimated to contribute ~34 % of the total wattage at closure, but decays quickly to nearly zero for the majority of the regulatory time period) (Kicker 2019, Sarathi 2019). In WIPP PA, Pu is assumed to be in either the Pu(III) or Pu(IV) oxidation state and solubility is assumed to be different for these two oxidation states. In PA calculations, solubilities (i.e., the amounts of dissolved radionuclides) are calculated by multiplying

baseline solubilities by an uncertainty factor (colloidal contributions also factor into the total dissolved amounts, but are ignored here for simplicity).

For Pu(III), the baseline solubility (parameter SOLMOD3:SOLCOH) is 1.78E-7 mol/liter (L) (baseline solubilities vary depending on the brine volume and type, but a constant brine volume and Castile brine is assumed here for simplicity) and mean uncertainty factor is 0.640 (parameter SOLMOD3:SOLVAR) for a calculated mean solubility of (1.78E-7)*(100.640) = 7.77E-7 mol/L. For Pu(IV), the baseline solubility is 5.44E-8 mol/L (parameter SOLMOD4:SOLCOH) and mean uncertainty factor is -0.00486 (parameter SOLMDO4:SOLVAR) for a calculated mean solubility of 5.38E-8 mol/L. Because Pu(III) and Pu(IV) are assumed to each be present in half of the vectors, we average the two mean solubilities here for a result of 4.15E-7 mol/L. It is noted that brine saturation factors into calculating dissolved and wetted masses. In PA calculations, brine saturation varies with time, location in the repository, and BRAGFLO scenario. For simplicity and to avoid assuming repository location or scenario, the time-averaged mean saturations reported in Table 19 of Day (2019b) for the waste panel, south rest-of repository, and north rest-of-repository in scenarios S1-BF, S2-BF, S4-BF, and S6-BF are averaged here for a result of 0.271.

Comparison of Non-Wetted Inventory to Dissolved and Wetted Inventories

The total inventory of Pu-238, Pu-239, and Pu-240 in Ci in the CRA-2019 were 9.42E+05, 8.70E+05, and 3.16E+05 (parameters PU238:INVCHD, PU239:INVCHD, and PU240:INVCHD, respectively) or 55 kilograms (kg), 14032 kg, and 1392 kg, respectively, for a total of 15479 kg of Pu. The average dissolved mass of Pu is calculated based on Equation 4 from Day (2019a) (waste volume taken from BRAGFLO grid; porosity is the initial waste area porosity of 0.848, parameter WAS_AREA:POROSITY):

Mass (dissolved) = (Volume Waste) x (Porosity) x (Brine Saturation) x (Solubility) x (1000 L/m_3) x (Molecular Weight)

Mass (dissolved) = (438139 m_3) x (0.848) x (0.271) x (4.15E-07 mol/L) x (1000 L/m_3) x (0.269 kg/mol) = 11 kg of dissolved Pu.

The average wetted mass of Pu is calculated by assuming (as in Equation 6 in Day 2019a) that it is the difference between the total inventory and dissolved inventory multiplied by the brine saturation, or (15479 – 11 kg)*(0.271) = 4194 kg of wetted Pu. The estimated mass of nonwetted plutonium is calculated by subtracting the dissolved and wetted masses from the total mass: 15479 – 11 – 4194 = 11274 kg of non-wetted Pu.

Conclusion

The estimated amount of non-wetted radionuclides exceeds the amounts of dissolved and wetted radionuclides currently considered in the brine radiolysis model used in the CRA-2019 PA calculation. Additionally, there is evidence supporting G-values of non-wetted radionuclides that exceed those of dissolved and wetted radionuclides. Therefore, the potential exists for an additional effect on the order of the effect already considered. For a complete model, further investigation would be required to estimate the fraction of the non-wetted radionuclides that may be exposed to humid air (i.e., all particles of non-wetted radionuclides may not be fully exposed to air), as well as the amount of energy transferred to the relatively thin water layer for radiolysis. It is DOEs position that these factors would greatly reduce the amount of gas generation from the bounding calculation provided. Also note that increasing the rate of gas generation due to radiolysis beyond what was implemented in the CRA-2019

has been shown to result in decreased releases (see Figure 3 response to GEOCHEM-17c above, in which up to about 30% additional gas is generated). Therefore, explicitly including a contribution to brine radiolysis from non-wetted radionuclides may increase repository pressures, but ultimately decrease estimated releases.

References

Day, B. 2019a. Reassessment of Need and Parameter Justification for Modeling Gas Generation due to Radiolysis of Brine and Cellulose/Plastic/Rubber in WIPP for CRA-2019. Carlsbad, NM. Sandia National Laboratories. ERMS 570873.

Day, B. 2019b. Analysis Package for Salado Flow in the 2019 Compliance Recertification Application Performance Assessment (CRA-2019 PA). Carlsbad, NM. Sandia National Laboratories. ERMS 571368.

Kicker, D. 2019. Radionuclide Inventory Screening Analysis for the 2019 Compliance Recertification Application Performance Assessment (CRA-2019 PA). Carlsbad, NM. Sandia National Laboratories. ERMS 571659.

LaVerne, J. and L. Tandon. 2003. H2 Production in the Radiolysis of Water on UO2 and Other Oxides. Journal of Physical Chemistry B 107:13623-13628.

Le Caër, S. 2011. Water Radiolysis: Influence of Oxide Surfaces on H2 Production Under Ionizing Radiation. Water 3:235-253.

Sarathi, R. 2019. Analysis Package for Actinide Mobilization and Salado Transport in the 2019 Compliance Recertification Application Performance Assessment (CRA-2019 PA). Carlsbad, NM. Sandia national Laboratories. ERMS 571371.

Viers, D., J. Berg and M. Crowder. 2012. The Effect of Plutonium Dioxide Water Surface Coverage on the Generation of Hydrogen and Oxygen. MIS Program Report. Los Alamos National Laboratory. LA-UR-12-22377.

EPA Evaluation of Response

The DOE response was satisfactory, however, additional investigation required for future PAs.

CC3-GEOCHEM-21 Gas Generation by Radiolysis of Non-CPR Waste Materials

WIPP Compliance Recertification Application 2019 Appendix-GEOCHEM (Geochemistry)

EPA Question (from EPA Completeness Comment Package 3)

Please provide an analysis of the relative significance of radiolytic gas generation from other waste forms in the repository besides the CPR presented in Day (2019), including: 1) hydrated minerals, such as clays in waste soils; 2) solidified inorganic wastes; 3) solidified organic wastes; and 4) cements.

Day (2019) provided a screening analysis for omission of radiolytic gas generation from CPR. However, there may be radiolytic gas generation associated with other materials in the WIPP inventory. Radiolytic hydrogen gas generation has been reported for montmorillonite clay (e.g., Fourdrin et al. 2013),

solidified inorganic wastes, solidified organic wastes (e.g., Barber et al. 2001), and cements (e.g., Bouniol and Bjergbakke 2008). Screening analyses should be provided for these wastes to indicate whether they could significantly contribute to gas pressures in the WIPP repository environment.

Barber, D.B., K.P. Carney, P.R. Hart, D.G. Cummings, M.T. Sayer, D.L. Hendrix, K.T. Shirley, and J.C. Demirgian. 2001. The determination of the rate of hydrogen generation from transuranic 003 type organic sludge. Waste Management Conference 2001, Tucson, Arizona.

Bouniol, P. and E. Bjergbakke. 2008. A comprehensive model to describe radiolytic processes in cement medium, Journal of Nuclear Materials 372:1-15.

Day, B. 2019. Reassessment of need and parameter justification for modeling gas generation due to radiolysis of brine and cellulose/plastic/rubber in WIPP for CRA-2019. Sandia National Laboratories, Carlsbad, New Mexico. ERMS 570873.

Fourdrin, C., H. Aarrachi, C. Latrille, S. Esnouf, F. Bergaya and S. Le Caer. 2013. Water radiolysis in exchanged-montmorillonites: the H_2 production mechanisms. Environmental Science and Technology 47:9530-9537

DOE Response (from DOE Response Package 7)

The DOE response to CC3-GEOCHEM-19 will be used to show that radiolytic contributions from the irradiation of hydrated minerals, solidified inorganics, solidified organics, and cements will continue to be screened out for CRA-2019 based on the relative inventory quantities of each of these materials and due to matrix depletion.

The analysis in CC3-GEOCHEM-19 assumes all emitted energy from non-wetted radionuclides is used in radiolysis of CPR. If the additional four materials are considered as possible targets for radiolysis, the emitted energy would then be divided according to the relative quantity of each material in the WIPP inventory (Table 6). In this consideration, the alpha deposition energy is distributed between the CPR and non-CPR materials by using a mass-weighted average G-value.

Table 6 CH and RH Inventory for CRA-2019[a]

Material	CH Mass (kg)	RH Mass (kg)	Total Mass (kg)
Cements[b]	1.76×10^6	2.08×10^3	1.76×10^6
Solidified Inorganic Material	1.21×10^7	3.61×10^4	1.21×10^7
Solidified Organic Material	5.28×10^6	3.70×10^3	5.28×10^6
Soil	4.99×10^6	1.90×10^4	5.01×10^6
CPR[c]	1.49×10^7	1.11×10^6	1.60×10^7
Total Inventory	$\mathbf{3.90 \times 10^7}$	$\mathbf{1.17 \times 10^6}$	$\mathbf{4.01 \times 10^7}$

(a) Table values summarized from Van Soest (2018).
(b) The cement totals here reflect only those reported by the TRU waste sites. The emplaced portion is accounted for in the Solidified Inorganic Material, Solidified Organic Material, and Other Inorganic Materials categories in Table 5-5 of Van Soest (2018).
(c) CPR inventory includes both waste materials and packaging materials.

Day (2019) reported an initial G(gas)-value for CPR of 1.24 molecules/100 eV. Fourdrin et al. (2013) obtained G(H_2)-values for montmorillonite clay ranging from 1.2 x 10^{-8} to 4.7 x 10^{-8} mol/J (0.116 to 0.453 molecules/100 eV).

Barber et al. (2001) found an experimentally derived G(H_2)-value for solidified organic material (sludge sorbed into an inert gypsum or calcium silicate matrix) of 5.4 ± 3.5 molecules/100 eV. The authors report that this value is too large to realistically represent radiolytic production of hydrogen gas from this system. While this type of material is not well-characterized, the authors expected to observe G-values ranging from 1-1.5 molecules/100 eV.

INEEL (1999) used a cement proxy (Envirostone) as a material representative of the solidified inorganics typically found in TRU mixed waste. Since Envirostone is a cement-like matrix with a high water content, the experimentally obtained values found in INEEL (1999) are also representative of the behavior of TRU waste cements. The G(H_2)-value for Envirostone was found by INEEL (1999) to range from 0.27 to 0.58 molecules/100 eV. This range of values agrees well with the G(H_2)-value of 0.41 molecules/100 eV from radiolysis of cement reported by Bouniol and Bjergbakke (2008).

A summary of G-values is listed in Table 7. An assumed G-value has been selected for each material from the upper bounds of the observed G-value range. The assumed G-value will be used for a bounding value on the gas generation potential of these materials.

Table 7 Summary of G-Values

Material Type	G-Value Range (molecules/100 eV)	Assumed G-Value (molecules/100 eV)
CPR	1.24	1.24
Cement	0.27 – 0.58	0.58
Solidified Inorganic Material	0.27 – 0.58	0.58
Solidified Organic Material	1 – 1.5	1.5
Soil	0.116 – 0.453	0.453

Combining the G-values in Table 7 with the inventory quantities from Table 6 gives the inventory-weighted G-values listed in Table 8. The cumulative G-value for CPR plus the four additional materials is 0.948, which is significantly less than the initial G-value of CPR evaluated by Day (2019) and in the response to CC3-GEOCHEM-19. It is noted that the Waste and Packaging Material "Other Inorganic Materials" contains cement, adding that mass into this analysis with the same G-value as cement would further lower the weighted G-value.

As reported by Day (2019) and further examined in CC3-GEOCHEM-19a, the G-value of CPR is expected to decrease to non-impactful levels due to matrix depletion in a short time frame relative to the WIPP regulatory period. Matrix depletion is the reduction in the effective G-value of a material over time. This occurs because the hydrogen-containing molecules in the irradiation zone, which are radiolytically degraded to form hydrogen gas, are depleted.

Matrix depletion has also been observed in non-CPR radiolysis (INEEL 1999). Similarly, the G-value of the heterogeneous material mixture comprising the materials listed in Table 7 would be expected to decrease with time in a manner similar to the G-values of CPR reported in Day (2019) and as described in the response to CC3-GEOCHEM-19a. As shown with the SMIC2 analysis in CC3-GEOCHM-19b, radiolysis with a G-value less than 0.3 is not impactful to the WIPP PA results. For CPR materials, the G-value reached a non-impactful level of < 0.3 within 100 years at the activity concentrations described in Zerwekh (1979), and within 200 years at the activity concentrations described in CC3-GEOCHEM-19a. Using these calculations as an approximation of the behavior of the heterogeneous material mixture,

the weighted G-value of the material mixture would decrease from its initial value of 0.948 to less than the non-impactful G-value in a similarly short period of time. Therefore, radiolysis of these materials is shown to be low relative to the processes described in CC3-GEOCHEM-19a, and can be screened out due to low impact.

Table 8 Inventory-Weighted G-Values

Material Type	Fraction of Total Inventory[(a)]	G-Value[(b)] (molecules/100 eV)	Weighted G-Value (molecules/100 eV)
CPR	0.3983	1.24	0.4939
Cement	0.0438	0.58	0.0254
Solidified Inorganic Material	0.3015	0.58	0.1749
Solidified Organic Material	0.1315	1.5	0.1973
Soil	0.1248	0.453	0.0565
Total	1.0000	--	**0.9480**

(a) Based on total inventory from Table 6.
(b) Based on Assumed G-Value from Table 7.

References

Barber, D., K. Carney, P. Hart, D. Cummings, M. Sayer, D. Hendrix, K. Shirley and J. Demirgian. 2001. The determination of the rate of hydrogen generation from transuranic 003 type organic sludge. Waste Management Conference 2001, Tucson, Arizona.

Bouniol, P. and E. Bjergbakke. 2008. A comprehensive model to describe radiolytic processes in cement medium. Journal of Nuclear Materials 372:1-15.

Day, B. 2019. Reassessment of need and parameter justification for modeling gas generation due to radiolysis of brine and cellulose/plastic/rubber in WIPP for CRA-2019. Sandia National Laboratories, Carlsbad, New Mexico. ERMS 570873.

Fourdrin, C., H. Aarrachi, C. Latrille, S. Esnouf, F. Bergaya and S. Le Caer. 2013. Water radiolysis in exchanged-montmorillonites: the H2 production mechanisms. Environmental Science and Technology 47:9530-9537.

Idaho National Engineering and Environmental Laboratory. 1999. TRUCPACT-II matrix depletion program final report. Bechtel BWXT Idaho, LLC. Idaho Falls, ID. INEEL/EXT-99-0987.

Van Soest, G. 2018. Performance assessment inventory report-2018. Los Alamos National Laboratory Carlsbad Operations. Carlsbad, NM. LA-UR-18-31882.

Zerwekh, A. 1979. Gas generation from radiolytic attack of TRU-contaminated hydrogenous waste. Los Alamos National Laboratory, Los Alamos, NM. LA-7674-MS.

EPA Evaluation of Response

The DOE response was satisfactory.

CC4-SOTERM-8 Pu(III) Intrinsic Colloid Concentrations

WIPP Compliance Recertification Application 2019 Appendix-SOTERM (Actinide Chemistry Source Term)

EPA Question (from EPA Completeness Comment Package 4)

Please address the following discrepancies identified in Pu(III) intrinsic colloid concentrations from the tables presented in Reed et al. (2019) as well as their effects on the PA:

CC4-SOTERM-8a. **Resolution of Instrinsic Colloid Concentrations**

Please resolve the discrepancy between intrinsic colloid concentrations cited on page 23 and in Table A-1 of Reed et al. (2019). The Pu(III) intrinsic colloid concentration (1.5 × 10-9 M) cited in the discussion on page 23 differs from the corresponding concentration in Table A-1 (1.49 × 10-8 M). The higher concentration in Table A-1 appears to be correct, based on the data presented in Figure 4-4 of Reed et al. (2013).

DOE Response (from DOE Response Package 7)

The plutonium data presented in Table A-1 (Reed et al., 2019) are slightly off. To reconcile inconsistencies over the past ten years, a re-analysis of these data going back to the original Inductively Coupled Plasma Mass Spectrometry (ICP-MS) data was performed and is given in Table 1 (Reed 2020). These connect and supersede what was done for CRA-2014 and CRA-2019 as imprecise designations were used between the two analysis sets.

Table 1. Final/Corrected Values for CONCINT from the Pu(III) Data for CRA-2019

Experiment	[Pu] at 10 nm filtration (M)*	[Pu] at 2.5 nm filtration (M)*	Estimated $[Pu]_{intrinsic}$ (M)*
Pu-FEC-G72 GWB brine, pC_{H+} = 7.71	1.1×10^{-8}	1.1×10^{-9}	9.9×10^{-9}
Pu-FEC-E82 ERDA-6 brine, pC_{H+} = 8.34	#9.9×10^{-8}	4.1×10^{-10}	9.5×10^{-9}
Pu-FEC-2 ERDA-6 brine, pC_{H+} = 9.11	#4.7×10^{-9}	9.7×10^{-10}	3.7×10^{-9}
Pu-FE23OX-2 ERDA-6 brine, pC_{H+} = 9.12	5.2×10^{-9}	7.3×10^{-10}	4.5×10^{-9}
Pu-FEC-E10 ERDA-6 brine, pC_{H+} = 9.54	#2.1×10^{-9}	5.7×10^{-10}	1.5×10^{-9}
* uncertainty from ICP-MS is ± 10%; based on replicate reproducibility this was increased to ± 30-80%. # average of two values obtained at through the different filtration protocols			

In this configuration, the recommended An(III) intrinsic colloid concentration should have been $9.9 \pm 3.0 \times 10^{-9}$ M (highest value) rather than $9.5 \pm 2.9 \times 10^{-9}$. This is comparable to an average colloidal concentration of $6.4 \pm 1.9 \times 10^{-9}$ M for the whole data set. All of these numbers are within the uncertainty of each other.

Reference

Reed, D.T. 2020. Supporting Document: Justification for the Pu(III) Intrinsic Colloid parameter (CONCINT) Based on Plutonium Filtration Data. Los Alamos National Laboratory, Carlsbad New Mexico. Los Alamos Report LAUR 20-29679.

CC-4 SOTERM-8b. **Effects on Repository Releases Due to Higher Am:CONCINT Parameter**

Please assess the effects on repository releases due to a higher AM:CONCINT parameter as a result of the changes in the previous question. If the Pu(III) intrinsic colloid concentration of 1.49 × 10^{-8} M identified in Table A-1 (Reed et al. 2019) is correct, the maximum observed Pu(III) intrinsic colloid concentration will increase from 9.5 × 10^{-9} M to 1.49 × 10^{-8} M. Using the oxidation state analogy, the AM:CONCINT parameter for the concentration of Am(III) intrinsic colloids will increase to 1.49 × 10^{-8} M.

DOE Response

A change to an An(III) intrinsic colloid (CONCINT) contribution of 9.9 ± 3.0 × 10^{-9} M rather than 9.5 ± 2.9 × 10-9 would have a negligible effect on the An(III) contribution to the mobile actinide concentration source term. These are effectively the same number. Additionally, they only contribute ~ 0.1% (see CRA 2019, Appendix SOTERM Table 23) of the total mobile concentration used in PA.

CC4-SOTERM-8c. **Explanation of Differences in Pu(III) Data**

Please explain the differences in some of the Pu(III) data presented by Reed et al. (2019), and data previously included in Reed et al. (2013) (see table below). Please explain whether the 2019 data are a correction of the 2013 data or if the 2013 data are from different samples that were excluded from the 2019 data. Also, please explain the reasons for the data correction or exclusion.

Pu(III) Intrinsic Colloid and Dissolved Concentration Data

pcH	*Pu(III) intrinsic colloid (M)*	*Pu(III) dissolved (M)*	*Brine*	*Source*
7	*9.53E-09*	*4.08E-10*	*GWB*	*Reed et al. (2019) Table A-1*
7.7	*1.00E-08*	*1.10E-09*	*GWB*	*Reed et al. (2013) Table 4-4*
8.3	*l.49E-08*	*1.14E-09*	*ERDA-6*	*Reed et al. (2019) Table A-1*
8.4	*1.20E-08*	*4.10E-10*	*ERDA-6*	*Reed et al. (2013) Table 4-4*

Reed, D.T., J.S. Swanson, J.F. Lucchini and M.K. Richmann. 2013. Intrinsic, Mineral and Microbial Colloid Enhancement Parameters for the WIPP Actinide Source Term. LCO-ACP-18, Revision 0. Los Alamos National Laboratory, Carlsbad, New Mexico.

Reed, D., J. Swanson and F. Stanley. 2019. LANL/ACRSP Parameter Recommendations for the CRA-2019 Deferred Performance Assessment LCO-ACP-18, Revision 0. Los Alamos National Laboratory, Carlsbad, New Mexico.

DOE Response

The correct data are shown in Table 1 that is part of answer SOTERM-8a. Those shown in Table A-1 (Reed et al., 2019) are incorrectly reported and represent data that were evaluated in a different way.

References

Reed, D., J. Swanson, J. Lucchini and M. Richmann. 2013. Intrinsic, Mineral and Microbial Colloid Enhancement Parameters for the WIPP Actinide Source Term. Los Alamos National Laboratory, Carlsbad, New Mexico. LCO-ACP-18, Revision 0.

Reed, D., J. Swanson and F. Stanley. 2019. LANL/ACRSP Parameter Recommendations for the CRA-2019 Deferred Performance Assessment. Los Alamos National Laboratory, Carlsbad, New Mexico. LCO-ACP-18, Revision 0.

EPA Evaluation of Response

The DOE response was adequate. A technical exchange following up on these comments was held in December 2020.

CC4- SOTERM-9 Th(IV) Intrinsic Colloid Concentrations Error

WIPP Compliance Recertification Application 2019 Appendix-SOTERM (Actinide Chemistry Source Term)

EPA Question (from EPA Completeness Comment Package 4)

Please evaluate the effects on predicted repository releases as a result of increasing the TH:CONCINT, NP:CONCINT, PU:CONCINT, and U:CONCINT parameters to 3.08 × 10-6 M.

In a previous evaluation of colloid concentrations obtained from the Th(IV) filtration data (USEPA 2017), the Agency accepted DOE's explanation that two samples from the Reed et al. (2013) experiment E10C3-1 (ERDA-6 brine from oversaturation) were likely too far from equilibrium solubility to reliably determine Th(IV) intrinsic colloid concentrations (see table below). However, the Agency found that dissolved Th(IV) concentrations in samples from oversaturation in GWB brine (experiment G8C2-1) were very close to equilibrium based on EQ3/6 modeled concentrations (see table below), so these samples should be included in the calculation of Th(IV) intrinsic colloid concentrations. The Agency also noted that the intrinsic colloid parameters should reflect upper bounding values (USEPA 2017).

The 10 nm-filtered Th(IV) concentration data in Table A-1 of Reed et al. (2019) are incorrect and are actually the 5 nm-filtered data from Borkowski (2012, page 19). Using the correct Borkowski (2012) data for samples from the experiments close to equilibrium solubility in GWB (two samples each from UG8C0-2, G8C2-1, and UG9C2-2, see table below), the upper bounding value for Th(IV) intrinsic increases to 3.08 × 10-6 M (highlighted in yellow). This value is significantly higher than the TH:CONCINT value of 4.3 × 10-8 M used for the CRA-2019 DPA. The Th(IV) intrinsic colloid concentration of 3.08 × 10-6 M is consistent with the upper bound observed for Th(IV) intrinsic colloids in NaCl and MgCl2 brine experiments reported by Altmaier et al. (2004) and consequently is a reasonable upper bound for TH:CONCINT. Based on the

assumption that actinides in the same oxidation state will have similar chemical behavior that was used by Reed et al. (2019), the values of the intrinsic colloid parameters for Pu(IV), Np(IV), and U(IV) will also increase to 3.08 × 10-6 M.

Th(IV) Colloidal and Dissolved Concentrations (Borkowski 2012) and Modeled Dissolved Th(IV) Concentrations (CRA-2019 Appendix SOTERM, Table SOTERM-30)

Brine	Experiment	pcH	Th(IV) Intrinsic Colloids (M)	Dissolved Th(IV) (M)
GWB	UG8CO-2 (1)	8.13	3.58E-08	1.41E-08
GWB	UG8CO-2 (2)	8.13	3.97E-08	1.27E-08
GWB	G8C2-1 (1)	8.54	3.00E-06	6.17E-08
GWB	G8C2-1 (2)	8.54	3.08E-06	5.43E-08
GWB	UG9C2-2 (1)	9.11	9.40E-09	3.63E-08
GWB	UG9C2-2 (2)	9.11	2.24E-08	2.68E-08
GWB modeled baseline solubility				5.45E-08
ERDA-6	E10C3-1 (1)	9.18	1.08E-06	5.02E-07
ERDA-6	E10C3-1 (2)	9.18	7.56E-07	8.14E-07
ERDA-6 modeled baseline solubility				5.44E-08

Altmaier, M., V. Neck, and T. Fanghänel. 2004. Solubility and colloid formation of Th(IV) in concentrated NaCl and $MgCl_2$ solution. Radiochimica Acta 92:537-543.

Borkowski, M. 2012. Numerical Values for Graphs Presented in Report LCO-ACP-08, Rev. 0, Entitled Solubility of An(IV) in WIPP Brine: Thorium Analog Studies in WIPP Simulated Brine, and for Graphs. Published in: Borkowski, M., et al. Radiochimica Acta 98 (9-11), 577-582, (2010). LA-UR- 12-26640; LANLCO ACRSP ACP-01/2012, Rev. 0. Los Alamos National Laboratory, Carlsbad, New Mexico.

Reed, D., J. Swanson, and F. Stanley. 2019. LANL/ACRSP Parameter Recommendations for the CRA-2019 Deferred Performance Assessment, LCO-ACP-18, Revision 0. Los Alamos National Laboratory, Carlsbad, New Mexico.

U.S.E.P.A. (United States Environmental Protection Agency). 2017. Technical Support Document For Section 194.24, Evaluation Of The Compliance Recertification Actinide Source Term, Gas Generation, Backfill Efficacy, Water Balance And Culebra Dolomite Distribution Coefficient Values. Office of Radiation and Indoor Air, Washington, D.C., EPA-HQ-OAR-2014- 0609, June 2017.

DOE Response (from DOE Response Package 7)

The WIPP project position on intrinsic colloids through the CRA-2009 was based on the colloid enhancement factors developed at the time of the CCA. The values for the intrinsic colloid enhancement factors (CONCINT) were zero for Th(IV), U(IV), Np(IV) and 1×10^{-9} M (based on a null result) for Pu(IV) and approved by the EPA in the CCA, CRA-2004, and CRA-2009. The DOE review completed for CRA-2014 concluded that this long-held CCA position was no longer defensible given the further state of understanding about actinide behavior in brine (Reed et al., 2013). The two most important reasons for this were: 1) the chemistry of U(IV) and Np(IV) in brines is very analogous to Pu(IV) and all three of these oxidation states should have a similar colloidal behavior; and 2) it was clear that the intrinsic colloids being formed were not classical

“electrostatic” colloids and the factors leading to their formation were not well understood. For this reason, the DOE decided to establish a more robust, conservative, but reasonable project position for the CONCINT parameter. This led to an increase in the intrinsic colloidal enhancement factor for all the An(IV) actinides to a value of 2×10^{-8} M that was based on an estimate using the results of the long-term thorium solubility studies which was the only An(IV) data available to the project at that time. This approach was accepted by the EPA with the direction to consider a wider set of pH values for CRA-2019 using the same calculational approach and thorium data (Reed et al. 2013, 2019). This recommendation was implemented in CRA-2019 leading to an increase of the enhancement parameter to a value of 4.3×10^{-8} M. The overall effect of the changes completed in CRA-2014 and CRA-2019 was to increase the colloid enhancement parameters for all of the An(IV) actinides in WIPP PA.

The use of thorium to simulate actinide(IV) solubility is a conservatism built into the WIPP model (this overestimates An(IV) solubility by a factor of ~100). U(IV) and Np(IV) more accurately simulate the solubility of Pu(IV). The colloidal behavior of thorium is also dissimilar to U(IV), Np(IV), and Pu(IV) as its tendency towards hydrolysis, which is a key to defining its colloidal behavior, is significantly weaker than the other An(IV) actinides. Modeling An(IV) colloidal enhancement parameters on Th(IV) colloidal concentrations adds additional layers of conservatism which is desirable from a the viewpoint of performance assessment, but not desirable from the viewpoint of accurately predicting actinide behavior under repository conditions. The DOE funded an Institute for Nuclear Waste Disposal (INE) report to assess this issue for CRA-2019 and develop an experimental strategy for using U(IV) and Np(IV) as an improved analog for Pu(IV) chemistry (Altmaier et al., 2017). The many difficulties and high metastability found in using thorium data as an analog for An(IV) solubility have been discussed extensively by the DOE (CRA-2014, Appendix SOTERM Section 3.3; CRA-2019, Appendix SOTERM Section 5.4; CRA-2019 DOE response CC1-SOTERM-4) and discussed extensively with the EPA during the past several years. It is for these many reasons that the DOE has been very selective in using thorium data for the estimation of the CONCINT colloidal enhancement parameters and ideally this parameter should be based on U(IV), Np(IV) or Pu(IV) data where colloids are much less likely to be formed.

For the CRA-2019 CONCINT parameter recommendations to WIPP PA the EPA is correct in pointing out that what was identified as 5 nm-filtration data in the Borkowski 2012 report was used (Borkoswki et al., 2012). The Amicon ultrafiltration filters do not have a hard cutoff as implied in the Borkowski report and there is in fact overlap between the size distribution ranges in the 10K and 30K Molecular Weight Cut-Off (MWCO) filters used (https://www.sigmaaldrich.com/technical-documents/articles/biology/nanoparticleultrafiltration.html). This was an unfortunate inconsistency in the implementation of the CRA- 2019 changes that leads to a relatively small error in the calculated parameter value of CONCINT. This parameter error is considered small when compared to the solubility being known only to within an order of magnitude.

The DOE does not agree however with the EPA that the CONCINT parameter should be set to the highest observed value reported in the Borkowski concentration data. In the EPA table provided, it is quite clear that there is a strong hysteresis between experiments that were approached from undersaturation with those that were approached from oversaturation. For experiments UG8CO and UG9C2, both undersaturation experiments, the colloidal fraction is ~ 4

x 10^{-8} M and 1.5 x 10^{-8} M respectively. In contrast, the colloidal fraction for experiments G8C2, and E10C3, which were approached from oversaturation, are 3 x 10^{-6} M and 9 x 10^{-7} M respectively – as much as 200 times higher. This type of meta-stability and disparity in much of the thorium data, which extends beyond the data summarized by the EPA, is why the DOE believes the thorium undersaturation data provide a more reasonable upper bound to the colloidal enhancement of U(IV), Np(IV) and Pu(IV) in calculating actinide release.

Lastly, the DOE does not agree that the Altmaier publication (Altmaier et al., 2004) provides a good estimate of the intrinsic colloidal behavior of thorium in brine systems. This paper was part of the many discussions with the EPA since CRA-2009 and there have also been many follow up discussions with INE researchers to reconcile the results they have seen in simplified brine systems with those observed by the WIPP in simulated brines. The results of these discussions, and the DOE explanation for the observed differences, were summarized previously (CRA-2014, Appendix SOTERM Section 3.3). The colloids observed in Altmaier et al. (2004) were in fact most likely mineral (Mg-precipitate associated) and not intrinsic due to the likely precipitation of some Mg phases in their system. A very different behavior has been consistently observed in simulated WIPP brine where both the concentration of intrinsic colloids and apparent solubility decreases with time. In these WIPP studies, there was also no Mg-associated mineral colloid formation. The DOE has speculated that this is likely due to a metastability between the colloidal and soluble fraction but in fact this process is not well understood and cannot be reliably predicted.

The DOE continues to acknowledge that the use of thorium data to determine the An(IV) intrinsic colloid enhancement parameter is not ideal and certainly far from perfect. Thorium is simply not a good analog for the colloidal behavior of U(IV), Np(IV) and most importantly Pu(IV). There are project-specific data in the U(IV)-EDTA system in WIPP Brine (Yalcintas et al., 2019) and in the thorium-EDTA biosorption data that show that there are essentially no colloids present in these systems. For CRA-2019, however the DOE is following the path agreed to with the EPA that preserves a reasonable but more robust project position on the values for the CONCINT parameter until there is greater clarity on the key and critical factors that define the colloidal enhancement of U(IV), Np(IV) and Pu(IV) intrinsic colloids in WIPP brine. Note that WIPP PA uses an element specific CONCINT value taken as the maximum of the oxidation state specific values, therefore the CONCINT value for Uranium (U:CONCINT) takes on the higher U(VI) value of 1.4 x 10^{-6} M.

References

Altmaier, M., V. Neck and T. Fanghänel. 2004. Solubility and colloid formation of Th(IV) in concentrated NaCl and MgCl2 solution. *Radiochimica Acta* 92:537-543.

Altmaier, M., D. Fellhauer, X. Gaona and E. Yalcintas. 2017. Assessment of Np(IV) and U(IV) as Improved Analogs for Pu(IV) in High Ionic-Strength Brine Systems. KIT-INE Report.

Borkowski, M. 2012. Numerical Values for Graphs Presented in Report LCO-ACP-08, Rev. 0, Entitled Solubility of An(IV) in WIPP Brine: Thorium Analog Studies in WIPP Simulated Brine and for Graphs. Published in: Borkowski, M., et al. Radiochimica Acta 98 (9-11), 577-582, (2010). Los Alamos National Laboratory, Carlsbad, New Mexico. LANL-CO ACRSP ACP-01/2012, Rev. 0. LAUR-12-26640.

Reed, D., J. Swanson, J.F. Lucchini and M. Richmann. 2013. Intrinsic, Mineral and Microbial Colloid Enhancement Parameters for the WIPP Actinide Source Term. Los Alamos National Laboratory, Carlsbad, NM. LCO-ACP-18. LA-UR 13-20858.

Reed, D., J. Swanson and F. Stanley. 2019. LANL/ACRSP Parameter Recommendations for the CRA-2019 Deferred Performance Assessment. Los Alamos National Laboratory, Carlsbad, New Mexico. LCO-ACP-18, Revision 0.

U.S. Department of Energy. 2014. Title 40 CFR Part 191 Subparts B and C. Compliance Recertification Application for the Waste Isolation Pilot Plant (March), Appendix SOTERM. Carlsbad Field Office, Carlsbad, NM. DOE/WIPP 2014-3503.

U.S. Department of Energy. 2019. Title 40 CFR Part 191 Subparts B and C. Compliance Recertification Application for the Waste Isolation Pilot Plant (March), Appendix SOTERM. Carlsbad Field Office, Carlsbad, NM. DOE/WIPP.

Yalcintas, E., X. Gaona, M. Richmann, K. Dardenne, M. Altmaier and D. Reed. 2019. Spectroscopy and Solubility of U(IV) in Dilute to Concentrated NaCl Solutions in the Presence of EDTA at pH_m 1-11. Los Alamos National Laboratory, Carlsbad, NM. Los Alamos Report LA-UR-19-28330.

EPA Evaluation of Response

The DOE response was satisfactory. Explanatory information was provided as requested.

CC4- SOTERM-10 Th(IV) Concentration Data Revisions

WIPP Compliance Recertification Application 2019 Appendix-SOTERM (Actinide Chemistry Source Term)

EPA Question (from EPA Completeness Comment Package 4)

Please explain the differences between Th(IV) data presented for two samples by Reed et al. (2013 and 2019), and data presented by Borkowski (2012) (see table below). Please explain whether the Reed et al. (2013 and 2019) data are a correction of the Borkowski (2012) data or if the Reed et al. (2013 and 2019) data represent different samples than the Borkowski (2012) samples.

Th(IV) Intrinsic Colloid and Dissolved Concentration data

pcH	Th(IV) intrinsic colloid (M)	Th(IV) dissolved (M)	Brine	Source
9.1	3.60E-08	1.00E-08	GWB	Reed et al. (2013) Table A2-1, Reed et al. (2019) Table A-2
9.1	2.70E-08	2.20E-08	GWB	Reed et al. (2013) Table A2-1, Reed et al. (2019) Table A-2
9.11	9.40E-09	3.63E-08	GWB	Borkowski (2012)
9.11	2.24E-08	2.68E-08	GWB	Borkowski (2012)

Borkowski, M. 2012. Numerical Values for Graphs Presented in Report LCO-ACP-08, Rev. 0, Entitled Solubility of An(IV) in WIPP Brine: Thorium Analog Studies in WIPP Simulated Brine, and for Graphs.

Published in: Borkowski, M., et al. Radiochimica Acta 98 (9-11), 577- 582, (2010). LA-UR- 12-26640; LANL-CO ACRSP ACP-01/2012, Rev. 0. Los Alamos National Laboratory, Carlsbad, New Mexico.

Reed, D.T., J.S. Swanson, J.F. Lucchini and M.K. Richmann. 2013. Intrinsic, Mineral and Microbial Colloid Enhancement Parameters for the WIPP Actinide Source Term, LCO-ACP-18, Revision 0. Los Alamos National Laboratory, Carlsbad, New Mexico.

Reed, D., J. Swanson and F. Stanley. 2019. LANL/ACRSP Parameter Recommendations for the CRA-2019 Deferred Performance Assessment, LCO-ACP-18, Revision 0. Los Alamos National Laboratory, Carlsbad, New Mexico.

DOE Response (from DOE Response Package 7)

The data for the first two samples (Reed et al. 2013 and 2019) in the table provided by the EPA response are transposed in their columns. The slight difference in value between these samples and those listed in Borkowski 2012 are due to differences from rounding. The corrected EPA table should look like the following:

pcH	Th(IV) intrinsic colloid (M)	Th(IV) dissolved (M)	Brine	Source
9.1	1.0E-8	3.6E-8	GWB	Reed et al. (2013) Table A2-1, Reed et al. (2019) Table A-2
9.1	2.2E-8	2.7E-8	GWB	Reed et al. (2013) Table A2-1, Reed et al. (2019) Table A-2
9.11	9.40E-09	3.63E-08	GWB	Borkowski (2012)
9.11	2.24E-08	2.68E-08	GWB	Borkowski (2012)

The Th(IV) dissolved concentrations were determined by the ICP-MS results after filtering the samples with a 30kD filters (pore size ~10 nm). The Th(IV) intrinsic colloid concentrations were determined by subtracting the dissolved fraction from the 10nm filtered concentrations. These values were corroborated with the original data package (ACP-09-123). There is in fact no difference between the Reed at al., 2013/2019 data and those presented in Borkowski et al., 2012.

References

Borkowski, M. 2012. Data Package entitled: Thorium-19 for LCO-ACP-17 Report and two RDFs for technical and QA Review. September 27, 2012. ACP-09-123.

Borkowski, M. 2012. Numerical Values for Graphs Presented in Report LCO-ACP-08, Rev. 0, Entitled Solubility of An(IV) in WIPP Brine: Thorium Analog Studies in WIPP Simulated Brine, and for Graphs. Published in: Borkowski, M., et al. Radiochimica Acta 98 (9-11), 577-582, (2010). Los Alamos National Laboratory, Carlsbad, New Mexico. LANL-CO ACRSP ACP-01/2012, Rev. 0. LA-UR- 12-26640.

Reed, D., J. Swanson, J.F. Lucchini and M. Richmann. 2013. Intrinsic, Mineral, and Microbial Colloid Enhancement Parameters for the WIPP Actinide Source Term. Los Alamos National Laboratory, Carlsbad, NM. LCO-ACP-18, LA-UR 13-20858.

Reed, D., J. Swanson and F. Stanley. 2019. LANL/ACRSP Parameter Recommendations for the CRA-2019 Deferred Performance Assessment. Los Alamos National Laboratory, Carlsbad, New Mexico. LCO-ACP-18, Revision 0.

EPA Evaluation of Response

The DOE response was satisfactory. Explanatory information was provided as requested.

CC4- SOTERM-11 Th(IV) Mineral Fragment Colloid Parameter

WIPP Compliance Recertification Application 2019 Appendix-SOTERM (Actinide Chemistry Source Term)

EPA Question (from EPA Completeness Comment Package 4)

Please assess whether the mineral fragment colloid parameter for Th(IV) (TH:CONCMIN) should be increased from 2.6 × 10-8 M to an upper bounding value of 6.2 × 10-7 M.

Two samples measuring Th(IV) solubility in oversaturated GWB (Borkowski 2012, experiment G8C2-1) had Th(IV) concentrations of 3.3 × 10-7 M and 6.2 × 10-7 M in the size range consistent with the mineral fragment colloid size range (10 nm to 450 nm, see table below, samples are highlighted in yellow).

Th(IV) Mineral Fragment Colloid and Dissolved Concentration Data

Brine	Experiment	pcH	Th(IV) 450 nm filtration (M)	Th(IV) 10 nm filtration (M)	Th(IV) mineral fragment colloids (M)	Th(IV) dissolved (M)
GWB	UG8C0-2(1)	8.13	5.47×10^{-8}	4.99×10^{-8}	4.8×10^{-9}	1.41×10^{-8}
GWB	UG8C0-2(2)	8.13	5.07×10^{-8}	5.24×10^{-8}	0	1.27×10^{-8}
GWB	G8C2-1(1)	8.54	3.68×10^{-6}	3.06×10^{-6}	6.2×10^{-7}	6.17×10^{-8}
GWB	G8C2-1(2)	8.54	3.46×10^{-6}	3.13×10^{-6}	3.3×10^{-7}	5.43×10^{-8}
GWB	UG9C2-2(1)	9.11	4.95×10^{-8}	4.57×10^{-8}	3.8×10^{-9}	3.63×10^{-8}
GWB	UG9C2-2(2)	9.11	4.60×10^{-8}	4.92×10^{-8}	0	2.68×10^{-8}
ERDA-6	E10C3-1(1)	9.18	1.58×10^{-6}	1.58×10^{-6}	0	5.02×10^{-7}
ERDA-6	E10C3-1(2)	9.18	1.58×10^{-6}	1.57×10^{-6}	1×10^{-8}	8.14×10^{-7}

Borkowski, M. 2012. Numerical Values for Graphs Presented in Report LCO-ACP-08, Rev. 0, Entitled Solubility of An(IV) in WIPP Brine: Thorium Analog Studies in WIPP Simulated Brine, and for Graphs Published in Borkowski, M., et al. Radiochimica Acta 98 (9-11), 577- 582 (2010). LA-UR- 12-26640; LANLCO ACRSP ACP-01/2012, Rev. 0. Los Alamos National Laboratory, Carlsbad, New Mexico.

DOE Response (from DOE Response Package 7)

The WIPP project position on intrinsic colloids through the CRA-2009 was based on the colloid enhancement factors developed at the time of the CCA. For the mineral fragment enhancement

factor (CONCMIN), the parameter value was set to 2.6 × 10-8 M based on iron colloidal interactions found in some plutonium studies (Reed et al. 2013b). This mineral colloid value was re-affirmed based on the analysis of newer plutonium-Fe WIPP data (see data in Figures 4-3 and 4-4 and associated discussion in Section 4.2.3 in Reed et al., 2013) and the parameter values used in WIPP PA for CONCMIN were not changed in CRA-2014 or CRA-2019. In these applications, the original conceptualization of the CCA, that only iron mineral colloids were likely present, was not changed and the DOE does not propose to change this.

The thorium data summarized by the EPA in this comment is metastable (see the more detailed discussion in the CC4-SOTERM-9 DOE response) and difficult to interpret. There are in fact no identifiable mineral colloids in these thorium experiments (no Fe or precipitated brine components). For this important reason, these data should not be used as a basis for establishing CONCMIN.

References

Reed, D., J. Swanson, J.F. Lucchini and M. Richmann. 2013. Intrinsic, Mineral, and Microbial Colloid Enhancement Parameters for the WIPP Actinide Source Term. Los Alamos National Laboratory, Carlsbad, NM. LCO-ACP-18, LA-UR 13-20858.

Reed, D., M. Richmann and M. Borkowski. 2013b. Long-term Plutonium Speciation in Fe-Dominated High Ionic-Strength Brines. Proceedings of the Third International Workshop on Actinide and Brine Chemistry in a Salt-Based Repository (ABC-Salt III). Santa Fe, NM. LA-UR-15-21114, pg. 59.

EPA Evaluation of Response

The DOE response was satisfactory. The information was provided as requested.

CC4- SOTERM-12 Actinide(IV)-Silica Colloids

WIPP Compliance Recertification Application 2019 Appendix-SOTERM (Actinide Chemistry Source Term)

EPA Question (from EPA Completeness Comment Package 4)

Please evaluate and summarize in a writeup the possible importance of An(IV)-silicate colloids to mobilization of Th(IV), U(IV), and Pu(IV) in WIPP brines. Please include any relevant tables or figures in this write up as needed.

Recent publications, for example, Zänker et al. (2016), Neil et al. (2018), and Neil et al. (2019), have described the potential mobilization of +IV actinides by colloids that include structural An(IV) and silica. Possible formation of these colloids under WIPP repository conditions was not addressed in the CRA 2019.

Neill, T.M., K. Morris, C.I. Pearce, N.K. Sherriff, M.G. Burke, P.A. Chater, A. Janssen, L. Natrajan, and S. Shaw. 2018. Stability, composition, and core-shell particle structure of uranium(IV)-silicate colloids. Environmental Science and Technology 52:9118-9127.

Neill, T.M., K. Morris, C.I. Pearce, L. Abrahamsen-Mills, L. Kovarik, S. Kellet, B. Rigby, T. Vitova, B. Schacherl, and S. Shaw. 2019. Silicate stabilization of colloidal UO_2 produced by uranium metal corrosion. Journal of Nuclear Materials 526.

Zänker, H. S. Weiss, C. Henning, V. Brendler, and A. Ikeda-Ohno. 2019. Oxyhydroxy silicate colloids: a new type of waterborne actinide(IV) colloids. ChemistryOpen 5:174-182.

DOE Response (from DOE Response Package 6)

The U.S. Department of Energy (DOE) does not currently believe that silica is an important contributor to the intrinsic colloidal concentration of Th(IV), U(IV), Np(IV) and Pu(IV) in the mobile actinide source term. This view is predominantly based on DOE's understanding that silica is not a component of the Waste Isolation Pilot Plant (WIPP) brine and the amount of silica present in transuranic waste that could dissolve in WIPP brine is likely small but also not well established. Additionally, as of the 2019 Compliance Recertification Application (CRA) cutoff date (1/08/2018), there was no WIPP-relevant data/publications that clearly pointed to a potential role for silica in the formation of actinide colloids. Appendix WCA (DOE 1996) did not identify silica as a prevalent waste characteristic worthy of tracking. For these reasons, there are no WIPP-specific data that directly address this issue and the silica content of WIPP waste is not currently tracked/estimated as part of the inventory tracking process.

The review paper noted by the U.S. Environmental Protection Agency (Zänker et al., 2016) is a general review that is centered on low pH to near-neutral systems where some silica-enhanced colloid formation has been noted. This review mainly targets low ionic strength (<0.1 M) near-surface groundwater systems that tend to be in contact with silica-containing minerals which made its relevance to WIPP unclear.

The more recent post-CRA-2019 publications (Neill et al., 2018; Neill et al., 2019), however, extend specifically to higher pH (9-10.5) and repository considerations. It was established that under these pH conditions silica reacts with a hydrolyzed U(IV) to interfere with the precipitation process and amorphously coat the UO_2 core. This led to very small (< 20 nm but typically 2-5 nm in size) colloids that can significantly increase the colloidal concentration relative to a U(IV)-only system. These colloids were mostly observed at high silica concentration (> 1 mM) under anoxic conditions and all the work was at an ionic strength < 1M. It was speculated, however, that a similar process should also extend to lower silica concentrations. This nucleation process has some similarities to the structure of U-silicate minerals that are found extensively in nature and it was hypothesized that silica colloid formation may be a possible explanation and mechanism for the formation of these minerals.

These recent uranium data, because they may also impact Np(IV) and Pu(IV), are interesting and suggest that further evaluation of this colloidal issue by the WIPP project may be merited. It is not possible, based on only these studies, to project an impact on the WIPP case since the dependency of this process on [Si] was not clearly established and, perhaps more importantly, the effects of organic complexation and high ionic strength on the formation and long-term stability of the silica colloids was not investigated. The low silica concentrations, high ionic strength brines and presence of strong organic complexation all favor a low impact on the intrinsic colloid content of the actinide source term.

References

References with hyperlinks were provided in prior CRAs. The remainder of the reference documents will be provided in Enclosure 4 or as otherwise noted.

Zänker, H., S. Weiss, C. Henning, V. Brendler and A. Ikeda-Ohno. 2016. Oxyhydroxy silicate colloids: a new type of waterborne actinide(IV) colloids. ChemistryOPEN 5:174-182.

Neill, T., K. Morris, C. Pearce, N. Sherriff, M. Burke, P. Chater, A. Janssen, L. Natrajan and S. Shaw. 2018. Stability, composition, and core-shell particle structure of uranium(IV)-silicate colloids. Environmental Science and Technology 52:9118-9127.

Neill, T., K. Morris, C. Pearce, L. Abrahamsen-Mills, L. Kovarik, S. Kellet, B. Rigby, T. Vitova, B. Schacherl and S. Shaw. 2019. Silicate stabilization of colloidal UO2 produced by uranium metal corrosion. Journal of Nuclear Materials V 526.

U.S. Department of Energy (DOE). 1996. Title 40 CFR Part 191 Compliance Certification Application for the Waste Isolation Pilot Plant (October). 21 vols. Carlsbad Field Office, Carlsbad, NM. DOE/CAO-1996-2184.

EPA Evaluation of Response

The DOE response was partially adequate. A technical exchange was held December 2020, and additional investigation will be required for future PAs.

CC5-GEOCHEM-24 Inclusion of Calcite Precipitation in EQ3/6 Calculations

WIPP Compliance Recertification Application 2019 Appendix-GEOCHEM (Geochemistry)

EPA Question (from EPA Completeness Comment Package 5)

Please provide additional geochemical calculations to evaluate the impacts of calcite precipitation on WIPP brine and actinide solubilities. Use the minimum brine volume (1x) of both GWB and ERDA-6 brines with the following scenarios:

- *With calcite precipitation suppressed;*
- *With calcite precipitation until a calcite saturation index of 0.50 is achieved (if possible);*
- *With calcite precipitation until a calcite saturation index of 0.25 is achieved; and*
- *With calcite precipitation until a calcite saturation index of 0.0 is achieved.*

For these calculations:

- *Use anhydrite, halite, brucite, hydromagnesite5424, hibbingite, and cerussite as the initial starting minerals.*
- *Allow the most stable Am(III), Th(IV) and Np(V) solid phases to precipitate to equilibrium, along with phase 5, glauberite, borax, whewellite, and syngenite if these phases become saturated.*

Please include input and output files, spreadsheets, and any other material used to perform these calculations.

The approach used for the CRA-2019 DPA actinide solubility calculations (Domski and Sisk-Scott 2019) is described in detail by Domski (2019). There are noteworthy differences between the actinide solubility calculations in previous WIPP PAs and the CRA-2019 DPA, including: 1) dissolution of significant quantities of reactant phases and precipitation of relatively large amounts of more stable phases, 2) inclusion of lead and iron solids and aqueous species in the calculations, and 3) the assumption that calcite will precipitate to equilibrium from the WIPP brines under repository conditions.

Previous WIPP PAs (PAVT, PABC-2004, PABC-2009, and CRA-2014 PA) assumed the presence of the Salado minerals halite [NaCl(s)] and anhydrite [$CaSO_4$(s)] and the MgO hydration and carbonation products brucite [$Mg(OH)_2$(s)] and hydromagnesite [$Mg_5(CO_3)_4(OH)_2 \cdot 4H_2O$(s)], and equilibrated these minerals with brine containing Am(III), Th(IV), and Np(V). These FMT and EQ3/6 calculations included the dissolution and precipitation of fairly small amounts of solid phases and did not include calcite [$CaCO_3$(s)] precipitation. For the CRA-2019 DPA actinide solubility modeling calculations, Domski and Sisk-Scott (2019) included halite, anhydrite, brucite, and hydromagnesite as reactant phases, but also added litharge (PbO) and $Fe(OH)_2$-hex(s). Litharge and $Fe(OH)_2$-hex(s) were unstable under the modeled conditions, were completely dissolved, and large proportions of this lead and iron precipitated as cerussite [$PbCO_3$(s)] and hibbingite [$Fe_2Cl(OH)_3$(s)]. The choice of the starting mineral phases in the CRA-2019 DPA actinide solubility calculations raises some concerns.

One concern relates to the effects of the initial mineral phases on the amounts of water modeled in the calculations. In previous WIPP PA calculations, the initial reactant minerals were also present at equilibrium, with relatively small amounts of reaction required to achieve equilibrium solution concentrations. Consequently, changes in the mass of water in the calculations were fairly small. In the CRA-2019 DPA calculations, the unstable minerals litharge and $Fe(OH)_2$-hex(s) were included in the reactants and dissolved completely. These reactions resulted in the production of large quantities of water during conversion of Fe(OH)-hex(s) to hibbingite (Domski 2019, Table 12). The production of this large amount of water is not supported by the available WIPP data, because most of the iron in the repository will be initially present as metallic iron [Fe(s)], which will consume water via anoxic corrosion. Similarly, lead will initially be present in metallic form, and should consume water as it undergoes anoxic corrosion to form litharge.

Domski and Sisk-Scott (2019) assumed that all iron and lead would be present in the initial mineral phases as the corrosion products $Fe(OH)_2$-hex(s) and litharge and all of these materials are completely dissolved during the actinide solubility calculations. However, Domski (2019) did not present evidence demonstrating that the iron and lead corrosion rates would be sufficient to produce the amounts of oxidized iron and lead in the final reaction products.

Domski and Sisk-Scott (2019) assumed that all MgO would be hydrated in the form of brucite and hydromagnesite. This assumption introduces a large amount of water into the system, because initially, the MgO backfill will be present mainly as MgO that would consume water as it hydrates. MgO hydration rates are modeled in WIPP PA, but Domski (2019) does not demonstrate that MgO will hydrate quickly enough to provide the required amount of brucite for

reaction. Hydromagnesite is assumed in WIPP PA to form quickly and to control CO_2 fugacities in the repository. However, the availability of CO_2 to form hydromagnesite is a function of the CPR degradation rate, which is sampled in PA. Domski (2019) does not provide evidence that sufficient CO_2 will be generated so that the modeled large quantities of dissolved hydromagnesite will be available.

Actinide solubility calculations for the PAVT, PABC-2004, PABC-2009, and CRA-2014 PA were performed assuming that calcite would not precipitate from solution, with predicted calcite oversaturation after equilibration with Salado minerals, brucite, hydromagnesite, and actinide solid phases. In these previous PA calculations, phase 5 precipitation has been predicted from GWB brine, but not from ERDA-6 brine. The modeled absence of phase 5 precipitation from ERDA-6 brine in previous WIPP PAs is consistent with the results of WIPP MgO hydration and carbonation experiments (Snider and Xiong 2004, Deng et al. 2009).

CRA-2019 DPA EQ3/6 modeling calculations of dissolved Am(III), Th(IV), and Np(V) concentrations in GWB and ERDA-6 brines predict consumption of large amounts of water compared to the amounts predicted for CRA-2014 PA, particularly for ERDA-6 brine calculations (Domski 2019, Tables 8 and 9). Much of the water consumption predicted by the CRA-2019 DPA calculations is caused by brucite and hydromagnesite dissolution coupled with precipitation of calcite and phase 5. The CRA-2019 DPA actinide solubility calculations that predict extensive precipitation of phase 5 from ERDA-6 brine are inconsistent with the experimental data from WIPP MgO hydration experiments (Snider and Xiong 2004, Deng et al. 2009).

Oversaturation with respect to calcite is common in natural aqueous systems and is attributed to slow precipitation kinetics and inhibition of calcite precipitation by constituents that include magnesium, phosphate, sulfate, strontium, barium, lead, and organics (e.g., Katz et al. 1993, LeBron and Suarez 1996, Langmuir 1997, Zavarin and Doner 2005). Although calcite precipitation may occur from WIPP brines, it is likely that constituents in WIPP brines will cause some degree of calcite oversaturation to persist.

Although reaction-path calculations to examine the evolution of WIPP brines would be worthwhile, the actinide solubility calculations for the CRA-2019 DPA do not appear to accurately simulate expected WIPP processes and may not reliably indicate expected actinide solubilities. The defensibility of the actinide solubilities used in the CRA-2019 DPA would be greatly improved by conducting equilibrium solubility calculations similar to previous PA calculations. In these calculations, the starting materials should be the most stable phases, including halite, anhydrite, brucite, hydromagnesite, hibbingite, and cerussite. Because the extent of calcite precipitation is uncertain, a series of calculations should be performed to determine its effects. Re-evaluation of the actinide solubilities by assuming a reasonable amount of calcite oversaturation would more accurately simulate likely repository conditions and yield more defensible actinide solubilities.

Brush, L.H., Xiong, Y., Garner, J.W., Ismail, A., and Roselle, G.T. 2006. Consumption of carbon dioxide by precipitation of carbonate minerals resulting from dissolution of sulfate minerals in the Salado Formation in response to microbial sulfate reduction in the WIPP. Sandia National Laboratories, Carlsbad, New Mexico, ERMS 544785.

Deng, H., Xiong, Y., Nemer, M. and Johnsen, S. 2009. Experimental work conducted on MgO longterm hydration, 2008 milestone report. Sandia National Laboratories, Carlsbad, New Mexico, ERMS 551421.

Domski, P.S. 2019. Technical Aspects of the Baseline Solubility Model for the CRA-2019 PA. Sandia National Laboratories, Carlsbad, New Mexico, ERMS 571535.

Domski, P.S., and Sisk-Scott, C. 2019. Prediction of baseline actinide solubilities for CRA 2019 with an updated EQ3/6 Pitzer thermodynamic database, DATA0.FM4. Sandia National Laboratories, Carlsbad, New Mexico, ERMS 571178.

Katz, J.L., Reick, M.R., Herzog, R.E., and Parsiegla, K.I. 1993. Calcite growth inhibition by iron. Langmuir 9:1423-1430.

Langmuir, D. 1997. Aqueous Environmental Chemistry. Prentice Hall, Upper Saddle River, New Jersey.

Lebron, I., and Suarez, D.L. 1996. Calcite nucleation and precipitation kinetics as affected by dissolved organic matter at 25°C and pH > 7.5. Geochimica et Cosmochimica Acta, 60:2765-2776.

Snider, A.C, and Xiong, Y. 2004. Continuing investigations of the hydration and carbonation of Premier Chemical MgO. Sandia National Laboratories, Carlsbad, New Mexico, ERMS 537188.

Xiong, Y. 2006. Incorporation of amorphous calcium carbonate into the EQ3/6 HMY database and its modified version HML. Sandia National Laboratories, Carlsbad, New Mexico, ERMS 544629.

Zavarin, M., and Doner, H.E. 2005. Effect of P and Se(IV) on calcite precipitation inhibition. Soil Science 17:612-623.

DOE Response (from DOE Response Package 8)

The U.S. Department of Energy (DOE) does not consider the calcite saturation question relevant to completeness as this information has been provided to U.S. Environmental Protection Agency (EPA) previously (Domski, 2019). However, the DOE will re-summarize the end-member calcite saturation data necessary to derive the relationships of interest to the EPA. Additionally, DOE will demonstrate that EPA's request of changing the reactants does not influence the final equilibrium chemistry of the system.

The effect of calcite saturation and precipitation and its impact on actinide solubility was thoroughly investigated in Domski (2019) and additional EQ3/6 simulations are unnecessary to address this aspect of the CC5-GEOCHEM-24 comment. The EPA requested in comment CC5-GEOCHEM-24 that the DOE examine actinide solubility in Generic Weep Brine (GWB) and ERDA-6 at set values of the calcite saturation index (SI), the values of calcite SI that were of interest to the EPA included, SI = 0.0, 0.25, 0.50, and a case where calcite is suppressed. Domski (2019) has provided end-member results for the cases where the calcite saturation index is set to zero, and for the case where calcite is suppressed. These results can be found in columns 3 and 4 of Tables 8 and 9 in Domski (2019). For model scenarios with calcite suppression, saturation indices are

reported at equilibrium in output files *gwb2019.6o* and *erda2019.6o*[1] for GWB and Energy Research and Development Administration (ERDA) brines, respectively (see column 3 in Tables 8 and 9 from Domski (2019) for the file names). The final calcite equilibrium saturation indices were 1.70 and 1.71 for GWB and ERDA-6, respectively. Thus, these SI values correspond to the chemical data in column 3 of Tables 8 and 9 of Domski (2019), and the equilibrium calcite, SI = 0.0, corresponds to column 4 of Tables 8 and 9 of Domski (2019). With this information it is a simple matter to linear interpolate conservative actinide concentrations for calcite SI values of 0.25 and 0.50. Given that the range of concentrations for Am(+III), Th(+IV), and Np(+V) over this saturation index range is relatively small, the error that may be introduced by assuming a linear relationship between concentration and saturation index is also small.

The EPA also requested that hibbingite ($Fe_2Cl(OH)_3$) and cerussite ($PbCO_3$) be used as reactants, stating that these are the more "stable" reactant phases, rather than those chosen by Domski and Sisk-Scott (2019), $Fe(OH)_2$-Hex ($Fe(OH)_2$) and litharge (PbO), to represent iron and lead, respectively. Domski and Sisk-Scott (2019) and Domski (2019) demonstrated that $Fe(OH)_2$-Hex and litharge react on a mole to mole basis to form hibbingite and cerussite. Because of the mole per mole conversion of the iron and lead reactant to product phases, the inversion of the product phases for the reactant phases in the EQ6 simulations will not change the final equilibrium chemistry of the modeled system.

_____

[1] These EQ6 output files are included in Enclosure 4 and are also found archived on the Sandia National Laboratory (SNL) server at the following location: /cvs/CVSLIB/WIPP_EXTERNAL/CRA19_comments.

To provide objective evidence that using the "stable" phases for iron and lead as reactants have no impact on the equilibrium chemistry, the EQ6 input files for the minimum (1x) volume cases for GWB (*gwb_1x.6i*) and ERDA-6 (*erda_1x.6i*) brines were edited and the iron reactant was changed to hibbingite and the lead reactant changed to cerussite. The new files are *gwb_hc.6i* and *erda_hc.6i* for GWB and ERDA-6, respectively. The EQ6 input files were executed using the DATA0.FM4 database and the equilibrium results, i.e., the final step in the reaction path, were extracted, using the *GetEQdata.xls* macro into the spreadsheet *Compare_Pb&Fe_reactants.xlsx*[2]. The results of these simulations are shown in Tables GEOCHEM-24-1 and GEOCHEM-24-2 for GWB and ERDA-6, respectively. Note that the data
shown in Tables GEOCHEM-24-1 and GEOCHEM-24-2 originates from the final step in the EQ6 reaction path which represents the equilibrium conditions of the modeled system.

Contrary to the EPA's claim in CC5-GEOCHEM-24, "The defensibility of the actinide solubilities used in the Compliance Recertification Application (CRA)-2019 Deferred Performance Assessment (DPA) would be greatly improved by conducting equilibrium solubility calculations similar to previous PA calculations", reaction-path modeling does indeed provide the equilibrium chemistry and mineral assemblage of the modeled system. Equilibrium in a reaction path simulation is achieved when the system chemistry ceases to change with the addition of reactants, it is at this point where the EQ6 code terminates the simulation and records the final equilibrium state of the system. Reaction-path modeling using EQ6 has been in effect for the WIPP baseline actinide solubility calculations since CRA-2014 at which time the EQ3/6 code package replaced the Fracture-Matrix Transport (FMT) (Babb and Novak, 1995, 1997 and addenda; Wang, 1998) code for these calculations.

Inspection of Tables GEOCHEM-24-1 and GEOCHEM-24-2 reveals that the final equilibrium chemistry for both brines are identical regardless of whether the Domski and Sisk-Scott (2019) phases, or the EPA suggested iron and lead phases are used as a reactant.

---

[2] The EQ6 input and output files used to address this comment as well as processed output contained in the Excel file, and the Excel macro, are included in Enclosure 4 for EPA, and can be found archived on the SNL server at the following location: /nfs/data/CVSLIB/WIPP_EXTERNAL/ap153_solubility tech memo.

Table GEOCHEM-24-1. Comparison of GWB Equilibrium Chemistry Using the EPA Suggested Iron and Lead Reactants

Filename[1]	gwb_1x.6o	gwb_hc.6o
Fe and Pb Reactants	$Fe(OH)_2$-Hex, litharge	Hibbingite, cerussite
Parameter		
Pitzer pH	8.82	8.82
pcH	9.54	9.54
a(w)	0.732	0.732
(I)	7.56	7.56
Mass Solvent (kg)	0.609	0.609
(m)/(M) (L/kg.H_2O)	1.16	1.16
Concentration	**Molality**	**Molality**
Am (m)	1.88E-07	1.88E-07
B (m)	2.60E-01	2.60E-01
Br (m)	4.37E-02	4.37E-02
Ca (m)	1.26E-02	1.26E-02
Cl (m)	6.26E+00	6.26E+00
Fe (m)	3.03E-05	3.03E-05
K (m)	7.67E-01	7.67E-01

Filename[1]	gwb_1x.6o	gwb_hc.6o
Mg (m)	4.03E-01	4.03E-01
Na (m)	5.44E+00	5.44E+00
Np (m) [2]	4.66E-07	4.66E-07
Pb (m)	2.20E-02	2.20E-02
S (m)	2.68E-01	2.68E-01
Th (m)	6.31E-08	6.31E-08
HCO_3^- (m)	2.89E-04	2.89E-04
CO_2(g) Fugacity	2.02E-06	2.02E-06
Mineral Phase	**Saturation Index**	**Saturation Index**
$Am(OH)_3$(s)	0.00	0.00
Anhydrite	0.00	0.00
Brucite	0.00	0.00
Calcite	0.00	0.00
Cerussite(cr)	0.00	0.00
Glauberite	0.00	0.00
Halite	0.00	0.00
Hydromagnesite5424	0.00	0.00
KNpO2CO3	0.00	0.00
$Mg_3Cl(OH)_5.4H_2O$ (Phase 5)	0.00	0.00
Hibbingite	0.00	0.00
Syngenite	-0.261	-0.261
ThO_2(am)	0.00	0.00
Whewellite	0.00	0.00

[1] *gwb_1x.6o* is the EQ6 output file from Domski and Sisk-Scott (2019), *gwb_hc.6o* is the EQ6 output file using hibbingite and cerussite as reactants.

[2] There was a difference in the Np molality for GWB in the 12th decimal place, however, only 3 significant digits are reported to performance assessment which would go to the 9th decimal place for Np, thus, the difference is insignificant.

Table GEOCHEM-24-2. Comparison of ERDA-6 Equilibrium Chemistry Using the EPA Suggested Iron and Lead Reactants

Filename[1]	erda_1x.6o	erda_hc.6o
Fe and Pb Reactants	$Fe(OH)_2$-Hex, litharge	Hibbingite, cerussite
Parameter		
Pitzer pH	8.82	8.82
pcH	9.52	9.52
a(w)	0.732	0.732
(I)	7.50	7.50
Mass Solvent (kg)	0.168	0.168
(m)/molarity (L/kg.H_2O)	1.16	1.16
Concentration	**Molality**	**Molality**

Filename[1]	erda_1x.6o	erda_hc.6o
Am (m)	2.06E-07	2.06E-07
B (m)	3.26E-01	3.26E-01
Br (m)	6.56E-02	6.56E-02
Ca (m)	1.48E-02	1.48E-02
Cl (m)	6.04E+00	6.04E+00
Fe (m)	3.09E-05	3.09E-05
K (m)	5.78E-01	5.78E-01
Mg (m)	5.04E-01	5.04E-01
Na (m)	5.40E+00	5.40E+00
Np (m)	1.39E-06	1.39E-06
Pb (m)	2.18E-02	2.18E-02
S (m)	2.59E-01	2.59E-01
Th (m)	6.30E-08	6.30E-08
HCO_3- (m)	2.89E-04	2.89E-04
CO_2(g) Fugacity	2.02E-06	2.02E-06
Mineral Phase	**Saturation Index**	**Saturation Index**
$Am(OH)_3$(s)	0.00	0.00
Anhydrite	0.00	0.00
Borax	0.00	0.00
Brucite	0.00	0.00
Calcite	0.00	0.00
Cerussite(cr)	0.00	0.00
Glauberite	0.00	0.00
Halite	0.00	0.00
Hydromagnesite5424	0.00	0.00
$KNpO_2CO_3$	0.00	0.00
$Mg_3Cl(OH)_5.4H_2O$ (Phase 5)	0.00	0.00
Hibbingite	0.00	0.00
Syngenite	-0.493	-0.493
ThO_2(am)	0.00	0.00
Whewellite	0.00	0.00

[1] *erda_1x.6o* is the EQ6 output file from Domski and Sisk-Scott (2019), *erda_hc.6o* is the EQ6 output file using hibbingite and cerussite as reactants.

The mineral phase data provided in Tables GEOCHEM-24-1 and GEOCHEM-24-2 shows the equilibrium assemblage of phases present in each reacted brine system at equilibrium.

The reactant phases halite, anhydrite, brucite, hydromagnesite, and for iron and lead, either Fe(OH)2-Hex and litharge, or hibbingite and cerussite were all present at their scaled inventory masses at the start of the EQ6 simulations. The results shown in the above tables reveal that all the reactants are in equilibrium with the solutions (SI = 0.0), and that additional product phases are also at equilibrium, these include the actinide solubility limiting phases: borax, glauberite, phase 5, and whewellite. The lead and iron reactant/product phases hibbingite and cerussite are also in equilibrium with the solution. In the case where hibbingite and cerussite were reactants they did not dissolve during the reaction path but maintained equilibrium with the solution throughout the reaction path. Note, the EPA instructed that the mineral phases: phase 5, glauberite, borax, whewellite, and syngenite, be allowed to precipitate in the simulations, and

with the exception of syngenite all of them did form. Syngenite maintained undersaturation (SI<0) throughout the GWB and ERDA-6 reaction path simulations.

It remains the DOE's position that no changes to the solubility calculations raised in this comment are necessary for the CRA-2019 DPA.

References

Babb, S.C., and C.F. Novak. 1995. "WIPP PA User's Manual for FMT, Version 2.0." Albuquerque, NM: Sandia National Laboratories. ERMS 228119.

Babb, S.C., and C.F. Novak. 1997 and addenda. "User's Manual for FMT Version 2.3: A Computer Code Employing the Pitzer Activity Coefficient Formalism for Calculating Thermodynamic Equilibrium in Geochemical Systems to High Electrolyte Concentrations." Albuquerque, NM: Sandia National Laboratories. ERMS 243037.

Domski, P.S. 2019. Technical Aspects of the Baseline Solubility Model for the CRA-2019 PA. Sandia National Laboratories, Carlsbad, New Mexico, ERMS 571535.

Domski, P.S., and C. Sisk-Scott. 2019. Prediction of baseline actinide solubilities for CRA 2019 with an updated EQ3/6 Pitzer thermodynamic database, DATA0.FM4. Sandia National Laboratories, Carlsbad, New Mexico, ERMS 571178.

Wang, Y. 1998. "WIPP PA Validation Document for FMT (Version 2.4), Document Version 2.4." Carlsbad, NM: Sandia National Laboratories. ERMS 251587.

EPA Evaluation of Response

The DOE response was satisfactory; a follow up call was held with DOE in Feb. 2021.

CC5-GEOCHEM-25 Effects of Polyhalite on Modeled Brine Chemistry

WIPP Compliance Recertification Application 2019 Appendix-GEOCHEM (Geochemistry)

EPA Question (from EPA Completeness Comment Package 5)

Please evaluate whether including polyhalite [$K_2Ca_2Mg(SO_4)_4 \cdot 2H_2O(s)$] in the initial Salado minerals in the actinide solubility calculations significantly affects the modeling results. In the EQ3/6 calculations, please assume that the Salado mineralogy is 90% halite, 7.5% anhydrite, and 2.5% polyhalite. Please provide input and output files of all EQ3/6 calculations from this evaluation.

Polyhalite is a common mineral in the Salado Formation (Stein 1985, Brush 1990, Lambert 1992), and polyhalite dissolution may affect the dissolution and precipitation of other calcium-, sulfate-, and magnesium-bearing minerals. Polyhalite solubility data has been included in the FMT and EQ3/6 databases used for PA calculations, and Brush (1990) stated that polyhalite would be included in WIPP actinide solubility calculations. However, although polyhalite has been included in all WIPP PA FMT and EQ3/6 databases, it has not been included in the initial Salado minerals for actinide solubility calculations. Inclusion of this Salado mineral in the geochemical modeling

calculations will make the calculations more representative of likely repository conditions and improve the defensibility of the modeled actinide solubilities.

Brush, L.H. 1990. Test plan for laboratory and modeling studies of repository and radionuclide chemistry for the Waste Isolation Pilot Plant. Sandia National Laboratories, Carlsbad, New Mexico, ERMS 226015.

Lambert, S.J. 1992. Geochemistry of the Waste Isolation Pilot Plant (WIPP) site, southeastern New Mexico, USA. Applied Geochemistry 7:513-531.

Stein, C.L. 1985. Mineralogy in the Waste Isolation Pilot Plant (WIPP), Southeastern New Mexico: A preliminary investigation. Sandia National Laboratories, Albuquerque, New Mexico, SAND-85-0321.

DOE Response (from DOE Response Package 8)

It is the DOE's position that this EPA comment is not relevant to completeness. Additional EQ3/6 calculations are unnecessary to address CC5-GEOCHEM-25 because polyhalite is not part of the approved Waste Isolation Pilot Plant (WIPP) Chemical Conditions conceptual model, and is not included in the current analysis plan (Brush et al., 2012) used for the CRA-2019 DPA calculations.

In CC5-GEOCHEM-25 the EPA references a 30-year old document, Brush (1990), as stating that polyhalite would be included in the WIPP actinide solubility calculations, however, this document (Brush, 1990) was superseded long before the CRA-2019 DPA calculations were performed. The CRA-2019 DPA actinide solubility calculations were performed under the test plan AP-153, rev 1 (Brush et al., 2012) which only specifies halite and anhydrite as reactants representing the Salado Formation.

From Brush et al., (2012):

> "…as we will assume for this analysis that the Salado contains 90 wt % halite and 10 wt % anhydrite because the conceptual models for WIPP near-field chemistry include only halite and anhydrite (SCA, 2008)."

Polyhalite has not been included in the actinide solubility model for WIPP performance assessment from the Compliance Certification Application (CCA) onward. Edwards (2009) provides the "Verification of the Waste Isolation Pilot Plant Chemistry Conceptual Models", where the adequacy of the WIPP Chemical Conditions conceptual model was evaluated, and confirms, on page 2-11 in the second bullet, that "Equilibrium is assumed between the repository brine, waste, and the Salado minerals, halite, anhydrite, brucite, and magnesite.". Furthermore, minor changes as outlined on pages 2-12 and 2-13, "…were the only required modifications to DOE's CCA Chemical Conditions conceptual model.", and these changes did not include the addition of polyhalite to the model.

References

Brush, L.H. 1990. Test plan for laboratory and modeling studies of repository and radionuclide chemistry for the Waste Isolation Pilot Plant. Sandia National Laboratories, Carlsbad, New Mexico, ERMS 226015.

Brush, L.H., P.S. Domski, and Y.L. Xiong. 2012a. "Analysis Plan for WIPP Near-Field Geochemical Process Modeling." AP-153, Rev. 1, February 8, 2012. Carlsbad, NM: Sandia National Laboratories. ERMS 556960.

Edwards, J. 2009. Untitled letter with attachment to D.C. Moody concluding that the WIPP near-field chemical conceptual models have had only minor changes since the CCA and are still adequate for use in PA. February 3, 2009. Washington, DC: U.S. Environmental Protection Agency Office of Air and Radiation. ERMS# 563940

SCA (S. Cohen and Associates). 2008. "Verification of the Waste Isolation Pilot Plant Chemistry Conceptual Models, Final Report." September 19, 2008. Vienna, VA: S. Cohen and Associates.

EPA Evaluation of Response

The DOE response was satisfactory and follow up call was held with DOE in Feb. 2021.

CC5-GEOCHEM-26 Effects of Cements on Brine Chemistry

WIPP Compliance Recertification Application 2019 Appendix-GEOCHEM (Geochemistry)

EPA Question (from EPA Completeness Comment Package 5)

Please evaluate whether including portlandite [$Ca(OH)_2(s)$] in the actinide solubility calculations affects the predicted brine chemistry and actinide solubility modeling results. Please provide input and output files of all EQ3/6 calculations from this evaluation.

> *Portlandite is a component of cements included in WIPP waste and in repository seals. Previous evaluations of the likely effects of portlandite on brine pH were based on calculations that compared the amounts of magnesium in brine and polyhalite to the potential range of portlandite in the cements (EPA 2017, Section 6.4.3.2). Because the likely effects of portlandite on brine chemistry can be addressed using the EQ3/6 code and database, these effects should be calculated directly to develop more defensible actinide solubilities.*
>
> *EPA (U.S. Environmental Protection Agency) 2017. Evaluation of the Compliance Recertification Actinide Source Term, Gas Generation, Backfill Efficacy, Water Balance and Culebra Dolomite Distribution Coefficient Values. Docket No. EPA-HQ-OAR-2014-0609. U.S. Environmental Protection Agency. Washington, DC.*

DOE Response (from DOE Response Package 8)

> It is the DOE's position that evaluating the effect of cements on brine chemistry is not a completeness issue. Additional EQ3/6 simulations are unnecessary to address CC5-GEOCHEM-26 because cementitious materials are not considered for the purposes of actinide solubility or performance assessment. Appendix SOTERM (2019) Section 6.2 it is stated:

MgO will be present in sufficient quantity to achieve its design goal of buffering the pH and carbonate levels should brine inundation occur. Additionally, there is a sufficient MgO to cement ratio (>5) to mitigate the effects of cement on pH (Kienzler et al. 2016).

Using the inventory data from Van Soest (2018), which was used for the CRA-2019 DPA, the ratio of MgO to cement (by mass) is 5:1. If we consider that Portland cement contains 60-67% CaO by mass and convert to moles, the ratio of MgO to CaO increases to between 11.8 for 60% CaO and 10.5 for 67% CaO. In other words, the reactive constituent of the cement, the $Ca(OH)_2$, is not present in quantities that warrant concern for actinide solubility and, therefore, PA purposes. The calculation of the various ratios can be found in the spreadsheet: *CC5-GEOCHEM-26_Scaling of Solids_2019.xlsx* included in Enclosure 4 and can be found archived on the SNL server at the following location: /cvs/CVSLIB/WIPP_EXTERNAL/CRA19_comments

References

Kienzler, B., C. Borkel, V. Metz, and M. Schlieker. 2016. Lon-Term Interactions of Full-Scale Cemented Waste Simulates with Salt Brines. Karlsruhe Institute of Technology, Karlsruhe, Germany. KIT Scientific Reports #7721.

Van Soest, G. 2018. Performance Assessment Inventory Report – 2018, INV-PA-18, Rev. 0. LA36 UR-18-31882. Carlsbad, NM: Los Alamos National Laboratory – Carlsbad Operations.

EPA Evaluation of Response

The DOE response was satisfactory and a follow up call was held with DOE in Feb. 2021.

CC5-GEOCHEM-27 Incomplete Documentation Related to Pitzer Parameter Errors in DATA0.FM4

WIPP Compliance Recertification Application 2019 Appendix-GEOCHEM (Geochemistry)

EPA Question (from EPA Completeness Comment Package 5)

Please address the following questions regarding the parameter errors in the DATA0.FM4 database that were documented in Parameter Problem Reports 2019-004 through 2019-013 (Domski 2019a – 2019j):

GEOCHEM-27a.

Please provide the +III actinide solubilities in GWB and ERDA-6 brines that were calculated using the corrected Pitzer parameters for all five brine volumes used in PA.

DOE Response (from DOE Response Package 8)

The An(+III) solubilities as calculated in ERDA-6 and GWB brines using the updated Pitzer parameters are included in the following Excel spreadsheet and document, respectively.

F5F_Concentrations.xlsx

Domski, P.S. 2020. *Correction of the α_1 terms of three binary Pitzer parameter blocks in DATA0.FM4, PPR 2019-004 through 2019-013*. Sandia National Laboratories, Carlsbad, New Mexico. ERMS# 572559.

These files are included in Enclosure 4.

EPA Question

GEOCHEM-27b.

Please provide documentation describing the revised PA calculations performed to establish that the corrected +III actinide solubilities did not significantly affect PA results (Domski 2019a – 2019j). As part of this documentation, please include a copy of the following report:

Domski, P.H. 2020. Correction of the α_1 terms of three binary Pitzer parameter blocks in DATA0.FM4, PPR 2019-004 through 2019-013. Sandia National Laboratories, Carlsbad, New Mexico.

DOE Response

The document describing the revised PA calculations performed to establish the corrected An(+III) actinide solubilities and their impact on performance assessment may be found in the following document.

Kim, S., P. Domski, and L. Feng. 2020. *Impact Analysis of Corrected Actinide (III) Baseline Solubility Parameters on Performance Assessments.* Sandia National Laboratories, Carlsbad, New Mexico. ERMS# 572507.

The above document is included in Enclosure 4, as is the following document:

Domski, P.S. 2020. *Correction of the α_1 terms of three binary Pitzer parameter blocks in DATA0.FM4, PPR 2019-004 through 2019-013*. Sandia National Laboratories, Carlsbad, New Mexico. ERMS# 572559.

EPA Question

GEOCHEM-27c.

Please provide a copy of Parameter Problem Report 2019-003, which is referenced in Domski (2019a – 2019j).

DOE Response

Parameter Problem Report 2019-003 (Domski, 2019a), and its accompanying memorandum (Domski, 2019b) are included in Enclosure 4.

References

Domski, P.S. 2019a. Parameter Problem Report (PPR) 2019-003. Sandia National Laboratories, Carlsbad, New Mexico. ERMS# 572265.

Domski, P.S. 2019b. Correction of a Binary Pitzer Parameter in DATA0.FM4, PPR 2019-003. Sandia National Laboratories, Carlsbad, New Mexico. ERMS# 572172.

EPA Question

GEOCHEM-27d.

Please note the typographical errors in Domski (2019a – 2019j). In these documents, one of the ion pairs is listed as Ca^{2+}/$MgEDTA^{2-}$, but the correct ion pair is Mg^{2+}/$CaEDTA^{2-}$, based on the data in DATA0.FM4 and supporting documentation (Domski 2018).

Incorrect α_1 Pitzer parameter values were included in the DATA0.FM4 database for the Ca^{2+}/$EDTA^{4}$, Mg^{2+}/$MgEDTA^{2-}$ and Mg^{2+}/$CaEDTA^{2-}$ ion pairs. For these three ion pairs, an incorrect α_1 value of 2.0 was entered in the database instead of the correct value of 1.4. Domski (2019a – 2019j) stated that these incorrect Pitzer parameters affected the parameter values for +III actinide solubilities in GWB and ERDA-6 brines used in PA. However, the recalculated +III actinide solubilities were not provided, so the magnitude of the effects of the incorrect Pitzer parameters on modeled +III actinide solubilities cannot be determined based on the available information.

Domski (2019a – 2019j) stated that PA modeling with the updated +III actinide solubility parameters resulted in no impact to the CCDFGF plots of total +III actinides released from the repository. Review of the documentation of the modeling calculations and results is required for the Agency's evaluation of the adequacy and completeness of this assessment. Domski (2019a – 2019j) notes that issues related to the Pitzer parameters were discovered during an evaluation triggered by Parameter Problem Report PPR 2019-003, but a copy of this document was not provided.

A typographical error in one of the ion pairs was identified in Domski (2019a – 2019j), with Ca^{2+}/$MgEDTA^{2-}$ identified instead of the correct ion pair Mg^{2+}/$CaEDTA^{2-}$. This error is unimportant to PA, because the correct ion pair is included in the DATA0.FM4 database that was used in the CRA-2019 DPA.

Domski, P.S. 2018. Memo on the estimation of Pitzer parameters for the Mg^{2+}/$CaEDTA^{2-}$, Mg^{2+}/$MgEDTA^{2}$, and Ca^{2+}/$EDTA^{4-}$ pairs. Sandia National Laboratories, Carlsbad, New Mexico. ERMS 570855.

Domski, P.S. 2019a. Parameter Problem Report (PPR) 2019-1 004. Sandia National Laboratories, Carlsbad, New Mexico. ERMS 572492.

Domski, P.S. 2019b. Parameter Problem Report (PPR) 2019-005. Sandia National Laboratories, Carlsbad, New Mexico. ERMS 572493.

Domski, P.S. 2019c. Parameter Problem Report (PPR) 2019-006. Sandia National Laboratories, Carlsbad, New Mexico. ERMS 572494.

Domski, P.S. 2019d. Parameter Problem Report (PPR) 2019-007. Sandia National Laboratories, Carlsbad, New Mexico. ERMS 572495.

Domski, P.S. 2019e. Parameter Problem Report (PPR) 2019-008. Sandia National Laboratories, Carlsbad, New Mexico. ERMS 572496.

Domski, P.S. 2019f. Parameter Problem Report (PPR) 2019-009. Sandia National Laboratories, Carlsbad, New Mexico. ERMS 572497.

Domski, P.S. 2019g. Parameter Problem Report (PPR) 2019-010. Sandia National Laboratories, Carlsbad, New Mexico. ERMS 572498.

Domski, P.S. 2019h. Parameter Problem Report (PPR) 2019-011. Sandia National Laboratories, Carlsbad, New Mexico. ERMS 572499.

Domski, P.S. 2019i. Parameter Problem Report (PPR) 2019-012. Sandia National Laboratories, Carlsbad, New Mexico. ERMS 572500.

Domski, P.S. 2019j. Parameter Problem Report (PPR) 2019-013. Sandia National Laboratories, Carlsbad, New Mexico. ERMS 572501.

DOE Response

A memorandum of correction was written (Domski, 2020) and was included with the records package for Parameter Problem reports 2019-004 through 2019-013. This memo of correction notes the typographical error noted by EPA in CC5-GEOCHEM-27d. The memo is included in the Enclosure 4.

Reference

Domski, P.S. 2020. Memorandum of Correction for Parameter Problem Reports (PPR) 2019-004–2019-013. Sandia National Laboratories, Carlsbad, New Mexico. ERMS# 574281.

EPA Evaluation of Response

The DOE response was satisfactory, and the requested data provided.

CC6-GEOCHEM-28 Iron-Sulfate Pitzer Parameters and Solid Phases Not Included in DATA0.FM4

WIPP Compliance Recertification Application 2019 Appendix-GEOCHEM (Geochemistry)

EPA Question (from EPA Completeness Comment Package 6)

Please explain the absence from DATA0.FM4 of the iron-sulfate Pitzer parameters and iron-sulfate solid solubilities identified for inclusion in the revised EQ3/6 database by Jang (2017). Please address the

potential effects of omitting these parameters and solid solubilities on the actinide solubility calculations for the CRA-2019 DPA.

Kim et al. (2017) developed an internally consistent set of solid solubility constants, aqueous speciation stability constants, and Pitzer ion interaction parameters for ferrous iron in sodium chloride, sodium sulfate, and sodium carbonate solutions based on WIPP experimental data (Nemer et al. 2011). Jang (2017) identified solids, aqueous species, and Pitzer parameters for inclusion in the WIPP EQ3/6 database using the results of Kim et al. (2017). Some of these data are absent from DATA0.FM4 (Domski 2019):

- *α and β Pitzer parameters for Fe^{2+}/SO_4^{2-} and Fe^{2+}/HSO_4 interactions*
- *ϑ Pitzer parameters for H^+/ Fe^{2+} and SO_4^{2-}/HSO_4^- interactions*
- *ψ parameters for $Fe^{2+}/Na^+/SO_4^{2-}$, $Fe^{2+}/K^+/SO_4^{2-}$, and $Fe^{2+}/H^+/SO_4^{2-}$ interactions*
- *the stability constant for the $Fe(OH)_4^{2-}$ aqueous species*
- *solubility constants for the iron sulfate solids $FeSO_4$(s), $FeSO_4 \cdot 7H_2O$(s), $FeSO_4 \cdot H_2O$(s), and $FeSO_4 \cdot 4H_2O$(s)*

DOE did not provide justification for omitting these data.

The Pitzer parameters for the ferrous iron interactions with sulfate are part of the internally consistent data set developed by Kim et al. (2017). Sulfate is an important constituent in WIPP brines and in Salado minerals such as anhydrite. Consequently, the reasons for excluding the ferrous iron-sulfate Pitzer interaction parameters from the DATA0.FM4 database should be provided. In addition, the expected effects of the missing parameters on the actinide solubility calculations should be evaluated. Alternatively, the database should be updated to include these values along with an analysis of how these data impact the dissolved actinide solubility calculations.

Domski, P.S. 2019. An update to the EQ3/6 Pitzer thermodynamic database DATA0.FM1 with the creation of DATA0.FM4. Sandia National Laboratories, Carlsbad, New Mexico, ERMS 571052.

Jang, J. J. 2017. Solubility model for the Fe^{+2} - Mg^{+2} - Na^+ - Ca^{+2} - H^+ - Cl^- - oxalate^{-2} - EDTA^{-4} citrate^{-3} – H_2O systems. Sandia National Laboratories, Carlsbad, New Mexico, ERMS 568758.

Kim, S., C. Marrs, M. Nemer, and J-H Jang. 2017. Solubility model for ferrous iron hydroxide, hibbingite, siderite, and chukanovite in high saline solutions of sodium chloride, sodium sulfate, and sodium carbonate. ACS Earth Space Chem. 1:647−663.

Nemer, M.B., Y. Xiong, A.E. Ismail, and J.-H. Jang. 2011. Solubility of $Fe_2(OH)_3Cl$ (pure-iron endmember of hibbingite) in NaCl and Na_2SO_4 brines. Chemical Geology 280:26-32.

DOE Response (from DOE Response Package 10)

The absence of the iron-sulfate system in the DATA0.FM4 thermodynamic database was an unintentional oversight. This system is included in Kim et al. (2017) and should have been included in DATA0.FM4. Future revisions of the database will include this chemical system. This has been added to Enclosure 2, CRA-2019 Errata Tracking.

Had the iron-sulfate system been included in DATA0.FM4 for use in the Compliance Recertification Application (CRA)-2019 Deferred Performance Assessment (DPA) actinide solubility calculations, it would have had a negligible effect on the calculated actinide solubility values. Sulfate only forms weak complexes with the +III and +IV actinides included in DATA0.FM4, and iron does not form complexes with the actinides.

EPA Evaluation of Response

The DOE response was adequate. The omitted data should be added to the database for future PAs.

CC6-GEOCHEM-29 Adequacy of Lead Parameterization in DATA0.FM4

WIPP Compliance Recertification Application 2019 Appendix-GEOCHEM (Geochemistry)

EPA Question (from EPA Completeness Comment Package 6)

Please justify the absence of important lead data and calculations in the FM4 database. If the data are available, the following information related to the lead parameterization in DATA0.FM4 must be included before lead is included in actinide solubility calculations for WIPP PA:

- *Solid phases such as laurionite [Pb(OH)Cl(s)], hydrocerussite [$Pb_3(CO_3)_2(OH)_2$(s)], mendipite [$Pb_3O_2Cl_2$(s)], cotunnite [$PbCl_2$(s)], and galena [PbS(s)]*
- *Pitzer ion-interaction parameters for lead aqueous species*
- *Lead model verification by comparison of model-predicted concentrations to experimentally measured data*

The DATA0.FM4 database (Domski 2019) includes the solid phases litharge [PbO(s)], cerussite [$PbCO_3$(s)], phosgenite [$Pb_2CO_3Cl_2$(s)], and anglesite [$PbSO_4$], which can form from oxidation of metallic lead. Additional lead solid phases have been reported to form during corrosion of lead objects in marine environments, including laurionite [Pb(OH)Cl(s)], hydrocerussite [$Pb_3(CO_3)_2(OH)_2$(s)], mendipite [$Pb_3O_2Cl_2$(s)], and cotunnite [$PbCl_2$(s)], with galena [PbS(s)] formation reported under anaerobic conditions (MacLeod 1991). Felmy et al. (2000) also observed precipitation of $KCl{\cdot}2PbCl_2$(cr) and caracolite [$NaCl{\cdot}Na_2SO_4{\cdot}$ 2$PbSO_4$(cr)] from experiments with carbonate-free Salado (G-Seep) and Castile (ERDA-6) brines. DOE should address the potential formation of these solids and should include solubility data for potentially important solid phases in the EQ3/6 database.

The lead solid and aqueous species data in DATA0.FM4 were obtained from Powell et al. (2009). Powell et al. (2009) reviewed lead aqueous speciation and solids solubility data for the inorganic ligands OH^-, Cl^-, CO_3^{2-}, SO_4^{2-}, and PO_4^{3-}. This review included evaluation of the reliability of the stability constants and related publications, correlation of the data with ionic strength, use of the specific ion interaction theory to extrapolate the stability constants to an ionic strength of zero, and recommendation of aqueous speciation and solubility constants at 25°C and zero ionic strength. However, the data set has not been validated by comparing modeled aqueous speciation and solids solubility data to WIPP-relevant experimental aqueous speciation and solids solubility data.

The lead model included in DATA0.FM4 does not include Pitzer ion interaction parameters. Use of the Pitzer activity coefficient model to predict the solubilities of actinides in highly concentrated WIPP brines

is an important part of the actinide source term conceptual model (Wilson et al., 1996, SCA 2008). Considerable uncertainty is associated with the calculated aqueous lead concentrations and solid phase stabilities because the Pitzer model was not used. The extent of the uncertainties cannot be assessed because the results of validation calculations with the lead data in DATA0.FM4 were not provided.

Because lead aqueous speciation in DATA0.FM4 currently does not include complexation with organic ligands, including lead solids and aqueous species may not directly affect the results of the actinide solubility calculations. However, if large quantities of lead solids react, as modeled in the CRA-2019 DPA actinide solubility calculations, large amounts of water in the brines may be consumed or produced, influencing concentrations of organic ligands and other factors such as pH, which can affect actinide solubilities (see completeness comment CC5-GEOCHEM-24).

Domski, P.S. 2019. An update to the EQ3/6 Pitzer thermodynamic database DATA0.FM1 with the creation of DATA0.FM4. Sandia National Laboratories, Carlsbad, New Mexico, ERMS 571052.

Felmy, A. R., L. M. Onishi, N. S. Foster, J. R. Rustad, D. Rai, M. J. Mason. 2000. An aqueous thermodynamic model for the Pb_{2+} - Na_{+} - K_{+} - Ca_{2+} - Mg_{2+} - H_{+} - Cl_{-} - SO_{42-} - H_2O system to high concentration: Application to WIPP brines. Geochimica et Cosmochimica Acta, Vol. 64: 3615-3628.

MacLeod, I. 1991. Identification of corrosion products on non-ferrous metal artifacts recovered from shipwrecks. Studies in Conservation, 36:222-234.

Powell, K.J., P.L. Brown, R.H. Byrne, T. Gajda, G. Hefter, A.-K. Leuz, S. Sjöberg, and H. Wanner. 2009. Chemical speciation of environmentally significant metals with inorganic ligands. Part 3: The Pb_{2+}, + OH_{-}, Cl_{-}, CO_{32-}, SO_{42-}, and PO_{43-} systems (IUPAC Technical Report). Pure and Applied Chemistry, 81:2425-2476.

SC&A (S. Cohen & Associates). 2008b. Verification of the Waste Isolation Pilot Plant Chemistry Conceptual Models. Prepared for the U.S. Environmental Protection Agency Office of Radiation and Indoor Air, September 19, 2008.

Wilson, C., D. Porter, J. Gibbons, E. Oswald, G. Sjoblom, and F. Caporuscio. 1996. Conceptual Models Peer Review Report, Prepared for the U.S. Department of Energy, Carlsbad, New Mexico, July 1996, Docket No. A-93-02 Item II-G-1.

DOE Response (from DOE Response Package 10)

> The U.S. Department of Energy (DOE) recognizes the limitations of the Powell et al. (2009) lead system as implemented in DATA0.FM4 for CRA-2019 DPA, and discussed its limitations in Appendix GEOCHEM Section 3.3.7:
>
> > "A critical review of the lead solids and lead speciation reactions with inorganic ligands published as an International Union of Pure and Applied Chemistry (IUPAC) technical document (Powell et al., 2009) was
> > implemented for CRA-2019… Thus, the lead model used for CRA-2019 includes only thermodynamic data for lead inorganic aqueous complexes and lead solid phases with no accompanying Pitzer interaction parameters for the charged species."

With regard to the impact of the lead model on actinide solubility, Appendix GEOCHEM Section 3.3.7 states:

> "The lead speciation reactions in Table GEOCHEM-33 suggest that lead-chloride species will dominate the lead chemistry. Considering that chloride has an infinite source in the form of halite in the repository, combined with knowledge that there are no lead-organic reactions included in the database, the possibility of lead competing for organic ligands is eliminated, which is conservative because it will increase the actinide concentrations via organic complexation."

The DOE also noted in Appendix GEOCHEM Section 3.3.7:

> "The lead model of Powell et al. (2009) should be replaced with a more appropriate Pitzer model that includes lead speciation reactions with both inorganic and organic ligands to properly characterize the lead system in the WIPP."

The lead system parameters included in DATA0.FM4 were presented to and agreed upon with the U.S Environmental Protection Agency at the September 25, 2018 Technical Exchange Meeting. In a letter to DOE, Peake (2018) for Issue #35, "Lead" carries the status of "Resolved", and action that it may require further discussion. The DOE acknowledges the limitations of the lead model as implemented in DATA0.FM4 and will take steps to further develop and verify the model for future recertifications.

References

Peake, T. 2018. Letter to Mike Brown. Subject: 2018-12-17 E Letter to CBFO WIPP Issues Summary. U.S. Environmental Protection Agency, Center for Waste Management and Regulations. December 17, 2018.

Powell, K., P. Brown, R. Byrne, T. Gajda, G. Hefter, A.-K. Leuz, S. Sjöberg, and H. Wanner. 2009. Chemical speciation of environmentally significant metals with inorganic ligands. Part 3: The Pb^{2+}, OH^-, Cl^-, CO_3^{2-}, SO_4^{2-}, and PO_4^{3-} systems (IUPAC Technical Report). Pure and Applied Chemistry, 81:2425-2476.

EPA Evaluation of Response

The DOE response was adequate, however the lead data was rejected by EPA.

CC6-GEOCHEM-31 Comparison of Modeled and Experimental Glushinskite Data

WIPP Compliance Recertification Application 2019 Appendix-GEOCHEM (Geochemistry)

EPA Question (from EPA Completeness Comment Package 6)

Please provide figures that compare the experimentally measured solubilities of glushinskite [MgOxalate·2H_2O] in NaCl and $MgCl_2$ solutions to the modeled concentrations obtained using DATA0.FM4.

Figure 1 of Jang (2019) compared experimentally measured glushinskite solubilities to concentrations modeled using preliminary thermodynamic data. Some of these thermodynamic data were subsequently changed to improve the fit of the model to the experimental data. Please provide equivalent figures obtained using the final oxalate species data in DATA0.FM4.

Jang, J.J. 2019. AP-182, Analysis Plan for Derivation and Addition of Equilibrium Constants and Pitzer Interaction Parameters to the WIPP Geochemical Thermodynamic Database. Carlsbad, NM Sandia National Laboratories.

DOE Response (from DOE Response Package 10)

Figures 1 and 2 display the solubility of glushinskite [MgOxalate·2H_2O] in NaCl and $MgCl_2$ solutions, respectively, calculated by EQ3/6 using DATA0.FM4. The glushinskite solubility was calculated in NaCl and $MgCl_2$ solutions using EQ3/6 to speciate and equilibrate glushinskite with the solution compositions from the experiments (Jang 2019). The EQ3/6 input/out files, and the Excel file of the processed model output are included with the enclosure to this comment response.

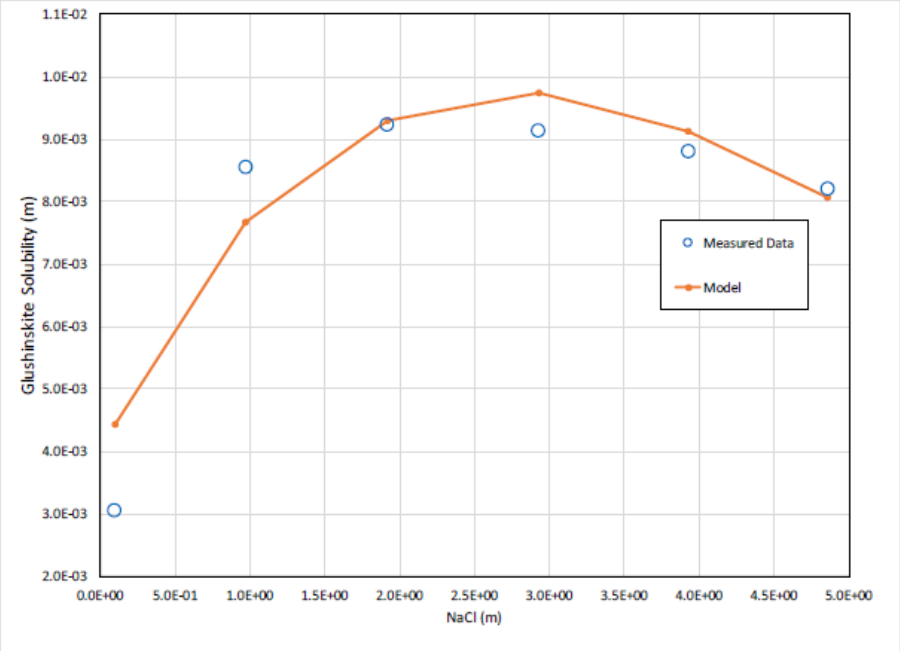

Figure 1. Glushinskite Solubility (m) in NaCl Solutions.

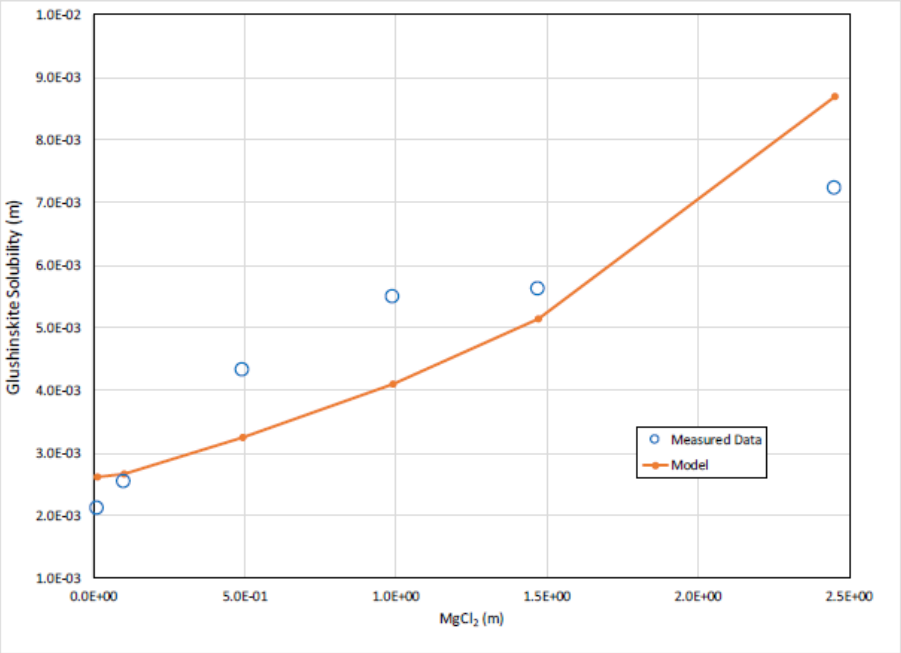

Figure 2. Glushinskite Solubility (m) in $MgCl_2$ Solutions.

EPA Evaluation of Response

The DOE response was satisfactory. The information was provided as requested.

CC6- GEOCHEM-32 Effects of Shielded Containers on Steel Surface Area per Unit Volume

WIPP Compliance Recertification Application 2019 Appendix-GEOCHEM (Geochemistry)

EPA Question (from EPA Completeness Comment Package 6)

Please explain why the steel surface area per unit volume remains unchanged (parameters REFCON:ASDRUM, REFCON:DRROOM, and REFCON:VROOM), despite an increased number of shielded containers for the CRA-2019 PA compared to the CRA-2014 PA.

> *The surface area of steel per unit repository volume (D_s = 11.2 m_2/m_3) is calculated for WIPP PA using:*
>
> *D_s= REFCON:ASDRUM × REFCON:DRROOM ÷ REFCON:VROOM*
>
> *Where:*
>
> *REFCON:ASDRUM is the surface area of steel associated with a waste disposal drum (6 m_2/drum)*
>
> *REFCON:DRROOM is the number of waste drums in a disposal room (6,800 drums)*
>
> *REFCON:VROOM is the volume of a disposal room (3,640 m_3)*

Calculations of D_s depend on the proportions of different wastes and waste containers in the repository (EPA 2017). The CRA-2019 PA iron-based metals and alloys inventory has increased by 14,000 metric tons since the CRA-2014 PA (see table), primarily because of increased RH packaging materials from shielded containers (DOE 2018). However, DOE has not addressed whether the increased number of shielded containers will significantly affect D_s. Because of the substantial increase in the number of RH shielded containers, DOE must provide information to support retaining the existing REFCON:ASDRUM, REFCON:DRROOM, and REFCON:VROOM parameters.

CRA-2014 PA and CRA-2019 PA Inventories of Iron-Based Metals and Alloys in Waste and Steel Packaging Materials

Parameter	CRA-2014 PA (kg)	CRA-2019 PA (kg)
CH Waste Iron-Based Metal and Alloys	10,900,000	14,100,000
CH Steel Packaging Materials	30,000,000	31,200,000
RH Waste Iron-Based Metal and Alloys	1,350,000	1,330,000
RH Steel Packaging Materials	6,860,000	16,500,000
Repository Total	49,110,000	63,130,000

Source: Table 5-5 of Van Soest (2012, 2018)

DOE (U.S. Department of Energy). 2018. Annual Transuranic Waste Inventory Report – 2018. Revision 0. U.S. Department of Energy, Carlsbad Field Office, DOE/TRU-18-3425.

EPA (U.S. Environmental Protection Agency). 2017. Evaluation of the Compliance Recertification Actinide Source Term, Gas Generation, Backfill Efficacy, Water Balance and Culebra Dolomite Distribution Coefficient Values. Docket No. EPA-HQ-OAR-2014-0609. U.S. Environmental Protection Agency. Washington, DC.

Van Soest, G.D. 2012. Performance Assessment Inventory Report – 2012. Los Alamos National Laboratory Carlsbad Operations INV-PA-12, Revision 0, LA-UR-12-26643.

Van Soest, G.D. 2018. Performance Assessment Inventory Report – 2018. Los Alamos National Laboratory Carlsbad Operations INV-PA-18, Revision 0, December 12, 2018.

DOE Response (from DOE Response Package 9)

In response to the U.S. Environmental Protection Agency (EPA) Comment 4-C-4 from the Compliance Recertification Application (CRA)-2014 (Shrader 2015), the U.S. Department of Energy (DOE) submitted the results of an analysis supporting the use of the parameters used to calculate the surface area of steel per unit volume (Ds) in Performance Assessment (PA) calculations. The analysis made two conservative estimates of steel surface area based on emplaced containers. Both estimates were shown to be lower than the currently implemented assumption based on PA parameterization, indicating that PA calculations currently overestimate steel surface area and thus overestimate gas generation due to iron corrosion.

No changes were made to the steel surface area calculation for the CRA-2019 PA. In discussion with the EPA prior to submittal of the CRA-2019, the DOE and EPA agreed that no change to the steel surface area calculation was needed for CRA-2019, but that the issue would be revisited periodically for future PAs as updates are made to the numbers of waste containers emplaced in the Waste Isolation Pilot Plant (WIPP).

However, we are able to make a general statement on the potential inclusion of additional shielded containers to the container inventory considered in DOE's response to EPA's comment 4-C-4 from the CRA-2014. We note that the response to the comment relied on the analysis of Day (2015), which was based upon the consideration of normalized steel surface areas for each container type currently emplaced in the WIPP. The steel surface area for shielded containers (4.39 m_2 in Table 3 of Day 2015) was shown to be below the average steel surface area over all container types (6.00 m_2 in same table). Thus, if additional shielded containers were added to the analysis of Day (2015), the overall surface area per drum equivalent would decrease, indicating that the currently implemented steel surface area continues to overestimate steel surface area in the repository and that PA calculations continue to overestimate gas generation due to iron corrosion.

References

Shrader, T. 2015. Response to the U.S. Environmental Protection Agency Letters Dated June 5, 2015 and July 30, 2015 Regarding the 2014 Compliance Recertification Application. U.S. Department of Energy Carlsbad Field Office.

Day, B. 2015. Memo to Records: Review of the Technical Basis for REFCON: ASDRUM, DRROOM, and VROOM Performance Assessment Analysis Parameters with Comparison to the Currently Emplaced Steel Surface Area per Unit Volume in the WIPP Repository. Sandia National Laboratories, Carlsbad, NM. ERMS 564670.

EPA Evaluation of Response

The DOE response was adequate.

CC6- GEOCHEM-33 Humid Steel Corrosion Parameter

WIPP Compliance Recertification Application 2019 Appendix-GEOCHEM (Geochemistry)

EPA Question (from EPA Completeness Comment Package 6)

Please explain the differences between the mean and standard deviation values for the humid steel corrosion parameter STEEL:HUMCORR in Zeitler (2018) and Kim and Feng (2019). Please also confirm that the correct distribution for STEEL:HUMCORR was entered into the parameter database and sampled for the CRA-2019 PA.

Appendix GEOCHEM (Section GEOCHEM-2.4.1) cites Zeitler (2018) as the source of the cumulative distribution for the humid steel corrosion parameter that was sampled in the CRA-2019 PA. The statistics for this cumulative distribution are compared in the table below to the statistics summarized by the input parameter report for the CRA-2019 (Kim and Feng 2019). The reported mean and standard deviation values in these documents are slightly different. Although

these differences are not expected to have affected the results of the CRA-2019 PA, DOE should explain the reasons for these differences and confirm that the correct cumulative distribution was sampled for the parameter STEEL:HUMCORR.

STEEL:HUMCORR		
Reference	Zeitler (2018, Table 2) ERMS 569807	Kim and Feng (2019) ERMS 571377
Mean	2.73E-16	2.43E-16
Median	1.90E-16	1.90E-16
St. Dev.	3.32E-16	2.47E-16
Minimum	0.00E+00	0.00E+00
Maximum	1.03E-15	1.03E-15

Kim and Feng. 2019. Input Parameter Report for the 2019 Compliance Recertification Application Performance Assessment (CRA-2019 PA), Revision 1. Sandia National Laboratories, Carlsbad, New Mexico, ERMS 571660.

Zeitler, T.R. 2018. Bounding Calculation of the Cumulative Distribution for STEEL:HUMCORR. Sandia National Laboratories, Carlsbad New Mexico, ERMS 569807.

DOE Response (from DOE Response Package 9)

The correct distribution for the humid steel corrosion parameter (STEEL:HUMCORR) was entered into the Performance Assessment (PA) parameter database (PAPDB) and sampled for the CRA- 2019 PA. The distribution for STEEL:HUMCORR is a cumulative distribution defined by individual data points rather than a mean and standard deviation. A mean and standard deviation were calculated by the PAPDB from the individual data points based on the appropriate statistical calculations for a cumulative distribution (consistent with how statistics have been calculated for all cumulative distributions in the PAPDB). The mean and standard deviation values are correctly reported in Kim and Feng (2019), but the values reported in Zeitler (2018) were calculated inconsistently with the statistical calculations for a cumulative distribution. The mean and standard deviation from Zeitler (2018) were not input into the parameter database. Also, for clarity, the mean and standard deviation for cumulative distributions are not used by the Latin- Hypercube Sampling (LHS) PA code when determining sampled parameter values.

References

Kim, S. and M. Feng. 2019. Input Parameter Report for the 2019 Compliance Recertification Application Performance Assessment (CRA-2019 PA), Revision 1. Sandia National Laboratories, Carlsbad, NM. ERMS 571377.

Zeitler, T. 2018. Bounding Calculation of the Cumulative Distribution for STEEL:HUMCORR. Sandia National Laboratories, Carlsbad NM. ERMS 569807.

EPA Evaluation of Response

The DOE response was satisfactory.

CC6- GEOCHEM-35 Omission of Brine Radiolysis Effects from Appendix GEOCHEM Discussions of Radiolysis and the Brine Production Model

WIPP Compliance Recertification Application 2019 Appendix-GEOCHEM (Geochemistry)

EPA Question (from EPA Completeness Comment Package 6)

Although brine radiolysis consumes brine, this process is not included in the Appendix GEOCHEM discussions of radiolysis (Section GEOCHEM-2.1.7) or the brine production process model (Section GEOCHEM-2.2). Please indicate whether the effects of radiolysis were included in the CRA-2019 PA calculations of brine volumes. If the effects of radiolysis on brine volumes were not included in the CRA-2019 PA, please evaluate the effects on repository releases of including radiolytic brine consumption.

The discussions of radiolysis in Sections GEOCHEM-2.1.7 and GEOCHEM-2.2 address the effects of radiolysis on gas generation rates, but the effects of radiolysis on brine consumption are not addressed in these sections. Day (2019) and Zeitler et al. (2019) discuss the parameters GLOBAL:GDEPFAC, GLOBAL:DECAYNRG, and GLOBAL GH2AVG for calculating H2(g) generation rates through brine radiolysis, but Day (2019) only parenthetically mentions brine consumption and Zeitler et al. (2019) does not discuss radiolytic brine consumption. Consequently, it is unclear whether brine consumption through radiolysis was included in CRA-2019 PA calculations of brine volumes.

Day, B. 2019. Reassessment of need and parameter justification for modeling gas generation due to radiolysis of brine and cellulose/plastic/rubber in WIPP for CRA-2019. Sandia National Laboratories, Carlsbad, New Mexico, ERMS 570873.

Zeitler, T.R., J. Bethune, S. Brunell, D. Kicker, and J. Long. 2019. Summary Report for the 2019 Compliance Recertification Application Performance Assessment (CRA-2019 PA). Revision 0. Sandia National Laboratories, Carlsbad, New Mexico, ERMS 571376.

DOE Response (from DOE Response Package 9)

> The brine consumption effect of radiolysis was included in the Compliance Recertification Application (CRA)-2019 Performance Assessment (PA) calculations of brine volumes and saturations, but not completely documented in Appendix GEOCHEM. Sections GEOCHEM-2.1.7 and GEOCHEM-2.2 correctly noted the inclusion of radiolysis of water as a gas generation mechanism in Waste Isolation Pilot Plant (WIPP) PA but omitted that the radiolysis of water is also included as a brine consumption reaction.
>
> Section GEOCHEM-2.2 references Day (2019) which describes the radiolytic H_2 generation rate as being equivalent to the brine consumption rate (i.e., one mole of gas produced for each net mole of water consumed). However, neither Section GEOCHEM-2.2 nor Day (2019) explicitly show the assumed radiolysis reaction incorporated into the BRAGFLO PA model (i.e., $H_2O(l) \rightarrow H_2(g)$; oxygen is assumed to react with metals in the waste and not contribute to gas production). In future descriptions of gas generation and brine production/consumption, explicit

description of the radiolytic effects will be included. For example, Equations GEOCHEM.2 (total gas generation rate) and GEOCHEM.3 (total brine production/consumption rate) will now include terms associated with radiolysis:

$$q_{rg} = q_{rgc} + q_{rgm} + q_{rgs} + q_{rgr} \text{ (updated GEOCHEM.2)}$$

$$q_{rb} = q_{rbc} + q_{rbs} + q_{rbm} + q_{rbh} + q_{rbhc} + q_{rbr} \text{ (updated GEOCHEM.3)}$$

where q_{rgr} and q_{rbr} are the brine radiolysis rates associated with gas generation and brine production/consumption, respectively, and the other terms are already defined in Appendix GEOCHEM. This change has been added to Enclosure 2, CRA-2019 Errata Tracking.

Also, additional equations will be included in Appendix GEOCHEM to describe the calculation of q_{rgr} and q_{rbr}. The q_{rgr} term is described in detail in Equation 7 in Day (2019) as R_{H2} and will be brought into Appendix GEOCHEM. Because the brine consumption rate is equal in absolute value to the gas generation rate, $q_{rbr} = -q_{rgr}$. This change has been added to Enclosure 2, CRA-2019 Errata Tracking.

Reference

Day, B. 2019. Reassessment of need and parameter justification for modeling gas generation due to radiolysis of brine and cellulose/plastic/rubber in WIPP for CRA-2019. Sandia National Laboratories, Carlsbad, New Mexico. ERMS 570873.

EPA Evaluation of Response

The DOE response was satisfactory; the omission was acknowledged in errata.

FC1-CCR-SOTERM-8, 9, 10 Nd(III) Colloids Data

WIPP Compliance Recertification Application 2019 Appendix-SOTERM (Actinide Chemistry Source Term)

EPA Question (from EPA Completeness Follow Up Comment Package 1)

Please explain the discrepancies in the reported Nd(III) colloids data described below, including the inconsistencies in listing filter pore sizes used, the previously reported lack of colloids in experimental solutions, and the mismatch in the number of relevant sequential filtration data sets reported in GWB and ERDA-6 brine. Please also provide the measured Nd(III) concentrations in all sequential filtration samples measured in GWB and ERDA-6 experiments between pcH 7.94 and pcH 10 from the experiments described by Borkowski et al. (2010).

Nd(III) filtration data cited by Reed et al. (2013) were attributed to Borkowski et al. (2010), including four solubility experiments in GWB and two solubility experiments in ERDA-6. Reed et al. (2019) included results from one of these experiments for the CRA-2019 colloid parameter evaluation. Figure 4-2 of Reed et al. (2013) is a graph of filtration data for 2 nm, 5 nm, 10 nm, 220 nm, and larger filter pore sizes, and there is evidence of intrinsic colloids based on the 10 nm and 2 nm filtration data. However, the Reed et al. (2013, 2019) data appear to be inconsistent with information in Borkowski et al. (2010). These possible inconsistencies could affect the defensibility of the Am(III) intrinsic colloid concentration parameter used in the CRA-2019:

1. *Borkowski et al. (2010 p. 29) stated that the filter pore sizes used in the experiments were 5 nm, 30 nm, and 220 nm, and these listed pore sizes do not include the 2 nm and 10 nm filter pore sizes cited by Reed et al. (2013, 2019)*

2. *Borkowski et al. (2010 p. 29) stated that "colloids or a fine particle suspension were not formed during the solubility experiments." This statement appears inconsistent with the data in Reed et al. (2013, Figure 4-2) and Reed et al. (2019, Table A-2)*

3. *Borkowski et al. (2010, Figure 4-2(A)) showed that there were five sets of sequential filtration samples from experiments in ERDA-6 between pcH 8 and 10, but Reed et al. (2013, Figure 4-2) included data from only two sets of sequential filtration samples in ERDA-6 at pcH 7.94 and 9.14*

4. *Data presented in Borkowski et al. (2010, Figure 4-2(B)) showed that there were three sets of sequential filtration samples from experiments in GWB between pcH 8 and 10, but Reed et al. (2013, Figure 4-2) included data from four sets of sequential filtration samples in GWB at pcH 8.20, 8.31, 8.53, and 8.55*

Borkowski, M., J.F. Lucchini, M.K. Richmann, and D.T. Reed. 2010. Actinide (III) Solubility in WIPP Brine: Data Summary and Recommendations. LA-UR 09-03222. Los Alamos National Laboratory, Los Alamos, New Mexico.

Reed, D.T., J.S. Swanson, J.F. Lucchini and M.K. Richmann. 2013. Intrinsic, Mineral and Microbial Colloid Enhancement Parameters for the WIPP Actinide Source Term. LCO-ACP-18, Revision 0, Los Alamos National Laboratory, Carlsbad, New Mexico.

Reed, D.T., J.S. Swanson and F. Stanley. 2019. Intrinsic, LANL/ ACRSP Parameter Recommendations for the CRA-2019 Deferred Performance Assessment. LCO-ACP-24, Revision 0, Los Alamos National Laboratory, Carlsbad, New Mexico. ERMS 571296.

DOE Response (from DOE Response Package 11)

The recommended intrinsic colloid enhancement parameters for Compliance Recertification Application (CRA)-2019 are described in Reed et al. (2019). These parameters were based on a specific set of analyses described in Reed et al. (2013) to evaluate the distribution of colloidal species in long-term solubility studies. For CRA-2019, the U.S. Department of Energy (DOE) agreed to honor the U.S. Environmental Protection Agency (EPA) request to simply re-interpret the CRA-2014 data over a broader pH range and re-calculate the enhancement parameters for these extended data sets. The DOE has already responded to EPA questions on the An(III) and An(IV) intrinsic colloid enhancement data selected (See DOE responses to EPA questions CC3-SOTERM-8 and CC3-SOTERM 9, 10, and 11). It is important to note that the An(III) intrinsic colloid parameter recommendations are based on Pu(III) data because it better represents Pu/Am ((III) in the Waste Isolation Pilot Plant (WIPP) model, not the Nd(III) data discussed in this comment (see discussion in Reed et al., 2013 and 2019). Additionally, the DOE provided a detailed review, explanation and assessment of the use of ultrafiltration within the Los Alamos actinide program (Reed, 2020). The DOE continues to believe that the An(III) intrinsic colloid parameter used for CRA-2019 is defensible.

The EPA, as discussed in Reed (2020), is correctly noting that although the same filters were used throughout the actinide program, they have been inconsistently designated in published reports. This is mainly due to changes in our understanding of the filter cut-off size ranges and nominal pore sizes over the past 15+ years since this work was initiated. In the Borkowski et al. (2009) report, filtrations were performed with a 0.22 µm, 100K and 30 K molecular weight cut-off (MWCO) Amicon ultrafilters. These are the same filter types and sizes that remain in use today within the actinide program. The sequential filtration, in the Borkowski et al. (2009) report, was done to evaluate the potential presence of colloidal species in the solubility study. In this report, these were referred to as 0.22 µm, ~ 30 nm and ~ 5 nm filtration sizes, respectively. These, in hindsight and with our current understanding, should have been designated as 0.22 µm, ~20 nm and ~ 10 nm filtration sizes, and these are the sizes that map into the parameter recommendations made in both CRA-2014 and CRA-2019.

The Nd(III) experiments were in fact analyzed for colloidal content in the 2012 evaluation (Reed et al., 2013). In this set of analyses, the experiments described in Borkowski et al. (2009), were re-analyzed in 2012 but no data were used from this report as its publication pre-dates the time of the re-analyses performed. In the end, the Pu(III) data, not the neodymium data, were the basis of the intrinsic colloid enhancement parameters recommended and the Nd(III) analysis was not carried forward to CRA-2019.

The EPA incorrectly believes that these data are inconsistent with each other. The conclusions stated in the Borkowski et al. (2009) report from the sequential filtration study were (See page 23 in the report):

> "All the neodymium concentrations determined in filtered samples and unfiltered samples (with one exception) were in good agreement and within experimental error. This indicates that colloids or a fine particle suspension were not formed during the solubility experiments. ..... Only one data point .... had a higher neodymium concentration. This data point corresponds to an unfiltered sample, where it is likely that a small grain of suspended solid was taken with the solution because of sample perturbation during the sampling process."

These data actually agree very well with the overall results of the 5-level sequential filtration study performed in 2012 where it was observed that intrinsic colloidal species were only noted at filtrations less than 10 nm. The finer levels of filtration used in 2012 were done in response to new information available to the project that <10 nm structural colloids could be forming in the brine systems under WIPP-relevant conditions (Burns et al., 2005; Soderholm et al., 2008). All in all, this is a good example of how changes in scientific understanding influences and drives needed changes within the WIPP Performance Assessment approach.

An answer to the specific questions raised by the EPA is also provided:

1. The DOE acknowledges that the designations used for filter sizes has changed over the years. See the explanation in the answer provided above and the more detailed description of the filters that have been used in Reed (2020).

2. This statement is consistent when the filter sizes are corrected and direct comparisons are made. As noted, there should have been no intrinsic colloidal species present at the

> 10 nm filtrations (30 K Amicon) performed in the Borkowski et al. (2009) study. This was also observed in the 2012 study where the intrinsic colloids observed were <10 nm in size.

3. There is no reason why the same experiments should have been analyzed. These analyses were done at very different times with different objectives and goals. The Reed et al. (2013) data are not from the Borkowski et al., (2009) report.

4. Same response as 3 above.

The benefit of doing new experiments and re-assessing project assumptions (in this case back to the time of the Compliance Certification Application) is that new understandings are reached and the WIPP project moves forward. The study done in 2012 improved our understanding of the colloidal contributions in WIPP-relevant systems, strengthened the defensibility of the WIPP safety case, and supersedes as well as extends the understanding that was described in the Borkowski report that is the subject of this EPA question.

References:

*Borkowski, M., J.F. Lucchini, M.K. Richmann, D. Reed. 2009. Actinide (III) Solubility in WIPP Brine: Data Summary and Recommendations. Los Alamos National Laboratory; Carlsbad, NM. LCO-ACP-08. LA 14360.

Burns, P.C., K. Kubatko, G. Sigmon, B.J. Fryer, J.E. Gagnon, M.R. Antonio and L. Soderholm. 2005. Actinyl Peroxide Nanospheres. Angew. Chem. Int. Ed., (44) 2135-2139.

Reed, D.T., J. Swanson, J.F. Lucchini, M. Richmann. 2013. Intrinsic, Mineral, and Microbial Colloid Enhancement Parameters for the WIPP Actinide Source Term. Los Alamos National Laboratory; Carlsbad, NM. LCO-ACP-18, LA-UR 13-20858.

Reed, D., J. Swanson, F. Stanley. 1 2019. LANL/ACRSP Parameter Recommendations for the CRA-2019 Deferred Performance Assessment. Los Alamos National Laboratory: Carlsbad, NM. LCO-ACP-24. LA-UR-19-22787.

Reed, D.T. 2020. Supporting Document Justification for the Pu(III) Intrinsic colloid Parameter (COMNCINT) Based on Plutonium Filtration Data. Los Alamos National Laboratory: Carlsbad NM. Los Alamos Report LAUR 20-29679.

Soderholm, L., P.M. Almond, S. Skanthakumar, R.E. Wilson and P.C. Burns. 2008. The Structure of the Plutonium Oxide Nanocluster $[Pu_{38}O_{56}Cl_{54}(H_2O)_8]_{14}$. Angew. Chem. (120) 304-308.

* This is the more fully published version of “Borkowski, M., J.F. Lucchini, M.K. Richmann, and D.T. Reed. 2010. Actinide (III) Solubility in WIPP Brine: Data Summary and Recommendations. LA-UR 09-03222. Los Alamos National Laboratory, Los Alamos, New Mexico” Cited by the EPA.

EPA Evaluation of Response

The DOE response was satisfactory.

FC2-CCR-GEOCHEM-32 Number of Shielded Containers Emplaced Up to December 31, 2017

WIPP Compliance Recertification Application 2019 Appendix-GEOCHEM (Geochemistry)

EPA Question (from EPA Completeness Follow Up Comment Package 2)

How many shielded containers have been placed in the repository as of December 31, 2017 (the inventory cutoff date for the CRA-2019 DPA)?

EPA recognizes that in a technical exchange following the 2014 WIPP recertification in November 2017, EPA and DOE agreed that no new recalculation of steel surface area was needed because there would not be a significant amount of new waste entering the repository for CRA-2019. EPA and DOE also agreed that this value would be revisited periodically as needed.

However, Van Soest (2018) reports an increased inventory of iron-based metals and alloys compared to Van Soest (2012). This inventory has increased the iron-based metals by 14,000 metric tons. EPA would like to confirm how many shielded containers were emplaced in the repository before the 2019-DPA cutoff date of December 31, 2017. This value will help EPA parse out what amount of that 14,000 MT is projected versus emplaced. It will also determine whether the steel surface area of the waste has significantly increased and whether a calculation is warranted.

EPA (US Environmental Protection Agency). 2017. Technical Exchange Meeting. Video Teleconference between EPA and DOE. Environmental Protection Agency Office of Radiation and Indoor Air, April 8, 2017.

Van Soest, G.D. 2012. Performance Assessment Inventory Report – 2012. Los Alamos National Laboratory Carlsbad Operations INV-PA-12, Revision 0, LA-UR-12-26643.

Van Soest, G.D. 2018. Performance Assessment Inventory Report – 2018. Los Alamos National Laboratory Carlsbad Operations INV-PA-18, Revision 0, December 12, 2018.

DOE Response (from DOE Response Package 13)

> There were nine shielded container assemblies emplaced in the repository as of December 31, 2017.

EPA Evaluation of Response

The DOE response was satisfactory. The information was provided as requested.

APPENDIX B

REVIEW OF PARAMETERS USED IN THE CRA-2019 PERFORMANCE ASSESSMENT THAT HAVE CHANGED SINCE THE CRA-2014 PERFORMANCE ASSESSMENT

TABLE OF CONTENTS

B1.0 INTRODUCTION....B-4
B2.0 APPROACH....B-5
B3.0 RESULTS....B-5
B3.1. Parameter Value Checks....B-5
B3.2. Parameter Documentation Checks....B-5
B3.3. Code/Database Interface Checks....B-6
B4.0 PARAMETER DATA ENTRY PROCESS REVIEW....B-55
B5.0 COMPUTING HARDWARE....B-55
B6.0 CONCLUSIONS....B-58
REFERENCES....B-58

LIST OF TABLES

Table B1. Parameter Value Checks for Parameters Used in the CRA-2019 PA that have Changed since the CRA-2014 PA

Table B2. Documentation Checks for Parameters Used in the CRA-2019 PA that have Changed since the CRA-2014 PA

Table B3. Code/Database Interface Test Results for Parameters Used in the CRA-2019 PA that have Changed since the CRA-2014 PA

Table B4. WIPP PA Solaris Cluster Nodes Used in the CRA-2019 PA

LIST OF ACRONYMS AND ABBREVIATIONS

CCDF	Complimentary Cumulative Distribution Function
CFR	*Code of Federal Regulations*
CH	Contact-Handled
CRA	Compliance Recertification Analysis
DOE or the Department	U.S. Department of Energy
EPA or the Agency	U.S. Environmental Protection Agency
ERMS	Electronic Record Management System
PA	Performance Assessment
PAPDB	Performance Assessment Parameter Database
PDE	Parameter Data Entry
RH	Remote-Handled
SAN	Storage Area Network
SNL	Sandia National Laboratories
WIPP	Waste Isolation Pilot Plan

B1.0 INTRODUCTION

Appendix B describes EPA's review of parameters used in the CRA-2019 Performance Assessment (PA) that have changed since the CRA-2014 PA. The results of this review document the Agency's evaluation of DOE's compliance with the requirements of 40 CFR 194.23(c)(4). Parameters used in WIPP PAs are maintained by Sandia National Laboratories (SNL) in the computerized Performance Assessment Parameter Database (PAPDB) for use in PA calculations. In addition to parameter values, the database includes metadata such as parameter names, units, and distribution characteristics. The PAPDB also identifies supporting documentation describing the historic use of the parameters and their values in previous analyses, changes that have been made to parameter values over time, and documentation of the technical basis for those values.

The parameters used in the WIPP PA consist of two parts, a material and a property of that material. Using the maximum mobilized concentration of americium on microbial colloids as an example, the material americium in the PAPDB is identified as AM, and the property consisting of the maximum mobilized concentration of actinide on microbial colloids is identified as CAPMIC. The maximum mobilized concentration of americium on microbial colloids is therefore identified in the PAPDB as AM:CAPMIC. By extension, the maximum mobilized concentration of neptunium on microbial colloids is identified in the PAPDB as NP:CAPMIC. The changes that have occurred since the CRA-2014 PA include the introduction of new materials, new properties, and changes in existing property values.

In addition to parameter management, the PAPDB allows WIPP PA codes PRELHS and MATSET to retrieve parameter data for use in PA. PRELHS is used to retrieve parameter data such as ranges, means, and distributions for subjectively uncertain (sampled) parameters. MATSET is used mainly to retrieve values for constant parameters, however, it also retrieves median values used as defaults in PA for parameters that have been assigned uncertainty distributions but are modeled as constants. Additional information can be found in the PAPDB Design Document (Long 2019a). PAPDB Version 3.00 was used for the CRA-2019 PA.

The changes to the PAPDB for the CRA-2019 PA were managed pursuant to Revision 2 of SNL's Nuclear Waste Management Procedure NP 9-2: *Parameters*, dated April 25, 2017. In summary, the process of entering database information into the PAPDB begins with a thorough review and documentation of the changes to the database since the previously approved baseline PA. For the CRA-2019 PA, the previously approved baseline was the CRA-2014 PA and the changes were documented in Kim and Feng (2019). Kim and Feng (2019) was then used as the source document for completing Parameter Data Entry forms NP 9-2-1. The completed forms were reviewed by DOE/SNL for accuracy and completeness before entering the changes into the PAPDB.

Section B2.0 provides an overview of the approach taken by EPA in performing the parameter review. The results of the review are presented in Section B3.0. Section B4.0 describes the Agency's review of SNL's procedural documentation, and Section B5.0 describes the computing hardware. The Agency's conclusions are presented in Section B6.0.

B2.0 APPROACH

The EPA's parameter review had a three part objective:

1) Parameter calue checks to confirm that the parameter values were accurately transcribed from the source documentation to the PAPDB;
2) Parameter documentation checks to confirm the metadata in the PAPDB was sufficient to trace the parameter value to its technical source documentation; and
3) Code/database interface checks to confirm that the correct parameter values were retrieved from the PAPDB for use in the CRA-2019 PA.

The PAPDB parameter database and associated metadata are maintained by SNL in Carlsbad, New Mexico. Hard copies of documentation supporting the parameters and their values are maintained in SNL's WIPP Records Center. The supporting documents are tracked by SNL's Electronic Record Management System (ERMS), through which a unique identifying number is assigned to each document.

The EPA's review of the PAPDB was conducted in the SNL offices in Carlsbad, New Mexico, during the week of August 9, 2021. The work began with an advance review of SNL's primary source document, Kim and Feng (2019), and the preparation of checklists based upon that document. The parameters that were changed for the CRA-2019 PA are listed in Table 2 of Kim and Feng (2019) and the values of those parameters used in the CRA-2019 PA are identified in other tables in their report. EPA's checklists identified the changed parameters and provided blanks for 1) confirming that the parameter values reported by Kim and Feng (2019) had been accurately entered into the PAPDB, 2) entering SNL's ERMS identification numbers for supporting source documents and evaluating the adequacy of those documents, and 3) confirming that the correct values were retrieved from the database.

B3.0 RESULTS

B3.1. Parameter Value Checks

The first step in EPA's review was to check that the values of the parameters that were changed for the CRA-2019 PA in the PAPDB were the same as those in the source document Kim and Feng (2019). The results of this check are documented in Table B1. The default value shown on the table for distributed parameters is the value used in analyses where the parameter is treated as a constant. Every changed value was found to have been correctly entered into the PAPDB.

B3.2. Parameter Documentation Checks

The next step was to check that the source documentation identified in the PAPDB was clearly linked to original source documents describing the rationale and technical basis for the changes. The results of this check are documented in Table B2. Most source documents were linked to parameters used in the CRA-2019 PA that had not been updated since the CRA-2014 PA, such as waste inventory activities. In those cases, the source documents applied directly to the CRA-2019 PA analysis. Other source documents were linked to parameters that were changed for

interim sensitivity analyses conducted between the CRA-2014 PA and the CRA-2019 PA and were retained unchanged for use in the CRA-2019 PA. In those cases, the source documents applied to the changes that were made for the interim analyses. The relevant analysis for each parameter was identified in the Kim and Feng (2019) source document and is included in Table B1.

Discrepancies were found between the PAPDB and the source documents in the second decimal place of the average values for the cumulative distributions of parameters STEEL:CORRMCO2 and STEEL:HUMCORR and results in differences in how the PAPDB calculates average values in comparison to how the source document did. However, these discrepancies were minor and did not affect the CRA-2019 PA results because the provided mean value was calculated separately off-line, only for reference purposes and was not used when sampling from the distribution. All changed parameters were found to be adequately linked to their source documentation.

B3.3. Code/Database Interface Checks

The third step was to confirm that the correct parameter values were retrieved from the PAPDB for use in the CRA-2019 PA. Some parameters were used in more than one code, for example, the parameter AM:CAPMIC was used in both the BRAGFLO and the PANEL codes. The results of this check are documented in Table B3. The Agency confirmed that the correct value was returned for every constant parameter in every applicable code and that the returned value for sampled parameters was appropriately within the range of the parameter distribution in every applicable code.

Table B1. Parameter Value Checks for Parameters Used in the CRA-2019 PA that have Changed since the CRA-2014 PA

Material Name	Property Name	Distribution Type	Value in Kim & Feng Table 2 ERMS 571660 Rev 1					Parameter Units	Original Analysis	Used in Code	Same Value in PAPDB?
			Constant or Mean	Other	Minimum	Maximum	Default Value				
AM	CAPMIC	Constant	2.30E-09	--	--	--	--	Moles/liter	CRA19	BRAGFLO, PANEL	Yes
AM	CONCINT	Constant	9.50E-09	--	--	--	--	Moles/liter	CRA19	BRAGFLO, PANEL	Yes
AM	PROPMIC	Constant	3.00E-02	--	--	--	--	None	CRA19	BRAGFLO, PANEL	Yes
AM241	DECAYNRG	Constant	5.64E+00	--	--	--	--	MeV	CRA19	BRAGFLO	Yes
AM241	INVCHD	Constant	1.13E+06	--	--	--	--	Curies	CRA19	BRAGFLO, PANEL	Yes
AM241	INVRHD	Constant	1.30E+04	--	--	--	--	Curies	CRA19	BRAGFLO, PANEL	Yes
AM241L	INVCHD	Constant	1.19E+06	--	--	--	--	Curies	CRA19	PANEL	Yes
AM241L	INVRHD	Constant	1.45E+04	--	--	--	--	Curies	CRA19	PANEL	Yes
AM243	INVCHD	Constant	2.24E+01	--	--	--	--	Curies	CRA19	PANEL	Yes
AM243	INVRHD	Constant	4.12E+02	--	--	--	--	Curies	CRA19	PANEL	Yes
BH_OPEN	RELP_MOD	Constant	1.10E+01	--	--	--	--	None	CRA19	BRAGFLO	Yes
BOREHOLE	TAUFAIL	Uniform	3.93E+01	--	1.60E+00	7.70E+01	3.93E+01	Pa	CRA14_SEN4	CUTTINGS_S	Yes
BOREHOLE	WUF	Constant	3.30E+00	--	--	--	--	None	CRA19	EPAUNI, PRECCDFGF, NUTS, PANEL	Yes
CAVITY_5	CAP_MOD	Constant	1.00E+00	--	--	--	--	None	CRA14_SEN4	BRAGFLO	Yes
CAVITY_5	COMP_RCK	Constant	0.00E+00	--	--	--	--	Pa^{-1}	CRA14_SEN4	BRAGFLO	Yes
CAVITY_5	KPT	Constant	0.00E+00	--	--	--	--	None	CRA14_SEN3	BRAGFLO	Yes
CAVITY_5	PCT_A	Constant	0.00E+00	--	--	--	--	Pa	CRA14_SEN4	BRAGFLO	Yes
CAVITY_5	PCT_EXP	Constant	0.00E+00	--	--	--	--	None	CRA14_SEN4	BRAGFLO	Yes
CAVITY_5	PC_MAX	Constant	1.00E+08	--	--	--	--	Pa	CRA14_SEN3	BRAGFLO	Yes
CAVITY_5	PORE_DIS	Constant	7.00E-01	--	--	--	--	None	CRA14_SEN3	BRAGFLO	Yes
CAVITY_5	POROSITY	Constant	1.00E+00	--	--	--	--	None	CRA14_SEN4	BRAGFLO	Yes
CAVITY_5	PO_MIN	Constant	1.01E+05	--	--	--	--	Pa	CRA14_SEN3	BRAGFLO	Yes
CAVITY_5	PRESSURE	Constant	1.01E+05	--	--	--	--	Pa	CRA14_SEN3	BRAGFLO	Yes

Table B1. Parameter Value Checks for Parameters Used in the CRA-2019 PA that have Changed since the CRA-2014 PA (Continued)

Material Name	Property Name	Distribution Type	Value in Kim & Feng Table 2 ERMS 571660 Rev 1					Parameter Units	Original Analysis	Used in Code	Same Value in PAPDB?
			Constant or Mean	Other	Minimum	Maximum	Default Value				
CAVITY_5	PRMX_LOG	Constant	-1.00E+01	--	--	--	--	log(m^2)	CRA14_SEN4	BRAGFLO	Yes
CAVITY_5	PRMY_LOG	Constant	-1.00E+01	--	--	--	--	log(m^2)	CRA14_SEN4	BRAGFLO	Yes
CAVITY_5	PRMZ_LOG	Constant	-1.00E+01	--	--	--	--	log(m^2)	CRA14_SEN4	BRAGFLO	Yes
CAVITY_5	RELP_MOD	Constant	1.10E+01	--	--	--	--	None	CRA14_SEN4	BRAGFLO	Yes
CAVITY_5	SAT_IBRN	Constant	0.00E+00	--	--	--	--	None	CRA14_SEN4	BRAGFLO	Yes
CAVITY_5	SAT_RBRN	Constant	0.00E+00	--	--	--	--	None	CRA14_SEN4	BRAGFLO	Yes
CAVITY_5	SAT_RGAS	Constant	0.00E+00	--	--	--	--	None	CRA14_SEN4	BRAGFLO	Yes
CF252	INVCHD	Constant	5.07E-01	--	--	--	--	Curies	CRA19	PANEL	Yes
CF252	INVRHD	Constant	1.76E+00	--	--	--	--	Curies	CRA19	PANEL	Yes
CM243	INVCHD	Constant	2.54E+00	--	--	--	--	Curies	CRA19	PANEL	Yes
CM243	INVRHD	Constant	3.61E+01	--	--	--	--	Curies	CRA19	PANEL	Yes
CM244	INVCHD	Constant	6.19E+03	--	--	--	--	Curies	CRA19	PANEL	Yes
CM244	INVRHD	Constant	3.32E+04	--	--	--	--	Curies	CRA19	PANEL	Yes
CM245	INVCHD	Constant	2.97E+00	--	--	--	--	Curies	CRA19	PANEL	Yes
CM245	INVRHD	Constant	2.15E+01	--	--	--	--	Curies	CRA19	PANEL	Yes
CM248	INVCHD	Constant	4.63E-01	--	--	--	--	Curies	CRA19	PANEL	Yes
CM248	INVRHD	Constant	1.31E+00	--	--	--	--	Curies	CRA19	PANEL	Yes
CS137	INVCHD	Constant	6.16E+02	--	--	--	--	Curies	CRA19	PANEL	Yes
CS137	INVRHD	Constant	2.50E+05	--	--	--	--	Curies	CRA19	PANEL	Yes
DRZ_OE_0	CAP_MOD	Constant	1.00E+00	--	--	--	--	None	CRA14_SEN4	BRAGFLO	Yes
DRZ_OE_0	COMP_RCK	Constant	7.41E-10	--	--	--	--	Pa^{-1}	CRA14_SEN4	BRAGFLO	Yes
DRZ_OE_0	KPT	Constant	0.00E+00	--	--	--	--	None	CRA14_SEN2	BRAGFLO	Yes
DRZ_OE_0	PCT_A	Constant	0.00E+00	--	--	--	--	Pa	CRA14_SEN4	BRAGFLO	Yes
DRZ_OE_0	PCT_EXP	Constant	0.00E+00	--	--	--	--	None	CRA14_SEN4	BRAGFLO	Yes
DRZ_OE_0	PC_MAX	Constant	1.00E+08	--	--	--	--	Pa	CRA14_SEN2	BRAGFLO	Yes
DRZ_OE_0	PORE_DIS	Constant	7.00E-01	--	--	--	--	None	CRA14_SEN2	BRAGFLO	Yes
DRZ_OE_0	POROSITY	Constant	1.29E-02	--	--	--	--	None	CRA14_SEN4	BRAGFLO	Yes
DRZ_OE_0	PO_MIN	Constant	1.01E+05	--	--	--	--	Pa	CRA14_SEN2	BRAGFLO	Yes
DRZ_OE_0	PRMX_LOG	Constant	-1.70E+01	--	--	--	--	log(m^2)	CRA14_SEN4	BRAGFLO	Yes

Table B1. Parameter Value Checks for Parameters Used in the CRA-2019 PA that have Changed since the CRA-2014 PA (Continued)

Material Name	Property Name	Distribution Type	Value in Kim & Feng Table 2 ERMS 571660 Rev 1					Parameter Units	Original Analysis	Used in Code	Same Value in PAPDB?
			Constant or Mean	Other	Minimum	Maximum	Default Value				
DRZ_OE_0	PRMY_LOG	Constant	-1.70E+01	--	--	--	--	$\log(m^2)$	CRA14_SEN4	BRAGFLO	Yes
DRZ_OE_0	PRMZ_LOG	Constant	-1.70E+01	--	--	--	--	$\log(m^2)$	CRA14_SEN4	BRAGFLO	Yes
DRZ_OE_0	RELP_MOD	Constant	4.00E+00	--	--	--	--	None	CRA14_SEN2	BRAGFLO	Yes
DRZ_OE_0	SAT_IBRN	Constant	1.00E+00	--	--	--	--	None	CRA14_SEN4	BRAGFLO	Yes
DRZ_OE_0	SAT_RBRN	Constant	0.00E+00	--	--	--	--	None	CRA14_SEN4	BRAGFLO	Yes
DRZ_OE_0	SAT_RGAS	Constant	0.00E+00	--	--	--	--	None	CRA14_SEN4	BRAGFLO	Yes
DRZ_OE_1	CAP_MOD	Constant	1.00E+00	--	--	--	--	None	CRA14_SEN4	BRAGFLO	Yes
DRZ_OE_1	COMP_RCK	Constant	7.41E-10	--	--	--	--	Pa^{-1}	CRA14_SEN4	BRAGFLO	Yes
DRZ_OE_1	KPT	Constant	0.00E+00	--	--	--	--	None	CRA14_SEN2	BRAGFLO	Yes
DRZ_OE_1	PCT_A	Constant	0.00E+00	--	--	--	--	Pa	CRA14_SEN4	BRAGFLO	Yes
DRZ_OE_1	PCT_EXP	Constant	0.00E+00	--	--	--	--	None	CRA14_SEN4	BRAGFLO	Yes
DRZ_OE_1	PC_MAX	Constant	1.00E+08	--	--	--	--	Pa	CRA14_SEN2	BRAGFLO	Yes
DRZ_OE_1	PORE_DIS	Constant	7.00E-01	--	--	--	--	None	CRA14_SEN2	BRAGFLO	Yes
DRZ_OE_1	POROSITY	Constant	1.29E-02	--	--	--	--	None	CRA14_SEN4	BRAGFLO	Yes
DRZ_OE_1	PO_MIN	Constant	1.01E+05	--	--	--	--	Pa	CRA14_SEN2	BRAGFLO	Yes
DRZ_OE_1	PRMX_LOG	Constant	-1.70E+01	--	--	--	--	$\log(m^2)$	CRA14_SEN4	BRAGFLO	Yes
DRZ_OE_1	PRMY_LOG	Constant	-1.70E+01	--	--	--	--	$\log(m^2)$	CRA14_SEN4	BRAGFLO	Yes
DRZ_OE_1	PRMZ_LOG	Constant	-1.70E+01	--	--	--	--	$\log(m^2)$	CRA14_SEN4	BRAGFLO	Yes
DRZ_OE_1	RELP_MOD	Constant	4.00E+00	--	--	--	--	None	CRA14_SEN2	BRAGFLO	Yes
DRZ_OE_1	SAT_IBRN	Constant	1.00E+00	--	--	--	--	None	CRA14_SEN4	BRAGFLO	Yes
DRZ_OE_1	SAT_RBRN	Constant	0.00E+00	--	--	--	--	None	CRA14_SEN4	BRAGFLO	Yes
DRZ_OE_1	SAT_RGAS	Constant	0.00E+00	--	--	--	--	None	CRA14_SEN4	BRAGFLO	Yes
DRZ_PC_0	CAP_MOD	Constant	1.00E+00	--	--	--	--	None	CRA14_SEN4	BRAGFLO	Yes
DRZ_PC_0	COMP_RCK	Constant	7.41E-10	--	--	--	--	Pa^{-1}	CRA14_SEN4	BRAGFLO	Yes
DRZ_PC_0	KPT	Constant	0.00E+00	--	--	--	--	None	CRA14_SEN3	BRAGFLO	Yes
DRZ_PC_0	PCT_A	Constant	0.00E+00	--	--	--	--	Pa	CRA14_SEN4	BRAGFLO	Yes
DRZ_PC_0	PCT_EXP	Constant	0.00E+00	--	--	--	--	None	CRA14_SEN4	BRAGFLO	Yes
DRZ_PC_0	PC_MAX	Constant	1.00E+08	--	--	--	--	Pa	CRA14_SEN3	BRAGFLO	Yes
DRZ_PC_0	PORE_DIS	Constant	7.00E-01	--	--	--	--	None	CRA14_SEN3	BRAGFLO	Yes

Table B1. Parameter Value Checks for Parameters Used in the CRA-2019 PA that have Changed since the CRA-2014 PA (Continued)

Material Name	Property Name	Distribution Type	Value in Kim & Feng Table 2 ERMS 571660 Rev 1					Parameter Units	Original Analysis	Used in Code	Same Value in PAPDB?
			Constant or Mean	Other	Minimum	Maximum	Default Value				
DRZ_PC_0	POROSITY	Constant	1.29E-02	--	--	--	--	None	CRA14_SEN4	BRAGFLO	Yes
DRZ_PC_0	PO_MIN	Constant	1.01E+05	--	--	--	--	Pa	CRA14_SEN3	BRAGFLO	Yes
DRZ_PC_0	PRMX_LOG	Constant	-1.70E+01	--	--	--	--	$\log(m^2)$	CRA14_SEN4	BRAGFLO	Yes
DRZ_PC_0	PRMY_LOG	Constant	-1.70E+01	--	--	--	--	$\log(m^2)$	CRA14_SEN4	BRAGFLO	Yes
DRZ_PC_0	PRMZ_LOG	Constant	-1.70E+01	--	--	--	--	$\log(m^2)$	CRA14_SEN4	BRAGFLO	Yes
DRZ_PC_0	RELP_MOD	Constant	4.00E+00	--	--	--	--	None	CRA14_SEN3	BRAGFLO	Yes
DRZ_PC_0	SAT_IBRN	Constant	1.00E+00	--	--	--	--	None	CRA14_SEN4	BRAGFLO	Yes
DRZ_PC_0	SAT_RBRN	Constant	0.00E+00	--	--	--	--	None	CRA14_SEN4	BRAGFLO	Yes
DRZ_PC_0	SAT_RGAS	Constant	0.00E+00	--	--	--	--	None	CRA14_SEN4	BRAGFLO	Yes
DRZ_PC_1	CAP_MOD	Constant	1.00E+00	--	--	--	--	None	CRA14_SEN4	BRAGFLO	Yes
DRZ_PC_1	COMP_RCK	Constant	7.41E-10	--	--	--	--	Pa^{-1}	CRA14_SEN4	BRAGFLO	Yes
DRZ_PC_1	KPT	Constant	0.00E+00	--	--	--	--	None	CRA14_SEN3	BRAGFLO	Yes
DRZ_PC_1	PCT_A	Constant	0.00E+00	--	--	--	--	Pa	CRA14_SEN4	BRAGFLO	Yes
DRZ_PC_1	PCT_EXP	Constant	0.00E+00	--	--	--	--	None	CRA14_SEN4	BRAGFLO	Yes
DRZ_PC_1	PC_MAX	Constant	1.00E+08	--	--	--	--	Pa	CRA14_SEN3	BRAGFLO	Yes
DRZ_PC_1	PORE_DIS	Constant	7.00E-01	--	--	--	--	None	CRA14_SEN3	BRAGFLO	Yes
DRZ_PC_1	POROSITY	Constant	1.29E-02	--	--	--	--	None	CRA14_SEN4	BRAGFLO	Yes
DRZ_PC_1	PO_MIN	Constant	1.01E+05	--	--	--	--	Pa	CRA14_SEN3	BRAGFLO	Yes
DRZ_PC_1	PRMX_LOG	Constant	-1.70E+01	--	--	--	--	$\log(m^2)$	CRA14_SEN4	BRAGFLO	Yes
DRZ_PC_1	PRMY_LOG	Constant	-1.70E+01	--	--	--	--	$\log(m^2)$	CRA14_SEN4	BRAGFLO	Yes
DRZ_PC_1	PRMZ_LOG	Constant	-1.70E+01	--	--	--	--	$\log(m^2)$	CRA14_SEN4	BRAGFLO	Yes
DRZ_PC_1	RELP_MOD	Constant	4.00E+00	--	--	--	--	None	CRA14_SEN3	BRAGFLO	Yes
DRZ_PC_1	SAT_IBRN	Constant	1.00E+00	--	--	--	--	None	CRA14_SEN4	BRAGFLO	Yes
DRZ_PC_1	SAT_RBRN	Constant	0.00E+00	--	--	--	--	None	CRA14_SEN4	BRAGFLO	Yes
DRZ_PC_1	SAT_RGAS	Constant	0.00E+00	--	--	--	--	None	CRA14_SEN4	BRAGFLO	Yes
GLOBAL	GDEPFAC	Uniform	2.50E-01	--	0.00E+00	5.00E-01	2.50E-01	None	CRA19	BRAGFLO	Yes
GLOBAL	GH2AVG	Constant	1.40E-02	--	--	--	--	molecule/eV	CRA19	BRAGFLO	Yes
GLOBAL	LAMBDAD	Constant	9.90E-03	--	--	--	--	$(km^{-2})(yr^{-1})$	CRA19	PRECCDFGF	Yes
GLOBAL	ONEPLG	Constant	4.03E-01	--	--	--	--	None	CRA19	PRECCDFGF	Yes

Table B1. Parameter Value Checks for Parameters Used in the CRA-2019 PA that have Changed since the CRA-2014 PA (Continued)

Material Name	Property Name	Distribution Type	Value in Kim & Feng Table 2 ERMS 571660 Rev 1					Parameter Units	Original Analysis	Used in Code	Same Value in PAPDB?
			Constant or Mean	Other	Minimum	Maximum	Default Value				
GLOBAL	PBRINE	Cumulative	2.63E-01	2.45E-01 median	4.00E-02	5.70E-01	2.63E-01	None	CRA14_SEN4	PRECCDFGF	Yes
GLOBAL	SRADO2	Constant	0.00E+00	--	--	--	--	mol O_2 / mol H_2	CRA19	BRAGFLO	Yes
GLOBAL	THREEPLG	Constant	2.66E-01	--	--	--	--	None	CRA19	PRECCDFGF	Yes
GLOBAL	TWOPLG	Constant	3.31E-01	--	--	--	--	None	CRA19	PRECCDFGF	Yes
NITRATE	QINIT	Constant	2.72E+07	--	--	--	--	Moles	CRA19	BRAGFLO	Yes
NP	CAPMIC	Constant	3.80E-08	--	--	--	--	Moles/liter	CRA19	PANEL	Yes
NP	CONCINT	Constant	4.30E-08	--	--	--	--	Moles/liter	CRA19	PANEL	Yes
NP	PROPMIC	Constant	2.10E-01	--	--	--	--	None	CRA19	PANEL	Yes
NP237	INVCHD	Constant	2.75E+01	--	--	--	--	Curies	CRA19	PANEL	Yes
NP237	INVRHD	Constant	6.96E+00	--	--	--	--	Curies	CRA19	PANEL	Yes
PA231	INVCHD	Constant	1.59E+01	--	--	--	--	Curies	CRA19	PANEL	Yes
PA231	INVRHD	Constant	1.04E-03	--	--	--	--	Curies	CRA19	PANEL	Yes
PB210	INVCHD	Constant	9.79E-01	--	--	--	--	Curies	CRA19	PANEL	Yes
PB210	INVRHD	Constant	1.45E+01	--	--	--	--	Curies	CRA19	PANEL	Yes
PCS_NO	CAP_MOD	Constant	1.00E+00	--	--	--	--	None	APCS	BRAGFLO	Yes
PCS_NO	COMP_RCK	Constant	0.00E+00	--	--	--	--	Pa^{-1}	APCS	BRAGFLO	Yes
PCS_NO	KPT	Constant	0.00E+00	--	--	--	--	None	APCS	BRAGFLO	Yes
PCS_NO	PCT_A	Constant	0.00E+00	--	--	--	--	Pa	APCS	BRAGFLO	Yes
PCS_NO	PCT_EXP	Constant	0.00E+00	--	--	--	--	None	APCS	BRAGFLO	Yes
PCS_NO	PC_MAX	Constant	1.00E+08	--	--	--	--	Pa	APCS	BRAGFLO	Yes
PCS_NO	PORE_DIS	Constant	7.00E-01	--	--	--	--	None	APCS	BRAGFLO	Yes
PCS_NO	POROSITY	Constant	1.80E-01	--	--	--	--	None	APCS	BRAGFLO	Yes
PCS_NO	PO_MIN	Constant	1.01E+05	--	--	--	--	Pa	APCS	BRAGFLO	Yes
PCS_NO	PRESSURE	Constant	1.01E+05	--	--	--	--	Pa	APCS	BRAGFLO	Yes
PCS_NO	PRMX_LOG	Constant	-1.10E+01	--	--	--	--	$\log(m^2)$	APCS	BRAGFLO	Yes
PCS_NO	PRMY_LOG	Constant	-1.10E+01	--	--	--	--	$\log(m^2)$	APCS	BRAGFLO	Yes
PCS_NO	PRMZ_LOG	Constant	-1.10E+01	--	--	--	--	$\log(m^2)$	APCS	BRAGFLO	Yes
PCS_NO	RELP_MOD	Constant	1.10E+01	--	--	--	--	None	APCS	BRAGFLO	Yes
PCS_NO	SAT_IBRN	Constant	0.00E+00	--	--	--	--	None	APCS	BRAGFLO	Yes

Table B1. Parameter Value Checks for Parameters Used in the CRA-2019 PA that have Changed since the CRA-2014 PA (Continued)

Material Name	Property Name	Distribution Type	Value in Kim & Feng Table 2 ERMS 571660 Rev 1					Parameter Units	Original Analysis	Used in Code	Same Value in PAPDB?
			Constant or Mean	Other	Minimum	Maximum	Default Value				
PCS_NO	SAT_RBRN	Constant	0.00E+00	--	--	--	--	None	APCS	BRAGFLO	Yes
PCS_NO	SAT_RGAS	Constant	0.00E+00	--	--	--	--	None	APCS	BRAGFLO	Yes
PHUMOX3	PHUMCIM	Constant	2.00E-01	--	--	--	--	None	CRA19	BRAGFLO, PANEL	Yes
PHUMOX3	PHUMSIM	Constant	2.00E-01	--	--	--	--	None	CRA19	BRAGFLO, PANEL	Yes
PHUMOX4	PHUMCIM	Constant	1.00E-02	--	--	--	--	None	CRA19	BRAGFLO, PANEL	Yes
PHUMOX4	PHUMSIM	Constant	1.00E-02	--	--	--	--	None	CRA19	BRAGFLO, PANEL	Yes
PM147	INVCHD	Constant	4.40E-01	--	--	--	--	Curies	CRA19	PANEL	Yes
PM147	INVRHD	Constant	2.54E+01	--	--	--	--	Curies	CRA19	PANEL	Yes
PU	CAPMIC	Constant	3.80E-08	--	--	--	--	Moles/liter	CRA19	BRAGFLO, PANEL	Yes
PU	CONCINT	Constant	4.30E-08	--	--	--	--	Moles/liter	CRA19	BRAGFLO, PANEL	Yes
PU	PROPMIC	Constant	2.10E-01	--	--	--	--	None	CRA19	BRAGFLO, PANEL	Yes
PU238	DECAYNRG	Constant	5.59E+00	--	--	--	--	MeV	CRA19	BRAGFLO	Yes
PU238	INVCHD	Constant	9.42E+05	--	--	--	--	Curies	CRA19	BRAGFLO, PANEL	Yes
PU238	INVRHD	Constant	2.25E+04	--	--	--	--	Curies	CRA19	BRAGFLO, PANEL	Yes
PU238L	INVCHD	Constant	9.42E+05	--	--	--	--	Curies	CRA19	PANEL	Yes
PU238L	INVRHD	Constant	2.25E+04	--	--	--	--	Curies	CRA19	PANEL	Yes
PU239	DECAYNRG	Constant	5.24E+00	--	--	--	--	MeV	CRA19	BRAGFLO	Yes
PU239	INVCHD	Constant	8.70E+05	--	--	--	--	Curies	CRA19	BRAGFLO, PANEL	Yes
PU239	INVRHD	Constant	4.22E+03	--	--	--	--	Curies	CRA19	BRAGFLO, PANEL	Yes
PU239L	INVCHD	Constant	1.19E+06	--	--	--	--	Curies	CRA19	PANEL	Yes
PU239L	INVRHD	Constant	7.63E+03	--	--	--	--	Curies	CRA19	PANEL	Yes
PU240	DECAYNRG	Constant	5.26E+00	--	--	--	--	MeV	CRA19	BRAGFLO	Yes

Table B1. Parameter Value Checks for Parameters Used in the CRA-2019 PA that have Changed since the CRA-2014 PA (Continued)

Material Name	Property Name	Distribution Type	Value in Kim & Feng Table 2 ERMS 571660 Rev 1					Parameter Units	Original Analysis	Used in Code	Same Value in PAPDB?
			Constant or Mean	Other	Minimum	Maximum	Default Value				
PU240	INVCHD	Constant	3.16E+05	--	--	--	--	Curies	CRA19	BRAGFLO, PANEL	Yes
PU240	INVRHD	Constant	3.16E+03	--	--	--	--	Curies	CRA19	BRAGFLO, PANEL	Yes
PU241	INVCHD	Constant	1.82E+06	--	--	--	--	Curies	CRA19	PANEL	Yes
PU241	INVRHD	Constant	4.53E+04	--	--	--	--	Curies	CRA19	PANEL	Yes
PU242	DECAYNRG	Constant	4.99E+00	--	--	--	--	MeV	CRA19	BRAGFLO	Yes
PU242	INVCHD	Constant	1.48E+02	--	--	--	--	Curies	CRA19	BRAGFLO, PANEL	Yes
PU242	INVRHD	Constant	1.59E+01	--	--	--	--	Curies	CRA19	BRAGFLO, PANEL	Yes
PU244	INVCHD	Constant	5.80E-03	--	--	--	--	Curies	CRA19	PANEL	Yes
PU244	INVRHD	Constant	2.82E-02	--	--	--	--	Curies	CRA19	PANEL	Yes
RA226	INVCHD	Constant	1.78E+00	--	--	--	--	Curies	CRA19	PANEL	Yes
RA226	INVRHD	Constant	1.85E+01	--	--	--	--	Curies	CRA19	PANEL	Yes
RA228	INVCHD	Constant	9.03E-02	--	--	--	--	Curies	CRA19	PANEL	Yes
RA228	INVRHD	Constant	4.55E-02	--	--	--	--	Curies	CRA19	PANEL	Yes
REFCON	STCO_31	Constant	0.00E+00	--	--	--	--	None	CRA14_SEN4	BRAGFLO	Yes
REFCON	STCO_32	Constant	0.00E+00	--	--	--	--	None	CRA14_SEN4	BRAGFLO	Yes
REFCON	STCO_35	Constant	0.00E+00	--	--	--	--	None	CRA14_SEN4	BRAGFLO	Yes
REFCON	STCO_36	Constant	0.00E+00	--	--	--	--	None	CRA14_SEN4	BRAGFLO	Yes
REFCON	STCO_43	Constant	0.00E+00	--	--	--	--	None	CRA14_SEN4	BRAGFLO	Yes
REFCON	STCO_46	Constant	0.00E+00	--	--	--	--	None	CRA14_SEN4	BRAGFLO	Yes
SM147	INVCHD	Constant	1.23E-09	--	--	--	--	Curies	CRA19	PANEL	Yes
SM147	INVRHD	Constant	9.40E-08	--	--	--	--	Curies	CRA19	PANEL	Yes
SOLMOD3	SOLCOH	Constant	1.78E-07	--	--	--	--	Moles/liter	CRA19	BRAGFLO, PANEL	Yes
SOLMOD3	SOLCOH2	Constant	1.63E-07	--	--	--	--	Moles/liter	CRA19	PANEL	Yes
SOLMOD3	SOLCOH3	Constant	1.58E-07	--	--	--	--	Moles/liter	CRA19	PANEL	Yes
SOLMOD3	SOLCOH4	Constant	1.54E-07	--	--	--	--	Moles/liter	CRA19	PANEL	Yes
SOLMOD3	SOLCOH5	Constant	1.52E-07	--	--	--	--	Moles/liter	CRA19	PANEL	Yes

Table B1. Parameter Value Checks for Parameters Used in the CRA-2019 PA that have Changed since the CRA-2014 PA (Continued)

Material Name	Property Name	Distribution Type	Value in Kim & Feng Table 2 ERMS 571660 Rev 1					Parameter Units	Original Analysis	Used in Code	Same Value in PAPDB?
			Constant or Mean	Other	Minimum	Maximum	Default Value				
SOLMOD3	SOLSOH	Constant	1.63E-07	- -	- -	- -	- -	Moles/liter	CRA19	BRAGFLO, PANEL	Yes
SOLMOD3	SOLSOH2	Constant	1.58E-07	- -	- -	- -	- -	Moles/liter	CRA19	PANEL	Yes
SOLMOD3	SOLSOH3	Constant	1.56E-07	- -	- -	- -	- -	Moles/liter	CRA19	PANEL	Yes
SOLMOD3	SOLSOH4	Constant	1.55E-07	- -	- -	- -	- -	Moles/liter	CRA19	PANEL	Yes
SOLMOD3	SOLSOH5	Constant	1.54E-07	- -	- -	- -	- -	Moles/liter	CRA19	PANEL	Yes
SOLMOD3	SOLVAR	Cumulative	6.40E-01	3.46E-01 median	-1.14E+00	2.97E+00	6.40E-01	None	CRA19	BRAGFLO, PANEL	Yes
SOLMOD4	SOLCOH	Constant	5.44E-08	- -	- -	- -	- -	Moles/liter	CRA19	BRAGFLO, PANEL	Yes
SOLMOD4	SOLCOH2	Constant	5.44E-08	- -	- -	- -	- -	Moles/liter	CRA19	PANEL	Yes
SOLMOD4	SOLCOH3	Constant	5.44E-08	- -	- -	- -	- -	Moles/liter	CRA19	PANEL	Yes
SOLMOD4	SOLCOH4	Constant	5.44E-08	- -	- -	- -	- -	Moles/liter	CRA19	PANEL	Yes
SOLMOD4	SOLCOH5	Constant	5.44E-08	- -	- -	- -	- -	Moles/liter	CRA19	PANEL	Yes
SOLMOD4	SOLSOH	Constant	5.45E-08	- -	- -	- -	- -	Moles/liter	CRA19	BRAGFLO, PANEL	Yes
SOLMOD4	SOLSOH2	Constant	5.45E-08	- -	- -	- -	- -	Moles/liter	CRA19	PANEL	Yes
SOLMOD4	SOLSOH3	Constant	5.45E-08	- -	- -	- -	- -	Moles/liter	CRA19	PANEL	Yes
SOLMOD4	SOLSOH4	Constant	5.45E-08	- -	- -	- -	- -	Moles/liter	CRA19	PANEL	Yes
SOLMOD4	SOLSOH5	Constant	5.45E-08	- -	- -	- -	- -	Moles/liter	CRA19	PANEL	Yes
SOLMOD4	SOLVAR	Cumulative	-4.86E-03	-9.96E-02 median	-2.01E+00	1.43E+00	-4.86E-03	None	CRA19	BRAGFLO, PANEL	Yes
SOLMOD5	SOLCOH	Constant	1.20E-06	- -	- -	- -	- -	Moles/liter	CRA19	PANEL	Yes
SOLMOD5	SOLCOH2	Constant	7.27E-07	- -	- -	- -	- -	Moles/liter	CRA19	PANEL	Yes
SOLMOD5	SOLCOH3	Constant	5.52E-07	- -	- -	- -	- -	Moles/liter	CRA19	PANEL	Yes
SOLMOD5	SOLCOH4	Constant	4.61E-07	- -	- -	- -	- -	Moles/liter	CRA19	PANEL	Yes
SOLMOD5	SOLCOH5	Constant	4.05E-07	- -	- -	- -	- -	Moles/liter	CRA19	PANEL	Yes
SOLMOD5	SOLSOH	Constant	4.02E-07	- -	- -	- -	- -	Moles/liter	CRA19	PANEL	Yes
SOLMOD5	SOLSOH2	Constant	2.83E-07	- -	- -	- -	- -	Moles/liter	CRA19	PANEL	Yes
SOLMOD5	SOLSOH3	Constant	2.42E-07	- -	- -	- -	- -	Moles/liter	CRA19	PANEL	Yes
SOLMOD5	SOLSOH4	Constant	2.21E-07	- -	- -	- -	- -	Moles/liter	CRA19	PANEL	Yes

Table B1. Parameter Value Checks for Parameters Used in the CRA-2019 PA that have Changed since the CRA-2014 PA (Continued)

Material Name	Property Name	Distribution Type	Value in Kim & Feng Table 2 ERMS 571660 Rev 1					Parameter Units	Original Analysis	Used in Code	Same Value in PAPDB?
			Constant or Mean	Other	Minimum	Maximum	Default Value				
SOLMOD5	SOLSOH5	Constant	2.09E-07	- -	- -	- -	- -	Moles/liter	CRA19	PANEL	Yes
SR90	INVCHD	Constant	8.18E+02	- -	- -	- -	- -	Curies	CRA19	PANEL	Yes
SR90	INVRHD	Constant	1.96E+05	- -	- -	- -	- -	Curies	CRA19	PANEL	Yes
STEEL	CORRMCO2	Cumulative	1.33E-14	1.12E-14 median	0.00E+00	7.92E-14	1.33E-14	m/s	CRA19	BRAGFLO	Yes
STEEL	HUMCORR	Cumulative	2.43E-16	1.90E-16	0.00E+00	1.03E-15	2.43E-16	m/s	CRA19	BRAGFLO	Yes
SULFATE	QINIT	Constant	4.73E+06	- -	- -	- -	- -	Moles	CRA19	BRAGFLO	Yes
TH	CAPMIC	Constant	3.80E-08	- -	- -	- -	- -	Moles/liter	CRA19	PANEL	Yes
TH	CONCINT	Constant	4.30E-08	- -	- -	- -	- -	Moles/liter	CRA19	PANEL	Yes
TH	PROPMIC	Constant	2.10E-01	- -	- -	- -	- -	None	CRA19	PANEL	Yes
TH229	INVCHD	Constant	3.80E-01	- -	- -	- -	- -	Curies	CRA19	PANEL	Yes
TH229	INVRHD	Constant	8.74E-01	- -	- -	- -	- -	Curies	CRA19	PANEL	Yes
TH230	INVCHD	Constant	3.98E-01	- -	- -	- -	- -	Curies	CRA19	PANEL	Yes
TH230	INVRHD	Constant	2.26E+00	- -	- -	- -	- -	Curies	CRA19	PANEL	Yes
TH230L	INVCHD	Constant	7.78E-01	- -	- -	- -	- -	Curies	CRA19	PANEL	Yes
TH230L	INVRHD	Constant	3.13E+00	- -	- -	- -	- -	Curies	CRA19	PANEL	Yes
TH232	INVCHD	Constant	9.60E-02	- -	- -	- -	- -	Curies	CRA19	PANEL	Yes
TH232	INVRHD	Constant	2.26E-02	- -	- -	- -	- -	Curies	CRA19	PANEL	Yes
U	CAPMIC	Constant	3.80E-08	- -	- -	- -	- -	Moles/liter	CRA19	PANEL	Yes
U	CONCINT	Constant	1.40E-06	- -	- -	- -	- -	Moles/liter	CRA19	PANEL	Yes
U	PROPMIC	Constant	2.10E-01	- -	- -	- -	- -	None	CRA19	PANEL	Yes
U233	INVCHD	Constant	1.10E+02	- -	- -	- -	- -	Curies	CRA19	PANEL	Yes
U233	INVRHD	Constant	1.72E+01	- -	- -	- -	- -	Curies	CRA19	PANEL	Yes
U234	INVCHD	Constant	4.77E+02	- -	- -	- -	- -	Curies	CRA19	PANEL	Yes
U234	INVRHD	Constant	9.70E+00	- -	- -	- -	- -	Curies	CRA19	PANEL	Yes
U234L	INVCHD	Constant	5.86E+02	- -	- -	- -	- -	Curies	CRA19	PANEL	Yes
U234L	INVRHD	Constant	2.69E+01	- -	- -	- -	- -	Curies	CRA19	PANEL	Yes
U235	INVCHD	Constant	4.56E+00	- -	- -	- -	- -	Curies	CRA19	PANEL	Yes
U235	INVRHD	Constant	1.85E+00	- -	- -	- -	- -	Curies	CRA19	PANEL	Yes

Table B1. Parameter Value Checks for Parameters Used in the CRA-2019 PA that have Changed since the CRA-2014 PA (Continued)

Material Name	Property Name	Distribution Type	Value in Kim & Feng Table 2 ERMS 571660 Rev 1					Parameter Units	Original Analysis	Used in Code	Same Value in PAPDB?
			Constant or Mean	Other	Minimum	Maximum	Default Value				
U236	INVCHD	Constant	4.24E-01	--	--	--	--	Curies	CRA19	PANEL	Yes
U236	INVRHD	Constant	2.53E-01	--	--	--	--	Curies	CRA19	PANEL	Yes
U238	INVCHD	Constant	3.92E+01	--	--	--	--	Curies	CRA19	PANEL	Yes
U238	INVRHD	Constant	3.13E+00	--	--	--	--	Curies	CRA19	PANEL	Yes
WAS_AREA	CELCCHW	Constant	1.47E+06	--	--	--	--	kg	CRA19	BRAGFLO	Yes
WAS_AREA	CELCRHW	Constant	0.00E+00	--	--	--	--	kg	CRA19	BRAGFLO	Yes
WAS_AREA	CELECHW	Constant	2.24E+05	--	--	--	--	kg	CRA19	BRAGFLO	Yes
WAS_AREA	CELERHW	Constant	0.00E+00	--	--	--	--	kg	CRA19	BRAGFLO	Yes
WAS_AREA	CELLCHW	Constant	4.10E+06	--	--	--	--	kg	CRA19	BRAGFLO	Yes
WAS_AREA	CELLRHW	Constant	1.70E+05	--	--	--	--	kg	CRA19	BRAGFLO	Yes
WAS_AREA	HYMAGCON	Uniform	1.70E-10	--	0.00E+00	3.40E-10	1.70E-10	mol/(kg*s)	CRA19	BRAGFLO	Yes
WAS_AREA	IRNCCHW	Constant	3.12E+07	--	--	--	--	kg	CRA19	BRAGFLO	Yes
WAS_AREA	IRNCRHW	Constant	1.65E+07	--	--	--	--	kg	CRA19	BRAGFLO	Yes
WAS_AREA	IRONCHW	Constant	1.41E+07	--	--	--	--	kg	CRA19	BRAGFLO	Yes
WAS_AREA	IRONRHW	Constant	1.33E+06	--	--	--	--	kg	CRA19	BRAGFLO	Yes
WAS_AREA	PLASCHW	Constant	5.32E+06	--	--	--	--	kg	CRA19	BRAGFLO	Yes
WAS_AREA	PLASRHW	Constant	4.14E+05	--	--	--	--	kg	CRA19	BRAGFLO	Yes
WAS_AREA	PLSCCHW	Constant	2.83E+06	--	--	--	--	kg	CRA19	BRAGFLO	Yes
WAS_AREA	PLSCRHW	Constant	4.68E+05	--	--	--	--	kg	CRA19	BRAGFLO	Yes
WAS_AREA	PLSECHW	Constant	1.55E+06	--	--	--	--	kg	CRA19	BRAGFLO	Yes
WAS_AREA	PLSERHW	Constant	0.00E+00	--	--	--	--	kg	CRA19	BRAGFLO	Yes
WAS_AREA	RUBBCHW	Constant	1.09E+06	--	--	--	--	kg	CRA19	BRAGFLO	Yes
WAS_AREA	RUBBRHW	Constant	5.12E+04	--	--	--	--	kg	CRA19	BRAGFLO	Yes
WAS_AREA	RUBCCHW	Constant	7.28E+04	--	--	--	--	kg	CRA19	BRAGFLO	Yes
WAS_AREA	RUBCRHW	Constant	5.73E+03	--	--	--	--	kg	CRA19	BRAGFLO	Yes
WAS_AREA	RUBECHW	Constant	4.79E+03	--	--	--	--	kg	CRA19	BRAGFLO	Yes
WAS_AREA	RUBERHW	Constant	0.00E+00	--	--	--	--	kg	CRA19	BRAGFLO	Yes

Table B2. Documentation Checks for Parameters Used in the CRA-2019 PA that have Changed since the CRA-2014 PA

Material Name	Property Name	Parameter Description	Primary Source Document ERMS No.	Supporting Document ERMS No.	EPA Comments
AM	CAPMIC	Americium; maximum mobilized concentration on microbial colloids	571150	571296	ERMS 571150 is the Analysis Plan for the CRA-2019 PA which describes this parameter and its use. The parameter value is described in ERMS 571296 and is based on work by Swanson (2019). The parameter values match.
AM	CONCINT	Americium; intrinsic colloid concentration parameter	571150	571296	The comments for AM:CAPMIC also apply to AM:CONCINT.
AM	PROPMIC	Americium; ratio of moles mobilized on microbial colloids to moles dissolved	571150	571296	The comments for AM:CAPMIC also apply to AM:PROPMIC.
AM241	DECAYNRG	Americium 241; radionuclide decay energy	571150	571244	ERMS 571150 is the Analysis Plan for the CRA-2019 PA which describes this parameter and its use. ERMS 571150 refers to source data found in Table 6 of the Radionuclide Inventory Screening Analysis for the CRA-2019 PA (ERMS 571244). The parameter values match.
AM241	INVCHD	Americium 241; scaled initial inventory in CH waste	571150	571244	ERMS 571150 is the Analysis Plan for the CRA-2019 PA which describes this parameter and its use. ERMS 571150 refers to source data found in Table 5 of the Radionuclide Inventory Screening Analysis for the CRA-2019 PA (ERMS 571244). The parameter values match and are copied from the 2018 Performance Assessment Inventory Report (ERMS 575699).
AM241	INVRHD	Americium 241; scaled initial inventory in RH waste	571150	571244	The comments for AM241:INVCHD also apply to AM241:INVRHD.
AM241L	INVCHD	Americium 241 Lumped with Plutonium 241; scaled initial inventory in CH waste	571150	571244	ERMS 571150 is the Analysis Plan for the CRA-2019 PA which describes this parameter and its use. ERMS 571150 refers to source data found in Table 7 of the Radionuclide Inventory Screening Analysis for the CRA-2019 PA (ERMS 571244). The parameter values match.
AM241L	INVRHD	Americium 241 Lumped with Plutonium 241; scaled initial inventory in RH waste	571150	571244	The comments for AM241L:INVCHD also apply to AM241L:INVRHD.
AM243	INVCHD	Americium 243; scaled initial inventory in CH waste	571150	571244	ERMS 571150 is the Analysis Plan for the CRA-2019 PA which describes this parameter and its use. ERMS 571150 refers to source data found in Table 3 of the Radionuclide Inventory Screening Analysis for the CRA-2019 PA (ERMS 571244). The parameter values match and are copied from the 2018 Performance Assessment Inventory Report (ERMS 575699).
AM243	INVRHD	Americium 243; scaled initial inventory in RH waste	571150	571244	The comments for AM243:INVCHD also apply to AM243:INVRHD.
BH_OPEN	RELP_MOD	Relative permeability model number for an open borehole	571150	- -	ERMS 571150 is the Analysis Plan for the CRA-2019 PA. The value of this parameter was revised as presented and justified in Section 2.1.14. The parameter values match and come from ERMS 570325.

Table B2. Documentation Checks for Parameters Used in the CRA-2019 PA that have Changed since the CRA-2014 PA (Continued)

Material Name	Property Name	Parameter Description	Primary Source Document ERMS No.	Supporting Document ERMS No.	EPA Comments
BOREHOLE	TAUFAIL	Shear strength of degraded waste in borehole wall	567353	- -	The CRA-2019 Input Parameter Report (ERMS 571660) identifies CRA2014_SEN4 as the original analysis in which the parameter BOREHOLE:TAUFAIL was changed. CRA2014_SEN4 is a sensitivity analysis requested by EPA to evaluate the effect on normalized releases resulting from changes to a set of input parameter values that included BOREHOLE:TAUFAIL. The SNL source document ERMS 567353 is a summary of parameters that were changed in the CRA2014_SEN4 analysis. ERMS 567353 identifies ERMS 567343 as documenting correspondence between EPA and DOE requesting the parameter value changes in the CRA2014_SEN4 analysis. The parameter values match.
BOREHOLE	WUF	Borehole; Waste Unit Factor	571150	571244	ERMS 571150 is the Analysis Plan for the CRA-2019 PA which describes this parameter and its use. ERMS 571150 refers to source data found in Table 1 and described in Section 2.2 of the Radionuclide Inventory Screening Analysis for the CRA-2019 PA (ERMS 571244). The parameter values match.
CAVITY_5	CAP_MOD	BRAGFLO startup material for PCS; -5 to 0 years; capillary pressure model number	567353	- -	The CRA-2019 Input Parameter Report (ERMS 571660) identifies CRA2014_SEN4 as the original analysis in which the value of CAVITY_5:CAP_MOD was changed. CRA2014_SEN4 is a sensitivity analysis requested by EPA to evaluate the effect on normalized releases resulting from changes to a set of input parameter values. The SNL source document ERMS 567353 states that the value of this parameter was changed by SNL to facilitate the CRA2014_SEN4 analysis. ERMS 571660 states that CAVITY_5 property values for the CRA-2019 PA are the same as those for CAVITY_4, which were used in the CRA-2014 PA and the parameter values match. ERMS 567353 cites ERMS 560298 as the source of this parameter value. ERMS 560298 was reviewed and found to adequately describe its source.
CAVITY_5	COMP_RCK	BRAGFLO startup material for PCS; -5 to 0 years; bulk compressibility	567353	- -	The comments for CAVITY_5: CAP_MOD also apply to CAVITY_5:COMP_RCK.
CAVITY_5	KPT	BRAGFLO startup material for PCS; -5 to 0 years, Flag to activate the permeability-determined threshold capillary pressure model	566607	- -	The CRA-2019 Input Parameter Report (ERMS 571660) identifies CRA2014_SEN3 as the original analysis in which the parameter CAVITY_5:KPT was added. CRA2014_SEN3 is a sensitivity analysis specified by EPA to evaluate the effect on normalized releases resulting from rapid creep closure and healing of all repository panel closures and adjacent DRZs as well as the Operations and Experimental Areas and their adjacent DRZs. The SNL primary source document ERMS 566607 is a summary of parameters added or changed in the CRA2014_SEN3 sensitivity analysis. CAVITY_5 was a new material developed for the CRA2014_SEN3 analysis. ERMS 566607 refers to ERMS 566571 for documentation of the correspondence between EPA and DOE requesting this analysis. ERMS 571660 states that CAVITY_5 property values for the CRA-2019 PA are the same as those for CAVITY_4, which were used in the CRA-2014 PA. The parameter values match.
CAVITY_5	PCT_A	BRAGFLO startup material for PCS; -5 to 0 years; threshold capillary pressure model linear parameter	567353	- -	The comments for CAVITY_5:CAP_MOD also apply to CAVITY_5:PCT_A.
CAVITY_5	PCT_EXP	BRAGFLO startup material for PCS; -5 to 0 years; threshold capillary pressure model exponential parameter	567353	- -	The comments for CAVITY_5:CAP_MOD also apply to CAVITY_5:PCT_EXP

Table B2. Documentation Checks for Parameters Used in the CRA-2019 PA that have Changed since the CRA-2014 PA (Continued)

Material Name	Property Name	Parameter Description	Primary Source Document ERMS No.	Supporting Document ERMS No.	EPA Comments
CAVITY_5	PC_MAX	BRAGFLO startup material for PCS; -5 to 0 years, maximum allowable capillary pressure	566607	- -	The comments for CAVITY_5:KPT also apply to CAVITY_5:PC-MAX.
CAVITY_5	PORE_DIS	BRAGFLO startup material for PCS; -5 to 0 years, Brooks-Corey pore distribution parameter	566607	- -	The comments for CAVITY_5:KPT also apply to CAVITY_5:PORE_DIS.
CAVITY_5	POROSITY	BRAGFLO startup material for PCS; -5 to 0 years, effective porosity	567353	- -	The comments for CAVITY_5:CAP_MOD also apply to CAVITY_5:POROSITY.
CAVITY_5	PO_MIN	BRAGFLO startup material for PCS; -5 to 0 years, minimum brine pressure for capillary model KPC=3	566607	- -	The comments for CAVITY_5:KPT also apply to CAVITY_5:PO_MIN.
CAVITY_5	PRESSURE	BRAGFLO startup material for PCS; -5 to 0 years, brine far-field pore pressure	566607	- -	The comments for CAVITY_5:KPT also apply to CAVITY_5:PRESSURE.
CAVITY_5	PRMX_LOG	BRAGFLO startup material for PCS; -5 to 0 years, log of intrinsic permeability, X-direction	567353	- -	The comments for CAVITY_5:CAP_MOD also apply to CAVITY_5:PRMX_LOG.
CAVITY_5	PRMY_LOG	BRAGFLO startup material for PCS; -5 to 0 years, log of intrinsic permeability, Y-direction	567353	- -	The comments for CAVITY_5:CAP_MOD also apply to CAVITY_5:PRMY_LOG.
CAVITY_5	PRMZ_LOG	BRAGFLO startup material for PCS; -5 to 0 years, log of intrinsic permeability, Z-direction	567353	- -	The comments for CAVITY_5:CAP_MOD also apply to CAVITY_5:PRMZ_LOG.
CAVITY_5	RELP_MOD	BRAGFLO startup material for PCS; -5 to 0 years; relative permeability model number	567353	- -	The comments for CAVITY_5:CAP_MOD also apply to CAVITY_5:RELP_MOD.
CAVITY_5	SAT_IBRN	BRAGFLO startup material for PCS; -5 to 0 years, initial brine saturation	567353	- -	The comments for CAVITY_5:CAP_MOD also apply to CAVITY_5:SAT_IBRN.
CAVITY_5	SAT_RBRN	BRAGFLO startup material for PCS; -5 to 0 years, residual brine saturation	567353	- -	The comments for CAVITY_5:CAP_MOD also apply to CAVITY_5:SAT_RBRN.

Table B2. Documentation Checks for Parameters Used in the CRA-2019 PA that have Changed since the CRA-2014 PA (Continued)

Material Name	Property Name	Parameter Description	Primary Source Document ERMS No.	Supporting Document ERMS No.	EPA Comments
CAVITY_5	SAT_RGAS	BRAGFLO startup material for PCS; -5 to 0 years, residual gas saturation	567353	- -	The comments for CAVITY_5:CAP_MOD also apply to CAVITY_5:SAT_RGAS.
CF252	INVCHD	Californium 252; scaled initial inventory in CH waste	571150	571244	ERMS 571150 is the Analysis Plan for the CRA-2019 PA which describes this parameter and its use. ERMS 571150 refers to source data found in Table 3 of the Radionuclide Inventory Screening Analysis for the CRA-2019 PA (ERMS 571244). The parameter values match and are copied from the 2018 Performance Assessment Inventory Report (ERMS 575699).
CF252	INVRHD	Californium 252; scaled initial inventory in RH waste	571150	571244	The comments for CF252:INVCHD also apply to CF252:INVRHD.
CM243	INVCHD	Curium 243; scaled initial inventory in CH waste	571150	571244	The comments for CF252:INVCHD also apply to CM243:INVCHD.
CM243	INVRHD	Curium 243; scaled initial inventory in RH waste	571150	571244	The comments for CF252:INVCHD also apply to CM243:INVRHD.
CM244	INVCHD	Curium 244; scaled initial inventory in CH waste	571150	571244	The comments for CF252:INVCHD also apply to CM244:INVCHD.
CM244	INVRHD	Curium 244; scaled initial inventory in RH waste	571150	571244	The comments for CF252:INVCHD also apply to CM244:INVRHD.
CM245	INVCHD	Curium 245; scaled initial inventory in CH waste	571150	571244	The comments for CF252:INVCHD also apply to CM245:INVCHD.
CM245	INVRHD	Curium 245; scaled initial inventory in RH waste	571150	571244	The comments for CF252:INVCHD also apply to CM245:INVRHD.
CM248	INVCHD	Curium 248; scaled initial inventory in CH waste	571150	571244	The comments for CF252:INVCHD also apply to CM248:INVCHD.
CM248	INVRHD	Curium 248; scaled initial inventory in RH waste	571150	571244	The comments for CF252:INVCHD also apply to CM248:INVRHD.
CS137	INVCHD	Cesium 137; scaled initial inventory in CH waste	571150	571244	The comments for CF252:INVCHD also apply to CS137:INVCHD.
CS137	INVRHD	Cesium 137; scaled initial inventory in RH waste	571150	571244	The comments for CF252:INVCHD also apply to CS137:INVRHD.
DRZ_OE_0	CAP_MOD	Capillary pressure model number for the DRZ around the OPS and EXP areas from -5 to 0 years	567353	- -	The CRA-2019 Input Parameter Report (ERMS 571660) identifies CRA2014_SEN4 as the original analysis in which the value of DRZ_OE_0:CAP_MOD was changed. CRA2014_SEN4 is a sensitivity analysis requested by EPA to evaluate the effect on normalized releases resulting from changes to a set of input parameter values. The SNL source document ERMS 567353 states that the value of this parameter was changed by SNL to facilitate the CRA2014_SEN4 analysis and provides the property values associated with this material. ERMS 571660 states that the property values for DRZ_OE_0 used in the CRA-2019 PA are the same as those used for DRZ_0 in the CRA-2014 PA. ERMS 567353 cites ERMS 560298 as the source of this parameter value. The parameter values match and ERMS 560298 was found to adequately describe their source.

Table B2. Documentation Checks for Parameters Used in the CRA-2019 PA that have Changed since the CRA-2014 PA (Continued)

Material Name	Property Name	Parameter Description	Primary Source Document ERMS No.	Supporting Document ERMS No.	EPA Comments
DRZ_OE_0	COMP_RCK	Bulk compressibility of the DRZ around the OPS and EXP areas from -5 to 0 years	567353	- -	The comments for DRZ_OE_0:CAP_MOD also apply to DRZ_OE_0:COMP_RCK.
DRZ_OE_0	KPT	Flag to activate the permeability-determined capillary pressure threshold model for the DRZ around the OPS and EXP areas from -5 to 0 years	565722	- -	The CRA-2019 Input Parameter Report (ERMS 571660) identifies CRA2014_SEN2 as the original analysis in which parameter DRZ_OE_0:KPT was added. CRA2014_SEN2 is a sensitivity analysis requested by EPA to evaluate the effect on normalized releases resulting from rapid creep closure and healing of the Operations and Experimental Areas and their adjacent DRZs. The SNL primary source document ERMS 565722 is a summary of parameters added or changed in the CRA2014_SEN2 analysis. DRZ_OE_0 is a new material developed for the CRA2014_SEN2 analysis. ERMS 565722 refers to ERMS 565676 for documentation of the correspondence between EPA and DOE requesting this analysis. The parameter values match.
DRZ_OE_0	PCT_A	Threshold capillary pressure model linear parameter for the DRZ around the OPS and EXP areas from -5 to 0 years	567353	- -	The comments for DRZ_OE_0:CAP_MOD also apply to DRZ_OE_0:PCT_A.
DRZ_OE_0	PCT_EXP	Threshold capillary pressure model exponential parameter for the DRZ around the OPS and EXP areas from -5 to 0 years	567353	- -	The comments for DRZ_OE_0:CAP_MOD also apply to DRZ_OE_0:PCT_EXP.
DRZ_OE_0	PC_MAX	Maximum allowable capillary pressure for the DRZ around the OPS and EXP areas from -5 to 0 years	565722	- -	The comments for DRZ_OE_0:KPT also apply to DRZ_OE_0:PC_MAX.
DRZ_OE_0	PORE_DIS	Brooks-Corey pore distribution parameter for the DRZ around the OPS and EXP areas from -5 to 0 years	565722	- -	The comments for DRZ_OE_0:KPT also apply to DRZ_OE_0:PORE_DIS.
DRZ_OE_0	POROSITY	Effective porosity of the DRZ around the OPS and EXP areas from -5 to 0 years	567353	- -	The comments for DRZ_OE_0:CAP_MOD also apply to DRZ_OE_0:POROSITY.
DRZ_OE_0	PO_MIN	Minimum brine pressure for capillary pressure model KPC =3, in the DRZ around the OPS and EXP areas from -5 to 0 years	565722	- -	The comments for DRZ_OE_0:KPT also apply to DRZ_OE_0:PO_MIN.

Table B2. Documentation Checks for Parameters Used in the CRA-2019 PA that have Changed since the CRA-2014 PA (Continued)

Material Name	Property Name	Parameter Description	Primary Source Document ERMS No.	Supporting Document ERMS No.	EPA Comments
DRZ_OE_0	PRMX_LOG	Log of intrinsic permeability, x-direction, in the DRZ around the OPS and EXP areas from -5 to 0 years	567353	- -	The comments for DRZ_OE_0:CAP_MOD also apply to DRZ_OE_0:PRMX_LOG.
DRZ_OE_0	PRMY_LOG	Log of intrinsic permeability, y-direction, in the DRZ around the OPS and EXP areas from -5 to 0 years	567353	- -	The comments for DRZ_OE_0:CAP_MOD also apply to DRZ_OE_0:PRMY_LOG.
DRZ_OE_0	PRMZ_LOG	Log of intrinsic permeability, z-direction, in the DRZ around the OPS and EXP areas from -5 to 0 years	567353	- -	The comments for DRZ_OE_0:CAP_MOD also apply to DRZ_OE_0:PRMZ_LOG.
DRZ_OE_0	RELP_MOD	Relative permeability model number for the DRZ around the OPS and EXP areas from -5 to 0 years	565722	- -	The comments for DRZ_OE_0:KPT also apply to DRZ_OE_0:RELP_MOD.
DRZ_OE_0	SAT_IBRN	Initial brine saturation in the DRZ around the OPS and EXP areas from -5 to 0 years	567353	- -	The comments for DRZ_OE_0:CAP_MOD also apply to DRZ_OE_0:SAT_IBRN.
DRZ_OE_0	SAT_RBRN	Residual brine saturation in the DRZ around the OPS and EXP areas from -5 to 0 years	567353	- -	The comments for DRZ_OE_0:CAP_MOD also apply to DRZ_OE_0:SAT_RBRN.
DRZ_OE_0	SAT_RGAS	Residual gas saturation in the DRZ around the OPS and EXP areas from -5 to 0 years	567353	- -	The comments for DRZ_OE_0:CAP_MOD also apply to DRZ_OE_0:SAT_RGAS.
DRZ_OE_1	CAP_MOD	Capillary pressure model number for the DRZ around the OPS and EXP areas from 0 to 10,000 years	567353	- -	The CRA-2019 Input Parameter Report (ERMS 571660) identifies CRA2014_SEN4 as the original analysis in which the value of DRZ_OE_1:CAP_MOD was changed. CRA2014_SEN4 is a sensitivity analysis requested by EPA to evaluate the effect on normalized releases resulting from changes to a set of input parameter values. The SNL source document ERMS 567353 states that the value of this parameter was changed by SNL to facilitate the CRA2014_SEN4 analysis and provides the property values associated with this material. ERMS 571660 states that the property values for DRZ_OE_1 used in the CRA-2019 PA are the same as those used for DRZ_1 in the CRA-2014 PA. ERMS 567353 cites ERMS 560298 as the source of this parameter value. The parameter values match and ERMS 560298 was found to adequately describe its source.

Table B2. Documentation Checks for Parameters Used in the CRA-2019 PA that have Changed since the CRA-2014 PA (Continued)

Material Name	Property Name	Parameter Description	Primary Source Document ERMS No.	Supporting Document ERMS No.	EPA Comments
DRZ_OE_1	COMP_RCK	Bulk compressibility of the DRZ around the OPS and EXP areas from 0 to 10,000 years	567353	- -	The comments for DRZ_OE_1:CAP_MOD also apply to DRZ_OE_1:COMP_RCK.
DRZ_OE_1	KPT	Flag to activate the permeability-determined capillary pressure threshold model for the DRZ around the OPS and EXP areas from 0 to 10,000 years	565722	- -	The CRA-2019 Input Parameter Report (ERMS 571660) identifies CRA2014_SEN2 as the original analysis in which the parameter DRZ_OE_1:KPT was added. CRA2014_SEN2 is a sensitivity analysis requested by EPA to evaluate the effect on normalized releases resulting from rapid creep closure and healing of the Operations and Experimental Areas and their adjacent DRZs. The SNL primary source document ERMS 565722 is a summary of parameters added or changed in the CRA2014_SEN2 analysis and the parameter values match. DRZ_OE_1 is a new material developed for the CRA2014_SEN2 analysis. ERMS 565722 refers to ERMS 565676 for documentation of the correspondence between EPA and DOE requesting this analysis.
DRZ_OE_1	PCT_A	Threshold capillary pressure model linear parameter for the DRZ around the OPS and EXP areas from 0 to 10,000 years	567353	- -	The comments for DRZ_OE_1:CAP_MOD also apply to DRZ_OE_1:PCT_A.
DRZ_OE_1	PCT_EXP	Threshold capillary pressure model exponential parameter for the DRZ around the OPS and EXP areas from 0 to 10,000 years	567353	- -	The comments for DRZ_OE_1:CAP_MOD also apply to DRZ_OE_1:PCT_EXP.
DRZ_OE_1	PC_MAX	Maximum allowable capillary pressure for the DRZ around the OPS and EXP areas from 0 to 10,000 years	565722	- -	The comments for DRZ_OE_1:KPT also apply to DRZ_OE_1:PC_MAX.
DRZ_OE_1	PORE_DIS	Brooks-Corey pore distribution parameter for the DRZ around the OPS and EXP areas from 0 to 10,000 years	565722	- -	The comments for DRZ_OE_1:KPT also apply to DRZ_OE_1:PORE_DIS.
DRZ_OE_1	POROSITY	Effective porosity of the DRZ around the OPS and EXP areas from 0 to 10,000 years	567353	- -	The comments for DRZ_OE_1:CAP_MOD also apply to DRZ_OE_1:POROSITY
DRZ_OE_1	PO_MIN	Minimum brine pressure for capillary pressure model KPC =3, in the DRZ around the OPS and EXP areas from 0 to 10,000 years	565722	- -	The comments for DRZ_OE_1:KPT also apply to DRZ_OE_1:PO_MIN.

Table B2. Documentation Checks for Parameters Used in the CRA-2019 PA that have Changed since the CRA-2014 PA (Continued)

Material Name	Property Name	Parameter Description	Primary Source Document ERMS No.	Supporting Document ERMS No.	EPA Comments
DRZ_OE_1	PRMX_LOG	Log of intrinsic permeability, x-direction, in the DRZ around the OPS and EXP areas from 0 to 10,000 years	567353	- -	The comments for DRZ_OE_1:CAP_MOD also apply to DRZ_OE_1:PRMX_LOG.
DRZ_OE_1	PRMY_LOG	Log of intrinsic permeability, y-direction, in the DRZ around the OPS and EXP areas from 0 to 10,000 years	567353	- -	The comments for DRZ_OE_1:CAP_MOD also apply to DRZ_OE_1: PRMY_LOG.
DRZ_OE_1	PRMZ_LOG	Log of intrinsic permeability, z-direction, in the DRZ around the OPS and EXP areas from 0 to 10,000 years	567353	- -	The comments for DRZ_OE_1:CAP_MOD also apply to DRZ_OE_1: PRMZ_LOG.
DRZ_OE_1	RELP_MOD	Relative permeability model number for the DRZ around the OPS and EXP areas from 0 to 10,000 years	565722	- -	The comments for DRZ_OE_1:KPT also apply to DRZ_OE_1:RELP_MOD.
DRZ_OE_1	SAT_IBRN	Initial brine saturation in the DRZ around the OPS and EXP areas from 0 to 10,000 years	567353	- -	The comments for DRZ_OE_1:CAP_MOD also apply to DRZ_OE_1:SAT_IBRN.
DRZ_OE_1	SAT_RBRN	Residual brine saturation in the DRZ around the OPS and EXP areas from 0 to 10,000 years	567353	- -	The comments for DRZ_OE_1:CAP_MOD also apply to DRZ_OE_1:SAT_RBRN.
DRZ_OE_1	SAT_RGAS	Residual gas saturation in the DRZ around the OPS and EXP areas from 0 to 10,000 years	567353	- -	The comments for DRZ_OE_1:CAP_MOD also apply to DRZ_OE_1:SAT_RGAS.
DRZ_PC_0	CAP_MOD	Capillary pressure model number for the DRZ around active panel closures from -5 to 0 years	567353	- -	The CRA-2019 Input Parameter Report (ERMS 571660) identifies CRA2014_SEN4 as the original analysis in which the value of DRZ_PC_0:CAP_MOD was changed. CRA2014_SEN4 is a sensitivity analysis requested by EPA to evaluate the effect on normalized releases resulting from changes to a set of input parameter values. The SNL source document ERMS 567353 states that the value of this parameter was changed by SNL to facilitate the CRA2014_SEN4 analysis and provides the property values associated with this material. ERMS 567353 cites ERMS 560298 as the source of this parameter value. The parameter values match and ERMS 560298 was found to adequately describe its source.

Table B2. Documentation Checks for Parameters Used in the CRA-2019 PA that have Changed since the CRA-2014 PA (Continued)

Material Name	Property Name	Parameter Description	Primary Source Document ERMS No.	Supporting Document ERMS No.	EPA Comments
DRZ_PC_0	COMP_RCK	Bulk compressibility of the DRZ around active panel closures from -5 to 0 years	567353	- -	The comments for DRZ_PC_0:CAP_MOD also apply to DRZ_PC_0:COMP_RCK.:
DRZ_PC_0	KPT	Flag to activate the permeability-determined capillary pressure threshold model for the DRZ around active panel closures from -5 to 0 years	566607	- -	The CRA-2019 Input Parameter Report (ERMS 571660) identifies CRA2014_SEN3 as the original analysis in which the parameter DRZ_PC_0:KPT was added. CRA2014_SEN3 is a sensitivity analysis specified by EPA to evaluate the effect on normalized releases resulting from rapid creep closure and healing of all repository panel closures and adjacent DRZs as well as the Operations and Experimental Areas and their adjacent DRZs. The SNL primary source document ERMS 566607 is a summary of parameters added or changed in the CRA2014_SEN3 sensitivity analysis and the parameter values match. DRZ_PC_0 is a new material developed for the CRA2014_SEN3 analysis. ERMS 566607 refers to ERMS 566571 for documentation of the correspondence between EPA and DOE requesting this analysis.
DRZ_PC_0	PCT_A	Threshold capillary pressure model linear parameter for the DRZ around active panel closures from -5 to 0 years	567353	- -	The comments for DRZ_PC_0:CAP_MOD also apply to DRZ_PC_0:PCT_A.
DRZ_PC_0	PCT_EXP	Threshold capillary pressure model exponential parameter for the DRZ around active panel closures from -5 to 0 years	567353	- -	The comments for DRZ_PC_0:CAP_MOD also apply to DRZ_PC_0:PCT_EXP.
DRZ_PC_0	PC_MAX	Maximum allowable capillary pressure for the DRZ around active panel closures from -5 to 0 years	566607	- -	The comments for DRZ_PC_0:KPT also apply to DRZ_PC_0:PC_MAX.
DRZ_PC_0	PORE_DIS	Brooks-Corey pore distribution parameter for the DRZ around active panel closures from -5 to 0 years	566607	- -	The comments for DRZ_PC_0:KPT also apply to DRZ_PC_0:PORE_DIS.
DRZ_PC_0	POROSITY	Effective porosity of the DRZ around active panel closures from -5 to 0 years	567353	- -	The comments for DRZ_PC_0:CAP_MOD also apply to DRZ_PC_0:POROSITY.
DRZ_PC_0	PO_MIN	Minimum brine pressure for capillary pressure model KPC =3, in the DRZ around active panel closures from -5 to 0 years	566607	- -	The comments for DRZ_PC_0:KPT also apply to DRZ_PC_0:PO_MIN.

Table B2. Documentation Checks for Parameters Used in the CRA-2019 PA that have Changed since the CRA-2014 PA (Continued)

Material Name	Property Name	Parameter Description	Primary Source Document ERMS No.	Supporting Document ERMS No.	EPA Comments
DRZ_PC_0	PRMX_LOG	Log of intrinsic permeability, x-direction, in the DRZ around active panel closures from -5 to 0 years	567353	- -	The comments for DRZ_PC_0:CAP_MOD also apply to DRZ_PC_0:PRMX_LOG.
DRZ_PC_0	PRMY_LOG	Log of intrinsic permeability, y-direction, in the DRZ around active panel closures from -5 to 0 years	567353	- -	The comments for DRZ_PC_0:CAP_MOD also apply to DRZ_PC_0:PRMY_LOG.
DRZ_PC_0	PRMZ_LOG	Log of intrinsic permeability, z-direction, in the DRZ around active panel closures from -5 to 0 years	567353	- -	The comments for DRZ_PC_0:CAP_MOD also apply to DRZ_PC_0:PEMZ_LOG.
DRZ_PC_0	RELP_MOD	Relative permeability model number for the DRZ around active panel closures from -5 to 0 years	566607	- -	The comments for DRZ_PC_0:KPT also apply to DRZ_PC_0:RELP_MOD.
DRZ_PC_0	SAT_IBRN	Initial brine saturation in the DRZ around active panel closures from -5 to 0 years	567353	- -	The comments for DRZ_PC_0:CAP_MOD also apply to DRZ_PC_0:SAT_IBRN.
DRZ_PC_0	SAT_RBRN	Residual brine saturation in the DRZ around active panel closures from -5 to 0 years	567353	- -	The comments for DRZ_PC_0:CAP_MOD also apply to DRZ_PC_0:SAT_RBRN.
DRZ_PC_0	SAT_RGAS	Residual gas saturation in the DRZ around active panel closures from -5 to 0 years	567353	- -	The comments for DRZ_PC_0:CAP_MOD also apply to DRZ_PC_0:SAT_RGAS.
DRZ_PC_1	CAP_MOD	Capillary pressure model number for the DRZ around active panel closures from 0 to 10,000 years	567353	- -	The CRA-2019 Input Parameter Report (ERMS 571660) identifies CRA2014_SEN4 as the original analysis in which the value of DRZ_PC_1:CAP_MOD was changed. CRA2014_SEN4 is a sensitivity analysis requested by EPA to evaluate the effect on normalized releases resulting from changes to a set of input parameter values. The SNL source document ERMS 567353 states that the value of this parameter was changed by SNL to facilitate the CRA2014_SEN4 analysis and provides the property values associated with this material. ERMS 567353 cites ERMS 560298 as the source of this parameter value. The parameter values match and ERMS 560298 was found to adequately describe its source.
DRZ_PC_1	COMP_RCK	Bulk compressibility of the DRZ around active panel closures from 0 to 10,000 years	567353	- -	The comments for DRZ_PC_1:CAP_MOD also apply to DRZ_PC_1:COMP_RCK.

Table B2. Documentation Checks for Parameters Used in the CRA-2019 PA that have Changed since the CRA-2014 PA (Continued)

Material Name	Property Name	Parameter Description	Primary Source Document ERMS No.	Supporting Document ERMS No.	EPA Comments
DRZ_PC_1	KPT	Flag to activate the permeability-determined capillary pressure threshold model for the DRZ around active panel closures from 0 to 10,000 years	566607	- -	The CRA-2019 Input Parameter Report (ERMS 571660) identifies CRA2014_SEN3 as the original analysis in which the parameter DRZ_PC_1:KPT was added. CRA2014_SEN3 is a sensitivity analysis specified by EPA to evaluate the effect on normalized releases resulting from rapid creep closure and healing of all repository panel closures and adjacent DRZs as well as the Operations and Experimental Areas and their adjacent DRZs. The SNL primary source document ERMS 566607 is a summary of parameters added or changed in the CRA2014_SEN3 sensitivity analysis and the parameter values match. DRZ_PC_1 is a new material developed for the CRA2014_SEN3 analysis. ERMS 566607 refers to ERMS 566571 for documentation of the correspondence between EPA and DOE requesting this analysis.
DRZ_PC_1	PCT_A	Threshold capillary pressure model linear parameter for the DRZ around active panel closures from 0 to 10,000 years	567353	- -	The comments for DRZ_PC_1:CAP_MOD also apply to DRZ_PC_1:PCT_A.
DRZ_PC_1	PCT_EXP	Threshold capillary pressure model exponential parameter for the DRZ around active panel closures from 0 to 10,000 years	567353	- -	The comments for DRZ_PC_1:CAP_MOD also apply to DRZ_PC_1:PCT_EXP.
DRZ_PC_1	PC_MAX	Maximum allowable capillary pressure for the DRZ around active panel closures from 0 to 10,000 years	566607	- -	The comments for DRZ_PC_1:KPT also apply to DRZ_PC_1:PC_MAX.
DRZ_PC_1	PORE_DIS	Brooks-Corey pore distribution parameter for the DRZ around active panel closures from 0 to 10,000 years	566607	- -	The comments for DRZ_PC_1:KPT also apply to DRZ_PC_1:PORE_DIS.
DRZ_PC_1	POROSITY	Effective porosity of the DRZ around active panel closures from 0 to 10,000 years	567353	- -	The comments for DRZ_PC_1:CAP_MOD also apply to DRZ_PC_1:POROSITY.
DRZ_PC_1	PO_MIN	Minimum brine pressure for capillary pressure model KPC =3, in the DRZ around active panel closures from 0 to 10,000 years	566607	- -	The comments for DRZ_PC_1:KPT also apply to DRZ_PC_1:PO_MIN.

Table B2. Documentation Checks for Parameters Used in the CRA-2019 PA that have Changed since the CRA-2014 PA (Continued)

Material Name	Property Name	Parameter Description	Primary Source Document ERMS No.	Supporting Document ERMS No.	EPA Comments
DRZ_PC_1	PRMX_LOG	Log of intrinsic permeability, x-direction, in the DRZ around active panel closures from 0 to 10,000 years	567353	- -	The comments for DRZ_PC_1:CAP_MOD also apply to DRZ_PC_1:PRMX_LOG.
DRZ_PC_1	PRMY_LOG	Log of intrinsic permeability, y-direction, in the DRZ around active panel closures from 0 to 10,000 years	567353	- -	The comments for DRZ_PC_1:CAP_MOD also apply to DRZ_PC_1:PRMY_LOG.
DRZ_PC_1	PRMZ_LOG	Log of intrinsic permeability, z-direction, in the DRZ around active panel closures from 0 to 10,000 years	567353	- -	The comments for DRZ_PC_1:CAP_MOD also apply to DRZ_PC_1:PRMZ_LOG.
DRZ_PC_1	RELP_MOD	Relative permeability model number for the DRZ around active panel closures from 0 to 10,000 years	566607	- -	The comments for DRZ_PC_1:KPT also apply to DRZ_PC_1:RELP_MOD.
DRZ_PC_1	SAT_IBRN	Initial brine saturation in the DRZ around active panel closures from 0 to 10,000 years	567353	- -	The comments for DRZ_PC_1:CAP_MOD also apply to DRZ_PC_1:SAT_IBRN.
DRZ_PC_1	SAT_RBRN	Residual brine saturation in the DRZ around active panel closures from 0 to 10,000 years	567353	- -	The comments for DRZ_PC_1:CAP_MOD also apply to DRZ_PC_1:SAT_RBRN.
DRZ_PC_1	SAT_RGAS	Residual gas saturation in the DRZ around active panel closures from 0 to 10,000 years	567353	- -	The comments for DRZ_PC_1:CAP_MOD also apply to DRZ_PC_1:SAT_RGAS.
GLOBAL	GDEPFAC	Energy deposition probability for wetted solid radionuclides	571150	- -	ERMS 571150 is the Analysis Plan for the CRA-2019 PA. The values for this parameter are described in Section 2.1.3 and listed in Table 2-5. The parameter values match and come from ERMS 570873.
GLOBAL	GH2AVG	Brine radiolysis G-value - $G(H_2)$	571150	- -	ERMS 571150 is the Analysis Plan for the CRA-2019 PA. The values for this parameter are described in Section 2.1.3 and listed in Table 2-5. The parameter values match and come from Reed et al. (1993).
GLOBAL	LAMBDAD	Drilling rate per unit area	571150	- -	ERMS 571150 is the Analysis Plan for the CRA-2019 PA. The values for this parameter are described in Section 2.1.11 and listed in Table 2-13. The parameter values match and come from DOE (2018).
GLOBAL	ONEPLG	Probability of having Plug Pattern 1	571150	- -	ERMS 571150 is the Analysis Plan for the CRA-2019 PA. The values for this parameter are described in Section 2.1.11 and listed in Table 2-13. The parameter values match and come from DOE (2018).

Table B2. Documentation Checks for Parameters Used in the CRA-2019 PA that have Changed since the CRA-2014 PA (Continued)

Material Name	Property Name	Parameter Description	Primary Source Document ERMS No.	Supporting Document ERMS No.	EPA Comments
GLOBAL	PBRINE	Probability that an intrusion borehole encounters pressurized Castile brine	567353	- -	The CRA-2019 Input Parameter Report (ERMS 571660) identifies CRA2014_SEN4 as the original analysis in which the value of GLOBAL:PBRINE was changed. CRA2014_SEN4 is a sensitivity analysis requested by EPA to evaluate the effect on normalized releases resulting from changes to a set of input parameter values. The SNL source document ERMS 567353 provides the property values associated with this material. ERMS 567353 cites ERMS 560298 as the source of this parameter value. The parameter values match and ERMS 560298 was found to adequately describe its source.
GLOBAL	SRADO2	Stoichiometric coefficient for O_2 from radiolysis	571150	- -	ERMS 571150 is the Analysis Plan for the CRA-2019 PA. The values for this parameter are described in Section 2.1.3 and listed in Table 2-5. The parameter values match and come from ERMS 570873.
GLOBAL	THREEPLG	Probability of having Plug Pattern 3	571150	- -	ERMS 571150 is the Analysis Plan for the CRA-2019 PA. The values for this parameter are described in Section 2.1.11 and listed in Table 2-13. The parameter values match and come from DOE (2018).
GLOBAL	TWOPLG	Probability of having Plug Pattern 2	571150	- -	ERMS 571150 is the Analysis Plan for the CRA-2019 PA. The values for this parameter are described in Section 2.1.11 and listed in Table 2-13. The parameter values match and come from DOE (2018).
NITRATE	QINIT	Nitrate; scaled initial inventory in waste	571150	571244	ERMS 571150 is the Analysis Plan for the CRA-2019 PA which describes this parameter and its use. ERMS 571150 refers to source data found in Section 6 and Appendix D, Table D-5 of the Radionuclide Inventory Screening Analysis for the CRA-2019 PA (ERMS 571244). The parameter values match and are copied from the 2018 Performance Assessment Inventory Report (ERMS 575699).
NP	CAPMIC	Neptunium; maximum mobilized concentration on microbial colloids	571150	571296	ERMS 571150 is the Analysis Plan for the CRA-2019 PA which describes this parameter and its use. The parameter value is described in ERMS 571296 and is based on work by Reed et al. (2013). The parameter values match.
NP	CONCINT	Neptunium; Americium; intrinsic colloid concentration parameter	571150	571296	The comments for NP:CAPMIC also apply to NP:CONCINT.
NP	PROPMIC	Neptunium; ratio of moles mobilized on microbial colloids to moles dissolved	571150	571296	The comments for NP:CAPMIC also apply to NP:PROPMIC.
NP237	INVCHD	Neptunium 237; scaled initial inventory in CH waste	571150	571244	ERMS 571150 is the Analysis Plan for the CRA-2019 PA which describes this parameter and its use. ERMS 571150 refers to data found in Table 3 of the Radionuclide Inventory Screening Analysis for the CRA-2019 PA (ERMS 571244). The parameter values match and are copied from the 2018 Performance Assessment Inventory Report (ERMS 575699).
NP237	INVRHD	Neptunium 237; scaled initial inventory in RH waste	571150	571244	The comments for NP237:INVCHD also apply to NP237:INVRHD.
PA231	INVCHD	Protactinium 231; scaled initial inventory in CH waste	571150	571244	The comments for NP237:INVCHD also apply to PA231:INVCHD.
PA231	INVRHD	Protactinium 231; scaled initial inventory in RH waste	571150	571244	The comments for NP237:INVCHD also apply to PA231:INVRHD.
PB210	INVCHD	Lead 210; scaled initial inventory in CH waste	571150	571244	The comments for NP237:INVCHD also apply to PB210:INVCHD.

Table B2. Documentation Checks for Parameters Used in the CRA-2019 PA that have Changed since the CRA-2014 PA (Continued)

Material Name	Property Name	Parameter Description	Primary Source Document ERMS No.	Supporting Document ERMS No.	EPA Comments
PB210	INVRHD	Lead 210; scaled initial inventory in RH waste	571150	571244	The comments for NP237:INVCHD also apply to PB210:INVRHD.
PCS_NO	CAP_MOD	Abandoned panel closure areas, Model number, capillary pressure model	568138	- -	The CRA-2019 Input Parameter Report (ERMS 571660) identifies the APCS as the original analysis in which the parameter PCS_NO:CAP_MOD was added. The SNL source document ERMS 568138 is the Analysis Plan for that analysis. The purpose of the APCS analysis is described in ERMS 568138 as demonstrating the effects on WIPP PA of incorporating the "APCS approach" for modeling abandoned panel closures. PCS_NO is a new material developed for the APCS analysis. The parameter values match and ERMS 568138 was found to adequately explain and justify the parameter values associated with this material.
PCS_NO	COMP_RCK	Abandoned panel closure areas; bulk compressibility	568138	- -	The comments for PCS_NO:CAP_MOD also apply to PCS_NO:COMP_RCK.
PCS_NO	KPT	Abandoned panel closure areas; flag to activate the permeability-determined capillary pressure threshold model	568138	- -	The comments for PCS_NO:CAP_MOD also apply to PCS_NO:KPT.
PCS_NO	PCT_A	Abandoned panel closure areas; threshold capillary pressure model linear parameter	568138	- -	The comments for PCS_NO:CAP_MOD also apply to PCS_NO:PCT_A.
PCS_NO	PCT_EXP	Abandoned panel closure areas; threshold capillary pressure model exponential parameter	568138	- -	The comments for PCS_NO:CAP_MOD also apply to PCS_NO:PCT_EXP.
PCS_NO	PC_MAX	Abandoned panel closure areas; maximum allowable capillary pressure	568138	- -	The comments for PCS_NO:CAP_MOD also apply to PCS_NO:PC_MAX.
PCS_NO	PORE_DIS	Abandoned panel closure areas; Brooks-Corey pore distribution parameter	568138	- -	The comments for PCS_NO:CAP_MOD also apply to PCS_NO:PORE_DIS.
PCS_NO	POROSITY	Abandoned panel closure areas, Effective porosity	568138	- -	The comments for PCS_NO:CAP_MOD also apply to PCS_NO:POROSITY.
PCS_NO	PO_MIN	Abandoned panel closure areas; minimum brine pressure for capillary model KPC=3	568138	- -	The comments for PCS_NO:CAP_MOD also apply to PCS_NO:PO_MIN.
PCS_NO	PRESSURE	Abandoned panel closure areas; brine far-field pore pressure	568138	- -	The comments for PCS_NO:CAP_MOD also apply to PCS_NO:PRESSURE.

Table B2. Documentation Checks for Parameters Used in the CRA-2019 PA that have Changed since the CRA-2014 PA (Continued)

Material Name	Property Name	Parameter Description	Primary Source Document ERMS No.	Supporting Document ERMS No.	EPA Comments
PCS_NO	PRMX_LOG	Abandoned panel closure areas; log of intrinsic permeability, X-direction	568138	- -	The comments for PCS_NO:CAP_MOD also apply to PCS_NO:PRMX_LOG.
PCS_NO	PRMY_LOG	Abandoned panel closure areas; log of intrinsic permeability, Y-direction	568138	- -	The comments for PCS_NO:CAP_MOD also apply to PCS_NO:PRMY_LOG.
PCS_NO	PRMZ_LOG	Abandoned panel closure areas; log of intrinsic permeability, Z-direction	568138	- -	The comments for PCS_NO:CAP_MOD also apply to PCS_NO:PRMZ_LOG.
PCS_NO	RELP_MOD	Abandoned panel closure areas; relative permeability model number	568138	- -	The comments for PCS_NO:CAP_MOD also apply to PCS_NO:RELP_MOD.
PCS_NO	SAT_IBRN	Abandoned panel closure areas; initial brine saturation	568138	- -	The comments for PCS_NO:CAP_MOD also apply to PCS_NO:SAT_IBRN.
PCS_NO	SAT_RBRN	Abandoned panel closure areas; residual brine saturation	568138	- -	The comments for PCS_NO:CAP_MOD also apply to PCS_NO:SAT_RBRN.
PCS_NO	SAT_RGAS	Abandoned panel closure areas; residual gas saturation	568138	- -	The comments for PCS_NO:CAP_MOD also apply to PCS_NO:SAT_RGAS.
PHUMOX3	PHUMCIM	Proportionality constant for humic colloids for +III actinides in Castile brine	571150	571250	ERMS 571150 is the Analysis Plan for the CRA-2019 PA which describes this parameter and its use. The parameter value is provided in ERMS 571250 and is based on calculations in ERMS 569599 and ERMS 567222. The parameter values match.
PHUMOX3	PHUMSIM	Proportionality constant for humic colloids for +III actinides in Salado brine	571150	571250	The comments for PHUMOX3:PHUMCIM also apply to PHUMOX3:PHUMSIM.
PHUMOX4	PHUMCIM	Proportionality constant for humic colloids for +IV actinides in Castile brine	571150	571250	The comments for PHUMOX3:PHUMCIM also apply to PHUMOX4:PHUMCIM.
PHUMOX4	PHUMSIM	Proportionality constant for humic colloids for +IV actinides in Salado brine	571150	571250	The comments for PHUMOX3:PHUMCIM also apply to PHUMOX4:PHUMSIM.
PM147	INVCHD	Promethium 147; scaled initial inventory in CH waste	571150	571244	ERMS 571150 is the Analysis Plan for the CRA-2019 PA which describes this parameter and its use. ERMS 571150 refers to data found in Table 3 of the Radionuclide Inventory Screening Analysis for the CRA-2019 PA (ERMS 571244). The parameter values match and are copied from the 2018 Performance Assessment Inventory Report (ERMS 575699).
PM147	INVRHD	Promethium 147; scaled initial inventory in RH waste	571150	571244	The comments for PM147:INVCHD also apply to PM147:INVRHD.

Table B2. Documentation Checks for Parameters Used in the CRA-2019 PA that have Changed since the CRA-2014 PA (Continued)

Material Name	Property Name	Parameter Description	Primary Source Document ERMS No.	Supporting Document ERMS No.	EPA Comments
PU	CAPMIC	Plutonium; maximum mobilized concentration on microbial colloids	571150	571296	ERMS 571150 is the Analysis Plan for the CRA-2019 PA which describes this parameter and its use. The parameter value is described in ERMS 571296 and is based on work by Reed et al. (2013). The parameter values match.
PU	CONCINT	Plutonium; intrinsic colloid concentration parameter	571150	571296	The comments for PU:CAPMIC also apply to PU:CONCINT.
PU	PROPMIC	Plutonium; ratio of moles mobilized on microbial colloids to moles dissolved	571150	571296	The comments for PU:CAPMIC also apply to PU:PROPMIC.
PU238	DECAYNRG	Plutonium 238; radionuclide decay energy	571150	571244	ERMS 571150 is the Analysis Plan for the CRA-2019 PA which describes this parameter and its use. ERMS 571150 refers to data found in Table 6 of the Radionuclide Inventory Screening Analysis for the CRA-2019 PA (ERMS 571244). The parameter values match.
PU238	INVCHD	Plutonium 238; scaled initial inventory in CH waste	571150	571244	ERMS 571150 is the Analysis Plan for the CRA-2019 PA which describes this parameter and its use. ERMS 571150 refers to data found in Table 3 of the Radionuclide Inventory Screening Analysis for the CRA-2019 PA (ERMS 571244). The parameter values match and are copied from the 2018 Performance Assessment Inventory Report (ERMS 575699).
PU238	INVRHD	Plutonium 238; scaled initial inventory in RH waste	571150	571244	The comments for PU238:INVCHD also apply to PU238:INVRHD.
PU238L	INVCHD	Plutonium 238 Equals Plutonium 238 Inventory; scaled initial inventory in CH waste	571150	571244	ERMS 571150 is the Analysis Plan for the CRA-2019 PA which describes this parameter and its use. ERMS 571150 refers to data found in Table 7 of the Radionuclide Inventory Screening Analysis for the CRA-2019 PA (ERMS 571244). The parameter values match.
PU238L	INVRHD	Plutonium 238 Equals Plutonium 238 Inventory; scaled initial inventory in RH waste	571150	571244	The comments for PU238L:INVCHD also apply to PU238L:INVRHD.
PU239	DECAYNRG	Plutonium 239, radionuclide decay energy	571150	571244	ERMS 571150 is the Analysis Plan for the CRA-2019 PA which describes this parameter and its use. ERMS 571150 refers to data found in Table 6 of the Radionuclide Inventory Screening Analysis for the CRA-2019 PA (ERMS 571244). The parameter values match.
PU239	INVCHD	Plutonium 239; scaled initial inventory in CH waste	571150	571244	ERMS 571150 is the Analysis Plan for the CRA-2019 PA which describes this parameter and its use. ERMS 571150 refers to data found in Table 3 of the Radionuclide Inventory Screening Analysis for the CRA-2019 PA (ERMS 571244). The parameter values match and are copied from the 2018 Performance Assessment Inventory Report (ERMS 575699).
PU239	INVRHD	Plutonium 239; scaled initial inventory in RH waste	571150	571244	The comments for PU239:INVCHD also apply to PU239:INVRHD.
PU239L	INVCHD	Plutonium 239 Lumped with Plutonium 240 and Plutonium 242; scaled initial inventory in CH waste	571150	571244	ERMS 571150 is the Analysis Plan for the CRA-2019 PA which describes this parameter and its use. ERMS 571150 refers to data found in Table 7 of the Radionuclide Inventory Screening Analysis for the CRA-2019 PA (ERMS 571244). The parameter values match.

Table B2. Documentation Checks for Parameters Used in the CRA-2019 PA that have Changed since the CRA-2014 PA (Continued)

Material Name	Property Name	Parameter Description	Primary Source Document ERMS No.	Supporting Document ERMS No.	EPA Comments
PU239L	INVRHD	Plutonium 239 Lumped with Plutonium 240 and Plutonium 242; scaled initial inventory in RH waste	571150	571244	The comments for PU239L:INVCHD also apply to PU239L:INVRHD.
PU240	DECAYNRG	Plutonium 240, radionuclide decay energy	571150	571244	ERMS 571150 is the Analysis Plan for the CRA-2019 PA which describes this parameter and its use. ERMS 571150 refers to data found in Table 6 of the Radionuclide Inventory Screening Analysis for the CRA-2019 PA (ERMS 571244). The parameter values match.
PU240	INVCHD	Plutonium 240; scaled initial inventory in CH waste	571150	571244	ERMS 571150 is the Analysis Plan for the CRA-2019 PA which describes this parameter and its use. ERMS 571150 refers to data found in Table 3 of the Radionuclide Inventory Screening Analysis for the CRA-2019 PA (ERMS 571244). The parameter values match and are copied from the 2018 Performance Assessment Inventory Report (ERMS 575699).
PU240	INVRHD	Plutonium 240; scaled initial inventory in RH waste	571150	571244	The comments for PU240:INVCHD also apply to PU240:INVRHD.
PU241	INVCHD	Plutonium 241; scaled initial inventory in CH waste	571150	571244	ERMS 571150 is the Analysis Plan for the CRA-2019 PA which describes this parameter and its use. ERMS 571150 refers to data found in Table 3 of the Radionuclide Inventory Screening Analysis for the CRA-2019 PA (ERMS 571244). The parameter values match and are copied from the 2018 Performance Assessment Inventory Report (ERMS 575699).
PU241	INVRHD	Plutonium 241; scaled initial inventory in RH waste	571150	571244	The comments for PU241:INVCHD also apply to PU2:INVRHD.
PU242	DECAYNRG	Plutonium 242, radionuclide decay energy	571150	571244	ERMS 571150 is the Analysis Plan for the CRA-2019 PA which describes this parameter and its use. ERMS 571150 refers to data found in Table 6 of the Radionuclide Inventory Screening Analysis for the CRA-2019 PA (ERMS 571244). The parameter values match.
PU242	INVCHD	Plutonium 242; scaled initial inventory in CH waste	571150	571244	ERMS 571150 is the Analysis Plan for the CRA-2019 PA which describes this parameter and its use. ERMS 571150 refers to data found in Table 3 of the Radionuclide Inventory Screening Analysis for the CRA-2019 PA (ERMS 571244). The parameter values match and are copied from the 2018 Performance Assessment Inventory Report (ERMS 575699).
PU242	INVRHD	Plutonium 242; scaled initial inventory in RH waste	571150	571244	The comments for PU242:INVCHD also apply to PU242:INVRHD.
PU244	INVCHD	Plutonium 244; scaled initial inventory in CH waste	571150	571244	ERMS 571150 is the Analysis Plan for the CRA-2019 PA which describes this parameter and its use. ERMS 571150 refers to data found in Table 3 of the Radionuclide Inventory Screening Analysis for the CRA-2019 PA (ERMS 571244). The parameter values match and are copied from the 2018 Performance Assessment Inventory Report (ERMS 575699).
PU244	INVRHD	Plutonium 244; scaled initial inventory in RH waste	571150	571244	The comments for PU244:INVCHD also apply to PU244:INVRHD.
RA226	INVCHD	Radium 226; scaled initial inventory in CH waste	571150	571244	ERMS 571150 is the Analysis Plan for the CRA-2019 PA which describes this parameter and its use. ERMS 571150 refers to data found in Table 3 of the Radionuclide Inventory Screening Analysis for the CRA-2019 PA (ERMS 571244). The parameter values match and are copied from the 2018 Performance Assessment Inventory Report (ERMS 575699).

Table B2. Documentation Checks for Parameters Used in the CRA-2019 PA that have Changed since the CRA-2014 PA (Continued)

Material Name	Property Name	Parameter Description	Primary Source Document ERMS No.	Supporting Document ERMS No.	EPA Comments
RA226	INVRHD	Radium 226; scaled initial inventory in RH waste	571150	571244	The comments for PU238:INVCHD also apply to RA226:INVRHD.
RA228	INVCHD	Radium 228; scaled initial inventory in CH waste	571150	571244	ERMS 571150 is the Analysis Plan for the CRA-2019 PA which describes this parameter and its use. ERMS 571150 refers to data found in Table 3 of the Radionuclide Inventory Screening Analysis for the CRA-2019 PA (ERMS 571244). The parameter values match and are copied from the 2018 Performance Assessment Inventory Report (ERMS 575699).
RA228	INVRHD	Radium 228; scaled initial inventory in RH waste	571150	571244	The comments for PU238:INVCHD also apply to RA228:INVRHD.
REFCON	STCO_31	Reference Constant; Stoichiometric coefficient for $FeOH_2$ sulfidation:H_2	567353	- -	The CRA-2019 Input Parameter Report (ERMS 571660) identifies CRA2014_SEN4 as the original analysis in which the value of REFCON:STCO_31 was changed. CRA2014_SEN4 is a sensitivity analysis requested by EPA to evaluate the effect on normalized releases resulting from changes to a set of input parameter values. The SNL source document ERMS 567353 states that the value of this parameter was changed at EPA's request. ERMS 567353 cites ERMS 560298 as the source of this parameter value, which matches the parameter value used for the CRA-2019 PA. Justification for the continued use of this parameter value in the CRA-2019 PA is documented in ERMS 570879 as being requested by EPA (ERMS 570585). Because the parameter update occurred for the CRA2014_SEN4 analysis, the parameter data entry form is located with the CRA2014_SEN4 documentation.
REFCON	STCO_32	Reference Constant, Stoichiometric coefficient for $FeOH_2$ sulfidation:H_2O	567353	- -	The comments for REFCON:STCO_31 also apply to REFCON:STCO_32.
REFCON	STCO_35	Reference Constant; Stoichiometric coefficient for $FeOH_2$ sulfidation:$FeOH_2$	567353	- -	The comments for REFCON:STCO_31 also apply to REFCON:STCO_35.
REFCON	STCO_36	Reference Constant; Stoichiometric coefficient for $FeOH_2$ sulfidation:FeS	567353	- -	The comments for REFCON:STCO_31 also apply to REFCON:STCO_36.
REFCON	STCO_43	Reference Constant; Stoichiometric coefficient for metallic Fe sulfidation:Fe	567353	- -	The comments for REFCON:STCO_31 also apply to REFCON:STCO_43.
REFCON	STCO_46	Reference Constant; Stoichiometric coefficient for metallic Fe sulfidation:FeS	567353	- -	The comments for REFCON:STCO_31 also apply to REFCON:STCO_46.
SM147	INVCHD	Samarium 147; scaled initial inventory in CH waste	571150	571244	ERMS 571150 is the Analysis Plan for the CRA-2019 PA which describes this parameter and its use. ERMS 571150 refers to data found in Table 3 of the Radionuclide Inventory Screening Analysis for the CRA-2019 PA (ERMS 571244). The parameter values match and are copied from the 2018 Performance Assessment Inventory Report (ERMS 575699).

Table B2. Documentation Checks for Parameters Used in the CRA-2019 PA that have Changed since the CRA-2014 PA (Continued)

Material Name	Property Name	Parameter Description	Primary Source Document ERMS No.	Supporting Document ERMS No.	EPA Comments
SM147	INVRHD	Samarium 147; scaled initial inventory in RH waste	571150	571244	The comments for SM147:INVCHD also apply to SM147:INVRHD.
SOLMOD3	SOLCOH	Solubility of +III actinides in the minimum volume of Castile brine	571150	571169	ERMS 571150 is the Analysis Plan for the CRA-2019 PA which describes this parameter and its use. The parameter value is provided in ERMS 571169 and is based on calculations described in ERMS 571011 and ERMS 571178. The parameter values match.
SOLMOD3	SOLCOH2	Solubility of +III actinides in 2x the minimum volume of Castile brine	571150	571169	The comments for SOLMOD3:SOLCOH also apply to SOLMOD3:SOLCOH2.
SOLMOD3	SOLCOH3	Solubility of +III actinides in 3x the minimum volume of Castile brine	571150	571169	The comments for SOLMOD3:SOLCOH also apply to SOLMOD3:SOLCOH3.
SOLMOD3	SOLCOH4	Solubility of +III actinides in 4x the minimum volume of Castile brine	571150	571169	The comments for SOLMOD3:SOLCOH also apply to SOLMOD3:SOLCOH4.
SOLMOD3	SOLCOH5	Solubility of +III actinides in 5x the minimum volume of Castile brine	571150	571169	The comments for SOLMOD3:SOLCOH also apply to SOLMOD3:SOLCOH5.
SOLMOD3	SOLSOH	Solubility of +III actinides in the minimum volume of Salado brine	571150	571169	The comments for SOLMOD3:SOLCOH also apply to SOLMOD3:SOLSOH.
SOLMOD3	SOLSOH2	Solubility of +III actinides in 2x the minimum volume of Salado brine	571150	571169	The comments for SOLMOD3:SOLCOH also apply to SOLMOD3:SOLSOH2.
SOLMOD3	SOLSOH3	Solubility of +III actinides in 3x the minimum volume of Salado brine	571150	571169	The comments for SOLMOD3:SOLCOH also apply to SOLMOD3:SOLSOH3.
SOLMOD3	SOLSOH4	Solubility of +III actinides in 4x the minimum volume of Salado brine	571150	571169	The comments for SOLMOD3:SOLCOH also apply to SOLMOD3:SOLSOH4.
SOLMOD3	SOLSOH5	Solubility of +III actinides in 5x the minimum volume of Salado brine	571150	571169	The comments for SOLMOD3:SOLCOH also apply to SOLMOD3:SOLSOH5.
SOLMOD3	SOLVAR	Solubility multiplier for +III oxidation state radionuclides	571150	571169	ERMS 571150 is the Analysis Plan for the CRA-2019 PA which describes this parameter and its use. The parameter value is provided in ERMS 571169 and is based on calculations described in ERMS 571169. The parameter values match.

Table B2. Documentation Checks for Parameters Used in the CRA-2019 PA that have Changed since the CRA-2014 PA (Continued)

Material Name	Property Name	Parameter Description	Primary Source Document ERMS No.	Supporting Document ERMS No.	EPA Comments
SOLMOD4	SOLCOH	Solubility of +IV actinides in the minimum volume of Castile brine	571150	571169	ERMS 571150 is the Analysis Plan for the CRA-2019 PA which describes this parameter and its use. The parameter value is provided in ERMS 571169 and is based on calculations described in ERMS 571011 and ERMS 571178. The parameter values match.
SOLMOD4	SOLCOH2	Solubility of +IV actinides in 2x the minimum volume of Castile brine	571150	571169	The comments for SOLMOD4:SOLCOH also apply to SOLMOD4:SOLCOH2.
SOLMOD4	SOLCOH3	Solubility of +IV actinides in 3x the minimum volume of Castile brine	571150	571169	The comments for SOLMOD4:SOLCOH also apply to SOLMOD4:SOLCOH3.
SOLMOD4	SOLCOH4	Solubility of +IV actinides in 4x the minimum volume of Castile brine	571150	571169	The comments for SOLMOD4:SOLCOH also apply to SOLMOD4:SOLCOH4.
SOLMOD4	SOLCOH5	Solubility of +IV actinides in 5x the minimum volume of Castile brine	571150	571169	The comments for SOLMOD4:SOLCOH also apply to SOLMOD4:SOLCOH5.
SOLMOD4	SOLSOH	Solubility of +IV actinides in the minimum volume of Salado brine	571150	571169	The comments for SOLMOD4:SOLCOH also apply to SOLMOD4:SOLSOH
SOLMOD4	SOLSOH2	Solubility of +IV actinides in 2x the minimum volume of Salado brine	571150	571169	The comments for SOLMOD4:SOLCOH also apply to SOLMOD4:SOLSOH2.
SOLMOD4	SOLSOH3	Solubility of +IV actinides in 3x the minimum volume of Salado brine	571150	571169	The comments for SOLMOD4:SOLCOH also apply to SOLMOD4:SOLSOH3.
SOLMOD4	SOLSOH4	Solubility of +IV actinides in 4x the minimum volume of Salado brine	571150	571169	The comments for SOLMOD4:SOLCOH also apply to SOLMOD4:SOLSOH4.
SOLMOD4	SOLSOH5	Solubility of +IV actinides in 5x the minimum volume of Salado brine	571150	571169	The comments for SOLMOD4:SOLCOH also apply to SOLMOD4:SOLSOH5.
SOLMOD4	SOLVAR	Solubility multiplier for +IV oxidation state radionuclides	571150	571169	ERMS 571150 is the Analysis Plan for the CRA-2019 PA which describes this parameter and its use. The parameter value is provided in ERMS 571169 and is based on calculations described in ERMS 571169. The parameter values match.
SOLMOD5	SOLCOH	Solubility of +V actinides in the minimum volume of Castile brine	571150	571169	ERMS 571150 is the Analysis Plan for the CRA-2019 PA which describes this parameter and its use. The parameter value is provided in ERMS 571169 and is based on calculations described in ERMS 571011 and ERMS 571178. The parameter values match.
SOLMOD5	SOLCOH2	Solubility of +V actinides in 2x the minimum volume of Castile brine	571150	571169	The comments for SOLMOD5:SOLCOH also apply to SOLMOD5:SOLCOH2.

Table B2. Documentation Checks for Parameters Used in the CRA-2019 PA that have Changed since the CRA-2014 PA (Continued)

Material Name	Property Name	Parameter Description	Primary Source Document ERMS No.	Supporting Document ERMS No.	EPA Comments
SOLMOD5	SOLCOH3	Solubility of +V actinides in 3x the minimum volume of Castile brine	571150	571169	The comments for SOLMOD5:SOLCOH also apply to SOLMOD5:SOLCOH3.
SOLMOD5	SOLCOH4	Solubility of +V actinides in 4x the minimum volume of Castile brine	571150	571169	The comments for SOLMOD5:SOLCOH also apply to SOLMOD5:SOLCOH4.
SOLMOD5	SOLCOH5	Solubility of +V actinides in 5x the minimum volume of Castile brine	571150	571169	The comments for SOLMOD5:SOLCOH also apply to SOLMOD5:SOLCOH5.
SOLMOD5	SOLSOH	Solubility of +V actinides in the minimum volume of Salado brine	571150	571169	The comments for SOLMOD5:SOLCOH also apply to SOLMOD5:SOLSOH
SOLMOD5	SOLSOH2	Solubility of +V actinides in 2x the minimum volume of Salado brine	571150	571169	The comments for SOLMOD5:SOLCOH also apply to SOLMOD5:SOLSOH2.
SOLMOD5	SOLSOH3	Solubility of +V actinides in 3x the minimum volume of Salado brine	571150	571169	The comments for SOLMOD5:SOLCOH also apply to SOLMOD5:SOLSOH3.
SOLMOD5	SOLSOH4	Solubility of +V actinides in 4x the minimum volume of Salado brine	571150	571169	The comments for SOLMOD5:SOLCOH also apply to SOLMOD5:SOLSOH4.
SOLMOD5	SOLSOH5	Solubility of +V actinides in 5x the minimum volume of Salado brine	571150	571169	The comments for SOLMOD5:SOLCOH also apply to SOLMOD5:SOLSOH5.
SR90	INVCHD	Strontium 90; scaled initial inventory in CH waste	571150	571244	ERMS 571150 is the Analysis Plan for the CRA-2019 PA which describes this parameter and its use. ERMS 571150 refers to data found in Table 3 of the Radionuclide Inventory Screening Analysis for the CRA-2019 PA (ERMS 571244). The parameter values match and are copied from the 2018 Performance Assessment Inventory Report (ERMS 575699).
SR90	INVRHD	Strontium 90; scaled initial inventory in RH waste	571150	571244	The comments for SR90:INVCHD also apply to SR90:INVRHD.
STEEL	CORRMCO2	Anoxic iron corrosion rate under brine-inundated conditions with no CO_2 present	571150	570869	ERMS 571150 is the Analysis Plan for the CRA-2019 PA which describes this parameter and its use. The parameter value is provided in ERMS 570869 and is based on calculations ERMS 565005. The source document parameter mean in ERMS 570869 differs slightly from the parameter value mean on the data entry form and in the PAPDB (1.35E-14 vs. 1.33E-14, respectively). This discrepancy is minor and does not affect the CRA-2019 PA because the mean is provided only for reference purposes and is not used when sampling from the cumulative distribution.

Table B2. Documentation Checks for Parameters Used in the CRA-2019 PA that have Changed since the CRA-2014 PA (Continued)

Material Name	Property Name	Parameter Description	Primary Source Document ERMS No.	Supporting Document ERMS No.	EPA Comments
STEEL	HUMCORR	Iron corrosion rate under humid conditions	571150	569807	ERMS 571150 is the Analysis Plan for the CRA-2019 PA which describes this parameter and its use. The parameter value is provided in ERMS 569807 and is based on data from ERMS 559077 and a methodology from ERMS 565009 and ERMS 565108. The source document parameter mean in ERMS 569807 differs slightly from the parameter value mean on the data entry form and in the PAPDB. The discrepancy is minor and does not affect the CRA-2019 PA because the mean is provided only for reference purposes and is not used when sampling from the cumulative distribution.
SULFATE	QINIT	Sulfate; scaled initial inventory in waste	571150	571244	ERMS 571150 is the Analysis Plan for the CRA-2019 PA which describes this parameter and its use. ERMS 571150 refers to data found in Section 6 and Appendix D, Table D-5 of the Radionuclide Inventory Screening Analysis for the CRA-2019 PA (ERMS 571244). The parameter values match and are copied from the 2018 Performance Assessment Inventory Report (ERMS 575699).
TH	CAPMIC	Thorium; maximum mobilized concentration on microbial colloids	571150	571296	ERMS 571150 is the Analysis Plan for the CRA-2019 PA which describes this parameter and its use. The parameter value is described in ERMS 571296 and is based on work by Reed et al. (2013). The parameter values match.
TH	CONCINT	Thorium; intrinsic colloid concentration parameter	571150	571296	The comments for TH:CAPMIC also apply to TH:CONCINT.
TH	PROPMIC	Thorium; ratio of moles mobilized on microbial colloids to moles dissolved	571150	571296	The comments for TH:CAPMIC also apply to TH:PROPMIC.
TH229	INVCHD	Thorium 229; scaled initial inventory in CH waste	571150	571244	ERMS 571150 is the Analysis Plan for the CRA-2019 PA which describes this parameter and its use. ERMS 571150 refers to data found in Table 3 of the Radionuclide Inventory Screening Analysis for the CRA-2019 PA (ERMS 571244). The parameter values match and are copied from the 2018 Performance Assessment Inventory Report (ERMS 575699).
TH229	INVRHD	Thorium 229; scaled initial inventory in RH waste	571150	571244	The comments for TH229:INVCHD also apply to TH229:INVRHD.
TH230	INVCHD	Thorium 230; scaled initial inventory in CH waste	571150	571244	ERMS 571150 is the Analysis Plan for the CRA-2019 PA which describes this parameter and its use. ERMS 571150 refers to data found in Table 3 of the Radionuclide Inventory Screening Analysis for the CRA-2019 PA (ERMS 571244). The parameter values match and are copied from the 2018 Performance Assessment Inventory Report (ERMS 575699).
TH230	INVRHD	Thorium 230; scaled initial inventory in RH waste	571150	571244	The comments for TH230:INVCHD also apply to TH230:INVRHD.
TH230L	INVCHD	Thorium 230 Lumped with Thorium 229; scaled initial inventory in CH waste	571150	571244	ERMS 571150 is the Analysis Plan for the CRA-2019 PA which describes this parameter and its use. ERMS 571150 refers to data found in Table 7 of the Radionuclide Inventory Screening Analysis for the CRA-2019 PA (ERMS 571244). The parameter values match.
TH230L	INVRHD	Thorium 230 Lumped with Thorium 229; scaled initial inventory in RH waste	571150	571244	The comments for TH230L:INVCHD also apply to TH230L:INVRHD.

Table B2. Documentation Checks for Parameters Used in the CRA-2019 PA that have Changed since the CRA-2014 PA (Continued)

Material Name	Property Name	Parameter Description	Primary Source Document ERMS No.	Supporting Document ERMS No.	EPA Comments
TH232	INVCHD	Thorium 232; scaled initial inventory in CH waste	571150	571244	ERMS 571150 is the Analysis Plan for the CRA-2019 PA which describes this parameter and its use. ERMS 571150 refers to data found in Table 3 of the Radionuclide Inventory Screening Analysis for the CRA-2019 PA (ERMS 571244). The parameter values match and are copied from the 2018 Performance Assessment Inventory Report (ERMS 575699).
TH232	INVRHD	Thorium 232; scaled initial inventory in RH waste	571150	571244	The comments for TH232:INVCHD also apply to TH232:INVRHD.
U	CAPMIC	Uranium; maximum mobilized concentration on microbial colloids	571150	571296	ERMS 571150 is the Analysis Plan for the CRA-2019 PA which describes this parameter and its use. The parameter value is described in ERMS 571296 and is based on work by Reed et al. (2013). The parameter values match.
U	CONCINT	Uranium; intrinsic colloid concentration parameter	571150	571296	The comments for U:CAPMIC also apply to U:CONCINT.
U	PROPMIC	Uranium; ratio of moles mobilized on microbial colloids to moles dissolved	571150	571296	The comments for U:CAPMIC also apply to U:PROPMIC.
U233	INVCHD	Uranium 233; scaled initial inventory in CH waste	571150	571244	ERMS 571150 is the Analysis Plan for the CRA-2019 PA which describes this parameter and its use. ERMS 571150 refers to data found in Table 3 of the Radionuclide Inventory Screening Analysis for the CRA-2019 PA (ERMS 571244). The parameter values match and are copied from the 2018 Performance Assessment Inventory Report (ERMS 575699).
U233	INVRHD	Uranium 233; scaled initial inventory in RH waste	571150	571244	The comments for U233:INVCHD also apply to U233:INVRHD.
U234	INVCHD	Uranium 234; scaled initial inventory in CH waste	571150	571244	The comments for U233:INVCHD also apply to U234:INVCHD.
U234	INVRHD	Uranium 234; scaled initial inventory in RH waste	571150	571244	The comments for U233:INVCHD also apply to U234:INVRHD.
U234L	INVCHD	Uranium 234 Lumped with Uranium 233; scaled initial inventory in CH waste	571150	571244	ERMS 571150 is the Analysis Plan for the CRA-2019 PA which describes this parameter and its use. ERMS 571150 refers to data found in Table 7 of the Radionuclide Inventory Screening Analysis for the CRA-2019 PA (ERMS 571244). The parameter values match.
U234L	INVRHD	Uranium 234 Lumped with Uranium 233; scaled initial inventory in RH waste	571150	571244	The comments for PU234L:INVCHD also apply to PU234L:INVRHD.
U235	INVCHD	Uranium 235; scaled initial inventory in CH waste	571150	571244	The comments for U233:INVCHD also apply to U235:INVCHD.
U235	INVRHD	Uranium 235; scaled initial inventory in RH waste	571150	571244	The comments for U233:INVCHD also apply to U235:INVRHD.
U236	INVCHD	Uranium 236; scaled initial inventory in CH waste	571150	571244	The comments for U233:INVCHD also apply to U236:INVCHD.
U236	INVRHD	Uranium 236; scaled initial inventory in RH waste	571150	571244	The comments for U233:INVCHD also apply to U236:INVRHD.

Table B2. Documentation Checks for Parameters Used in the CRA-2019 PA that have Changed since the CRA-2014 PA (Continued)

Material Name	Property Name	Parameter Description	Primary Source Document ERMS No.	Supporting Document ERMS No.	EPA Comments
U238	INVCHD	Uranium 238; scaled initial inventory in CH waste	571150	571244	The comments for U233:INVCHD also apply to U238:INVCHD.
U238	INVRHD	Uranium 238; scaled initial inventory in RH waste	571150	571244	The comments for U233:INVCHD also apply to U238:INVRHD.
WAS_AREA	CELCCHW	Mass of cellulosics in CH waste container materials	571150	571244	ERMS 571150 is the Analysis Plan for the CRA-2019 PA which describes this parameter and its use. ERMS 571150 refers to data described in Section 7 and listed in Table D-4 of the Radionuclide Inventory Screening Analysis for the CRA-2019 PA (ERMS 571244). The parameter values match and are copied from the 2018 Performance Assessment Inventory Report (ERMS 575699).
WAS_AREA	CELCRHW	Mass of cellulosics in RH waste container materials	571150	571244	The comments for WAS_AREA:CELCCHW also apply to WAS_AREA:CELCRHW.
WAS_AREA	CELECHW	Mass of cellulosics in CH waste emplacement materials	571150	571244	The comments for WAS_AREA:CELCCHW also apply to WAS_AREA:CELECHW.
WAS_AREA	CELERHW	Mass of cellulosics in RH waste emplacement materials	571150	571244	The comments for WAS_AREA:CELCCHW also apply to WAS_AREA:CELERHW.
WAS_AREA	CELLCHW	Mass of cellulosics in CH waste	571150	571244	The comments for WAS_AREA:CELCCHW also apply to WAS_AREA:CELLCHW.
WAS_AREA	CELLRHW	Mass of cellulosics in RH waste	571150	571244	The comments for WAS_AREA:CELCCHW also apply to WAS_AREA:CELLRHW.
WAS_AREA	HYMAGCON	Conversion rate of hydromagnesite to magnesite	571150	570879	ERMS 571150 is the Analysis Plan for the CRA-2019 PA which describes this parameter and its use. The parameter value was updated upon direction by EPA (ERMS 570585) as described and justified in ERMS 570879. The parameter values match.
WAS_AREA	IRNCCHW	Mass of iron containers for CH waste	571150	571244	The comments for WAS_AREA:CELCCHW also apply to WAS_AREA:IRNCCHW.
WAS_AREA	IRNCRHW	Mass of iron containers for RH waste	571150	571244	The comments for WAS_AREA:CELCCHW also apply to WAS_AREA:IRNCRHW.
WAS_AREA	IRONCHW	Mass of iron-based material in CH waste.	571150	571244	The comments for WAS_AREA:CELCCHW also apply to WAS_AREA:IRONCHW.
WAS_AREA	IRONRHW	Mass of iron-based material in RH waste.	571150	571244	The comments for WAS_AREA:CELCCHW also apply to WAS_AREA:IRONRHW.
WAS_AREA	PLASCHW	Mass of plastics in CH waste	571150	571244	The comments for WAS_AREA:CELCCHW also apply to WAS_AREA:PLASCHW.
WAS_AREA	PLASRHW	Mass of plastics in RH waste	571150	571244	The comments for WAS_AREA:CELCCHW also apply to WAS_AREA:PLASRHW.
WAS_AREA	PLSCCHW	Mass of plastic liners in CH waste containers	571150	571244	The comments for WAS_AREA:CELCCHW also apply to WAS_AREA:PLSCCHW.
WAS_AREA	PLSCRHW	Mass of plastic liners in RH waste containers	571150	571244	The comments for WAS_AREA:CELCCHW also apply to WAS_AREA:PLSCRHW.

Table B2. Documentation Checks for Parameters Used in the CRA-2019 PA that have Changed since the CRA-2014 PA (Continued)

Material Name	Property Name	Parameter Description	Primary Source Document ERMS No.	Supporting Document ERMS No.	EPA Comments
WAS_AREA	PLSECHW	Mass of plastic in CH waste emplacement materials	571150	571244	The comments for WAS_AREA:CELCCHW also apply to WAS_AREA:PLSECHW.
WAS_AREA	PLSERHW	Mass of plastic in RH waste emplacement materials	571150	571244	The comments for WAS_AREA:CELCCHW also apply to WAS_AREA:PLSERHW.
WAS_AREA	RUBBCHW	Mass of rubber in CH waste	571150	571244	The comments for WAS_AREA:CELCCHW also apply to WAS_AREA:RUBBCHW.
WAS_AREA	RUBBRHW	Mass of rubber in RH waste	571150	571244	The comments for WAS_AREA:CELCCHW also apply to WAS_AREA:RUBBRHW.
WAS_AREA	RUBCCHW	Mass of rubber in CH waste containers	571150	571244	The comments for WAS_AREA:CELCCHW also apply to WAS_AREA:RUBCCHW.
WAS_AREA	RUBCRHW	Mass of rubber in RH waste containers	571150	571244	The comments for WAS_AREA:CELCCHW also apply to WAS_AREA:RUBCRHW.
WAS_AREA	RUBECHW	Mass of rubber in CH waste emplacement materials	571150	571244	The comments for WAS_AREA:CELCCHW also apply to WAS_AREA:RUBECHW.
WAS_AREA	RUBERHW	Mass of rubber in RH waste emplacement materials	571150	571244	The comments for WAS_AREA:CELCCHW also apply to WAS_AREA:RUBERHW.

Key to ERMS Reference Numbers in Table B2

559077 Roselle 2013
560298 Kicker and Herrick 2013
565005 Zeitler and Hansen 2015a
565009 Zeitler and Hansen 2015b
565108 Zeitler and Hansen 2015c
565676 Peake 2016
565722 Day 2016
566571 Zeitler 2016a
566607 Zeitler 2016b
567222 Mariner 2016
567343 Zeitler 2016c
567353 Zeitler and Day 2016
568138 Zeitler and Day 2017
569599 Mariner 2018
569807 Zeitler 2018a
570325 Day 2018
570585 Peake 2018
570869 Zeitler 2018b
570873 Day 2019
570879 Zeitler 2019a
571011 Sisk-Scott 2019
571150 Zeitler 2019b
571169 Domski 2019
571178 Domski and Sisk-Scott 2019
571244 Kicker 2019
571250 Mariner 2019
571296 Reed et al.2019
571660 Kim and Feng 2019
575699 Van Soest 2018

Complete references are provided at the end of Appendix B.

Table B3. Code/Database Interface Test Results for Parameters Used in the CRA-2019 PA that have Changed since the CRA-2014 PA

Material Name	Property Name	Code	File Name	PAPDB Value	Same Value Returned?	Comments
AM	CAPMIC	BRAGFLO	lhs3_bf_CRA19_r1_v031.cdb	2.30E-09	Yes	The correct value was returned.
AM	CAPMIC	PANEL	lhs3_panel_CRA19_b1_r1_v031.cdb	2.30E-09	Yes	The correct value was returned.
AM	CONCINT	BRAGFLO	lhs3_bf_CRA19_r1_v031.cdb	9.50E-09	Yes	The correct value was returned.
AM	CONCINT	PANEL	lhs3_panel_CRA19_b1_r1_v031.cdb	9.50E-09	Yes	The correct value was returned.
AM	PROPMIC	BRAGFLO	lhs3_bf_CRA19_r1_v031.cdb	3.00E-02	Yes	The correct value was returned.
AM	PROPMIC	PANEL	lhs3_panel_CRA19_b1_r1_v031.cdb	3.00E-02	Yes	The correct value was returned.
AM241	DECAYNRG	BRAGFLO	lhs3_bf_CRA19_r1_v031.cdb	5.64E+00	Yes	The correct value was returned.
AM241	INVCHD	BRAGFLO	lhs3_bf_CRA19_r1_v031.cdb	1.13E+06	Yes	The correct value was returned.
AM241	INVCHD	PANEL	lhs3_panel_CRA19_b1_r1_v031.cdb	1.13E+06	Yes	The correct value was returned.
AM241	INVRHD	BRAGFLO	lhs3_bf_CRA19_r1_v031.cdb	1.30E+04	Yes	The correct value was returned.
AM241	INVRHD	PANEL	lhs3_panel_CRA19_b1_r1_v031.cdb	1.30E+04	Yes	The correct value was returned
AM241L	INVCHD	PANEL	lhs3_panel_CRA19_b1_r1_v031.cdb	1.19E+06	Yes	The correct value was returned.
AM241L	INVRHD	PANEL	lhs3_panel_CRA19_b1_r1_v031.cdb	1.45E+04	Yes	The correct value was returned.
AM243	INVCHD	PANEL	lhs3_panel_CRA19_b1_r1_v031.cdb	2.24E+01	Yes	The correct value was returned.
AM243	INVRHD	PANEL	lhs3_panel_CRA19_b1_r1_v031.cdb	4.12E+02	Yes	The correct value was returned.
BH_OPEN	RELP_MOD	BRAGFLO	lhs3_bf_CRA19_r1_v031.cdb	1.10E+01	Yes	The correct value was returned.
BOREHOLE	TAUFAIL	CUTTINGS_S	lhs3_cusp_CRA19_r1_v031.cdb	1.60 to 77.0	3.61E+01	Sampled value correctly lies within the sampled range of 1.60 to 77.0.
BOREHOLE	WUF	EPAUNI	epu_CRA19_ch_misc.inp epu_CRA19_rh_misc.inp	3.30E+00	Yes	The correct value was returned.
BOREHOLE	WUF	PRECCDFGF	lhs3_ccgf_CRA19_r1_v031.cdb	3.30E+00	Yes	The correct value was returned.
BOREHOLE	WUF	NUTS	ms_nut_CRA19_r1_s2_V030.cdb nut_iso_CRA19_r1_s2_V030.cdb	3.30E+00	Yes	The correct value was returned.
BOREHOLE	WUF	PANEL	lhs3_panel_CRA19_b1_r1_v031.cdb	3.30E+00	Yes	The correct value was returned.
CAVITY_5	CAP_MOD	BRAGFLO	lhs3_bf_CRA19_r1_v031.cdb	1.00E+00	Yes	The correct value was returned.
CAVITY_5	COMP_RCK	BRAGFLO	lhs3_bf_CRA19_r1_v031.cdb	0.00E+00	Yes	The correct value was returned.
CAVITY_5	KPT	BRAGFLO	lhs3_bf_CRA19_r1_v031.cdb	0.00E+00	Yes	The correct value was returned.
CAVITY_5	PCT_A	BRAGFLO	lhs3_bf_CRA19_r1_v031.cdb	0.00E+00	Yes	The correct value was returned.
CAVITY_5	PCT_EXP	BRAGFLO	lhs3_bf_CRA19_r1_v031.cdb	0.00E+00	Yes	The correct value was returned.

Table B3. Code/Database Interface Test Results for Parameters Used in the CRA-2019 PA that have Changed since the CRA-2014 PA (Continued)

Material Name	Property Name	Code	File Name	PAPDB Value	Same Value Returned?	Comments
CAVITY_5	PC_MAX	BRAGFLO	lhs3_bf_CRA19_r1_v031.cdb	1.00E+08	Yes	The correct value was returned.
CAVITY_5	PORE_DIS	BRAGFLO	lhs3_bf_CRA19_r1_v031.cdb	7.00E-01	Yes	The correct value was returned.
CAVITY_5	POROSITY	BRAGFLO	lhs3_bf_CRA19_r1_v031.cdb	1.00E+00	Yes	The correct value was returned.
CAVITY_5	PRMY_LOG	BRAGFLO	lhs3_bf_CRA19_r1_v031.cdb	-1.00E+01	Yes	The correct value was returned.
CAVITY_5	PRMZ_LOG	BRAGFLO	lhs3_bf_CRA19_r1_v031.cdb	-1.00E+01	Yes	The correct value was returned.
CAVITY_5	RELP_MOD	BRAGFLO	lhs3_bf_CRA19_r1_v031.cdb	1.10E+01	Yes	The correct value was returned.
CAVITY_5	SAT_IBRN	BRAGFLO	lhs3_bf_CRA19_r1_v031.cdb	0.00E+00	Yes	The correct value was returned.
CAVITY_5	SAT_RBRN	BRAGFLO	lhs3_bf_CRA19_r1_v031.cdb	0.00E+00	Yes	The correct value was returned.
CAVITY_5	SAT_RGAS	BRAGFLO	lhs3_bf_CRA19_r1_v031.cdb	0.00E+00	Yes	The correct value was returned.
CF252	INVCHD	PANEL	lhs3_panel_CRA19_b1_r1_v031.cdb	5.07E-01	Yes	The correct value was returned.
CF252	INVRHD	PANEL	lhs3_panel_CRA19_b1_r1_v031.cdb	1.76E+00	Yes	The correct value was returned.
CM243	INVCHD	PANEL	lhs3_panel_CRA19_b1_r1_v031.cdb	2.54E+00	Yes	The correct value was returned.
CM243	INVRHD	PANEL	lhs3_panel_CRA19_b1_r1_v031.cdb	3.61E+01	Yes	The correct value was returned.
CM244	INVCHD	PANEL	lhs3_panel_CRA19_b1_r1_v031.cdb	6.19E+03	Yes	The correct value was returned.
CM244	INVRHD	PANEL	lhs3_panel_CRA19_b1_r1_v031.cdb	3.32E+04	Yes	The correct value was returned.
CM245	INVCHD	PANEL	lhs3_panel_CRA19_b1_r1_v031.cdb	2.97E+00	Yes	The correct value was returned.
CM245	INVRHD	PANEL	lhs3_panel_CRA19_b1_r1_v031.cdb	2.15E+01	Yes	The correct value was returned.
CM248	INVCHD	PANEL	lhs3_panel_CRA19_b1_r1_v031.cdb	4.63E-01	Yes	The correct value was returned.
CM248	INVRHD	PANEL	lhs3_panel_CRA19_b1_r1_v031.cdb	1.31E+00	Yes	The correct value was returned.
CS137	INVCHD	PANEL	lhs3_panel_CRA19_b1_r1_v031.cdb	6.16E+02	Yes	The correct value was returned.
CS137	INVRHD	PANEL	lhs3_panel_CRA19_b1_r1_v031.cdb	2.50E+05	Yes	The correct value was returned.
DRZ_OE_0	CAP_MOD	BRAGFLO	lhs3_bf_CRA19_r1_v031.cdb	1.00E+00	Yes	The correct value was returned.
DRZ_OE_0	COMP_RCK	BRAGFLO	lhs3_bf_CRA19_r1_v031.cdb	7.41E-10	Yes	The correct value was returned.
DRZ_OE_0	KPT	BRAGFLO	lhs3_bf_CRA19_r1_v031.cdb	0.00E+00	Yes	The correct value was returned.
DRZ_OE_0	PCT_A	BRAGFLO	lhs3_bf_CRA19_r1_v031.cdb	0.00E+00	Yes	The correct value was returned.
DRZ_OE_0	PCT_EXP	BRAGFLO	lhs3_bf_CRA19_r1_v031.cdb	0.00E+00	Yes	The correct value was returned.
DRZ_OE_0	PC_MAX	BRAGFLO	lhs3_bf_CRA19_r1_v031.cdb	1.00E+08	Yes	The correct value was returned.

Table B3. Code/Database Interface Test Results for Parameters Used in the CRA-2019 PA that have Changed since the CRA-2014 PA (Continued)

Material Name	Property Name	Code	File Name	PAPDB Value	Same Value Returned?	Comments
DRZ_OE_0	PORE_DIS	BRAGFLO	lhs3_bf_CRA19_r1_v031.cdb	7.00E-01	Yes	The correct value was returned.
DRZ_OE_0	POROSITY	BRAGFLO	lhs3_bf_CRA19_r1_v031.cdb	1.29E-02	Yes	The correct value was returned.
DRZ_OE_0	PO_MIN	BRAGFLO	lhs3_bf_CRA19_r1_v031.cdb	1.01E+05	Yes	The correct value was returned.
DRZ_OE_0	PRMX_LOG	BRAGFLO	lhs3_bf_CRA19_r1_v031.cdb	-1.70E+01	Yes	The correct value was returned.
DRZ_OE_0	PRMY_LOG	BRAGFLO	lhs3_bf_CRA19_r1_v031.cdb	-1.70E+01	Yes	The correct value was returned.
DRZ_OE_0	PRMZ_LOG	BRAGFLO	lhs3_bf_CRA19_r1_v031.cdb	-1.70E+01	Yes	The correct value was returned.
DRZ_OE_0	RELP_MOD	BRAGFLO	lhs3_bf_CRA19_r1_v031.cdb	4.00E+00	Yes	The correct value was returned.
DRZ_OE_0	SAT_IBRN	BRAGFLO	lhs3_bf_CRA19_r1_v031.cdb	1.00E+00	Yes	The correct value was returned.
DRZ_OE_0	SAT_RBRN	BRAGFLO	lhs3_bf_CRA19_r1_v031.cdb	0.00E+00	Yes	The correct value was returned.
DRZ_OE_0	SAT_RGAS	BRAGFLO	lhs3_bf_CRA19_r1_v031.cdb	0.00E+00	Yes	The correct value was returned.
DRZ_OE_1	CAP_MOD	BRAGFLO	lhs3_bf_CRA19_r1_v031.cdb	1.00E+00	Yes	The correct value was returned.
DRZ_OE_1	COMP_RCK	BRAGFLO	lhs3_bf_CRA19_r1_v031.cdb	7.41E-10	Yes	The correct value was returned.
DRZ_OE_1	KPT	BRAGFLO	lhs3_bf_CRA19_r1_v031.cdb	0.00E+00	Yes	The correct value was returned.
DRZ_OE_1	PCT_A	BRAGFLO	lhs3_bf_CRA19_r1_v031.cdb	0.00E+00	Yes	The correct value was returned.
DRZ_OE_1	PCT_EXP	BRAGFLO	lhs3_bf_CRA19_r1_v031.cdb	0.00E+00	Yes	The correct value was returned.
DRZ_OE_1	PC_MAX	BRAGFLO	lhs3_bf_CRA19_r1_v031.cdb	1.00E+08	Yes	The correct value was returned.
DRZ_OE_1	PORE_DIS	BRAGFLO	lhs3_bf_CRA19_r1_v031.cdb	7.00E-01	Yes	The correct value was returned.
DRZ_OE_1	POROSITY	BRAGFLO	lhs3_bf_CRA19_r1_v031.cdb	1.29E-02	Yes	The correct value was returned.
DRZ_OE_1	PO_MIN	BRAGFLO	lhs3_bf_CRA19_r1_v031.cdb	1.01E+05	Yes	The correct value was returned.
DRZ_OE_1	PRMX_LOG	BRAGFLO	lhs3_bf_CRA19_r1_v031.cdb	-1.70E+01	Yes	The correct value was returned.
DRZ_OE_1	PRMY_LOG	BRAGFLO	lhs3_bf_CRA19_r1_v031.cdb	-1.70E+01	Yes	The correct value was returned.
DRZ_OE_1	PRMZ_LOG	BRAGFLO	lhs3_bf_CRA19_r1_v031.cdb	-1.70E+01	Yes	The correct value was returned.
DRZ_OE_1	RELP_MOD	BRAGFLO	lhs3_bf_CRA19_r1_v031.cdb	4.00E+00	Yes	The correct value was returned.
DRZ_OE_1	SAT_IBRN	BRAGFLO	lhs3_bf_CRA19_r1_v031.cdb	1.00E+00	Yes	The correct value was returned.
DRZ_OE_1	SAT_RBRN	BRAGFLO	lhs3_bf_CRA19_r1_v031.cdb	0.00E+00	Yes	The correct value was returned.
DRZ_OE_1	SAT_RGAS	BRAGFLO	lhs3_bf_CRA19_r1_v031.cdb	0.00E+00	Yes	The correct value was returned.
DRZ_PC_0	CAP_MOD	BRAGFLO	lhs3_bf_CRA19_r1_v031.cdb	1.00E+00	Yes	The correct value was returned.

Table B3. Code/Database Interface Test Results for Parameters Used in the CRA-2019 PA that have Changed since the CRA-2014 PA (Continued)

Material Name	Property Name	Code	File Name	PAPDB Value	Same Value Returned?	Comments
DRZ_PC_0	COMP_RCK	BRAGFLO	lhs3_bf_CRA19_r1_v031.cdb	7.41E-10	Yes	The correct value was returned.
DRZ_PC_0	KPT	BRAGFLO	lhs3_bf_CRA19_r1_v031.cdb	0.00E+00	Yes	The correct value was returned.
DRZ_PC_0	PCT_A	BRAGFLO	lhs3_bf_CRA19_r1_v031.cdb	0.00E+00	Yes	The correct value was returned.
DRZ_PC_0	PCT_EXP	BRAGFLO	lhs3_bf_CRA19_r1_v031.cdb	0.00E+00	Yes	The correct value was returned.
DRZ_PC_0	PC_MAX	BRAGFLO	lhs3_bf_CRA19_r1_v031.cdb	1.00E+08	Yes	The correct value was returned.
DRZ_PC_0	PORE_DIS	BRAGFLO	lhs3_bf_CRA19_r1_v031.cdb	7.00E-01	Yes	The correct value was returned.
DRZ_PC_0	POROSITY	BRAGFLO	lhs3_bf_CRA19_r1_v031.cdb	1.29E-02	Yes	The correct value was returned.
DRZ_PC_0	PO_MIN	BRAGFLO	lhs3_bf_CRA19_r1_v031.cdb	1.01E+05	Yes	The correct value was returned.
DRZ_PC_0	PRMX_LOG	BRAGFLO	lhs3_bf_CRA19_r1_v031.cdb	-1.70E+01	Yes	The correct value was returned.
DRZ_PC_0	PRMY_LOG	BRAGFLO	lhs3_bf_CRA19_r1_v031.cdb	-1.70E+01	Yes	The correct value was returned.
DRZ_PC_0	PRMZ_LOG	BRAGFLO	lhs3_bf_CRA19_r1_v031.cdb	-1.70E+01	Yes	The correct value was returned.
DRZ_PC_0	RELP_MOD	BRAGFLO	lhs3_bf_CRA19_r1_v031.cdb	4.00E+00	Yes	The correct value was returned.
DRZ_PC_0	SAT_IBRN	BRAGFLO	lhs3_bf_CRA19_r1_v031.cdb	1.00E+00	Yes	The correct value was returned.
DRZ_PC_0	SAT_RBRN	BRAGFLO	lhs3_bf_CRA19_r1_v031.cdb	0.00E+00	Yes	The correct value was returned.
DRZ_PC_0	SAT_RGAS	BRAGFLO	lhs3_bf_CRA19_r1_v031.cdb	0.00E+00	Yes	The correct value was returned.
DRZ_PC_1	CAP_MOD	BRAGFLO	lhs3_bf_CRA19_r1_v031.cdb	1.00E+00	Yes	The correct value was returned.
DRZ_PC_1	COMP_RCK	BRAGFLO	lhs3_bf_CRA19_r1_v031.cdb	7.41E-10	Yes	The correct value was returned.
DRZ_PC_1	KPT	BRAGFLO	lhs3_bf_CRA19_r1_v031.cdb	0.00E+00	Yes	The correct value was returned.
DRZ_PC_1	PCT_A	BRAGFLO	lhs3_bf_CRA19_r1_v031.cdb	0.00E+00	Yes	The correct value was returned.
DRZ_PC_1	PCT_EXP	BRAGFLO	lhs3_bf_CRA19_r1_v031.cdb	0.00E+00	Yes	The correct value was returned.
DRZ_PC_1	PC_MAX	BRAGFLO	lhs3_bf_CRA19_r1_v031.cdb	1.00E+08	Yes	The correct value was returned.
DRZ_PC_1	PORE_DIS	BRAGFLO	lhs3_bf_CRA19_r1_v031.cdb	7.00E-01	Yes	The correct value was returned.
DRZ_PC_1	POROSITY	BRAGFLO	lhs3_bf_CRA19_r1_v031.cdb	1.29E-02	Yes	The correct value was returned.
DRZ_PC_1	PO_MIN	BRAGFLO	lhs3_bf_CRA19_r1_v031.cdb	1.01E+05	Yes	The correct value was returned.
DRZ_PC_1	PRMX_LOG	BRAGFLO	lhs3_bf_CRA19_r1_v031.cdb	-1.70E+01	Yes	The correct value was returned.
DRZ_PC_1	PRMY_LOG	BRAGFLO	lhs3_bf_CRA19_r1_v031.cdb	-1.70E+01	Yes	The correct value was returned.
DRZ_PC_1	PRMZ_LOG	BRAGFLO	lhs3_bf_CRA19_r1_v031.cdb	-1.70E+01	Yes	The correct value was returned.

Table B3. Code/Database Interface Test Results for Parameters Used in the CRA-2019 PA that have Changed since the CRA-2014 PA (Continued)

Material Name	Property Name	Code	File Name	PAPDB Value	Same Value Returned?	Comments
DRZ_PC_1	RELP_MOD	BRAGFLO	lhs3_bf_CRA19_r1_v031.cdb	4.00E+00	Yes	The correct value was returned.
DRZ_PC_1	SAT_IBRN	BRAGFLO	lhs3_bf_CRA19_r1_v031.cdb	1.00E+00	Yes	The correct value was returned.
DRZ_PC_1	SAT_RBRN	BRAGFLO	lhs3_bf_CRA19_r1_v031.cdb	0.00E+00	Yes	The correct value was returned.
DRZ_PC_1	SAT_RGAS	BRAGFLO	lhs3_bf_CRA19_r1_v031.cdb	0.00E+00	Yes	The correct value was returned.
GLOBAL	GDEPFAC	BRAGFLO	lhs3_bf_CRA19_r1_v031.cdb	0.00 to 0.50	2.83E-01	Sampled value correctly lies within the sampled range of 0.00 to 0.50.
GLOBAL	GH2AVG	BRAGFLO	lhs3_bf_CRA19_r1_v031.cdb	1.40E-02	Yes	The correct value was returned.
GLOBAL	LAMBDAD	PRECCDFGF	lhs3_ccgf_CRA19_r1_v031.cdb	9.90E-03	Yes	The correct value was returned.
GLOBAL	ONEPLG	PRECCDFGF	lhs3_ccgf_CRA19_r1_v031.cdb	4.03E-01	Yes	The correct value was returned.
GLOBAL	PBRINE	PRECCDFGF	lhs3_ccgf_CRA19_r1_v031.cdb	0.04 to 0.57	5.00E-01	Sampled value correctly lies within the sampled range of 0.04 to 0.57.
GLOBAL	SRADO2	BRAGFLO	lhs3_bf_CRA19_r1_v031.cdb	0.00E+00	Yes	The correct value was returned.
GLOBAL	THREEPLG	PRECCDFGF	lhs3_ccgf_CRA19_r1_v031.cdb	2.66E-01	Yes	The correct value was returned.
GLOBAL	TWOPLG	PRECCDFGF	lhs3_ccgf_CRA19_r1_v031.cdb	3.31E-01	Yes	The correct value was returned.
NITRATE	QINIT	BRAGFLO	lhs3_bf_CRA19_r1_v031.cdb	2.72E+07	Yes	The correct value was returned.
NP	CAPMIC	PANEL	lhs3_panel_CRA19_b1_r1_v031.cdb	3.80E-08	Yes	The correct value was returned.
NP	CONCINT	PANEL	lhs3_panel_CRA19_b1_r1_v031.cdb	4.30E-08	Yes	The correct value was returned.
NP	PROPMIC	PANEL	lhs3_panel_CRA19_b1_r1_v031.cdb	2.10E-01	Yes	The correct value was returned.
NP237	INVCHD	PANEL	lhs3_panel_CRA19_b1_r1_v031.cdb	2.75E+01	Yes	The correct value was returned.
NP237	INVRHD	PANEL	lhs3_panel_CRA19_b1_r1_v031.cdb	6.96E+00	Yes	The correct value was returned.
PA231	INVCHD	PANEL	lhs3_panel_CRA19_b1_r1_v031.cdb	1.59E+01	Yes	The correct value was returned.
PA231	INVRHD	PANEL	lhs3_panel_CRA19_b1_r1_v031.cdb	1.04E-03	Yes	The correct value was returned.
PB210	INVCHD	PANEL	lhs3_panel_CRA19_b1_r1_v031.cdb	9.79E-01	Yes	The correct value was returned.
PB210	INVRHD	PANEL	lhs3_panel_CRA19_b1_r1_v031.cdb	1.45E+01	Yes	The correct value was returned.
PCS_NO	CAP_MOD	BRAGFLO	lhs3_bf_CRA19_r1_v031.cdb	1.00E+00	Yes	The correct value was returned.
PCS_NO	COMP_RCK	BRAGFLO	lhs3_bf_CRA19_r1_v031.cdb	0.00E+00	Yes	The correct value was returned.
PCS_NO	KPT	BRAGFLO	lhs3_bf_CRA19_r1_v031.cdb	0.00E+00	Yes	The correct value was returned.
PCS_NO	PCT_A	BRAGFLO	lhs3_bf_CRA19_r1_v031.cdb	0.00E+00	Yes	The correct value was returned.

Table B3. Code/Database Interface Test Results for Parameters Used in the CRA-2019 PA that have Changed since the CRA-2014 PA (Continued)

Material Name	Property Name	Code	File Name	PAPDB Value	Same Value Returned?	Comments
PCS_NO	PCT_EXP	BRAGFLO	lhs3_bf_CRA19_r1_v031.cdb	0.00E+00	Yes	The correct value was returned.
PCS_NO	PC_MAX	BRAGFLO	lhs3_bf_CRA19_r1_v031.cdb	1.00E+08	Yes	The correct value was returned.
PCS_NO	PORE_DIS	BRAGFLO	lhs3_bf_CRA19_r1_v031.cdb	7.00E-01	Yes	The correct value was returned.
PCS_NO	POROSITY	BRAGFLO	lhs3_bf_CRA19_r1_v031.cdb	1.80E-01	Yes	The correct value was returned.
PCS_NO	PO_MIN	BRAGFLO	lhs3_bf_CRA19_r1_v031.cdb	1.01E+05	Yes	The correct value was returned.
PCS_NO	PRESSURE	BRAGFLO	lhs3_bf_CRA19_r1_v031.cdb	1.01E+05	Yes	The correct value was returned.
PCS_NO	PRMX_LOG	BRAGFLO	lhs3_bf_CRA19_r1_v031.cdb	-1.10E+01	Yes	The correct value was returned.
PCS_NO	PRMY_LOG	BRAGFLO	lhs3_bf_CRA19_r1_v031.cdb	-1.10E+01	Yes	The correct value was returned.
PCS_NO	PRMZ_LOG	BRAGFLO	lhs3_bf_CRA19_r1_v031.cdb	-1.10E+01	Yes	The correct value was returned.
PCS_NO	RELP_MOD	BRAGFLO	lhs3_bf_CRA19_r1_v031.cdb	1.10E+01	Yes	The correct value was returned.
PCS_NO	SAT_IBRN	BRAGFLO	lhs3_bf_CRA19_r1_v031.cdb	0.00E+00	Yes	The correct value was returned.
PCS_NO	SAT_RBRN	BRAGFLO	lhs3_bf_CRA19_r1_v031.cdb	0.00E+00	Yes	The correct value was returned.
PCS_NO	SAT_RGAS	BRAGFLO	lhs3_bf_CRA19_r1_v031.cdb	0.00E+00	Yes	The correct value was returned.
PHUMOX3	PHUMCIM	BRAGFLO	lhs3_bf_CRA19_r1_v031.cdb	2.00E-01	Yes	The correct value was returned.
PHUMOX3	PHUMCIM	PANEL	lhs3_panel_CRA19_b1_r1_v031.cdb	2.00E-01	Yes	The correct value was returned.
PHUMOX3	PHUMSIM	BRAGFLO	lhs3_bf_CRA19_r1_v031.cdb	2.00E-01	Yes	The correct value was returned.
PHUMOX3	PHUMSIM	PANEL	lhs3_panel_CRA19_b1_r1_v031.cdb	2.00E-01	Yes	The correct value was returned.
PHUMOX4	PHUMCIM	BRAGFLO	lhs3_bf_CRA19_r1_v031.cdb	1.00E-02	Yes	The correct value was returned.
PHUMOX4	PHUMCIM	PANEL	lhs3_panel_CRA19_b1_r1_v031.cdb	1.00E-02	Yes	The correct value was returned.
PHUMOX4	PHUMSIM	BRAGFLO	lhs3_bf_CRA19_r1_v031.cdb	1.00E-02	Yes	The correct value was returned.
PHUMOX4	PHUMSIM	PANEL	lhs3_panel_CRA19_b1_r1_v031.cdb	1.00E-02	Yes	The correct value was returned.
PM147	INVCHD	PANEL	lhs3_panel_CRA19_b1_r1_v031.cdb	4.40E-01	Yes	The correct value was returned.
PM147	INVRHD	PANEL	lhs3_panel_CRA19_b1_r1_v031.cdb	2.54E+01	Yes	The correct value was returned.
PU	CAPMIC	BRAGFLO	lhs3_bf_CRA19_r1_v031.cdb	3.80E-08	Yes	The correct value was returned.
PU	CAPMIC	PANEL	lhs3_panel_CRA19_b1_r1_v031.cdb	3.80E-08	Yes	The correct value was returned.
PU	CONCINT	BRAGFLO	lhs3_bf_CRA19_r1_v031.cdb	4.30E-08	Yes	The correct value was returned.
PU	CONCINT	PANEL	lhs3_panel_CRA19_b1_r1_v031.cdb	4.30E-08	Yes	The correct value was returned.

Table B3. Code/Database Interface Test Results for Parameters Used in the CRA-2019 PA that have Changed since the CRA-2014 PA (Continued)

Material Name	Property Name	Code	File Name	PAPDB Value	Same Value Returned?	Comments
PU	PROPMIC	BRAGFLO	lhs3_bf_CRA19_r1_v031.cdb	2.10E-01	Yes	The correct value was returned.
PU	PROPMIC	PANEL	lhs3_panel_CRA19_b1_r1_v031.cdb	2.10E-01	Yes	The correct value was returned.
PU238	DECAYNRG	BRAGFLO	lhs3_bf_CRA19_r1_v031.cdb	5.59E+00	Yes	The correct value was returned.
PU238	INVCHD	BRAGFLO	lhs3_bf_CRA19_r1_v031.cdb	9.42E+05	Yes	The correct value was returned.
PU238	INVCHD	PANEL	lhs3_panel_CRA19_b1_r1_v031.cdb	9.42E+05	Yes	The correct value was returned.
PU238	INVRHD	BRAGFLO	lhs3_bf_CRA19_r1_v031.cdb	2.25E+04	Yes	The correct value was returned.
PU238	INVRHD	PANEL	lhs3_panel_CRA19_b1_r1_v031.cdb	2.25E+04	Yes	The correct value was returned.
PU238L	INVCHD	PANEL	lhs3_panel_CRA19_b1_r1_v031.cdb	9.42E+05	Yes	The correct value was returned.
PU238L	INVRHD	PANEL	lhs3_panel_CRA19_b1_r1_v031.cdb	2.25E+04	Yes	The correct value was returned.
PU239	DECAYNRG	BRAGFLO	lhs3_bf_CRA19_r1_v031.cdb	5.24E+00	Yes	The correct value was returned.
PU239	INVCHD	BRAGFLO	lhs3_bf_CRA19_r1_v031.cdb	8.70E+05	Yes	The correct value was returned.
PU239	INVCHD	PANEL	lhs3_panel_CRA19_b1_r1_v031.cdb	8.70E+05	Yes	The correct value was returned.
PU239	INVRHD	BRAGFLO	lhs3_bf_CRA19_r1_v031.cdb	4.22E+03	Yes	The correct value was returned.
PU240	INVCHD	PANEL	lhs3_panel_CRA19_b1_r1_v031.cdb	4.22E+03	Yes	The correct value was returned.
PU239L	INVCHD	PANEL	lhs3_panel_CRA19_b1_r1_v031.cdb	1.19E+06	Yes	The correct value was returned.
PU239L	INVRHD	PANEL	lhs3_panel_CRA19_b1_r1_v031.cdb	7.63E+03	Yes	The correct value was returned.
PU240	DECAYNRG	BRAGFLO	lhs3_bf_CRA19_r1_v031.cdb	5.26E+00	Yes	The correct value was returned.
PU240	INVCHD	BRAGFLO	lhs3_bf_CRA19_r1_v031.cdb	3.16E+05	Yes	The correct value was returned.
PU240	INVCHD	PANEL	lhs3_panel_CRA19_b1_r1_v031.cdb	3.16E+05	Yes	The correct value was returned.
PU240	INVRHD	BRAGFLO	lhs3_bf_CRA19_r1_v031.cdb	3.16E+03	Yes	The correct value was returned.
PU240	INVRHD	PANEL	lhs3_panel_CRA19_b1_r1_v031.cdb	3.16E+03	Yes	The correct value was returned.
PU241	INVCHD	PANEL	lhs3_panel_CRA19_b1_r1_v031.cdb	1.82E+06	Yes	The correct value was returned.
PU241	INVRHD	PANEL	lhs3_panel_CRA19_b1_r1_v031.cdb	4.53E+04	Yes	The correct value was returned.
PU242	DECAYNRG	BRAGFLO	lhs3_bf_CRA19_r1_v031.cdb	4.99E+00	Yes	The correct value was returned.
PU242	INVCHD	BRAGFLO	lhs3_bf_CRA19_r1_v031.cdb	1.48E+02	Yes	The correct value was returned.
PU242	INVCHD	PANEL	lhs3_panel_CRA19_b1_r1_v031.cdb	1.48E+02	Yes	The correct value was returned.
PU242	INVRHD	BRAGFLO	lhs3_bf_CRA19_r1_v031.cdb	1.59E+01	Yes	The correct value was returned.

Table B3. Code/Database Interface Test Results for Parameters Used in the CRA-2019 PA that have Changed since the CRA-2014 PA (Continued)

Material Name	Property Name	Code	File Name	PAPDB Value	Same Value Returned?	Comments
PU242	INVRHD	PANEL	lhs3_panel_CRA19_b1_r1_v031.cdb	1.59E+01	Yes	The correct value was returned.
PU244	INVCHD	PANEL	lhs3_panel_CRA19_b1_r1_v031.cdb	5.80E-03	Yes	The correct value was returned.
PU244	INVRHD	PANEL	lhs3_panel_CRA19_b1_r1_v031.cdb	2.82E-02	Yes	The correct value was returned.
RA226	INVCHD	PANEL	lhs3_panel_CRA19_b1_r1_v031.cdb	1.78E+00	Yes	The correct value was returned.
RA226	INVRHD	PANEL	lhs3_panel_CRA19_b1_r1_v031.cdb	1.85E+01	Yes	The correct value was returned.
RA228	INVCHD	PANEL	lhs3_panel_CRA19_b1_r1_v031.cdb	9.03E-02	Yes	The correct value was returned.
RA228	INVRHD	PANEL	lhs3_panel_CRA19_b1_r1_v031.cdb	4.55E-02	Yes	The correct value was returned.
REFCON	STCO_31	BRAGFLO	lhs3_bf_CRA19_r1_v031.cdb	0.00E+00	Yes	The correct value was returned.
REFCON	STCO_32	BRAGFLO	lhs3_bf_CRA19_r1_v031.cdb	0.00E+00	Yes	The correct value was returned.
REFCON	STCO_35	BRAGFLO	lhs3_bf_CRA19_r1_v031.cdb	0.00E+00	Yes	The correct value was returned.
REFCON	STCO_36	BRAGFLO	lhs3_bf_CRA19_r1_v031.cdb	0.00E+00	Yes	The correct value was returned.
REFCON	STCO_43	BRAGFLO	lhs3_bf_CRA19_r1_v031.cdb	0.00E+00	Yes	The correct value was returned.
REFCON	STCO_46	BRAGFLO	lhs3_bf_CRA19_r1_v031.cdb	0.00E+00	Yes	The correct value was returned.
SM147	INVCHD	PANEL	lhs3_panel_CRA19_b1_r1_v031.cdb	1.23E-09	Yes	The correct value was returned.
SM147	INVRHD	PANEL	lhs3_panel_CRA19_b1_r1_v031.cdb	9.40E-08	Yes	The correct value was returned.
SOLMOD3	SOLCOH	BRAGFLO	lhs3_bf_CRA19_r1_v031.cdb	1.78E-07	Yes	The correct value was returned.
SOLMOD3	SOLCOH	PANEL	lhs3_panel_CRA19_b1_r1_v031.cdb	1.78E-07	Yes	The correct value was returned.
SOLMOD3	SOLCOH2	PANEL	lhs3_panel_CRA19_b1_r1_v031.cdb	1.63E-07	Yes	The correct value was returned.
SOLMOD3	SOLCOH3	PANEL	lhs3_panel_CRA19_b1_r1_v031.cdb	1.58E-07	Yes	The correct value was returned.
SOLMOD3	SOLCOH4	PANEL	lhs3_panel_CRA19_b1_r1_v031.cdb	1.54E-07	Yes	The correct value was returned.
SOLMOD3	SOLCOH5	PANEL	lhs3_panel_CRA19_b1_r1_v031.cdb	1.52E-07	Yes	The correct value was returned.
SOLMOD3	SOLSOH	BRAGFLO	lhs3_bf_CRA19_r1_v031.cdb	1.63E-07	Yes	The correct value was returned.
SOLMOD3	SOLSOH	PANEL	lhs3_panel_CRA19_b1_r1_v031.cdb	1.63E-07	Yes	The correct value was returned.
SOLMOD3	SOLSOH2	PANEL	lhs3_panel_CRA19_b1_r1_v031.cdb	1.58E-07	Yes	The correct value was returned.
SOLMOD3	SOLSOH3	PANEL	lhs3_panel_CRA19_b1_r1_v031.cdb	1.56E-07	Yes	The correct value was returned.
SOLMOD3	SOLSOH4	PANEL	lhs3_panel_CRA19_b1_r1_v031.cdb	1.55E-07	Yes	The correct value was returned.
SOLMOD3	SOLSOH5	PANEL	lhs3_panel_CRA19_b1_r1_v031.cdb	1.54E-07	Yes	The correct value was returned.

Table B3. Code/Database Interface Test Results for Parameters Used in the CRA-2019 PA that have Changed since the CRA-2014 PA (Continued)

Material Name	Property Name	Code	File Name	PAPDB Value	Same Value Returned?	Comments
SOLMOD3	SOLVAR	BRAGFLO	lhs3_bf_CRA19_r1_v031.cdb	-1.14 to 2.97	0	Sampled value correctly lies within the sampled range of -1.14 to 2.97.
SOLMOD3	SOLVAR	PANEL	lhs3_panel_CRA19_b1_r1_v031.cdb	-1.14 to 2.97	0	Sampled value correctly lies within the sampled range of -1.14 to 2.97.
SOLMOD4	SOLCOH	BRAGFLO	lhs3_bf_CRA19_r1_v031.cdb	5.44E-08	Yes	The correct value was returned.
SOLMOD4	SOLCOH	PANEL	lhs3_panel_CRA19_b1_r1_v031.cdb	5.44E-08	Yes	The correct value was returned.
SOLMOD4	SOLCOH2	PANEL	lhs3_panel_CRA19_b1_r1_v031.cdb	5.44E-08	Yes	The correct value was returned.
SOLMOD4	SOLCOH3	PANEL	lhs3_panel_CRA19_b1_r1_v031.cdb	5.44E-08	Yes	The correct value was returned.
SOLMOD4	SOLCOH4	PANEL	lhs3_panel_CRA19_b1_r1_v031.cdb	5.44E-08	Yes	The correct value was returned.
SOLMOD4	SOLCOH5	PANEL	lhs3_panel_CRA19_b1_r1_v031.cdb	5.44E-08	Yes	The correct value was returned.
SOLMOD4	SOLSOH	BRAGFLO	lhs3_bf_CRA19_r1_v031.cdb	5.45E-08	Yes	The correct value was returned.
SOLMOD4	SOLSOH	PANEL	lhs3_panel_CRA19_b1_r1_v031.cdb	5.45E-08	Yes	The correct value was returned.
SOLMOD4	SOLSOH2	PANEL	lhs3_panel_CRA19_b1_r1_v031.cdb	5.45E-08	Yes	The correct value was returned.
SOLMOD4	SOLSOH3	PANEL	lhs3_panel_CRA19_b1_r1_v031.cdb	5.45E-08	Yes	The correct value was returned.
SOLMOD4	SOLSOH4	PANEL	lhs3_panel_CRA19_b1_r1_v031.cdb	5.45E-08	Yes	The correct value was returned.
SOLMOD4	SOLSOH5	PANEL	lhs3_panel_CRA19_b1_r1_v031.cdb	5.45E-08	Yes	The correct value was returned.
SOLMOD4	SOLVAR	BRAGFLO	lhs3_bf_CRA19_r1_v031.cdb	-2.01 to 1.43	-5.56E-01	Sampled value correctly lies within the sampled range of -2.01 to 1.43.
SOLMOD4	SOLVAR	PANEL	lhs3_panel_CRA19_b1_r1_v031.cdb	-2.01 to 1.43	-5.56E-01	Sampled value correctly lies within the sampled range of -2.01 to 1.43.
SOLMOD5	SOLCOH	PANEL	lhs3_panel_CRA19_b1_r1_v031.cdb	1.20E-06	Yes	The correct value was returned.
SOLMOD5	SOLCOH2	PANEL	lhs3_panel_CRA19_b1_r1_v031.cdb	7.27E-07	Yes	The correct value was returned.
SOLMOD5	SOLCOH3	PANEL	lhs3_panel_CRA19_b1_r1_v031.cdb	5.52E-07	Yes	The correct value was returned.
SOLMOD5	SOLCOH4	PANEL	lhs3_panel_CRA19_b1_r1_v031.cdb	4.61E-07	Yes	The correct value was returned.
SOLMOD5	SOLCOH5	PANEL	lhs3_panel_CRA19_b1_r1_v031.cdb	4.05E-07	Yes	The correct value was returned.
SOLMOD5	SOLSOH	PANEL	lhs3_panel_CRA19_b1_r1_v031.cdb	4.02E-07	Yes	The correct value was returned.
SOLMOD5	SOLSOH2	PANEL	lhs3_panel_CRA19_b1_r1_v031.cdb	2.83E-07	Yes	The correct value was returned.
SOLMOD5	SOLSOH3	PANEL	lhs3_panel_CRA19_b1_r1_v031.cdb	2.42E-07	Yes	The correct value was returned.
SOLMOD5	SOLSOH4	PANEL	lhs3_panel_CRA19_b1_r1_v031.cdb	2.21E-07	Yes	The correct value was returned.

Table B3. Code/Database Interface Test Results for Parameters Used in the CRA-2019 PA that have Changed since the CRA-2014 PA (Continued)

Material Name	Property Name	Code	File Name	PAPDB Value	Same Value Returned?	Comments
SOLMOD5	SOLSOH5	PANEL	lhs3_panel_CRA19_b1_r1_v031.cdb	2.09E-07	Yes	The correct value was returned.
SR90	INVCHD	PANEL	lhs3_panel_CRA19_b1_r1_v031.cdb	8.18E+02	Yes	The correct value was returned.
SR90	INVRHD	PANEL	lhs3_panel_CRA19_b1_r1_v031.cdb	1.96E+05	Yes	The correct value was returned.
STEEL	CORRMCO2	BRAGFLO	lhs3_bf_CRA19_r1_v031.cdb	0.00 to 7.92E-14	1.05E-14	Sampled value correctly lies within the sampled range of 0.00 to 7.92E-14.
STEEL	HUMCORR	BRAGFLO	lhs3_bf_CRA19_r1_v031.cdb	0.00 to 1.03E-15	4.50E-16	Sampled value correctly lies within the sampled range of 0.00 to 1.03E-15.
SULFATE	QINIT	BRAGFLO	lhs3_bf_CRA19_r1_v031.cdb	4.73E+06	Yes	The correct value was returned.
TH	CAPMIC	PANEL	lhs3_panel_CRA19_b1_r1_v031.cdb	3.80E-08	Yes	The correct value was returned.
TH	CONCINT	PANEL	lhs3_panel_CRA19_b1_r1_v031.cdb	4.30E-08	Yes	The correct value was returned.
TH	PROPMIC	PANEL	lhs3_panel_CRA19_b1_r1_v031.cdb	2.10E-01	Yes	The correct value was returned.
TH229	INVCHD	PANEL	lhs3_panel_CRA19_b1_r1_v031.cdb	3.80E-01	Yes	The correct value was returned.
TH229	INVRHD	PANEL	lhs3_panel_CRA19_b1_r1_v031.cdb	8.74E-01	Yes	The correct value was returned.
TH230	INVCHD	PANEL	lhs3_panel_CRA19_b1_r1_v031.cdb	3.98E-01	Yes	The correct value was returned.
TH230	INVRHD	PANEL	lhs3_panel_CRA19_b1_r1_v031.cdb	2.26E+00	Yes	The correct value was returned.
TH230L	INVCHD	PANEL	lhs3_panel_CRA19_b1_r1_v031.cdb	7.78E-01	Yes	The correct value was returned.
TH230L	INVRHD	PANEL	lhs3_panel_CRA19_b1_r1_v031.cdb	3.13E+00	Yes	The correct value was returned.
TH232	INVCHD	PANEL	lhs3_panel_CRA19_b1_r1_v031.cdb	9.60E-02	Yes	The correct value was returned.
TH232	INVRHD	PANEL	lhs3_panel_CRA19_b1_r1_v031.cdb	2.26E-02	Yes	The correct value was returned.
U	CAPMIC	PANEL	lhs3_panel_CRA19_b1_r1_v031.cdb	3.80E-08	Yes	The correct value was returned.
U	CONCINT	PANEL	lhs3_panel_CRA19_b1_r1_v031.cdb	1.40E-06	Yes	The correct value was returned.
U	PROPMIC	PANEL	lhs3_panel_CRA19_b1_r1_v031.cdb	2.10E-01	Yes	The correct value was returned.
U233	INVCHD	PANEL	lhs3_panel_CRA19_b1_r1_v031.cdb	1.10E+02	Yes	The correct value was returned.
U233	INVRHD	PANEL	lhs3_panel_CRA19_b1_r1_v031.cdb	1.72E+01	Yes	The correct value was returned.
U234	INVCHD	PANEL	lhs3_panel_CRA19_b1_r1_v031.cdb	4.77E+02	Yes	The correct value was returned.
U234	INVRHD	PANEL	lhs3_panel_CRA19_b1_r1_v031.cdb	9.70E+00	Yes	The correct value was returned.
U234L	INVCHD	PANEL	lhs3_panel_CRA19_b1_r1_v031.cdb	5.86E+02	Yes	The correct value was returned.
U234L	INVRHD	PANEL	lhs3_panel_CRA19_b1_r1_v031.cdb	2.69E+01	Yes	The correct value was returned.

Table B3. Code/Database Interface Test Results for Parameters Used in the CRA-2019 PA that have Changed since the CRA-2014 PA (Continued)

Material Name	Property Name	Code	File Name	PAPDB Value	Same Value Returned?	Comments
U235	INVCHD	PANEL	lhs3_panel_CRA19_b1_r1_v031.cdb	4.56E+00	Yes	The correct value was returned.
U235	INVRHD	PANEL	lhs3_panel_CRA19_b1_r1_v031.cdb	1.85E+00	Yes	The correct value was returned.
U236	INVCHD	PANEL	lhs3_panel_CRA19_b1_r1_v031.cdb	4.24E-01	Yes	The correct value was returned.
U236	INVRHD	PANEL	lhs3_panel_CRA19_b1_r1_v031.cdb	2.53E-01	Yes	The correct value was returned.
U238	INVCHD	PANEL	lhs3_panel_CRA19_b1_r1_v031.cdb	3.92E+01	Yes	The correct value was returned.
U238	INVRHD	PANEL	lhs3_panel_CRA19_b1_r1_v031.cdb	3.13E+00	Yes	The correct value was returned.
WAS_AREA	CELCCHW	BRAGFLO	lhs3_bf_CRA19_r1_v031.cdb	1.47E+06	Yes	The correct value was returned.
WAS_AREA	CELCRHW	BRAGFLO	lhs3_bf_CRA19_r1_v031.cdb	0.00E+00	Yes	The correct value was returned.
WAS_AREA	CELECHW	BRAGFLO	lhs3_bf_CRA19_r1_v031.cdb	2.24E+05	Yes	The correct value was returned.
WAS_AREA	CELERHW	BRAGFLO	lhs3_bf_CRA19_r1_v031.cdb	0.00E+00	Yes	The correct value was returned.
WAS_AREA	CELLCHW	BRAGFLO	lhs3_bf_CRA19_r1_v031.cdb	4.10E+06	Yes	The correct value was returned.
WAS_AREA	CELLRHW	BRAGFLO	lhs3_bf_CRA19_r1_v031.cdb	1.70E+05	Yes	The correct value was returned.
WAS_AREA	HYMAGCON	BRAGFLO	lhs3_bf_CRA19_r1_v031.cdb	0.00 to 3.40E-10	2.23E-10	Sampled value correctly lies within the sampled range of 0.00 to 3.40E-10.
WAS_AREA	IRNCCHW	BRAGFLO	lhs3_bf_CRA19_r1_v031.cdb	3.12E+07	Yes	The correct value was returned.
WAS_AREA	IRNCRHW	BRAGFLO	lhs3_bf_CRA19_r1_v031.cdb	1.65E+07	Yes	The correct value was returned.
WAS_AREA	IRONCHW	BRAGFLO	lhs3_bf_CRA19_r1_v031.cdb	1.41E+07	Yes	The correct value was returned.
WAS_AREA	IRONRHW	BRAGFLO	lhs3_bf_CRA19_r1_v031.cdb	1.33E+06	Yes	The correct value was returned.
WAS_AREA	PLASCHW	BRAGFLO	lhs3_bf_CRA19_r1_v031.cdb	5.32E+06	Yes	The correct value was returned.
WAS_AREA	PLASRHW	BRAGFLO	lhs3_bf_CRA19_r1_v031.cdb	4.14E+05	Yes	The correct value was returned.
WAS_AREA	PLSCCHW	BRAGFLO	lhs3_bf_CRA19_r1_v031.cdb	2.83E+06	Yes	The correct value was returned.
WAS_AREA	PLSCRHW	BRAGFLO	lhs3_bf_CRA19_r1_v031.cdb	4.68E+05	Yes	The correct value was returned.
WAS_AREA	PLSECHW	BRAGFLO	lhs3_bf_CRA19_r1_v031.cdb	1.55E+06	Yes	The correct value was returned.
WAS_AREA	PLSERHW	BRAGFLO	lhs3_bf_CRA19_r1_v031.cdb	0.00E+00	Yes	The correct value was returned.
WAS_AREA	RUBBCHW	BRAGFLO	lhs3_bf_CRA19_r1_v031.cdb	1.09E+06	Yes	The correct value was returned.
WAS_AREA	RUBBRHW	BRAGFLO	lhs3_bf_CRA19_r1_v031.cdb	5.12E+04	Yes	The correct value was returned.
WAS_AREA	RUBCCHW	BRAGFLO	lhs3_bf_CRA19_r1_v031.cdb	7.28E+04	Yes	The correct value was returned.

Table B3. Code/Database Interface Test Results for Parameters Used in the CRA-2019 PA that have Changed since the CRA-2014 PA (Continued)

Material Name	Property Name	Code	File Name	PAPDB Value	Same Value Returned?	Comments
WAS_AREA	RUBCRHW	BRAGFLO	lhs3_bf_CRA19_r1_v031.cdb	5.73E+03	Yes	The correct value was returned.
WAS_AREA	RUBECHW	BRAGFLO	lhs3_bf_CRA19_r1_v031.cdb	4.79E+03	Yes	The correct value was returned.
WAS_AREA	RUBERHW	BRAGFLO	lhs3_bf_CRA19_r1_v031.cdb	0.00E+00	yes	The correct value was returned.

B4.0 PARAMETER DATA ENTRY PROCESS REVIEW

The parameter data entry process and controls were evaluated by reviewing the PDE forms used as the basis for data entry into the PAPDB, in accordance with SNL Nuclear Waste Management Procedure NP 9-2 Rev 2: *Parameters*. As noted above, this procedure was most recently updated in April 2017. This procedure prescribes the processes for developing, documenting, controlling, and changing parameters used in compliance-level and programmatic PA calculations performed by SNL in support of the WIPP. Parameter values are required to be developed and documented in accordance with approved, procedurally driven planning documents. NP 9-2 Rev 2 provides detailed instructions for entering or changing a parameter value in the PAPDB. Responsibilities for checking and approval are clearly defined and appropriate. No concerns regarding this procedure were identified.

Each PDE form for the parameters that are new or have been changed since the CRA-2014 PA was inspected by the Agency for completeness to confirm that all appropriate blanks were filled in and the necessary signatures were provided. The accuracy of the data entry process was checked by visually comparing the information on a subset of the forms with the information shown in the PAPDB. EPA did not consider it necessary to compare parameter values on every PDE form with those in the PAPDB because the PDE is an intermediate transcription between the values in Kim and Feng (2019) and those in the PAPDB. EPA confirmed the accuracy of this transcription process by directly comparing the PAPDB with Kim and Feng (2019). EPA's review of selected PDE forms found that they were completely and correctly filled out. Handwritten changes were found on several forms correcting the associated metadata. These hand entries were dated and initialed by the originator of the form or by another responsible individual and were, therefore, acceptable.

B5.0 COMPUTING HARDWARE

The CRA-2019 PA calculations were executed on the WIPP PA Solaris Cluster. Twenty Oracle/SUN nodes were configured to share the same disk array using Storage Area Network (SAN) technology for efficient disk utilization and data storage and management. This allowed for highly distributed processing while providing for integrated data access. The WIPP PA Solaris Cluster runs the Oracle Solaris 11 operating system (Long 2019b). The node name, hardware description, CPU information, operation system, and number of CPUs for each node are provided in Table B4.

The parameters changed for the CRA-2019 PA are used by the BRAGFLO, PANEL, CUTTINGS_S, EPAUNI, PRECCDFGF, and NUTS WIPP PA Codes.

- Brine and gas flow in and around the repository and in overlying formations are calculated using the BRAGFLO suite of codes (PREBRAG, BRAGFLO, and POSTBRAG) in conjunction with several utility codes. The entire set of calculations is performed for three replicates. Each replicate includes six scenarios (S1-S6) designed to cover a range of drilling intrusion types and times. For each replicate/scenario combination, calculations are performed for 100 vectors of uncertain model input parameters.

- Actinide mobilization in WIPP brines as dissolved species and sorbed to colloids are calculated with the PANEL code run in "concentration" mode, referred to here as PANEL_CON. This information is needed to compute the amount of radionuclides available for transport away from the repository in direct brine releases to the surface or in brines migrating to the accessible environment via subsurface pathways. Three replicates of the mobilization calculations were performed for the CRA-2019 PA.

- The total volume of radionuclide-contaminated solids that may reach the surface during a drilling intrusion event is calculated by the CUTTINGS_ S code.

- The EPAUNI code calculates the decay of the radionuclide components in each inventory waste stream over the 10,000-year regulatory period for use in calculating direct solids releases. These calculations are deterministic, so multiple replicates and vectors of uncertain parameters are not used. Calculations are performed for both contact-handled (CH) and remote-handled (RH) waste.

- The complementary cumulative distribution functions (CCDFs) for radionuclide releases to the accessible environment are constructed using the PRECCDFGF/CCDFGF code suite.

- Radionuclide transport in the Salado for single intrusion conditions is calculated using the NUTS code. Three replicate calculations were performed for the CRA-2019 PA.

Sampling of uncertain parameters used by the various process model codes is performed with the PRELHS and LHS codes. PRELHS reads information about the ranges and distributions of the uncertain parameters from the PAPDB and formats this information for LHS. The LHS code implements the sampling algorithms. LHS is executed once per replicate. Additional run control information is provided by Long (2019b).

Table B4. WIPP PA Solaris Cluster Nodes Used in the CRA-2019 PA

Node	Hardware Type	Number of CPUs	CPU	Operating System
GD	Oracle/SUN X6270 m2	24	x86(GenuineIntel 206C2 family 6 model 44 step 2 clock 3458 MHz)	Oracle Solaris 11
IRON	Oracle/SUN X6270 m2	24	x86(GenuineIntel 206C2 family 6 model 44 step 2 clock 3458 MHz)	Oracle Solaris 11
VH	Oracle/SUN X6270 m2	24	x86(GenuineIntel 206C2 family 6 model 44 step 2 clock 3458 MHz)	Oracle Solaris 11
PF	Oracle/SUN X6270 m2	24	x86(GenuineIntel 206C2 family 6 model 44 step 2 clock 3458 MHz)	Oracle Solaris 11
BLS	Oracle/SUN X6270 m2	24	x86(GenuineIntel 206C2 family 6 model 44 step 2 clock 3458 MHz)	Oracle Solaris 11
BEP	Oracle/SUN X6270 m2	24	x86(GenuineIntel 206C2 family 6 model 44 step 2 clock 3458 MHz)	Oracle Solaris 11
GDF	Oracle/SUN X6270 m2	24	x86(GenuineIntel 206C2 family 6 model 44 step 2 clock 3458 MHz)	Oracle Solaris 11

DC5	Oracle/SUN X6270 m2	24	x86(GenuineIntel 206C2 family 6 model 44 step 2 clock 3458 MHz)	Oracle Solaris 11
LZ	Oracle/SUN X6270 m2	24	x86(GenuineIntel 206C2 family 6 model 44 step 2 clock 3458 MHz)	Oracle Solaris 11
ZP	Oracle/SUN X6270 m2	24	x86(GenuineIntel 206C2 family 6 model 44 step 2 clock 3458 MHz)	Oracle Solaris 11
BC	Oracle/SUN X4-2B	48	x86(GenuineIntel 306E4 family 6 model 62 step 4 clock 2693 MHz)	Oracle Solaris 11
BOS	Oracle/SUN X4-2B	48	x86(GenuineIntel 306E4 family 6 model 62 step 4 clock 2693 MHz)	Oracle Solaris 11
CHI	Oracle/SUN X4-2B	48	x86(GenuineIntel 306E4 family 6 model 62 step 4 clock 2693 MHz)	Oracle Solaris 11
FOG	Oracle/SUN X4-2B	48	x86(GenuineIntel 306E4 family 6 model 62 step 4 clock 2693 MHz)	Oracle Solaris 11
HP	Oracle/SUN X4-2B	48	x86(GenuineIntel 306E4 family 6 model 62 step 4 clock 2693 MHz)	Oracle Solaris 11
JA	Oracle/SUN X4-2B	48	x86(GenuineIntel 306E4 family 6 model 62 step 4 clock 2693 MHz)	Oracle Solaris 11
ML	Oracle/SUN X4-2B	48	x86(GenuineIntel 306E4 family 6 model 62 step 4 clock 2693 MHz)	Oracle Solaris 11
RE	Oracle/SUN X4-2B	48	x86(GenuineIntel 306E4 family 6 model 62 step 4 clock 2693 MHz)	Oracle Solaris 11
UH	Oracle/SUN X4-2B	48	x86(GenuineIntel 306E4 family 6 model 62 step 4 clock 2693 MHz)	Oracle Solaris 11
ZZ	Oracle/SUN X4-2B	48	x86(GenuineIntel 306E4 family 6 model 62 step 4 clock 2693 MHz)	Oracle Solaris 11
SAN	Dell PowerEdge R820	64	x86(GenuineIntel 206D7 family 6 model 45 step 7 clock 2400 MHz)	Oracle Solaris 11

B6.0 CONCLUSIONS

No database problems were identified in this review that had an effect on the results of the CRA-2019 PA analysis. EPA's review confirmed that all parameter values used in the analysis were accurately transcribed from the source documentation to the PAPDB, that the metadata in the PAPDB was sufficient to trace the parameter value to its technical source documentation; and that the correct parameter values were retrieved from the PAPDB for use in the CRA-2019 PA. The controlling procedure for parameter data entry, SNL Nuclear Waste Management Procedure NP 9-2 Rev 2: *Parameters*, was reviewed and found to provide detailed instructions for entering or changing a parameter value in the PAPDB. Responsibilities for checking and approval were clearly defined and appropriate. No concerns regarding this procedure were identified. In addition, the Parameter Data Entry forms were found to be completely and correctly completed and accurately transcribed the parameter information used in the CRA-2019 PA. EPA's review of the parameters used in the CRA-2019 PA that were changed since the CRA-2014 PA resulted in no adverse findings.

REFERENCES

Day, B.A. 2016. A Summary of Parameters to be Implemented in the CRA2014_SEN2 PA. Sandia National Laboratories, Carlsbad, NM. March. ERMS 565722.

Day, B.A. 2018. Impact Analysis for BRAGFLO 6.03 Software Problem Report, SPR 18-002. Sandia National Laboratories. Carlsbad, NM. ERMS 570325.

Day, B.A. 2019. Reassessment of Need and Parameter Justification for Modeling Gas Generation Due to Radiolysis of Brine and Cellulose/Plastic/Rubber in WIPP for CRA-2019. Sandia National Laboratories, Carlsbad, NM. February. ERMS 570873.

DOE (U.S. Department of Energy) 2018. Delaware Basin Monitoring Annual Report, September 2018. DOE/WIPP-18-2308 Rev. 1. Carlsbad Field Office, Carlsbad, New Mexico. September.

Domski, P. 2019. Th(IV), Np(V), and Am(III) Baseline Solubilities and Th(IV) and Am(III) Solubility Uncertainties for the CRA-2019 PA. Sandia National Laboratories, Carlsbad, NM. April. ERMS 571169.

Domski, P. and C. Sisk-Scott 2019. Prediction of Baseline Actinide Solubilities for CRA-2019 with an Updated EQ3/6 Pitzer Thermodynamic Database, DATA0.FM4. Sandia National Laboratories, Carlsbad, NM. April. ERMS 571178.

Kim, S. and L. Feng. 2019. Input Parameter Report for the 2019 Compliance Recertification Application Performance Assessment (CRA-2019 PA), Rev. 1. Sandia National Laboratories, Carlsbad, NM. ERMS 571660.

Kicker, D. and C. Herrick 2013. Parameter Summary Report for the 20-14 Compliance Recertification Application. Sandia National Laboratories, Carlsbad, NM. June. ERMS 560298.

Kicker, D. 2019. Radionuclide Inventory Screening Analysis for the 2019 Compliance Recertification Application Performance Assessment (CRA-2019 PA). Sandia National Laboratories, Carlsbad, NM. April. ERMS 571244.

Long, J. 2017. Nuclear Waste Management Procedure NP 9-2, Parameters, Revision 2. Sandia National Laboratories, Carlsbad, NM. ERMS 568008.

Long, J. 2019a. Design Document/User's Manual/Implementation Document for PAPDB Version 3.00, Document Version 3.00. Sandia National Laboratories, Carlsbad, NM. ERMS 570734.

Long, J. 2019b. Computational Code Execution and File Management for the 2019 Compliance Recertification Application Performance Assessment (CRA-2019 PA). Sandia National Laboratories, Carlsbad, NM. ERMS 571375.

Mariner, P. 2016. Actinide(IV)-Humic Complexation in the WIPP Performance Assessment. Sandia National Laboratories, Carlsbad, NM. October. ERMS 567222.

Mariner, P. 2018. Actinide(III)-Humic Complexation in the WIPP Performance Assessment. Sandia National Laboratories, Carlsbad, NM. March. ERMS 569599.

Mariner, P. 2019. A Summary of Humic Colloid Parameter Values to be Implemented in the CRA-2019 Deferred Performance Assessment. Sandia National Laboratories, Carlsbad, NM. April. ERMS 571250.

Peake, T. 2016. Subject: EPA Requested SEN2 -12 Sensitivity Analysis Parameters. U.S. Environmental Protection Agency, Washington, D.C. September. ERMS 565676.

Peake, T. 2018. Subject: Accepting Resolutions to CRA-2014 Issues Table. U.S. Environmental Protection Agency, Washington, D.C. October. ERMS 570585.

Reed, D.T., S. Okajima, L.H. Brush, and M.A. Molecke. 1993. Radiolytically Induced Gas Production in Plutonium-Spiked WIPP Brine. Materials Research Society Symposium Proceedings (pp. 431-38). Vol. 294. Warrendale, PA: Materials Research Society.

Reed, D.T., J.S. Swanson, J.F. Lucchini, and M.K. Richmann 2013. Intrinsic, Mineral and Microbial Colloid Enhancement Parameters for the WIPP Actinide Source term. LCO-ACP-18. Los Alamos National Laboratory Carlsbad Operations. Carlsbad, New Mexico. February.

Reed, D.T., J. Swanson, and F. Stanley 2019. LANL/ACRSP Parameter Recommendations for the CRA-2019 Deferred Performance Assessment, Revision 1. LA-UR-19-22787. Los Alamos National Laboratory, Carlsbad, NM. ERMS 571296.

Roselle, G. T. 2013. Determination of Corrosion Rates from Iron/Lead Corrosion Experiments to be used for Gas Generation Calculations. Sandia National Laboratories, Carlsbad, NM. ERMS 559077.

Sisk-Scott, C. 2019. Calculation of Organic-Ligand Concentrations for the WIPP CRA-2019 Deferred PA. Sandia National Laboratories, Carlsbad, NM. February. ERMS 571011.

Swanson, J.S. 2019. Review of the Microbial Colloid Contribution to the WIPP Actinide Source Term. LA-OR-19-22310. Los Alamos National Laboratory Carlsbad Operations. Carlsbad, New Mexico. March.

Van Soest, G.D. 2018. Performance Assessment Inventory Report-2018. Los Alamos National Laboratory Carlsbad Operations. Carlsbad, NM. LA-UR-18-31882. ERMS 575699.

Zeitler, T.R. and C. Hansen. 2015a. Cumulative Distribution for STEEL:CORRMC02. Sandia National Laboratories, Carlsbad, NM. ERMS 565005.

Zeitler, T.R. and C. Hansen. 2015b. Cumulative Distribution for STEEL:HUMCORR. Sandia National Laboratories, Carlsbad, NM. ERMS 565009.

Zeitler, T.R. and C. Hansen. 2015c. Updated Calculation of the Cumulative Distribution for STEEL:HUMCORR. Sandia National Laboratories, Carlsbad, NM. ERMS 565108.

Zeitler, T.R. 2016a. Communications between the EPA and the DOE Regarding Panel Closure Sensitivity Study. Sandia National Laboratories, Carlsbad, NM. July. ERMS 566571.

Zeitler, T.R. 2016b. A Summary of Parameters to be Implemented in the CRA2014_SEN3 PA. Sandia National Laboratories, Carlsbad, NM. July. ERMS 566607.

Zeitler, T.R. 2016c. Communications between the EPA and the DOE Regarding CRA14_SEN4 Sensitivity Study, Rev. 1. Sandia National Laboratories, Carlsbad, NM. November. ERMS 567343.

Zeitler, T.R. and B.A. Day 2016. A Summary of Parameters to be Implemented in the CRA14_SEN4 PA. Sandia National Laboratories, Carlsbad, NM. November. ERMS 567353.

Zeitler, T.R. and B.A. Day 2017. Analysis Plan for the Assessment of Abandoned Panel Closures in South End of Repository and Lack of Waste Emplacement in Panel 9. Sandia National Laboratories, Carlsbad, NM. July. ERMS 568138.

Zeitler, T.R. and B.A. Day, J. Bethune, R. Sarathi, and J. Long 2017. Assessment of Abandoned Panel Closures in South End of Repository and Lack of Waste Emplacement in Panel 9. Sandia National Laboratories, Carlsbad, NM. August. ERMS 568459.

Zeitler, T.R. 2018a. Bounding Calculation of the Cumulative Distribution for STEEL:HUMCORR. Sandia National Laboratories, Carlsbad, NM. April. ERMS 569807.

Zeitler, T.R. 2018b. Cumulative Distribution for STEEL:CORRMCO2 for the CRA-2019 PA. Sandia National Laboratories, Carlsbad, NM. December. ERMS 570869.

Zeitler, T.R. 2019a. A Summary of EPA/DOE Defined Parameters to be Implemented in the CRA-2019 PA. Sandia National Laboratories, Carlsbad, NM. January. ERMS 570879.

Zeitler, T.R. 2019b. Analysis Plan for the 2019 WIPP Compliance Recertification Application Performance Assessment. Sandia National Laboratories, Carlsbad, NM. March. ERMS 571150.